UNCLASSIFIED

AD NUMBER

ADB121965

NEW LIMITATION CHANGE

TO

Approved for public release, distribution unlimited

FROM

Distribution authorized to U.S. Gov't. agencies and their contractors; Critical Technology; APR 1988. Other requests shall be referred to Air Force Astronautics Laboratory, Air Force Space Technology Center, Space Division, ATTN: TSTR, Edwards AFB, CA 93523-5000.

AUTHORITY

AFAL ltr dtd 17 Jan 1989

THIS PAGE IS UNCLASSIFIED

DTIC FILE COPY

(2)

AFAL-TR-88-004 AD:

AD-B121 965

Air Augmented Rocket Propulsion Concepts

DTIC
ELECTE
MAY 1 9 1988
S D
H

Final Report
for the period
1 Sept 1986 to
30 January 1988

April 1988

Authors:
R. W. Foster
W. J. D. Escher
J. W. Robinson

Astronautics Corporation of America
Technology Center
5800 Cottage Grove Road
Madison, WI 53716

ACA TER05675A
F04611-86-C-0094

WARNING: This document contains technical data whose export is restricted by the Arms Export Control Act (Title 22, U.S.C., Sec 2751 et seq.) or the Export Administration Act of 1979, as amended. Title 50, U.S.C., App. 2401, et seq. Violations of these export laws are subject to severe criminal penalties. Disseminate in accordance with the provisions of AFR 80-34.

Distribution authorized to U.S. Government agencies and their contractors; Critical Technology, April 1988. Other requests for this document must be referred to AFAL/TSTR, Edwards AFB, CA 93523-5000.

DESTRUCTION NOTICE: Destroy by any method that will prevent disclosure of contents or reconstruction of the document.

prepared for the: **Air Force Astronautics Laboratory**

Air Force Space Technology Center
Space Division, Air Force Systems Command
Edwards Air Force Base,
California 93523-5000

88 5 13 142

FOREWORD

This final report was submitted by Astronautics Corporation of America, Madison, WI on completion of contract F04611-86-C-0094 with the Air Force Astronautics Laboratory (AFAL), Edwards AFB, CA. AFAL Project Manager was Raymond Klucz.

This report has been reviewed and is approved for release and distribution in accordance with the distribution statement on the cover and on the DD Form 1473.

Raymond S. Klucz

RAYMOND S. KLUCZ
Project Manager

RICHARD S. MATLOCK
Chief, Applications Analysis Branch

FOR THE COMMANDER

DAVID J. DLKOWSKI, Major, USAF
Deputy Director
Aerospace Vehicle Systems Division

REPORT DOCUMENTATION PAGE

1a. REPORT SECURITY CLASSIFICATION Unclassified	1b. RESTRICTIVE MARKINGS
2a. SECURITY CLASSIFICATION AUTHORITY	3. DISTRIBUTION/AVAILABILITY OF REPORT Authorized to U.S. Govt agencies and their contractors; Critical Technology, April 1988. Other requests for this document must be referred to AFAL/TSTR, Edwards AFB CA 93523-5000.
2b. DECLASSIFICATION/DOWNGRADING SCHEDULE	
4. PERFORMING ORGANIZATION REPORT NUMBER(S) ACA TER05675A	5. MONITORING ORGANIZATION REPORT NUMBER(S) AFAL-TR-88-004
6a. NAME OF PERFORMING ORGANIZATION Astronautics Corporation of America - Technology Center 6b. OFFICE SYMBOL (If applicable)	7a. NAME OF MONITORING ORGANIZATION Air Force Astronautics Laboratory
6c. ADDRESS (City, State and ZIP Code) 5800 Cottage Grove Road Madison, WI 53716	7b. ADDRESS (City, State and ZIP Code) Edwards Air Force Base CA 93523-5000
8a. NAME OF FUNDING/SPONSORING ORGANIZATION 8b. OFFICE SYMBOL (If applicable)	9. PROCUREMENT INSTRUMENT IDENTIFICATION NUMBER F04622-86-C-0094
8c. ADDRESS (City, State and ZIP Code)	10. SOURCE OF FUNDING NOS. PROGRAM ELEMENT NO. 65808F; PROJECT NO. 3058; TASK NO. 00; WORK UNIT NO. 6B
11. TITLE (Include Security Classification) Air Augmented Rocket Propulsion Concepts (U)	
12. PERSONAL AUTHOR(S) Foster, R.W., Escher, W.J.D. and Robinson, J.W.	
13a. TYPE OF REPORT Final	13b. TIME COVERED FROM 860901 TO 880130
14. DATE OF REPORT (Yr., Mo., Day) 88/4	15. PAGE COUNT 281
16. SUPPLEMENTARY NOTATION An Investigation of Rocket Based Combined Cycle (RBCC) Engine Systems Applied to Single Stage to Orbit (SSTO) Space Transportation Systems	

17. COSATI CODES		
FIELD	GROUP	SUB. GR.
21	08	
22	02	

18. SUBJECT TERMS (Continue on reverse if necessary and identify by block number)
Air Augmented Rockets, Ramjets, Scramjets, SSTO, Orbit on Demand, Combined Cycle Engines, Space Vehicles,

19. ABSTRACT (Continue on reverse if necessary and identify by block number)

This report presents the results of a study of five combined cycle propulsion systems capable of accelerating a single stage vehicle with lifting surfaces from ground launch to Earth orbit. The engines studied were airbreathing, rocket based combined cycle (RBCC) engines. "Combined Cycle" engines integrate airbreathing and rocket propulsion systems into a single engine system.

These engines transition from initial air-augmented rocket mode takeoff and initial acceleration to ramjet to scramjet and finally to rocket propulsion to orbital insertion velocity.

Engine systems, engine/vehicle integration, vehicle structure, propellant storage systems and thermal protection system (TPS) design, sizing and weight estimation, overall performance on various trajectories, and ground support systems were studied. A technology assessment, subscale engine test plan, development program plan and life cycle costs estimates are presented.

Keywords=!

20. DISTRIBUTION/AVAILABILITY OF ABSTRACT UNCLASSIFIED/UNLIMITED ☐ SAME AS RPT. ☒ DTIC USERS ☐	21. ABSTRACT SECURITY CLASSIFICATION Unclassified
22a. NAME OF RESPONSIBLE INDIVIDUAL Raymond Klucz	22b. TELEPHONE NUMBER (Include Area Code) (805)275-5401 22c. OFFICE SYMBOL VSAB

DD FORM 1473, 83 APR EDITION OF 1 JAN 73 IS OBSOLETE.

TABLE OF CONTENTS

		PAGE NO.
1.0	INTRODUCTION	1
1.1	Study Overview	1
1.2	Vehicles Systems Requirements	2
1.3	Engine Systems Study	3
1.4	Study Goals and Findings	7
1.4.1	Propulsion System	7
1.4.2	Life Cycle Cost Estimate	8
1.4.3	Scaling of Configurations	10
1.5	Recommended Future Work	10
1.6	Approach	12
1.6.1	The Design Task Scope	12
1.6.2	Study Approach	12
1.7	Contents of the Report	12
2.0	AIR-AUGMENTED ROCKET SYSTEMS - ROCKET BASED COMBINED CYCLE ENGINE SYSTEMS - BRIEF REVIEW OF PRIOR WORK	17
2.1	Introduction	17
2.2	Air-Augmented Rockets	18
2.3	The Work Carried Out by the Marquardt Corp.	21
2.4	Thermal Choke and Fixed and Variable Exit Geometry Considerations	23
2.5	A Review of Some Relevant Experimental Investigations	24
2.6	NASA Langley Research Center HRE Project	27
3.0	ROCKET BASED COMBINED CYCLE PROPULSION SYSTEMS	29
3.1	Mission Profile	29
3.2	Multi Mode Performance Over the Mission Profile	30
3.3	Reference Ascent Flight Path	32
3.4	Engine Selection	32
3.4.1	Ejector Scramjet	35
3.4.2	Supercharged Ejector Scramjet	37
3.4.3	ScramLACE	37
3.4.4	Supercharged ScramLACE	40
3.4.5	Recycled Supercharged ScramLACE	40
3.5	Net Jet Specific Impulse	40
3.6	Effective Specific Impulse and I*	44
3.7	RBCC Engines Configuration and Performance	44
3.7.1	Physical Arrangement	44
3.7.2	Performance	44
3.7.3	Weight	45
3.7.4	Specific Impulse Performance	45
3.7.5	Thrust Performance	45
3.8	Approach to Discussion of Subsystems	47

DTIC COPY INSPECTED 1

ession For
GRA&I
TAB
nounced
tification
By
Distribution/
Availability Codes
Dist | Avail and/or Special
A-2 | 57

TABLE OF CONTENTS

		PAGE NO.
3.9	The Inlet Subsystem	47
3.9.1	Axisymmetric Design	48
3.9.2	Discrete Versus Annular Configurations	50
3.9.3	Force Accounting	52
3.9.4	"Second Stage" Compression	55
3.9.5	An Alternate Design Approach - the Ramp Inlet	56
3.10	Fan Subsystem	56
3.10.1	Assets	56
3.10.2	Liabilities	56
3.10.3	Stowage Options	58
3.10.4	Performance	59
3.10.5	Fan Subsystem Performance Upgrading	59
3.11	Rocket Subsystem	61
3.11.1	Capabilities Required	61
3.11.2	Design Approach	62
3.11.3	Operation	65
3.12	Ramjet Subsystem	71
3.13	Scramjet Subsystem	72
3.14	Air Liquifaction Subsystem	75
3.14.1	Assets	75
3.14.2	Liabilities	75
3.14.3	Requirements	75
3.14.4	The Fouling Problem	77
3.14.5	Conclusion	79
3.15	Slush Hydrogen Utilization	79
3.15.1	Benefits	79
3.15.2	Liabilities	84
3.15.3	Present Technology Development Efforts	84
3.16	Engine Structure, Materials, Processes and Weights	84
3.16.1	Structure, Materials and Processes	84
3.16.2	Fan Subsystem Weights - An Example	87
3.16.3	The Air Liquefaction Subsystem Example	87
3.16.4	Subsystems Weights Estimation Factors	87
3.16.5	125 Klb SLS Thrust Engine Weights	87
3.16.6	T/W Comparisons to Turbomachinery Based Engines	87
3.16.7	Engine Subsystems Conceptual Layouts	94
4.0	**ENGINE/VEHICLE INTEGRATION**	**101**
4.1	Engine Envelopes	101
4.2	Engine Weights vs Thrust Level	101
4.3	Engine Attachment Points	101
4.4	Engine/Vehicle Integration Considerations	101
5.0	**THE VEHICLE SYSTEM**	**107**
5.1	Approach to Discussion of the Vehicle System	107

TABLE OF CONTENTS

			PAGE NO.
5.2	Design Approach		107
	5.2.1	Vehicle Requirements	107
	5.2.2	Winged Axisymmetric Configuration	107
	5.2.3	Aerosurface Sizing	108
	5.2.4	Takeoff and Landing Attitude	108
5.3	Thermal Protection System (TPS), Structure and Materials		109
	5.3.1	TPS Requirements	109
	5.3.2	Design Approach	113
	5.3.3	Materials	119
5.4	Vehicle Systems		119
	5.4.1	Work Breakdown Structure and Unique Systems	119
	5.4.2	Autonomous Operation	122
	5.4.3	The Crew Module	127
5.5	Weight Estimation		127
5.6	500 klbm RBCC/SSTO Vehicle Concept Drawing		130
6.0	VEHICLE PERFORMANCE ANALYSIS		147
6.1	Introduction		147
6.2	Performance Analysis Requirements		147
	6.2.1	Trajectory Analysis Approach	147
	6.2.2	Vehicle Mass Build-up, Geometric Sizing and Payload Determination Software Requirements	148
6.3	Characteristics of the Trajectory Analysis Program Selected		148
	6.3.1	DOF36 Trajectory Simulation Program Discussion	149
	6.3.2	Trajectory Simulation Post Processing	153
6.4	Analysis Methodology and Findings		153
	6.4.1	Engine Performance Estimation Approach	157
	6.4.2	Vehicle Mass Properties	169
	6.4.3	Vehicle Aerodynamic Analysis Methodology	169
	6.4.4	Definition of Reference Trajectory	175
	6.4.5	Matrix of Core Variables Studied	175
	6.4.6	Sensitivity Studies Performed	180
6.5	Point Design Vehicle Configuration Selection and Performance		193
	6.5.1	Selection of Point Design TOGW/GLOW	193
	6.5.2	Point Design Engine Selection	193
	6.5.3	Scramjet/Rocket Transition Velocity Selection	195
	6.5.4	Strake Size	195

TABLE OF CONTENTS

			PAGE NO.
6.6	Point Design Vehicle Sensitivities		195
	6.6.1	Isp Sensitivity	195
	6.6.2	Drag Sensitivity	198
	6.6.3	Weight Estimate Sensitivity	198
	6.6.4	Other Characteristics of the Point Design Vehicle	198
6.7	Vertical Takeoff Considerations		203
	6.7.1	Thrust Vector Controll	203
	6.7.2	Vertical Takeoff and Landing Maneuver	205
	6.7.3	Vertical Takeoff and Landing Flight Path	206
	6.7.4	Time to Flying Speed	206
6.8	Propellant Consumption for Both Vertical and Horizontal Landing Maneuvers with or without "Go-Around"		206
	6.8.1	Vertical Landing	206
	6.8.2	Horizontal Landing Capabilities	211
6.9	The Effect of Orbital Inclination on Payload and Landing Capabilities		211
6.10	The Effect of Orbital Inclinaiton on Payload		211
6.11	Post Deorbit Cruise and Landing Effect of Non-Polar Orbit		211
6.12	On-Orbit Refueling		212
6.13	Aerodynamics and Stability Investigations of Similar Configurations by NASA Langley Research Center		212
7.0	GROUND OPERATIONS		217
7.1	Shuttle Ground Operations - Baseline		217
7.2	The Simplification Due to SSTO Operations		217
7.3	The Five Day Turnaround Goal		217
7.4	The Concept of Autonomous Operation		220
7.5	The Requirements for Autonomous Operation		223
8.0	TECHNOLOGY ASSESSMENT		227
8.1	Engine Subsystems		228
	8.1.1	Inlet Subsystem	228
	8.1.2	Fan Subsystem	228
	8.1.3	Rocket Subsystem	229
		8.1.3.1 Air-Augmented Rocket (AAR) Mode	229
		8.1.3.2 Rocket Mode	230
		8.1.3.3 Non-Rocket Modes	230
	8.1.4	Ramjet Subsystem	230
	8.1.5	Scramjet Subsystem	231
	8.1.6	Air Liquefaction Subsystem	231
	8.1.7	Slush Hydrogen Subsystem	232

TABLE OF CONTENTS

			PAGE NO.
8.2	Vehicle Systems		232
	8.2.1	Aerodynamic Characteristics	232
	8.2.2	Control System	232
	8.2.3	Vertical Landing	233
	8.2.4	Vehicle Structure	233
	8.2.5	Aeroheating and Thermal Protection System	233
	8.2.6	Acoustic Environment	233
9.0	**SUBSCALE ENGINE TEST PLAN**		235
9.1	Introduction		235
9.2	Subscale Engine Size		235
9.3	The Role of Ground and Flight Testing		236
9.4	Streamtube Engines		236
9.5	After Streamtube Engine Research		238
9.6	Cost and Schedule		239
10.0	**DDT&E PHASE PLAN**		241
10.1	Ground Rules		241
10.2	DDT&E Program		242
	10.2.1	Program Element 1	242
	10.2.2	Program Element 2	244
	10.2.3	Program Element 3	245
	10.2.4	Program Element 4	245
	10.2.5	Program Element 5	246
	10.2.6	Program Element 6	246
	10.2.7	Program Element 7	247
	10.2.8	Program Element 8	247
	10.2.9	Program Element 9	248
11.0	**LIFE CYCLE COSTS ANALYSIS**		249
11.1	Approach		249
11.2	Comparison Base Line		249
11.3	MMAG Cost Model Description		249
	11.3.1	Applications	249
	11.3.2	Required Inputs	250
	11.3.3	Generated Outputs	252
11.4	Ground Rules and Assumptions		252
11.5	Findings		252
	11.5.1	DDT&E Costs	252
	11.5.2	Production Phase Costs	252
	11.5.3	Operations Phase	252
	11.5.4	Life Cycle Cost	255

TABLE OF CONTENTS

			PAGE NO.
12.0	CONCLUSIONS AND RECOMMENDATIONS		257
	12.1 Principal Conclusions		257
	12.2 Recommended Approach		260
	12.3 Tasks		260
	12.3.1	Task 1 - Thrust Vector Lift/Aerodynamic Lift Study	260
	12.3.2	Task 2 - Upgrade Aerodynamics and Trajectory Analysis Findings	261
	12.3.3	Task 3 - Forebody, Base Drag and Rocket Mode Computational Fluid Dynamic Study	261
	12.3.4	Task 4 - Vehicle, Propulsion and Ground Support Systems Design Problem	262
	12.3.5	Task 5 - Takeoff and Landing Mode Trades	263
	12.3.6	Task 6 - Upgrade Life Cycle Costs Analysis	264
REFERENCES			265
GLOSSARY			269

FIGURE	LIST OF FIGURES	PAGE
Figure 1	Five RBCC Engine Types Evaluated	4
Figure 2	Basic Attributes of Rocket Based Combined Cycle Engine Vehicles	6
Figure 3	Comparison of RBCC/SSTO Vehicles to Multi-Stage All-Rocket Systems	9
Figure 4	Payload as a Percent of Dry Weight - A System Hardware Cost Indicator	8
Figure 5	The Commercial Aircraft Development Process	13
Figure 6	A Simplified Space Vehicle Design/Development Process	14
Figure 7	Study Tasks and Work Flow	15
Figure 8	Simplest Form of Air Augmentation of a Rocket Propulsion System	19
Figure 9	The Rocket Engine Nozzle Ejector (RENE) Concept	19
Figure 10	Ram-Rocket with Simultaneous Mixing and Combustion (SMC)	22
Figure 11	Ejector Ramjet with Diffusion and Afterburning (DAB)	22
Figure 12	Air-Augmented Rocket with Thermal Choke	23
Figure 13	Marquardt 18" Diameter Subscale Test Engine	25
Figure 14	Marquardt Mach 6 Ejector Scramjet Test Engine	25
Figure 15	Marquardt 18" Diameter Flight Weight Regeneratively Cooled Hydrogen Ramjet	26
Figure 16	Hypersonic Research Engine	27
Figure 17	Mission Scenarios Studied	30
Figure 18	Multi-Mode Engine Performance over the Mission Profile	32
Figure 19	Reference Trajectory Showing Non-Supercharged Operating Modes	33
Figure 20	Reference Trajectory Showing Fan Supercharged Operating Modes	34
Figure 21	RBCC Engines Configuration Matrix	35
Figure 22	Engine #10 - Ejector Scramjet - ESJ	36
Figure 23	Multi-Mode Operation - Ejector Scramjet Engines (#10 and #22)	36
Figure 24	Engine #12 - Supercharged Ejector Scramjet - SESJ	38
Figure 25	Multi-Mode Operation - Supercharged Ejector Scramjet Engines (#12, #30 and #32)	38
Figure 26	Engine #22 - ScramLACE - SL	39
Figure 27	Engine #30 - Supercharged ScramLACE-SSL	39
Figure 28	Engine #32 - Recycled Supercharged ScramLACE-RSSL	41
Figure 29	Rocket Engine Specific Impulse Calculation Parameters	42
Figure 30	Airbreathing Engine Net Jet Specific Impulse Calculation Parameters	42
Figure 31	Specific Impulse Over the Ascent Profile by Engine Type and Operating Mode	43
Figure 32	Thrust Over the Ascent Profile by Operating Mode	46
Figure 33	Axisymmetric Vehicle at 100% Capture	49
Figure 34	Capture Area Limits for Non-Axisymmetric and Axisymmetric Vehicles	49

FIGURE	LIST OF FIGURES	PAGE
Figure 35	Effects of Positive Angle of Attack Flight on an Axisymmetric Vehicle	50
Figure 36	"Pod" and "Annular" Engine Integration Approaches	51
Figure 37	"Square" vs. "Round" Engine Modules Integration Approaches	51
Figure 38	Aerodynamic Forces and Propulsion Forces	53
Figure 39	Nominal Capture Area Schedule	54
Figure 40	Axisymmetric Mixed External/Internal Compression Inlet	55
Figure 41	Ramp Inlet Design Concept	57
Figure 42	Ramp Positioning Schedule	57
Figure 43	Five Fan Stowage Options	58
Figure 44	Effect on Thrust and Isp of Increasing Hydrogen Flow into the Afterburner	60
Figure 45	Rocket Exhaust Mixing Length	63
Figure 46	Dual Concentric Annular Bell Combustion Chamber	64
Figure 47	Air Augmented Rocket Mode Diagram	65
Figure 48	Liquid Hydrogen/Liquid Air System Specific Impulses	67
Figure 49	Thrust Augmentation in Ejector Mode During the Early Portion of the Ascent Trajectory	68
Figure 50	Ramjet Mode Diagram	67
Figure 51	Shifting Scramjet Fuel Injection Approach	70
Figure 52	Rocket Mode - High Nozzle Exit Area Ratio	70
Figure 53	Scramjet Isp Performance Comparisons - This Study vs. 1960's Estimates for Hydrogen Fuel	73
Figure 54	Scramjet Mode Performance (All Engines)	74
Figure 55	Basic Liquid Air Cycle Engine (LACE)	76
Figure 56	RamLACE Engine	76
Figure 57	The "Recycle" Process in Engine #32	78
Figure 58	The Technologies Involved in Air Liquefaction	78
Figure 59	LACE Engine Thrust Performance With and Without Fouling Alleviation	80
Figure 60	Atmospheric Water Content and a Function of Altitude and Air Temperature	80
Figure 61	Icing Contamination Induced Airflow Area Blockage with Time	81
Figure 62	Contamination Induced Decrease in Overall Heat Transfer Coefficient with Time	81 81
Figure 63	Simulated Ascent Trajectory Heat Exchanger Contamination Test Results	82
Figure 64	Slush Hydrogen Heat Capacity and Density Relationships	83
Figure 65	Thrust to Weight Ratio for RBCC Engine Systems and Various Contemporary Aircraft	92
Figure 66	Subsystem Weight as a Percentage of Installed Engine Weight - Engine #10 - Ejector Scramjet	93
Figure 67	Subsystem Weight as a Percentage of Installed Engine Weight - Engine #30 - Supercharged ScramLACE	93

FIGURE	LIST OF FIGURES	PAGE
Figure 68	Conceptual Subsystems Arrangement for Engine #30 and #32 - Supercharged ScramLACE and Recycled Supercharged ScramLACE	95
Figure 69	Conceptual Subsystems Arrangement for Engine #12 - Supercharged Scramjet	97
Figure 70	Conceptual Subsystems Arrangement for Engine #10 - Ejector Scramjet	99
Figure 71	Size/Thrust Relationships for Non-Supercharged and Supercharged RBCC Engines for Various Sea Level Static Thrust Rated Engines	102
Figure 72	1995 Technology Availability Date (TAD) Thrust to Weight Ratios	103
Figure 73	Conical Shock Positions	104
Figure 74	Vehicle/Propulsion System Integration Approach	105
Figure 75	Effect of Decreasing Engine Thrust Rating and Increasing Number of Engines	106
Figure 76	Radiation Equilibrium Temperatures on Vehicle Nose and Leading Edges	110
Figure 77	Reentry Trajectories Envelope	110
Figure 78	Thermal Protection System Design Characteristics	111
Figure 79	Distribution of Aerothermal Heating Regions	113
Figure 80	External Insulation Multiwall TPS	115
Figure 81	Metallic Standoff TPS Concept	116
Figure 82	Hot Metallic Structure TPS Concept	118
Figure 83	Actively Cooled Wing/Fin Leading Edge TPS Concept	118
Figure 84	Active vs. Passive Cooling Weight Tradeoffs	120
Figure 85	RBCC/SSTO Vehicle System Work Breakdown Structure	121
Figure 86	Hierarchical Relationship Between a Generic Spaceborne Expert System and Subsystem Expert System	126
Figure 87	Interface Between Spaceborne Expert System and Ground Support System	128
Figure 88	Generic Spaceborne Expert System (SES)	129
Figure 89	Crew Module Conceptual Design	129
Figure 90	Vehicle Weight Breakdown by Major System with Propellants - 500 klbm Vehicle - Engine #10 -25% Strakes	131
Figure 91	Vehicle Weight Breakdown by Major System without Propellants - 500 klbm Vehicle - Engine #10 - 25% Strakes	132
Figure 92	Vehicle Weight Breakdown by Major System with Propellants - 500 klbm Vehicle - Engine #30 - 25% Strakes	133
Figure 93	Vehicle Weight Breakdown by Major System without Propellants - 500 lkbm Vehicle - Engine #30 - 25% Strakes	134
Figure 94	Vehicle Weight Breakdown by Major System with Propellants - 500 klbm Vehicle - Engine #10 - 50% Strakes	135
Figure 95	Vehicle Weight Breakdown by Major System without Propellants - 500 klbm Vehicle - Engine #10 - 50% Strakes	136
Figure 96	500 klbm Baseline Vehicle - Engine #10 - 50% Strakes Equivalent Wing Area - Mach 15 Scramjet Transition VTOHL Conceptual Layout	145
Figure 97	A Typical DOF36 Output Printout	151

FIGURE	LIST OF FIGURES	PAGE
Figure 98	Performance Graph File Output	154
Figure 99	Weights and Forces Graph File Output	155
Figure 100	Typical FUELVOL Output File	157
Figure 101	The Trajectory Analysis Process	156
Figure 102	NASA LaRC Generic Slender Wing Vehicle Drag Breakdown	170
Figure 103	A Zero-Lift Drag Curve for the RBCC/SSTO Vehicles	170
Figure 104	Various Strake Configurations Studied	172
Figure 105	Axial Force Coefficient of the Axisymmetric Configuration	172
Figure 106	Subsonic Lift Coefficient Characteristics of Slender Delta Wings	174
Figure 107	Normal Force Coefficient of the Axisymmetric Configuration	174
Figure 108	Reference Ascent Trajectory	176
Figure 109	Initial Portion of the Flight Path for HTO and VTO Modes of Takeoff	176
Figure 110	Payload vs. Engine Type and Strake Size for a 956 klbm Vehicle at 10% and 15% Strake Sizes	178
Figure 111	Payload vs. Engine Type and Strake Size for a 956 klbm Vehicle at 20% and 25% Strake Sizes	179
Figure 112	RBCC Engine Types Evaluated	181
Figure 113	Payload vs. Engine Type - Airbreathing Termination at Mach 20 with Full Capture at Mach 25	183
Figure 114	Payload vs. Engine Type - Airbreathing Termination and full Capture at Mach 15	183
Figure 115	Payload vs. Full Capture and Rocket Out Mach Number for Varying TOGW/GLOW Weight Classes	184
Figure 116	Payload vs. Full Capture and Rocket Out Mach Number for Various Engine Types	184
Figure 117	Sensitivity of Mass to Orbital Condition to Vehicle Drag	187
Figure 118	Effect of +/- 10% Isp by Propulsion Mode on Payload	188
Figure 119	Vehicle Weight History for all Five RBCC Engine Types Studied	188
Figure 120	Payload vs. % Variation in Weight Estimates	190
Figure 121	I* and Payload vs. Engine Types	190
Figure 122	Payload vs. TOGW and Engine Type	194
Figure 123	Payload vs. Full Capture Mach Number for Engines #10,#30 and #32	194
Figure 124	Angle of Attack vs. Mach Number for Varying Strake Sizes	196
Figure 125	Payload vs. Strake Size for the Baseline Vehicle	196
Figure 126	Effect of +/- 10% Isp Variation on Payload for the Baseline Vehicle	197
Figure 127	Payload vs. % Change in Drag Estimates for the Baseline Vehicle	197
Figure 128	Baseline Vehicle Weight Characteristics vs. Time	199
Figure 129	Baseline Vehicle Performance	201
Figure 130	Baseline Vehicle Weights and Forces	202
Figure 131	Baseline Vehicle Endurance vs. Cruise Mach Number	204
Figure 132	Baseline Vehicle Range vs. Cruise Mach Number	204
Figure 133	Single Axis Thrust Vector Control System Demonstrated as Part of the USAF "Integrated High Performance Turbine Engine Technology" (IHPTET) Program	205
Figure 134	Vertical Takeoff and Landing Attitude Maneuvers	207

FIGURE	LIST OF FIGURES	PAGE
Figure 135	"ZOOM" Maneuver for Vertical Landing - Minimum Energy Maneuver	208
Figure 136	Constantly Decreasing Altitude Vertical Landing Maneuver	208
Figure 137	Time History of Vertical Attitude Takeoff and Landing Maneuvers for the TEMCO Model 39	209
Figure 138	Propellant Requirements for Zero Horizontal and Vertical Velocity Landing	210
Figure 139	1995 TAD Payload vs. Orbital Inclination	212
Figure 140	LaRC Axisymmetric Model Configuration	213
Figure 141	RBCC/SSTO Vehicle with Annular Engine Installation	213
Figure 142	LaRC Oil Flow Tests at Mach 10 and Varying Angles of Attack	215
Figure 143	NASA LaRC Elevoned Cone - Longitudinal Stability	216
Figure 144	Baseline Vehicle and Ground System Work Breakdown Structure	218
Figure 145	National Space Transportation System Vandenberg Launch Site Operations Flow	218
Figure 146	Shuttle STS Landing and Launch Work Schedule	219
Figure 147	A Single Stage Orbiter Landing and Launch Operations Flow	219
Figure 148	An SSTO Version of the Shuttle STS Ground Operations Flow	221
Figure 149	RBCC/SSTO Landing to Launch Alert Operations Schedule	221
Figure 150	The Generic Spaceborne Expert System (SES)	224
Figure 151	Interface Between the SES and the Ground Support System	224
Figure 152	Technologies Related to Air-Augmented Rocket Systems	227
Figure 153	A Streamtube Engine Rig	237
Figure 154	Various Streamtube Engine Rig Building Blocks	237
Figure 155	Flight Test Program Schedule and Budget	240
Figure 156	DOD Research & Development Category System	241
Figure 157	Engine DDT&E Program Plan	243
Figure 158	DDT&E Cost Element	253
Figure 159	Vehicle and Engine Production Element	253
Figure 160	Operations and Support Element	254
Figure 161	Vehicle and Engines Life Cycle Cost	254
Figure 162	500 klbm Axisymmetric Baseline Vehicle Configuration	258
Figure 163	RBC/SSTO Vehicles Payload vs. TOGW/GLOW	259
Figure 164	RBCC/SSTO Vehicles Scramjet Transition Velocity vs. Rocket Out Mach Number for Various TOGW/GLOW Weights	259

LIST OF TABLES

TABLE		PAGE
Table 1	Representative Hydrogen/Oxygen Rocket Specific Impulses	71
Table 2	NAS7-377 Composite Materials Comparative Weight Analysis	86
Table 3	Subsystem Weight Estimation Factors	88
Table 4	1985 TAD Weight Breakdown by Engine Subsystem Weight and Percentage of Uninstalled Engine Weight	89
Table 5	1995 TAD Weight Breakdown by Engine Subsystem Weight and Percentage of Uninstalled Engine Weight	90
Table 6	Summary Engine Weight Statement for All 5 RBCC Engines	91
Table 7	Aerodynamic Peak Heat Rates and Temperatures	111
Table 8	Comparison of Multiwall TPS Design Approaches	115
Table 9	Comparison of Metallic Standoff TPS Design Approaches	116
Table 10	State-of-the-Art Materials Candidates	120
Table 11	Near Term Material Candidates	121
Table 12	1995 TAD 500 klbm - Engine #10 - 50% Strakes - Vehicle Weight and Sizing Report with Liquid Hydrogen	137-140
Table 13	1995 TAD 500 klbm - Engine #10 - 50% Strakes - Vehicle Weight and Sizing Report with Slush Hydrogen	141-144
Table 14a	Specific Impulse Performance for Engine #10 - Ejector Scramjet	159
Table 14b	Thrust Performance for Engine #10 - Ejector Scramjet	160
Table 15a	Specific Impulse Performance for Engine #12 - Supercharged Ejector Scramjet	161
Table 15b	Thrust Performance for Engine #12 - Supercharged Ejector Scramjet	162
Table 16a	Specific Impulse Performance for Engine #22 - Ejector ScramLACE	163
Table 16b	Thrust Performance for Engine #22 - Ejector ScramLACE	164
Table 17a	Specific Impulse Performance for Engine #30 - Supercharged ScramLACE	165
Table 17b	Thrust Performance for Engine #30 - Supercharged ScramLACE	166
Table 18a	Specific Impulse Performance for Engine #32 - Recycled Supercharged ScramLACE	167
Table 18b	Thrust Performance for Engine #32 - Recycled Supercharged ScramLACE	168
Table 19	Ascent Flight Time to 50 nmi Orbit Prior to Hohmann Transfer to 100 mni Orbit	191
Table 20	Net Payload Fractions for 956 klbm Vehicle with Mach 25	192

Table 21	Total Propellant Mass Fractions and Tanked O/F Ratios for 956 klbm Vehicle	192
Table 22	Weight Comparison of the LaRC Shuttle II Directly Scaled to 500 klbm vs a 500 klbm RBCC/SSTO Vehicle	200
Table 23	Thermal Protection System	251

Section 1.0

INTRODUCTION

This section presents a brief overview of:

- Study scope
- Vehicle system requirements
- Mission requirements
- Engine systems studied
- Study goals and findings
- Life cycle cost analysis assumptions and findings
- Scaling of configurations of various takeoff gross weight/gross lift off weight (TOGW/GLOW) vehicle classes
- Recommendations for future work
- Study approach
- Contents of the report

1.1 Study Overview

The "Combined Cycle" engines that are the subject of study here integrate airbreathing and rocket propulsion systems into a single engine system. These types of engines are referred to as being "Rocket Based Combined Cycle" engine systems or RBCC engines. These engines transition from initial air-augmented rocket mode takeoff and initial acceleration to ramjet to scramjet and finally to rocket propulsion to orbital insertion velocity.

Limited study of rocket based combined cycle engine systems was carried out in the 1960s under USAF and NASA sponsorship. These studies focused primarily on missile, aircraft and multiple stage space transportation systems. This report focuses on single-stage-to-orbit (SSTO) vehicle systems powered by rocket based combined cycle (RBCC) engine systems.

A significant effort in hypersonic propulsion is presently included in the National Aerospace Plane (NASP) or X-30 project. The overall design approach of the NASP/X-30 vehicles is inferred to be based upon non-axisymmetric vehicle configurations, i.e., similar to conventional aircraft geometries. This study, for reasons that will be discussed later, focuses on axisymmetric designs, similar to most rocket propelled vehicles, but with lifting surfaces.

The study effort focused on the analysis of past work in the field of rocket based combined cycle engine systems, the selection of five RBCC engines for further evaluation and an investigation of design approach alternatives which integrate these engines into a vehicle system. The vehicle integration study considered engine/vehicle integration alternatives, vehicle structure and subsystems concepts including propellant tank designs (integral and non-integral), thermal protection systems (TPS), and crew compartment and payload module integration. A number of candidate designs evolved from this effort. For these candidate configurations, trajectory and aerothermodynamic analyses were conducted in support of the TPS design.

The study also assessed the technology requirements unique to the axisymmetric RBCC designs. A subscale engine development and vehicle development plan were prepared. The findings of these tasks provided the information needed to carry out a preliminary life cycle cost analysis.

The cost analysis carried out in this study of the axisymmetric RBCC vehicle system is different from that of aircraft cost analysis. In the axisymmetric vehicle configuration studied, the

DDT&E production and operations costs were calculated based on axisymmetric rocket propelled vehicle systems costs models. Because of the use of the axisymmetric design approach, there is a significant reduction in the number of unique parts requirements in comparison to non-axisymmetric configurations. In non-axisymmetric structures, such as those used in aircraft, unique parts are required for the upper left, upper right, lower left and lower right portions of the vehicle structural systems. By way of illustration, the Shuttle orbiter structure is comprised of approximately 70% unique parts (Ref. 1). This fact has a meaningful impact on design costs, production tooling, processes and materials costs and the wide variety of structural test requirements. The axisymmetric vehicle design considerd in this study uses a large number of engine systems when compared to conventional aircraft of all-rocket vehicles, from eight to twelve or more. This provides not only redundancy in flight operations but should also reduce the costs associated with engine design, development testing, qualification and production by virtue of the smaller size of all engine components and the larger manufacturing run or lot size in comparison to aircraft and all-rocket vehicles of equivalent gross weight.

1.2 Vehicle System Requirements

The overall goals of the project were to determine the applicability of airbreathing rocket based combined cycle engine systems to rapid response space transportation mission requirements, and to determine their ability to satisfy those requirements at an affordable cost. "Affordable" was defined as being an operations and support cost of less than one tenth the present Space Shuttle system operations and launch support costs. The target mission assigned was a 10,000 lbm payload delivered to a 100 nmi circular polar orbit with a two man crew.

As an initial project task, the general vehicle system requirements were expanded to include the following:

1. A vehicle operational life of 20 years.
2. Approximately 50 flights per year.
3. Both horizontal and vertical takeoff options were to be studied with both horizontal and vertical landing options considered for each takeoff mode.
4. A fully reusable vehicle including the thermal protection system. The use of expendable materials, other than propellants and pressurants, was not allowed.
5. Hydrogen and oxygen propellants only.
6. Minimum use of non-recoverable high pressure gas, minimum use of helium. The use of nitrogen and air was permitted.
7. Minimum logistic support requirements.
8. The vehicle system operational support requirements should be met in a minimum duration prelaunch operation.
9. Propellant loading operations would be of minimum complexity and require a minimum of time to accomplish. Defueling and systems safeing operations should meet the same requirements.
10. Minimum ground equipment.
11. A minimum of ground support personnel should be required in terms of both number and skill level. The use of automated support systems was to be considered.
12. Minimum ground electrical power requirement.
13. The vehicle takeoff and landing surface requirements should be able to be met at existing CONUS bases.
14. The vehicle should be capable of standing on "Alert" status for several days with "topping".
15. There should be a minimum of support personnel and equipment requirements to maintain "Alert" status.

16. The vehicle should be capable of "On Demand Launch" immediately from the "Alert" status.
17. The vehicle should be capable of all weather operation.
18. The vehicle systems should be designed to be as highly autonomous as possible.

1.3 Engine Systems Studied

The five engine systems selected for study in this project were derived from the findings of the NASA sponsored study carried out by The Marquardt Company in the mid 1960s (Fig. 1 Ref. 2). In this study, The Marquardt Company, assisted by the Rocketdyne Division of North American Rockwell and Lockheed-California Company, investigated 36 variations of rocket based combined cycle engine systems.

An early objective of the analysis portion of the current study was to reevaluate the 36 configurations studied by Marquardt and to select the most promising configurations for study in this project. As a result of this reevaluation, five engine systems, illustrated in Fig. 1, were selected for further study. The numerical identification of each engine used in this study is based upon the numerical identifiers developed in Ref. 2.

Engine 10 - Ejector Scramjet

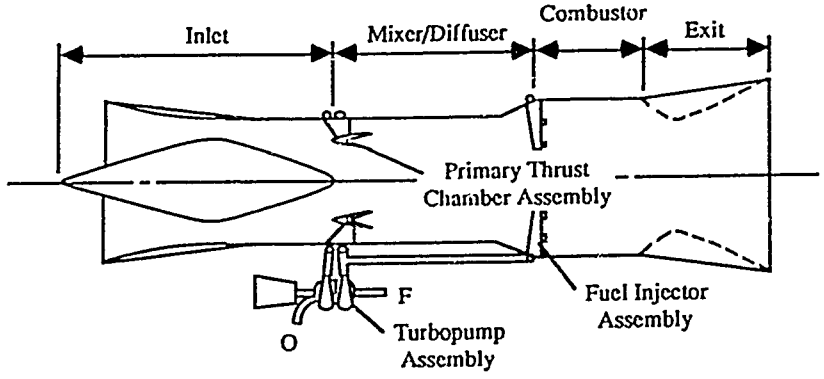
The ejector scramjet is the simplest and lightest configuration studied and has the highest thrust-to-weight ratio of the five engines. It also has the least new technology demands. Its liabilities are a lower specific impulse capability which not only results in an increase in total vehicle weight for a given payload but also has the highest propellant flow rate requirement for the cruise and landing operations phases of the orbital mission. The rocket system, when operated either in the ejector mode, or, in the latter phases of flight, in the rocket mode to orbital insertion, utilized liquid oxygen and liquid hydrogen.

Engine 12 - Supercharged Ejector Scramjet

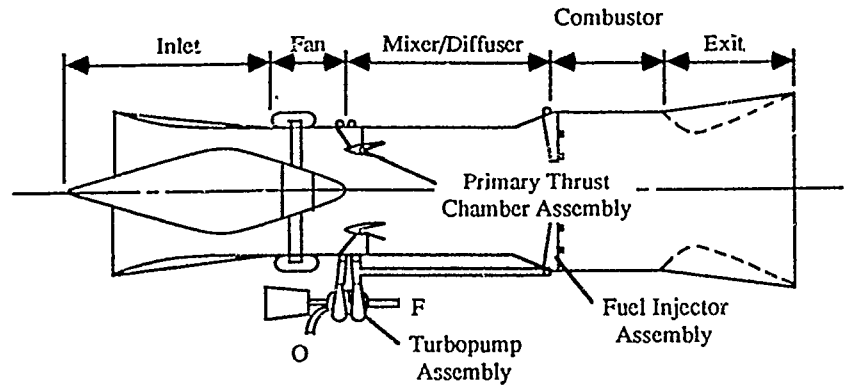
Engine 12 is configured identically to Engine 10 except that a supercharging fan is added between the downstream section of the inlet system and before the rocket ejector station. The advantages of this configuration are a slight performance increase in ejector mode specific impulse performance but primarily in sharply decreased fuel consumption in flyback and landing modes. These advantages are obtained at the expense of increased system complexity associated with the turbomachinery required to drive the fan system, the fan system itself, and the necessity to remove the fan from the engine flowpath at high flight speeds. In addition to the system complexity increase, the fan system represents additional weight to the engine system, and decreased thrust-to-weight ratio and increased vehicle inert weight. As in the Engine 10 configuration, the all rocket mode operation is based on liquid oxygen and liquid hydrogen.

Engine 22 - ScramLACE

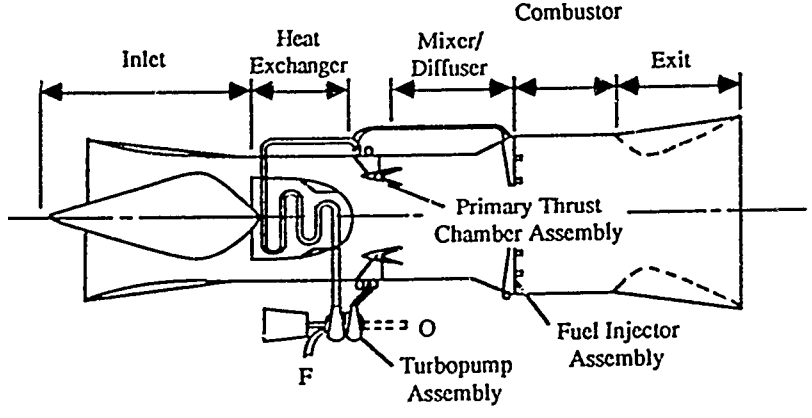
Engine 22 is Engine 10 with the liquid oxygen replaced by liquid air produced in flight by an air liquefaction subsystem operating only during the ejector mode portion of the flight. Operation to orbital insertion using rocket mode is based on liquid hydrogen and liquid oxygen as in the case of Engines 10 and 12. This capability reduces the weight of oxygen required and reduces TOGW/GLOW. The primary disadvantage of this system is, again, the addition of another complex, heavy subsystem, the air liquefaction system, which decreases thrust-to-weight ratio and increases vehicle TOGW/GLOW. As in the case in Engine 10, this engine has reduced powered descent and landing capability in comparison to Engine 12.



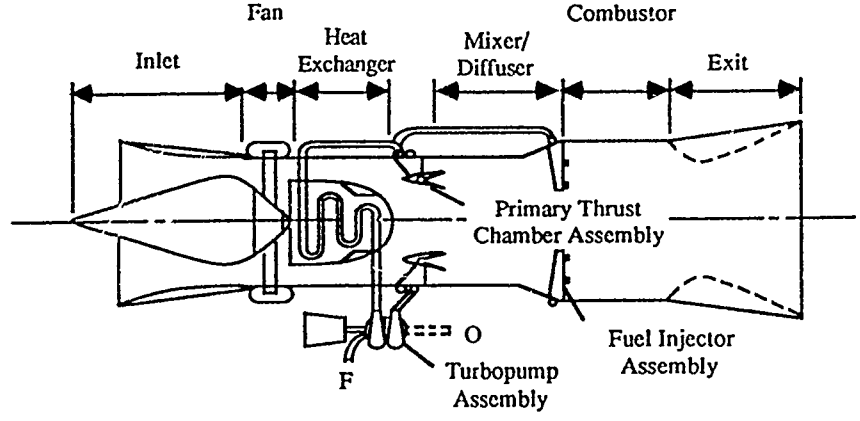
Ejector Scramjet
Engine #10



Supercharged Ejector Scramjet
Engine #12



ScramLACE
Engine #22



Supercharged ScramLACE
(Both Recycled and Non-Recycled)
Engine #30 and #32

Fig. 1 Five RBCC Engine Types Evaluated

Engine 30 - Non-Recycled Supercharged ScramLACE

The Engine 30 configuration consists of Engine 22 with the addition of the supercharging turbofan. This engine adds the complications of both an air liquefaction system, as in Engine 22, and the fan system as in Engine 12. The advantage obtained is increased performance in powered descent and landing over Engine 22.

Engine 32 - Recycled Supercharged Ejector ScramLACE

In Engines 22 and 30, the heat sink used by the air liquefaction subsystem is derived from the liquid hydrogen flow to the rocket ejector subsystem. The flow rate of hydrogen required to sustain the required liquid air flow rate exceeds the demand of the engine operating in ejector mode. This results in these engines operating in a non-optimum, fuel rich mode in plenum burning. In the "Recycled" configuration, the hydrogen in the vehicle system is not normal boiling point hydrogen but "slush" hydrogen - a 50/50 mixture of liquid and solid hydrogen. The air liquefaction process in ejector mode is augmented by added hydrogen flow a portion of which is returned to the vehicle hydrogen tank. This process results in the production of hydrogen at approximately 120 degree R which is "recycled" to the main hydrogen propellant tank and recooled by the larger thermal sink provided by the slush hydrogen. The engine can operate in its ejector mode at near optimum mixture ratio.

Engine 32 provides the highest specific impulse in the ejector mode through air liquefaction at a more optimum engine overall mixture ratio and a high specific impulse in the powered descent and landing phases of the orbital missions through use of the fan subsystem. These capabilities are bought at the price of further complexity and weight which yields the lowest thrust-to-weight ratio of the five engines studied. Further, slush hydrogen technology is not, at present, developed technology and additional work is required in its production, handling and use in systems of this type. Work on this problem is presently being undertaken in support of the NASP Technology Maturation Program, and therefore the use of slush hydrogen cannot be ruled out at this time.

The definition of powered descent and landing capability as used here includes "go-around" capability and self-ferry capability.

While an original goal of the study was to select the most promising engines for more detailed analysis, it became apparent early in the study that vehicle/propulsion design choices would be largely dictated by mission requirements (e.g., takeoff/landing mode) that must be met as specified by the ultimate user of the system. For this reason, all five alternative configurations were carried forward for analysis. The primary differences among the five engine systems were their specific impulse and thrust performance characteristics during ejector mode and total weight of the candidate engine configurations. All five candidates shared the same performance characteristics in terms of thrust and specific impulse in ramjet, scramjet and final rocket mode to orbital insertion, as well as fan mode.

These engine design alternatives open up numerous design choices not previously available in more conventional propulsion systems, such as all-rocket or airbreathing turbomachinery based systems. The range of alternatives, together with the basic attributes of air-augmented rocket based combined cycle engine systems in an SSTO configuration, are illustrated in Fig. 2.

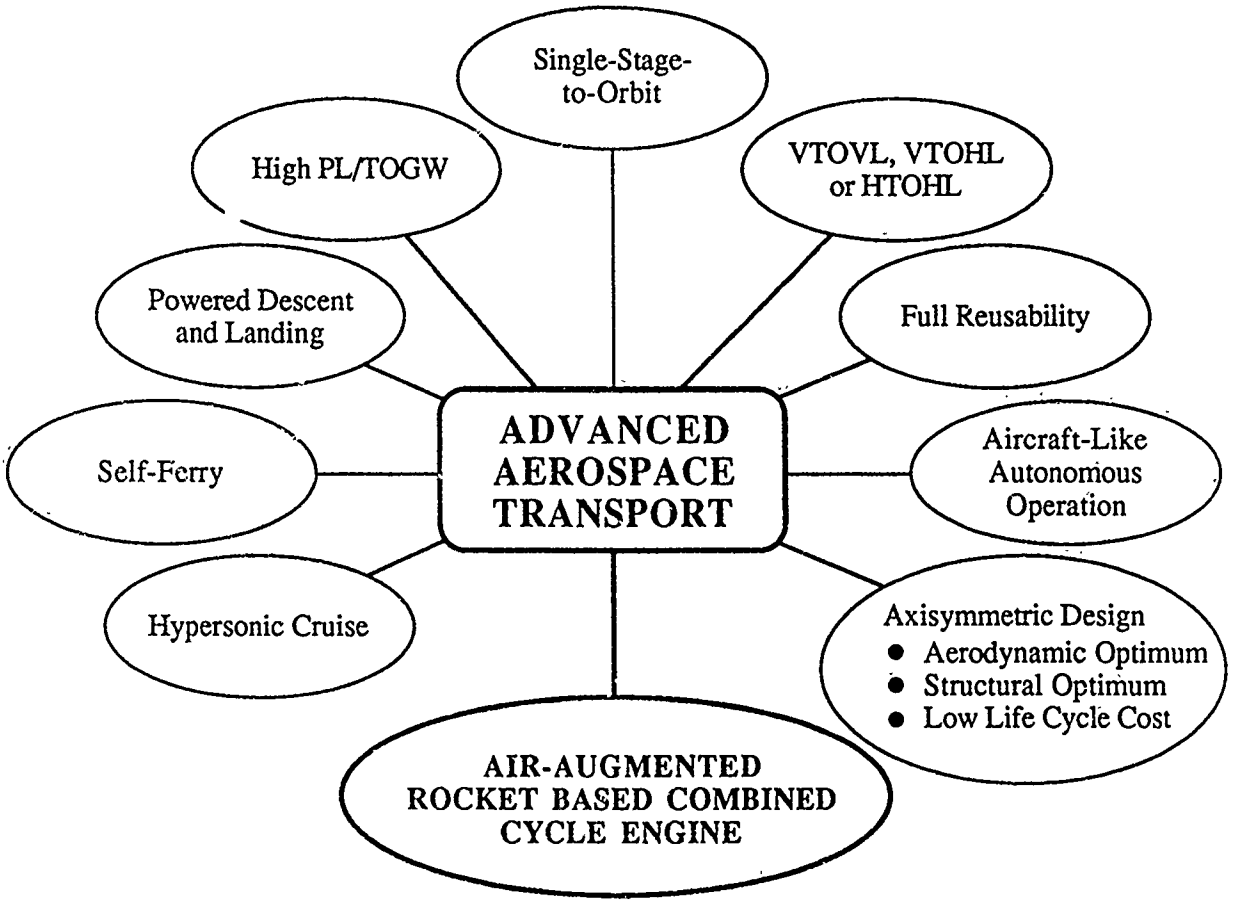


Fig. 2 Basic Attributes of Rocket Based Combined Cycle Engine Vehicles

The principle conclusions reached with regard to these five engine system/vehicle designs in orbital missions were:

- The baseline mission requirements, and other orbital mission requirements, could be met by any of the five engine systems studied at approximately 500 klbm TOGW/GLOW.

- All five engine configurations can provide for powered descent and landing. However, go-around capability and self-ferry capability requirements are best met by the inclusion of a fan subsystem. The fan can effectively serve as a "supercharger" for the rocket ejector mode, based on either liquid oxygen or liquid air as the oxidizer, and can also support a unique fan-ramjet operating mode for intermediate acceleration, cruise, landing and self-ferry requirements. The engineering challenge of fan integration, and more importantly its physical stowage out of the flow path at high flight speeds, remains to be addressed in detail and, in the opinion of the study team, remains a "vexing" problem.

- A significant finding of this study, which is unique to the SSTO approach investigated here, rather than multi-stage vehicles previously investigated in the work reported in Ref.

2, is that air liquefaction does not appear to be particularly advantageous in terms of payload delivery capability. Air liquefaction is not required to achieve the target mission case in particular.

- Air liquefaction systems capable of meeting the requirements of Engines 22, 30, and 32 are not presently available. The problems presented by this technology include safe, reliable partitioning of the liquid hydrogen coolant from the air flow, and, more significantly, prevention of fouling of the heat exchanger by ice formation from the inducted air.

- A portion of the payload performance enhancement achieved through the use of slush hydrogen in the SSTO missions is due to the higher density of that fuel which reduces wetted tank area required and vehicle gross weight. This means that slush hydrogen can also be applied advantageously to non-recycled and non-air liquefaction propulsion systems in SSTO missions.

- The improved engine weight achieved through the incorporation of manufacturing materials and processes that are assumed to become available for development applications in the 1995 time frame are critically important to achieving the high payload fractions projected in this study.

1.4 Study Goals and Findings

1.4.1 Propulsion System

The parameter of I*, or "Total Mission Effective Specific Impulse" is an important parameter in evaluating the performance of airbreathing systems. I* accounts for both aerodynamic drag and gravity losses along the complete flight path and will be discussed further in Section 3.0.

A goal of this study was to find a combination of RBCC propulsion systems and vehicle configurations that could provide a total mission effective specific impulse, or I*, of at least 600 seconds over the full trajectory of an orbital vehicle system. The finding of the study indicated that an I* of from 650 to 800 seconds could be expected from RBCC engine systems in the axisymmetric vehicle configurations that were studied.

A further objective of the study was to establish whether or not RBCC systems could provide single-stage-to-orbit vehicles with useful payload capability at TOGW/GLOW weights in practical ranges. The study concluded that the target payload of 10 klbm to a 100 nmi polar orbit could be delivered by a vehicle of approximately 500 klbm gross weight. This payload capability in this gross weight class vehicle significantly exceeds that deliverable by equivalent gross weight vehicles powered by all-rocket systems.

A further goal was to establish whether or not this performance could be achieved by rocket subsystems operating at low combustion pressure and capable of long useful life without replacement. The study found that liquid hydrogen/liquid oxygen rocket subsystems operating at a combustion pressure of 2000 psi and liquid hydrogen/LAIR rocket systems operating at a combustion pressure of 1000 psi with a maximum main engine flow path pressure of 150 psi could meet the mission requirements.

A final goal of the study was to establish whether or not this capability could be provided in a system with operations and operations support costs per pound of payload delivered to orbit of approximately 1/10 or less that of the current Space Shuttle system. The study found that this

appears to be possible when these engines are combined with axisymmetric, "rocket like" configurations.

Payload comparisons of the three vehicle configurations studied in this project to historical and co .temporary all-rocket systems are presented in Fig. 3. A significant measure of the performance of any orbital system is the percent of total dry weight represented by payload. This is a measure of the cost of hardware brought to the launch stand per pound of payload delivered to orbit. Comparisons of a 500 klbm, a 1 Mlbm, and a 1.5 Mlbm axisymmetric RBCC vehicle to a 2.6 Mlbm pounds mass two-stage all-rocket system are presented in Fig. 4. Again the potential performance advantage of the RBCC system against the all-rocket alternative is clearly apparent.

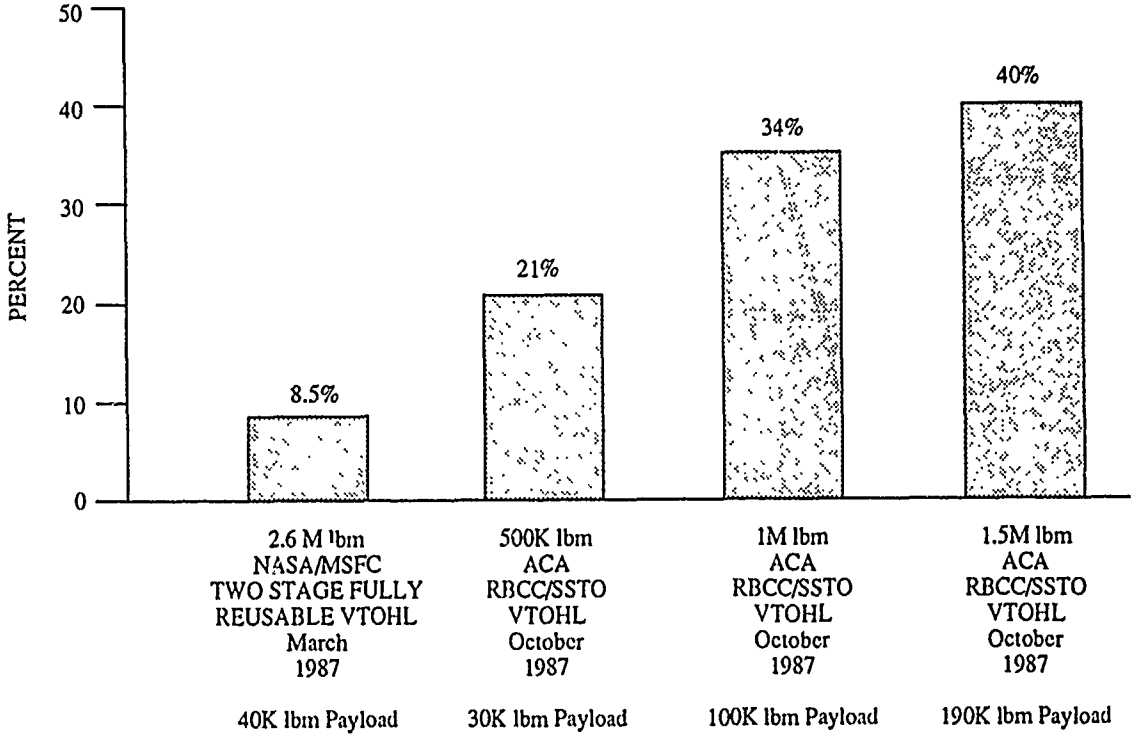


Fig. 4 Payload as a Percent of Dry Weight - A System Hardware Cost Indicator

1.4.2 Life Cycle Cost Estimate

A preliminary life cycle cost estimate for a representative configuration of an RBCC/SSTO vehicle using a life cycle cost analysis methodology developed for the Space Transportation Architecture (STAS) study was developed by MMGA. The cost estimates are representative of the LCC to be expected by combining airbreathing RBCC propulsion into axisymmetric structures similar to those characteristic of STAS all-rocket vehicle systems. This

Engine #10 - Ejector Scramjet - 25% Strakes - VTO -1995 TAD
Rocket Transition at Mach 15
Liquid Hydrogen

100 nmi Orbit from the EasternTest Range at a
Nominal 30° Orbital Inclination

Vehicle	TOGW lbm	Payload lbm	Payload/TOGW percent
Saturn V	6,000,000	330,000	5.5
Shuttle	4,160,000	45,000	1.1
Titan 34D	1,500,000	27,600	1.8
Titan 4	1,500,000	40,000	2.6
ESJ/1500	1,500,000	190,000	12.6
ESJ/1000	1,000,000	100,000	10.0
ESJ/500	500,000	30,000	6.0

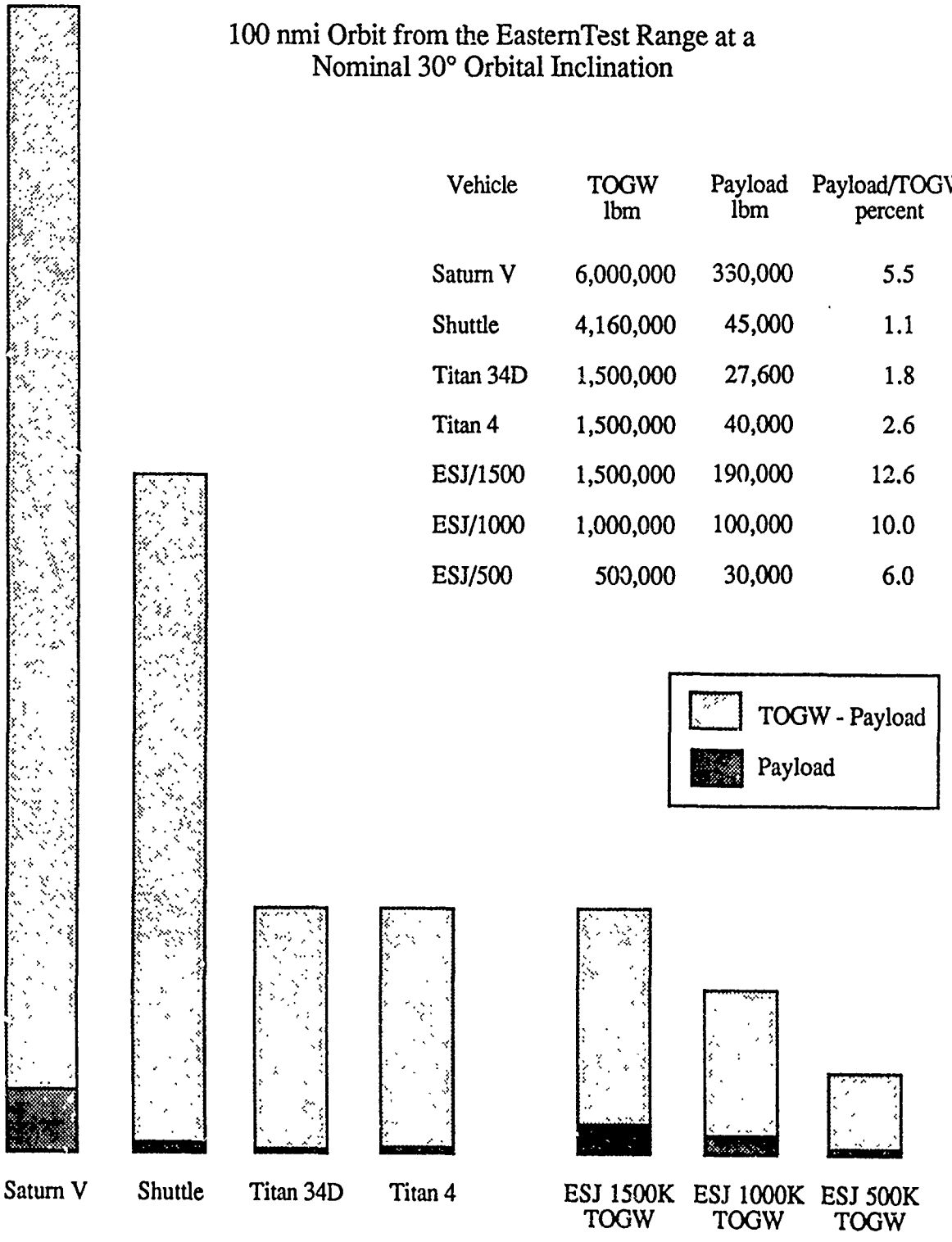


Fig. 3 Comparison of RBCC/SSTO Vehicles to Multi-Stage All-Rocket Systems

LCC estimate does not include those costs that would be incurred in technology development prior to the beginning of the DDT&E phase, nor the personnel and equipment cost reductions that might be achieved by the autonomous design approach required to be studied and discussed in Section 7.0. The ground rules and assumptions used in the LCC analysis were as follows:

- Fiscal year 1987 dollars
- 440 klbm TOGW vehicle
- Structures and engines life - 1000 flights
- Engine - Recycled Supercharged ScramLACE (Engine 32)
- Stage-up reliability = 0.996
- Stage-down reliability = 0.996
- Mission success = 0.992
- DDT&E phase - 1995 to 2002
- IOC date to 2005
- 5 test vehicles in the DDT&E phase
- 2 main operating bases (WTR and ETR)
- Cost of LH_2 = $2.00 per pound
- Cost of LOX = $0.05 per pound
- Cost of slush LH_2 = $4.00 per pound
- Normal turnaround time for ground operations processing = 5 days (1 shift per day)
- New launch site facilities:
  - Vehicle service facility
  - Operations control center
  - Propellant servicing area
- Cost associated with payload operations not included
- No new landing pads or landing strips constructed.
- STAS Mission Model Civil Option II/DOD Option 2
- Vehicle capability of 32 klbm LEO at 28.5 degrees inclination with 100% manifest load factor
- DDT&E engine cost of 2 billion dollars, first unit cost of 81 million dollars
- Payload loss cost expressed as a function of flight rate, payload capability, reliability and payload dollars per pound.

The basis of comparison with the present Space Shuttle System is operations and operations support cost. On this basis, the RBCC/SSTO vehicle LCC costs analysis indicated an operations and operations support cost of $160 per pound of payload to orbit compared to $2,646 per pound of payload to orbit for the present Shuttle vehicle with both vehicles in a 28.5 degree inclined 100 nmi orbit.

1.4.3 Scaling of Configurations

This study evaluated three different vehicles in terms of takeoff gross weight. These were vehicles of 500 klbm, 1 Mlbm and 1.5 Mlbm. There was no apparent reason why the larger vehicles would not be nearly direct scale-ups of the lower gross weight vehicle designs. It would appear that in the specific context considered here, the design experience gained in lower gross weight vehicles should be extensively and directly applicable to larger gross weight systems.

1.5 Recommended Future Work

In subsequent discussions presented here, it will be noted that the present state of knowledge of the subsystems comprising RBCC engine systems is adequate to support further development of such engines. The primary technical risk lies in the scramjet subsystem but more

significantly in the problem of integration of these subsystems into a single RBCC engine system capable of achieving orbital velocity.

Before any reasonably supportable decisions can be made as to the cost/benefit of undertaking sub-scale or full-scale RBCC engine development, additional study needs to be carried out at the vehicle systems level to more firmly establish the potential benefits, and risks, associated with the application of this type of engine to space transportation systems.

Several of these areas of technological uncertainty are presently planned to be addressed in the NASP Technology maturation Program and NASP Generic Technology Options Program. Others are being, or will be, investigated under activities being carried out under the USAF's Forecast II Technology Initiative Program. However, there are subjects unique to the RBCC/SSTO vehicle system that will not be addressed in these efforts. It is in these subject areas that future work is suggested.

Briefly summarized here, and discussed in Section 12.0, it is recommended that further work be carried out that would:

1. Investigate the effects on vehicle performance of varying the angular relationship between the vehicle longitudinal axis, thrust axis and wing chord line rather then using the fixed, parallel relationship investigated in this study. The objective of this work would be to establish the extent to which vehicle angle of attack might be reduced and payload performance improved by increasing the use of the aerodynamic surfaces to provide lift and reducing the propellant use by reducing engine thrust vector contribution to lift. An aeroheating model should be incorporated into this trajectory analysis work and should be used to further define optimum trajectories.

2. Use CFD analysis, or other numerical analysis techniques, investigate three fluid dynamic problems:

   - flow on the vehicle forebody during orbital ascent as influenced by angle-of-attack

   - base drag and flow characteristics of the truncated conical aftbody from zero velocity, sea level conditions to orbital velocity and altitude conditions

   - high altitude operation of the rocket subsystem in a manner that would enable further expansion of the rocket combustion products to the engine duct wall, in the divergent nozzle section of the engine and on the vehicle aftbody.

3. Investigate the flight dynamics, control requirements and propellant consumption characteristics of alternative vertical landing maneuvers.

4. Carry the vehicle and propulsion systems design definitions to a further level of detail for a specific TOGW/GLOW weight vehicle, RBCC engine system and vehicle takeoff and landing mode.

5. Based on the findings of the above studies, further detail the aerodynamic characteristics and trajectory performance analysis using higher fidelity analytical tools.

6. Provide a second iteration of the system life cycle costs estimates.

1.6 Approach

1.6.1 The Design Task Scope

The portion of the work carried out in this project consisted of a preliminary design task. The place that such a design task occupies in the context of the overall life cycle of an airplane development program is illustrated in Fig. 5. The workflow illustrated in this figure is not an "ideal" process, it is the requirement for the real process of developing a reliable aircraft system.

The work carried out in this project is comprised of the preliminary steps in the "very conservative design" process illustrated in that figure. This study departs from this "conservative" model in that the vehicle design studied here requires the use of highly advanced technologies that must be matured by the vehicle DDT&E work phase.

The overall process comprising that design process is illustrated in Fig. 6 which covers the problems of developing an integrated vehicle and propulsion system design. Again, this model is an overview of the real requirements of this process.

The work carried out in this study is represented by the activities A through J in Fig. 6. The next logical steps in the development of the design of the systems studied here are to refine the findings of the activities A through J and to carry out tasks K, N and O to provide a preliminary design of a selected engine/vehicle design configuration in a specific TOGW/GLOW class vehicle.

1.6.2 Study Approach

The study approach is illustrated in Fig. 7 and consisted of 10 tasks.

Tasks 1 and 2 provided an assessment of prior and current work in the field of RBCC systems and vehicle system designs applicable to the missions under study in this project. The output of these two tasks was used to provide both a starting basis for the design technologies to be applied and a first quantification of the propulsion system and vehicle system requirements. Tasks 3 and 4 provided an initial characterization of the engine systems and the vehicle configurations to be used.

In Task 5, quantitative information required to design an integrated propulsion system/vehicle system to a sufficient level of detail to support performance analysis was developed. In Tasks 6 and 7, the analytical tools required to analyze vehicle system performance in orbital missions and to characterize the sizing, mass characteristics and vehicle geometries were developed and applied to the baseline vehicle systems previously developed in Task Five. The results of these two tasks, with an emphasis on the performance of alternative RBCC engine systems selected, comprised a portion of the work accomplished.

The activities carried out in Tasks 8, 9 and 10 provided documentation of the findings related to propulsion and vehicle system design, an identification of the critical technology assessment requirements of both the engine and vehicle systems, a preliminary propulsion system subscale engine development plan and vehicle system development plan and a life cycle cost analysis.

1.7 Contents of the Report

Air-augmented rocket systems is a generic term descriptive of a wide variety of alternative design approaches that utilize atmospheric air to improve the performance of rocket

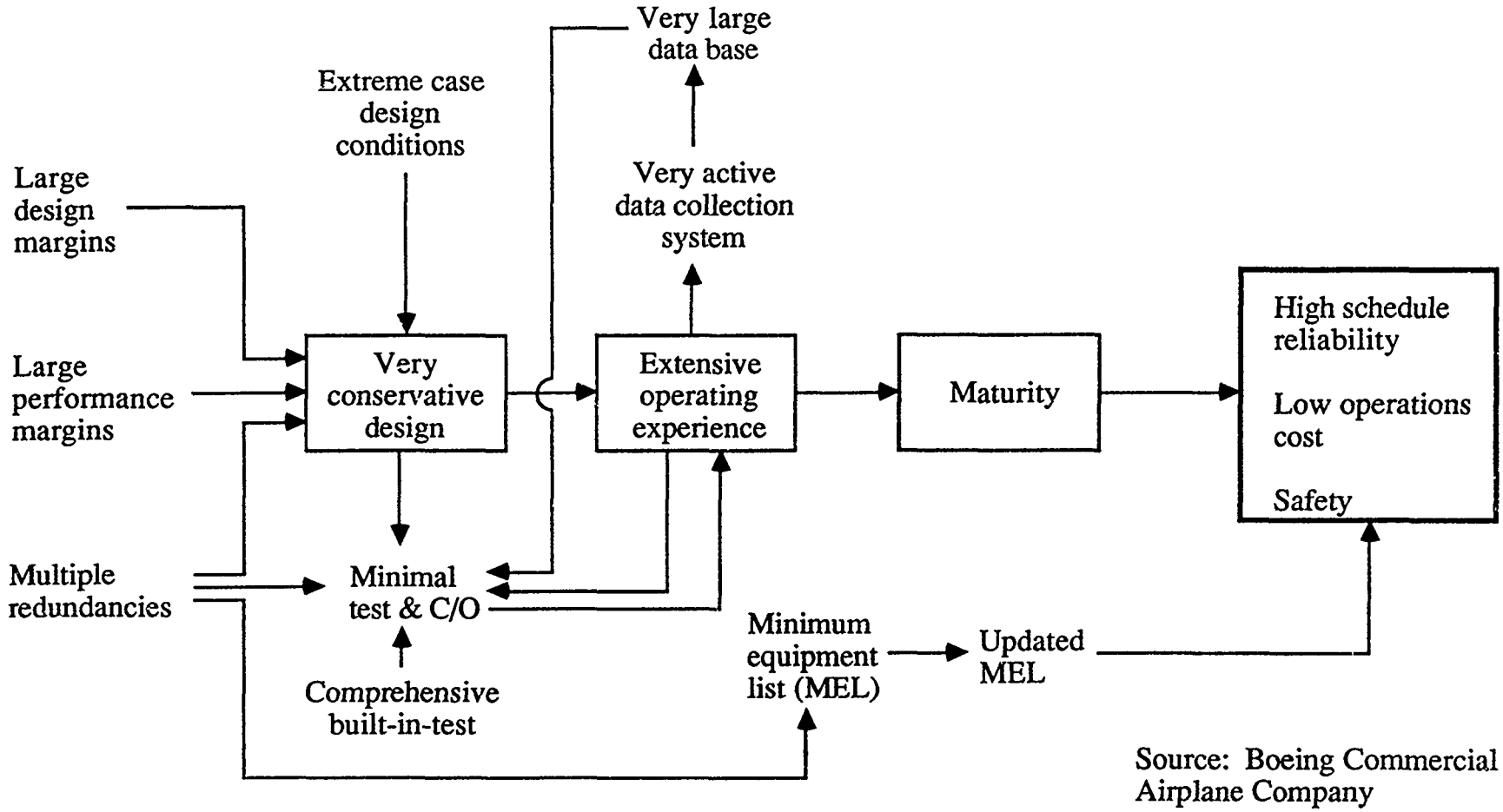
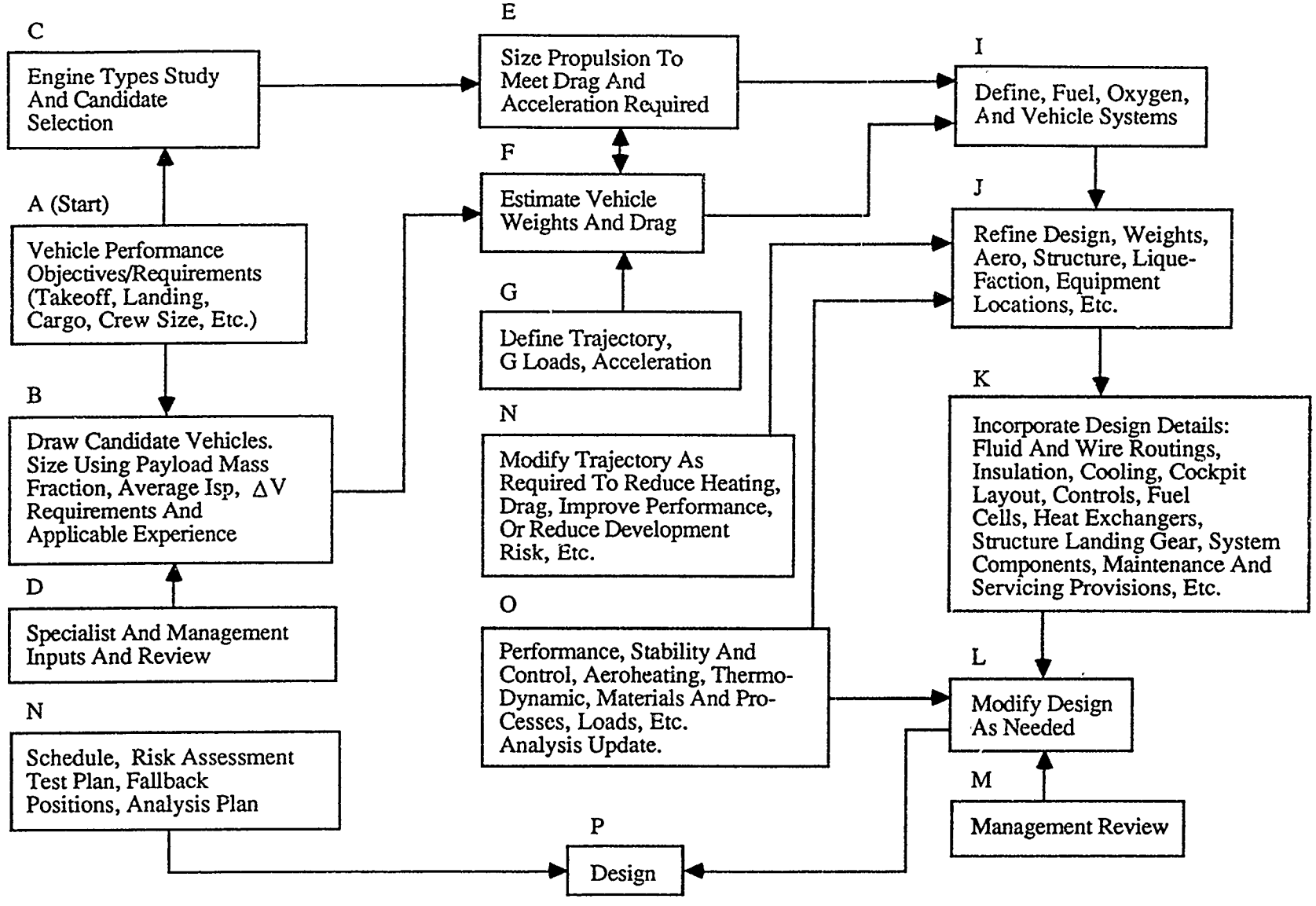


Fig. 5 The Commercial Aircraft Development Process



Source: General Dynamics

Fig. 6 A Simplified Space Vehicle Design/Development Process

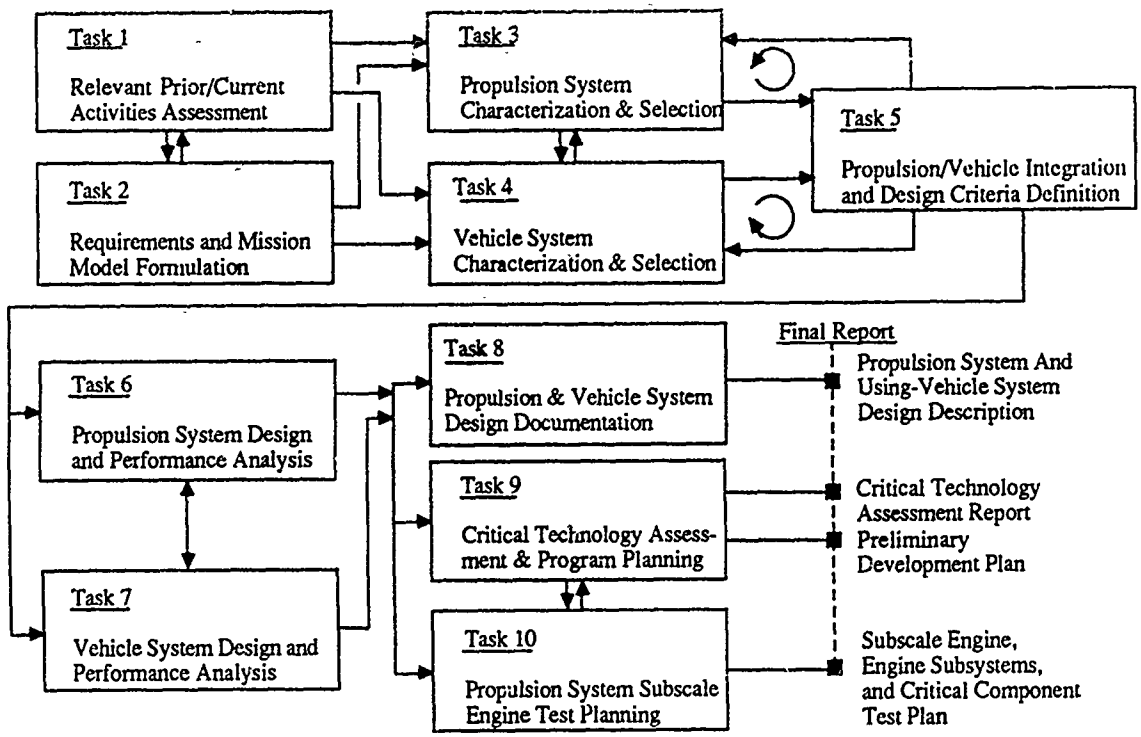


Fig. 7 Study Tasks and Work Flow

systems. Within this broad category of systems, the work carried out under NASA contract by The Marquardt Corporation and its subcontractor team, which formed the base of departure for this study, analyzed the relative performances of air-augmented rocket systems optimized over the flight spectrum from zero velocity to approximately Mach 12. The work carried out in this study extends that effort to orbital velocity by extending the performance estimates using now available performance estimates for scramjet propulsion to higher Mach numbers, and also provides for the use of an all-rocket mode from termination of scramjet propulsion to orbital insertion conditions. A brief discussion of representative theoretical and experimental work carried out in the study of air-augmented rocket engine cycles is presented in Section 2.0. Section 3.0 discusses rocket based combined cycle propulsion systems in the five configurations studied in this project.

Sections 4.0 and 5.0 consider the problems associated with engine/vehicle integration and vehicle systems designs capable of meeting the SSTO mission requirements. The most significant findings resulting from this study are presented in Section 6.0 - Vehicle Performance Analysis. In this Section, the findings regarding the performance of the five candidate engine systems flying an SSTO trajectory are analyzed and comparative and sensitivity analyses are presented.

In Section 7.0, the ground support system requirements for the proposed vehicle are presented at a preliminary system definition level.

These sections, Sections 1.0 through 7.0, provided documentation of the propulsion and vehicle systems findings.

Sections 8.0, 9.0 and 10.0 present, respectively, documentation of the results of the technology assessment study, subscale engine test planning requirements and an overall vehicle development program plan, the remaining three required data items.

The subject of life cycle costing is treated in Section 11.0 and is based upon the findings developed by the study and previously discussed in Sections 1.0 through 10.0.

The report ends with conclusions and recommendations for future activities that would further develop the design definition of this family of space transportation vehicles.

Section 2.0

AIR-AUGMENTED ROCKET SYSTEMS - ROCKET BASED COMBINED CYCLE ENGINE SYSTEMS - BRIEF REVIEW OF PRIOR WORK

2.1 Introduction

During the past three decades, the objectives that have been sought to be achieved in the space propulsion field have evolved from the problem of placing ten and fifty pound payloads in orbit to placing thousands of pounds of payload in orbit or on earth escape trajectories. These objectives have been achieved. They are now being replaced with another set of objectives, i.e., reduced cost, high reliability and improved operational flexibility. It is toward this new set of goals that this study effort is directed.

A clear statement of what will be required to achieve these goals and objectives is contained in the Advanced Launch System work statement (Ref. 3). In this Statement of Work, the contractor is required to:

> "...Develop both the objectives vehicle and interim vehicle and operations systems design which have the potential for substantially reduced costs, increased reliability, and perational flexibility in providing space transportation. Determine elements of the objective launch system that could be available for use earlier than 1998 without compromising the ultimate goal of a ten-fold cost reduction. Identify and describe all interim vehicle and operation systems and a support structure used in the growth period to the objective ALS. Conduct vehicle and operations trade studies to support the proposed system. All designs should include logistics, supportability, security, and environmental planning. Unique approaches to meet the objectives are encouraged. Continuation of current operational practices and/or current technologies is not a requirement. The status quo should only be maintained when shown to be the most cost effective way to achieve the objective."

Information available in the open literature indicates that the ALS system will be based upon conventional all-rocket propulsion technology. It is suggested that an airbreathing rocket based combined cycle propulsion system represents an alternative design approach capable of meeting this new generation of goals to a greater extent than they can be met with all-rocket designs. However, rocket propulsion technology has evolved to a state where it can be considered a "mature" technology and the risks associated with attempting to achieve this current set of goals and objectives can be assessed with reasonable confidence.

Statements have been frequently made to the effect that rocket based combined cycle engine systems are "immature" technologically and that there is a high risk associated with attempting to apply this type of propulsion system to space transportation systems. It is suggested that this statement is incorrect. It would be more properly stated that the risk is "unknown" rather than "high". RBCC propulsion systems are systems that integrate a number of propulsion systems which are normally thought of as complete systems in themselves but which, in RBCC systems, are subsystems of a single propulsion system. There are two different types of technological risks associated with RBCC systems. The first is the risk that any individual propulsion subsystem may or may not be able to be designed to achieve its functioning objectives. The second type of risk is the risk associated with integrating these propulsion subsystems into the single engine system. These two types of risks should be considered individually.

The individual propulsion technologies integrated into an RBCC system are:

- Rocket technology
- Ramjet technology
- Scramjet technology

The rocket system technology requirements and ramjet technology requirements have been demonstrated to be possible using hydrogen and oxygen as propellants. Scramjet technology cannot be considered "mature" but, as will be described subsequently in this section, this propulsion mode is not required to operate to full orbital velocity. The findings of this study indicate that payload to orbit optimizes at a scramjet termination velocity of approximately Mach 15. The principal technological risk associated with the individual propulsion subsystems is found primarily in the scramjet subsystem operating from Mach 8 to Mach 15. This risk or uncertainty remains to be assessed.

The major technological uncertainty is found in the problem of INTEGRATION of the individual propulsion subsystems into a single RBCC propulsion system. As will be discussed in Section 6.0, the simplest configuration of an RBCC engine, the Ejector Scramjet configuration, is capable of meeting the mission requirements implicit in this study.

There is a third element of risk that has not been discussed. This is the risk associated with providing performance improvements in the basic RBCC Ejector Scramjet engine configuration. These improvements include the addition of a fan supercharger system, the use of air liquefaction and the use of slush hydrogen. While the fan subsystem offers a significant opportunity to improve the flyback and landing performance, including go around and self-ferry, this capability is not a critical requirement to achieving the basic orbital mission. Further, as will also be discussed in Section 6.0, the use of air liquefaction and slush hydrogen technologies provide performance improvements, but these improvements are less significant then for multi-staged vehicle systems, and are judged not critical, to achieving that same orbital mission. These risks might more properly be judged as pre-planned product improvement (PPI) risks. They are not risks or uncertainties associated with carrying out the basic mission.

The objective of this section is to outline the basic work that has been accomplished in the field of RBCC propulsion technology. The work of MMAG in the field of simple ducted rocket systems, in the late 1950s, and the work of The Marquardt Corporation, in the mid-1960s, provides a means of presenting both the technological basis for these engine systems and a general measure of the status of RBCC propulsion integration.

2.2 Air-Augmented Rockets

The concept of air-augmentation of rocket engines is not new. Investigations have been carried out on variations of this approach in ducted rocket, ram-rocket, and various rocket powered ejector forms.

The objectives sought by such systems are to increase the thrust-to-weight ratio of the rocket propulsion system and to increase the specific impulse by appropriately using the atmosphere through which the vehicle passes. In this discussion, five different configurations of air-augmented rocket systems will be introduced. The order of their presentation is established by the order in which they provide improved thrust and Isp performance and operating capabilities over increasing Mach numbers.

The simplest form of air-augmentation of a rocket propulsion system is illustrated in Fig. 8. The idea is to install a simple, fixed geometry, lightweight shroud around a rocket engine.

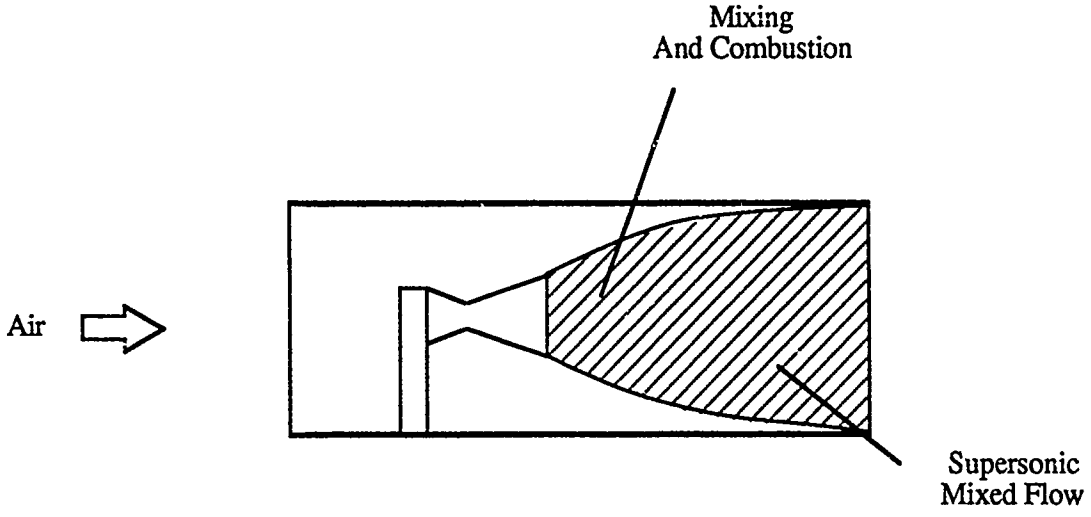


Fig. 8 Simplest Form of Air Augmentation of a Rocket Propulsion System

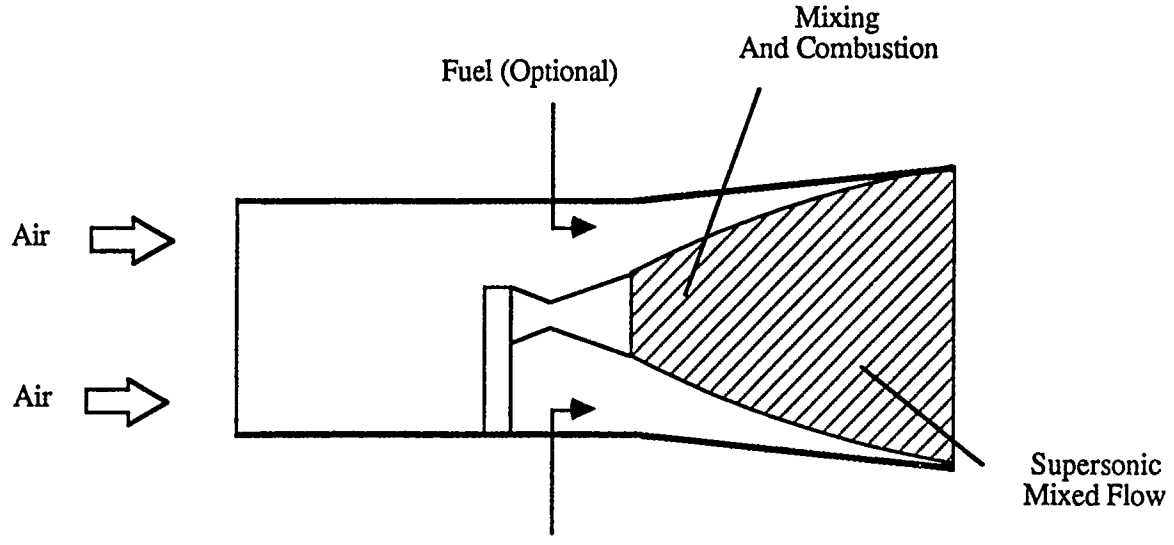


Fig. 9 The Rocket Engine Nozzle Ejector (RENE) Concept

Since rocket engines normally operate with fuel-rich exhausts, these exhausts have chemical energy which is normally unavailable to the rocket engine system itself. This lightweight shroud assembly permits additional combustion to be carried out in the shrouded exhaust stream when the atmospheric air mixes with the fuel rich exhaust and is further expanded in a divergent nozzle which is a part of that shroud. This process produces additional thrust and increased Isp derived from the expansion process on the additional expansion surfaces.

The basic limitation of this design approach is that it loses efficiency as flight velocity increases and at speeds slightly near Mach 1 begins to be a penalty on the performance of these systems through simple ram-drag effects. The method of implementation of this system is to use the shroud only during the early portion of flight and to jettison it before Mach 1. MMAG studied this approach in the late 1950s in their RENE (Rocket Engine Nozzle Ejector) project.

This work was carried out in three phases. In the first phase, the performance of simple ducted rockets from Mach 0 to 1.0 was considered. In the second phase, the RENE concept which evolved from the initial studies was subjected to experimental investigation. The third phase considered improvements on the RENE system with the objective of achieving a better understanding of the pumping characteristics of such systems and the problem of reducing the mixing chamber length.

The initial system studied was a simple ejector. The idea, at that time, was to augment the rocket thrust at takeoff and during flight up to Mach numbers about 0.8. It was planned to jettison the constant area ejector at about that speed. The aim was modest; to increase the average first stage Isp by five to ten seconds. This increase was to occur through the use of a larger area ratio rocket nozzle. NASA Langley Research Center, carried out experimental wind tunnel investigations using MMAG furnished equipment. These tests were made using a hydrogen peroxide rocket engine system in 1959 and were successful as reported by Schmeer and Simonson (Ref. 4). The takeoff thrust was augmented by as much as 14%. This value was consistent with that given for constant-area mixing theory.

Further tests were planned by MMAG to use a LOX/RP-1 rocket engine system, but, when constant area theory was applied, it was found that no theoretical augmentation values could be computed. This represented a technological turning point for MMAG. A literature search revealed no published analysis investigating what happens when low rocket propellant to inlet air mass ratios are used in constant-area ducts. MMAG's study was also limited to certain ground rules. These rules were:

1. The device was required to be simple - variable geometry inlets and exits were excluded.

2. The device had to be lightweight. This requirement made it necessary to deviate from the usual air/rocket exhaust mass-flow ratios of 5 to 20. MMAG confined their studies to values between 1 and 4.

Constant pressure mixing gave valid theoretical solutions - but, in order to secure constant pressure mixing over a range of Mach numbers and altitudes, a variable exit, or variable inlet, or both are required. A clue was given regarding a suitable design in that the mixing chamber for the constant pressure case was in many cases divergent. MMAG then attempted a modification to the mixing theory which resulted in the augmentation system called "Rocket Engine Nozzle Ejector" or RENE. The difference between a simple air-augmented rocket and the RENE design approach is illustrated in Fig. 8 and 9. MMAG found that the solution of the continuity equation for the constant pressure flow process provided two solutions, one subsonic and the other supersonic. If the subsonic solution (the usual one) is used, a variable exit is required because of the differences between the ambient pressure and the pressure after mixing. A further difficulty made the choice of the supersonic exit conditions a tenuous one. The literature gave no hint that

such a solution was physically possible. However, it also showed that no tests had been made at low mass ratios. Analysis indicated substantial thrust augmentation was possible with the supersonic RENE model (Ref. 4). Under USAF sponsorship, the Martin RENE design was tested at the Arnold Engineering Development Center. The experimental test was successful (Ref. 5) and rocket thrust and Isp augmentation was about 55%, 5% higher than the theory had predicted.

The thrust augmentation system which evolved to the RENE design, differed from the basic air-augmented ducted rocket in that:

1. The mixing chamber is conically divergent rather than cylindrical.

2. The air to rocket propellant flow is relatively small (approximately 3.0 in the RENE case compared to 20 in the conventional ducted rocket case.)

3. A supersonic exhaust exists after mixing.

The low air to rocket propellant mass flow ratio of RENE permitted a relatively small shroud. The characteristics of a supersonic exhaust and a divergent mixing chamber provided reasonably high thrust augmentation over a large flight spectrum with a fixed ejector nozzle.

2.3 The Work Carried Out by the Marquardt Corporation

Further study, expanding on the work carried out by MMAG, identified additional options in the approaches to design of rocket based systems using air-augmentation. An early variation was the ram-rocket, illustrated in Fig. 10, which varied from the RENE design approach in that the combined air and rocket fuel flow was subsonic rather than supersonic at the end of the mixing section. In this configuration, when additional fuel is introduced into the subsonic mixed flow and combustion is allowed to occur simultaneously with mixing, the resulting subsonic flow stream can then be passed through a convergent/divergent nozzle and expanded to supersonic velocities. This approach was called the "simultaneous mixing and combustion" approach or SMC.

An alternative approach (Fig. 11) was to mix a non-fuel rich supersonic rocket ejector drive jet with subsonic air stream and to further expand the combined flow stream in such a manner as increase static pressures and, at this point, to introduce additional fuel into that combined flow stream and then to expand the total flow stream through a convergent/divergent nozzle. This approach was called "diffusion and afterburning" or DAB.

In the 1965-67 NASA supported research into air-augmented rocket systems under contract NAS7-377 issued to the Marquardt Corporation. This project consisted of the three stages of evaluation of alternative design approaches to air-augmented rocket systems. During the first phase, 36 different engine cycles were identified. During the second phase, these 36 candidates were screened down to 12 on a basis of analytical criteria developed during the first phase. A principal criteria was the ability of these engines to deliver payload to orbit using a set of reference trajectories. Comparative mission analyses were performed for engines using simultaneous mixing and combustion (SMC) and diffusion and afterburning (DAB) with both engine systems beginning in air-augmented rocket operation with a transitioning to subsonic combustion ramjet operation in the flight velocity regime of 2,000 to 3,000 feet per second.

The SMC cycles exhibited consistently lower engine specific impulse at low Mach numbers with only slight gains in engine thrust-to-weight ratio relative to the DAB cycles. This resulted in slightly, but consistently, lower overall mission performance for the SMC cycles compared to the DAB cycles. This performance superiority of the DAB cycle, coupled with a number of significant advantages relative to engine mechanization and multimode operation

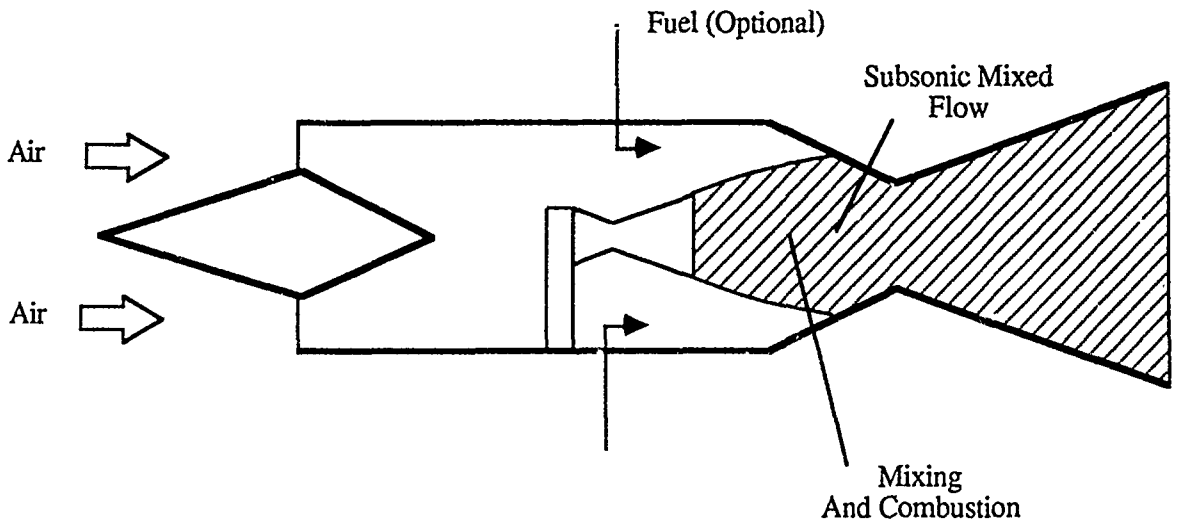


Fig. 10 Ram-Rocket with Simultaneous Mixing and Combustion (SMC)

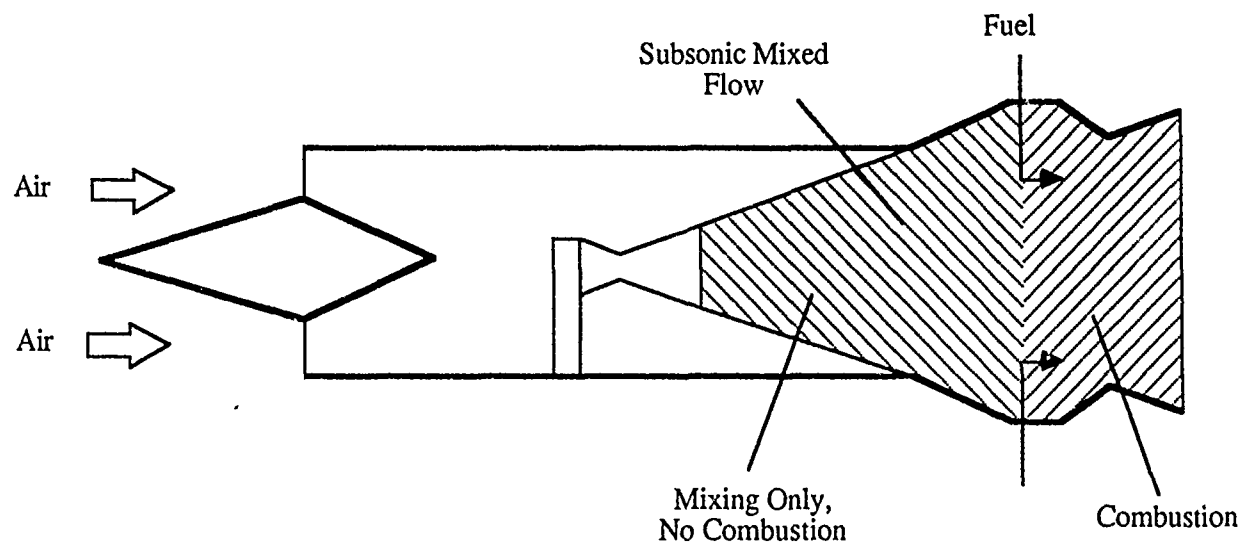


Fig. 11 Ejector Ramjet with Diffusion and Afterburning (DAB)

provided the basis for a screening out a significant number of the engine candidates investigated in the first phase of the Marquardt program.

2.4 Thermal Choke and Fixed and Variable Exit Geometry Considerations

Figure 11 illustrates an ejector ramjet DAB design approach. In this design approach illustrated, a convergent/divergent nozzle assembly is required to achieve final expansion of the engine exhaust products stream.

The propulsion system sought must be capable of providing thrust at velocities at which ramjet technology cannot be applied. In this flight regime, a supersonic combustion ramjet is required. In a supersonic combustion ramjet, where the flow stream through the engine is always at supersonic velocity, a convergent nozzle section is not optimum.

It is possible to design extensively variable exhaust nozzle assemblies. These types of assemblies are complex and heavy. The problem is further complicated by the fact that that geometry in this case must change in such a manner as to remove the convergent section of the nozzle in scramjet mode - not just change the exhaust area of a divergent section.

A different approach which has been demonstrated in the field of ramjet propulsion systems is the use of a "thermal choke". A thermal choke is created by scheduling the heat release rate in the subsonic, constant pressure mixed flow combustion passage in such a fashion as to establish a local sonic condition in what would otherwise be a divergent passage and to create the conditions for supersonic expansion on the remaining portion of the divergent nozzle. This approach is illustrated in Fig. 12. The advantage of this approach is that it enables a virtual throat to be established in the engine's divergent flow path and expansion to supersonic velocity to be accomplished without the requirement for a physical convergent nozzle section as illustrated in Fig. 11.

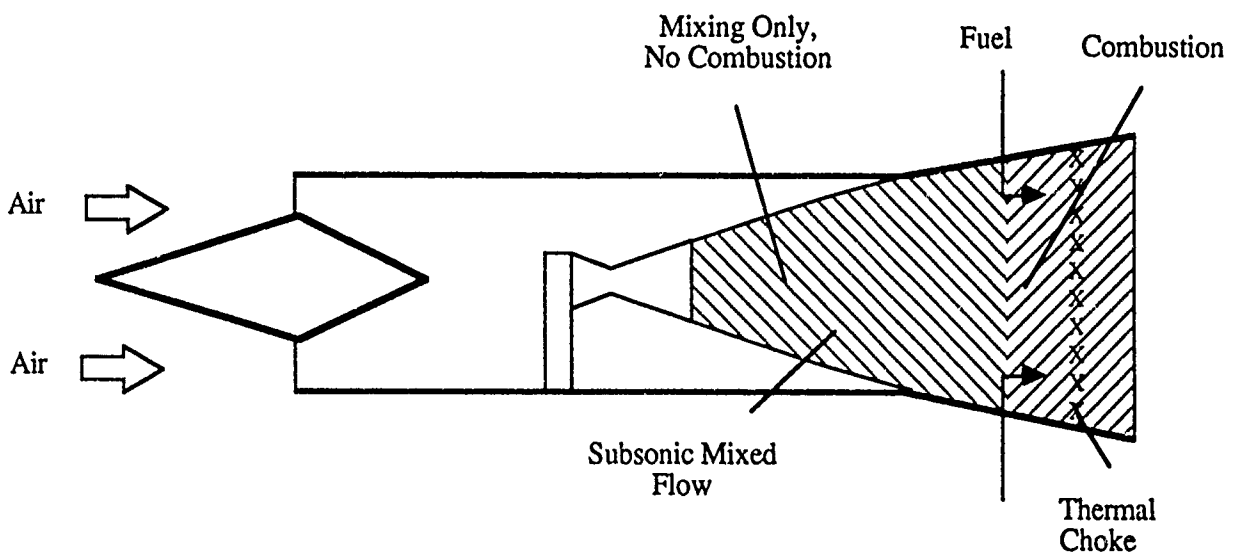


Fig. 12 Air-Augmented Rocket with Thermal Choke

In its investigation of the fixed exit version of RBCC engine configurations, the Marquardt Corporation found that, for acceleration operation along the reference flight paths investigated, the performance of the vehicle system in terms of payload delivered to orbit was only modestly compromised while engine weight and complexity was reduced in comparison to the variable nozzle case.

It was concluded that variable exit geometry carried a significant weight and complexity penalty due to the realities of variable nozzle design. Further, the performance change in terms of inert weight to payload ratio was relatively small. The total system inert weight per unit weight of payload was reduced from 22 pounds for the variable exit geometry to 21 pounds for the fixed exit system.

It must be noted that these findings were based on the performance of variable exit nozzles in two-stage to orbit vehicles. The use of the scramjet propulsion system was terminated at approximately Mach 12 in these vehicles. In the vehicle systems being studied in this report, scramjet propulsion is much more significant to achieving orbital performance than in the Marquardt case. Supersonic combustion ramjet mode operation above Mach 6 does not require or use variable exit geometry. In other words, any variable exit would be held wide open for this speed range (Ref. 2). The Marquardt findings appear to indicate that, in the missions studied here where scramjet operation is required up to Mach 15, the use of variable exit geometry is not justified in terms of increased system weight and complexity.

The RBCC engine design approach illustrated in Fig. 12 provides a combined cycle design with variable inlet geometry, fixed combustion geometry and fixed exit geometry capable of propelling a vehicle system to orbital velocity. This design approach provides acceleration from zero initial velocity using the rocket ejector mode transitioning to ramjet mode using the thermal choke approach and transitioning to supersonic combustion mode using the fixed geometry exit and vehicle aftbody expansion and finally transitioning to rocket mode to orbital insertion conditions.

2.5 A Review of Some Relevant Experimental Investigations

In the early 1960s, the Marquardt Corporation, under USAF sponsorship, tested hydrogen/air and hydrogen/oxygen ejector ramjet systems (Ref. 6). These investigations were carried out using clusters of 8 rocket thrust chambers operating stoichiometrically at 500 psia combustion pressures at an O/F = 8. Hydrogen was injected into the afterburner section which also served as a ramjet combustor. A variable geometry nozzle was employed in the series of boilerplate subscale engines. A representative subscale test engine of 18 inches diameter is illustrated in Fig. 13. Engine tests were successfully conducted at sea level/static conditions and direct-connect simulated flight conditions up to Mach 2.2. Predicted performance was demonstrated in Ejector mode through transition to ramjet mode and on ramjet mode. The capability for a controllable mode transition from ejector to ramjet was experimentally demonstrated.

In the late 1960s, an experimental program using storeable propellants was successfully run by Marquardt using a subscale fixed-geometry engine from static velocity to a maximum free stream velocity of approximately Mach 6 along a typical acceleration path (Fig. 14). The experimental hardware was tested under conditions using gaseous hydrogen fuel with gaseous oxygen as the oxidizer in the primary rocket to demonstrate ejector, ramjet, and scramjet modes of operation. Smooth transitions between operational modes were accomplished primarily by varying the location and amount of fuel supplied at the several fuel injection stations. The thermal choking mechanism was shown to be effective in controlling the inlet normal shock location over a wide range of operating conditions.

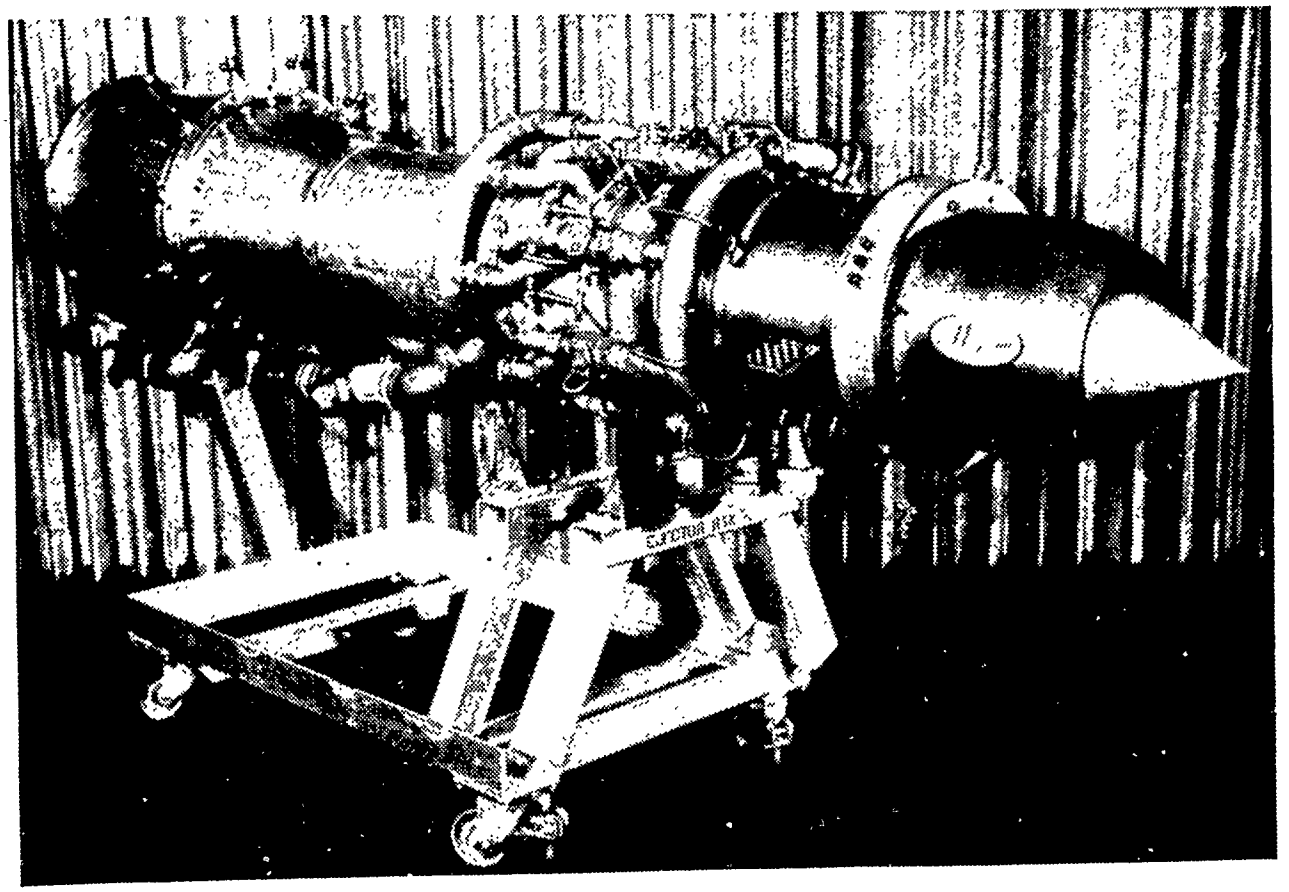


Fig. 13 Marquardt 18" Diameter Subscale Test Engine

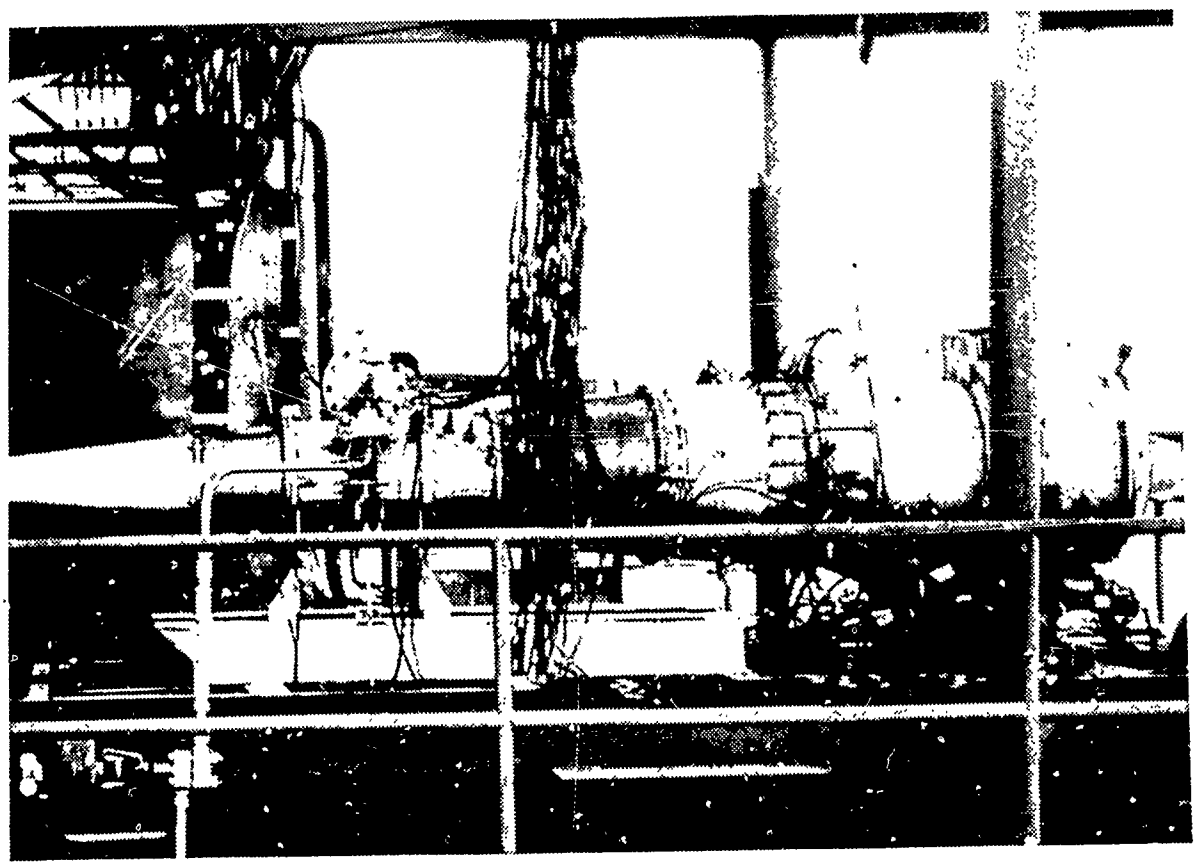


Fig. 14 Marquardt Mach 6 Ejector Scramjet Test Engine

The problems encountered in this Ejector Scramjet experimental program should also be noted. The engine performance was found to be approximately 40% below the predicted value at sea level conditions due to a 15 to 20% loss in inlet total pressure associated with inadvertent choking of the inlet throat. In addition, cycle performance was below the predicted levels at all comparable test conditions due primarily to poor inlet recovery in the test engine indicating an area requiring further research. Good agreement was obtained between predicted trends and experimental results with factored deficiencies substantiating cycle performance analysis methods. Overall engine combustion efficiencies were in the range of 72 to 87% for the ejector mode, 67 to 85% for the ramjet mode, and about 80% for scramjet operation. These values were less than the efficiency goals of 90% in the ejector mode and scramjet mode, due to inadequate secondary fuel penetration. A summary report on the 1966 experimental investigations is presented in Ref. 7.

Fig. 15 shows an 18 inch diameter, regeneratively-cooled, flightweight hydrogen-fueled ramjet/scramjet engine built and tested by researchers at the Marquardt Company in the period 1962 to 1968. This work, sponsored by the Aero Propulsion Laboratory, WPAFB was supported

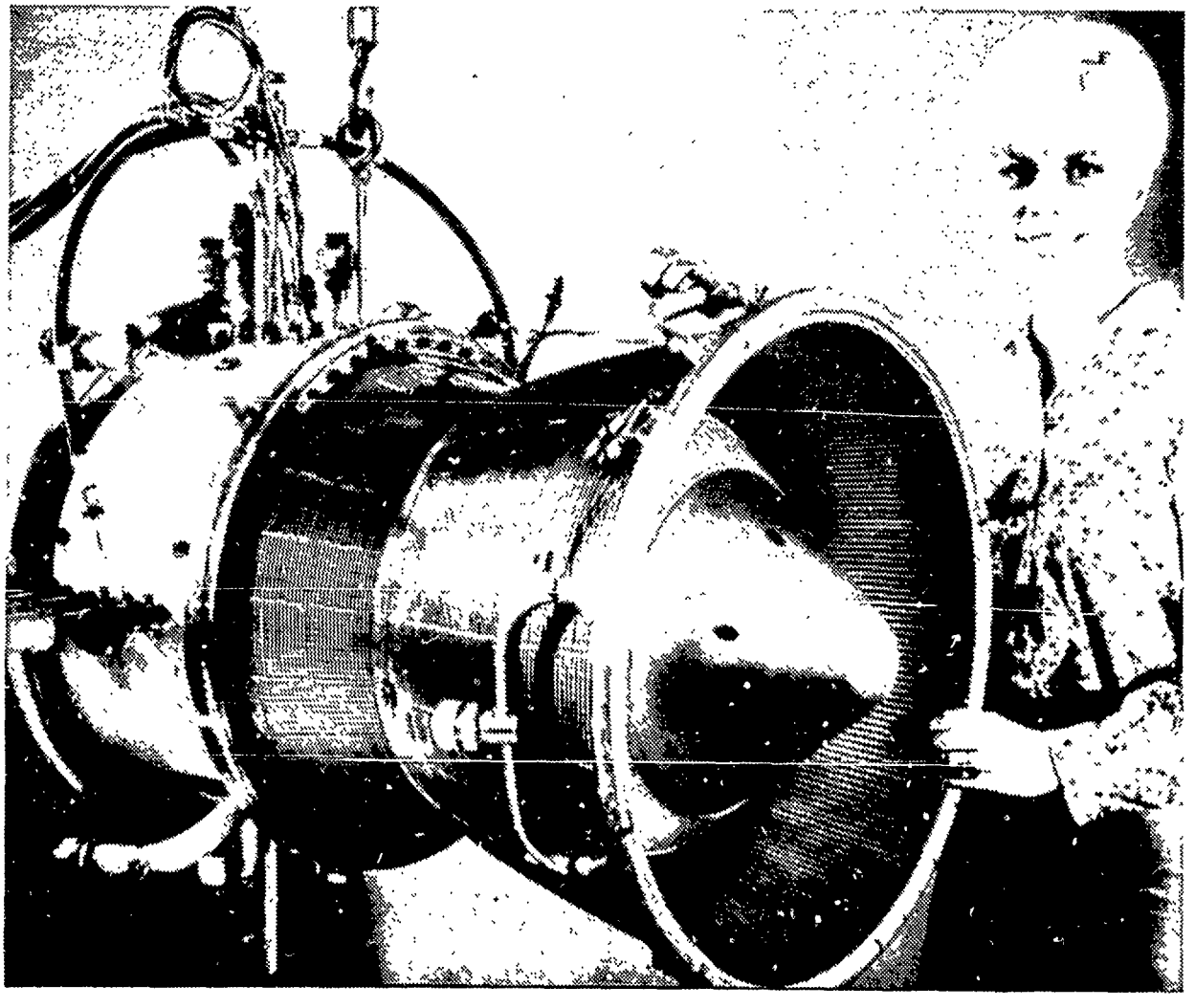


Fig. 15 Marquardt 18" Diameter Flight Weight Regeneratively Cooled Hydrogen Ramjet

over this period under the "hypersonic ramjet" exploratory research program. The variable-geometry exit nozzle engine construction shown here was successfully direct-connect tested from Mach 6 to Mach 8 simulated flight conditions achieving high combustion efficiencies in a very short combustion length. It also demonstrated adequate cooling capability as required for sustained, multiple reuse operations.

2.6 NASA Langley Research Center HRE Project

Another subscale engine test program of direct relevance to this project was the 7-year $40 million NASA-Langley/Garrett Airsearch Hypersonic Research Engine (HRE - Fig. 16) project. This effort concluded around 1975. Originally intended to be flight-tested on the X-15 research aircraft, several versions of the HRE in flight-weight regeneratively cooled hardware were extensively ground-facility tested in NASA high speed tunnels.

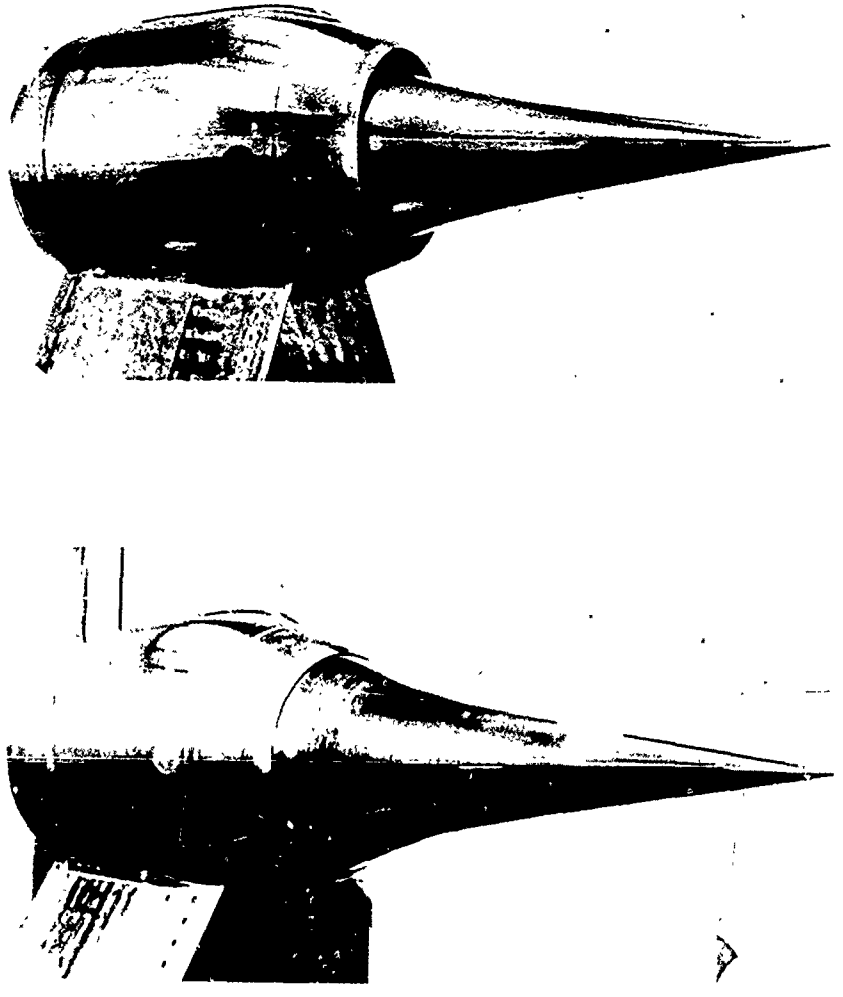


Fig. 16 Hypersonic Research Engine

The HRE engine had an inlet cowl diameter of approximately 19 inches, a maximum diameter of about 28 inches and a length of 87 inches. It was tested over a simulated high-altitude free-jet speed range from Mach 4 to Mach 7 in the NASA Lewis Plumbrook Station facility. In tests, the HRE Aerodynamic Integration Model (AIM) validated the performance predictions for the engine over the range from Mach 4 to Mach 7 operating in both the subsonic and supersonic combustion ramjet modes.

An equivalent test engine, the Structural Aerodynamic Model (SAM), was tested for structural integrity and regenerative cooling adequacy in the 8-foot high-temperature wind tunnel at the Langley Research Center. The unit came through with severe-condition cyclic testing with no significant problems. However, an ultimate limitation in thermal cycles was noted as inherent in the specific actively cooled structural design of the engine. Since that time, it has been reported that alternative design approaches have been identified that can reduce or eliminate that problem. A summary report of this important project is presented in Reference 8.

In the opinion of the present investigators, the technology status of RBCC engine systems is nearly adequate at the component/subsystem level. The principal area of uncertainty, again at the subsystem level, lies in scramjet combustion at flight speeds of up to Mach 15 over airbreathing orbital ascent trajectories. This knowledge of component/subsystem technology is adequate to support an advanced development program with the objectives of investigating the technology of INTEGRATION of these components and subsystems into a single RBCC candidate engine configuration. As information would be developed by an advanced development program, a basis could be established upon which to determine the desirability, costs and risks associated with proceeding into a DDT&E effort.

It is directly relevant to note that a priority objective of the NASP program is to carry out extensive investigation of scramjet propulsion in support of the development of the X-30 aircraft. The findings from this technology development effort will be directly applicable to the advanced development program suggested here. The focus should be upon the application of this type of propulsion system to space transportation systems with significant payload capability that would naturally follow the implementation of the X-30 project.

Section 3.0

ROCKET BASED COMBINED CYCLE PROPULSION SYSTEMS

This section presents a discussion of:

- the basic orbital mission profile
- how the five selected rocket based combined cycle engine systems operate over that mission profile
- the advantages and disadvantages of axisymmetric design of RBCC powered vehicles from the propulsion system standpoint
- the individual subsystems comprising the five RBCC engine configurations studied

3.1 Mission Profile

The basic mission studied was ascent to a 100 nmi polar orbital condition, deorbit, descent and landing as illustrated in Fig. 17.

One of the unique advantages of RBCC propulsion systems is a thrust-to-weight ratio sufficiently high to permit vertical takeoff and landing operation. In this study both horizontal, or "conventional" takeoff and landing and vertical takeoff and landing were considered.

Following takeoff, the vehicle flies an airbreathing and lifting trajectory starting initially with either straight ejector mode operation or supercharged ejector mode operation. This mode is maintained to approximately Mach 3.

At Mach 3, the RBCC propulsion system converts to either fan-ramjet and then to ramjet in supercharged variations or directly to conventional ramjet in non-supercharged variations. The vehicle flies the lifting ascent trajectory in this mode from Mach 3 to approximately Mach 6 with fan stowage required at approximately Mach 3.5 to 4. The stowage limit is dependent upon the design characteristics and performance of the fan subsystem.

Scramjet mode of operation begins at Mach 6 and is maintained to a flight velocity of approximately Mach 15. As will be subsequently discussed, one of the significant findings of this study was that scramjet propulsion to orbital velocity, or Mach 25, is not necessarily advantageous regardless of the availability of that technology.

The transition to all-rocket propulsion at around Mach 15 begins the final phase of the ascent profile to Mach 25 at approximately 300,000 feet. From this altitude, a Hohmann transfer maneuver is carried out to insert the vehicle into a 100 nmi polar orbit or otherwise inclined orbit, at a velocity of approximately 25,600 feet per second.

The vehicle then remains in orbit for some mission period that will be determined by the thermal insulation characteristics of the main propellant tanks. In this study, allowance was made for life support systems materials requirements for an on-orbit mission time of 15 days.

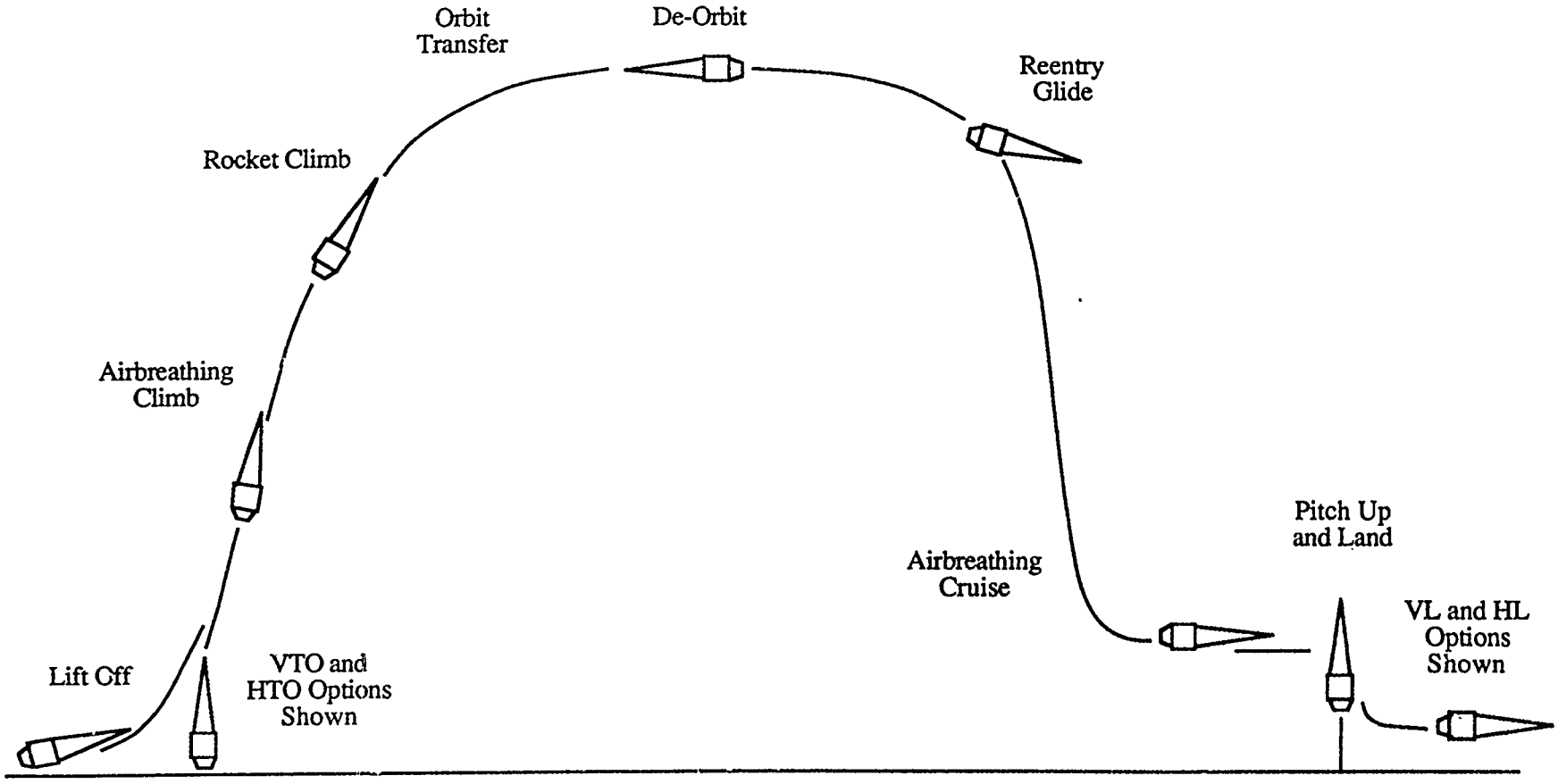


Fig. 17 Mission Scenarios Studied

The orbital mission is terminated by a retro-fire providing approximately 300 feet per second velocity decrement to the vehicle. A glide reentry and deceleration maneuver is accomplished to bring the vehicle to either supersonic or subsonic speed.

Depending upon the remaining available propellants and the engine variations used, all propulsion modes can be used for cruise flight.

Two landing options are available. First the "conventional" horizontal landing maneuver or, because of the thrust-to-weight available from RBCC systems, a vertical landing maneuver can be employed.

3.2 Multi-Mode Performance Over the Mission Profile

Fig. 18 presents the "Net-Jet" specific impulse performance for each of the propulsion modes through the mission, previously described and illustrated in Fig. 17, over the flight velocity spectrum from 0 velocity to orbital velocity.

This figure is of central importance in understanding the advantages of RBCC propulsion systems. For those readers working in the field of rocket propulsion, the approach to determining net-jet specific impulse as used in airbreathing systems will be discussed.

For an arbitrary ascent flight-path, the net-jet specific impulse level of each of the propulsion subsystems of the RBCC system are shown as a function of flight speed up to orbital conditions. These various propulsion subsystem specific impulse performance trends are shown as solid lines. The relative thickness of the lines defines, qualitatively, the thrust-to-weight ratio achievable in each mode as augmented by the use of atmospheric air at increasing flight velocities.

Note that both ramjet and scramjet performance curves in Figure 18 move progressively with speed from low thrust-to-weight ratios to higher values, and then revert to low values, as well as reduced specific impulse. On the other hand the "rocket" curve shows a steady, high thrust intensiveness over the full speed range, but with a relatively low Isp which may increase with altitude due to the ability to employ higher expansion ratio nozzles, not due to any effect to air-augmentation.

What RBCC engine systems do is to utilize the engine subsystem with the highest performance at the particular flight velocity and altitude conditions of an arbitrary mission or, specifically, an orbital mission. The path through these propulsion modes in an RBCC propelled vehicle is shown by the hatched operating path in Fig. 18. The RBCC engine type flight path illustrated in this Figure is based upon the use of RBCC configuration 12 - Supercharged Ejector Scramjet. As will be discussed subsequently, engines operating with air liquefaction are capable of delivering approximately 3,200 seconds specific impulse at liftoff.

Figure 18 illustrates an initial ascent path using an air-augmented rocket, transition to ramjet followed by transition to scramjet and final transition to orbital conditions under all-rocket propulsion. Upon retro-fire for deorbit, and descent to atmospheric flight, the point of "entry" is shown in Fig. 18 and the illustration of the flight path should be interpreted in the reverse order used for depicting the ascent path. That is the vehicle enters and goes towards lower velocity regimes on ramjet propulsion progressing to either fan ramjet or fan only operation for landing. In subsonic cruise/loiter flight and powered landing, RBCC engines may be operated "dry" with fan only operation or augmented with hydrogen afterburning plus fan operation. The range of specific impulses that can be achieved in these modes are from 6,000 to 22,000 seconds with this upper range being quite significant in providing the ability to meet the requirements of flyback and landing maneuvers and go-around maneuvers.

Example: Supercharged Ejector Scramjet (Engine #12)

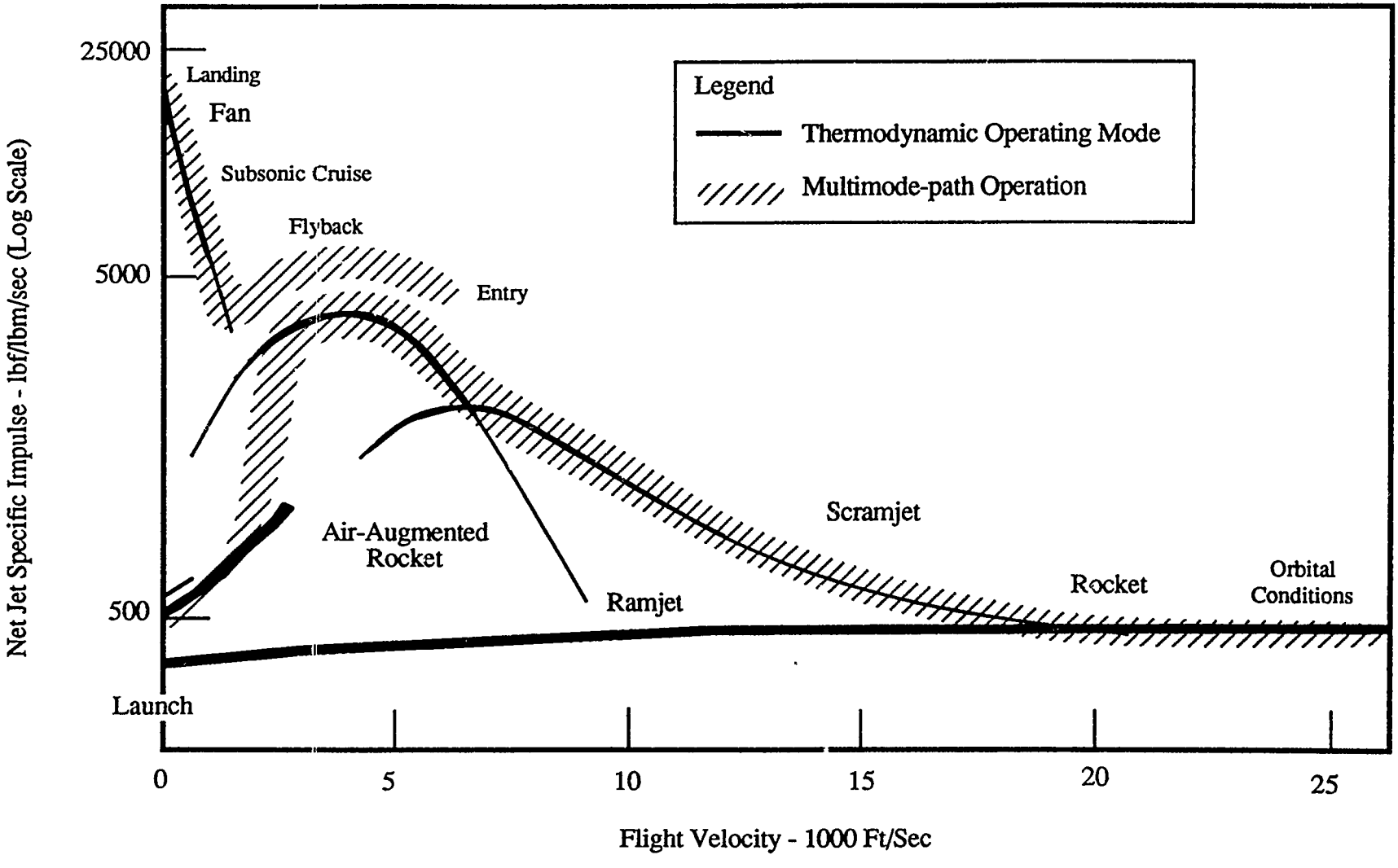


Fig. 18 Multi-Mode Engine Performance over the Mission Profile

The preceding two figures have presented the baseline orbital mission and its related velocity requirement and the net-jet specific impulse performance of the propulsion subsystems comprising RBCC engine systems over that same velocity range.

3.3 Reference Ascent Flight Path

Fig. 19 and 20 illustrate the reference ascent flight path used in this study and place the various propulsion subsystem modes of operation in the context of the total orbital ascent flight profile. Figure 19 illustrates the mode changes associated with non-supercharged RBCC systems and Figure 20 illustrates that of fan supercharged RBCC systems. These two figures illustrate a significant finding of the study, i.e., that the optimum transition point from scramjet mode to rocket mode is in the flight regime around Mach 15. This finding will be discussed further in Section 6.0.

3.4 Engine Selection

The principal database that provided performance information on candidate RBCC systems was that produced by NASA Contract NAS7-377 (Ref. 2). In that project, thirty-six (36) engines were studied within the "Class 0" phase. Of these 36 engines, a down selection process was carried out and yielded twelve (12) RBCC "Class 1" systems. These twelve systems were variations about a single "parent" multimode composite engine concept; the afterburning cycle, air-augmented rocket/ramjet system. These twelve engines were subgrouped into non-air liquefaction systems, of which there were four, and air liquefaction systems, of which there were eight.

The basis for screening of these engine systems included the following criteria:

- High payload performance
- High operational flexibility across the mission profile
- Ease of development in terms of major facility requirements for engine tests

Of the twelve engines selected using these criteria, five incorporated the scramjet mode which is essential to meeting the orbital mission requirements that were the subject of this study. These five engines were:

Engine 10 - the Ejector Scramjet - ESJ

Engine 12 - the Supercharged Ejector Scramjet - SESJ

Engine 22 - the ScramLACE - SL

Engine 30 - the Supercharged ScramLACE - SSL

Engine 32 - the Recycled Supercharged ScramLACE - RSSL

The matrix presented in Fig. 21 is presented to illustrate the fact that the five RBCC engine configuration variations derive from the configuration of Engine 10/ESJ. The first variation is the addition of fan supercharging. The second variation is the use of air liquefaction to produce liquid air for the rocket ejector mode rather than requiring vehicle contained liquid oxygen. The final variation is the use of slush hydrogen to support the air liquefaction process and to enable the engine system to be run at a closer to optimum mixture ratio in the rocket

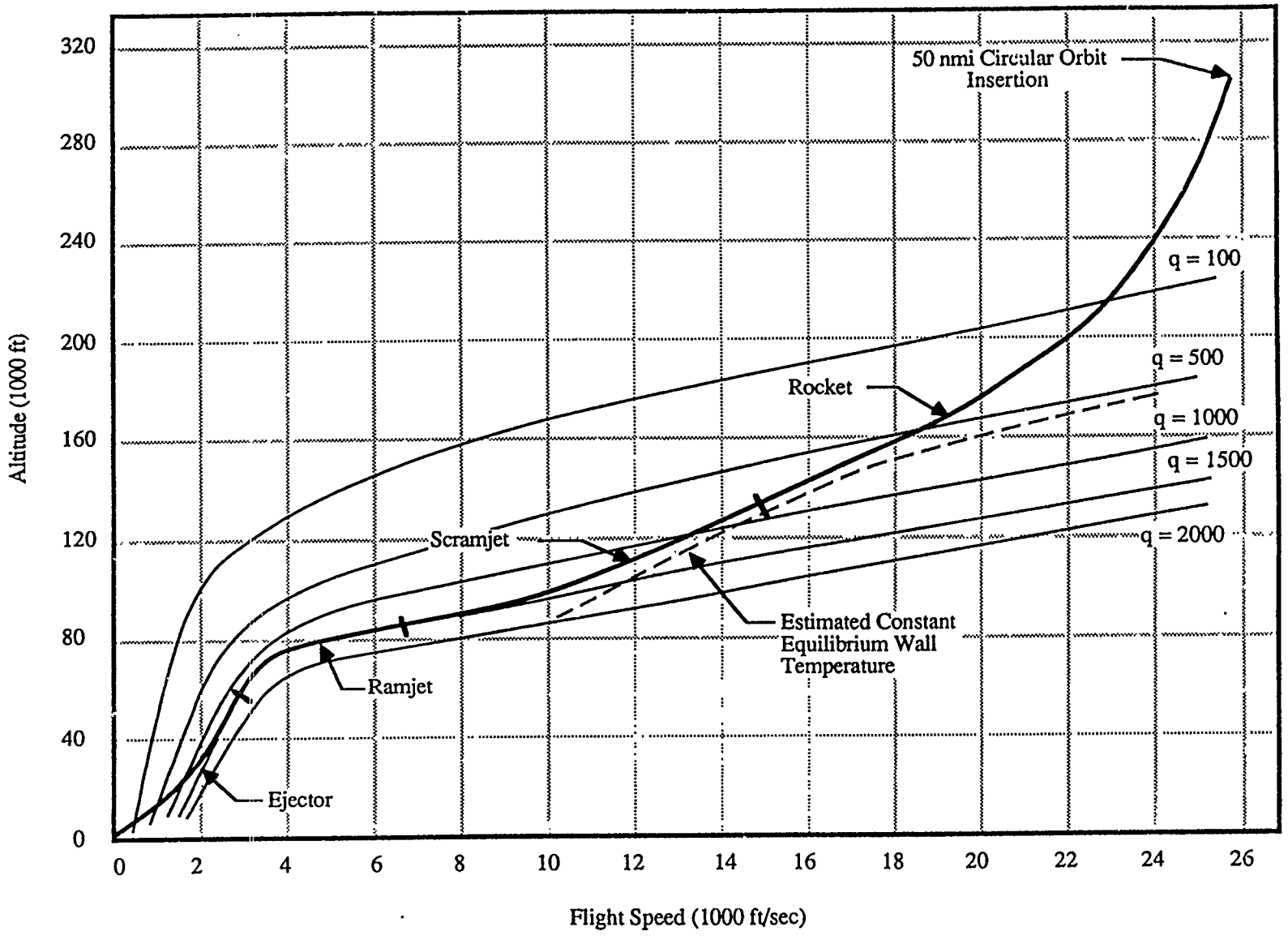


Fig. 19 Reference Trajectory Showing Non-Supercharged Operating Modes

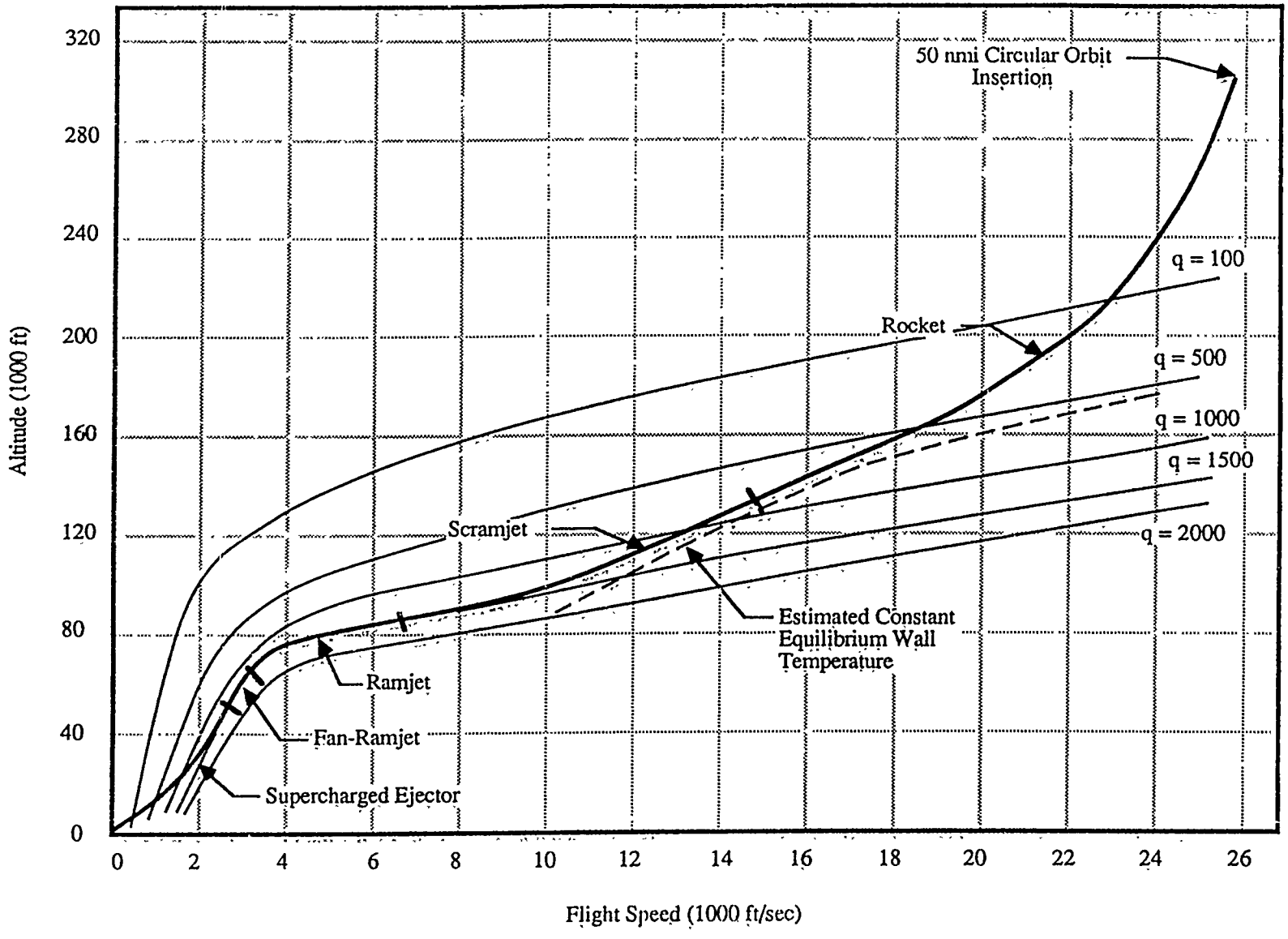


Fig. 20 Reference Trajectory Showing Fan Supercharged Operating Modes

Engine Variant Type

Name	ESJ	SESJ	SL	SSL	RSSL
Number	#10	#12	#22	#30	#32
Technical Features					
Ejector	X	X	X	X	X
Supercharger		X		X	X
LH_2/LO_2	X	X			
LH_2 /LAIR			X	X	X
Slush H_2 (Recycle)					X
Ramjet	X	X	X	X	X
Scramjet	X	X	X	X	X
Rocket	X	X	X	X	X

Fig. 21 RBCC Engines Configuration Matrix

ejector mode when compared to operation using non-recycled liquid hydrogen for air liquefaction and injection of the excess liquid hydrogen supply into the main engine combustor. All these ejector variations operate only in the initial portion of the flight below Mach 3.5 to 4.

The operation of the various propulsion subsystems comprising each RBCC engine configuration are integrated over the full orbital mission profile in the following manner:

3.4.1 Ejector Scramjet

A very simplified schematic of the Ejector Scramjet configuration is presented in Fig. 22 and the operating modes are illustrated in Fig. 23.

In Ejector Mode, the engine operates at high-thrust for liftoff and acceleration to Mach 2 to 3. The rocket primaries are at full thrust using hydrogen/oxygen propellants, and the afterburner is operating at local stoichiometric conditions at full flow.

The engine transitions to Ramjet Mode which provides an intermediate thrust level for supersonic to hypersonic acceleration with a thermal choke expansion mechanism. The rocket

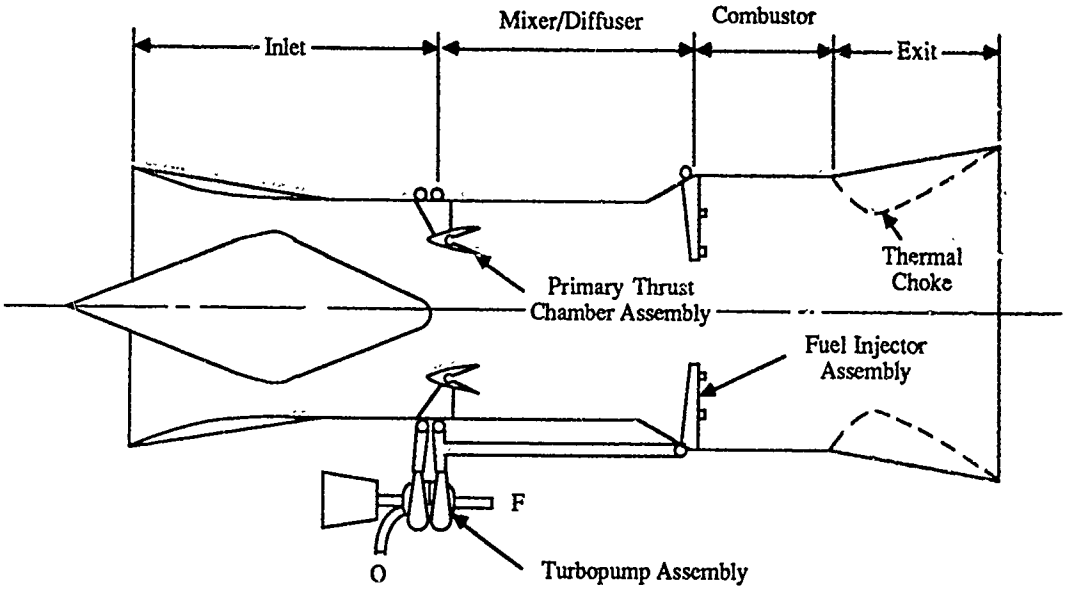


Fig. 22 Engine #10 - Ejector Scramjet - ESJ

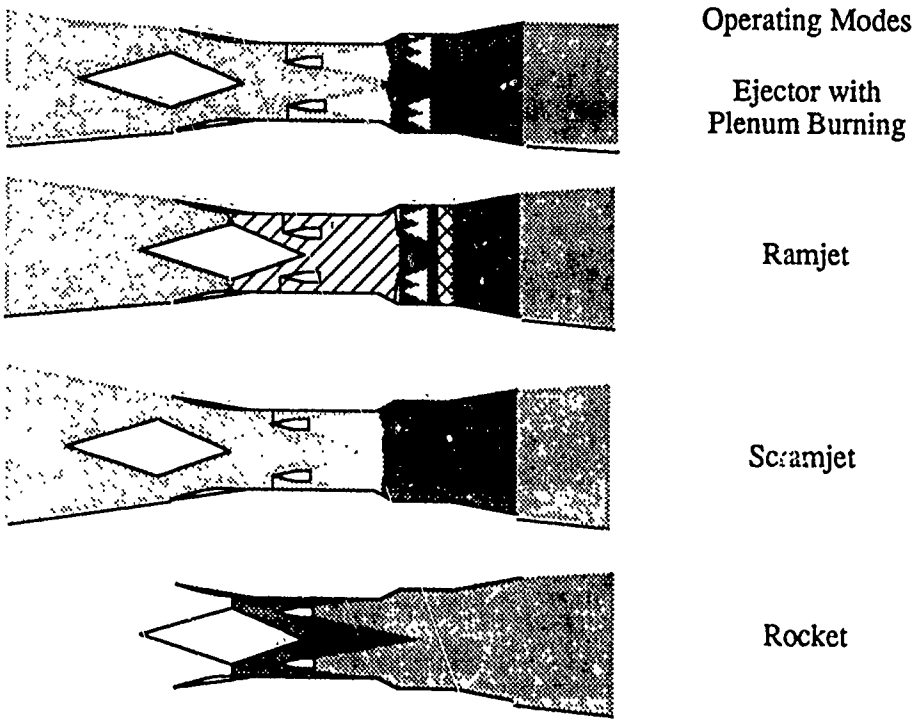


Fig. 23 Multi-Mode Operation - Ejector Scramjet Engines (#10 and #22)

primaries are off, while the ramjet combustor operates at near stoichiometric conditions and achieves a flight maximum combustion pressure of 150 psia.

The engine transitions to Scramjet Mode for continued airbreathing acceleration. The thermal choke is no longer needed, or, if a variable geometry exit is used, it is in a wide-open position. Hydrogen fueled injection is programmed forward in the duct now flowing all-supersonically. This transition of the hydrogen injection point is not noted in the schematic but will be discussed subsequently. The rocket primaries serve as an injection station with combustion taking place in the constant area and diverging ducts and expansion initiated in the nozzle and completed on the aft-body of the vehicle.

At approximately Mach 15, the engine transitions to rocket mode with the inlet physically closed, the rocket primaries operating on hydrogen/oxygen propellant and controlled thrust settings, and the exhaust gases expanded in the divergent portion of the duct and on the vehicle aftbody.

On return and landing, cruise, go-around, and landing capability is provided to the extent permitted by available propellants, by ramjet mode operation, and by ejector mode operation with or without plenum burning.

3.4.2 Supercharged Ejector Scramjet

See Fig. 24 and 25.

At the start of flight, the fan is at full power, the rocket primaries are at full rated thrust using hydrogen/oxygen propellants, the afterburner is operating at local stoichiometric conditions at full flow.

In the Fan Ramjet/Ramjet Mode, the engine transitions from fan/ejector mode to fan/ramjet mode in which only the fan and the ramjet system is operating. As engine inlet recovery temperature rises and the pressure contribution of the fan drops as flight velocity increases, the fan system is shut down and must be effectively stowed clear of the engine flow duct. The engine then transitions to scramjet mode and finally rocket mode for orbital insertion.

In the descent and landing phase of the flight, the fan is unstowed and can be operated with or without plenum burning to provide high specific impulse and sufficient thrust for subsonic loiter/landing of the vehicle. With the fan mode and plenum burning, the thrust produced is adequate to meet the requirements for vertical landing.

3.4.3 ScramLACE

See Fig. 26 and 23.

Operation of the air liquefaction system is initiated supplying liquid air to the rocket primaries which operate on hydrogen/liquid air (LAIR) throughout the ejector mode. The afterburner burns fuel-rich at full flow because of the excess hydrogen supply required by the air liquefaction system. Liquid air is consumed as it is produced.

The rocket primaries and air liquefaction system are shut down and the engine transitions to ramjet mode at near stoichiometric conditions.

As in the previous two engine configurations, the engine transitions to scramjet mode and rocket mode to achieve final orbital insertion.

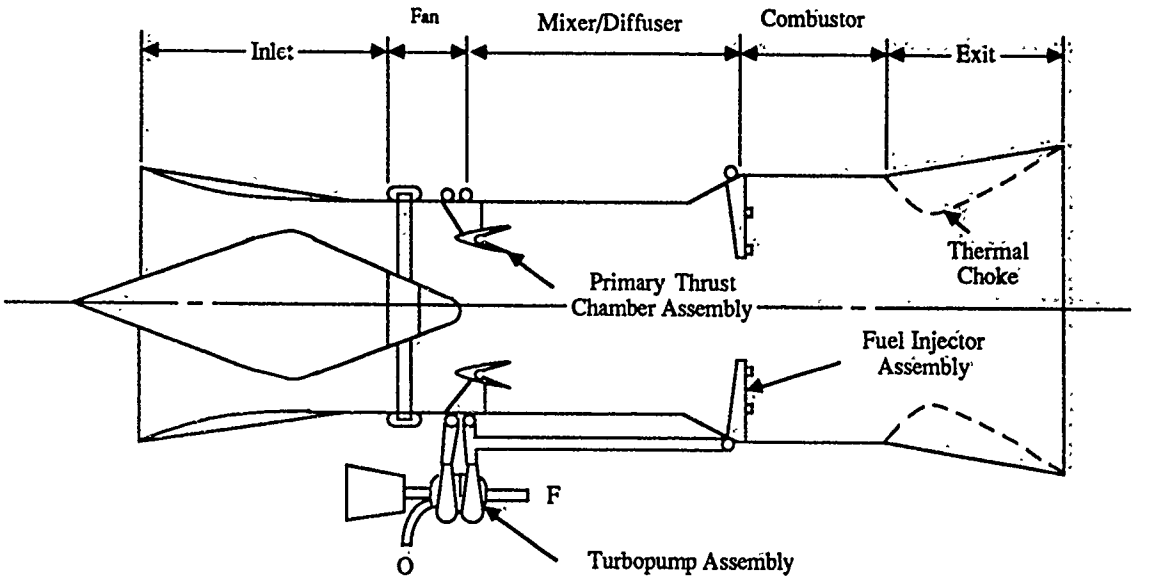


Fig. 24 Engine #12 - Supercharged Ejector Scramjet - SESJ

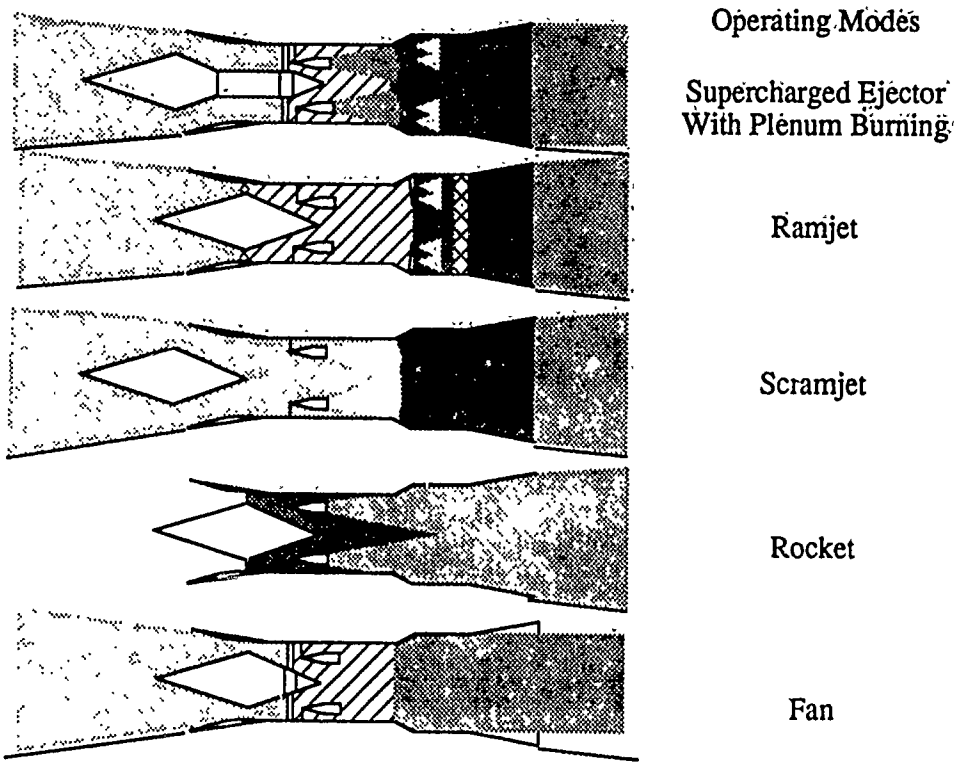


Fig. 25 Multi-Mode Operation - Supercharged Ejector Scramjet Engines - (#12, #30 and #32)

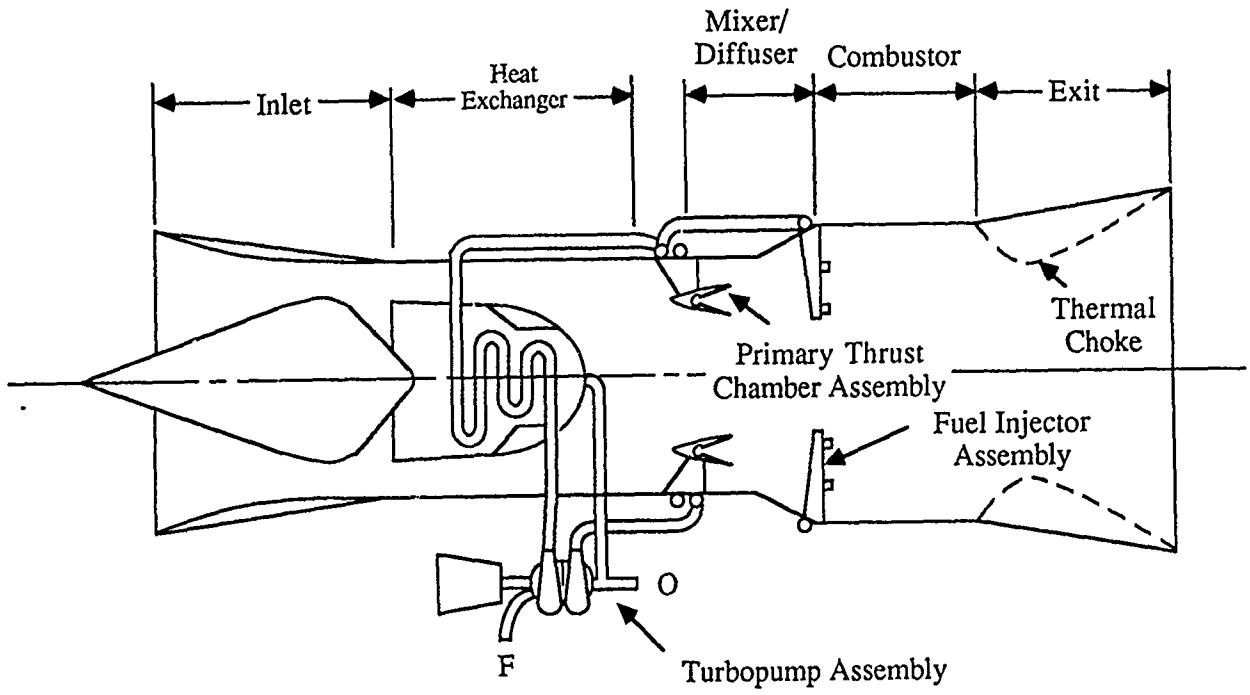


Fig. 26 Engine #22 - ScramLACE - SL

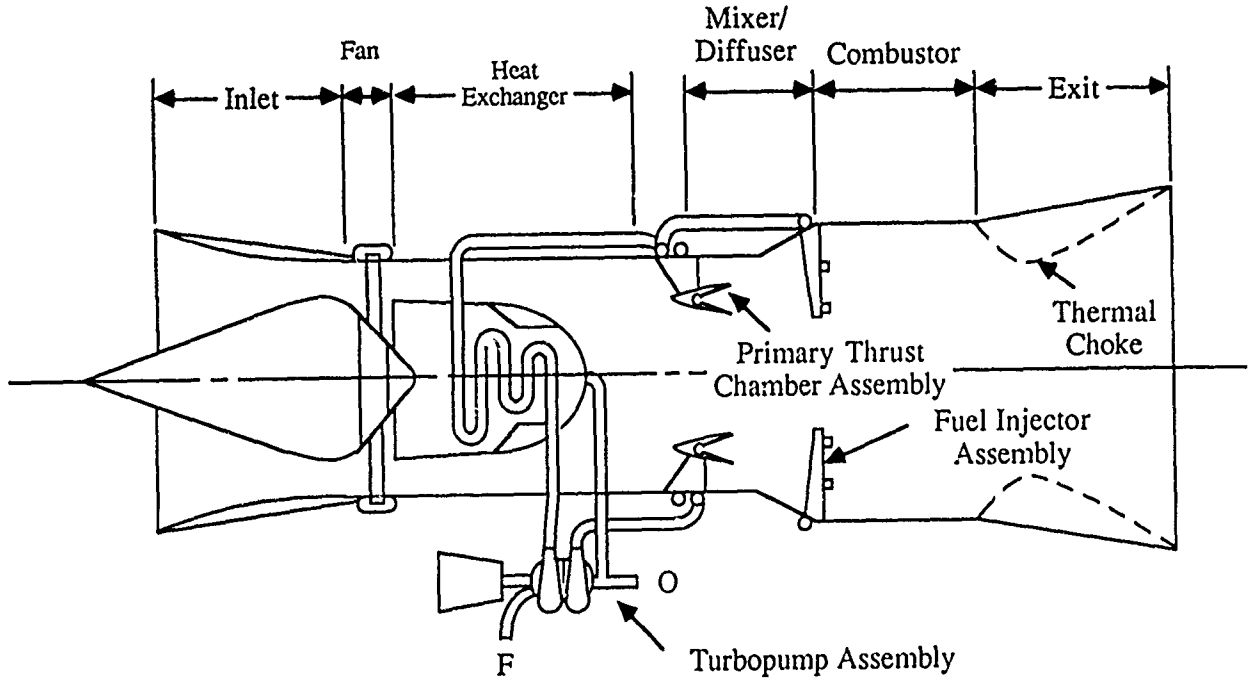


Fig. 27 Engine #30 - Supercharged ScramLACE - SSL

For landing, ejector operation with plenum burning can produce sufficient thrust to meet the requirements of a vertical landing maneuver. However, in this mode, as in the ejector scramjet mode, the specific impulse performance provided by the fan system is not available.

3.4.4 Supercharged ScramLACE

See Fig. 27 and 25.

The air liquefaction system is placed in operation and the rocket primaries go the full rated thrust using hydrogen/liquid air (LAIR) propellants, the afterburner burns fuel-rich because of the excessive hydrogen production from the air liquefaction system and liquefied air is consumed as it is produced by the rocket primaries.

With the fan system, the fan continues to operate at full power with hydrogen combustion in the ramjet. The fan is shut down and stowed as temperature rise and fan pressure rise contribution drops. With the termination of rocket ejector primary combustion, the ramjet is then operating at near stoichiometric mixture ratio. The engine transitions to scramjet and rocket mode to orbital insertion in the same manner that the preceding three engines described.

On landing, the fan mode with or without plenum burning is available to support cruise operations, go-around and horizontal landing. Fan mode with plenum burning is available to support vertical landing.

3.4.5 Recycled Supercharged ScramLACE

See Fig. 28 and 25.

At mission start, the air liquefaction system is operated and the rocket primaries are at full rated thrust using hydrogen/LAIR propellants. The afterburner is operating at near stoichiometric mixture ratio. This is achieved by recycling a portion of the liquid air condenser hydrogen flow back to the hydrogen fuel tank where it is reliquefied by direct contact with subcooled slush hydrogen. This flow path is illustrated in Fig. 28. The engine converts to fan ramjet, ramjet, scramjet and finally rocket mode as in all other cases.

As with all fan configured variations, fan operation with and without plenum burning is available to support both vertical and horizontal landing maneuvers.

3.5 Net Jet Specific Impulse

The method of computation of the value of specific impulse that is used in the basic ballistic equation to compute vehicle velocity capability is computed in two different manners for rocket engines and airbreathing engines. It is imperative that those persons used to the rocket engine methodologies for computing specific impulse understand the different approach in computing net-jet specific impulse. This is the value of specific impulse used to compute velocity capability based on specific impulse and vehicle mass ratio.

In all subsequent discussions presented in this report, unless otherwise noted, specific impulse will be assumed to be net-jet specific impulse, except in the final all-rocket mode of orbital flight or where noted.

In rocket engine systems (Fig. 29), two basic specific impulse computation methods are used. The first is the computation of "thrust chamber" specific impulse. This is derived by dividing the gross thrust, F, by the total oxidizer and fuel flow rates to the thrust chamber. "Engine" specific impulse is derived by dividing that same gross thrust by the total propellant

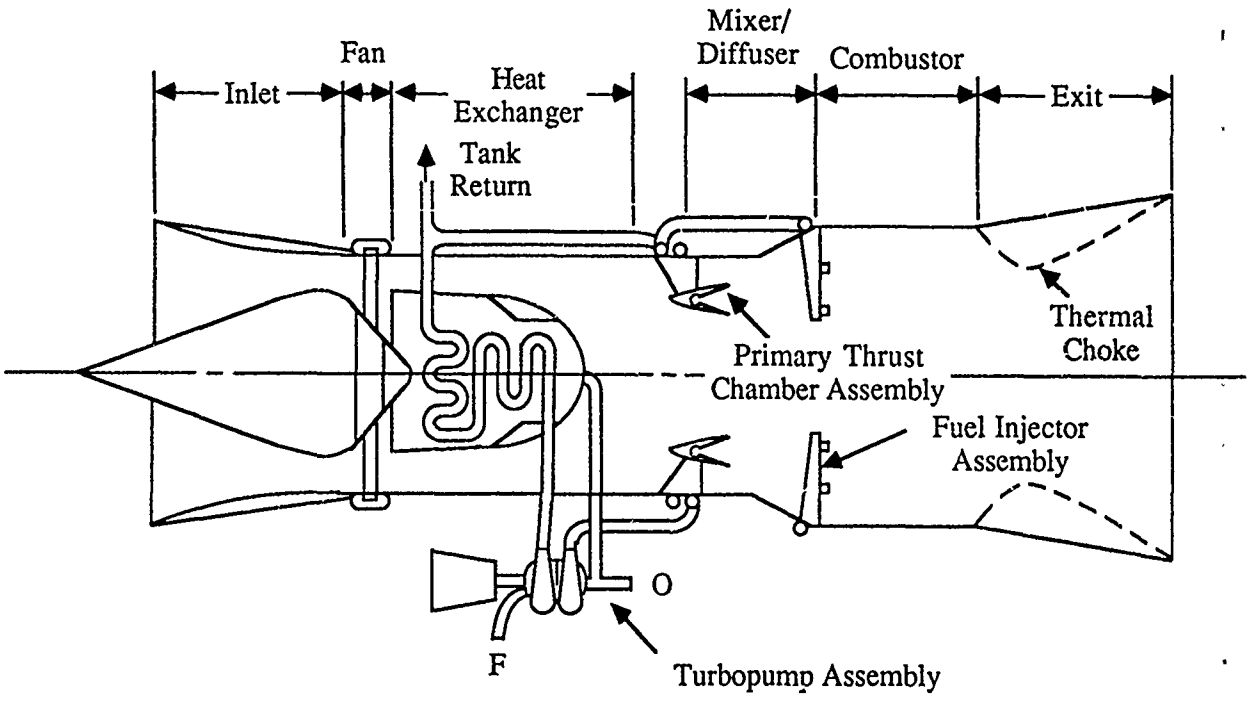


Fig. 28 Engine #32 - Recycled Supercharged ScramLACE - RSSL

flow rate to the engine system which also includes the propellant flow rate required to operate the turbopump system and any related propellant driven systems required to support engine operations. The various components of total drag do not enter into the calculation.

In airbreathing engines (Fig. 30), two factors operate to significantly increase the same specific impulse values. First, no vehicle borne liquid oxidizer flow is required to operate the engine system in conventional airbreathing systems such as those using turbomachinery. This situation does not always apply in RBCC systems which combine both rocket mode operation, where a vehicle borne liquid oxidizer is required, with airbreathing operation, where there is no vehicle borne liquid oxidizer. The second reason is that ram drag is subtracted from gross thrust to yield "net jet thrust". Ram drag accounts for the momentum penalty associated with taking the engine air flow on-baord the vehicle It is this thrust value that is divided by the fuel flow rate to yield "net jet" specific impulse. The physical relationships in this approach are illustrated in Fig. 30. The turbopump illustrated operates on a combustion of fuel and intake air. To be accurate in measuring the net jet specific impulse, the drag associated with turbopump inlet air compression would not be deducted from the total inlet drag in the computation.

An important point is that the additional drag on vehicle areas other than the inlet area is treated in the same manner in both the rocket and the airbreathing case. Similarly, base drag is treated in the same manner in both cases. Skin drag is also treated the same way in both cases.

The significance of this consideration is found in the fact that the work done on the engine airflow stream to overcome ram drag provides the initial work of compression, the first step of the thermodynamic cycle of the overall vehicle/engine propulsion system. The remaining steps are the combustion step and expansion step carried out in the combustion chamber and nozzle assembly respectively.

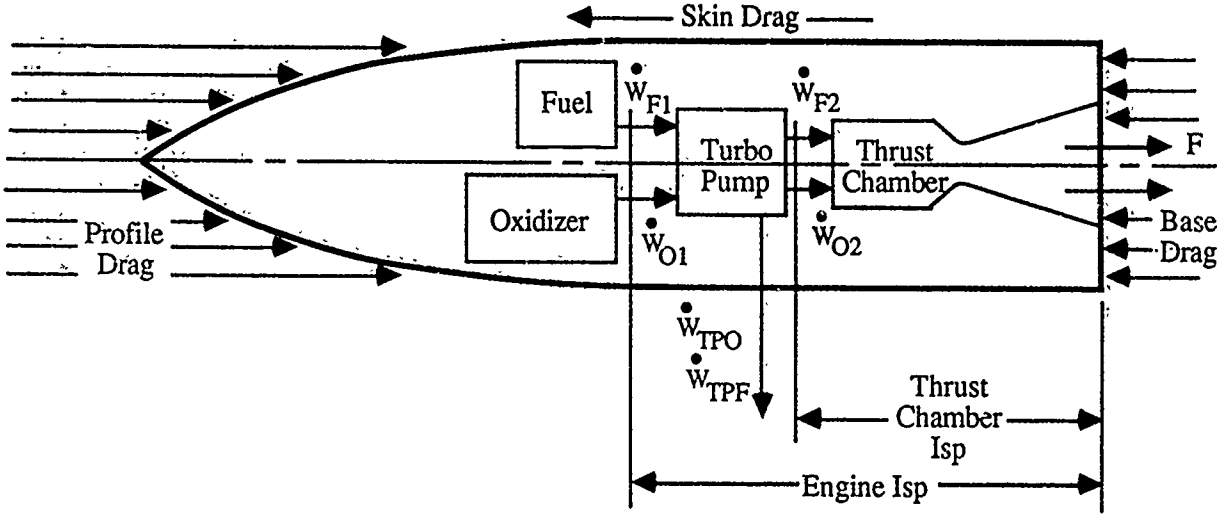


Fig. 29 Rocket Engine Specific Impulse Calculation Parameters

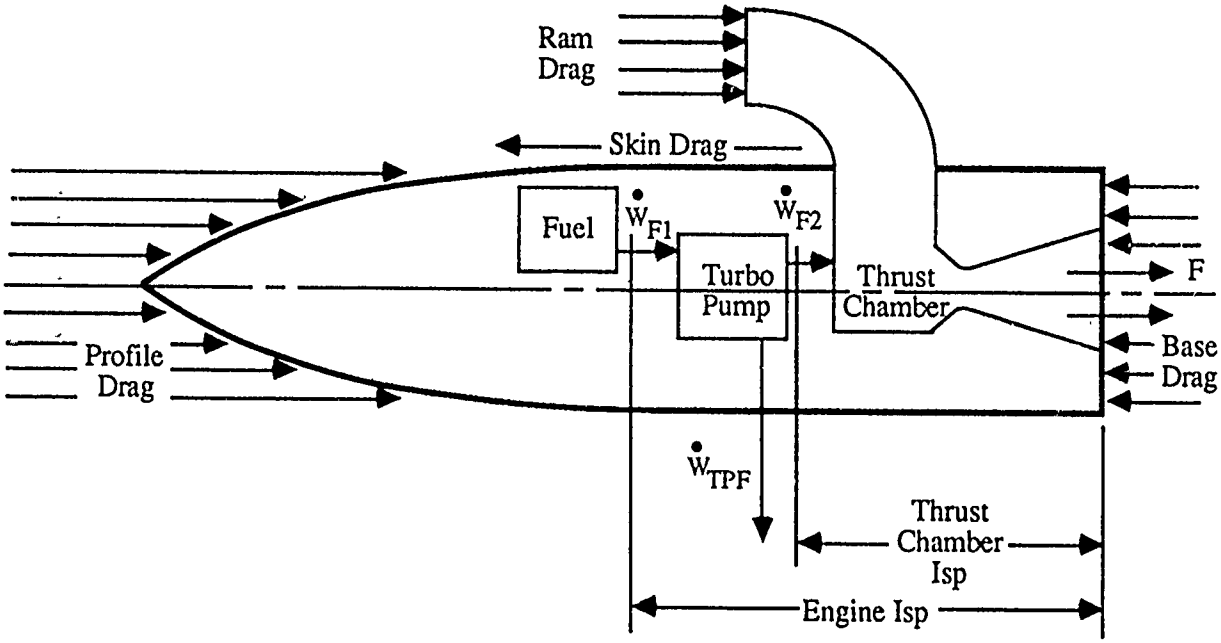


Fig. 30 Airbreathing Engine Net Jet Specific Impulse Calculation Parameters

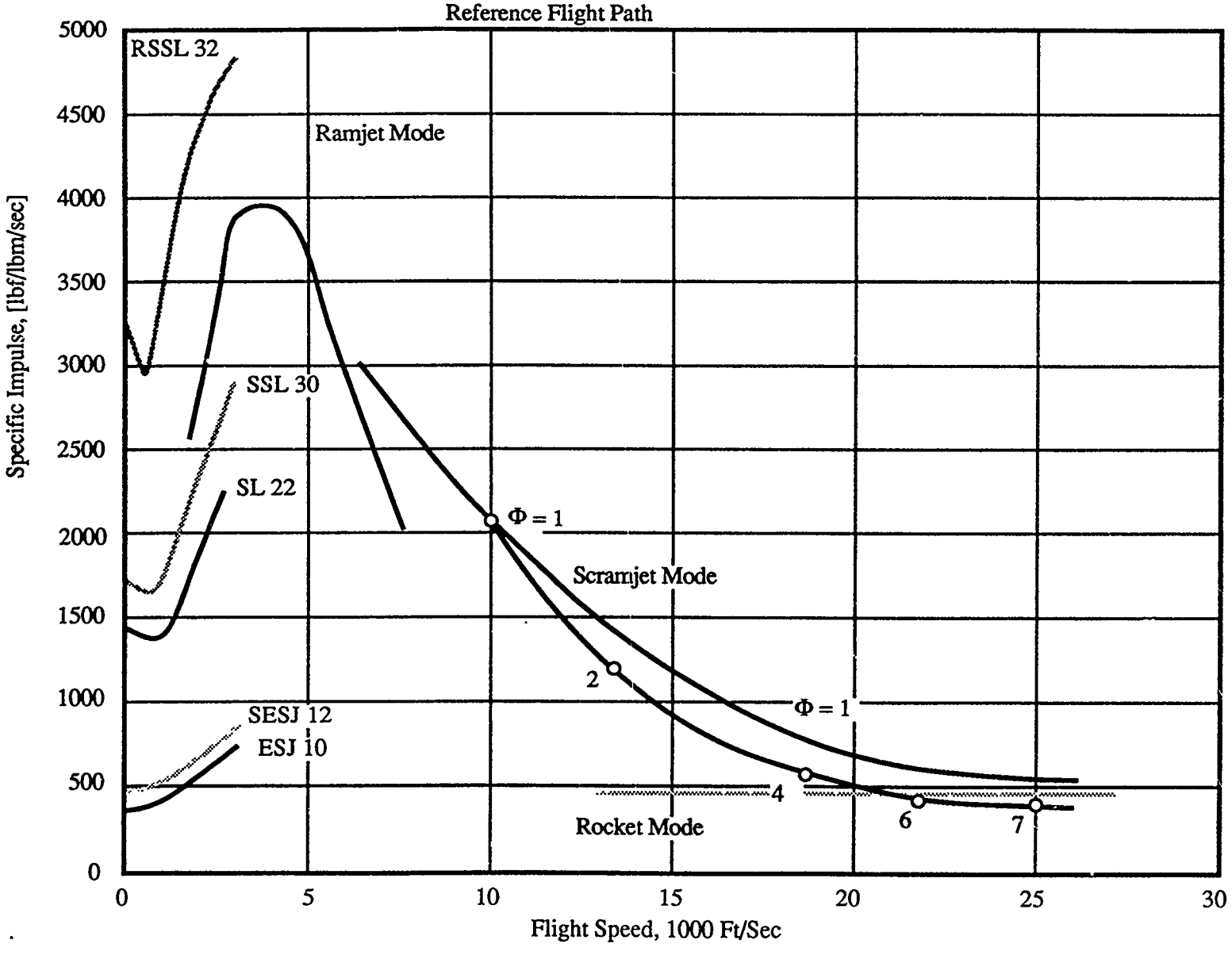


Fig. 31 Specific Impulse Over the Ascent Profile by Engine Type and Operating Mode

This leads us toward the vehicle configuration being reported on here. This configuration is one that makes maximum use of the work done to overcome drag to provide work of inlet air compression which then enables the remaining steps of the engine cycle to be completed. What is sought is a vehicle design that will as closely as possible achieve a configuration that is "all inlet" and, as will be discussed, also "all exit".

3.6 Effective Specific Impulse and I*

The ideal rocket equation:

$$V_{final} = g\ Isp\ \ln (M_0/M_i)$$

expresses the final velocity that would be achieved by a vehicle using a rocket propulsion system providing the specific impulse Isp as a function of the initial mass M_θ and final mass of the vehicle M_i without the effect of gravity or aerodynamic drag.

When that ideal velocity is reduced due to the effects of drag and gravity along a specific flight path, another specific impulse can be computed that, when placed in that same ballistic equation, will yield the actual delta Vs with drag and gravity losses. This specific impulse value is referred to as the "effective specific impulse" or Ieff. This is an instantaneous value along the flight path.

A third specific impulse value which is used here is the "equivalent effective specific impulse" or I*. This specific impulse value, when substituted into that same ballistic equation, provides a single specific impulse value that can be used to predict the final velocity of the vehicle with both drag and gravitational velocity losses. It is a form of overall value rather than an instantaneous value as in I_{eff}. The form of the ideal ballistic equation using I* becomes:

$$V_{final} = g\ I^*\ \ln (M_0/M_i)$$

3.7 RBCC Engines Configuration and Performance

3.7.1 Physical Arrangement

The physical arrangement of the engine subsystems as proposed in the NAS7-377 baseline study (Ref. 2) was extensively modified in this effort. Where the baseline study focused on a 250 Klb sea level static thrust engine, in this study this engine design was downsized to 125 Klb (SLS) and 65 Klb (SLS) thrust rated engines.

By selecting these three thrust ratings, weight estimates could be prepared for vehicles using propulsion modules with 65 Klb thrust engines in the 500 klbm TOGW vehicles, 125 Klb thrust rating engines in the 1 Mlbm TOGW vehicles and 250 Klb in the1.5 Mlbm TOGW vehicles.

3.7.2 Performance

The thrust and Isp performance of the five engine cycles studied in the NAS7-377 project were basically retained with two exceptions.

Scramjet Isp and thrust performance were reestimated on the basis of information available in the literature, supported by discussions with persons presently working in this field, to extend the baseline estimates from Mach 12 to the values required in this study, i.e., Mach 25.

The performance in Fan Mode was upgraded using more currently developed technology from a number of studies of high bypass ratio turbofan systems including specifically hydrogen and oxygen burning turbofan systems as studied recently by the Garrett Corporation for the Lockheed California Company (Ref. 9).

3.7.3 Weight

The weight estimates developed by the NAS7-377 project were based upon a technology availability date (TAD) of 1965. These weight estimates were revised in light of the developments that have occurred since 1965 in materials and manufacturing processes. The use of composite materials technology has a significant impact upon these weight estimates. The conclusions reached with regard to propulsion system and vehicle system weights will be discussed further in this section. Two technology availability dates were considered in this study. These were a TAD of 1985 and a TAD of 1995.

3.7.4 Specific Impulse Performance

Fig. 31 illustrates the specific impulse trends along the reference flight path for each of the five RBCC engine type examined in the study. The four ascent operating modes are: (1) rocket ejector or supercharged ejector mode, (2) ramjet mode, (3) scramjet mode, (4) rocket mode. Two scramjet trend lines are shown: (1) for stoichiometric or unity equivalence ratio combustion and (2) for fuel-rich operation up to seven times stoichiometric. This shift to fuel-rich operation is required to maintain adequate scramjet thrust as will be shown in the thrust performance chart to be discussed next. Isp for dry fan operation, and fan with plenum burning, on the return and landing maneuver is not shown in this figure but will be discussed separately.

The primary difference in the five engine concepts examined is found in the initial rocket ejector mode of operation. The Isp spread is significant with the non-air-liquefaction systems, the ejector scramjet and supercharged ejector scramjets, starting at near-rocket levels and increasing with speed. The higher Isp levels shown by the remaining three engines are due to the use of air liquefaction and hydrogen recycle.

For the initial flight speed regime up to ramjet transition, at about 3,000 feet/sec, the engine specific impulse levels range from near-rocket levels to those associated with an afterburning turbojet cycle (on the order of 5,000 secs). It is important to note that this increase in performance is available over only a small portion of the SSTO total flight profile speed range and is acquired at the expense of added engine complexity, cost and, most importantly, weight. The trade-off in terms of payload performance will be discussed subsequently.

It is important for the reader to note that this specific impulse chart is "net-jet" based. Further, these performance curves are valid only on the reference trajectory flight path previously discussed.

3.7.5 Thrust Performance

In terms of thrust performance, all five engine types studied were essentially directly comparable. Fig. 32 illustrates the thrust performance of all five engine systems for a nominal 250 Klb (SLS) design thrust engine flying on the reference trajectory. Thrust for dry fan and fan with plenum burning on the return and landing maneuver are not shown in this figure but will be discussed separately.

In the initial rocket ejector mode, thrust as well as specific impulse increases rapidly with speed, momentarily doubling in the case of thrust. A fuel-rich operating schedule is required in scramjet mode, otherwise the loss of thrust would be precipitous.

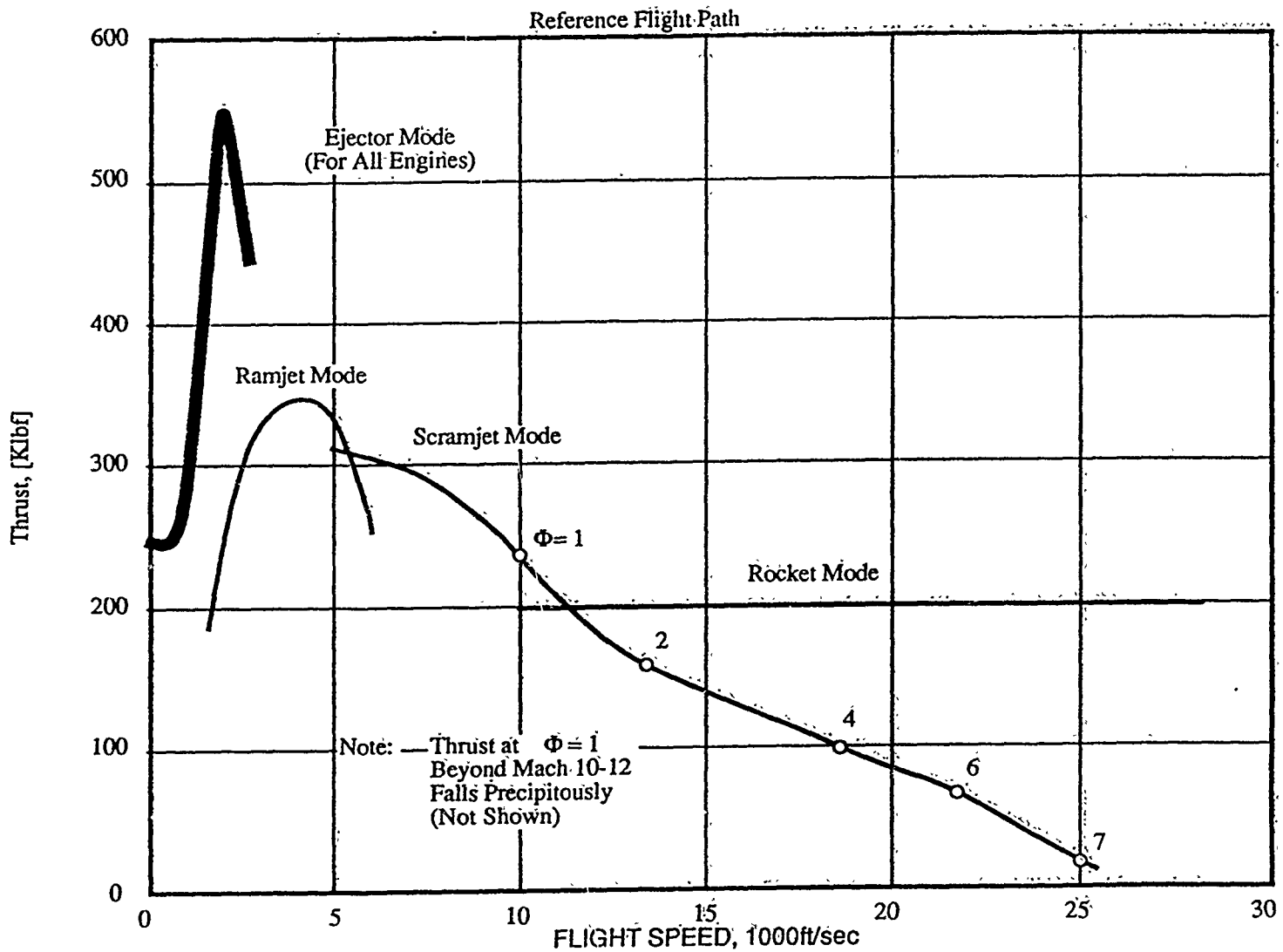


Fig. 32 Thrust Over the Ascent Profile by Operating Mode

3.8 Approach to Discussion of Subsystems

The five engine systems studied all have four subsystems in common. These are the inlet subsystem, the rocket subsystem, the ramjet subsystem, and the scramjet subsystem.

These four subsystems are all integrated into a single engine system with the major structural assembly being the mixer/diffuser/combustor/nozzle assembly. Each variation of configuration, that yields one of the five engine systems, is created from the baseline Ejector Scramjet by the use of:

- A stowable fan and its drive system
- The use of air liquefaction
- The use of slush hydrogen

In the subsequent section, each of the major subsystems comprising the RBCC engine system are discussed in the order suggested by the fact that all five engines represent combinations of basic subsystems. These subsystems are discussed in the following order:

- Inlet subsystem
- Fan subsystem
- Rocket subsystem
- Ramjet subsystem
- Scramjet subsystem
- Nozzle subsystem
- Air liquefaction subsystem
- Slush hydrogen utilization
- Engine structures and materials and engine weights

At the conclusion of this section, three preliminary design concepts illustrating design approaches to the five engine variations are presented only for the purposes of illustration of a conceptual mechanization of the technologies involved as many alternatives remain to be investigated further.

3.9 The Inlet Subsystem

The air inlet subsystem of all the candidate RBCC engine systems must function from an initial flight velocity of Mach 0 to Mach 25. This is a significant engineering challenge particularly with respect to achieving the maximum inlet capture area and high inlet efficiency over the varying geometrical requirements of the inlet system as a function of speed.

As will be seen in subsequent discussions, the weight of the RBCC propulsion system comprises a significant portion, from 40 to 50 percent, of the total inert weight of the vehicle design studied. Of the total propulsion system weight, nearly 50% is engine inlet subsystem weight.

Much work remains to be done on inlet subsystems that must operate between the Mach 0 and Mach 15 velocities associated with orbital ascent profiles. Of particular concern is the handling of the inlet boundary layer and real gas effects. With regard to handling of the inlet boundary layer, conversations carried out under this project with personnel of the NASA Langley Research Center indicated the general opinion that the inlet boundary layer should not be ingested at below low Mach number supersonic velocities and probably should be ingested at the higher supersonic and hypersonic velocities. A significant technological subproblem exists with regard to sealing moving surfaces in the hypersonic velocity flight regime.

The problems associated with the operation of RBCC engine systems are similar to those encountered by turboramjet or other turbomachinery based systems designed to operate at these flight velocities. There is a difference in that requirement for uniform air flow in the transonic region may be less stringent for RBCC systems than for turbomachine systems. An additional complexity, however, is that there is probably a need to affect complete closure of the inlet system following airbreathing termination in order to prevent exhaust gas recirculation from the primary rocket units in all-rocket mode in the main engine duct and to eliminate the necessity of cooling the engine's internal surfaces during reentry.

3.9.1 Axisymmetric Design

The design goal for the vehicle systems under study here is to achieve the maximum utilization of the drag work through the mechanism of using this work to achieve compression in the engine inlet. The design configuration that does this to the maximum extent feasible is illustrated in Fig. 33. Here the vehicle forebody provides the basis for the first step in compression and, in the axisymmetric configuration, is capable of achieving a theoretical capture area of 100% but which, in practical inlets, is usually a maximum of 70%, the value used in this study. This condition, versus the case for a nonaxisymmetric vehicle, is illustrated in Fig. 34.

In the axisymmetric design approach, the engine compression process is divided into two steps. The first step is carried out on the forebody of the vehicle and the flow processes associated with this step establish the conditions at the inlet of the second stage of inlet compression.

A number of undesirable situations are created that increase in significance with increasing angle-of-attack on the conical forebody (Fig. 35). These problems are largely associated with the reduced forebody compression on the top side of the vehicle due to a decrease in the effective cone angle. This is accompanied by a thickened boundary layer which may lead to inlet flow distortion and unstart conditions in the engine systems themselves. Local vorticity may be developed which would contribute to nonuniform flow into the engine system. Finally there is a problem of conical crossflow around the forebody of the vehicle at sustained angles-of-attack.

In the vehicle systems studied in this project, as will be discussed in Section 6.0, the performance analysis was based upon a propulsion system thrust vector colinear with the chord lines of the lifting surfaces with both the thrust line and chord line parallel to the longitudinal axis of the vehicle. Under these conditions, significant angles-of-attack were indicated to be required over the full ascent profile. What was not studied, because of the limitations of resources for this project, were vehicle systems where the thrust vector and lifting surfaces chord lines could be varied from the longitudinal axis of the vehicle. This is a subject that should receive additional study at the first opportunity.

In addition to this basically different approach to thrust and lift scheduling, the following offer possible alternative solutions to the problem:

- The use of additional lifting surface area with the drawbacks of weight and drag.
- Fixed positive angle of incidence or variable angle of incidence with the drawback of additional weight and system complexity.
- Flying a trajectory characterized with higher dynamic pressure which has significant impact on aeroheating and structural weight.

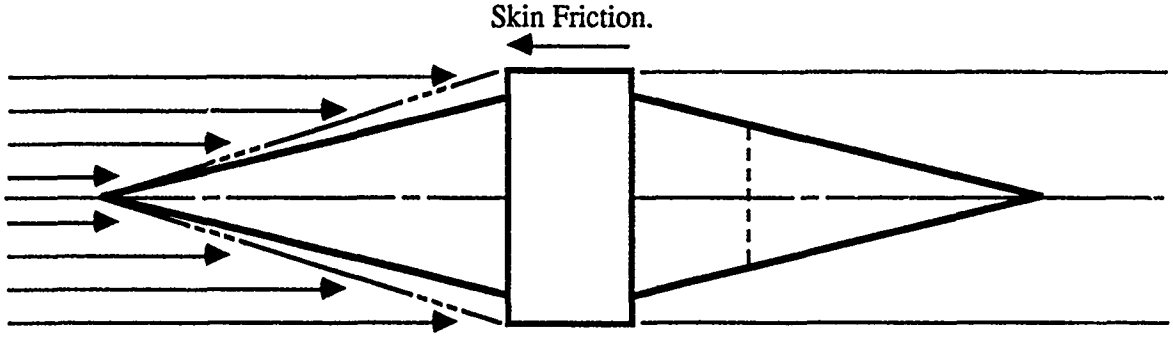


Fig. 33 Axisymmetric Vehicle at 100% Capture

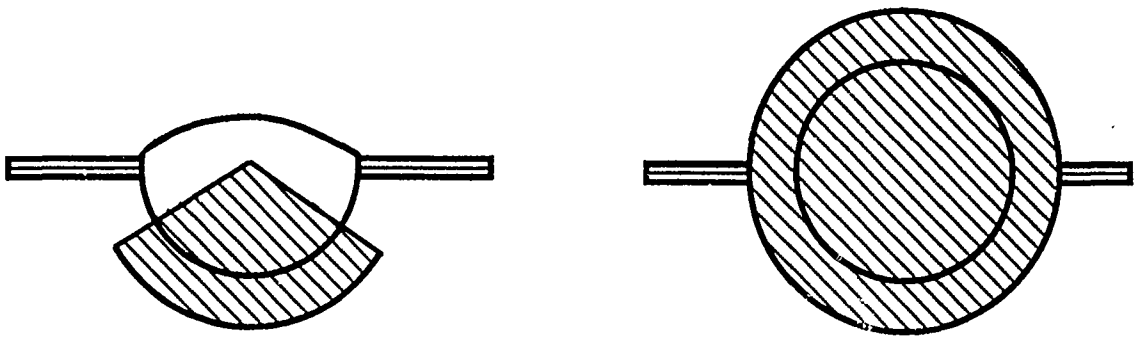


Fig. 34 Capture Area Limits for Non-Axisymmetric and Axisymmetric Vehicles

Statement Of Problem: At Angle-of-Attack Conditions Generally Required for Lifting Ascent Flight Paths, Leeward-Side Engine Inlets are Exposed to Degraded-Quality Airflow Conditions Which Can Adversely Affect Engine Performance and Operation

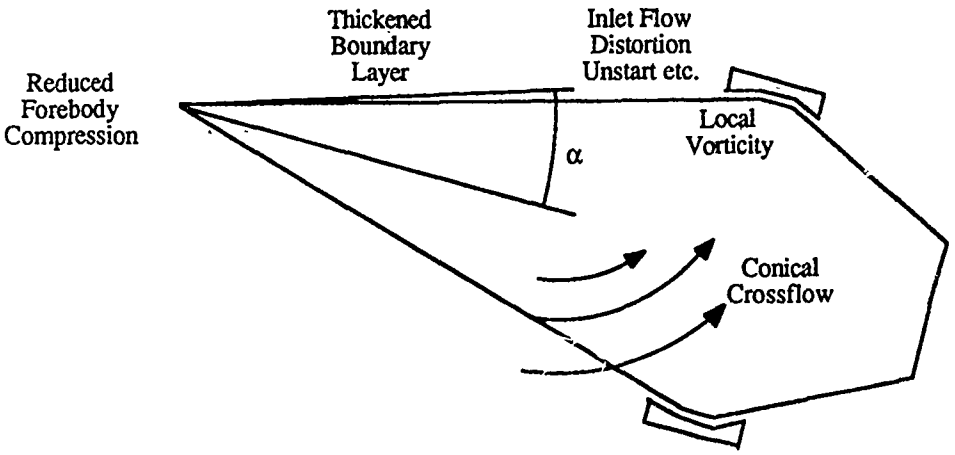


Fig. 35 Effects of Positive Angle of Attack Flight on an Axisymmetric Vehicle

- The use of an articulated forebody with additional system complexity, weight penalties and unknown effectiveness.
- Increasing the tolerance of the vehicle to flow asymmetries through various mechanisms that are speculative at this time.

3.9.2 Discrete Versus Annular Configurations

As has been previously discussed, an objective of the axisymmetric design is to enable us to achieve a maximum capture area. In so doing, the maximum advantage is taken of the work done in overcoming vehicle ram drag and applying it to the initial compression step for the engine system.

The two extreme alternatives of vehicle configuration are illustrated in Fig. 36. This is, on the one hand, the use of engine "pods" or modules positioned on a maximum diameter station of the vehicle. The second is the completely annular approach with the same engine location.

One advantage of the pod mounted system is the ability to avoid ingesting the boundary layer. However, this situation exists in both the low supersonic flight regime and the hypersonic flight regime. In the first, avoiding boundary layer ingestion is desirable but at the higher flight speeds the opinion is that the boundary layer should be ingested and use made of it because of the work of compression that has gone into it in its flow path over the forebody. A second advantage is that it enables the use of circular engine cross sections which would in turn provide minimum engine weight. However, Kumar (Ref. 10) has studied the combination of circular

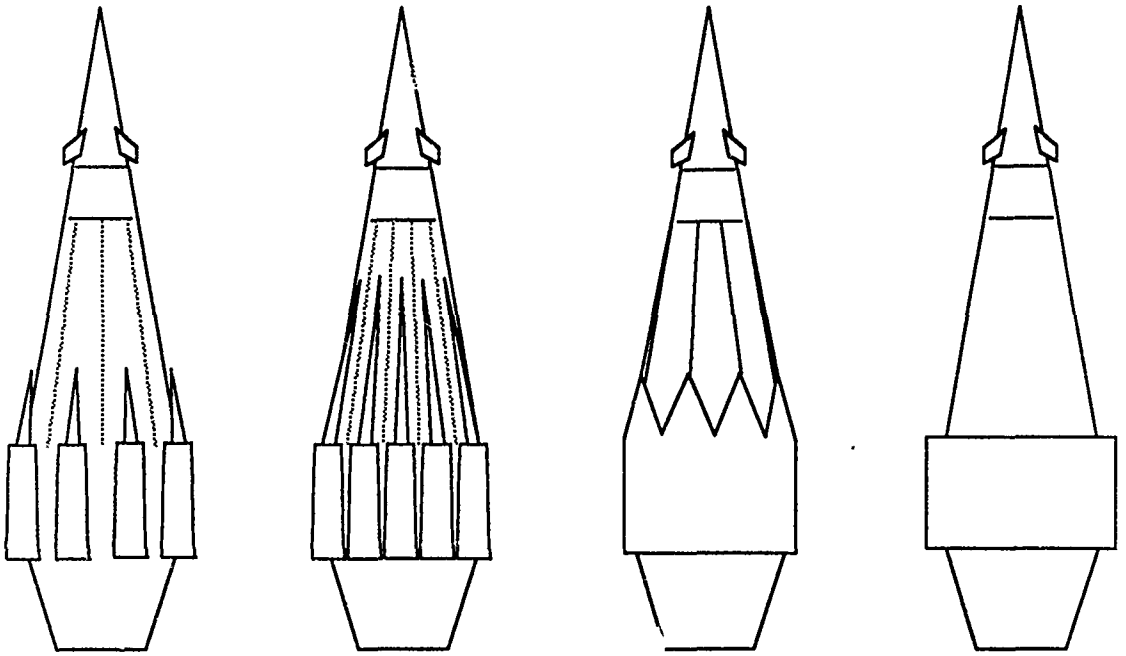


Fig. 36 "Pod" and "Annular" Engine Integration Approaches

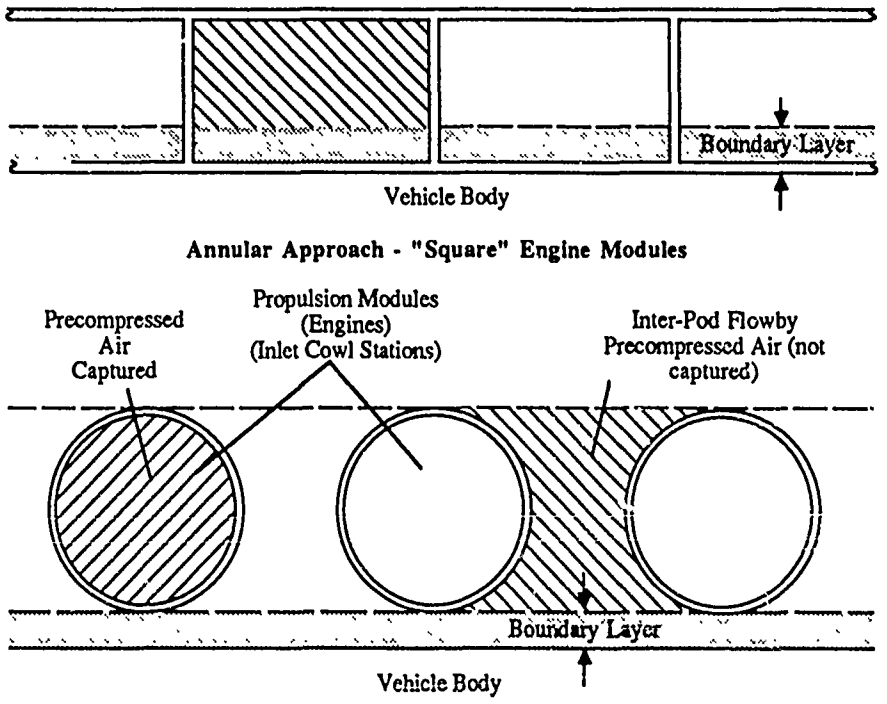


Fig. 37 "Square" vs. "Round" Engine Modules Integration Approaches

engine cross sections with rectangular inlet sections. Kumar's paper indicates that this approach may be practicable and would enable the minimum weight circular engine configurations to be incorporated into an annular inlet system.

The second alternative is the use of rectangular inlet sections and engines over the full circumference of the conical forebody. A possible disadvantage of this approach is that, unless that special provisions are made, the boundary layer will be ingested at all flight speeds. The weight impact of the use of rectangular engine designs would have to be considered.

These two situations are illustrated in Fig. 37.

3.9.3 Force Accounting

An axisymmetric vehicle and "annular" inlet configuration is presented in Fig. 38 with two idealized zero angle-of-attack flight conditions presented by the two halves of the figure above and below the vehicle center line.

Above the center line, the lower-than-design-speed situation is presented. Only a portion of the full-stream tube is taken into the engine inlet to maintain the operation of the engine cycle. The drag work that goes into the air that is not ingested into the engine system operates on the vehicle and must be handled as a drag force in the force accounting for the total vehicle system. The force of drag caused by the air that is ingested into the engine system is not charged to that account since that drag is already included in the calculation of net jet specific impulse and thrust as has been discussed previously. This is taken into account in the inlet efficiency assumptions.

Further, at low altitude, the exhaust gases will not expand completely on the aftbody of the vehicle system, which is our goal as was previously discussed, and will create base drag which must also be accounted for as a drag force in the force accounting for the entire vehicle.

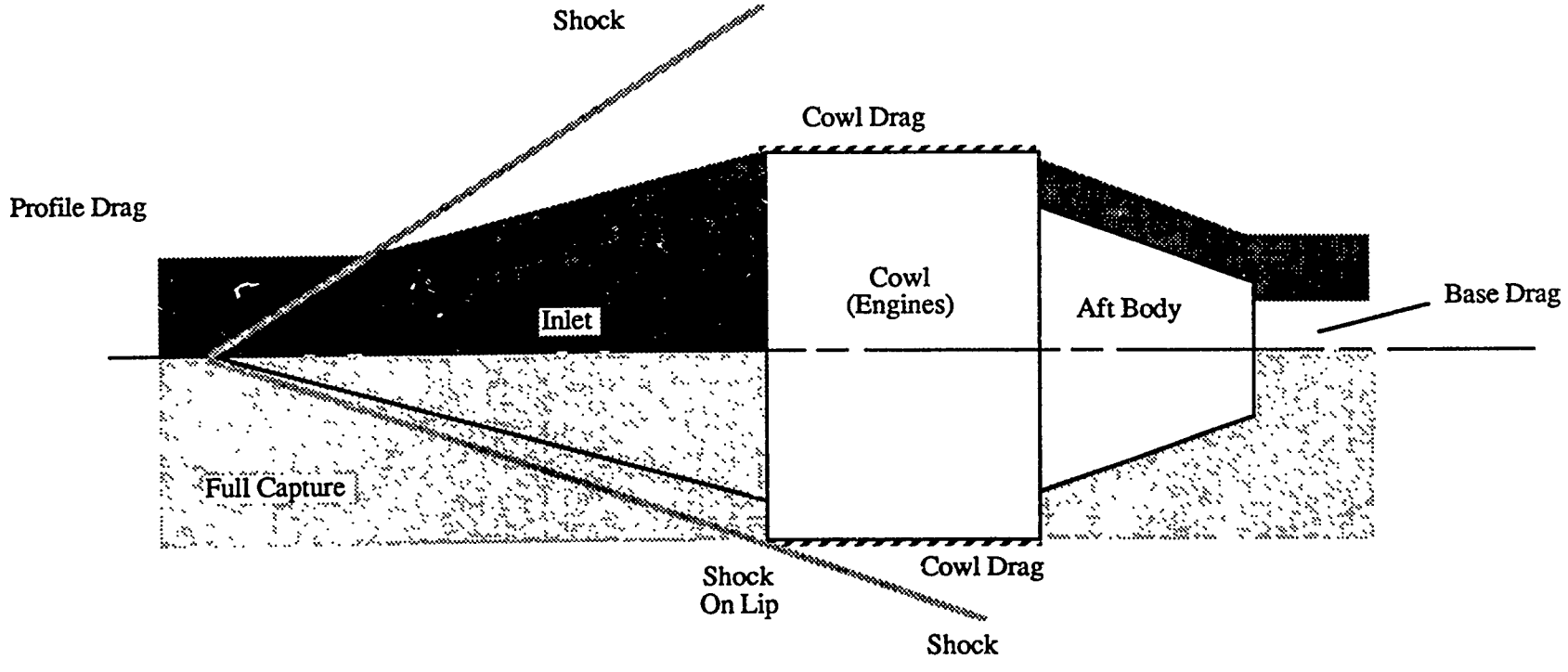
Below the center line, the optimum situation is represented. This is the instantaneous condition, that exists at the end of scramjet propulsion, where the vehicle shock is on the lip of the inlet and the maximum practical capture of 70% of vehicle cross sectional area is achieved. Again it must be noted that this is an instantaneous condition. Under this condition, all ram drag force is on the engine inlet and this force is accounted for in the net jet specific impulse performance measure. This force is therefore not deducted from the drag account in the overall force accounting system. If this were done, it would be an incorrect double accounting of drag. Only cowl drag exists in this idealized case.

Further, at the lower atmospheric pressure encountered in high altitude flight, the exhaust gases flow full over the base of the vehicle and base drag is zero. However, the most significant aspect of this discussion is not the condition that exists at zero velocity or at scramjet termination but the condition that exists in between.

As velocity increases, the effectiveness with which the inlet system captures the air flowing over the forebody increases. This benefit begins to be accumulated in the Mach 1 to 2 region and progresses to the flight velocity at which the shock reaches the inlet lip. This effect is illustrated in the nominal capture area schedule presented in Fig. 39. As has been previously mentioned, this study uses a "practical" value of 70% as a maximum capture percentage rather than a 100% capture which is the ideal.

At Lower Than Design Speed:

Drag Includes Profile Drag, Spillage Drag, Cowl and Base Drag Components



At Design Speed:

Drag is Spillage Drag and Cowl Drag

Fig. 38 Aerodynamic Forces and Propulsion Forces

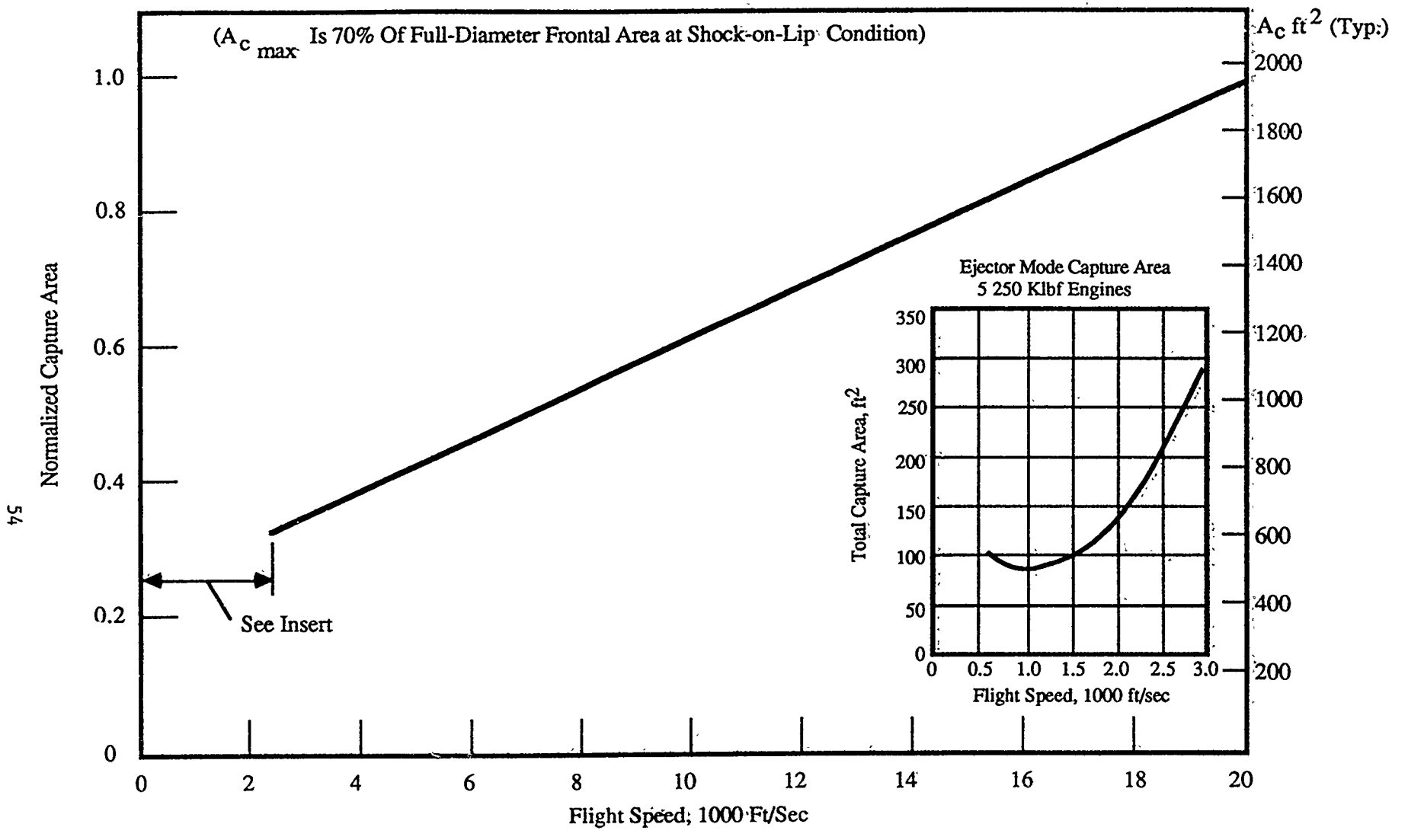
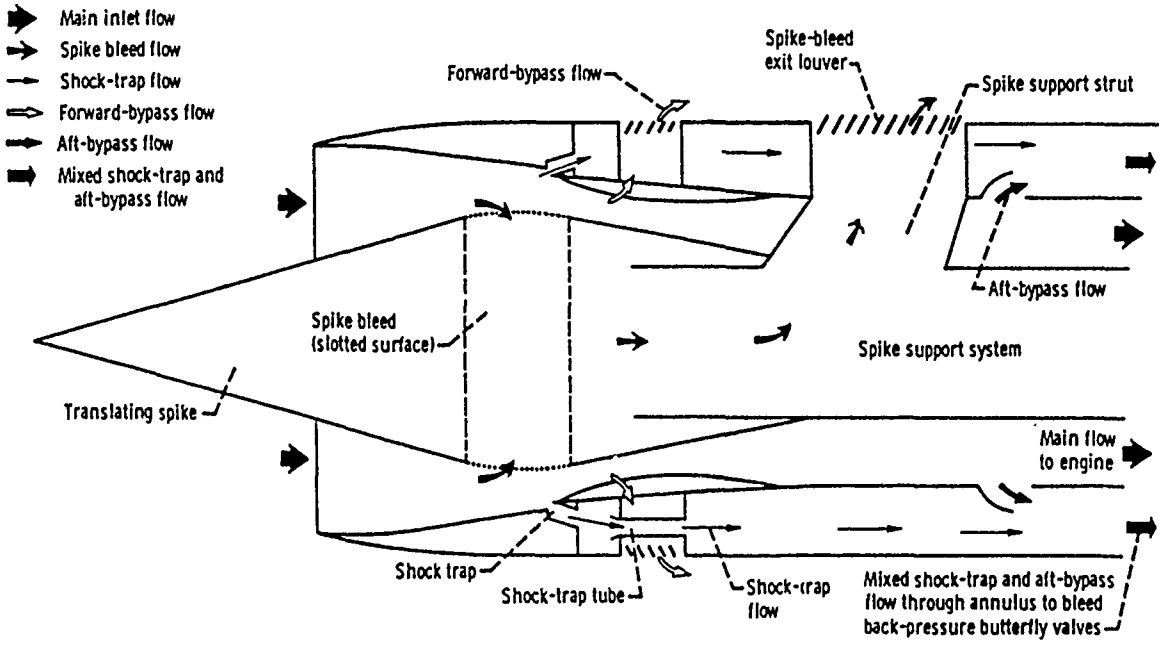


Fig. 39 Nominal Capture Area Schedule

3.9.4 "Second Stage" Compression

The forebody compression process does not provide adequate compression or compression control to support the operation of RBCC engine systems over the full range of Mach numbers encountered in the orbital ascent flight profile. A "second stage" of compression is required. This second stage of compression is provided by the engine inlet system.

It is instructive to examine a state-of-the-art supersonic inlet to gain a better understanding of the requirements that must be considered for engine inlets being studied in this effort. The simplified schematic diagram presented in Fig. 40 shows the axisymmetric mixed external/internal compression inlet used in the YF-12 aircraft (Ref. 11). This inlet system operates up to a flight speed of over Mach 3. It must operate during the aircraft acceleration period to that flight cruise velocity.



Source: NASA Conference Publication 2054

Fig. 40 Axisymmetric Mixed External/Internal Compression Inlet

This inlet must provide a means of maintaining a stable shock front just downstream of the minimum cross sectional area station of the inlet system. In order to accomplish this, the inlet plug must be capable of translational motion and must incorporate an active shock positioning system involving such control elements as a "shock trap", high speed acting bypass-flow control doors and boundary layer bleed.

There is an additional requirement that might have to be met in the inlet design for the vehicle system under study here. This is the requirement to physically close off the inlet section for two purposes. First, in the all-rocket mode transition to orbital insertion, the inlet might have to be physically closed to prevent recirculating flow developing as a result of engine operation in the main engine duct. It may be necessary to introduce turbopump exhaust gases into the flow duct to provide some minimal pressure in the engine duct to assure proper expansion of the rocket exhaust products into the flow engine duct and through the main engine exhaust nozzle. Additionally, it might be found highly desirable to physically close off the inlet during vehicle reentry to eliminate the need for active cooling in the engine system during this otherwise non-propulsive phase.

3.9.5 An Alternate Design Approach - The Ramp Inlet

In the NAS7-377 project (Ref. 2), an alternate design approach was developed that has the capability of responding to the diverse requirements that have been discussed. This is the two-dimensional, moving ramp, mixed compression type variable geometry inlet. The mechanical construction of this inlet is illustrated in Fig. 41. The schedule of positioning of this inlet design over the full flight velocity spectrum is illustrated in Fig. 42.

The two-dimensional ramp type inlet was selected in the baseline NAS7-377 study as being generally superior in terms of inlet performance particularly in scramjet mode, vehicle integration, and closure in all-rocket mode to the separate "spike" inlet discussed up to this point. However, its design requires the use of advanced materials and manufacturing techniques required for low weight, internal and external boundary layer control, cooling, reliability of actuation and control of the inlet contour with adequate dynamic response in order to meet the requirements discussed previously using the YF-12 inlet design as an example.

3.10 Fan Subsystem

3.10.1 Assets

The assets of the fan system are:

- When used to supercharge the rocket-ejector mode of operation, an Isp increase of up to 12% at sea level static conditions can be achieved.
- In the descent and landing phase of the orbital mission, the use of the fan could provide cruise and horizontal landing thrust with Isp's up to 35,000 seconds.
- With plenum burning, sufficient thrust is developed to permit vertical landing. However, the Isp performance drops to approximately 4,000 seconds at a fan pressure ratio of 1.6.

3.10.2 Liabilities

At flight velocities in the range of Mach 3.5, the reduction in pressure rise contributed by the fan system, together with the rising recovery temperatures in the inlet section, dictate that the fan must be removed from the engine duct and stowed. For use in the descent phase, it must be unstowed and redeployed.

The mechanism for accomplishing this has the following penalties:

- The problem of fan stowage, and redeployment, presents significant engineering design challenges.

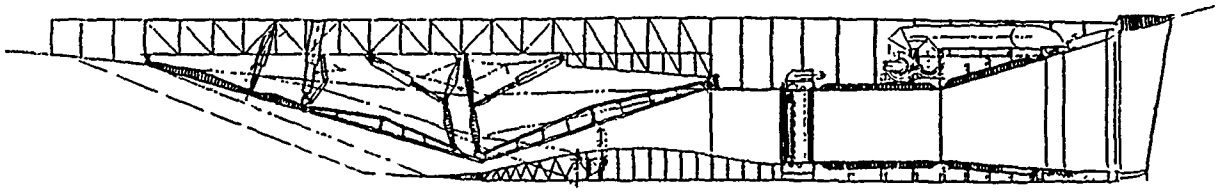
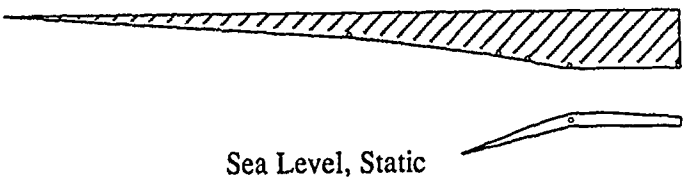
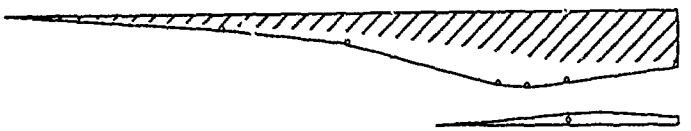


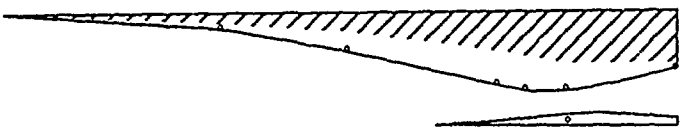
Fig. 41 Ramp Inlet Design Concept



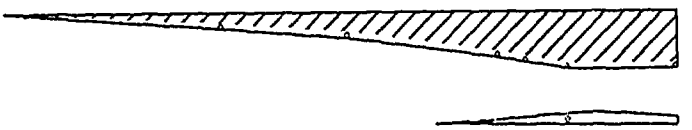
Sea Level, Static



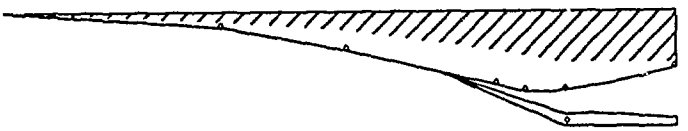
Subsonic Combustion M_0 3.25



Subsonic Combustion M_0 6



Supersonic Combustion M_0 6-15



Rocket Mode & Entry

Fig. 42 Ramp Positioning Schedule

- The added weight of the fan system reduces the payload capability of the vehicle system.
- The implementation of the stowage and deployment scheme requires a circular cross section engine at the fan station.
- The use of the fan increases system complexity and system cost.

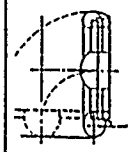
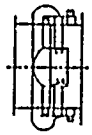
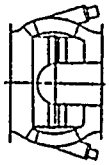
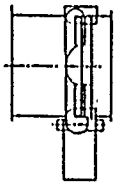
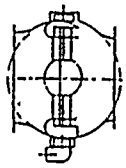
All these liabilities must be balanced against the advantages provided by the fan subsystem in flyback and landing maneuvers, particularly vertical landing maneuvers.

3.10.3 Stowage Options

The Marquardt Corporation studied five candidate stowage options (Ref. 12)(Fig. 43). These five options represent, from a physical motion or design standpoint, as being a reasonably exhaustive set of examples.

Five different criteria were used to rank these options without regard to the flight velocity performance requirements. These options were reexamined in terms of the requirements for RBCC systems in orbital ascent missions. Because of the requirement for a completely clear engine duct during scramjet mode operation, the windmilling and bypass options were eliminated.

The three remaining options, off-axis swinging, in-plane rotation and in-place rotation were judged to be acceptable candidates. In subsequent discussions, the in-place rotation approach will be used but only by way of example.

NOTE: THE LOWER THE POINTS ASSIGNED THE HIGHER THE PREFERENCE INDICATED	OFF-AXIS SWINGING	WINDMILLING	BYPASS	IN PLANE ROTATION	IN PLACE ROTATION
					
WEIGHT ASSESSMENT	5	1	2	3	4
RELIABILITY	3	1	2	3	3
MAINTAINABILITY	3	1	2	3	3
RECURRING COST	4	1	2	3	3
ADAPTABILITY TO EITHER FAN DRIVE TIP-TURBINE OR SHAFT	3	1	2	3	3
EFFECT OF INSTALLED PERFORMANCE	5	1	2	2	3

SOURCE: THE MARQUARDT CORPORATION

Fig 43 Five Fan Stowage Options

3.10.4 Performance

The primary advantage of the fan system is to improve the thrust and specific impulse performance of the RBCC engine in the rocket ejector mode and to provide high specific impulse during the descent and landing phase of the overall mission. It is particularly significant to note the performance of the fan system operating in both "dry" or non-afterburning condition and with afterburning in the engine plenum.

Fig. 44 presents the effect of increasing hydrogen injection mass flowrate into the afterburner in a representative sukpercharged RBCC engine system.

As can be seen, the maximum thrust augmentation ratio increases sharply with subsonic flight speed, which permits increasing afterburner equivalence ratios to be used. The very significant reduction in specific impulse with any augmentation is notable. At sea level, the Isp of the dry fan mode is approximately 22,000 seconds dropping to 4000 seconds and below for afterburner equivalence ratios greater then 0.2.

3.10.5 Fan Subsystem Performance Upgrading

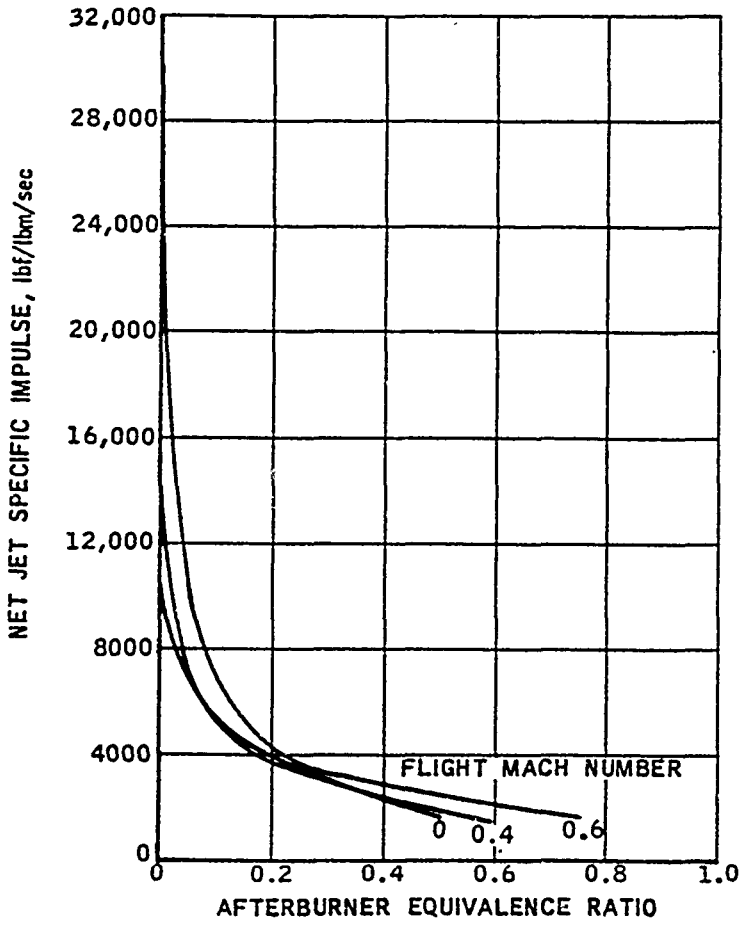
In the time that has elapsed since the baseline study was completed, significant improvement has been made in the field of high speed turbomachinery. These advances were studied in terms of their effect on the design of fan supercharged RBCC propulsion systems in the present study.

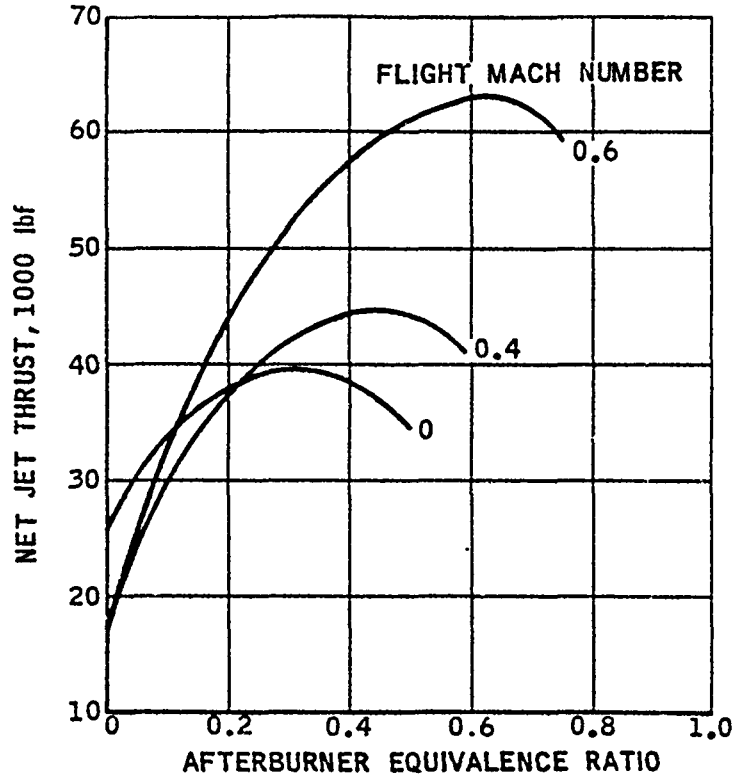
The most directly relevant work was found in an investigation carried out by the Garrett AiResearch Corporation for the Lockheed California Company as cited in Ref. 9. The Garrett Corporation studied a conventional twin-spool forward-fan configuration operating on hydrogen fuel in the power turbo section.

The differences between the baseline study and the Garrett findings are as follows:

- Bypass ratios were roughly comparable at 10:1 for the Garrett study and 9.6:1 for the NAS7-377 study.
- Power turbine rotor temperature was increased from 2,300 F in the baseline study to 2,700 F in the Garrett study.
- Overall fan-drive gas generator pressure ratio was increased from 13:1 in the baseline study to 40:1 in the Garrett study.
- Fan pressure ratio was increased from 1.3:1 in the baseline case to 1.6:1 in the Garrett study.
- Thrust achievable by a fan system of comparable diameter was increased from 20,000 lb operating in the dry mode to 31,000 lb in this study design.
- Sea level static specific impulse was increased from 22,000 seconds to 35,000 seconds.

The weight of the Garrett turbofan subsystem was approximately 4,000 pounds. It had a thrust/weight ratio of 8.1 with a fan diameter of 80 inches and an engine length of 120 inches. The reader should take note of the fan length which has a significant impact on the problems of stowage and redeployment of the fan subsystem.





(Source: Ref. 2)

Fig. 44 Effect on Thrust and Isp of Increasing Hydrogen Flow into the Afterburner

The increased thrust is achieved through two mechanisms. First, the increase in fan pressure ratio. However, the major portion of the thrust increase comes from the ability to increase the afterburner equivalence ratio.

The 10,000 plus seconds increase in sea level static Isp over the database value is due to the increase in the maximum power turbine rotor temperature from 2,300 F to 2,700 F and the cycle pressure ratio from 13:1 to 40:1.

This high performance is achieved by the use of state-of-the-art technology. Further, there is a design challenges accompanying the increase in fan overall length required over the lower pressure ratio designs characterized by the use of less advanced technology. If conventional configuration fan systems are incorporated into RBCC systems, they begin to more closely approach turbomachinery based combined cycle engine systems. In doing this, both the light weight and system simplicity of RBCC engine systems are progressively sacrificed.

The previous discussion should provide an illustration of the problems faced by alternative turbomachinery based combined cycle engine systems in comparison to RBCC engine systems. The larger, heavier, more complex turbo systems must somehow be removed from the flowpath, or the flowpath must be removed from the turbine system, at high supersonic and hypersonic flight speeds. To do this, two options are available. First, bypassing the turbo system itself. However, the problem associated with this is that the flowpath undergoes significant angular deviation in leaving the engine centerline and returning to the engine centerline which produces a negative impact on scramjet performance. The second option is to have the turbomachinery located in a completely different flowpath using large bypass doors to provide access to the inlet of the turbomachinery system and exhaust back to the engine flowline for scramjet operation. In both approaches, the "doors" must be opened and closed and effectively sealed and probably integrated into the engine coolant system in scramjet combustion mode.

3.11 Rocket Subsystem

3.11.1 Capabilities Required

The rocket subsystem of the RBCC engine must be designed to meet a set of unique requirements:

- In the initial ejector phase of flight, the engine operates as an air jet, or ejector, pump deriving the pumping power from the rocket subsystem which provides the primary jet. The inducted air is the secondary flow which is pumped by the rocket subsystem to achieve the thermodynamic objectives previously discussed in Section 2.0.

- In the design approach proposed here, the rocket subsystem also serves as a fuel injector station in scramjet operation providing heated hydrogen fuel to the combustion process.

- In the final phase of orbital ascent, the rocket subsystem must operate with further expansion in the engine duct and engine exhaust nozzle unit to provide the velocity increment from approximately Mach 15 to final insertion in the target orbit.

In Engine 10, the Ejector Scramjet, and in Engine 12 the Supercharged Ejector Scramjet, liquid oxygen is used as the oxidizer in both the rocket ejector mode and final rocket mode. In Engine 22, the ScramLACE, Engine 30, the Supercharged ScramLACE and in Engine 32, the Recycled Supercharged ScramLACE Engine, the oxidizer in the rocket ejector mode is liquid air and in the final rocket mode is liquid oxygen. This creates a requirement in Engines 22, 30 and 32 for dual oxidizer operation. This will increase the injector system complexity but is judged to be within the state-of-the-art.

The vehicle ejector subsystem must perform as a primary drive jet generator for what is basically a rocket driven ejector or jet pump. The ejector design must achieve full mixing between the rocket primary jet and the inlet air secondary jet in the shortest mixing length possible in order to achieve a minimum engine weight.

3.11.2 Design Approach

In Fig. 45, it can be seen that if a single conventional rocket thrust chamber is used to drive the rocket ejector, a mixing length of eight to ten duct diameters is needed to achieve full flow mixing. This results in high engine weight and a difficult configuration to integrate into a vehicle structure at any reasonable thrust level rating.

By using a multiplicity of individual rocket units, the air/rocket-exhaust shear area is significantly increased in proportion to the main duct diameter circumference. What is being done here is simply putting a number of single ducts, ten in the first case illustrated, into a single package. The mixing of each individual rocket is still accomplished in eight to ten "duct" diameters but this design effectively places ten ducts into a single flow tube. This approach can be extended further to a higher number of individual rocket units as illustrated in the third case shown in Fig. 45. By the use of fifty primary rocket units, the mixing section length can be approximately one duct diameter.

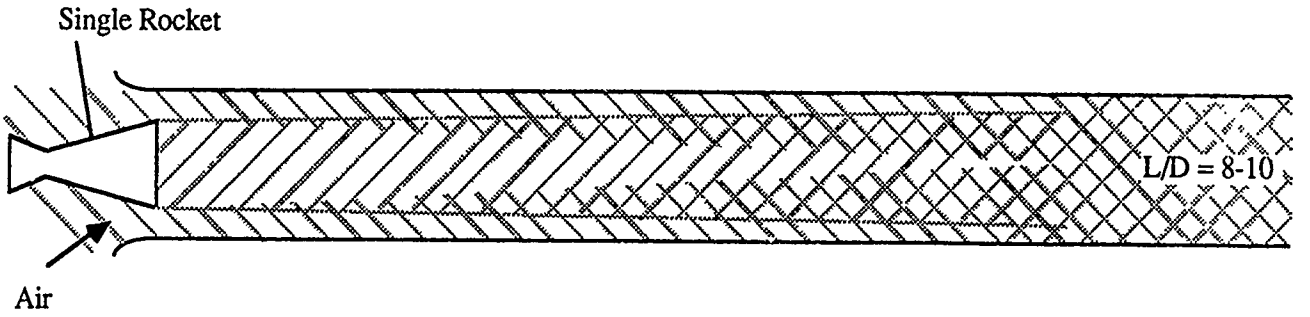
The mechanization of fifty small engines into a single tube may be impractical. Alternatively, the same mixing result can be accomplished using annular combustion chambers in the engine duct as illustrated in Figure 45. The 50 small engine ejector system desired is replaced by an equivalent "dual concentric" system of two annular combustion chambers.

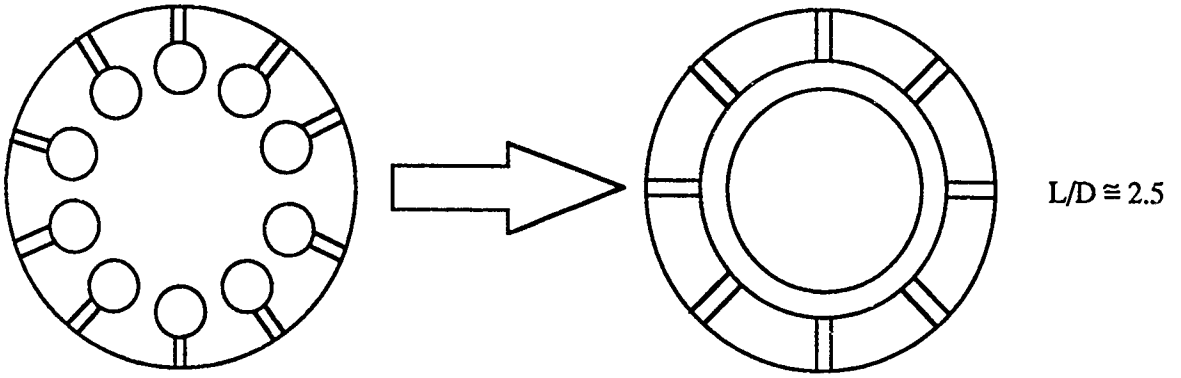
The multiple bell rocket approach was reduced to practice by the Martin Company and The Marquardt Corporation in the 1960s as previously discussed in Section 2.0. The performance of the hardware validated the analytical approaches developed by Marquardt and there is little technological uncertainty associated with a mixing characteristics of the multiple bell design approach.

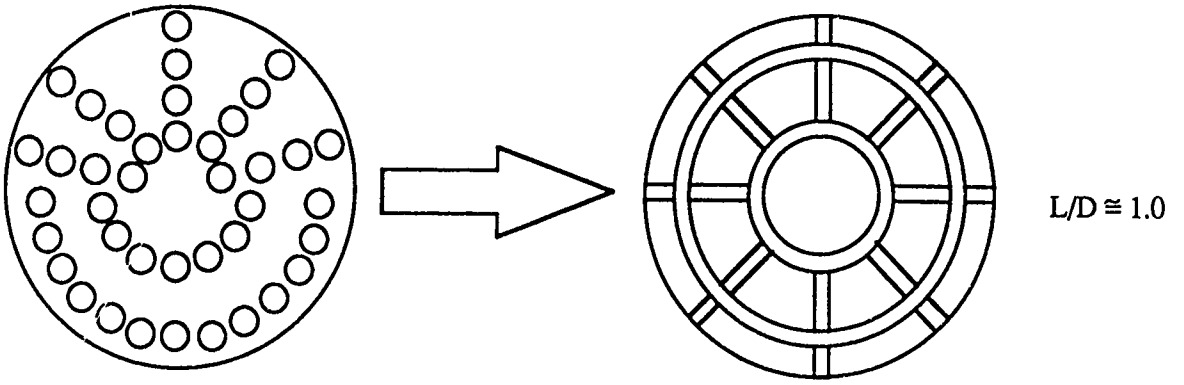
The annular bell configuration was first suggested by Martin Marietta Denver Aerospace for its RENE design. A conceptual design of a dual concentric rocket ejector drive unit developed in the NAS7-377 study is illustrated in Fig. 46. In the design approaches considered in this study, the rocket ejector unit remains in a flow passage for the full duration of the flight and must be actively cooled during the high Mach number portions of orbital ascent when the rocket subsystem is not operating. Removal and stowage of the rocket ejector was not considered because of the role it can play as a scramjet injection station.

The basic advantage of this design approach is that there are two, as opposed to 250, separate combustors to install and operate. The design is also symmetrical and provides a more uniformly concentric exhaust flow within the mixer section than would be provided by the fifty individual thrust chamber design approach.

Annular thrust chamber designs have a considerable R&D hardware test background. Extensive work was carried out under USAF and NASA funding in the 1960s in conjunction with thrust chamber designs to support Rocketdyne's "Aerospike" rocket engine design concept.

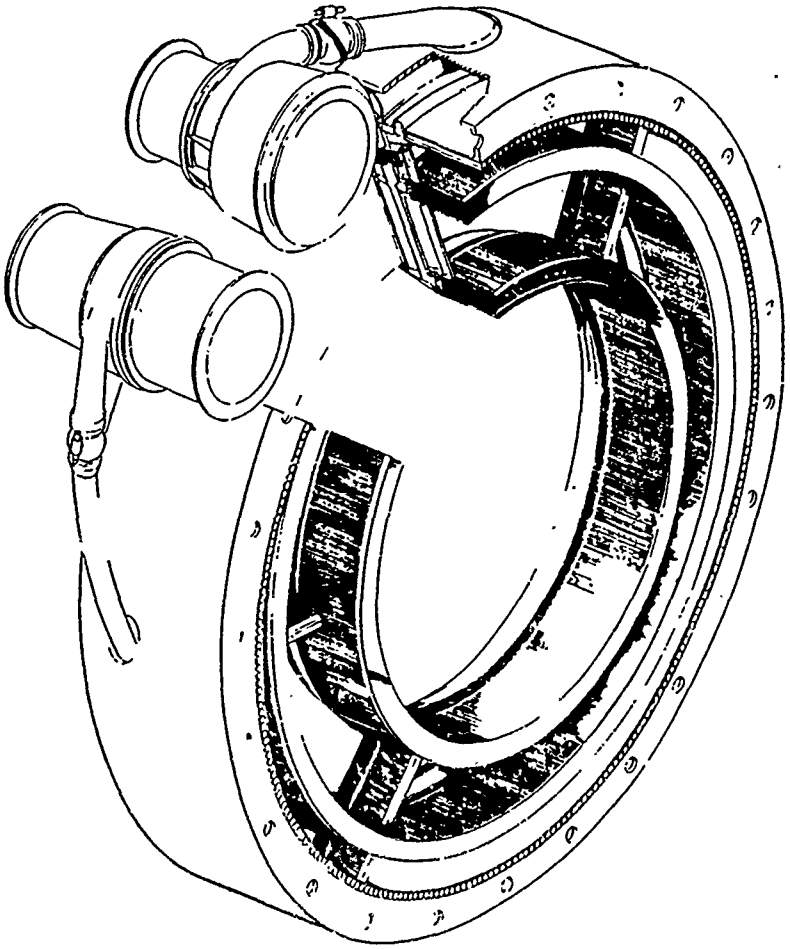






Source: NAS7-377

Fig. 45 Rocket Exhaust Mixing Length (Source: Ref. 2)



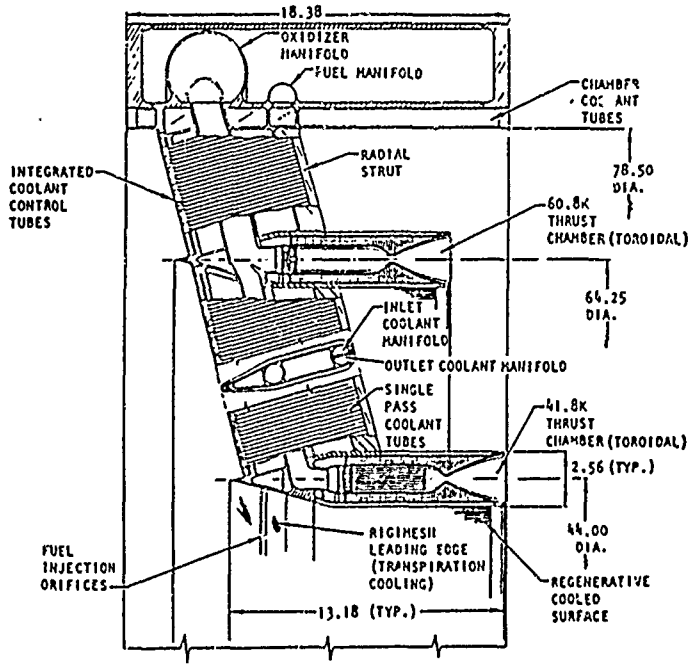


Fig. 46 Dual Concentric Annular Bell Combustion Chamber (Source: Ref. 2)

3.11.3 Operation

The rocket ejector subsystem operates in three of the four propulsion modes. First, it provides the primary ejector drive jet in rocket ejector mode. Second, it provides a forward located injection station for injection of hydrogen in Scramjet mode. Finally, it functions as a rocket engine in a large expansion ratio configuration to provide vehicle propulsion from the termination of scramjet combustion to orbital insertion.

In the air-augmented rocket mode, illustrated in Fig. 47, the rocket unit primary jet system operates on liquid oxygen and hydrogen in Engine 10 and Engine 12 configurations. Engines 22, 30 and 32 operate on liquid air and hydrogen. In both cases, the rocket subsystem operates at stoichiometric or slightly lean conditions to provide a completely oxidized exhaust jet that will not support further combustion in the engine duct. This supports a "mixing-only" process in the engine duct which develops into a diffused subsonic flow at the maximum engine cycle pressure. This flow is partially expanded in the divergent section of the engine at which point hydrogen fuel injection takes place. Stoichiometric combustion occurs in the total air flow over a very short distance in the expanding section of the duct due to hydrogen's high flame speed. At that point, the flow is either choked by a converging/diverging nozzle section or, as in the case studied here, by the heat-addition process that leads to thermal choking. Supersonic flow expansion then takes place in the remainder of the divergent duct from the choke/shock and further expansion can occur on the aftbody of the vehicle.

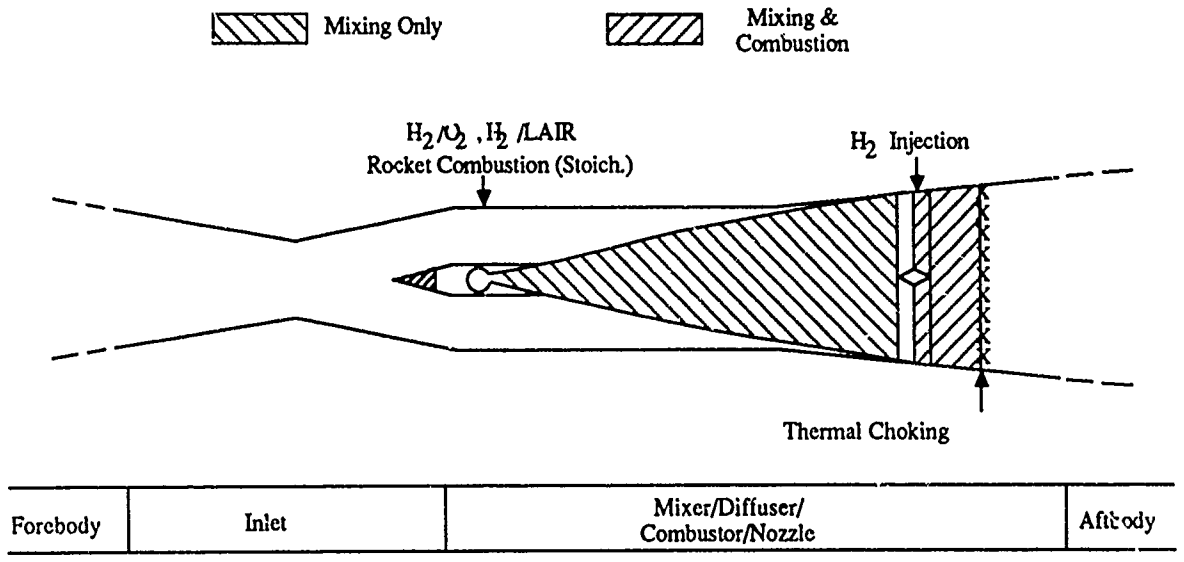


Fig. 47 Air Augmented Rocket Mode Diagram

In the baseline configuration (Ref. 2) of the liquid hydrogen/liquid oxygen rocket ejector primaries, the engines operated at 2000 psia combustion pressure, a stoichiometric mixture ratio of 8:1 (O/F), and a nozzle area ratio of 12.5:1. This produces an exhaust pressure of

approximately 18 psi. The specific impulse provided by this design will be approximately 350 seconds measured as a rocket thrust chamber specific impulse and not a net jet specific impulse. At the combustion pressure proposed, properly designed rocket engines should be capable of operating many hundreds of hours or more without replacement.

The baseline (Ref. 2) liquid air (LAIR) and liquid hydrogen rocket subsystem was designed to operate at a combustion pressure of 1000 psia, a stoichiometric mixture ratio of approximately 34:1 (A/F) and a nozzle area ratio of 9.6. This yielded a nozzle exit pressure of 10.6 psia at an engine specific impulse of 205 seconds. The operating life of the H_2/LAIR rocket engine system should exceed the operating life of H_2/LO_2 engine systems due to the lower combustion pressure, lower flow velocities, lower peak pressures and lower heat flux rates. However, it must be remembered that the LH_2/LAIR thrust chambers will be operated on LO_2 in the final rocket mode propulsion phase of the orbital ascent trajectory.

As has been discussed previously, a subject of study here is the performance of the various engine subsystems in airbreathing RBCC propulsion systems. This can be measured in terms of the specific impulse value that must be used in solving the ballistic equation to determine the flight velocity increment that can be developed by each propulsion subsystem. It is necessary to understand the differences in the methods of measuring Isp performance for LOX and LAIR rocket engine subsystems as they would be measured in the vehicle systems that are being considered here.

In liquid oxygen systems, the rocket engine and thrust chamber specific impulse values are determined by dividing the gross thrust produced by the rocket engine by the total liquid oxygen and liquid hydrogen flow rates.

Using this method to compute the engine specific impulse of liquid air based systems, the result shown in Fig. 48 in the upper plot is obtained.

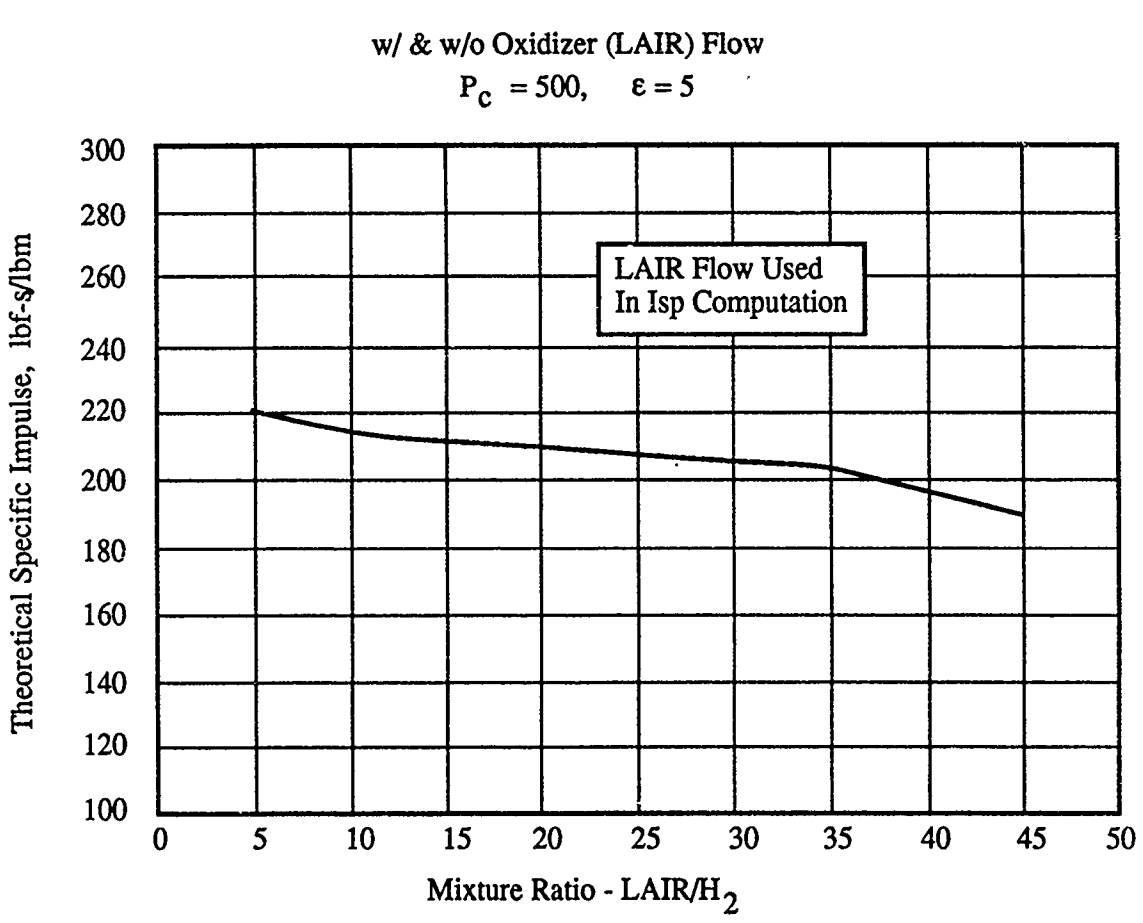
In the LAIR system, liquid air is not stored on board the vehicle and its mass does not enter into the definition of Isp as used in the ballistic equation. Measured from the ballistic equation standpoint of Isp, the performance of liquid air systems is very significantly increased as illustrated in the lower plot of Fig. 48. Again it should be noted that this specific impulse value is rocket specific impulse, not net jet. Further, this Isp does not consider drag or gravitational losses.

Both liquid oxygen and liquid air based rocket subsystem specific impulses are further increased by the use of the air augmentation design approaches as discussed previously in Section 2.0.

In Fig. 49, the thrust augmentation provided by air-augmentation of the rocket subsystem is illustrated as a function of flight velocity. Bear in mind that ejector mode operation is terminated at about Mach 2.5.

The thrust augmentation provided by flight velocity for liquid oxygen based systems is illustrated by the O/F curve for a value of 8:1. As can be seen, the thrust augmentation at termination represents roughly a doubling of the SLS thrust and thus roughly a doubling in the engine Isp.

In ramjet mode, as illustrated in Fig. 50, the rocket subsystem is not functioning. The supersonic external air flow is efficiently shocked down through the forebody compression and by the mixed compression inlet system previously discussed. The rocket subsystem is exposed to higher temperature gas at approximately 100 psi in subsonic flow and must be suitably protected thermally to withstand these conditions. Combustion is continued in the plenum burning mode



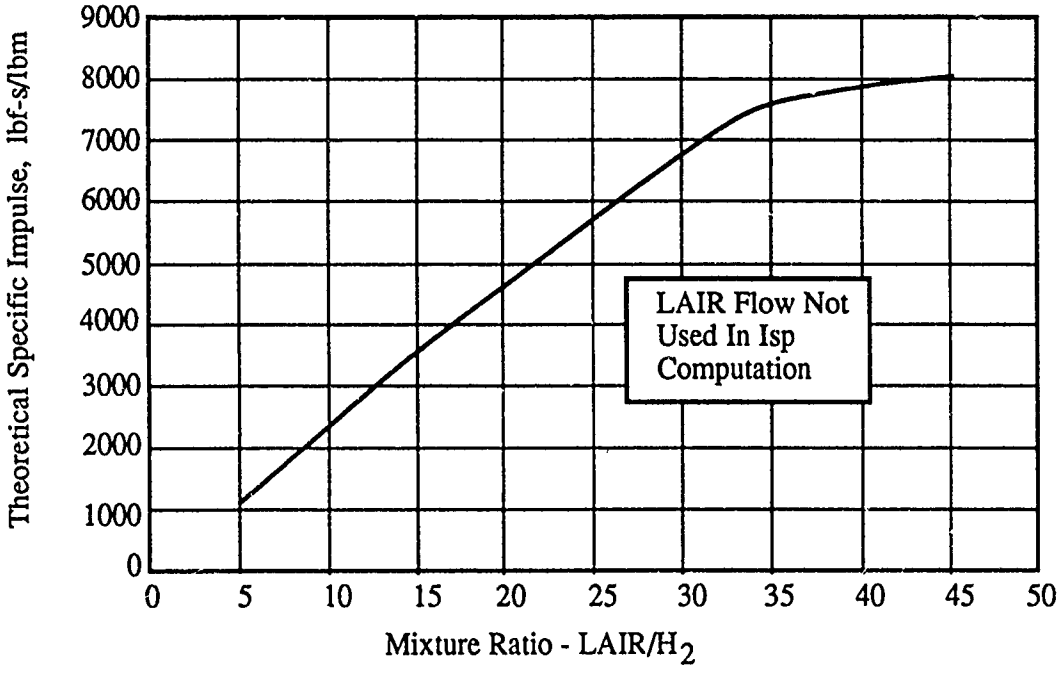


Fig. 48 Liquid Hydrogen/Liquid Air System Specific Impulses (Source: Ref. 2)

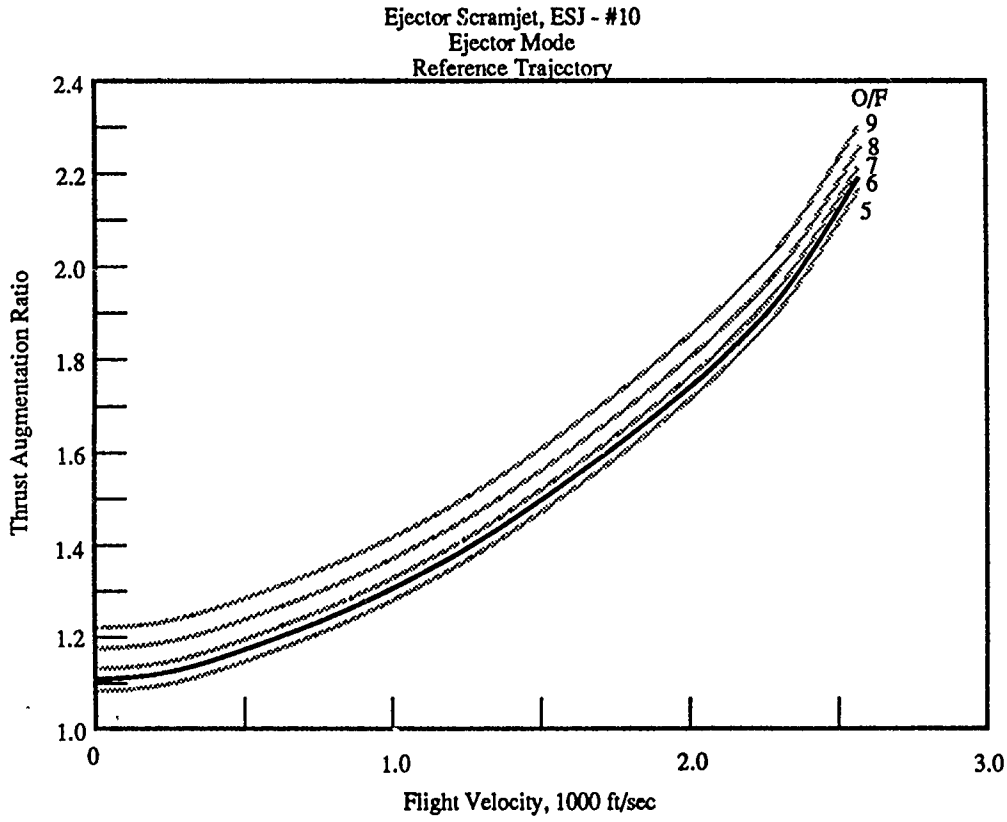


Fig. 49 Thrust Augmentation in Ejector Mode During the Early Portion of the Ascent Trajectory

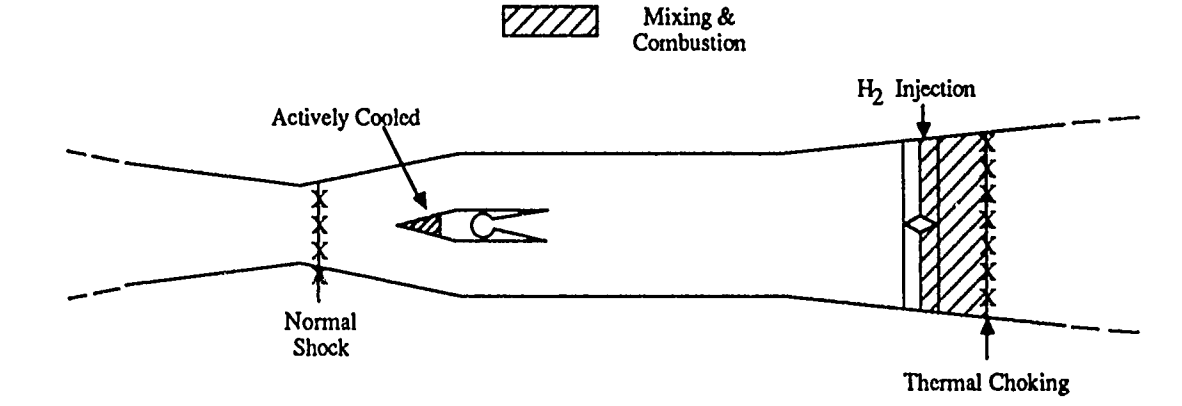


Fig. 50 Ramjet Mode Diagram

established initially in the ejector ramjet mode. A thermal choke is maintained and the expansion process to supersonic velocities occurs in the divergent section downstream of this station and on the vehicle aftbody surfaces. Static backpressure decreases with increasing altitude, and, at about Mach 6 flight speed, the engine transitions from ramjet to scramjet operation.

As flight velocity increases through the ramjet mode, the engine inlet throat section progressively decreases in area and the combustion process typically takes place at continuously increasing static pressures. At some point in this process, the duct flow transitions from subsonic to sonic to supersonic. Because of the finite amount of time required to accomplish combustion in hydrogen/air systems, the fuel injection station must be moved forward progressively as vehicle velocity further increases. In the design approach considered in this study, a combination of aft station injection progressing to rocket subsystem fuel injection, as illustrated in Fig. 51, is used in the "low-speed" scramjet regime in the range of approximately Mach 6 to 10. The general objective is to move the distributed heat-release zone gradually forward to increase the cycle contraction ratio (the free stream capture area divided by the duct heat-release cross-sectional area) while maintaining an optimal local internal-duct supersonic flow Mach number. Thermal choking, obviously, must be avoided. This is primarily a "low speed" scramjet problem.

In the "high-speed" flight regime, say from Mach 10 to 15 or possibly higher, the fuel injection process must be moved further forward, shown here schematically as wall injection from the inlet throat section plus continuing rocket unit subsystem flow. The scramjet process now takes place at maximal available contraction ratio. Also, the duct length available for combustion is now the maximum. There will be severe heating on the upstream portion of the rocket subsystem which must be relieved by an effective cooling system. In engines of the diameter being considered here, wall mounted injection systems cannot provide the depth of jet penetration required to maintain efficient combustion over the entire flow duct diameter. This problem is common to all supersonic combustion engine systems and is not unique to RBCC propulsion systems.

Rocket mode operation takes over as scramjet mode thrust and specific impulse decrease along the flight path. At the point of transition to all-rocket operation, present understanding of the problem indicates that the inlet must be closed off and the rocket unit operated on hydrogen and oxygen in the closed engine duct.

Under these conditions, i.e., very low ambient pressure, the rocket subsystem exhaust is highly underexpanded by the rocket nozzles designed for lower altitude and velocity conditions in ejector mode operation.

What is desired, in the configuration studied here, is to efficiently achieve further expansion out to the engine duct walls which, in the sealed inlet configuration, will provide additional thrust. If the expansion process can be carried out further in the divergent nozzle section and on the vehicle aftbody, further specific impulse augmentation can be expected (Fig. 52).

It is probable that the engine turbopump exhaust products can be advantageously routed to the closed off inlet section of the duct to prevent rocket exhaust recirculation interferences in the high area ratio expansion process in the aft end of the engine. This approach has been indicated to be required by related research carried out by the Rocketdyne Corporation as reported in Ref. 13.

By using the engine duct as a nozzle extension to the basic rocket subsystem nozzles, the expansion ratio should be able to be increased to approximately 200:1. Further expansion on the vehicle aftbody could significantly increase this expansion ratio.

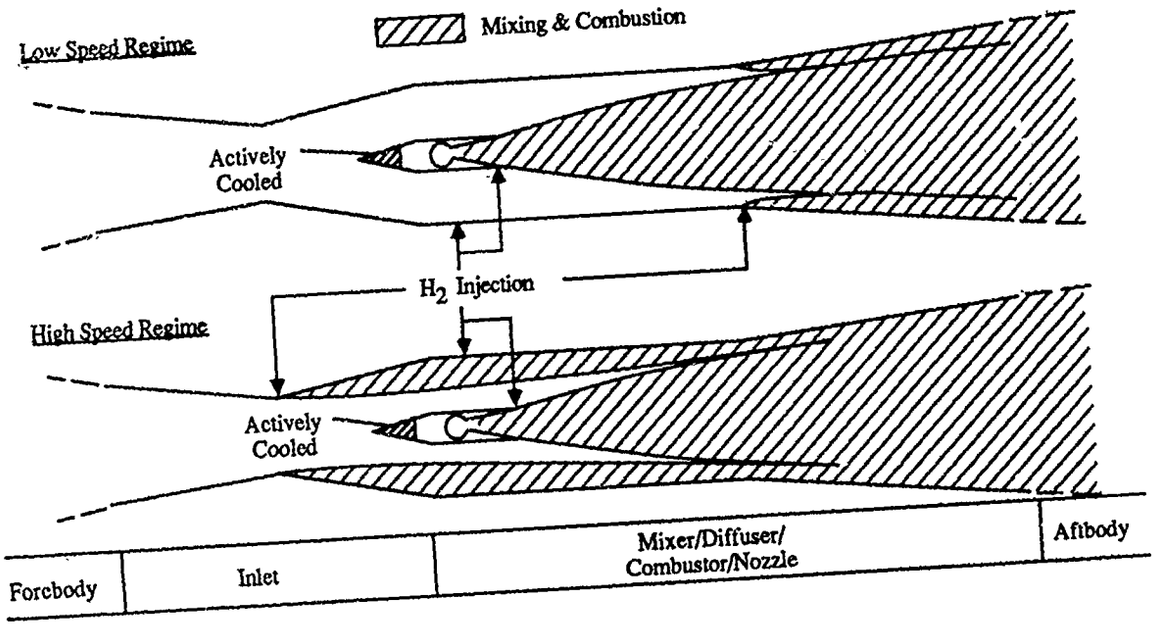


Fig. 51 Shifting Scramjet Fuel Injection Approach

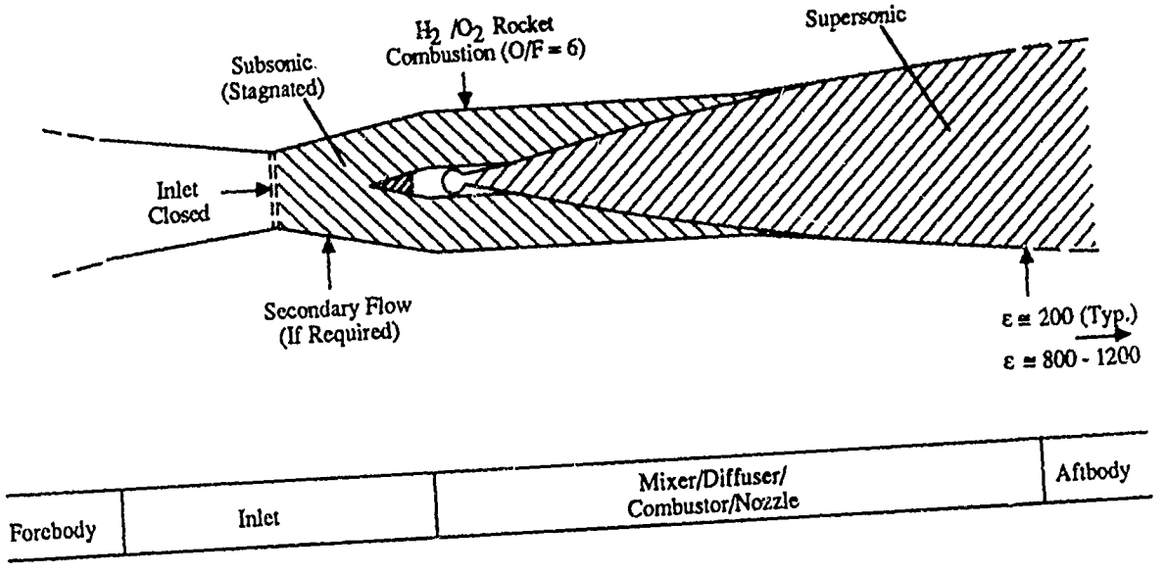


Fig. 52 Rocket Mode - High Nozzle Exit Area Ratio

This design approach should be investigated by experimental work aimed at the particular configuration studied here. Such an investigation should be given priority equivalent to that of the previously discussed problem of uniform vehicle forebody compression as affected by angle-of-attack.

Table 1 presents representative liquid hydrogen and liquid oxygen rocket engine and thrust chamber Isp performance that has been delivered by four real engine systems and two theoretical high expansion ratio engine systems. An engine Isp value of 470 seconds was used as the baseline in this study. As will be discussed in Section 6.0, sensitivity analyses were run on this Isp value.

Table 1 Representative H_2/O_2 Rocket Specific Impulses

Engine Type	Engine Isp sec	Thrust Chamber Isp sec	Altitude ft	Area Ratio A_e/A_t
1. J-2*	435	443	60,000 +	40
2. M-1*	428	433.4	-	40
3. RL10A-3-3*	444	-	200,000	40
4. SSME*	453	-	Vacuum	77.5
5. SSME-150+**	475	-	Vacuum	200
6. OTV Propulsion "Advanced Engine"	485	-	Vacuum	-

* Liquid Propellant Engine Manual, Chemical Propulsion Information Agency, Johns Hopkins University, Applied Physics Laboratory, Laural, Md., October 1982
** Sayles, G. and Moszee, R., Scale Up of Single Stage to Orbit Vehicles, AFRPL paper, 25 September 1985

Table 1 Representative Hydrogen/Oxygen Rocket Specific Impulses

3.12 Ramjet Subsystem

Ramjet technology is supported by a very extensive database covering both analytical methods and actual engine development, manufacturing and flight use. Specifically with regard to the use of liquid hydrogen as a ramjet fuel, The Marquardt Corporation carried out experimental investigations involving a flight weight, regeneratively cooled ramjet operating to Mach 8 ground simulated flight speeds. This work has been previously discussed in Section 2.0.

Successful ramjet combustion has been demonstrated in very short combustion lengths on the order of less than one foot. Experimental work has shown high combustion efficiencies approaching 98%.

In the applications studied here, the principal difference between conventional ramjet engine designs and the design for the RBCC engine system is that retractable fuel injector/flameholder units must be provided. These units cannot be left in the hypersonic flow field during scramjet mode.

In the design approach proposed in this study, a physical convergent/divergent nozzle will not be used. As previously discussed, a thermal-choke will be established in the engine nozzle section and supersonic expansion will take place from that station. Further, as substantiated by the findings of the baseline NAS7-377 study, Ref. 2, fixed exit nozzle geometry will be used.

3.13 Scramjet Subsystem

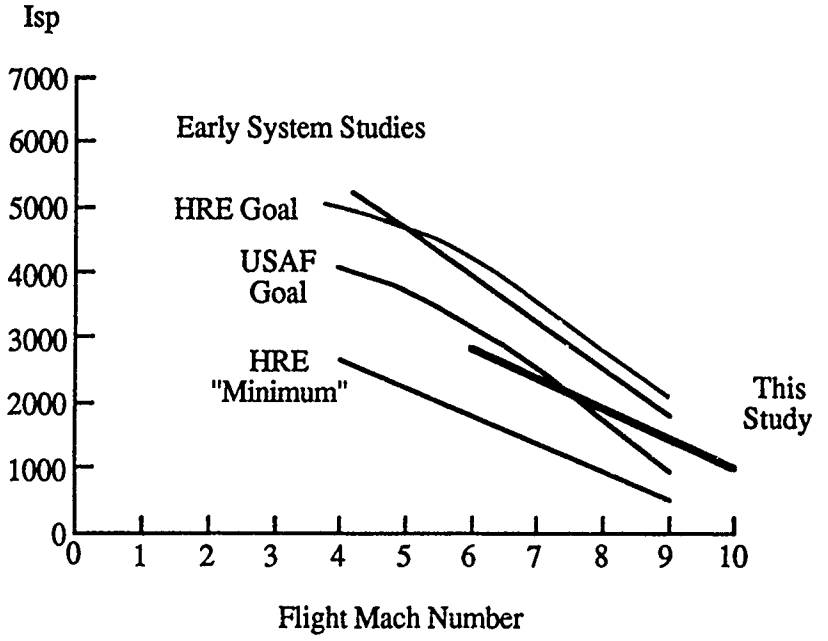
In the time period between the development of scramjet performance estimates used in the baseline NAS7-377 study and the present date, significant additional information has become available on scramjet propulsion. This more current data has been used to revise the baseline study estimates of specific impulse and thrust in scramjet mode operation (Ref. 14 to 19).

The two charts presented in Fig. 53 provide a backdrop of scramjet specific impulse performance estimates taken from the literature of the 60's and compare them to more current estimates. Two overlapping flight speed ranges are presented.

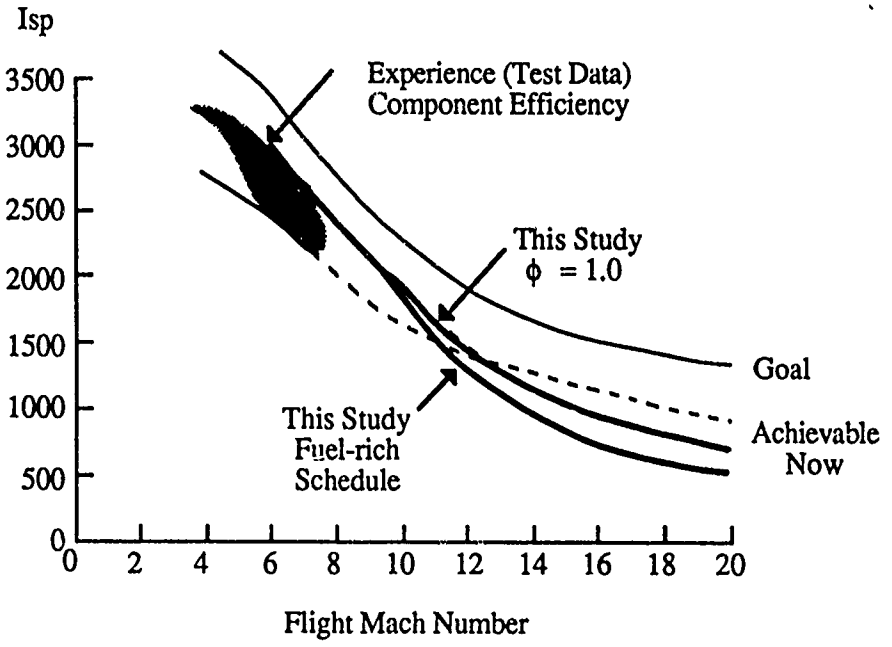
On the top chart, selected "goal" and "minimum" performance trends are noted along with some early system study results. The HRE (Hypersonic Research Engine) program, previously discussed, accomplished ground-test performance somewhat above the "minimum" curve at simulated Mach numbers of 4 and 7. This engine design was compromised in various ways by the expectation of flight-testing on the X-15 research aircraft. Later ground tests at Langley Research Center on an improved "vehicle integrated" engine geometry achieved substantially higher performance.

The bottom chart derives from USAF work and reflects both "goal" and "achievable now (ca. 1985)" trends based on available experimental results and analytical extensions. Experimental results are illustrated in the shaded zone encompassing steady-state ground-test results while the higher-speed trendlines are based on short-duration (milliseconds) pulse-facility testing results. It can be seen that the estimates used in the present study are well below the "achievable now" dashed curve at flight speeds beyond about Mach 12. Presumably, this suggests that this study is somewhat conservative at the high speed end. However, there is a critical lack of credible high-speed experimentally-derived scramjet performance data. At the present time, the X-30 project activities include a significant amount of work aimed at filling this information gap.

The scramjet mode net jet specific impulse and thrust coefficient performance used to support the study's trajectory analysis work, to be described in Section 6.0, are illustrated in Fig. 54. For flight speeds beyond Mach 10, two curves are provided: (1) stoichiometric, or unity equivalence ratio, and (2) fuel-rich progression with speed with equivalence ratio rising from one through seven. The strong effect on thrust of the fuel-rich progression is apparent in the diverging thrust coefficient trends. The degrading effect on specific impulse is fairly marked at the low- and mid-speed range conditions but fairly moderate at speeds in excess of about Mach 20. The reader is reminded, as discussed in previous sections and as will be further discussed in section 6.0, that the scramjet mode of operation was found to optimize at a termination of approximately Mach 15 in RBCC/SSTO vehicle systems.

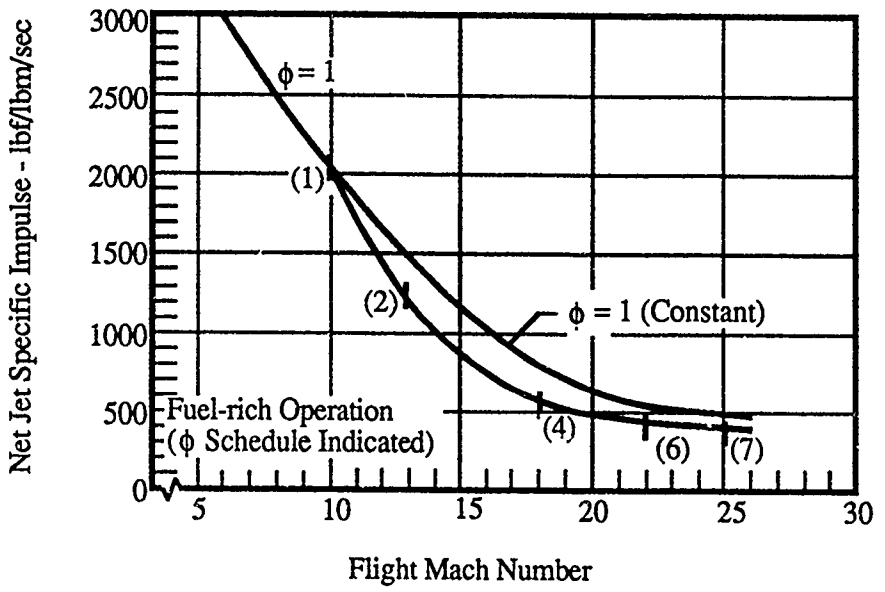


Source: NASA-LeRC



Source: AFWAL-APL

Fig. 53 Scramjet Isp Performance Comparisons - This Study vs. 1960's Estimates for Hydrogen Fuel



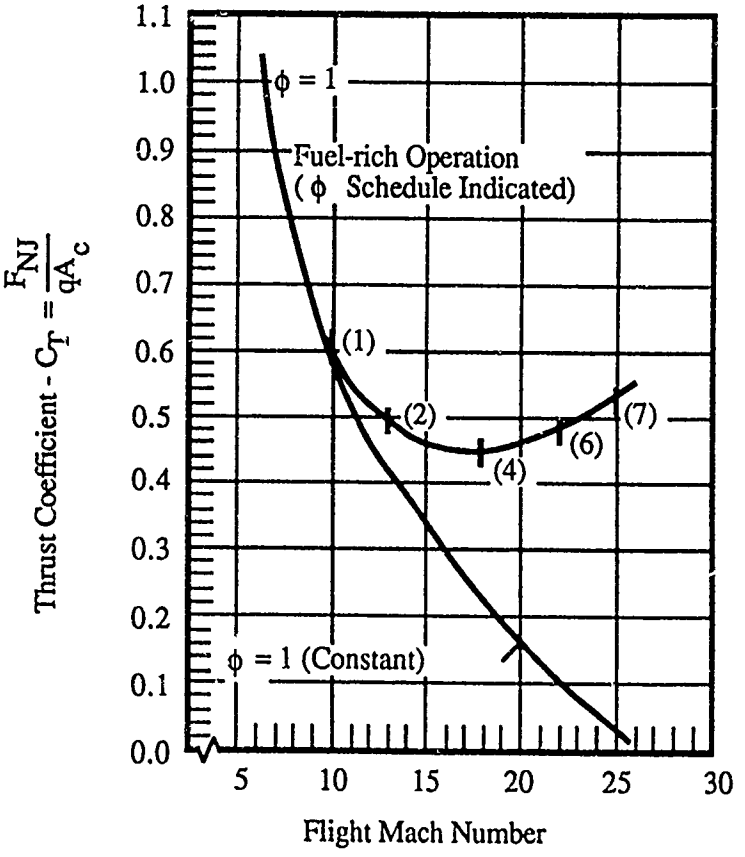


Fig. 54 Scramjet Mode Performance (All Engines)

3.14 Air Liquefaction Subsystem

3.14.1 Assets

The air liquefaction subsystem operates only during the rocket ejector phase of flight.

By using liquid air rather than liquid oxygen, the specific impulse in the ejector mode is raised from 420 seconds to approximately 1,400 seconds.

When fan supercharging is used, the specific impulse is increased from 1400 to 1700 seconds. With the addition of hydrogen recycling, it is raised to 2700 seconds without supercharging and 3200 seconds with supercharging.

A further advantage is found in that liquid air/liquid hydrogen engines operate effectively at lower combustion pressures, reduced gas velocities, lower combustion temperatures and an overall lower heat flux rate profile. Finally, the elimination of the need for liquid oxygen to support the rocket ejector mode significantly decreases vehicle TOGW/GLOW. However, liquid oxygen is still required for the final transition from scramjet termination to orbital insertion.

3.14.2 Liabilities

The use of liquid air systems adds significant weight to the engine system. In this study, it represents approximately 23 to 30% of the uninstalled weight.

The system also introduces increased system complexity and cost.

The principal current operational liability of air liquefaction using liquid hydrogen is the susceptibility of such systems to ice-fouling in the liquefying heat exchanger systems.

Finally, a potential for leakage between the hydrogen circuit and the air circuit in the heat exchanger system exists which consequently introduces an additional element of risk in the operation of such systems unless specific steps are taken to eliminate this potential problem.

As will be discussed in Section 6.0, the significant weight increase that accompanies the use of air liquefaction systems acts to reduce the payload performance improvement potential of this approach.

This technology is presently being studied further under programs sponsored by AFWAL Aero Propulsion Laboratory. Developments in this field that will result from that project should be considered in any future work carried out on RBCC engine systems utilizing air liquefaction.

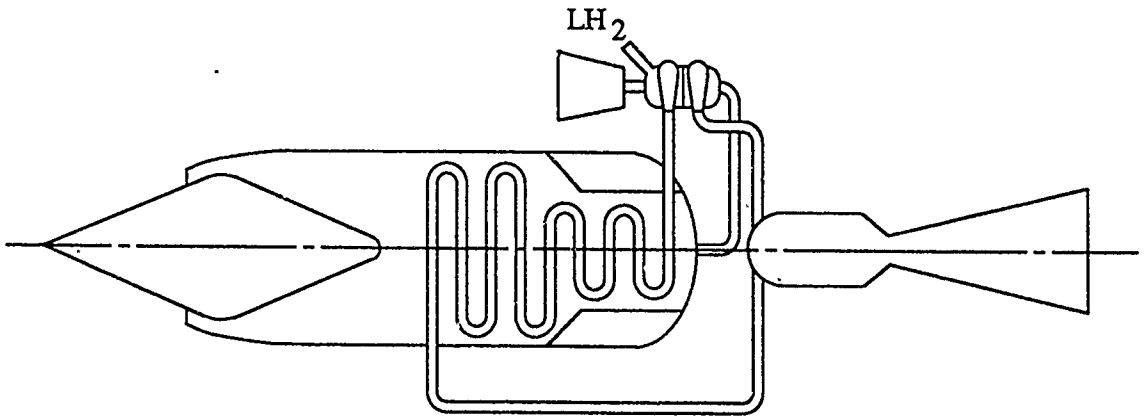
3.14.3 Requirements

The basic Liquid Air Cycle Engine (LACE) as originated by researchers at the Marquardt Corporation in the mid-1950s is a specific engine design. In this report, as the term LACE is applied to the rocket ejector subsystem of the complete RBCC engine, basic LACE in not meant to be implied.

The original LACE engine design is illustrated in Fig. 55. This was a rocket engine system that operated on hydrogen and used liquid air as an oxidizer. In operating in a vehicle from takeoff conditions through a nominal flightpath regime to approximately Mach 6, all the liquid hydrogen fuel consumed by the engine was used to cool and liquefy all the inlet air. The warmed up hydrogen and the liquid air (LAIR) produced in the heat exchanger were burned in a

I_s is for Sea Level Static Conditions

ϕ = Net Engine Equivalence Ratio



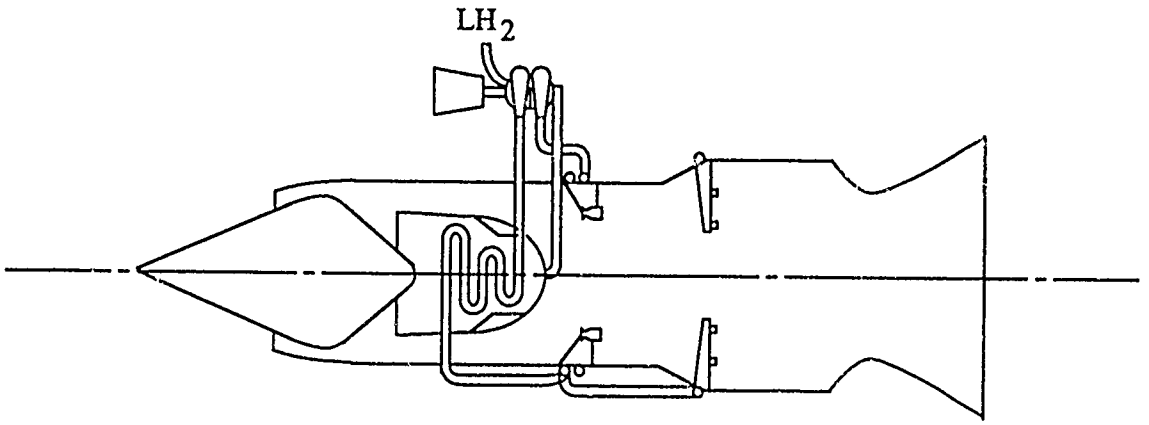
Basic LACE $I_s = 1000$

$\phi = 8$

Fig. 55 Basic Liquid Air Cycle Engine (LACE)

I_s is for Sea Level Static Conditions

ϕ = Net Engine Equivalence Ratio



RamLACE $I_s = 1400$

$\phi = 4.5$

Fig. 56 RamLACE Engine

single rocket-type combustor to produce thrust. Experimental engines using this design were constructed and operated that verified the analytical findings.

Basic LACE is characterized by net jet thrust and sea level static specific impulse levels of performance around approximately 1,000 seconds at a net engine equivalence ratio of 8. Basic LACE has some crucial limitations that must be considered. Basic LACE does not offer high specific-impulse acceleration/cruise-power operation competitive with conventional ramjet/scramjet mode operation. It is intrinsically limited to an upper-high speed of about Mach 6 at which point the Isp and thrust performance fall off dramatically due to sharply increased ram-drag penalties. Higher airstream recovery temperatures involved in higher speed operation which adversely affect the air liquefaction heat exchanger performance and weights.

In the baseline study carried out under Contract NAS7-377, Basic LACE was investigated and subsequently screened out for lack of payload performance. A "ramjet version" referred as RamLACE, operating at a net engine equivalent ratio of 4.5 and producing specific impulse performances in the range of 1400 seconds was also considered. This design extended the speed range over which LACE could be used to higher Mach numbers. The RamLACE configuration is illustrated in Fig. 56.

By the use of the thermal choke approach to support expansion in a straight duct, an engine design was developed that could extend the flight velocity spectrum into the scramjet velocity range - the ScramLACE design.

The final air liquefaction variation of LACE requires the use of subcooled, or "slush", hydrogen to provide a larger low temperature heat sink in a given vehicle geometry. This enables the engine to be operated at closer to stoichiometric conditions rather than the very fuel-rich operation required when conventional hydrogen is used for the purpose of air liquefaction. In this cycle, the warmed up hydrogen is returned to the slush hydrogen main propellant tank. This constitutes a "recycle" of the liquid hydrogen provided to the air liquefaction system, and the recycled hydrogen is reliquefied by the remaining slush hydrogen in that main propellant tank. This "recycle" process is carried out in Engine 32 as illustrated in Fig. 57.

Technologically, air liquefaction systems are more complicated than one could infer from the simple problem of liquefying air using hydrogen in a simple heat exchanger. Fig. 58 illustrates the numerous technologies that can be applied to provide variations of the basic, simple air liquefaction system. The use of para/ortho hydrogen conversion catalysts increase the thermal sink capability of liquid hydrogen or slush hydrogen. The liquid air may be subject to further processing in a system referred to as ACES, Air Collection Enrichment System, which removes the nitrogen component to varying degrees and passes on a liquid product with a higher oxygen to nitrogen ratio.

3.14.4 The Fouling Problem (Ref. 20)

In flying the reference trajectory, whether using vertical takeoff mode or horizontal takeoff mode, the vehicle operates in the ejector mode for approximately 80 to 100 seconds and rises from an altitude of sea level conditions to approximately 50,000 feet at ejector mode termination.

Air liquefaction heat exchangers are subject to atmospheric constituents fouling. The principal "contaminants" are water in the form of vapor or as droplets, carbon dioxide and argon. Water-ice fouling of heat exchangers is mainly associated with low-altitude atmospheric flight conditions as will be experienced in the rocket ejector mode of the orbital ascent trajectory discussed here. Carbon dioxide and argon fouling is related to high-speed, high-altitude vehicle

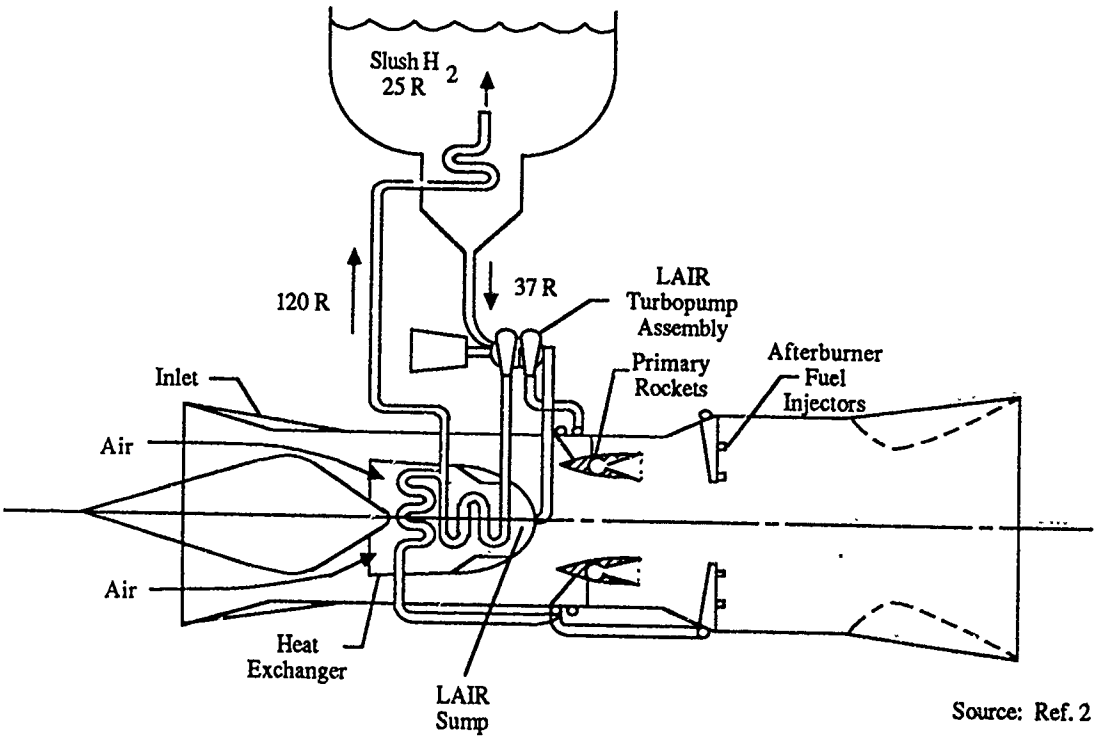


Fig. 57 The "Recycle" Process in Engine #32

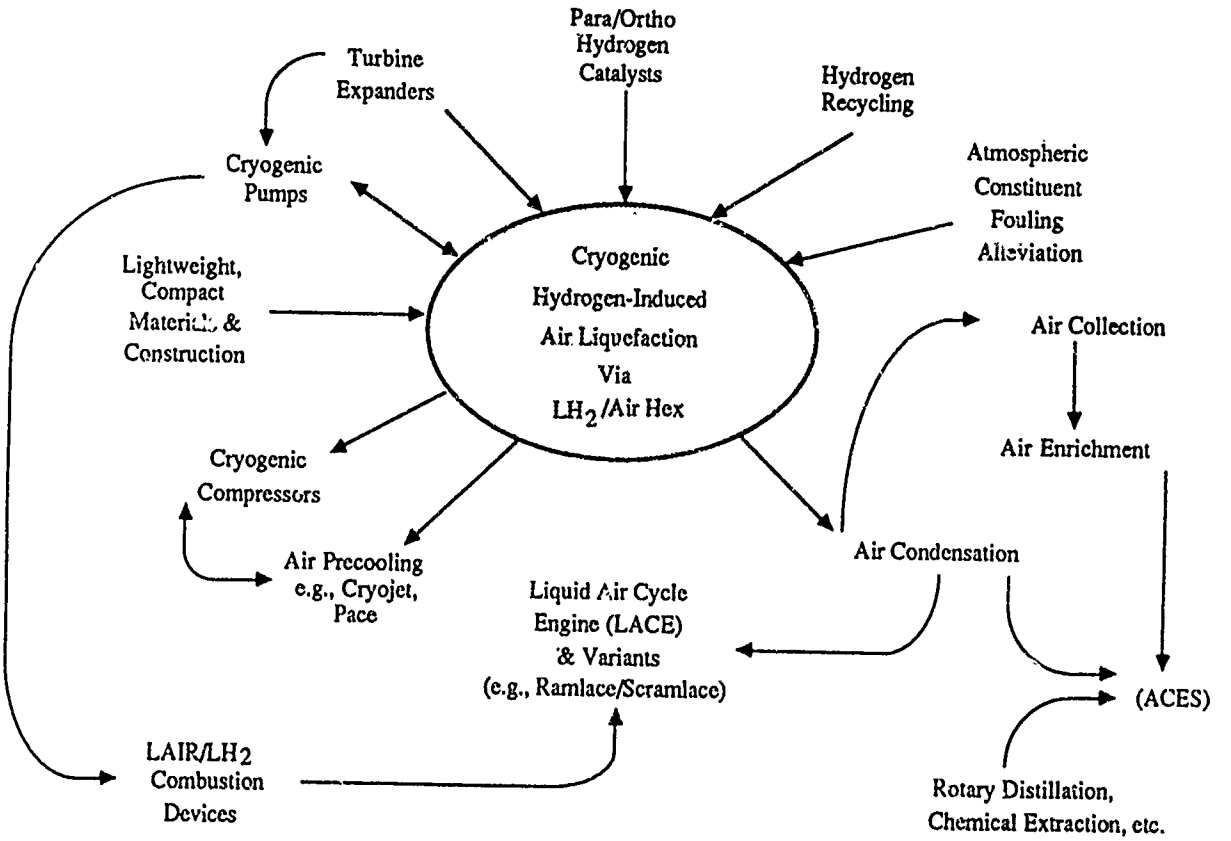


Fig. 58 The Technologies Involved in Air Liquefaction

UNCLASSIFIED



AD NUMBER

B121 765

CLASSIFICATION CHANGES

TO

FROM

AUTHORITY

AFNL 3+r
17 Jan 74

THIS PAGE IS UNCLASSIFIED

operation. This type of fouling is not a significant subject of concern in the RBCC engine cycles studied.

The problem of heat exchanger fouling is a two part issue in terms of performance degradation: (1) physical blockage of airflow passages by solids which form and adhere to the exposed heat-exchanger active surfaces and (2) reduction in heat-transfer rates caused by the insulating action of the ice deposited. Blockages cause an increased air flow pressure drop leading to reduced airflow rates through the heat exchanger, while reduction in heat-transfer rates cause a loss in heat exchanger effectiveness. Both these phenomona lead to a reduction in air liquefied per unit hydrogen flow. This in turn diminishes engine thrust and specific impulse and can lead to engine failure. Fig. 59 shows engine thrust levels versus time for a set of engine runs with a small LACE system. Two of these runs used an icing alleviation scheme that involves the injection/recovery of ethylene glycol. The near vertical curve downward shows the precipitous decay in thrust caused by ice-fouling of the heat exchanger with a normal absolute humidity level of 0.01 lb water/lb dry air. As can be seen from Fig. 60 this corresponds to a 60 degree F, 100% relative humidity day at sea level conditions or one-third of the water vapor level of a 90 degree F, 100% relative humidity day. It is highly probable that higher humidities would be encountered in real operational conditions of the vehicles being studied here. The relative effectiveness of the de-icing-fluid system in resisting fouling action of the ice build-up is clear from the remaining two thrust/time curves shown.

Fig. 61 and 62 show the increase in airflow area blockage and the decrease in heat-transfer coefficient during a run at constant sea level conditions. The specific humidity of 0.01 is a relatively low value when compared to those conditions that would be encountered in the real operation of RBCC engine powered vehicles. These runs did not consider flight conditions where the vehicle could encounter cloud-contained water droplets or direct precipitation. This would particularly compromise the all-weather flight capability of RBCC engine propelled vehicles.

Fig. 63 presents a simulated ascent trajectory heat exchanger icing contamination performance curve.

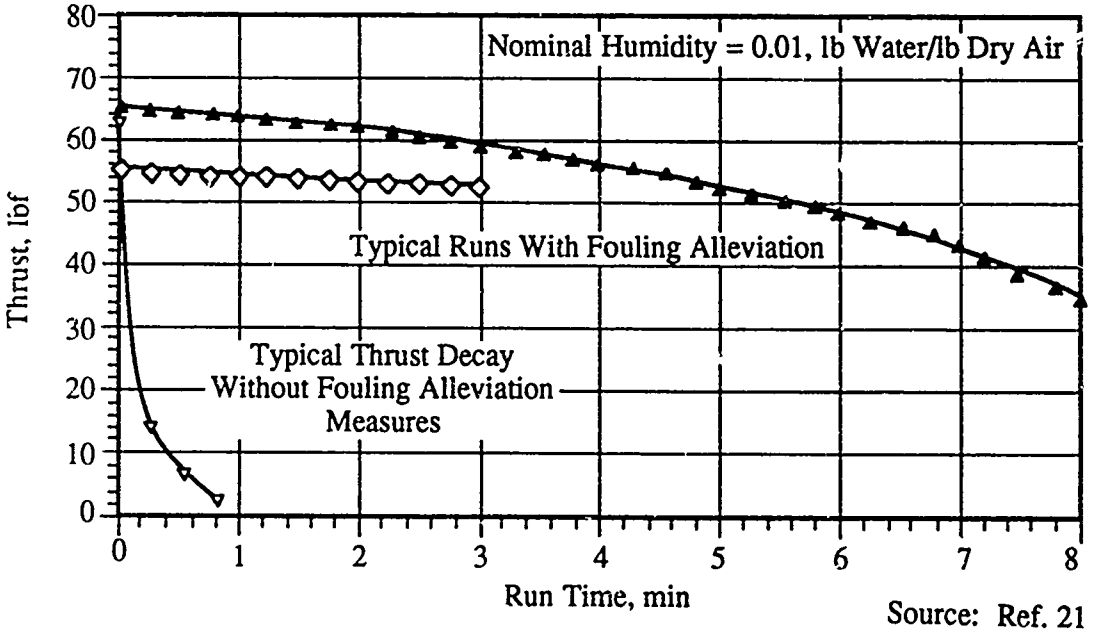
3.14.5 Conclusions

When the benefits that air liquefaction subsystems offer are considered in terms of payload pounds to orbit on the reference trajectory studied here, they produce a measurable but not significant performance increase. With the reservation that further study should be done in this area, our conclusion is that the technological risk associated with elimination of the ice-fouling problem together with the other technology development problems that must be solved to practically implement such systems does not presently appear to justify their use in RBCC/SSTO vehicle systems.

3.15 Slush Hydrogen Utilization

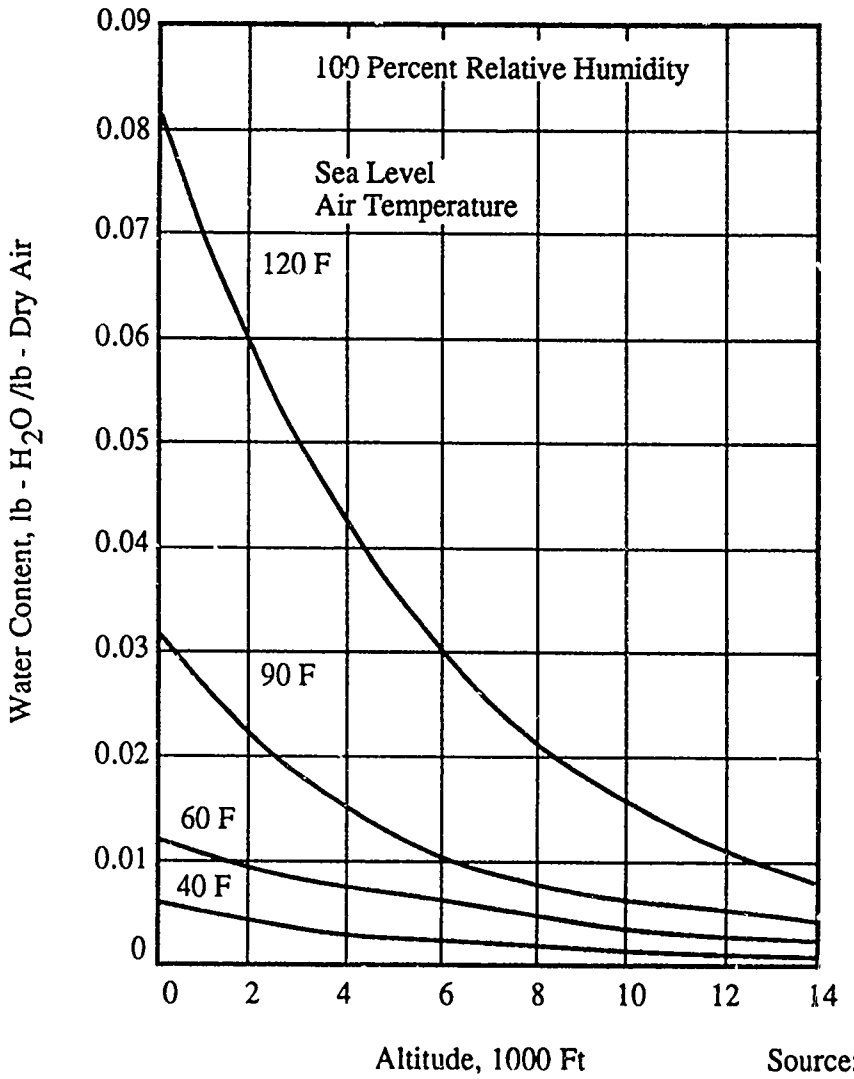
3.15.1 Benefits

Sixty percent slush hydrogen, the maximum percentage practically producable and handleable, has approximately a 15% higher density than normal boiling point (NBP) hydrogen. It also has approximately 20% lower enthalpy than NBP hydrogen. (Fig. 64)(Ref. 22)



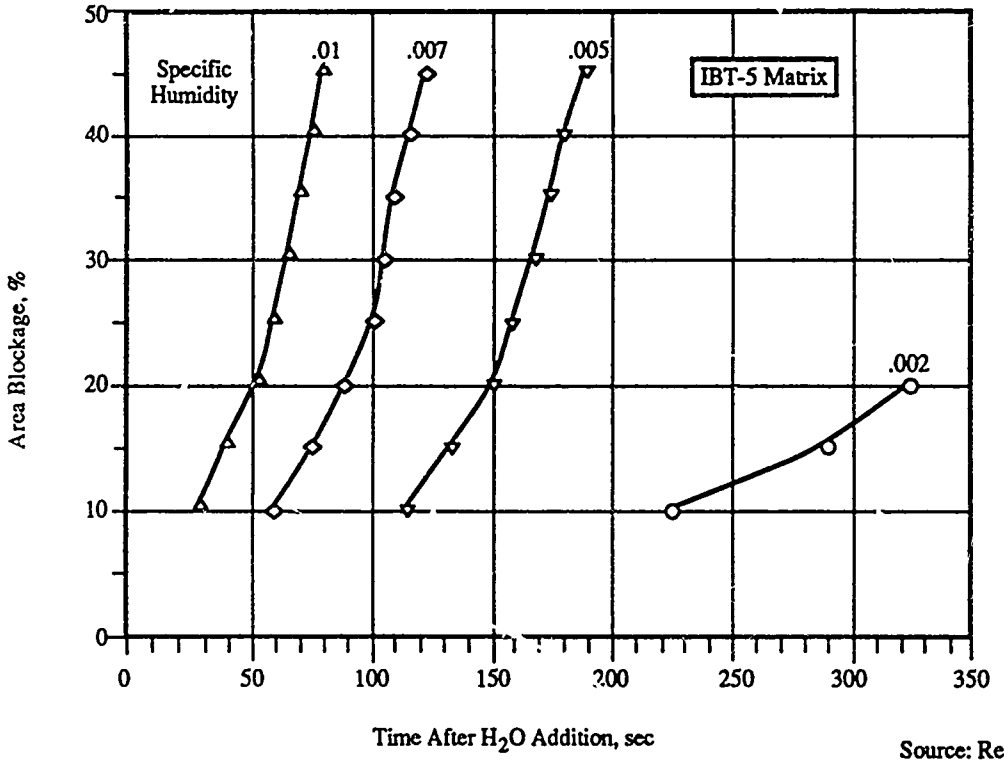
Source: Ref. 21

Fig. 59 LACE Engine Thrust Performance With and Without Fouling Alleviation



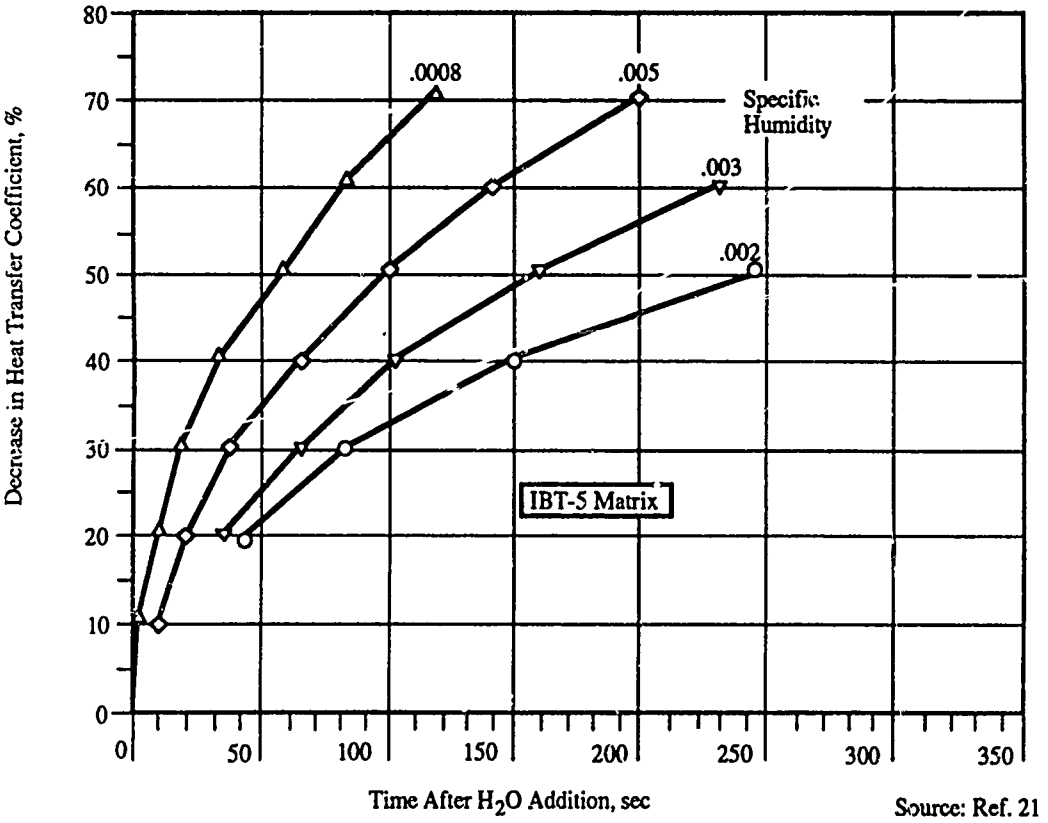
Source: Ref. 21

Fig. 60 Atmospheric Water Content and a Function of Altitude and Air Temperature



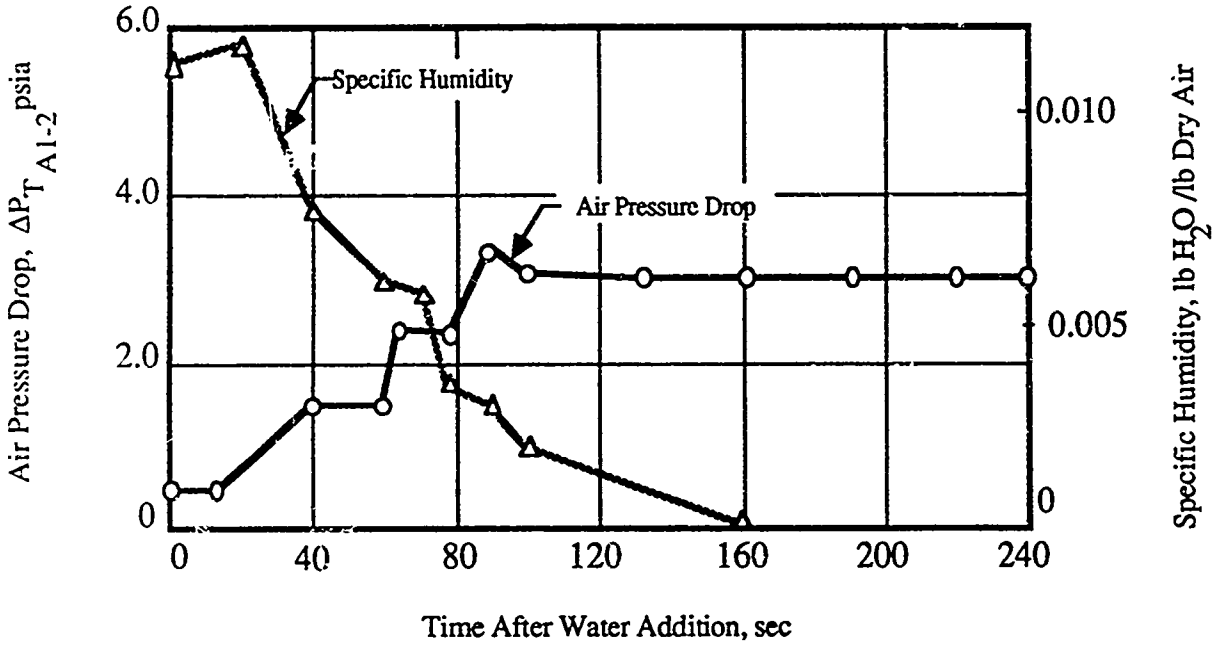
Source: Ref. 21

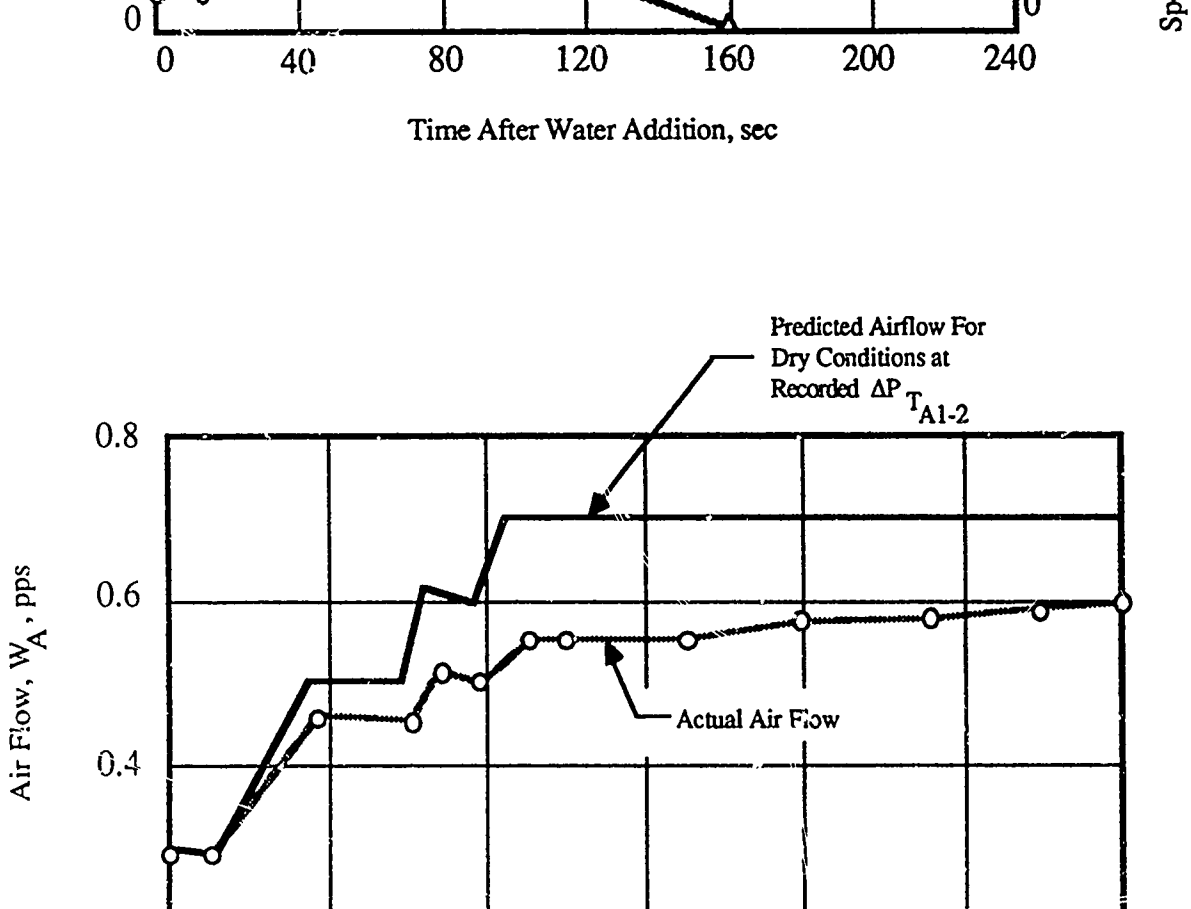
Fig. 61 Icing Contamination Induced Airflow Area Blockage with Time



Source: Ref. 21

Fig. 62 Contamination Induced Decrease in Overall Heat Transfer Coefficient with Time





Source: Ref. 21

Fig. 63 Simulated Ascent Trajectory Heat Exchanger Contamination Test Results

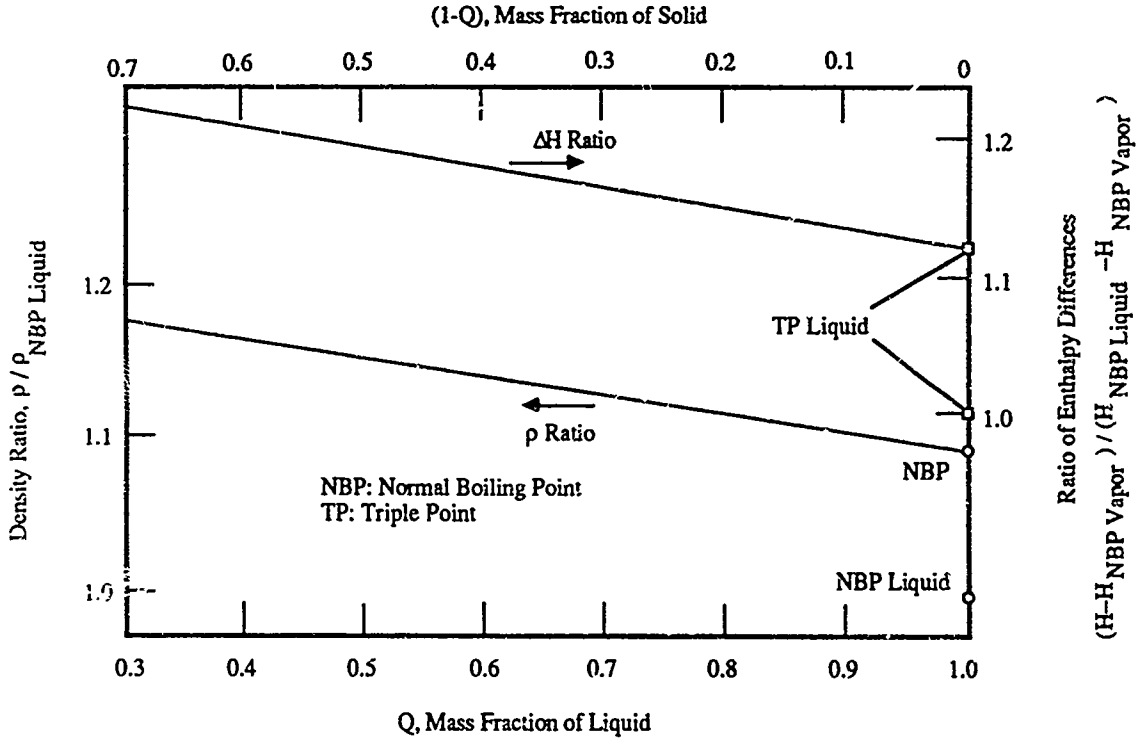


Fig. 64 Slush Hydrogen Heat Capacity and Density Relationships

Judged from the perspective of the RBCC/SSTO mission requirements, the use of slush hydrogen permits a decrease in vehicle frontal area, tank volume and thus tank wetted area and structural weight. This slightly reduces drag but the most significant effect is structural weight reduction as will be discussed in Section 6.0.

A point that is frequently not considered in this mission context, or similar mission situations, is that the slush state is not required to be maintained for the full flight duration. It only needs to be maintained to that point in the trajectory where 15% of the volume of the tanked hydrogen has been consumed. This will leave sufficient tank volume to contain all the NBP hydrogen that could be produced by the conversion of slush H_2 to NBP H_2. In the vehicles studied here, this time ranges from 60 seconds in the 1 Mlbm TOGW/GLOW vehicle with Engine 22 to 98 seconds for a 500 klbm vehicle using Engine 10.

This apparent advantage is reduced in its significance when ground operations are considered. The requirements of the vehicle system studied here include the ability to remain on "alert" status for significant periods of time. This would require the slush hydrogen to be maintained in the vehicle propellant tank for extended periods.

It is highly unlikely that the hydrogen propellant tank insulation properties would lead to a conversion of slush to NBP hydrogen in the relatively short time period in which 15% of the hydrogen propellant volume is consumed. In the vehicles under study here, less than two minutes would be required to achieve 15 % H_2 tank emptying.

It would be advantageous to retain slush hydrogen after ascent flight termination in order to extend the "on-station" operating time available. Design specific trade studies would have to be carried out to quantify the slush hydrogen advantage vs. on-board active refrigeration or a combination of both.

3.15.2 Liabilities

The production, transfer, storage and use technologies of slush hydrogen are not developed technologies at this time.

3.15.3 Present Technology Development Efforts

The principal effort in the development of slush hydrogen technology in this country today is an effort just being undertaken by the NASA Lewis Research Center.

In September of 1987, LeRC held a pre-solicitation conference on the subject of "Slush Hydrogen Technology Maturation for the National Aerospace Plane". The overall technology maturation program plan is comprised of six elements:

1. Flight system technology
2. Production of storage technology
3. Production
4. Storage and transfer
5. Prototype flight tank
6. Safety

The work that will be accomplished by the LeRC program should be closely monitored in the future for its applicability to RBCC/SSTO vehicle systems.

3.16 Engine Structure, Materials, Processes and Weights

3.16.1 Structure, Materials and Processes

The starting point for the estimate of engine weights for the five RBCC engines studied was the NAS7-377 (Ref. 2) structure, materials, processes and weights findings. These estimations were first modified to incorporate technology development from the 1967 study date to a Technology Availability Date (TAD) of 1985. The 1985 TAD baseline estimates were then extrapolated to a 1995 TAD date - the date of start of the DDT&E phase proposed in this study.

At the time the initial weight estimates were prepared in 1967, both the Marquardt Corporation and Rocketdyne Corporation had actual hardware experience in the construction of the propulsion subsystems involved. Besides Rocketdyne's broad experience in rocket engine systems, the Marquardt Corporation had constructed and operated a subscale, flight-weight, regeneratively-cooled hydrogen-fueled hypersonic ramjet test engine which was discussed earlier in Section 2.0.

Representative materials used in the 1967 study included:

- Hastalloy X
- Titanium Wire-Wrap
- 5 Al-2.5 Sn Titanium Honeycomb
- RENE 41 Honeycomb
- 2024-T4 and 2219-T89 Aluminum Honeycomb

Representative joining/bonding techniques used were:

- Conventional welding and brazing
- Furnace and quartz-lamp braze
- Polyimide, Polybenzimidazole Adhesives
- Mechanical Fasteners (e.g., bolted honeycomb panels)

In the baseline 1965 study extension phase, the use of composite materials in future engine systems was considered. An example of a single assembly weight analysis carried out at that time is presented in Table 2. This table presents sample calculations of the structural weight of a 2-dimensional inlet ramp moving-panel component. Both the baseline study materials and composite materials were compared in this piece-by-piece study.

By replacing facesheets of the various honeycomb panels in the inlet with Al-B or Ni-SiC composite materials, a weight saving of greater than 16 pounds could be accomplished. This is more than 50 percent of the replaced facesheet weight. Considering the complete panels, including hinges, edge closers, attached structures and leading edges, the facesheet weight savings represent better than 32 percent of the complete inlet plate structural weight (excluding the center body and actuation system).

For the RBCC engine systems considered in this study, with the 1995 TAD, the following materials were considered as being representative:

- Aluminides of titanium, iron and nickel
- Metal matrix composite materials
  - Silicon carbide reinforced titanium aluminide
  - Tungsten fiber reinforced iron-based superalloy
  - Graphite reinforced copper
- Non-metal matrix composite materials
  - Graphite reinforced PMR-15 polyimide
  - Carbon/carbon materials
- Rapid solidification processed metals, alloys and intermetallics
- Refractory metals (e.g., Columbium)

Representative forming processes developed since the 1967 baseline that are now available and that will be available for the 1995 TAD include:

- Superplastic forming
- High-energy forming (e.g., explosive forming)
- Cryostretch forming
- Composite filament winding
- Electrochemical milling

Representative joining techniques include:

- Diffusion bonding
- Electron beam welding
- Laser welding
- Advanced adhesive compounds

Table 2 NAS7-377 Composite Materials Comparative Weight Analysis

2-D Inlet Panel Materials Substitution Study

Inlet Substructure	Conventional Material Weight		Composite Material Weight	Weight Saved
Forward Ramp Plate Face Sheets	Titanium Stainless Steel	= 9.4 lbs = 7.5 lbs	2.7 lbs	6.7 lbs 4.8 lbs
Aft Ramp Plate Face Sheets	Hastalloy X	= 6.6 lbs	3.2 lbs	3.4 lbs
Cowl Plate Face Sheets	Hastalloy X and Stainless Steel	= 10.7 lbs	5.2 lbs	5.5 lbs
Side Plate Face Sheets	Hastalloy X and Stainless Steel	= 6.2 lbs	3.2 lbs	3.0 lbs
Honeycomb Core, Leading Edges, Edge Closures, Hinging, and Corner Connectors (no face sheet weights)	Inconel 718 Inco and Ti (6 Al 4 V)	= 18.4 lbs = 15.9 lbs	does not apply	does not apply
Total Weights: Face Sheets Only		32.9 lbs 31.0 lbs	14.3 lbs	18.6 lbs 16.7 lbs
Complete Plates *		51.3 lbs	32.7 lbs	18.6 lbs

By replacing face sheets on the various honeycomb panels in the inlet with Al-B or Ni-SiC composite materials, a weight saving of greater than 16 pounds can be accomplished. This is more than 50% of the replaced face sheet weight.

Source: Ref. 2

*Considering the complete panels, including hinges, edge closures, attach structures and leading edges, the facesheet weight savings represent better than 32% of the complete inlet plate structure weight (excluding the centerbody and actuation system).

3.16.2 Fan Subsystem Weights - An Example

An example of 1967 TAD/1985 TAD weight estimate for the fan subsystem specific weights was adjusted from those documented in the 1967 database to a 1985 weight estimate and a 1995 TAD weight estimate. This was done by increasing the 1967 baseline weight by 35% based on higher pressure ratio fan technology using current technology materials and fabrication processes. This 1985 weight estimate was then reduced by the same amount, 35%, as the estimated advancement that will be achieved by 1995 technology yielding a net weight of 0.88 over the baseline study.

The 1995 TAD weight estimation for the Fan Subsystem is based on the assumption that the present AFWAL Integrated High Performance Turbine Engine Technology (IHPTET) program will continue to be supported and will provide the means of achieving significant weight reductions in the fan subsystem.

3.16.3 The Air Liquefaction Subsystem Example

As a second example, the baseline study weight estimate for the air liquefaction subsystem was reduced by 15 percent for a 1985 TAD weight estimate on the basis of:

- The use of fan supercharging of the air liquefaction system
- Improved heat exchanger technology currently available
- The use of a pressure-balanced containment vessel
- Recent developments in ortho-hydrogen/para-hydrogen converting catalyst materials

For the 1995 TAD, the 1985 TAD air liquefaction subsystem weight was reduced an additional 15% on the basis of improvements that will be achieved in these same areas of technology.

3.16.4 Subsystems Weights Estimation Factors

Table 3 presents the subsystem weight estimation factors applied to the 1967 TAD to create the 1985 TAD weights and the factors applied to the 1985 TAD weight to create the 1995 TAD weights together with the basis upon which these factors were developed.

3.16.5 125 Klb SLS Thrust Engine Weights

Table 4 presents the weight breakdown by engine subsystem weight and percentage of uninstalled engine weight. At the top of each column, the engine's design air-to-rocket flow ratios are listed for the design-condition rocket ejector mode operation in terms of secondary air flow rate to primary rocket propellant flow rate.

Table 5 presents these same weight estimations for a 1995 TAD.

Table 6 presents a summary engine weight statement covering all five RBCC 1995 TAD engine systems in the same 125 Klb thrust SLS engine systems which were developed using the approach discussed in the preceding paragraph.

3.16.6 T/W Comparisons to Turbomachinery Based Engines

Fig. 65 compares the thrust-to-weight ratio and aircraft takeoff thrust loading of the five RBCC engine system configurations studied in comparison to contemporary turbomachinery

Table 3 Subsystem Weight Estimation Factors

Subsystem	1965 → 1985 Factor	Basis	1985 → 1995 Factor	Basis
Fan Stowage	1.35	Higher Pressure Ratio Fan, Larger Airbreathing Gas Generator	0.65	USAF IHPTET Program Technologies, Materials Advancements, and High Temperature and Pressure Ratio Power Turbines
Air Liquefaction	0.85	Materials and Heat Transfer Advancement Reduces Catalyst Weight	0.85	Limited Materials Gains and Improved Heat Exchanger Technology
Primary Rocket	1.05 0.95	Engines 22, 30, & 32 for Dual Oxidizer Injector & Materials Engines 10 & 12 for Materials	0.85	Limited Materials Gains and Lighter Turbopumps from SSME Technology
Mixer/Diffuser/ Combustor	1.25	Longer Diffuser	0.70	Materials Advancements
Exit Nozzle and Centerbody	1.30	Variable Nozzle and Stowable Ramjet Fuel Injector	0.75	Materials Advancements
Strut and Piping	1.00		0.90	Materials Advancements
Contingency and Controls	1.00		0.85	Materials and Control Technology Advancement
Inlet	0.70	Quasi-fixed Axisymmetric Inlet vs. 2-D Ramp	0.80	Materials Advancements

$$\text{Weight Estimation Factor} = \frac{\text{1985 TAD Weight}}{\text{NAS7-377 Weight}} \text{ or } \frac{\text{1995 TAD Weight}}{\text{1985 TAD Weight}}$$

Table 4 1985 TAD Weight Breakdown by Engine Subsystem Weight and Percentage of Uninstalled Engine Weight

125 KLB Thrust (SLS) - 1985 TAD

(All Weights in lbm)
Technology Availability D 1985

125 klbf Engines	#10 ESJ	#12 SESJ	#22 SL	#30 SSL	#32 RSSL
w_s/w_p	1.5	1.9	1.5	2.0	2.0
Subsystem					
Fan/Gas Generator/Stowage	--	2086 (31%)	--	2499 (27%)	2604 (24%)
Air Liquefaction	--	--	2107 (29%)	1925 (21%)	2554 (24%)
Primary Rocket	1447 (31%)	1195 (18%)	1780 (24%)	1147 (12%)	1607 (15%)
Mixer/Diffuser/Combustor	1235 (26%)	1302 (19%)	1220 (17%)	1246 (13%)	1258 (12%)
Exit Nozzle/Centerbody	1400 (30%)	1322 (19%)	1275 (17%)	1292 (14%)	1279 (12%)
Strut & Piping	204 (4%)	295 (4%)	319 (4%)	405 (4%)	465 (4%)
Controls & Contingency	429 (9%)	619 (9%)	671 (9%)	851 (9%)	977 (9%)
Uninstalled Engine	4715 (100%)	6819 (100%)	7372 (100%)	9365 (100%)	10744 (100%)
Thrust/Weight (unin.)	26.5	18.3	17.0	13.3	11.0
Inlet	4474	4474	4474	4474	4474
Installed Engine	9189	11293	11846	13839	15218
Thrust/Weight (in.)	13.6	11.1	10.6	9.0	8.2

Table 5 1995 TAD Weight Breakdown by Engine Subsystem Weight and Percentage of Uninstalled Engine Weight

125 KLB Thrust (SLS) - 1995 TAD

(All Weights in lbm)
Technology Availability Date: 1995

125 klbf Engines	#10 ESJ	#12 SESJ	#22 SL	#30 SSL	#32 RSSL
w_s/w_p	1.5	1.9	1.5	2.0	2.0
Subsystem					
Fan/Gas Generator/Stowage	--	1356 (27%)	--	1624 (23%)	1693 (20%)
Air Liquefaction	--	--	1791 (30%)	1636 (23%)	2171 (26%)
Primary Rocket	1230 (33%)	1016 (20%)	1513 (25%)	975 (14%)	1366 (16%)
Mixer/Diffuser/Combustor	865 (24%)	911 (18%)	854 (14%)	872 (12%)	881 (11%)
Exit Nozzle/Centerbody	1050 (28%)	992 (20%)	956 (16%)	969 (13%)	959 (12%)
Strut & Piping	184 (5%)	266 (5%)	287 (5%)	365 (5%)	419 (5%)
Controls & Contingency	365 (10%)	526 (10%)	570 (10%)	723 (10%)	830 (10%)
Uninstalled Engine	3694 (100%)	5067 (100%)	5971 (100%)	7164 (100%)	8319 (100%)
Thrust/Weight (unin.)	33.8	24.7	21.0	17.5	15.0
Inlet	3579	3579	3579	3579	3579
Installed Engine	7273	8646	9550	10743	11898
Thrust/Weight (in.)	17.2	14.5	13.1	11.6	10.5

Table 6 Summary Engine Weight Statement for All 5 RBCC Engines

1995 vs 1985 TAD Comparison

		125 KLB (SLS) Engines				
		#10 ESJ	#12SESJ	#22 SL	#30 SSL	#32 RSSL
Uninstalled Engine	1985:	4715	6819	7372	9365	10744
	1995:	3694	5067	5971	7164	8319
Uninstalled Thrust/Weight	1985:	26.5	18.3	17.0	13.3	11.6
	1995:	33.8	24.7	21.0	17.5	15.0
Installed Engine	1985:	9189	11293	11846	13839	15218
	1995:	7273	8646	9550	10743	11898
Installed Thrust/Weight	1985:	13.6	11.1	10.6	9.0	8.2
	1995:	17.2	14.5	13.1	11.6	10.5

based engine systems. Figures 66 and 67 present the distribution of subsystem weight as a percentage of installed engine weight for Engines 10 and 30. These two figures provide a

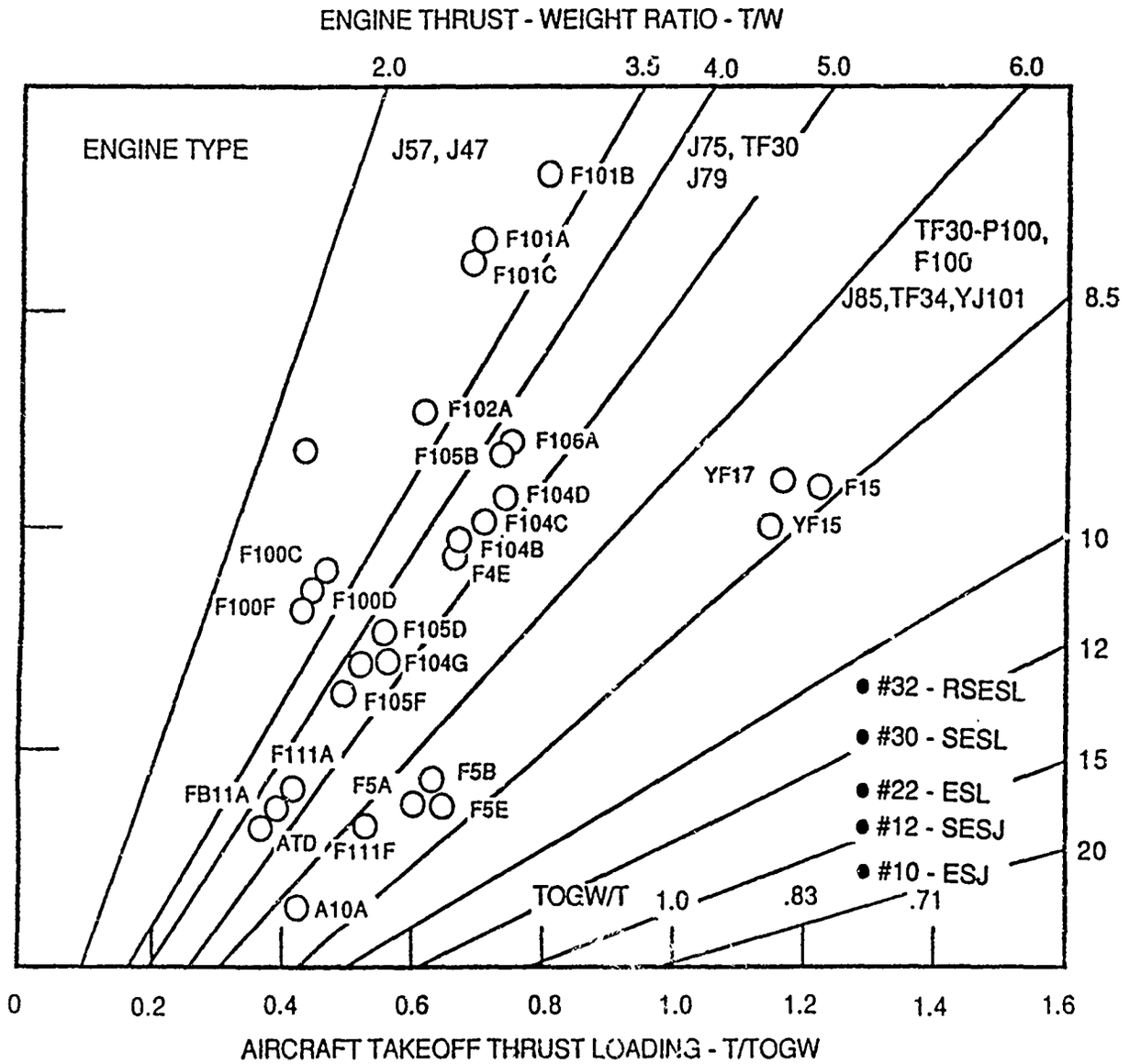


Fig. 65 Thrust to Weight Ratio for RBCC Engine Systems and Various Contemporary Aircraft

graphic comparison of the thrust-to-weight effect of the installation of the fan/drive gas generator/stowage subsystem and the air liquefaction subsystem on the weight distribution of the 125 Klb thrust baseline engine 10 system.

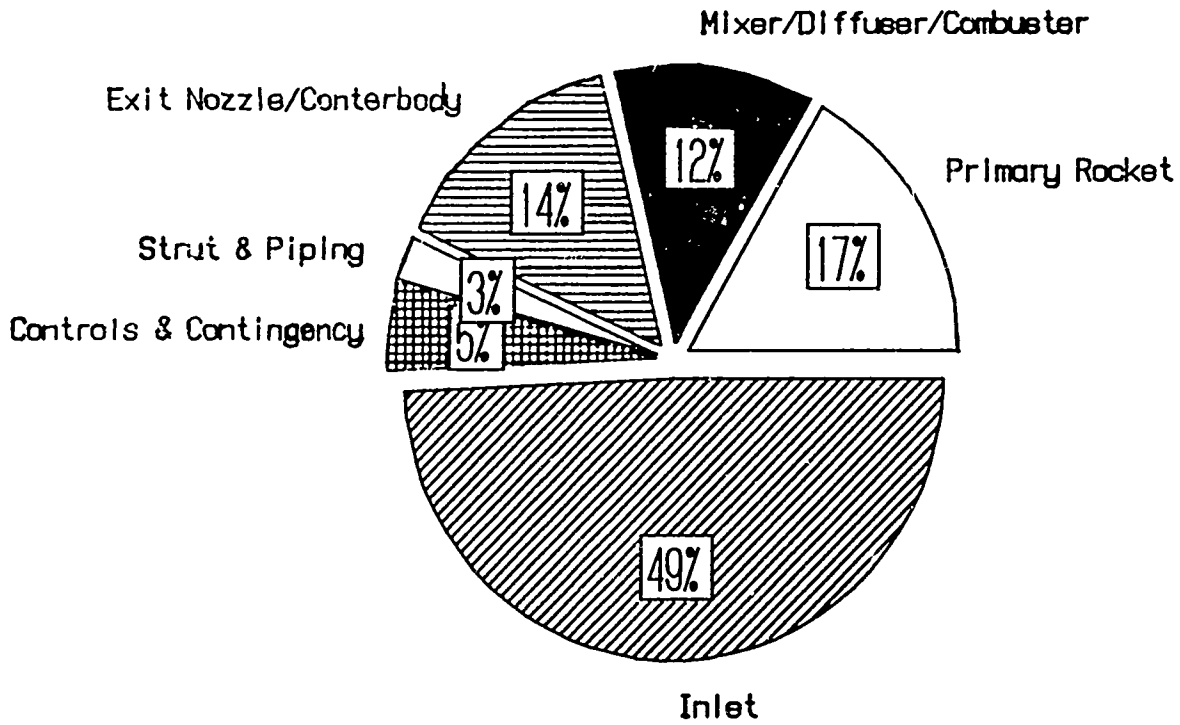


Fig. 66 Subsystem Weight as a Percentage of Installed Engine Weight - Engine #10 - Ejector Scramjet

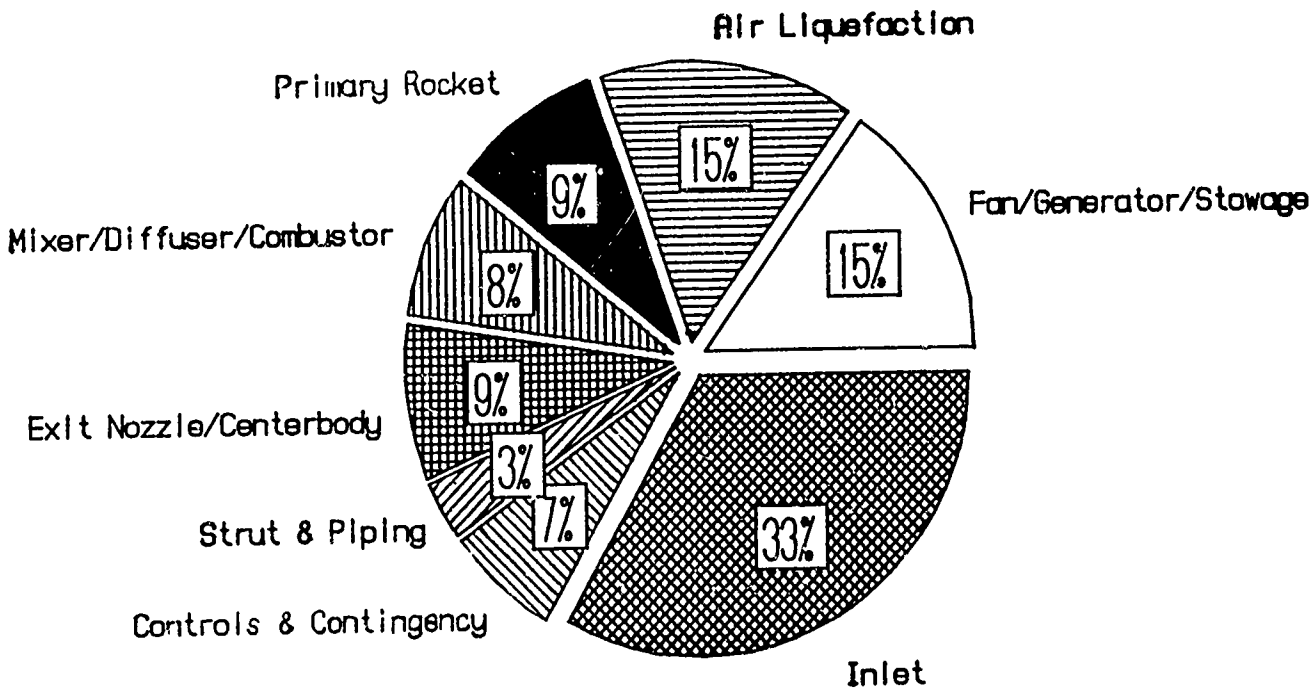


Fig. 67 Subsystem Weight as a Percentage of Installed Engine Weight - Engine #30 - Supercharged ScramLACE

3.16.7 Engine Subsystems Conceptual Layouts

Figures 68 to 70 are conceptual layouts showing possible arrangements of the major components in the RBCC engine concepts studied. These figures should not be taken as design recommendations. They serve to illustrate the varying degrees of technical complexity and the design integration problems that must be solved for each engine type.

In Figure 68 a conceptual layout of the two most complex RBCC engine configurations is presented. These two engines, 30, - the Supercharged ScramLACE Engine and 32 - the Recycled Supercharged ScramLACE Engine, include both supercharging and air liquefaction in Engine 30, and the use of recycling of slush hydrogen feed in Engine 32 which does not impact on the basic Engine 30 configuration but does result in increased engine weight. Engine 22 - the ScramLACE engine consists of this same configuration without the fan/supercharger subsystem.

Figure 69 illustrates a conceptual configuration for Engine 12 - the Supercharged Ejector Scramjet engine. The major difference in this configuration is the elimination of the air liquefaction subsystem.

Figure 70 presents the conceptual design of the simplest of the five RBCC engine configurations studied. This is Engine 10 - the Ejector Scramjet Engine. This engine does not have either the fan/supercharger subsystem, air liquefaction subsystem or recycle.

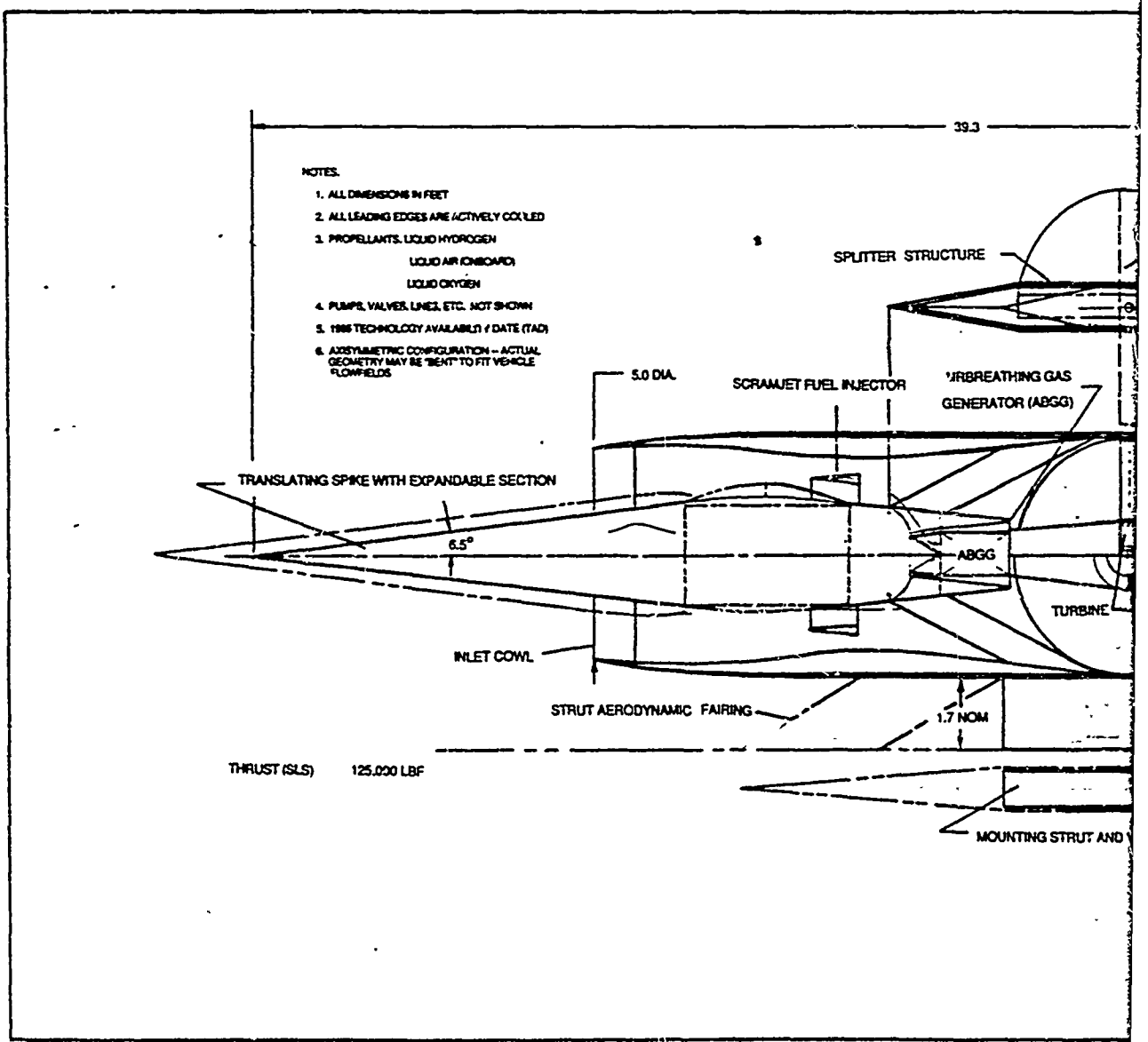
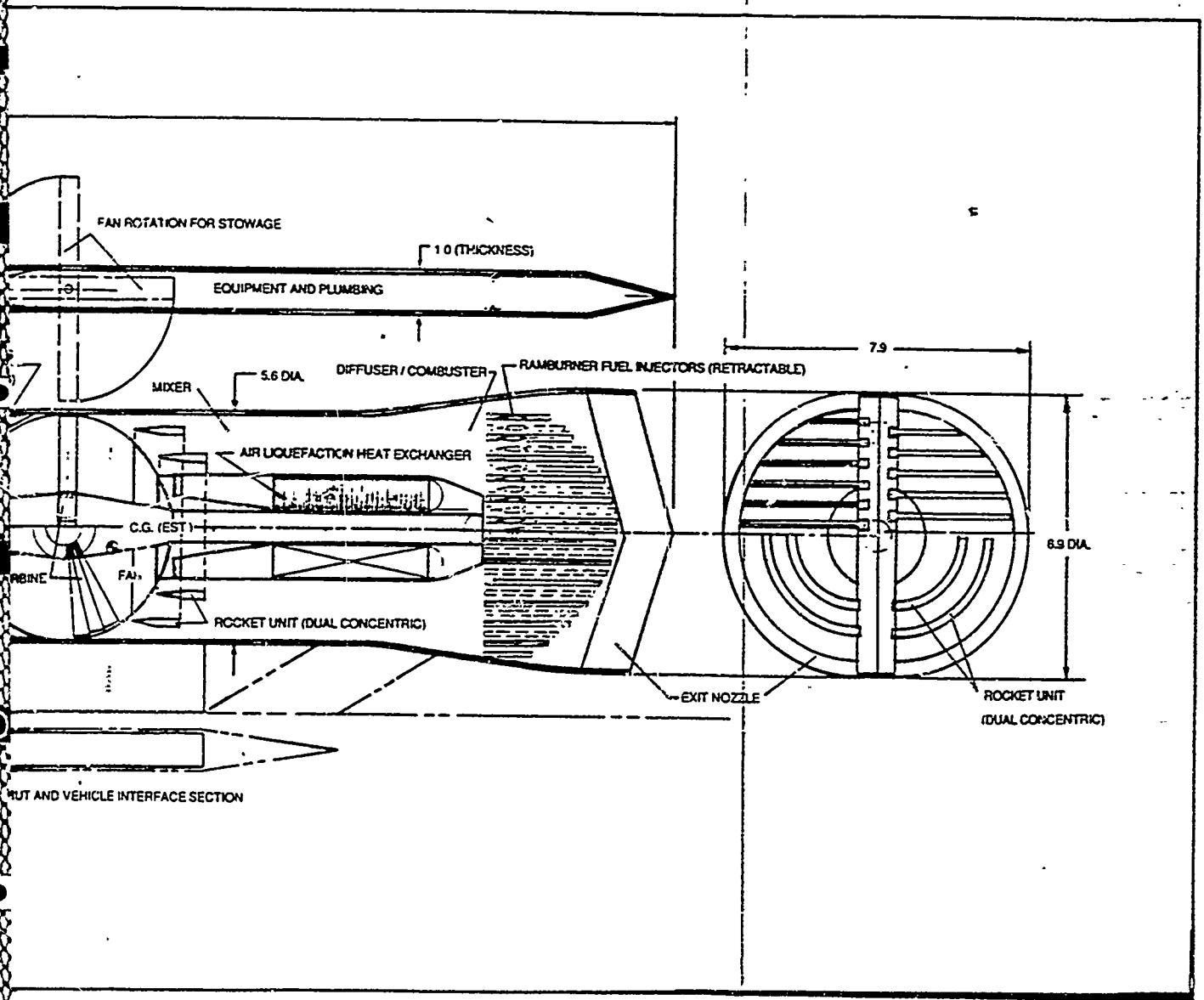


Fig. 68 Conceptual Subsystems Arrangement for Engine #30 and #32 - Supercharged ScramLACE and Recycled Supercharged ScramLACE



UT AND VEHICLE INTERFACE SECTION

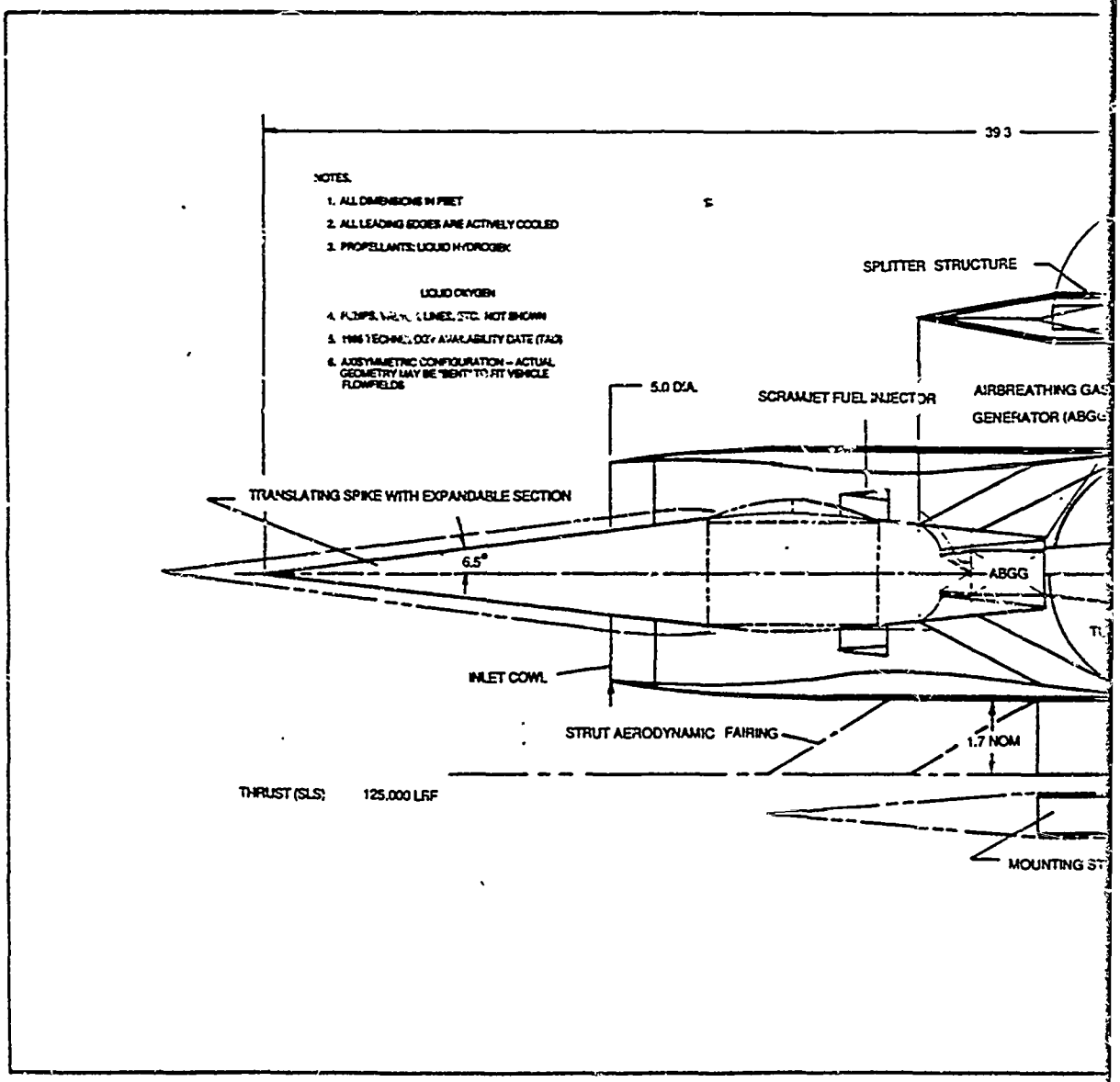
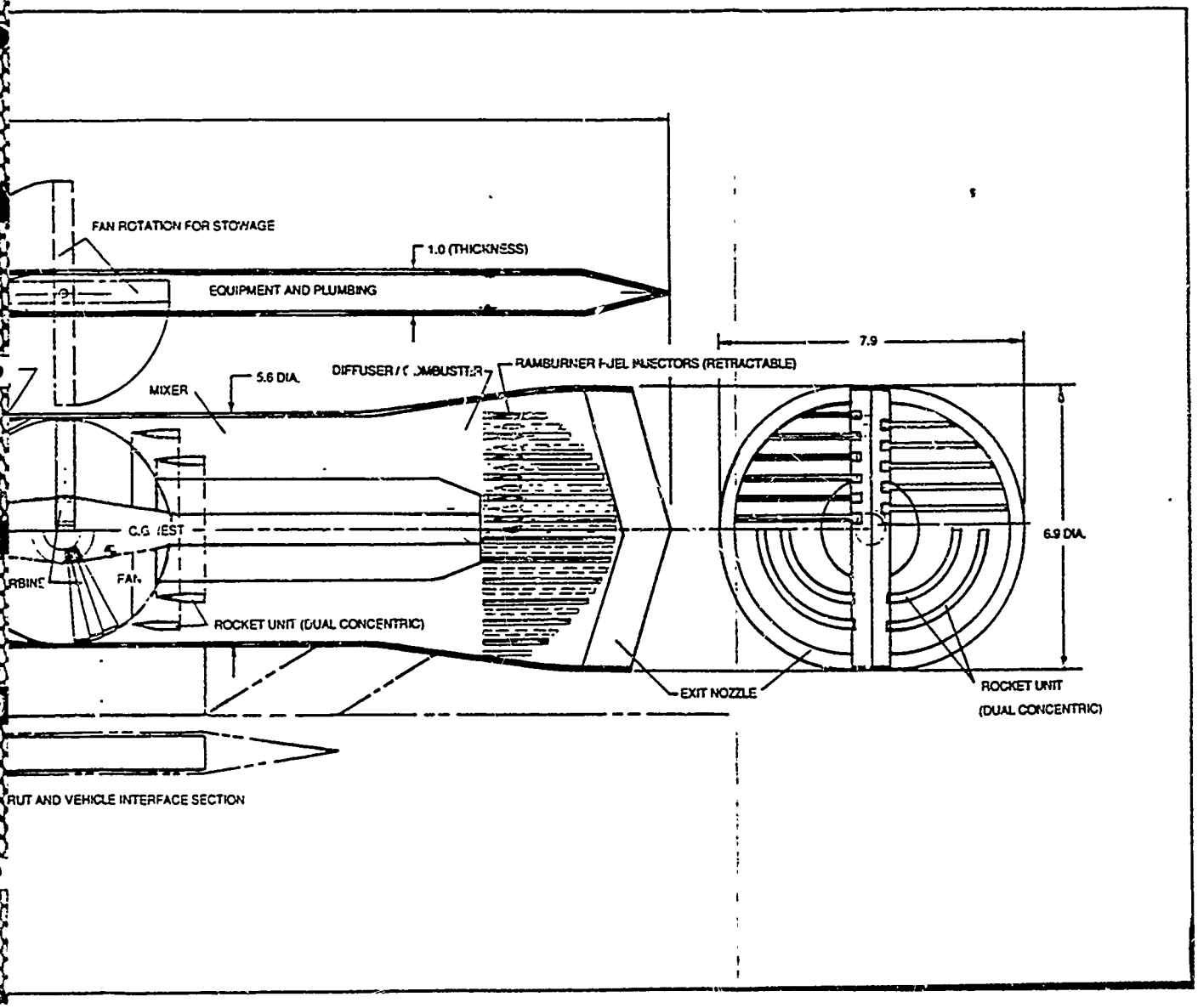


Fig. 69 Conceptual Subsystems Arrangement for Engine #12 - Supercharged Scramjet


FAN ROTATION FOR STOWAGE
1.0 (THICKNESS)
EQUIPMENT AND PLUMBING
7.9
MIXER
5.6 DIA.
DIFFUSER / COMBUSTOR
RAMBURNER FUEL INJECTORS (RETRACTABLE)
C.G. TEST
6.9 DIA.
FAN
ROCKET UNIT (DUAL CONCENTRIC)
EXIT NOZZLE
ROCKET UNIT
(DUAL CONCENTRIC)
RUT AND VEHICLE INTERFACE SECTION

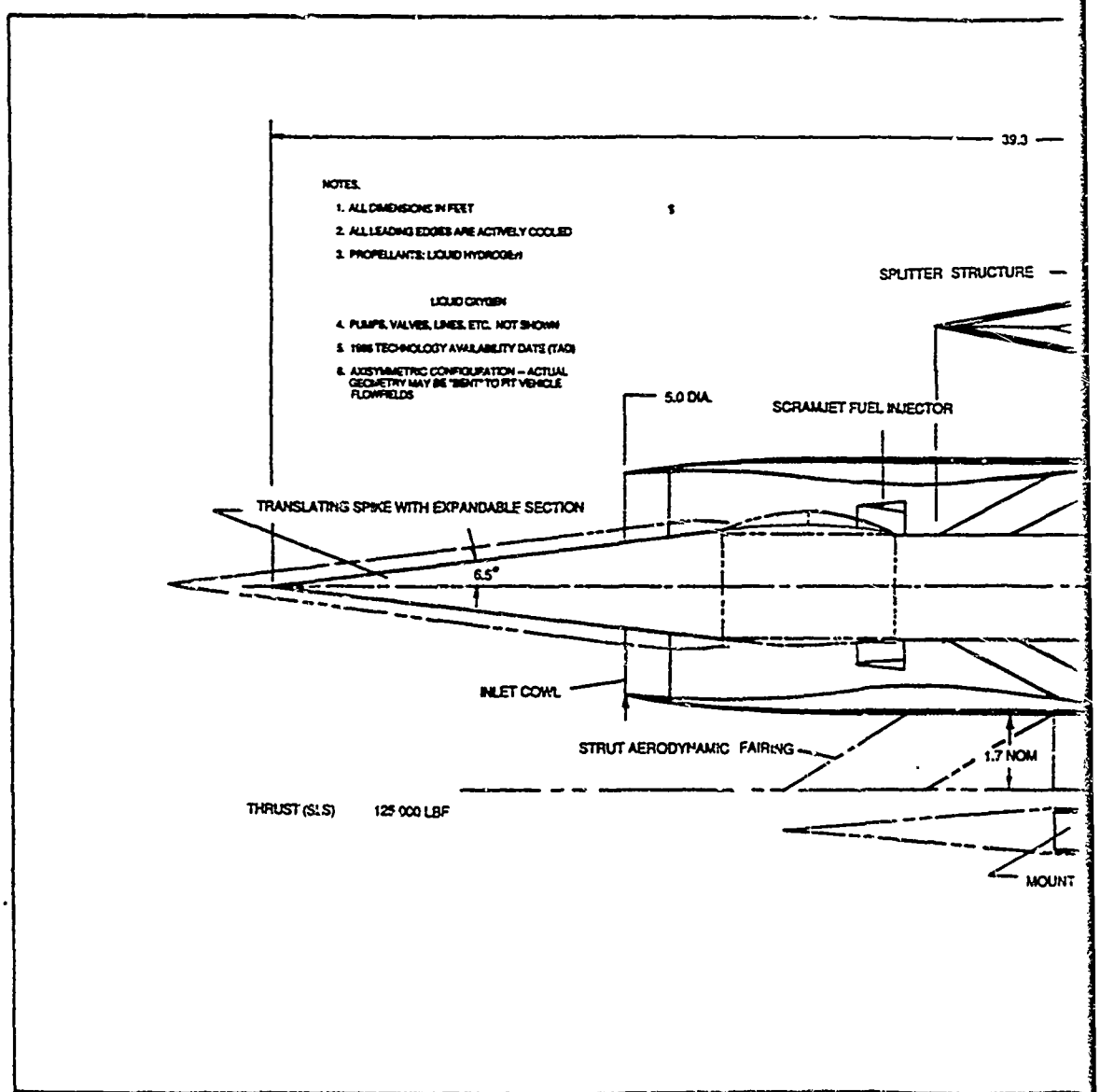
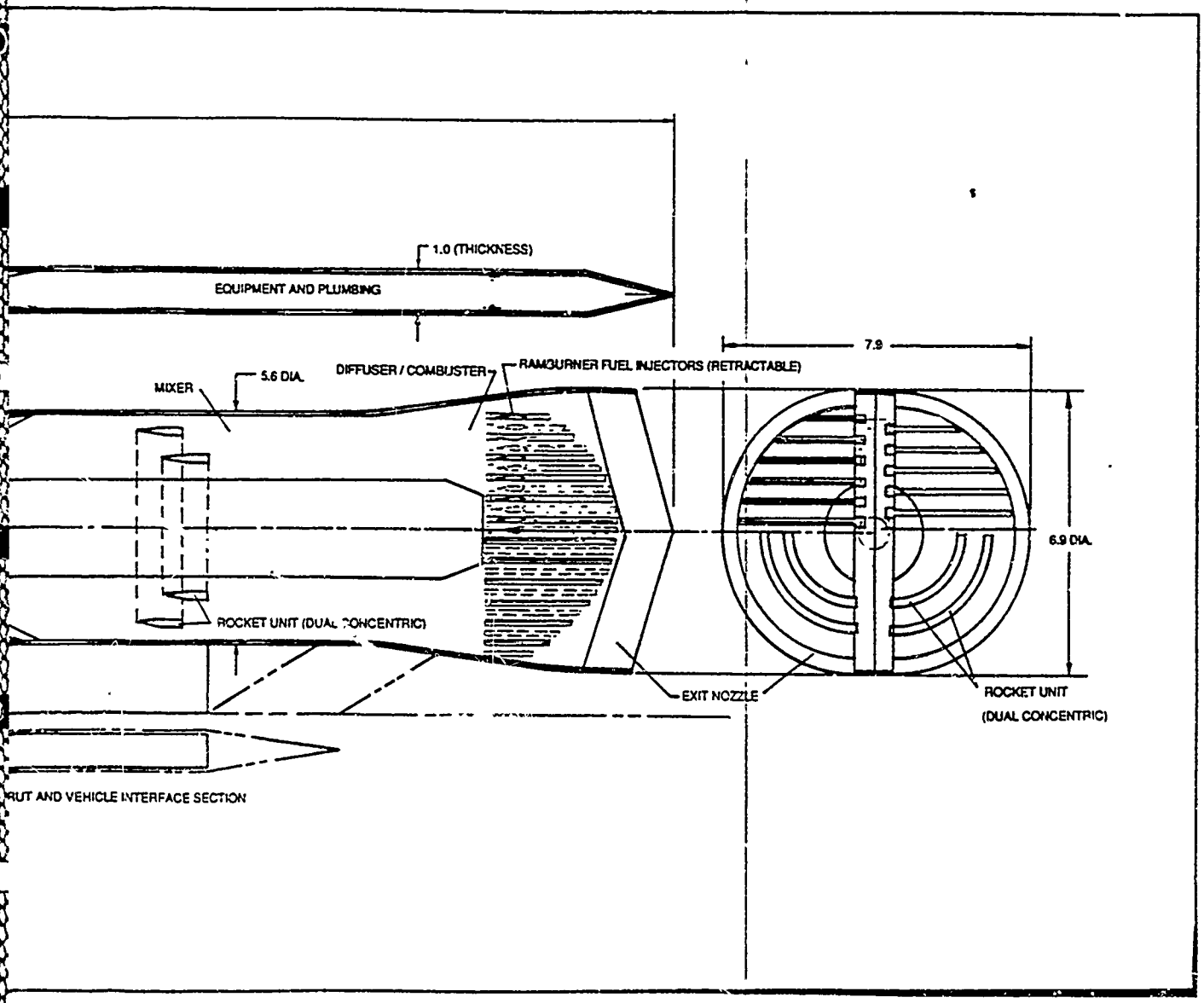


Fig. 70 Conceptual Subsystems Arrangement for Engine #10 - Ejector Scram


1.0 (THICKNESS)
EQUIPMENT AND PLUMBING
7.9
MIXER
5.6 DIA.
DIFFUSER / COMBUSTER
RAMBURNER FUEL INJECTORS (RETRACTABLE)
6.9 DIA.
ROCKET UNIT (DUAL CONCENTRIC)
EXIT NOZZLE
ROCKET UNIT
(DUAL CONCENTRIC)
RUT AND VEHICLE INTERFACE SECTION

Section 4.0

ENGINE/VEHICLE INTEGRATION

This section discusses the approaches available to integrate RBCC engines into vehicle structural designs.

4.1 Engine Envelopes

Fig. 71 presents a comparison of the engine envelopes for both fan equipped and non-fan equipped RBCC engines for the baseline 250 Klb sea level static (SLS) baseline configuration, the 125 Klb SLS thrust and the 65 Klb SLS thrust rated engines.

The configuration illustrated incorporates an axisymmetric spike inlet. The overall lengths presented are from the spike tip to the engine exhaust plane. The two significant diameters given are for the mixer section and exit nozzle of essentially circular configured engines. In the case of annular engines, an equivalence in the circular cross sectional area would be maintained in all thrust readings.

4.2 Engine Weights vs. Thrust Level

The engine weight estimates developed in the baseline NAS7-377 study were for 250 Klb SLS thrust rated engines. These weights were modified, as has been discussed in the previous section, to incorporate both the basic design changes developed in this study and the improvements in technology anticipated to be available by 1995 that could be applied to reducing the RBCC engine system weights. It was necessary to scale these weights from the baseline value of 250 Klb to the 125 Klb and 65 Klb thrust rating engines.

This was done by taking the thrust vs. weight engine characteristics as a function of engine thrust level that were developed in the baseline study and updating them to the 1995 TAD weight estimates The resulting T/W plots are presented in Fig. 72 for all five RBCC engine types.

4.3 Engine Attachment Points

Two engine attachment points are proposed. The principal thrust pickup attachment point will be located at the rocket ejector subsystem station. The second attachment point, and thrust pickup point, will be located at the beginning of the expansion section of the engine.

4.4 Engine/Vehicle Integration Considerations

In integrating RBCC engine systems into a vehicle structure, a first consideration is the vehicle forebody conical shock geometry as a function of flight speed. Ideally the inlet outside diameter at the maximum diameter station vehicle should lie just inside the conical shock at the maximum airbreathing flight speed; that is, at the selected scramjet/rocket mode transition point.

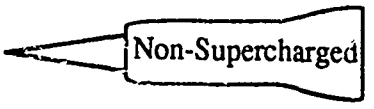
In Fig. 73, zero angle-of-attack conical shock positions are shown as a function of flight Mach number for an eight degree half angle slender cone. For a true conical (axisymmetric) vehicle at hypersonic flight speeds, the thin shock layer within which the inlet cowl surface has to be fitted is obvious from this figure.

65 klb (SLS)

L = 25.7 ft

D_{mix} = 4.02 ft

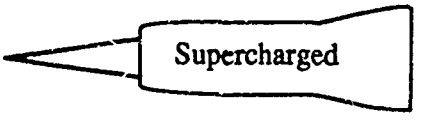
D_{max} = 5.10 ft



L = 29.2 ft

D_{mix} = 4.02 ft

D_{max} = 5.10 ft

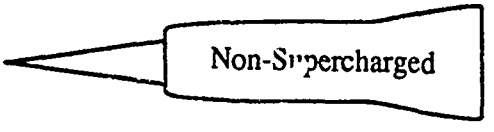


125 klb (SLS)

L = 34.2 ft

D_{mix} = 5.42 ft

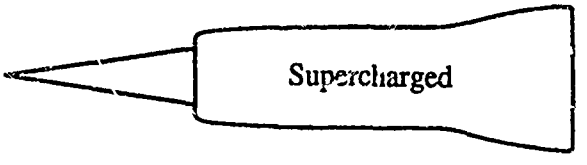
D_{max} = 6.48 ft



L = 40.5 ft

D_{mix} = 5.42 ft

D_{max} = 6.48 ft

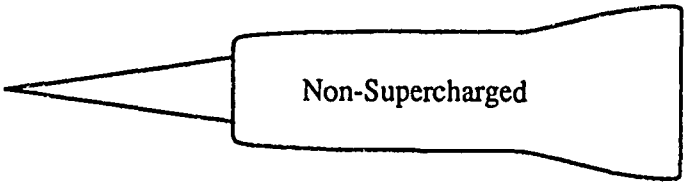


250 klb (SLS)

L = 48.4 ft

D_{mix} = 7.67 ft

D_{max} = 9.17 ft



L = 57.25 ft

D_{mix} = 7.67 ft

D_{max} = 9.17 ft

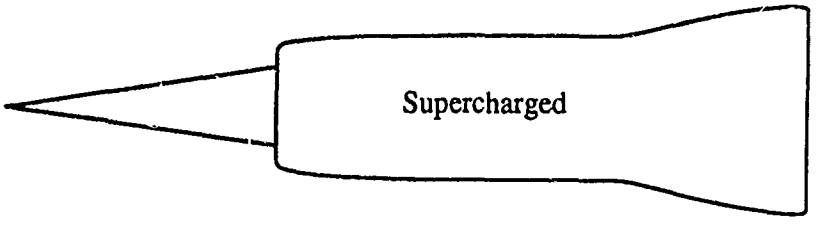


Fig. 71 Size/Thrust Relationships for Non-Supercharged and Supercharged RBCC Engines for Various Sea Level Static Thrust Rated Engines

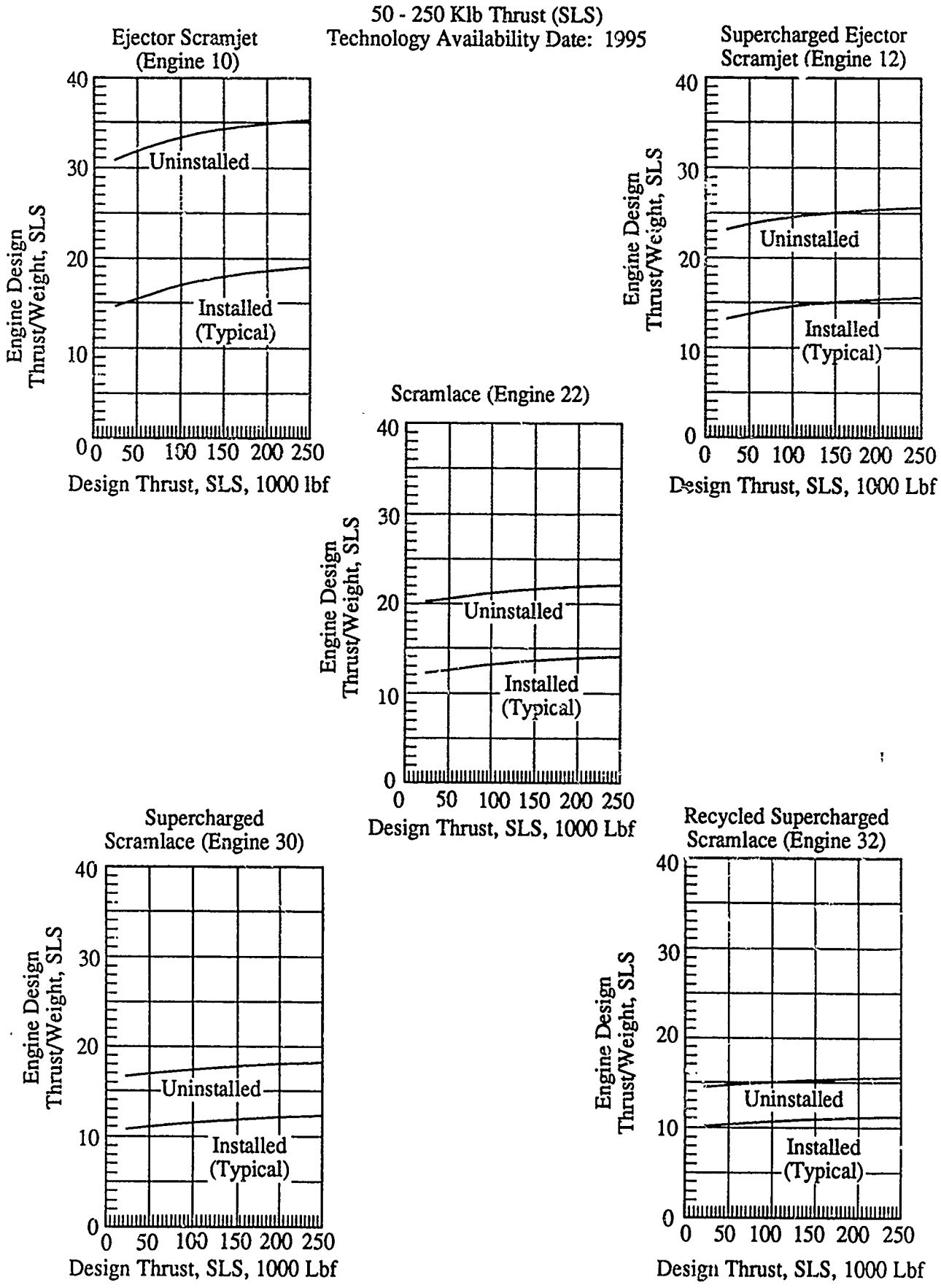


Fig. 72 1995 Technology Availability Date (TAD) Thrust to Weight Ratios

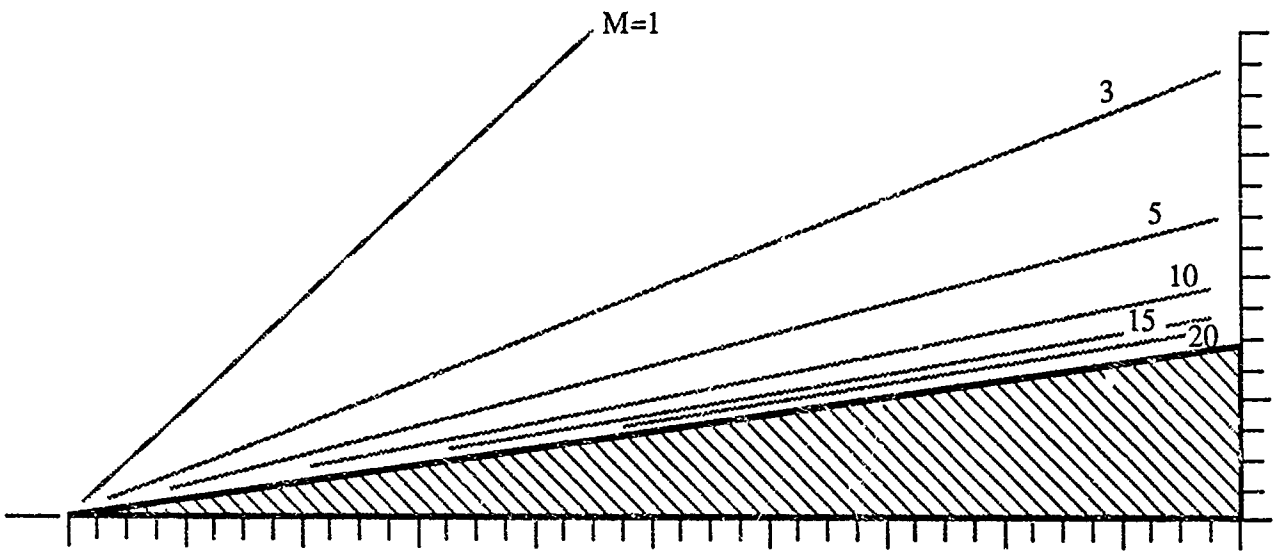


Fig. 73 Conical Shock Positions

There are two extremes in the vehicle/propulsion system integration approach. These are illustrated in Figure 74. The first approach is the "discrete" approach where individual engines are modularly mounted at the maximum diameter station of the axisymmetric vehicle structure. The second approach is the "annular" approach. The effects of decreasing individual engine thrust rating and increasing the number of engines for a given vehicle is illustrated in Figure 75. It can be seen that the discrete engine approach carried out with a small number of engines makes the possibility of achieving high thrust/capture in the inlet section difficult, if not impractical, to achieve. As the number of engines increase, and the individual engine thrust rating decreases with slowly increasing engine weight, an annular configuration can be approached even with discrete circular cross section engines as illustrated in the twelve engine case.

The advantages of the annular approach include the fact that, at shock-on-lip design condition, the full vehicle stream-tube (equal to the frontal area) is being captured with the exception of that percentage spillage loss and other losses encountered in real systems. A true annular engine, i.e., one composed of engines of arched rectangular cross section, can be used to implement an annular enginesystem. It has already been noted that this configuration can be created by using side-by-side circular cross section engines. Both square and circular cross section engine modules could be used in an annular configuration. The use of circular cross section engines is required for the use of fan supercharging. A further disadvantage of rectangular cross section engines is the increased weight when compared to circular cross section engines. A contribution to hoop strength should be provided by a full circular annular inlet

structure where that hoop strength would be developed over the engine outside diameter. Analysis of the weight impact of the use of rectangular cross section engines versus circular cross section engines remains a subject for future study in the axisymmetric configuration proposed here.

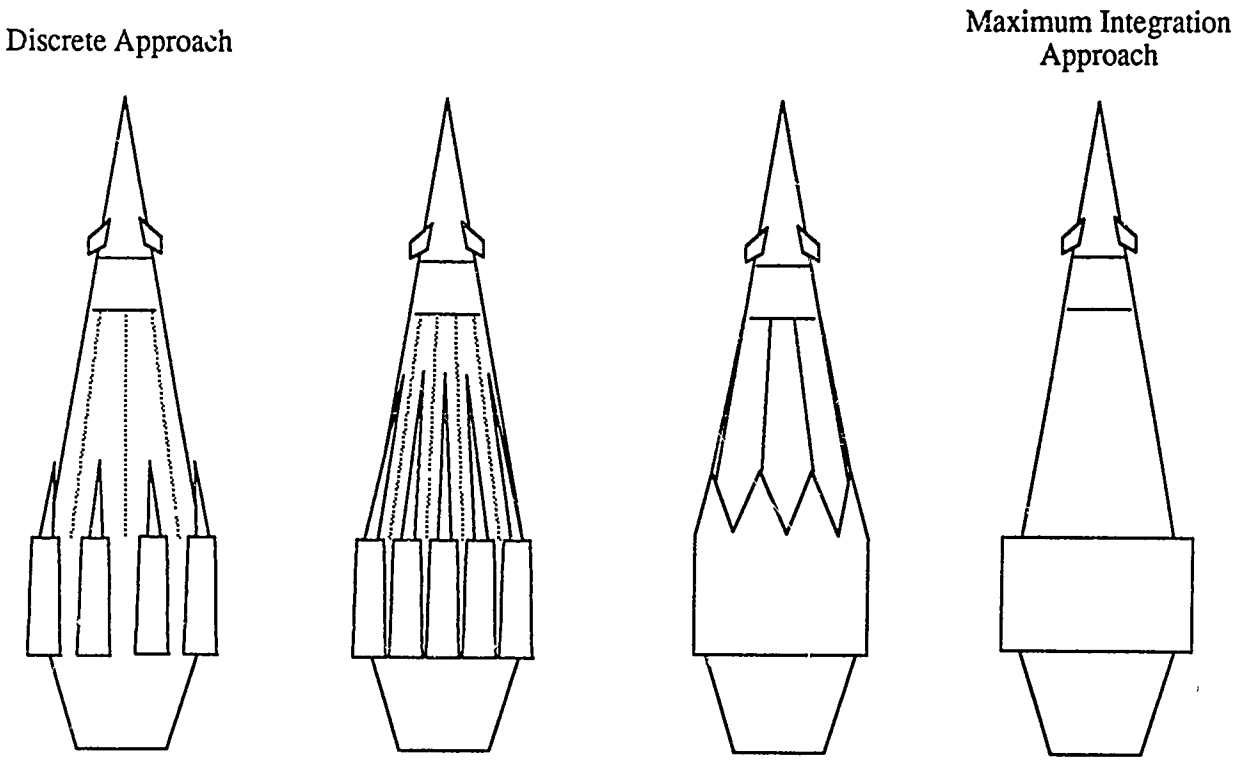
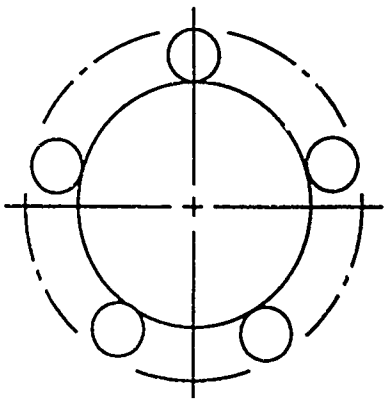


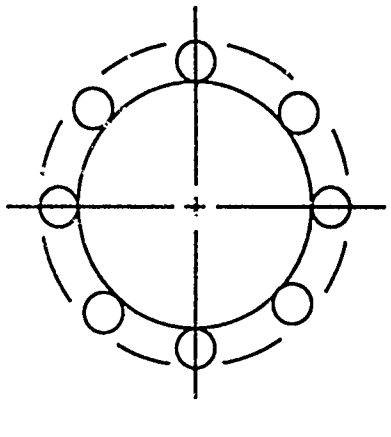
Fig. 74 Vehicle/Propulsion System Integration Approach

Engine Number and Size Impact on Vehicle Size
Engine 32 - 956 klbm TOGW/GLOW



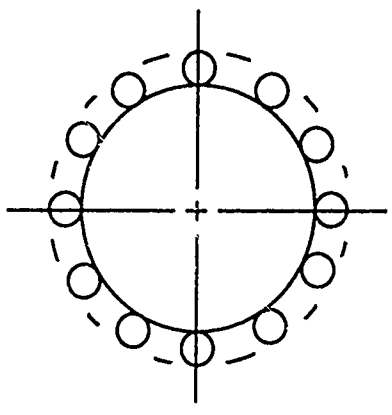
Fuselage O.D. - 32.3 ft
Engine O.D. - 7.7 ft
Vehicle O.D. - 47.7 ft
Vehicle Length - 270 ft
Eng. Wt. Installed - 145 205 lbm

5 Engines



Fuselage O.D. - 32.3 ft
Engine O.D. - 6.1 ft
Vehicle O.D. - 44.5 ft
Vehicle Length - 270 ft
Eng. Wt. Installed - 149 430 lbm

8 Engines



Fuselage O.D. - 32.3 ft
Engine O.D. - 5.0 ft
Vehicle O.D. - 42.5 ft
Vehicle Length - 270 ft
Eng. Wt. Installed - 154 129 lbm

12 Engines

Fig. 75 Effect of Decreasing Engine Thrust Rating and Increasing Number of Engines

Section 5.0

THE VEHICLE SYSTEM

5.1 Approach to Discussion of the Vehicle System

The first part of this section discusses the logic behind the basic vehicle design approach. The approach to the design of the thermal protection system, which is integral with the basic vehicle structural system and forms a major portion of the total vehicle structure, is then considered. A brief review of the subsystems comprising the total vehicle system is presented. The use of a "Spaceborne Expert Systems", or SES, to support autonomous operation of vehicle and ground support systems, and the crew module and its life support system, is presented.

A discussion of the methodology used to develop the vehicle weight estimates is presented along with a brief overview of the weight estimates that were developed to support performance analysis work to be described in Section 6.0. A preliminary design concept drawing of the baseline 500 klbm TOGW vehicle system will be presented.

5.2 Design Approach

5.2.1 Vehicle Requirements

The vehicle is required to deliver a two-man crew, in a crew compartment with escape capability, and 10,000 lbm payload to a 100 nmi polar orbit. The vehicle is a single stage configuration using liquid hydrogen and liquid oxygen propellants. It is to be a fully reusable vehicle capable of autonomous operation to the maximum extent practical. The study considered both horizontal and vertical takeoff and horizontal and vertical landing. The vehicle system level requirements were previously discussed in Section 1.0.

5.2.2 Winged Axisymmetric Configuration

The vehicle flies a lifting, accelerating trajectory. It is not designed for extended hypersonic cruise. The basic configuration studied uses highly swept delta wing sections or "strakes". The vehicle fuselage studied is a circularly axisymmetric structure consisting of a nominal eight degree half angle conical forebody and a 16 degree half angle conical aftbody truncated at approximately the 40 percent station of the aftbody.

This approach was selected in order to:

1. Provide maximum feasible airflow capture area.
2. Provide a minimum drag configuration.
3. Provide the maximum feasible exhaust nozzle area ratio for scramjet and high altitude rocket engine operation.
4. Provide an intrinsically balanced thrust vector.
5. Provide the lightest weight pressure vessel design.
6. Provide the simplest fabrication approach through the use of circular cross sections which eliminate the upper left, upper right, lower left and lower right unique part shapes characteristics of non-axisymmetric, or aircraftlike, designs.
7. Permit multiple use of basic parts.
8. Reduce the scale and a number of tooling item requirements.
9. Provide the capability to use differential throttling for attitude control by taking advantage of the high speed of response of rocket engines to propellant flow variations and the high

speed of response of ramjets and scramjets to fuel and air flow variations within the limitations of the inlet control system.

The disadvantages of this configuration are reduced lift and lift/drag ratio in comparison to more aerodynamically efficient, non-axisymmetric, lifting body and wing body shapes.

5.2.3 Aerosurface Sizing

Horizontal takeoff aircraft typically have their lifting surfaces sized by the runway liftoff conditions selected, determined by the capabilities of the wheels, tires and braking systems in this case.. Rotation and liftoff speed and angle-of-attack limitations are primary considerations in wing area sizing. The lifting surface sizes for HTO configurations used in this study were based upon a 350 mile per hour ground speed and a 15 degree angle-of-attack at liftoff. This ground speed is approximately 100 miles per hour beyond the present state-of-the-art in aircraft wheels, tires and brakes. Development of 350 mile per hour takeoff capability is presently an objective considered in the NASP technology maturation program.

Vertical takeoff vehicles, on the other hand, do not depend on initial aerodynamic lift. Lifting surface sizes are then established primarily on the basis of either posts takeoff angle-of-attack limitations or other specific mission requirements unless other conditions predominate, as will be discussed.

In this study, angle-of-attack considerations are more significant in that not only are the lifting surfaces involved, but also the maintenance of uniform airflow to the engine inlets in the axisymmetric configuration. As wing area is increased, the angle-of-attack at any particular point in this trajectory is reduced. As has been discussed previously the ability of the axisymmetric configuration to operate effectively with varying angles-of-attack is a problem that requires further study. At this point, our study indicates that the minimum acceptable strake size, not considering the effect of angle-of-attack on inlet flow, will be somewhere between 25 percent and 50 percent of body diameter. In the 500 klbm TOGW baseline vehicle system studied, the 50% strake configuration operated with a maximum angle-of-attack of eight degrees at the Mach 15 scramjet to rocket transition point beyond which angle-of-attack ceases to be of any significance to the propulsion system since the inlet subsystem is no longer functioning.

5.2.4 Takeoff and Landing Attitude

Using a vertical takeoff attitude provides several advantages:

- No runway is required for launch
- Vehicle gross weight is not constrained by the runway surface loading limitations
- There is no intersection of the vehicle produced shock cone with the ground during the early stages of ascent.
- Lighter takeoff gear might be used, but the extent of this difference compared to the HTO landing gear systems requires additional study to be quantified since there are several interacting factors that may tend to minimize this advantage.

With vertical landing, the basic advantage of eliminating the runway requirement is retained.

From the standpoint of landing gear weight, horizontal takeoff and landing (HTOHL) implies a gear weight of approximately 3% of GLOW dictated by gross takeoff weight that must be borne by the gear. In the VTOHL design, where the takeoff weight is borne by a ground launch structure, and there is no takeoff gear, the landing gear is sized by the empty weight, the VTOHL landing gear elements are estimated to weigh about 1% of GLOW.

With regard to engine subsystem weight in an SSTO mission, the engine thrust rating and engine weight is determined primarily by the thrust requirements in the intermediate and high Mach number ranges, not takeoff thrust requirements. Hence, VTOHL and HTOHL engine weights should be comparable. More detailed investigation of this subject is recommended.

With regard to tankage and structural weights, not including tahe landing gear weight, the HTOHL and VTOHL vehicles should again be comparable if the dominating loads are flight accelerations and flight aerodynamic and aeroheating loads.

To summarize, in conventional situations wing sizing is set by takeoff speed requirements in HTOHL operations and lower wing areas are required to support that same operation in a VTOHL vehicle. In the vehicle design being considered here, the unique requirement for maintaining a uniform inlet air flow about the full circumference of the vehicle dictates that wing sizing will be selected on the basis of angle-of-attack limitations, not takeoff maneuver requirements. The vertical takeoff vehicle will be comparable to the horizontal takeoff vehicle in flyback maneuvers, and cruise flight because their comparable wing areas will produce comparable L/D ratios. The VTOHL vehicle will be lighter by the difference between the HTOHL takeoff/landing gear weight and the VTOHL landing gear weight. In a VTOVL vehicle, the vertical landing maneuver is a very fuel consuming maneuver. The VL maneuver might also require structural design provisions that will result in a higher inert weight then in the VTOHL case. This disadvantage of higher propellant consumption must be weighed against the increased utility, or benefit, the user of such systems might derive from having an orbital transportation system capable of operating without runways.

5.3 Thermal Protection System (TPS), Structure and Materials

5.3.1 TPS Requirements

The most stringent aeroheating conditions that the thermal protection system is expected to encounter will occur at approximately 190,000 feet at Mach 25 during the ascent portion of the flight. Fig. 76 presents a plot of radiation equilibrium temperature on a twelve inch radius nose and a three inch radius leading edge surface at various angles-of-attack, altitude and Mach number. Increasing sweep back angle reduces the leading edge equilibrium temperature. The nose and leading edge conditions constitute the most stringent TPS material challenges within the overall TPS system.

Radiation equilibrium conditions assume that heat transfer into a surface is balanced by radiation of that same surface back into space. For thin metallic surfaces insulated internally, the assumption of radiation equilibrium conditions provides a means of comparing alternative trajectories in terms of aeroheating rather than the much more complex and design specific analysis of other approaches. For the reentry maneuver, angle-of-attack can be traded against dynamic pressure. High angle-of-attack reentries require less aggressive, lower dynamic pressure reentry paths. Fig. 77 presents the envelope of reentry that bounds all the vehicle conceptual designs studied.

The peak aerodynamic heating and radiation equilibrium temperatures for the conceptual designs studied here are shown in Table 7 for the ascent and reentry flight phases. For ascent, the peak heating occurs, as noted, at M=25, altitude 191,500 feet and a two degree angle-of-attack. For reentry, the peak heating occurs at M=24, altitude 240,000 feet and a forty degree angle-of-attack.

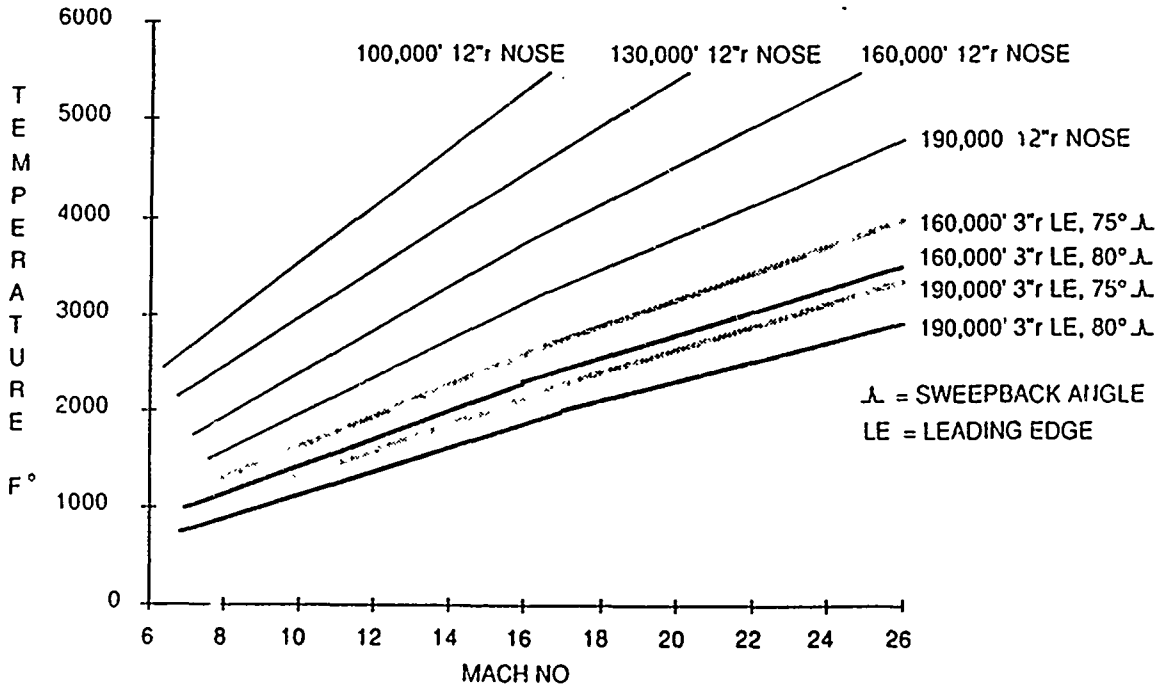


Fig. 76 Radiation Equilibrium Temperatures on Vehicle Nose and Leading Edges

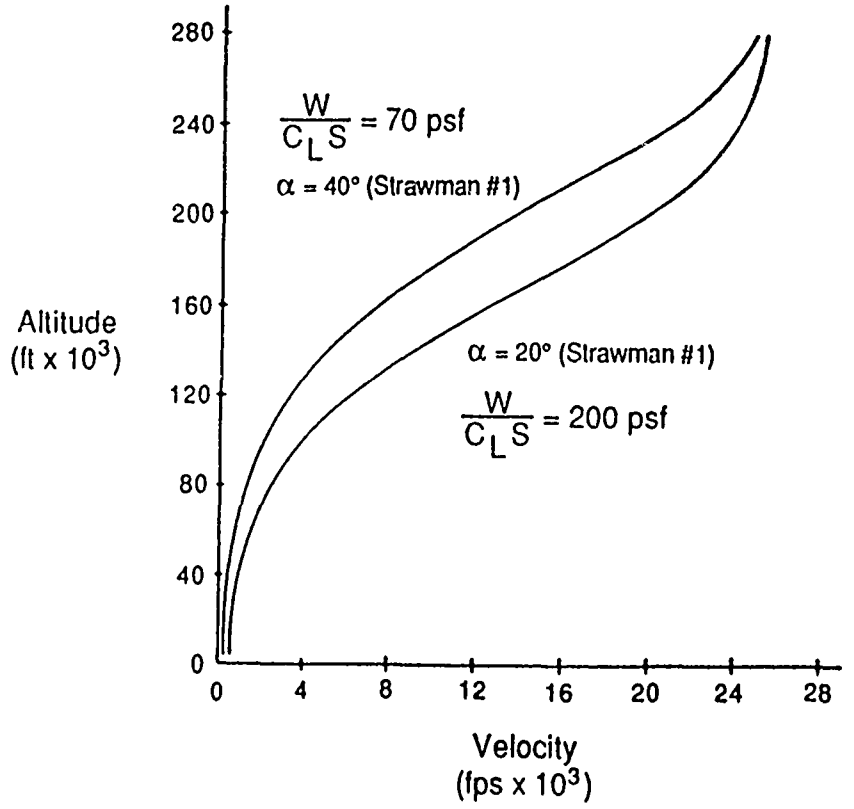


Fig. 77 Reentry Trajectories Envelope

Table 7 Aerodynamic Peak Heat Rates and Temperatures

	Ascent M=25 A=191,500 ft 2° Angle of Attack		Entry M=24 A=240,000 ft 40° Angle of Attack	
	q $\frac{BTU}{Ft^2 - sec}$	T °F	q $\frac{BTU}{Ft^2 - sec}$	T °F
Stagnation Point	263.60	4593	82.60	3320
2 ft aft	22.08	2258	14.55	1989
20 ft aft	6.18	1517	4.07	1322
100ft aft	27.34	2407	2.91	1177
Strake Edges	55.86	2968	100.19	3507

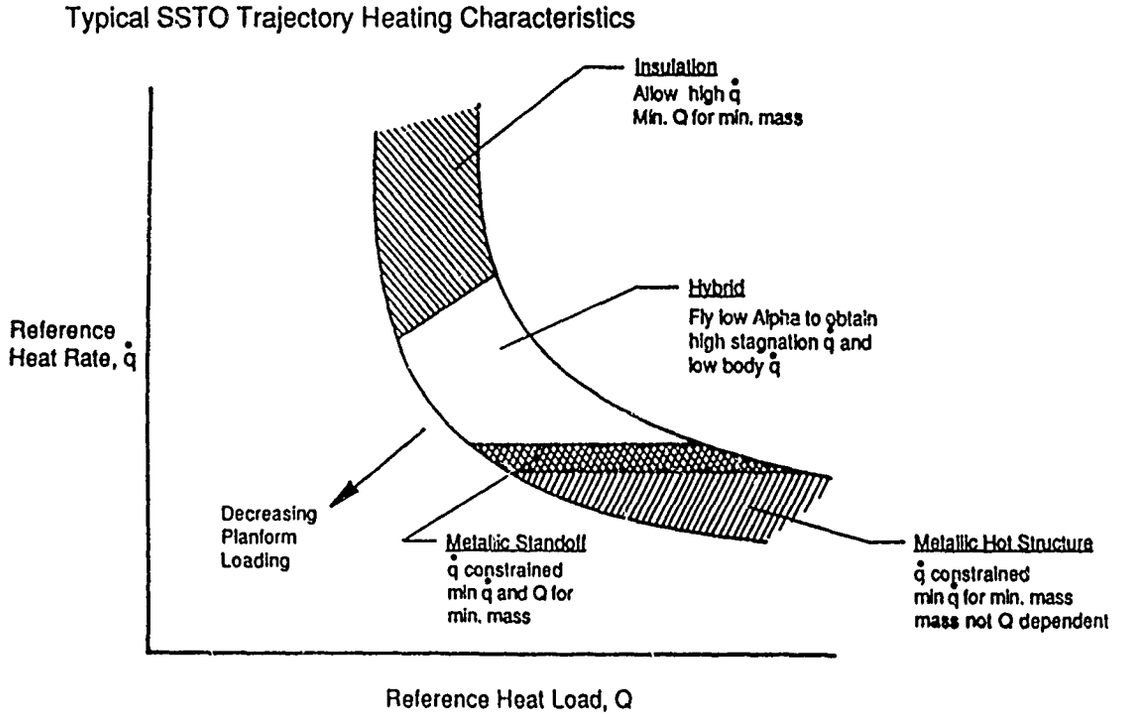


Fig. 78 Thermal Protection System Design Characteristics

Except for the leading edge of the most windward strake, the reentry heating is less severe than the ascent heating. Reentry at a lower angle-of-attack would result in achieving lower altitudes while at high velocities creating a more severe aeroheating problem.

The thermal protection system requirements are defined by both the maximum heat flux rate (Btu/in^2-sec) and the total integrated heat load that can be absorbed by the vehicle structure and propellant mass where propellant mass is used in an active TPS approach. A design maximized for heat flux is usually not optimized for heat load. The ascent and reentry trajectories can be tailored to shift the heat flux and heat loading at any point on the vehicle. Fig. 78 presents the TPS concepts favored in different regions of the heat rate-heat load envelope.

TPS Design Guidelines

The TPS design guidelines developed by MMAG for the RBCC/SSTO configuration vehicles studied were:

- 30% of the vehicle will be exposed to temperatures greater than 1800 F.
- 20% of the vehicle will be exposed to temperatures between 1300 F and 1800 F.
- 30% of the vehicle will be exposed to temperatures between 800 F and 1300 F.
- 20% of the vehicle will be exposed to temperatures less than 800 F.

Weight estimates for the TPS system were based upon a 1.5 lb/ft^2 surface area in areas with temperatures above 1300 F. The backface temperature limit was placed at 350 F except for hot metallic structures. The external emissivity for all surfaces materials was assumed to be 0.8. It was assumed that there would be negligible to no water retention by fiberous insulations and that these insulations could survive runway and ice debris impacts, turnaround handling and all weather conditions. It was desired that the design should be amendable to rapid inspection and recertification for flight use.

The TPS system incorporated estimates of technology capabilities that will be available in the 1990s in terms of design, manufacturing and assembly. The goals appear to be feasible by using currently available titanium alloys and material processing which readily improves thermal properties of the selected base material.

The vehicle was divided into four regions based on the temperatures and heat range that would be encountered in the flight profile, which are consistent with generally accepted data for similar vehicles. Titanium alloy materials are extensively used in the region where the temperature is less than 800 F. Titanium alloy is also used in the region between 800 F and 1300 F by using a titanium which has been ion implanted with a noble metal such as platinum. This results in the ability to avoid the use of heavier thermal protection systems in these two vehicle regions.

The distribution of these four regions on the conceptual vehicle fuselage structure is illustrated in Fig. 79. The wing structure leading edges encounter zone C conditions followed by zone B and zone A conditions progressing toward the trailing edges.

The backface surface temperatures of the TPS system is assumed to be 350 F primarily due to the thermal limitations of internal insulators. Current materials for cryogenic insulators are polyurethane (175 F maximum) and polymethacrylimide (400 F maximum) foams. Polymethacrylimide foam was selected for use as the primary cryogenic insulator to minimize the TPS and structure requirements weights.

ZONE A: T < 800° F (Upper aft fuselage)

ZONE B: 800° F < T < 1800° F (Lower fuselage, Fwd upper fuselage, Empennage)

ZONE C: T > 1800° F (Leading edges, Adiabatic Expansion Surfaces)

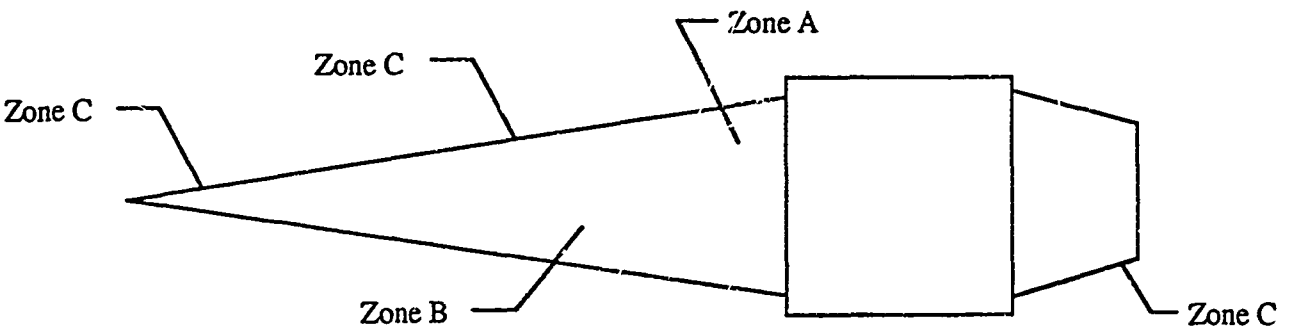


Fig. 79 Distribution of Aerothermal Heating Regions

Since the heat flux which a candidate TPS material can tolerate is directly related to emittance, a high emittance of 0.8 is assumed to provide for higher temperature capability in the TPS. Studies have indicated that under service conditions the emissivity of heat shield materials tends to decrease as the number of missions increase and appears to be related to exposure modified surface effects and physical surface changes.

5.3.2 Design Approach

In vehicle structural systems of the type being considering here, there are two classes of thermal protection systems. These are the "passive" and "active" systems. Of these two technologies, passive systems have reached a higher state of development when compared to active systems. No system has been designed and demonstrated in the mission environment studied here.

The Shuttle Orbiter TPS system design is primarily a design for reentry. The ascent trajectory for the Shuttle system is a non-lifting trajectory which does not encounter the extremes of temperature and dynamic pressure or the durations of high temperature exposure that will be encountered in the RBCC/SSTO vehicle system systems flying an air-breathing powered lifting ascent trajectory.

This study has focused primarily on passive thermal protection systems since these systems are the most developed. These systems offer the highest probability of successful application in the 1995 time frame as required by the DDT&E phase start date specified for this study. Active systems, which are currently being investigated for applications of the type considered here, are discussed briefly.

There are many alternative design approaches to passive thermal protection systems that are applicable to high velocity vehicles. There are three general categories into which passive TPS systems can be placed. A fourth category of passive TPS systems is hybrid TPS systems which are a combination of external insulation with the two remaining types of TPS systems. The key considerations for TPS design are the external surface temperatures associated with the peak heat rate and the total heat load transmitted to the vehicle structure and propellant mass. These four systems are discussed below.

EXTERNAL INSULATION SYSTEMS consist of both low and high temperature reusable surface insulation (LRSI, HRSI). This type of system is being used on the Shuttle. It is a system which incorporates insulating tiles on the external vehicle surfaces, is generally non-load carrying, and has high temperature capabilities (LRSI - 1400 F; HRSI - 2400 F) and acts as a heat sink.

METALLIC STANDOFF SYSTEMS consist of systems which incorporate a radiative metallic outer surface insulated from, and attached to, the main structure of the vehicle. This type of system operates by radiating some of the heat away and absorbing the remainder into the heat sink provided by the insulation.

HOT METALLIC STRUCTURE SYSTEMS are systems which directly expose the load carrying structure to the heat source and may incorporate a load carrying metallic heat shield. Hot metallic structures generally do not have TPS, rather, the structure itself is designed to radiate most of the heat encountered to the atmosphere.

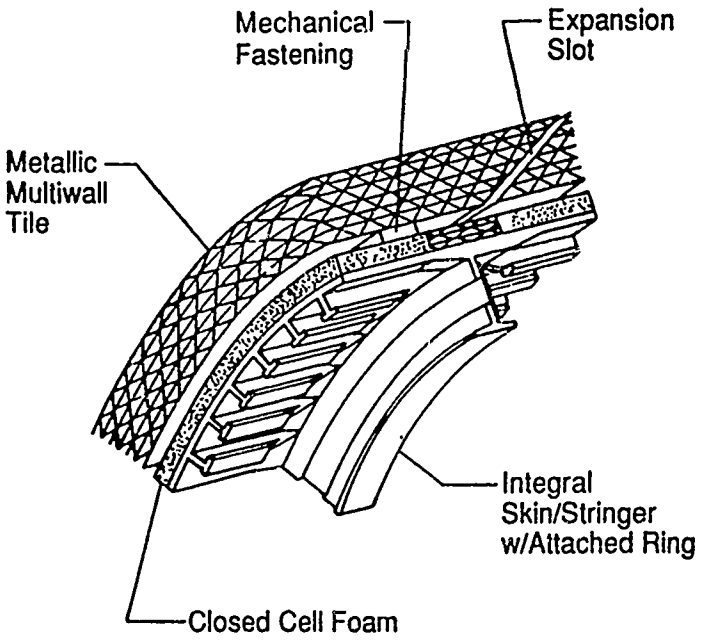
HYBRID SYSTEMS are systems which employ high temperature external insulation in the stagnation regions of the vehicle and a metallic system over the remainder of the vehicle's lower surface. This type of system is designed to take advantage of the vehicle's heating characteristics for low angle-of-attack entries.

The external insulation concept known as "multiwall TPS" is illustrated in Fig. 80 and is a candidate for use in temperature zones up to 1800 F for extended use. To date, research has focused on flat, all-titanium configurations which are limited to temperatures below 1000 F. Effort has been extended to include curved surfaces and higher temperature concepts. Preliminary estimates indicate that these concepts, which offer the inherent durability of metallic systems, are mass competitive with the RSI system currently used in the Shuttle.

Table 8 presents a comparison of three multiwall TPS design approaches to LRSI and HRSI. As compared to the study estimate of 1.5 lbm/ft^2 for the TPS, the multiwall TPS offers a very good possibility of reducing weight by up to 40% in selective high temperature areas by using the SuperAlloy and hybrid SuperAlloy/Titanium multiwall TPS in place of HRSI or LRSI. One unique feature of the multiwall TPS is the ability to have the design specifically tailored to a given range of temperatures.

Fig. 81 illustrates the metallic standoff TPS concept. The metallic standoff concept is applicable to the moderate and high temperature zones. One of the most weight competitive of all TPS concepts, this concept is attractive where integral tank/fuselage weight reduction requirements are significant. The honeycomb panel cells can be pumped to remove the air to further improve the insulation characteristics of the panel.

The standoff TPS concept uses a heat shield supported by metal supports which penetrate a non-load bearing insulation. The flexible standoffs bend as the shield expands when heated imposing little restraint or thermal stress on the structure.

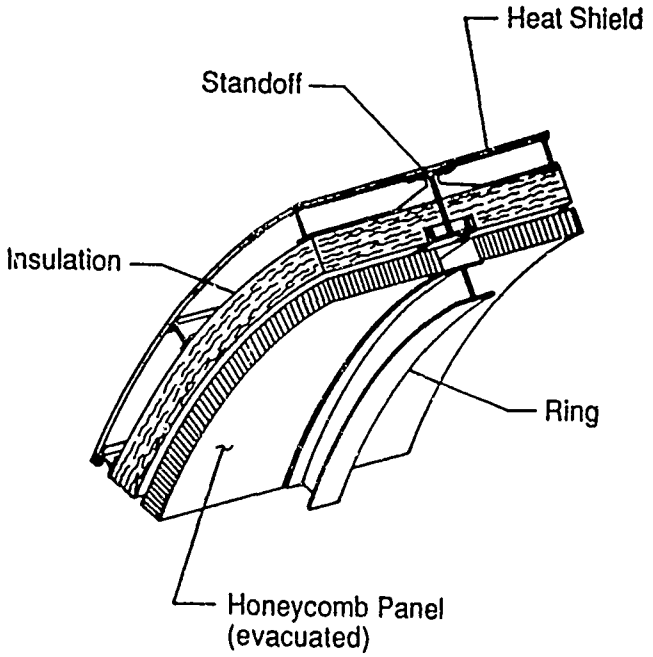


- Heat Exposure Zone: A & B
- To be tested on Shuttle
- Replacable
- More durable than RSI
- Mass efficient with LRSI
- Current Weight = 1.39 lbm/ft^2
- Projected Weight = 0.88 to 1.0 lbm/ft^2

Fig. 80 External Insulation Multiwall TPS

Table 8 Comparison of Multiwall TPS Design Approaches

	WEIGHT lbm/ft^2	MAX. TEMP. °F
HRSI	2.6	2400
Standoff TPS (SuperAlloy)	2.2	2400
Standoff TPS (SuperAlloy) (Evacuated Panels)	1.6	2400



- Heat Exposure Zone: B & C
- Allows extensive use of composite materials
- Applicable to Integral tank/ fuselage concepts
- Current Weight = 2.2 lbm/ft^2 (avg)
- Projected Weight = 1.6 lbm/ft^2

Fig. 81 Metallic Standoff TPS Concept

Table 9 Comparison of Metallic Standoff TPS Design Approaches

MAX. TEMP. °F	WEIGHT lbm/ft^2	
1400	1.05	LRSI
1000	1.39	Titanium M/W (Vented)
1000	0.88	Titanium M/W (Evacuated)
2400	2.6	HRSI
2000	1.5	SuperAlloy M/W

Initial tests of this design concept has indicated that service temperatures up to 2400 F are possible. A second generation has been produced with as much as 34% mass savings over initial designs. Once again, the standoff concept must be compared to the Shuttle RSI TPS. This is done in Table 9.

As compared to the study estimate of 1.5 lbm/ft^2 for the TPS in the design concept studied, the standard TPS concept, even using the evacuated panels, still fall short of meeting our weight goal. Weight goals could be met by using a graphite/polyimide foam insulation as opposed to polymethacrylimide foam and using graphite/epoxy or better graphite/polyimide honeycomb main structure in place of an aluminum or titanium structure.

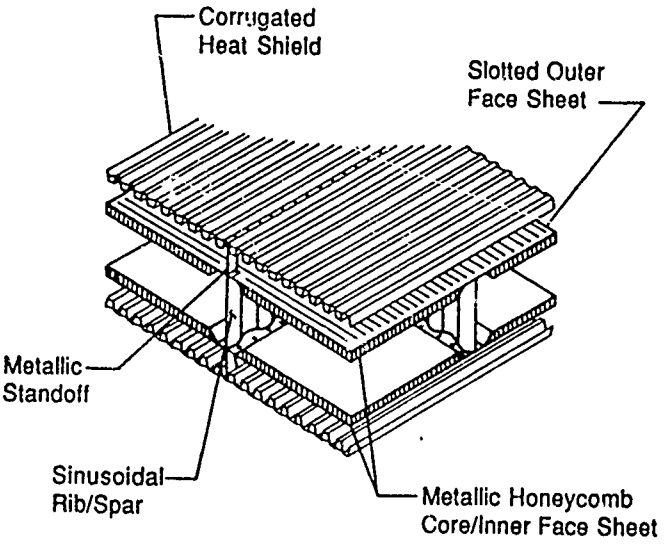
The hot metallic structure concept illustrated in Fig. 82 is a candidate for moderate to high temperature zones on the study vehicle. This concept consists of a non-insulated main structure which is made up of high temperature monolithic and/or SuperAlloy metals along with a SuperAlloy heat shield which radiates most of the heat load. The main structure core is shown as honeycomb panels connected by corrugated sheet ribs and spars. The unique capability of this design is to vary the material type within the zones of the panels. Inner layers and cores can be made from sheet titanium whereas exterior face sheets can be made from SuperAlloys which incorporate slots which control thermal expansion loads when exposed to high surface temperatures. This concept allows the outer facesheet and corrugated heat shield to achieve equilibrium at the very high temperatures. This hot structure concept is not yet as weight competitive as other passive concepts, but is becoming more competitive as the new lightweight, high temperature materials are evolving. Current state-of-the-art concepts weights range from 6.4 to 8 lbm/ft^2 plan area. The projected near-art weight is 4.0 to 5.2 lbm/ft^2. The state-of-the-art concept falls short of the 4.4 lbm/ft^2 weights used for zones B and C in the vehicle weight estimates considered here. The near art concept centers on the study weight for hot structures. This is encouraging but it is only possible due to the ability to bond dissimilar metals by the liquid interface diffusion (LID) or superplastic forming diffusion bonding (SPF/DB) methods.

All the passive methods discussed can be applied to wing structures. It would be helpful to consider wing structures as a basis for introducing a discussion of active cooling systems.

When the ascent or reentry heating energy is partially dissipated by auxiliary cooling, the system is considered to be an actively cooled system. The possible options for active coolant utilization in a given cross section extend from outside the exterior protection layer, using such methods as transpiration cooling, to direct protection of the innermost structural members. This latter method, in conjunction with an effective layer of insulation between the metallic heat shield and the load carrying structure, with integrated coolant channels, has been selected as a baseline concept for discussion. This approach is illustrated in Fig. 83.

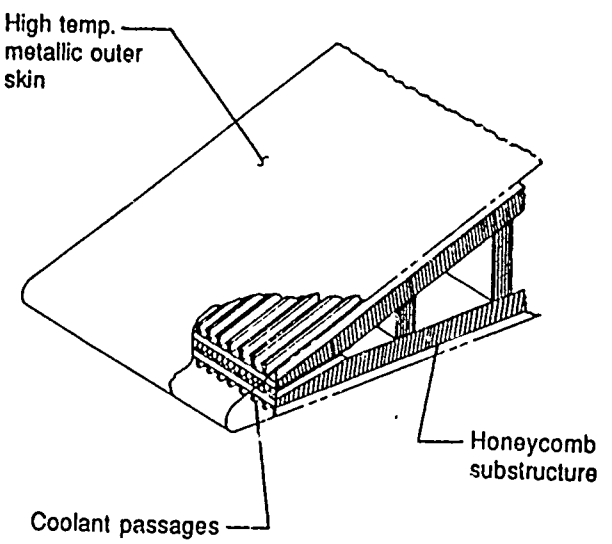
Coolant loops for active cooling designs can be closed, open, or combinations of both with the closed loop implying continuous recycling of the same fluid from the heat source to a heat exchanger. Any combination of loops, when used during an extended heating period, requires a final open loop, in which either an expendable fluid is externally vented overboard or the accumulated heat is dumped into a heat sink or is radiated away by a coolside exterior radiating surfaces.

Typical coolants considered for the heat shield system loops are: water/glycol mixtures, silicone liquids, liquid metals, ram air, various gases, liquid fuel, and commercial refrigerants. In the design concept illustrated, leading edges exposed to stagnation heating from the airflow are impingement cooled. The coolant is injected through a slot in the coolant inlet manifold and impinges on the inside surface of the leading edge which then turns the coolant around to flow around the component surface.



- Heat Exposure Zone: B & C
- Usable on wing, empenage & fin structures
- Requires Superplastic Forming/ Diffusion Bonding (SPF/DF) for High temp. assembly
- Not yet mass competitive with other passive TPS systems
- Slotting relieves thermal stresses in outer face sheet
- Current Weight = 6.4 to 8.0 lbm/ft^2
- Projected Weight = 4.0 to 5.2 lbm/ft^2

Fig. 82 Hot Metallic Structure TPS Concept



- Heat Exposure Zone: C
- Continuous closed loop cooling system can be used for short heating periods
- Closed loop & open loop cooling systems can be combined for extended heating periods
- Coolants: water/glycol, liq. metals, ram air, fuel or commercial refrigerants
- Projected Weight = 2.5 to 3.1 lbm/ft^2

Fig. 83 Actively Cooled Wing/Fin Leading Edge TPS Concept

Present projected weights for panels containing active cooling systems versus the weights of passive systems are illustrated in Fig. 84. This plot illustrates the weights and thicknesses required by the active and passive systems using the parameters of total local heat rate and total heating period or maximum heating rate. The criteria for the protective inner structure was that this region would not exceed 200 F at any time, including the extended post-heating soaking period.

As can be seen, weight penalties for the passive approach are two to three times that of active systems. The weight sensitivity to the length of heating period is considerable for the passive systems. The weights of the active systems are more sensitive to variations in maximum heating rates. Significantly less insulation thickness is required in the active systems.

5.3.3 Materials

Table 10 presents a list of materials that are considered state-of-the-art for vehicle applications. These candidates are divided into four material classes: (1) monolithic metals, (2) SuperAlloy metals, (3) organic composites, and (4) metal matrix composites. The maximum recommended service temperatures for each material are presented.

The Shuttle currently uses a wide variety of these materials successfully. On the most recent flights, parts constructed of Boron/Aluminum have been successfully tested. Use of Boron/Aluminum parts yields a five percent savings in overall weight and has up to a three-fold increase in ultimate tensile strength as compared to 2024-T42 Aluminum.

In the field of superalloys, studies have indicated that lack of creep strength was a possible design constraint for metallic TPS. Further studies have shown that by using an advanced thermomechanical process, the creep strength of Hynes 188 was improved by 50%. This advanced thermomechanical processing involves severely cold-working a sheet of material prior to a high temperature (2100 F) solution anneal.

The rapid progress made in materials research has brought the materials listed in Table 11 very close to availability for practical application, and in some cases, materials on the list are available for current application with limitations on fabrication, economics, and other factors.

These materials are divided into monolithic metals, organic and metal matrix composites. Although SuperAlloys are not listed, work in the area of a new generation of oxide coatings may extend the use of SuperAlloys into high temperature areas that are currently not possible because of oxidation limitations.

Some materials, specifically aluminum/lithium, are being used on a limited basis on civilian commercial aircraft. Aluminum/lithium offers an 11% mass savings because of reduced material density at a strength level consistent with current aluminum materials. Another material is titanium which has been enhanced by ion implantation of platinum. The principal limitation with this material is the lack of sufficiently large facilities to manufacture the material in a cost effective manner and in sheet sizes that will be required to fabricate an RBCC/SSTO vehicle

5.4 Vehicle Systems

5.4.1 Work Breakdown Structure and Unique Systems

Fig. 85 presents a work breakdown structure developed for the RBCC/SSTO vehicle system. The design of the majority of the subsystems comprising the vehicle system are not unique to the RBCC/SSTO concept. These subsystems have been demonstrated in flight

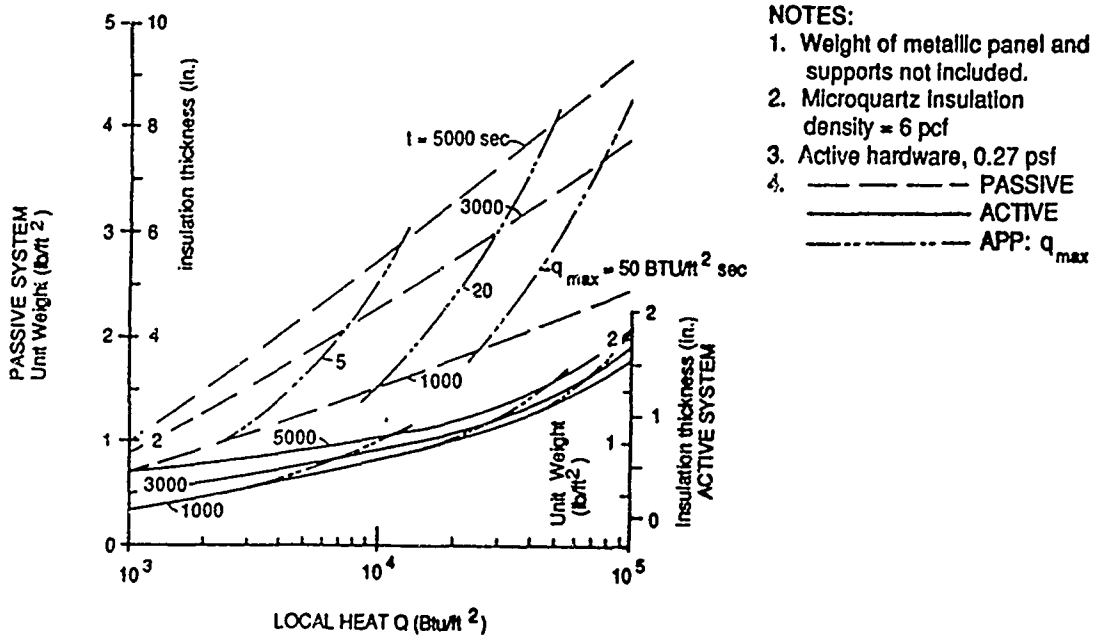


Fig. 84 Active vs. Passive Cooling Weight Tradeoffs

Table 10 State-of-the-Art Materials Candidates

Monolithic Metals	Max. Temp. °F
Aluminum	350
Titanium	750
Super Alloys	
Inconel 618,718, 625	1300,1200,1600
Rene '41	1600
Haynes 188 *	1800
L-605	1800
Haynes 188 (w/lanthanum)	2000
TD NiCr	2200
Columbium (coated)	2400
Organic Composites	
Graphite/Epoxy	300
LRSI (LI-900)	1400
HRSI (LI-2200)	2400
Carbon-Carbon	2600
Metal Matrix Composites	
Boron/Aluminum	550

* Using advanced thermomechanical processing

Table 11 Near Term Material Candidates

Monolithic Metals	Max. Temp. °F
Aluminum Lithium	350
Titanium **	1300
Organic Composites	
Boron/Epoxy	350
Graphite/Bismaleimide	600
Graphite/Polyimide	700
Advanced Carbon-Carbon	2600
FRCI (Fibrous Refractory Comp. Insul.)	3000
Metal Matrix Composites	
Borsic/Aluminum	500
Graphite/Aluminum	500
Silicon Carbide/Aluminum	600
Polycrystalline Alumina/Aluminum	600
Graphite/Magnesium	600
Boron-Carbon/Magnesium	800
Silicon Carbide/Magnesium	800
Silicon Carbide/Titanium **	1600
Borsic/Titanium	1350

** Ion Implanted with Noble metals, eg. Platinum

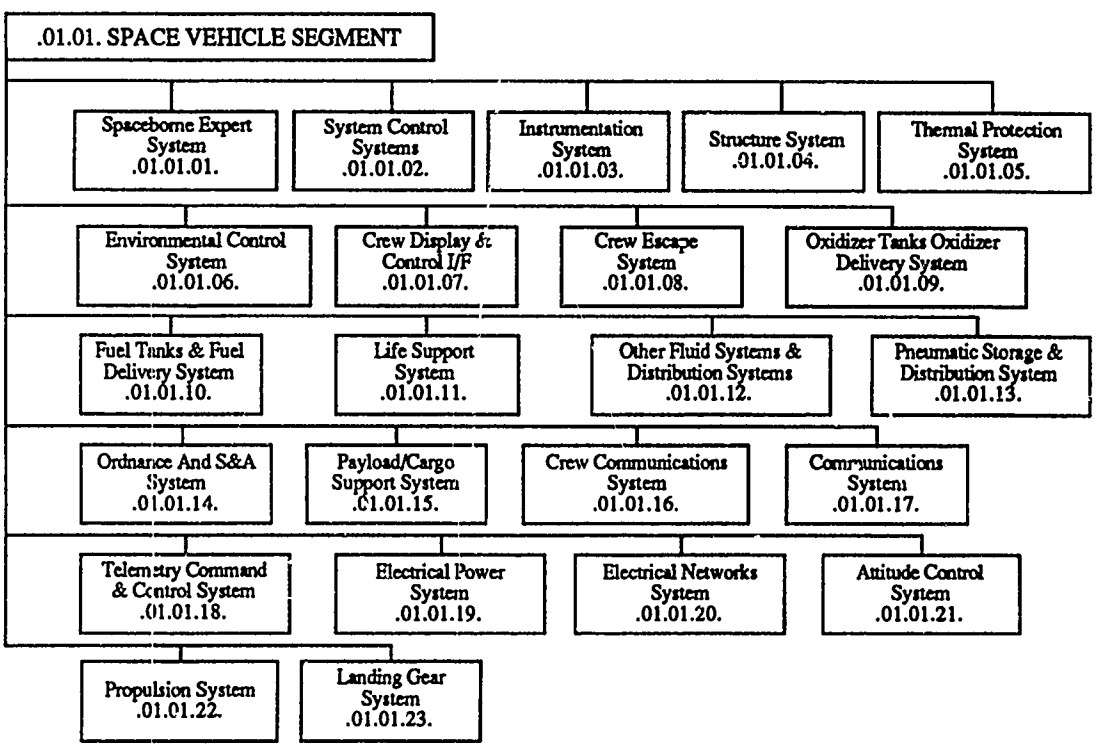


Fig. 85 RBCC/SSTO Vehicle System Work Breakdown Structure

operation in the Shuttle and improvements on these designs are a continuing subject for investigation by NASA, the USAF and the NASP project.

With regard to systems that are unique to the RBCC/SSTO vehicle and the axisymmetric design approach, the Propulsion System and Thermal Protection System have been discussed. In the discussion here, two additional

systems that are unique to the RBCC/SSTO design being studied will be focused on. These two systems are the "Spaceborne Expert System", or SES, and the "Crew Module". The crew module contains:

- Major portion of the SES
- Vehicle control and instrumentation system
- Environmental control system
- Crew display and control interface
- Crew escape system
- Crew communications and ground communications systems
- Telemetry command and control system
- A major portion of the vehicle electrical power system

5.4.2 Autonomous Operation

The extent to which advanced control technologies could be applied to support autonomous operation of a RBCC/SSTO vehicle system was investigated. The objectives sought to be achieved by the use of these control technologies to provide autonomous operation of the vehicle system to the greatest extent practical are:

1. Reduce life cycle costs
2. Prevent catastrophic failure
3. Increase personnel safety
4. Improve system reliability and increase the probability of mission success

Past State of Knowledge

In the 1950's, space vehicles were almost exclusively operated as systems with near zero redundancy in essentially serial sequences of events. Critical component operating time logs were kept on only a very limited number of components found primarily in the guidance, navigation and control systems. Time or accumulated cycles data for less complex components and subsystems were typically not gathered. Trend data tracking systems for component, subassembly or assembly performance trends from receiving inspection to pre-flight test and checkout were not developed or used.

An early use of computer based test and checkout was made in the ATLAS system in ground systems manufactured by Consolidated Systems Corporation. More extensive use was made in the APOLLO system using the Packard Bell PB-250 computer controlled Automatic Checkout Equipment (ACE) system in SA-I pre-static and post-static acceptance testing and the RCA 110A computer and the Advanced Test or Launch Language (ATOLL) developed specifically for APOLLO systems in system test and checkout, acceptance static firing, and flight firing operations.

None of this past work approached the comprehensive scope of work implicit in the concept of the autonomous operations.

Approaches such as Built-In Test Equipment (BITE) and Built-In-Test (BIT) systems were introduced into aircraft systems, for example Lockheed's Versatile Automatic Test Equipment (VATE), in approximately the same time frame.

In the early 1960's, work on more complex launch and space vehicle systems, expanding on the APOLLO lessons learned, was carried out as studies at the Marshall Space Flight Center. For example; under the On-Board Test and Checkout Data Management System (OCDMS) project which involved Boeing Aerospace, the General Electric Company's Apollo Support Department and Planning Research Corporation. This approach considered the problem of design of autonomous systems in such missions as the Mobile Lunar Laboratory System (MOLAB) and the Manned Mars Squadron Mission explored by MSFC in the mid-1960's

Steady progress has been made in aircraft systems during the 1960's and 70's and work in this field continues to produce improvement in both military aircraft and civilian transport aircraft MTBF and MTTR performance.

In space launch systems and space vehicle systems, significant advances in test and checkout and flight control systems design have not been made. The state-of-the-art in such systems is typically represented by such vehicles as Delta, Atlas, and Titan launchers and the Space Shuttle - all designed around the 1970's or earlier technology.

No systems have been developed or used to date to support ground operations, much less flown, that contain the level of technology implicit in the autonomous control of RBCC/SSTO vehicles studied in this project

The Present State of Knowledge

Significant work on the problem of autonomous vehicle systems, or semi-autonomous systems, has only recently begun to be undertaken. Among these efforts is the "ADAPT" technology being developed for Space Station and STAS. Additionally representative of these activities are such recent government procurement actions as the following:

- May 1986 - Kennedy Space Center - Automatic Flight Inspection System
- May 1986 - MSFC - Avionics Concepts for Heavy Lift Cargo Vehicles
- March 1987 - WPAFB - Adaptive Guidance, Navigation and Control for the Ascent Phase of Space Transportation Vehicles (Exploratory Development)
- March 1987 - WPAFB - Multi-Path Redundant Avionics Suite (Exploratory Development)
- July 1987 - WPAFB - Space Transportation Analysis and Decision Support Expert Systems
- October 1987 - LeRC - Future Propulsion Systems Life Management Systems

Another example of current work in this same area of investigation, but with emphasis primarily on the early phases of the vehicle of aircraft life cycle, is the DoD Computer Aided Logistics System (CALS) and its companion program at WPAFB - Unified Life cycle Engineering (ULCE). In these related projects, there are data base acquisition systems in the DDT&E phase that could support the development of autonomous control systems through the manufacturing and operations phases but without provision for such applications. Rather these two projects focus on optimizing engineering and design in the DDT&E phase to provide the best

design possible in terms of producibility and operability with minimum logistics support requirements.

Associated with the CALS/ULCE project is another USAF project designed to standardize the information developed by CAE/CAD/CAM systems that is descriptive of the product undergoing development. This interface approach is known as the Product Definition Data Interface or PDDI. A description of PDDI given by **Design News**, April 1987 is that "PDDI can be thought of as a rigorous way of defining the minimum data that must be passed along to serve any integrated parts manufacturing system".

A common thread that runs through these projects is the emphasis on subsystems in the DDT&E and manufacturing phases or the operations phase, but not both. Consideration of the impact of such systems on the overall vehicle system during its full life cycle are not being studied.

In the working group reports resulting from the workshop held at NASA/LeRC in August of 1987 on the subject of Future Propulsion Systems Life Management Systems, NASA terminology was roughly equivalent to the autonomous operation problem being discussed here, and one theme was repeated frequently. This is that work carried out related to such systems must be carried out with consideration of their operation in the complete launch vehicle or space vehicle life cycle context. Further, the LMS is critically dependent upon the development of a large knowledge base and that that knowledge base development must begin in the DDT&E phase and cover the full life cycle of the system in which it will operate.

Related points were brought out by the Boeing Company in its 1986 "Shuttle Ground Operations Efficiency and Technologies Study". In this study, Boeing made the following comments:

- "Future vehicles, beginning with the design concept phase, must put life cycle costs ahead of performance"
- "Operational requirements must be a part of the early design phase if recurring launch operations costs are to be reduced significantly. Over-all vehicle integration must be emphasized early (emphasis in original) if the life cycle costs are to be controlled"
- "Both manned and unmanned vehicles must use vehicle BIT/BITE for ground checkout and countdown (eliminate most checkout GSE) at the launch site"
- "Large, complex launch control centers must be eliminated. Massive ground/vehicle data and control lines must go away"

Another indicator of the trend in future aerospace systems is found in the developing dissatisfaction with vehicle data bus systems designed to meet that requirements of MIL-STD-1553. Lockheed has recently proposed a bus specification that would provide very significant data rate increases in comparison to 1553 bus systems to support the data requirements of near-future spaceborne and airborne systems, exemplified by the Advanced Technology Fighter (ATF) project, which are generally foreseen as including AI/E systems in a variety of applications.

Artificial Intelligence and SES

The potential role of "artificial intelligence" and the subclass of AI systems - "expert systems" - have been given significant attention in the projects that have been recently started and discussed previously. It must be noted that a significant contribution can be made by already available computational techniques, methods and equipment. One of the significant limitations

of AI systems in the present state-of-the-art is the speed of execution of AI and expert systems programs. While significant improvements have been made in artificial intelligence and expert (AI/E) language systems, and supporting computational hardware, the speed of operation of these systems is not presently adequate in some complex decision making processes that must be executed in milliseconds and this requirement occurs quite frequently in the types of systems this study is concerned with.

The principal advantages claimed by AI/E technology, when compared to conventional approaches, are the ability to:

- Use abstractions, concepts and symbols
- Adapt to an environment and to learn from it
- Use imprecisely specified information
- Accept changes in the information available
- Tolerate erroneous or unexpected information

The reader familiar with modern process control systems programming techniques, and hardware systems, would realize that many of these capabilities can be implemented without the use of algorithms specifically designed as AI/E algorithms.

In the problem context here, all the approaches that are possible, conventional process control computational techniques, artificial intelligence techniques, expert system techniques, etc., operate, in some way or another, by interpreting the conditions in the vehicle system and subsystems through measuring devices, by having an "intelligent" algorithm that works with the knowledge of the vehicle system and subsystem status and which can then take action through controls or "effectors" to change or not change the conditions that exist in the vehicle system and its subsystems. The particular problem is that such systems must run in "real-time". Further, the intelligent algorithm must work with "knowledge" of the vehicle system and its subsystems. Beside the intelligent algorithm, a "knowledge base" descriptive of the details of operation of the vehicle system and its subsystems to a very fine level of detail is required. Such a knowledge base must evolve as the vehicle system design itself evolves and knowledge becomes available concerning the details of operation of all the subsystems comprising the total vehicle system. The problem of developing this knowledge base is referred to as "knowledge engineering" and represents a most difficult portion of the problem of developing autonomous systems that will meet the goals desired for vehicles of the type considered here. The efforts aimed towards developing the knowledge base required must be carried out by methods that are capable of supporting the acquisition and ordering of such expert knowledge "growing" over time with the development of the vehicle system and all supporting systems.

The intelligent algorithms that might be applied using the knowledge base discussed remain only most superficially defined at this time.

The SES is not a single device but rather a combination of activities, hardware of various forms, knowledge in the form of information that is compatible with the hardware elements of the system, all combined progressively over the full life cycle of the vehicle system beginning in the DDT&E phase and ending in the operation phase.

A hierarchial and communications relationship between a generic spaceborne expert system and subsystem expert systems is illustrated in Fig. 86. This is a view of the organization of the system as it would most probably operate in flight.

In any systems test and checkout operation, prelaunch or postlaunch, and in all flight servicing operations prior to launch, the vehicle borne portion of the SES must interface with the ground support equipment systems and maintenance and repair systems. The design that should

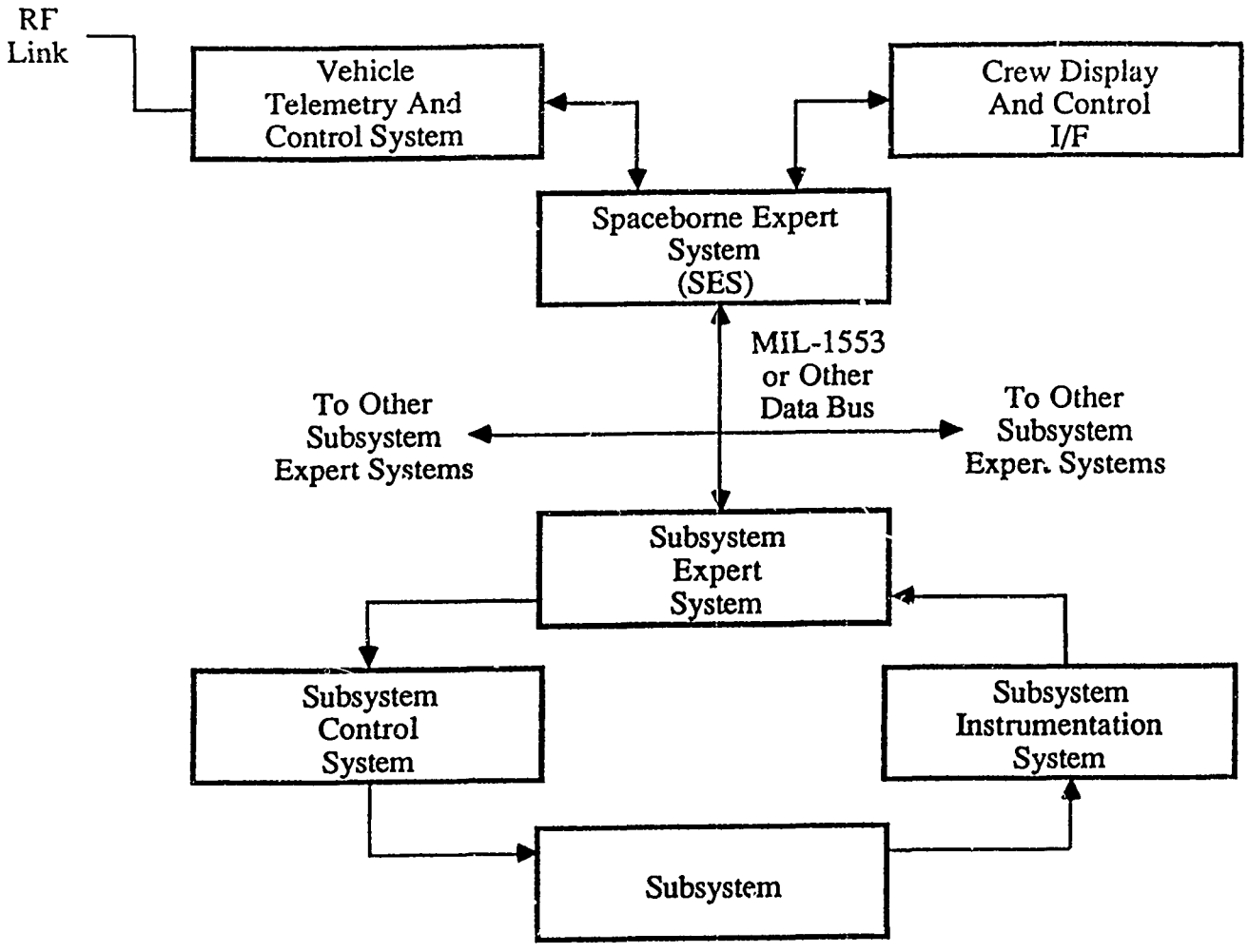


Fig. 86 Hierarchical Relationship Between a Generic Spaceborne Expert System and Subsystem Expert System

be pursued for RBCC/SSTO vehicles is one that will provide a maximum integration of ground and vehicle borne equipment systems all under the control of the vehicle borne SES. In these operations, the requirement for real-time control must be met but these requirements are probably less stringent than those that will be encountered in flight operations. The relationship of such an autonomous system with the ground support system is illustrated in Fig. 87.

A very simplified illustration of the basic elements of a generic SES or Subsystem Expert System (SUBES) is presented in Fig. 88. The three principal technological problems that must be addressed in the future are implicit in this figure. These are the development of the expert system algorithms, development of the knowledge base descriptive of both the vehicle borne systems, ground systems and other systems that will be under control of the expert system, and the development of the hardware compatible with the intelligent algorithm and knowledge base capable of meeting the requirements of real-time control of complex operations involving many events occurring at high speed.

5.4.3 The Crew Module

A conceptual design of the Crew Module is presented in Fig. 89. The pressurized crew compartment consists of a side-by-side arrangement with dual controls and instrument displays. Avionics, avionics support racks, environmental control and life support systems are located forward of the instrument display panel.

Avionics for the RBCC/SSTO Crew Module consist of integrated vehicle and ground systems control equipment and software systems which incorporate distributed computers and redundant data buses in a network architecture as previously discussed and illustrated.

Weight estimations developed for the crew module of the RBCC/SSTO baseline design provide life support system consumables sufficient for 15 days.

5.5 Weight Estimation

The approach to the estimation of weights of the five candidate RBCC engine systems was discussed in Section 2.0. In previously parts of this section, the MMAG approach to the estimation of weight for the thermal protection system and its supporting structure has been discussed. Additional guidelines that were used in developing the vehicle weight estimation were:

- Surface control - 0.5 lb/ft^2 x 20% of the exposed wing area and fin area
- RCS system equal of surface controls
- Wiring equals 2 lb/ft extending the length and width of the vehicle
- Fixed weight includes cockpit, avionics, antennas and the environmental control and life support system
- APU hardware equal 1% of gross vehicle weight
- Landing gear weight equal 3% of gross weight (HTOL) or 2% of gross weight (VTOL)
- The engine weights were provided by ACA and presented previously in Section 2.0.
- Residuals and unusable fluids were 0.5% of fuel weight
- Consumables for the APU and RCS were 1.5% of usable fuel
- Consumables for the environmental control and life support systems were 500 lbm

Based on the findings of the performance analysis, weight and sizing studies carried out during this project, a baseline vehicle gross weight of 500 klbm was selected. Further, as will also be discussed in Section 6.0, Engines 10 - Ejector Scramjet and Engine 30 - the Supercharged ScramLACE were selected as being representative of the simplest and most complex RBCC

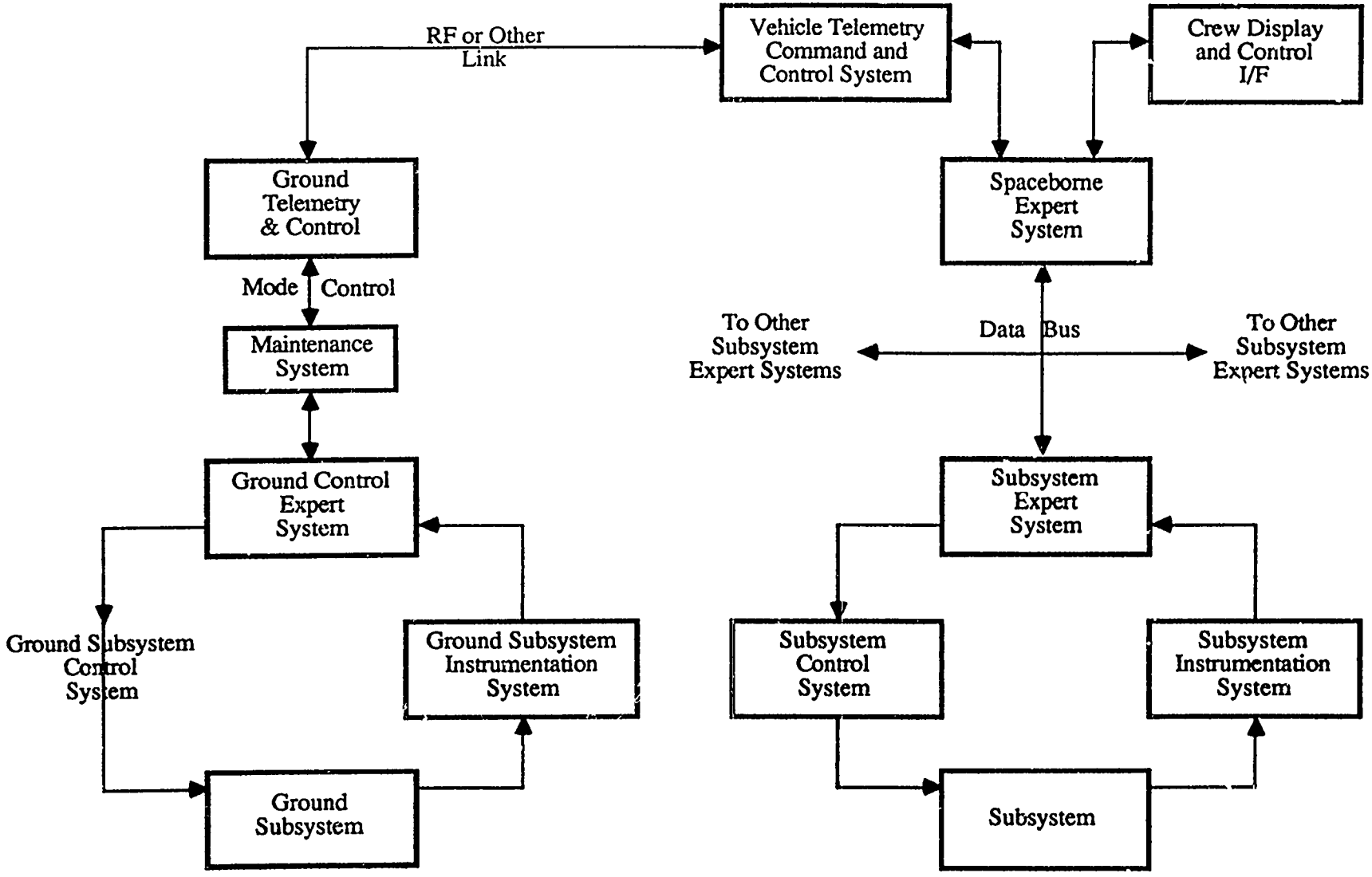


Fig. 87 **Interface Between Spaceborne Expert System and Ground Support System**

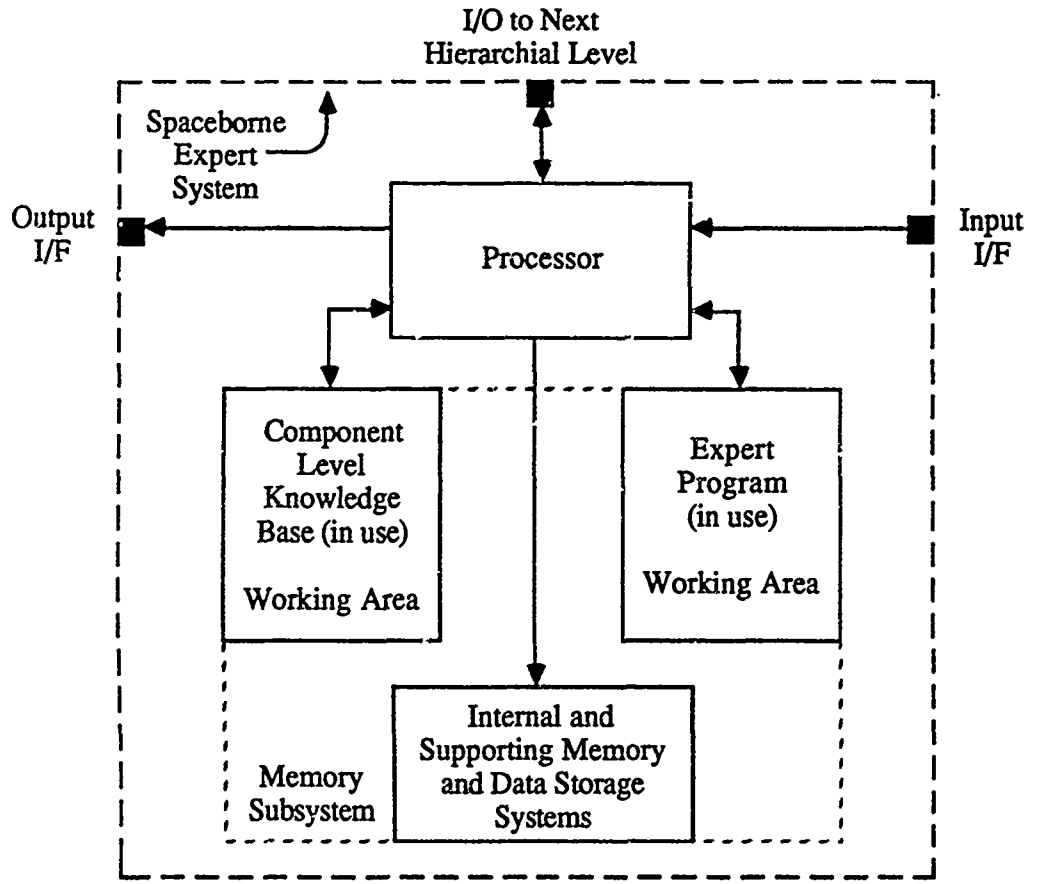


Fig. 88 Generic Spaceborne Expert System (SES)

Characteristics:

# of Crew - 2

Weight:

Structure	-	940
TPS	-	490
Avionics	-	1000
Crew Support	-	2000
Total		4430lb

Size:

* Length	-	30'
* Minor Dia	-	4' I.D.
* Major Dia	-	9.25' I.D.

Volume - 1100 cuft

*Based on Strawman 1

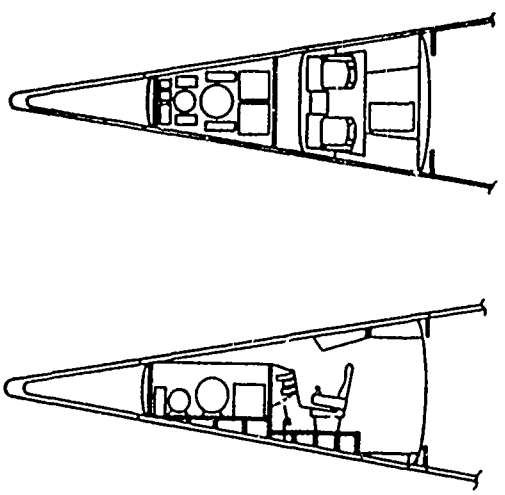


Fig. 89 Crew Module Conceptual Design

engine configurations with Engine 10 being the baseline engine in a VTOHL system with 50% strakes or equivalent wing area.

The problem of the effect of angle-of-attack on the inlet air conditions in the axisymmetric configuration is judged to be of great significance. For this reason, the baseline configuration employs 50% strakes rather than the 25% strake size. The 25% strake size is adequate to meet the lifting requirements of the ascent trajectory but in doing so incurs unacceptably high angles-of-attack in the judgement of the study team. Vehicle performance, in terms of the effect of strake size on peak angle-of-attack, is discussed in further detail in Section 6.0.

In Fig. 90 and 91, the distribution of weight by systems in the 500 klbm GLOW vehicles powered by Engine 10, and for Engine 30 in Fig. 92 and 93, with 25% strakes, VTOHL and full capture and rocket mode at M=15 is presented. These weight distributions are given with and without propellants to enable the reader to see the distribution of weight within the dry vehicle and the distribution of dry weight within the fully fueled vehicle.

In Fig. 94 and 95, the same weight breakdown for the baseline Engine 10 vehicle system using the 50% of vehicle diameter strake size is presented. This configuration appears, based on the analysis carried out to date, to be nearly an optimum for this particular vehicle configuration.

Tables 12 and 13 present the weight, center of gravity and sizing analysis for the Engine 10 powered baseline vehicle configuration with 50% strakes and rocket mode transition at Mach 15 using both conventional hydrogen (run #S105015V.500) and slush hydrogen (run #S105015V.5SL).

5.6 500 klbm RBCC/SSTO Vehicle Concept Drawing

Fig. 96 presents a preliminary design concept drawing of the 500 klbm RBCC/SSTO point design vehicle. Selection of this gross weight and the use of the Ejector Scramjet in the point design was made as a result of the findings regarding vehicle performance that will be presented in the next section.

This drawing should be interpreted only in the most general terms. Many questions remain open regarding the particular vehicle design approaches that will result in an optimum design. The use of an annular inlet, as shown in Fig. 96, is only one of a range of alternative approaches all of which should be further investigated. The use of fuselage length strakes, the approach initially used, is now open to question based on the findings developed during this study. More conventional wing forms now appear appropriate.

VEHICLE WEIGHT BREAKDOWN WITH PROPELLANTS
500K VEHICLE - #10 - 25% STRAKES - VTO
FULL CAPTURE & ROCKET @ M=15

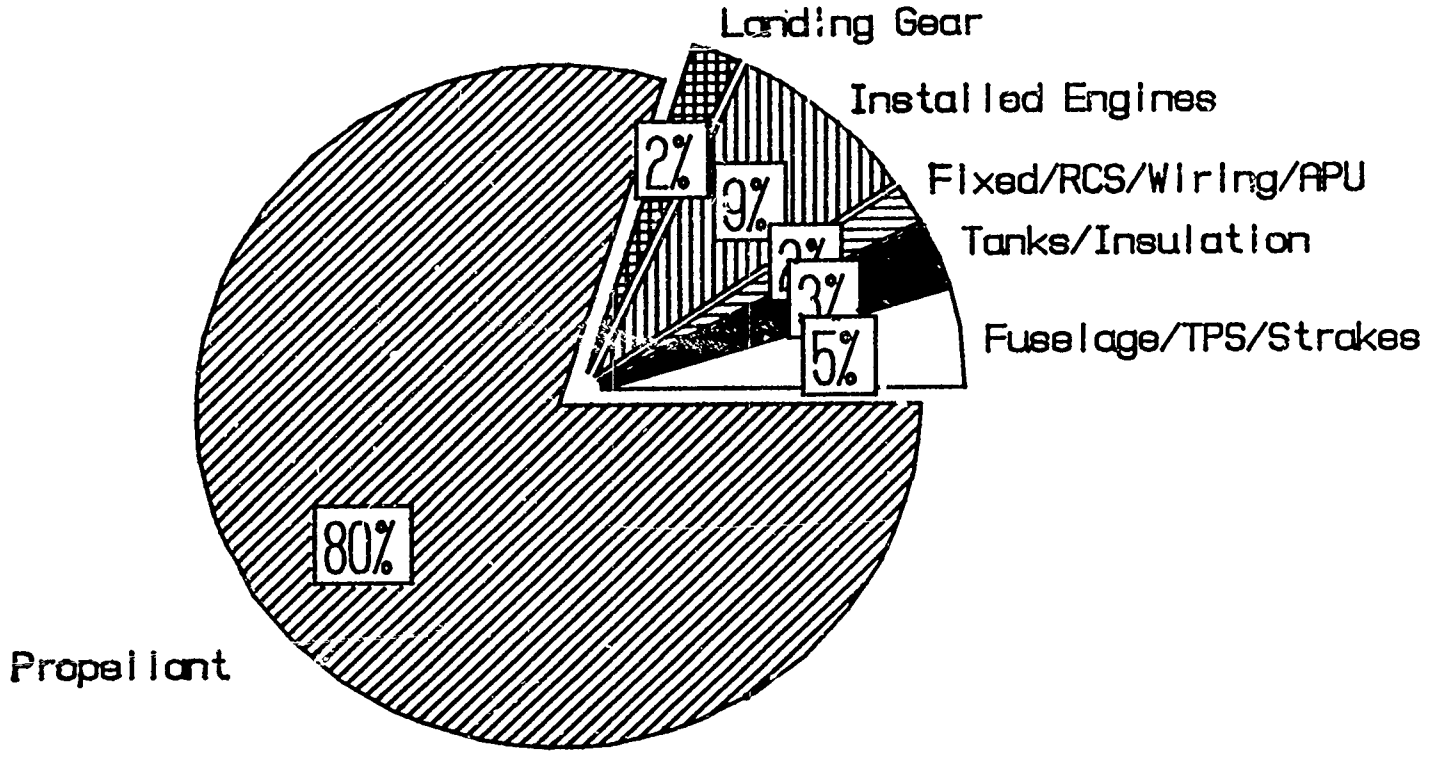


Fig. 90 Vehicle Weight Breakdown by Major System with Propellants - 500 klbm Vehicle - Engine #10 - 25% Strakes

VEHICLE WEIGHT BREAKDOWN WITHOUT PROPELLANTS
500K VEHICLE - #10 - 25% STRAKES - VTO
FULL CAPTURE & ROCKET @ M=15

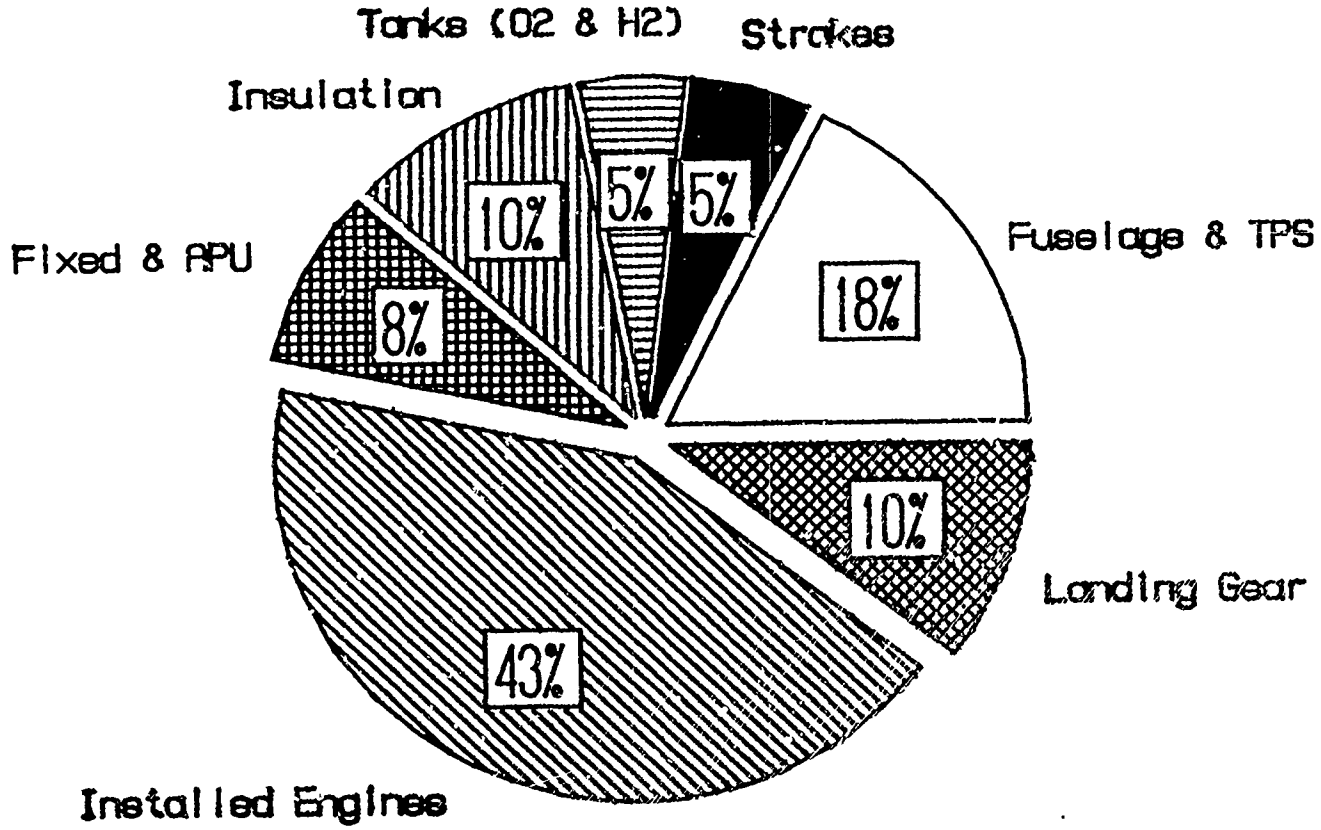


Fig. 91 Vehicle Weight Breakdown by Major System without Propellants - 500 klbm Vehicle - Engine #10 - 25% Strakes

VEHICLE WEIGHT BREAKDOWN WITH PROPELLANTS
500K VEHICLE - #30 - 25% STRAKES - VTO
FULL CAPTURE & ROCKET @ M=15

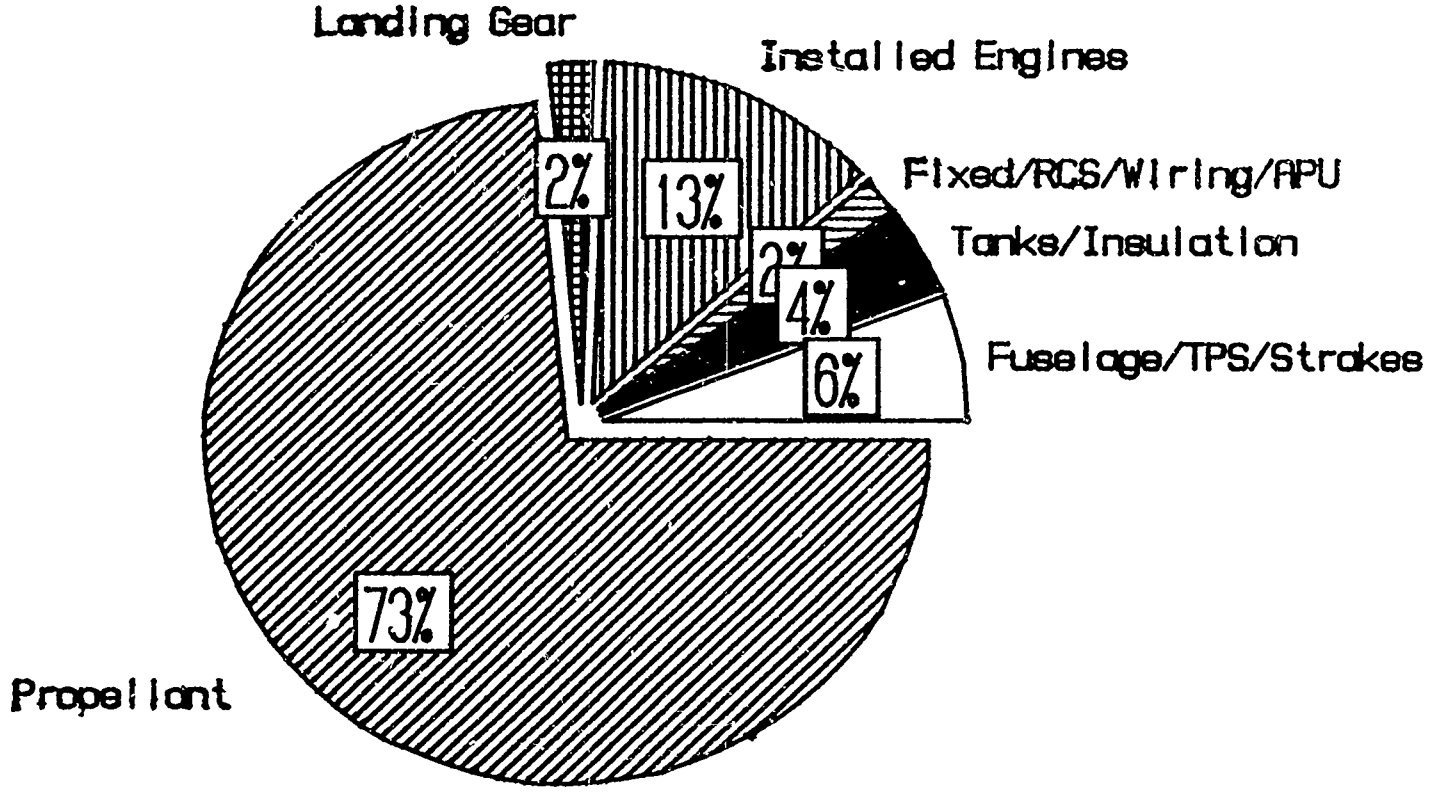


Fig. 92 Vehicle Weight Breakdown by Major System with Propellants - 500 Klbm Vehicle - Engine #30 - 25% Strakes

VEHICLE WEIGHT BREAKDOWN WITHOUT PROPELLANTS
500K VEHICLE - #30 - 25 % STRAKES - VTO
FULL CAPTURE & ROCKET @ M=15

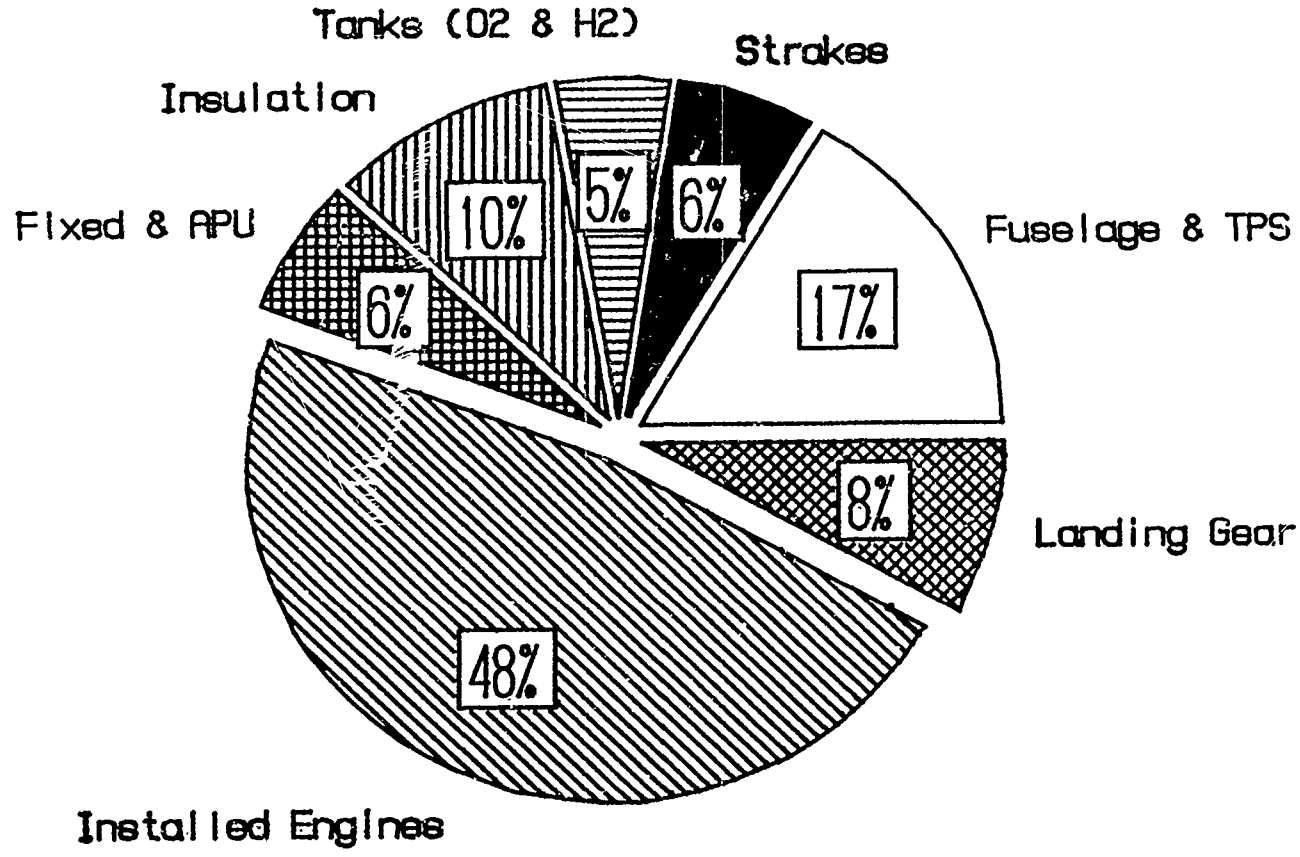


Fig. 93 Vehicle Weight Breakdown by Major System without Propellants - 500 klbm Vehicle - Engine #30 - 25% Strakes

VEHICLE WEIGHT BREAKDOWN WITH PROPELLANTS
500K VEHICLE - #10 - 50% STRAKES - VTO
FULL CAPTURE & ROCKET @ M=15

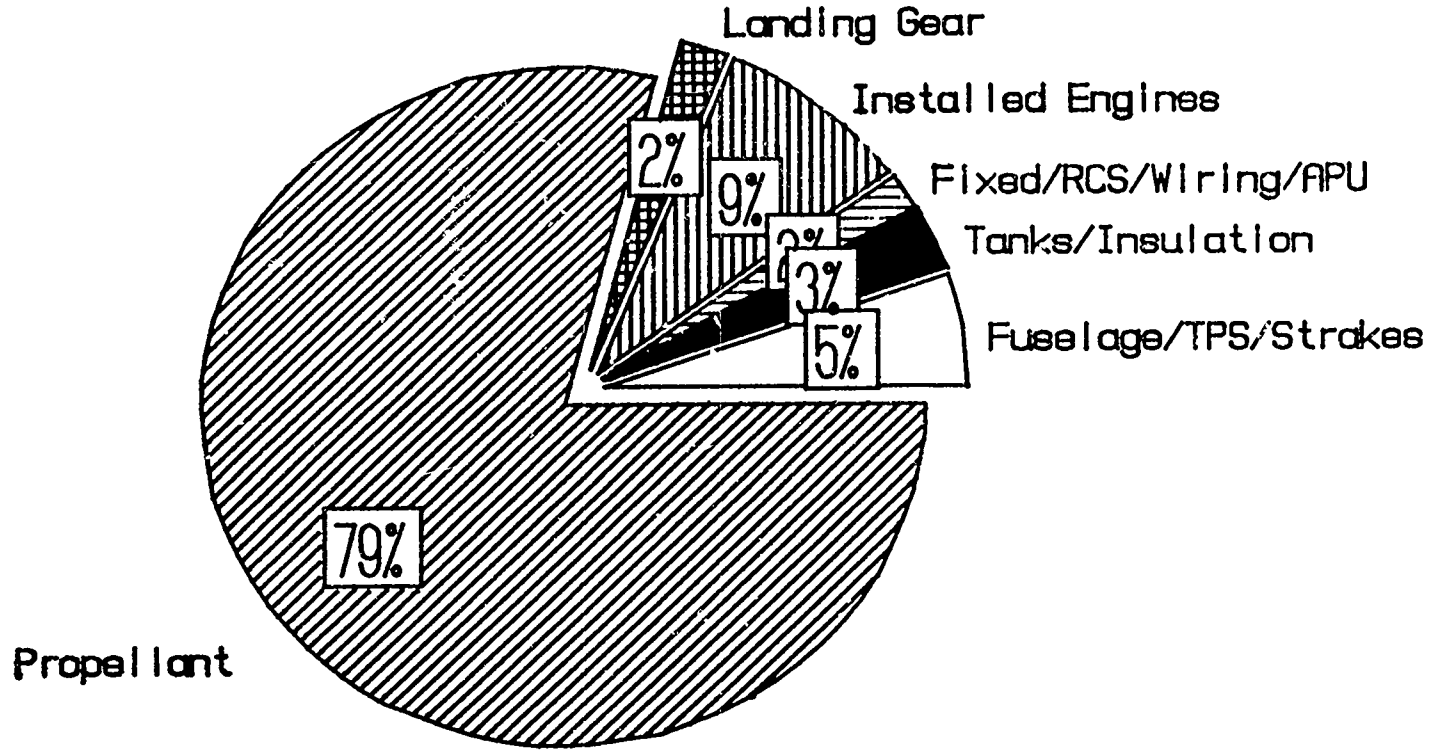


Fig. 94 Vehicle Weight Breakdown by Major System with Propellants - 500 klbm Vehicle - Engine #10 - 50% Strakes

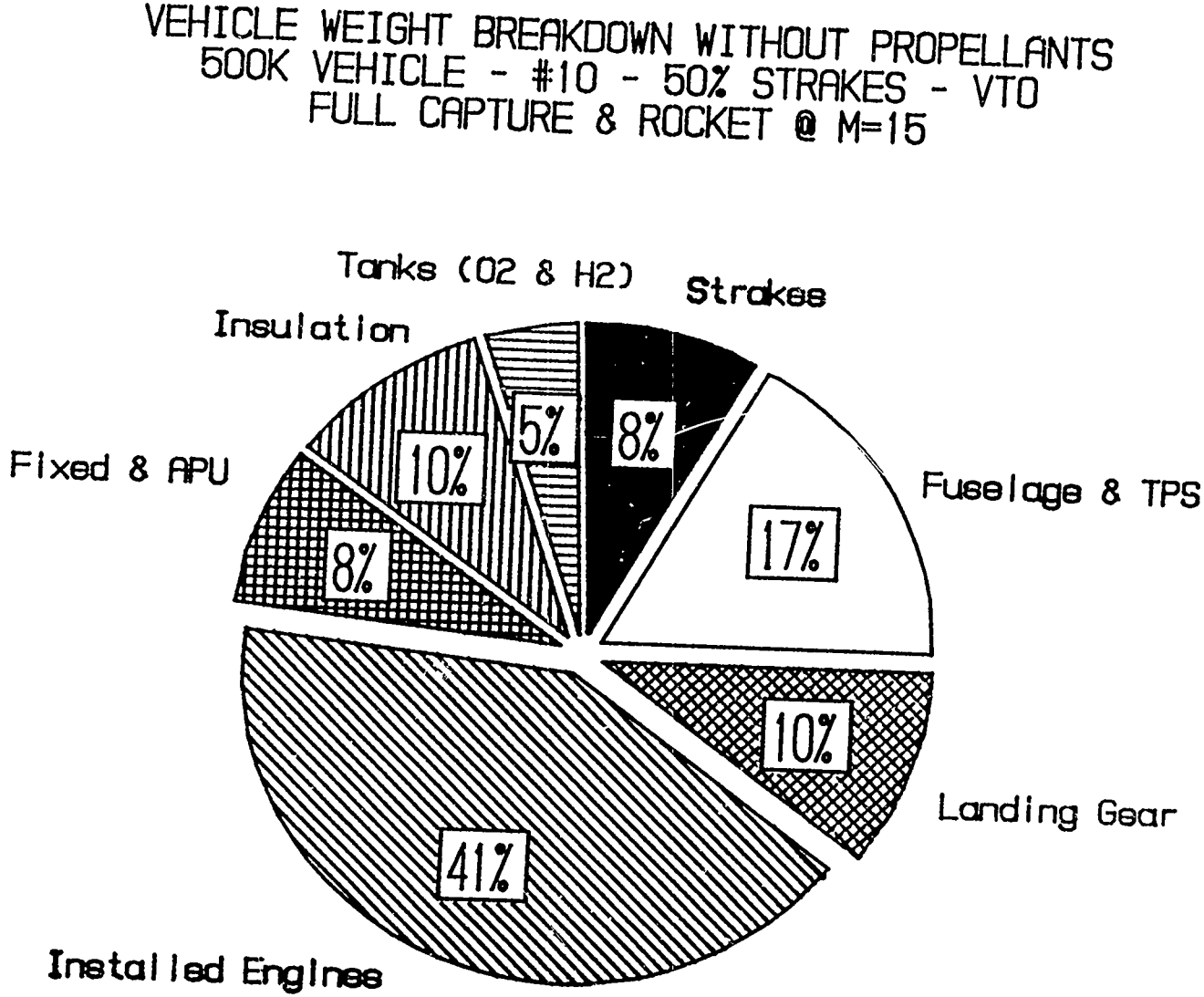


Fig. 95 Vehicle Weight Breakdown by Major System without Propellants - 500 klbm Vehicle - Engine #10 - 50% Strakes

Table 12 1995 TAD 500 klbm - Engine #10 - 50% Strakes - Vehicle Weight and Sizing Report with Liquid Hydrogen

Vehicle Sizing Data for 1995

Vehicle Name: Strawman 1 **Configuration :S105015V.500**

Program Name: Air Augmented Rocket

Date: 12-03-1987

Nose Cone Data:

Length = 9.8′
Nose Cap Radius = 1′
Major Outside Diameter = 4.5′
Wetted Area = 98 sqft
Structure Weight = 179 lb
C.G. = Sta 67.4

Crew Compartment Data:

Length = 17.8′
Minor Outside Diameter = 4.5′
Major Outside Diameter = 9.5′
Wetted Area = 393 sqft
Structure Weight = 719 lb
C.G. = Sta 237.3

Fixed Weight = 3,000 lb
C.G. = Sta 190.5

Crew Weight = 440 lb
C.G. = Sta 292.9

Oxidizer Area Data:

Length = 30.2′
Minor Outside Diameter = 9.5′
Major Outside Diameter = 18.0′
Wetted Area = 1,316 sqft
Structure Weight = 2,408 lb C.G. = Sta 531.1

Tank Weight = 531 lb C.G. = Sta 596.5

Oxidizer Weight = 258,011 lb C.G. = Sta 604.1

Tank Insulation Weight = 1,602 lb C.G. = Sta596.5

Small Dome Height = 3.5′
Small Dome Diameter (I.D.) = 10.0′
Tank Frustum Length = 21.0′
Large Dome Height = 5.6′
Large Dome Diameter (I.D.) = 15.9′

Tank Volume = 3,741 cuft

Scramjet Transition Velocity = Mach 15
Vertical Takeoff and Horizontal Landing

Table 12 1995 TAD 500 klbm - Engine #10 - 50% Strakes - Vehicle Weight and Sizing Report with Liquid Hydrogen (Cont'd)

Configuration :S105015V.500 Page 2

Fuel Area Data:

Length = 82.6'
Minor Outside Diameter = 18.0'
Major Outside Diameter = 33.6'
Surface Area = 6,842 sqft
Structure Weight = 12,521 lb C.G. = Sta 1233.7

Tank Weight = 4,018 lb C.G. = Sta 1175.1

Fuel Weight = 121,359 lb C.G. = Sta 1199.2

Tank Insulation Weight = 8,183 lb C.G. = Sta 1175.1

Small Dome Height = 6.9'
Small Dome Diameter (I.D.) = 19.4'
Tank Frustum Length = 48.7'
Large Dome Height = 16.5'
Large Dome Diameter (I.D.) = 33.1'

Tank Volume = 28,306 cuft

Payload Bay Area:

Length = 10'
Wetted Area = 648 sqft
Structural Weight = 1,186 lb
C.G. = Sta 0.0

Payload C. G. = Sta 1619.1

Engine Area Data:

Engine Type = 10
# of Engines = 8
Total Engine Weight = 40,880 lb C.G. = Sta 1275.4

Strake Area Data:

Strake Length = 58.5'
Surface Area (ea) = 568 sqft
Total Weight = 8,309 lb
C.G. = Sta 749.4

Table 12 1995 TAD 500 klbm - Engine #10 - 50% Strakes - Vehicle Weight and Sizing Report with Liquid Hydrogen (Cont'd)

Configuration :S105015V.500 Page 3

Misc. Component Data:

APU Weight = 5,000 lb C.G. = Sta 78.6

Landing Gear Weight = 10,000 lb C.G. = Sta 1395.6

Wiring Weight = 382 lb

RCS & Control Weight = 454 lb

Overall Vehicle Data:

Length = 140.4'

Tank Structure O.D. = 33.6'
Diameter to Outside of Strakes = 50.4'
Diameter to Outside of Engines = 42.6'
Max. Fuselage Diameter = 50.4'

Nose Cone Angle = 16.0 deg.
Tail Cone Angle = 20.0 deg.

Sizing based on Liquid Fuel

Propellant Weight & Volume Break Down

Fuel:

Ascent	115,505 lb	26,132 cuft
Hohman Transfer	329 lb	74 cuft
ACS	25 lb	6 cuft
Retrofire	351 lb	79 cuft
Boiloff & Resvs	149 lb	34 cuft
Flyback	5,000 lb	1,131 cuft
Total	121,359 lb	27,457 cuft

Oxidizer:

Ascent	252,928 lb	3,557 cuft
Hohman Transfer	1,917 lb	27 cuft
ACS	152 lb	2 cuft
Retrofire	2,122 lb	30 cuft
Boiloff & Resvs	891 lb	13 cuft
Total	258,011 lb	3,629 cuft

Ascent Fuel Weight Includes :
1% Addition for Residuals and Unusable Fluids
1.5% Addition of the Usable Fuel for the APU, RCS, and ECS

Table 12 1995 TAD 500 klbm - Engine #10 - 50% Strakes - Vehicle Weight and Sizing Report with Liquid Hydrogen (Cont'd)

Configuration :S105015V.500 Page 4

Vehicle Weight Summary:

Component Name	Component Weight (lb)
Fuselage & TPS	17,012 lb
Strakes	8,309 lb
Tanks (02 & H2)	4,549 lb
Insulation	9,785 lb
Fixed	3,000 lb
RCS & Controls	454 lb
Wiring	382 lb
APU	5,000 lb
Engines & Inst	40,880 lb
Landing Gear	10,000 lb
Dry Weight	99,370 lb
Propellant	374,370 lb
Payload	
Net	20,820 lb
Flyback	5,000 lb
Crew	440 lb
Gross Veh. Weight	500,000 lb

Fuel Mass Fraction = 75.9 %
Payload/Glow Ratio = 0.053
Payload/Dry Weight Ratio = 0.264

Dry Weight C.G. = Sta 1064.7
Gross Weight C.G. = Sta 882.1

Table 13 1995 TAD 500 klbm - Engine #10 - 50% Strakes - Vehicle Weight and Sizing Report with Slush Hydrogen

Vehicle Sizing Data for 1995

Vehicle Name: Strawman 1 **Configuration :S105015V.5SL**

Program Name: Air Augmented Rocket

Date: 12-03-1987

Nose Cone Data:

Length = 9.8′
Nose Cap Radius = 1′
Major Outside Diameter = 4.5′
Wetted Area = 98 sqft
Structure Weight = 179 lb
C.G. = Sta 67.4

Crew Compartment Data:

Length = 17.8′
Minor Outside Diameter = 4.5′
Major Outside Diameter = 9.5′
Wetted Area = 393 sqft
Structure Weight = 719 lb
C.G. = Sta 237.3

Fixed Weight = 3,000 lb
C.G. = Sta 190.5

Crew Weight = 440 lb
C.G. = Sta 292.9

Oxidizer Area Data:

Length = 30.2′
Minor Outside Diameter = 9.5′
Major Outside Diameter = 18.0′
Wetted Area = 1,315 sqft
Structure Weight = 2,406 lb C.G. = Sta 531.0

Tank Weight = 531 lb C.G. = Sta 596.4

Oxidizer Weight = 257,803 lb C.G. = Sta 603.9

Tank Insulation Weight = 1,601 lb C.G. = Sta 596.4

Small Dome Height = 3.5′
Small Dome Diameter (I.D.) = 10.0′
Tank Frustum Length = 21.0′
Large Dome Height = 5.6′
Large Dome Diameter (I.D.) = 15.9′

Tank Volume = 3,738 cuft

Scramjet Transition Velocity = Mach 15
Vertical Takeoff and Horizontal Landing

Table 13 1995 TAD 500 klbm - Engine #10 - 50% Strakes - Vehicle Weight and Sizing Report with Slush Hydrogen (Cont'd)

Configuration :S105015V.5SL Page 2

Fuel Area Data:

Length = 77.7'
Minor Outside Diameter = 18.0'
Major Outside Diameter = 32.4'
Surface Area = 6,258 sqft
Structure Weight = 11,453 lb C.G. = Sta 1199.2

Tank Weight = 3,505 lb C.G. = Sta 1139.6

Fuel Weight = 122,153 lb C.G. = Sta 1162.2

Tank Insulation Weight = 7,417 lb C.G. = Sta 1139.6

Small Dome Height = 6.9'
Small Dome Diameter (I.D.) = 19.4'
Tank Frustum Length = 44.4'
Large Dome Height = 15.9'
Large Dome Diameter (I.D.) = 31.9'

Tank Volume = 24,692 cuft

Payload Bay Area:

Length = 10'
Wetted Area = 648 sqft
Structural Weight = 1,186 lb
C.G. = Sta 0.0

Payload C. G. = Sta 1559.4

Engine Area Data:

Engine Type = 10
# of Engines = 8
Total Engine Weight = 40,880 lb C.G. = Sta 1219.9

Strake Area Data:

Strake Length = 53.9'
Surface Area (ea) = 504 sqft
Total Weight = 7,373 lb
C.G. = Sta 744.8

Table 13 1995 TAD 500 klbm - Engine #10 - 50% Strakes - Vehicle Weight and Sizing Report with Slush Hydrogen (Cont'd)

Configuration :S105015V.5SL Page 3

Misc. Component Data:

APU Weight = 5,000 lb C.G. = Sta 78.6

Landing Gear Weight = 10,000 lb C.G. = Sta 1340.2

Wiring Weight = 368 lb

RCS & Control Weight = 403 lb

Overall Vehicle Data:

Length = 135.4'

Tank Structure O.D. = 32.4'
Diameter to Outside of Strakes = 48.5'
Diameter to Outside of Engines = 41.4'
Max. Fuselage Diameter = 48.5'

Nose Cone Angle = 16.0 deg.
Tail Cone Angle = 19.0 deg.

Sizing based on Slush Fuel

Propellant Weight & Volume Break Down

Fuel:

Ascent	116,303 lb	22,804 cuft
Hohman Transfer	327 lb	64 cuft
ACS	25 lb	5 cuft
Retrofire	349 lb	68 cuft
Boiloff & Resvs	149 lb	29 cuft
Flyback	5,000 lb	980 cuft
Total	122,153 lb	23,952 cuft

Oxidizer:

Ascent	252,742 lb	3,555 cuft
Hohman Transfer	1,909 lb	27 cuft
ACS	151 lb	2 cuft
Retrofire	2,113 lb	30 cuft
Boiloff & Resvs	888 lb	12 cuft
Total	257,803 lb	3,626 cuft

Ascent Fuel Weight Includes :
1% Addition for Residuals and Unusable Fluids
1.5% Addition of the Usable Fuel for the APU, RCS, and ECS

Table 13 1995 TAD 500 klbm - Engine #10 - 50% Strakes - Vehicle Weight and Sizing Report with Slush Hydrogen (Cont'd)

Configuration :S105015V.5SL Page 4

Vehicle Weight Summary:

Component Name	Component Weight (lb)
Fuselage & TPS	15,942 lb
Strakes	7,373 lb
Tanks (02 & H2)	4,036 lb
Insulation	9,019 lb
Fixed	3,000 lb
RCS & Controls	403 lb
Wiring	368 lb
APU	5,000 lb
Engines & Inst	40,880 lb
Landing Gear	10,000 lb
Dry Weight	96,020 lb
Propellant	374,956 lb
Payload	
Net	23,584 lb
Flyback	5,000 lb
Crew	440 lb
Gross Veh. Weight	500,000 lb

Fuel Mass Fraction = 76.0 %
Payload/Glow Ratio = 0.058
Payload/Dry Weight Ratio = 0.302

Dry Weight C.G. = Sta 1027.3
Gross Weight C.G. = Sta 866.4

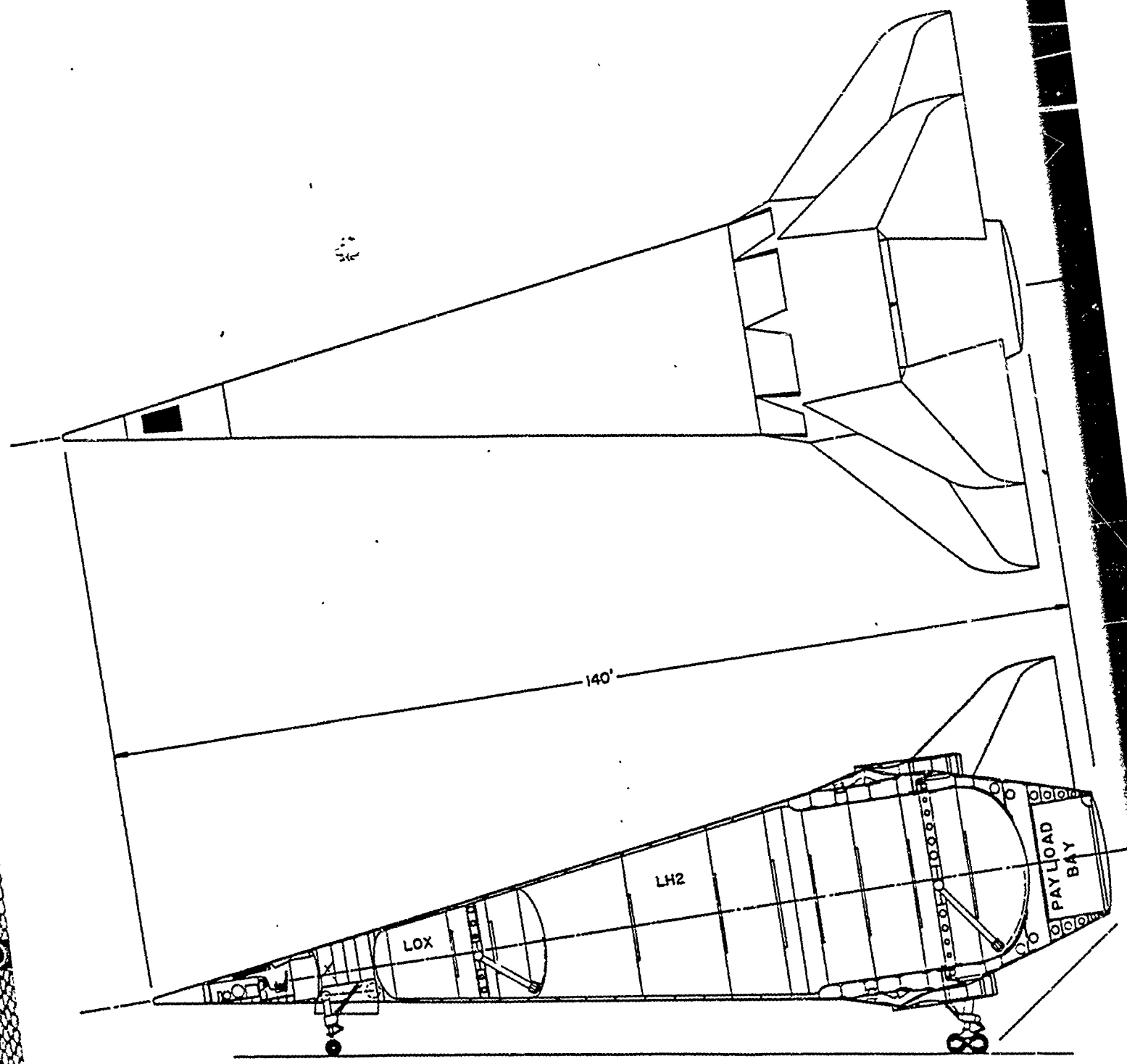
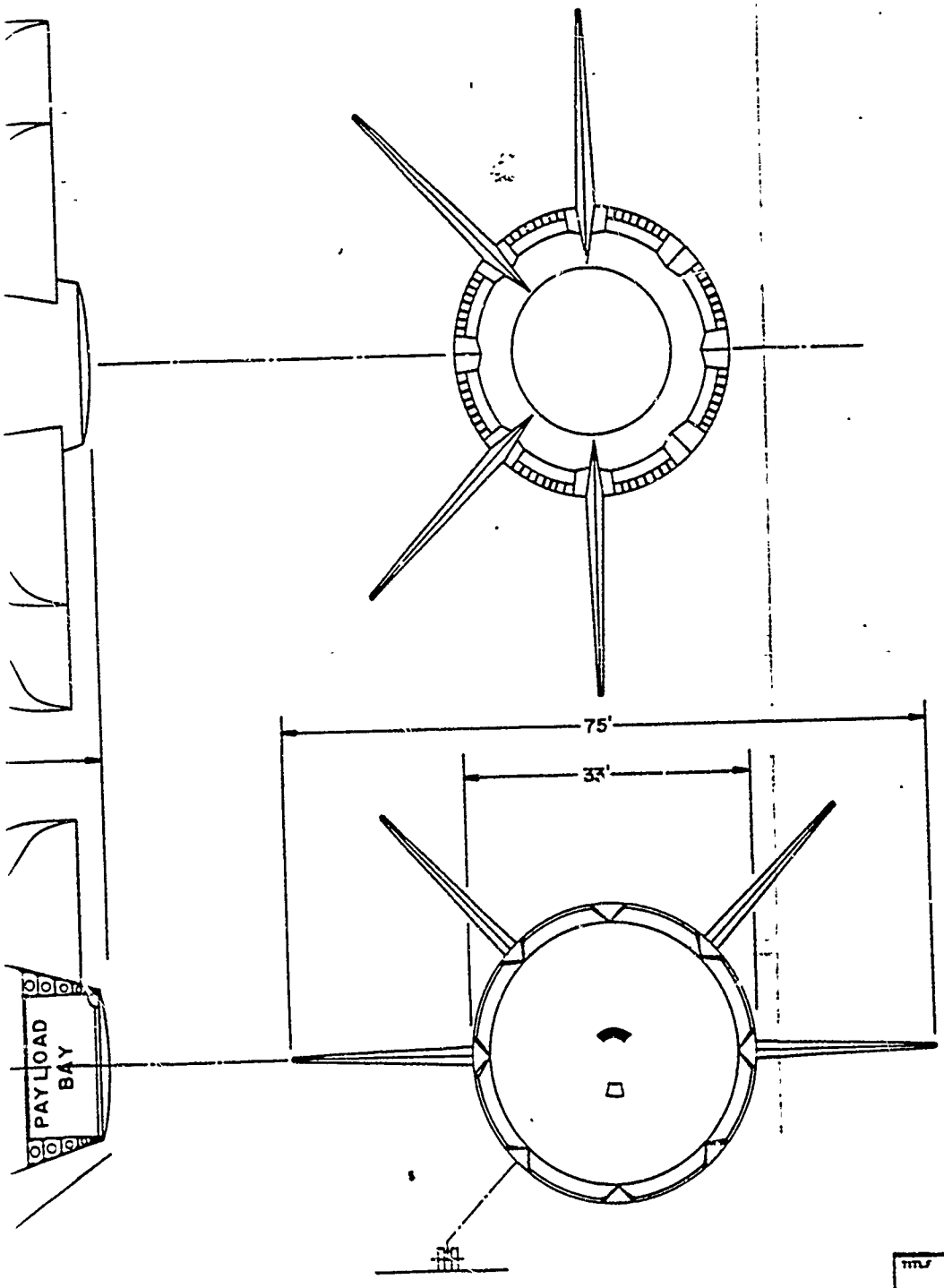


Fig. 96 500 klbm Baseline Vehicle - Engine #10 - 50% Strakes Equivalent V
Area - Mach 15 Scramjet Transition - VTOHL Conceptual Layout



500 klbm TOGW/GLOW
RBCC/SSTO Vehicle

quivalent Wing
l Layout

2

Section 6.0

VEHICLE PERFORMANCE ANALYSIS

6.1 Introduction

The preceding sections have presented the study findings regarding the five alternative configurations of Rocket Based Combined Cycle Engine systems, vehicle integration considerations and the findings of the vehicle analysis and conceptual design task. This section presents the findings resulting from the flight performance analysis carried out based on the vehicle design definition resulting from these tasks.

6.2 Performance Analysis Requirements

The scope of work of this project required that a simulation system be obtained, modified and implemented that would provide the ability to model the effects of changes in engine performance, vehicle weights and other parameters.

The ability to estimate vehicle subsystem mass build-up and to determine a range of vehicle geometric characteristics was also required. The mass build-up estimates were required to include, for comparison purposes, the capability to provide a quantified determination of the vehicles' ability to deliver discretionary payload to a 100 nmi polar orbits. The geometric characteristics were required to enable the aerodynamic characteristics to be determined for various vehicle configurations.

Finally, the results of the use of the performance analysis tools to be used in the project had to provide output data in formats that would be easily understood and adequate to comparatively analyze the engine and vehicle systems of interest.

6.2.1 Trajectory Analysis Approach

The simulation system approach developed for this project essentially decouples the trajectory simulation from the vehicle mass build-up estimation and vehicle sizing software. The single exception is in the Hohmann transfer maneuver propellants which required a comparatively small iteration operation to correct.

This enables the engine system performance to be compared between alternative RBCC engine configurations in terms of the total mass delivered to orbit. This approach permitted the effects of lift, drag, and velocity loss due to gravity to be identified for trajectory variations using each engine type without having to consider the variation in dry weight produced by various alternative vehicle structural design approaches. Vehicle dry weight could then be subtracted from the mass delivered to orbit and the payload weight available could then be determined.

Trajectory Analysis Software Requirements

The trajectory analysis software selected had to provide the capability of simulating horizontal and vertical takeoff, ascent to local orbital conditions at approximately 200,000 feet and 100 nmi altitude orbital insertion of each RBCC/SSTO alternative vehicle configuration studied.

Since the type of RBCC engines being studied have specific impulse levels which range from rocket specific impulses of 470 to net jet airbreathing specific impulses of 4595 sec,

trajectory analysis software which restricts engine performance input to a single average value, or a few discrete values, is not adequate for the study of these types of engines. Variable engine performance input was considered to be a trajectory analysis software requirement.

The present study required quantification of the payload benefit derived from the air-augmented rocke engine design approach studied. This quantification was directly related to the vehicle system aerodynamics which varied for each engine alternative. This required the ability of the software to accept variable vehicle aerodynamic characteristics, such as C_L and C_D, as functions of Mach Number and angle-of-attack.

Another reason for the variable aerodynamic characteristics requirement was that the primary engine performance database, the findings of the NAS7-377 project, contain net-jet specific impulse and net-jet thrust data. That is, the engine performance data already accounted for engine inlet induced ram-drag, and, to avoid double drag accounting, the engine captured airflow induced drag had to be subtracted from the total vehicle drag which is conventionally an aerodynamic parameter, not a propulsion related parameter.

The requirement of variable trajectory path capability was needed to isolate the effects deriving from the trajectory itself since airbreathing engine performance is directly tied to flight conditions and each of the various engine/vehicle combinations had a different optimum trajectory definition.

The trajectory analysis software also had to have the capability of computing effective specific impulse, I_{eff}, and equivalent effective specific impulse, I*. Effective specific impulse is the instantaneous value of specific impulse which accounts for vehicle drag and gravity forces acting along the vehicle velocity vector.

Practical Considerations

Practical considerations placed obvious restrictions on the trajectory analysis software eventually selected. A tradeoff between software acquisition, implementation and operation costs and accuracy had to be made. For these reasons, several smaller, faster, non-optimizing personal computer programs were analyzed to determine their applicability to the trajectory analysis requirements.

A personal computer based program, DOF36 written by the Air Force Wright Aeronautical Laboratory/Aeropropulsion Laboratory (AFWAL/APL), was selected for primary use on this project. DOF36 fulfilled all of the aforementioned trajectory analysis requirements, but did not have the capability of calculating vehicle subsystem mass-buildup, sizing and payload determination estimation. Separate software to accomplish these calculations was needed and was provided by MMAG.

6.2.2 Vehicle Mass Build-up, Geometric Sizing and Payload Determination Software Requirements

Vehicle mass build-up and sizing programs tend to be very vehicle design concept specific. That is, the programs are built around specific vehicle geometric and structural characteristics. The vehicle mass build-up and sizing programs were written by MMAG for the axisymmetric straked cone configuration chosen for the baseline vehicle system in this study.

6.3 Characteristics of the Trajectory Analysis Program Selected

The basic characteristics of the trajectory analysis, vehicle mass build-up, sizing and payload determination software chosen for use on this project will now be discussed.

DOF36 was developed by the Air Force Wright Aeronautical Laboratory (AFWAL/POPA) and was employed as the primary trajectory analysis tool. Development of the application methodology was done by MMAG staff and used by both ACA and MMAG to provide a basis for jointly carrying out the analysis of the effect of integration of the engine systems, for which ACA was primarily responsible, and the vehicle systems, for which MMAG was primarily responsible.

Application specific programs were written by MMAG staff and were used jointly by MMAG and ACA to provide vehicle mass build-up, sizing and payload determination capabilities for the study.

6.3.1 DOF36 Trajectory Simulation Program Discussion

DOF36, a three or six degree-of-freedom (DOF) trajectory simulation which uses a circular, non-rotating Earth model is briefly discussed below. Separate documentation exists in the form of a DOF36 Program Users Manual and an Analysis Development Document (see Ref.s 23 and 24.

Program Environment and Program Inputs

DOF36 is an ANSI (American National Standards Institute) Standard FORTRAN 77 source code program which operates on a math coprocessor supported personal computer within a DOS (Disk Operating System) environment.

Keyboard entries call the desired engine, aerodynamic and fuel flow files, which are in the form of unformatted ASCII text files and are described in more detail below. Keyboard responses also indicate whether or not output and graph files, also described below, are to be created.

Input file

The input file is used to call the desired aerodynamic and engine Isp files, as well as to specify simulation timing parameters, vehicle control dynamic parameters, engine cycle and vehicle guidance events, and to initialize all remaining simulation parameters. The aerodynamic and engine Isp files will bediscussed separately.

The control data section provides input of the number of simulation degrees-of-freedom, the control system type and the required control loop time constants and gains. The relatively limited scope of the study, the preliminary nature of the design concepts explored, as well as the project requirement for mainly comparative system trajectory performance analysis did not require the use of the 6-Degree-Of-Freedom (6-DOF) capability of DOF36. Therefore, DOF36 was used in this study exclusively in its 3-DOF mode.

Of the four control system types available in DOF36, pitch/roll aerodynamic control, pitch/yaw aerodynamic control, pitch roll thrust vector control (TVC) and pitch/yaw TVC, pitch yaw aerodynamic control was selected for use in this study. This was selected because multiple plane control, i.e., roll or yaw control, was not relevant to orbital ascent flight and the costs in project time that a multi-axis analysis would require were not considered to be justifiable for a design analysis of this type.

The Lguide, Hguide and Vguide sections provide input of planar guidance laws for the longitudinal, horizontal and vertical planes, respectively. The longitudinal guidance laws

available for selection in DOF36 include commanded Mach number, commanded speed, commanded longitudinal g's, and a no fuel flow/coast mode.

The Takeoff data section inputs horizontal takeoff data, including velocity at the initiation of pitch-up, the takeoff commanded vertical plane acceleration, and the relative longitudinal acceleration assumed during takeoff which is then implemented until the vehicle lifts off the runway. The velocity at the initiation of pitch-up maneuver and the takeoff commanded vertical plane acceleration were selected such that the actual takeoff velocity did not exceed 350 mi/hr while the initial relative longitudinal acceleration was held constant for all engine/vehicle configurations at 1.3 g.

The Takeoff data section is omitted when simulating vertical takeoff. Instead, the initial vehicle flight path angle is specified to be 90-degrees, and, shortly after takeoff, a pitch-down maneuver is commanded.

Aero file

The Aero file provides tabular input of vehicle aerodynamic characteristics and the associated aerodynamic reference area. The aerodynamic characteristics contained in the aero file are the following:

- the pitch plane and yaw plane angle-of-attack induced lift coefficients
- the pitch plane lift coefficient at zero angle-of-attack
- the angle-of-attack induced drag coefficient
- and the drag altitude/Reynolds number correction

Engine file

The engine file specifies the type of engine performance data to be input and provides for tabular input of that data. The types of engine performance data acceptable as engine file input to DOF36 include:

- thrust coefficient as a function of propellant mass flowrate, Mach number, and altitude
- specific impulse as a function of propellant mass flowrate, Mach number, and altitude
- and specific impulse as a function of engine equivalence ratio, Mach number, and altitude.

Since specific impulse data as a function of flight velocity and altitude was available from the baseline study database, specific impulse as a function of propellant mass flowrate, Mach number, and altitude was chosen as the mode of engine performance input used in the engine file. Because engine performance was derived from the database for discrete engine operating modes and for a reference trajectory, the latter making engine performance an implicit function of altitude, specific impulse was entered into the engine file as a function of Mach number only. Study of the effect of specific impulse variation with engine throttle setting or propellant mass flowrate was considered to be beyond the resources available for this study.

FFMAX file

The FFMAX file provides the tabular input of maximum fuel flow rate as a function of Mach number. The ability of DOF36 to accept and process the FFMAX file resulted from a

```
1          6 D - O - F   S U M M A R Y   O U T P U T
0     RUN TITLE:  ENGINE 32, FULL CAP & ROCKET @ M-15, 16 deg, 54.9 ft DIA, 25% STR
0                 AERODYNAMIC FILE ----- A322515V.956
0                 ENGINE FILE ---------- E3215V.956
0                 INPUT FILE ----------- I322515V.956
0                 FFMAX FILE ----------- FF3215V.956
0                 SUMMARY FILE --------- O322515V.956


+++++ RUN SUMMARY +++++
 ENGINE 32, FULL CAP & ROCKET @ M-15, 16 deg, 54.9 ft DIA, 25% STR
 TERMINATION CONDITION = 101
      FINAL CONDITIONS:
      TIME=    690.31     ALT =  187949.2     MACH=     24.30
      M1  = 956000.00     M2  = 344767.75     MR  =    2.7729
      ISPE=    786.88     ISPA=   1192.99     ISPT= 0.7291950720E+09

1/////   6  D - O - F   OUTPUT SUMMARY   /////                    PAGE   1

     TIME ALTITUDE  MACH   SPEED     Q   GAMMA ALPHA     WEIGHT   W-DOT   ISP   THRUST    IEFF   IRAT   GCB-1
     0.00      0.0  0.00     1.0  0.00 90.00  0.00  956000.00 1000.00 3219.8 1297235.7     0.0   0.00    1.36
     5.00    145.7  0.05    56.6  0.03 90.13  0.00  954001.00  396.81 3709.9 1273691.6   826.0   0.26    1.33
     9.14    470.4  0.09   101.8  0.08 90.71 -0.01  952353.87  353.29 3201.7 1131130.5   811.9   0.25    1.19
     9.14    470.4  0.09   101.8  0.08 90.71 -0.01  952353.87  353.29 3201.7 1131130.5?????????????    1.19
    10.00    560.7  0.10   108.7  0.10 90.90 -0.14  952031.87  391.09 3200.5 1251676.7   641.6   0.20    1.31
    15.00   1227.9  0.14   157.6  0.20 91.60 -1.06  950090.00  385.70 3191.6 1231005.7   744.1   0.23    1.29
    20.00   2131.4  0.18   203.3  0.32 90.94 -2.17  948174.31  380.62 3183.3 1211614.4   703.2   0.22    1.27
    25.00   3255.1  0.22   245.7  0.45 87.33 -3.30  946283.31  375.84 3175.5 1193472.5   660.1   0.21    1.26
    30.00   4576.5  0.26   285.7  0.59 80.04 -4.17  944415.56  371.27 3168.0 1176171.9   629.6   0.20    1.24
    35.00   6047.4  0.30   327.9  0.74 67.58 -4.47  942571.06  366.40 3160.0 1157812.7   670.0   0.21    1.22
    40.00   7560.8  0.35   383.2  0.97 50.36 -3.88  940754.00  359.99 3149.5 1133785.9   890.6   0.28    1.19
    45.00   8927.3  0.43   466.9  1.38 31.32 -2.28  938976.44  350.33 3133.7 1097815.7  1375.9   0.44    1.15
    45.36   9014.6  0.44   475.4  1.42 29.98 -2.12  938839.87  318.37 3132.1  997158.0  1816.5   0.58    1.05
    45.36   9014.6  0.44   475.4  1.42 29.98 -2.12  938839.87  318.37 3132.1  997158.0?????????????    1.05
    49.00   9758.4  0.52   559.8  1.93 17.60  1.70  937594.31  342.23 3127.7 1070384.6  1977.4   0.63    1.12
    54.00  10409.4  0.65   701.8  2.97  8.51  7.84  935879.25  343.83 3160.7 1093612.0  2409.2   0.76    1.13
    59.00  11000.2  0.77   826.8  4.04 11.01 11.67  934156.31  345.24 3227.6 1114316.1  2108.7   0.65    1.13
    64.00  12221.0  0.84   899.2  4.60 22.12  9.42  932427.75  346.10 3256.0 1126900.6  1215.4   0.37    1.10
    69.00  14274.2  0.92   975.3  5.06 28.08  3.19  930694.94  347.04 3287.2 1140776.2  1271.0   0.39    1.04
    74.00  16585.2  1.01  1060.3  5.55 24.94  1.90  928956.75  348.85 3323.3 1159339.2  1413.1   0.43    1.00
    79.00  18901.2  1.11  1152.6  6.07 25.23  2.80  927189.87  358.05 3369.3 1206361.7  1506.9   0.45    1.08
    84.00  21535.6  1.22  1255.8  6.59 26.63  2.62  925374.00  368.57 3421.8 1261175.7  1636.7   0.48    1.18
    89.00  24499.2  1.35  1372.6  7.10 26.65  2.30  923501.50  380.74 3482.7 1326014.6  1791.7   0.51    1.25
    94.00  27693.9  1.50  1504.7  7.61 26.03  2.31  921563.50  394.81 3553.0 1402778.6  1954.5   0.55    1.34
    99.00  31110.3  1.67  1654.7  8.13 25.10  2.29  919584.44  396.72 3735.0 1481729.9  2168.7   0.58    1.45
   104.00  34720.8  1.87  1826.0  8.64 23.87  2.45  917595.94  398.75 3948.8 1574585.4  2460.6   0.62    1.57
   109.00  38441.7  2.09  2025.0  8.98 20.67 -1.71  915597.12  400.55 4144.3 1660002.5  2835.8   0.68    1.68
   114.00  41727.7  2.33  2251.4  9.48 15.49  0.37  913590.94  401.96 4304.7 1730314.0  3207.6   0.75    1.76
   119.00  44769.3  2.57  2489.7 10.02 15.40  5.19  911578.69  401.91 4454.9 1790505.6  3359.6   0.75    1.83
   124.00  48409.1  2.82  2730.3 10.11 16.00  2.31  909578.25  398.19 4561.2 1816211.5  3404.2   0.75    1.87
   129.00  52090.9  3.08  2983.8 10.12 13.53  0.18  907407.62  474.15 3710.8 1759456.2  3296.9   0.89    1.82
   134.00  55372.9  3.36  3247.9 10.24 10.82  1.90  905011.31  484.52 3746.3 1815139.5  3105.2   0.83    1.89
   139.00  58456.9  3.64  3518.3 10.36 10.43  4.37  902569.62  489.19 3743.4 1831216.9  3110.6   0.83    1.92
   144.00  61708.0  3.92  3791.5 10.29  9.56  2.12  900127.87  487.50 3698.2 1802856.4  3134.8   0.85    1.90
   149.00  64681.6  4.20  4066.1 10.26  7.68  1.45  897725.44  470.11 3624.7 1703973.7  3190.0   0.88    1.80
   154.00  67183.0  4.46  4325.7 10.30  5.97  2.65  895429.00  448.03 3545.8 1588650.4  3153.0   0.89    1.68
   159.00  69332.8  4.71  4569.7 10.36  5.15  4.48  893205.19  443.75 3457.8 1534373.6  3049.8   0.88    1.62
   164.00  71396.1  4.94  4803.9 10.37  4.80  4.72  890989.94  442.34 3371.0 1491143.7  2932.1   0.87    1.58
   169.00  73393.1  5.17  5035.8 10.35  4.33  4.23  888765.06  449.69 3274.9 1472669.6  2882.3   0.88    1.57
   174.00  75248.5  5.41  5268.6 10.37  3.80  4.62  886491.06  459.91 3175.0 1460198.5  2824.0   0.89    1.56
   179.00  76973.8  5.63  5495.4 10.38  3.42  5.29  884203.87  445.07 3099.0 1379277.9  2729.2   0.88    1.47
   184.00  78590.2  5.84  5704.3 10.35  3.01  4.68  882053.37  415.56 3042.9 1264518.4  2666.8   0.88    1.35
   189.00  80007.1  6.03  5898.3 10.34  2.43  4.45  880042.37  393.14 2991.2 1175961.7  2640.9   0.88    1.25
   194.00  81180.8  6.22  6084.1 10.40  1.97  6.13  878074.81  393.88 2943.4 1159331.7  2580.8   0.88    1.24
   199.00  82249.9  6.39  6260.3 10.45  1.91  8.05  876103.69  394.58 2898.1 1143512.0  2436.3   0.84    1.23
   204.00  83379.9  6.56  6429.6 10.44  2.02  8.10  874126.69  397.75 2854.7 1135454.0  2329.7   0.82    1.22
   209.00  84573.9  6.73  6603.0 10.40  1.99  7.07  872119.12  405.30 2810.3 1139039.6  2343.2   0.83    1.23
   214.00  85732.6  6.91  6782.3 10.38  1.80  6.50  870073.19  413.11 2764.5 1142045.7  2372.9   0.86    1.24
   219.00  86794.9  7.09  6963.7 10.40  1.60  7.05  867986.94  421.76 2718.0 1146351.9  2349.5   0.86    1.24
   224.00  87796.3  7.27  7143.9 10.43  1.52  8.07  865854.87  431.05 2671.9 1151705.9  2276.3   0.85    1.26
   229.00  88812.2  7.45  7322.5 10.43  1.55  8.47  863676.69  440.23 2628.2 1156160.7  2203.7   0.84    1.27
   234.00  89868.5  7.62  7502.5 10.41  1.55  8.06  861457.37  446.74 2580.3 1152723.2  2175.5   0.84    1.27
   239.00  90921.1  7.80  7685.3 10.39  1.45  7.46  859210.19  452.15 2533.7 1145619.9  2175.1   0.86    1.26
   244.00  91910.4  7.99  7869.6 10.38  1.30  7.48  856935.81  457.61 2486.7 1137942.1  2161.2   0.87    1.26
1/////   6  D - O - F   OUTPUT SUMMARY   /////                    PAGE   2

     TIME ALTITUDE  MACH   SPEED     Q   GAMMA ALPHA     WEIGHT   W-DOT   ISP   THRUST    IEFF   IRAT   GCB-1
   249.00  92825.1  8.17  8052.7 10.41  1.19  8.17  854630.25  464.71 2440.0 1133893.4  2111.9   0.87    1.26
   254.00  93710.7  8.35  8232.9 10.42  1.16  8.86  852288.87  471.82 2394.1 1129573.0  2041.6   0.85    1.26
   259.00  94615.1  8.52  8411.4 10.42  1.17  8.92  849912.37  478.51 2348.6 1123852.7  1987.3   0.85    1.25
   264.00  95538.2  8.70  8590.4 10.39  1.15  8.42  847509.31  482.74 2303.2 1111825.5  1964.4   0.85    1.25
   269.00  96436.6  8.87  8770.4 10.38  1.06  7.98  845085.00  486.99 2257.4 1099340.2  1953.4   0.87    1.23
   274.00  97270.9  9.05  8950.1 10.38  0.95  8.13  842638.62  492.15 2211.8 1088523.1  1926.1   0.87    1.23
   279.00  98045.5  9.23  9127.7 10.40  0.87  8.82  840159.50  499.50 2166.6 1082200.9  1873.6   0.86    1.22
   284.00  98803.8  9.40  9302.2 10.42  0.87  9.43  837643.87  506.71 2122.2 1075348.6  1808.9   0.85    1.22
   287.01  99269.4  9.50  9408.1 10.42  0.88  9.53  836009.69  461.60 2095.3  967203.1  1771.5   0.85    1.09
   287.01  99269.4  9.50  9408.1 10.42  0.88  9.53  836089.69  461.60 2095.3  967203.1?????????????    1.09
   288.00  99425.4  9.53  9439.9 10.41  0.89 10.42  835607.37  510.01 2087.3 1064535.9  1712.7   0.82    1.21
   293.00 100310.2  9.68  9595.4 10.31  1.13 13.37  833069.06  505.46 2048.2 1035267.5  1589.4   0.78    1.18
   298.00 101460.2  9.83  9742.3 10.06  1.41 12.25  830552.25  501.24 2011.8 1008383.9  1508.4   0.75    1.16
   303.00 102790.9  9.97  9896.2  9.73  1.49  9.72  828056.94  496.84 1973.9  980735.9  1589.6   0.81    1.13
   308.00 104117.4 10.12 10056.8  9.43  1.38  8.17  825566.87  500.75 1934.4  968639.6  1657.9   0.86    1.12
   313.00 105323.5 10.28 10219.8  9.19  1.20  8.42  823048.56  506.48 1895.4  959989.2  1657.6   0.87    1.11
   318.00 106408.3 10.42 10379.7  9.00  1.08  9.78  820502.75  511.81 1859.2  951556.2  1605.0   0.86    1.11
```

Fig. 97 A Typical DOF36 Output Printout

study team modification to the program as received from AFWAL. Since DOF36 originally calculated required thrust with a constant, user input fuel flowrate, the program modification was performed to limit the program calculated thrust profile to that dictated by the engine performance database. This change and the associated FFMAX calculation procedure will be further described.

Program Internal Processing

DOF36 first initializes all simulation parameters and then reads in, and performs linear interpolation on, the basic input data. Acceleration components are then calculated in the simulation's inertial reference frame. The program then calculates the required inertial reference frame control force acceleration vector and converts the difference between this control force acceleration vector and the actual accelerations to a dynamic control loop error signal. This error signal is then converted into time rates of change of the simulation's independent variables, e.g., angle-of-attack and flight path angle. With the time rates of change of these independent variables known, the program then performs second-order Runge-Kutta integration in order to update the respective simulation variables. Finally, the program checks the status of guidance and engine cycle events and checks the program built-in stop conditions, then either loops back to the input data interpolation step with now updated variable values, or terminates the simulation.

Program Outputs

Some of the more important simulation parameters, such as time, angle-of-attack, and Mach number are printed to the computer monitor during program execution. All of the simulation parameters are then output to an ASCII text output file which is then easily converted to hard copy. Fig. 97 presents a portion of a typical DOF36 output file printout.

The data and associated engineering units which are contained in the output file includes:

time [s]
altitude [ft]
Mach number [--]
speed [ft/s]
dynamic pressure [lb_f/in^2]
flight path angle [deg]
angle-of-attack [deg]
vehicle mass [lbm]
fuel mass flowrate [lbm/s]
effective specific impulse [lb_f-s/lbm]
the ratio of specific impulse to effective specific impulse [--]
axial force [lb_f]
cumulative axial impulse [lb_f]
net thrust [lb_f]
total net thrust impulse [lb_f]
normal force [lb_f]
longitude [deg]
latitude [deg]
heading [deg]
range ground track [nmi]
relative vertical acceleration [--]
relative horizontal acceleration [--]
relative longitudinal acceleration [--]

6.3.2 Trajectory Simulation Post Processing

DOF36 Output Plotting

The original version of DOF36 was also modified to create an output data file which would better lend itself to graphing of the data. This graph file was post processed to make it readable by a commercial graphics software package which ultimately plotted various trajectory simulation parameters against Mach number for engine/vehicle system comparison purposes. An example of this graphic output is presented in Fig. 98 and 99.

FUELVOL Program

Fig. 100 presents a typical output from the trajectory simulation program post-processor program named FUELVOL. FUELVOL is a short, in-house written FORTRAN program designed to both calculate the ascent flight hydrogen/oxygen split based on engine type, engine operating mode and time, and to estimate the liquid hydrogen (LH_2) and liquid oxygen (LO_2) tank sizes for the simulated vehicle.

The program user inputs the engine type and the trajectory simulation calculated vehicle mass and time of ejector mode/ramjet mode transition, of scramjet mode/rocket mode transition, and at local orbital conditions. For the non-air-liquefaction engines analyzed in this study (Engines 10 and 12), the oxygen mass flowrate during the engine ejector mode was also required by the program. Based on all of the engines' nominally selected rocket mode oxygen/hydrogen combustion mass ratio of 6.0, the initial, intermediate, and final vehicle mass ratios were calculated. The time spent in each of the engine operating modes, the propellant flow rates, and the time required for the vehicle to reach local orbital conditions were calculated. The program then calculated the mass and volume hydrogen/oxygen split and thus provided a preliminary geometrical sizing of the vehicle's frustum LH_2 and LO_2 tanks. The program was also able to calculate hydrogen volumes and determine tank sizes when slush hydrogen, which is required for Engine 32, was used for any or all of the five engines studied.

Vehicle Geometrical Sizing Program

Once the vehicle hydrogen/oxygen mass ratio had been determined from the FUELVOL program just described, this and other data, were entered into the vehicle geometric sizing program. The other data required by the sizing program included the vehicle takeoff gross weight; the vehicle takeoff attitude; the number and type of engines and their associated 1985 and 1995 TAD weights and center of gravity stations; the vehicle strake size; the quality of the hydrogen fuel used (i.e., slush or liquid); and the desired non-optimum factors to be applied to the vehicle structural elements and tanks.

Based on the MMAG derived vehicle mass property determination methodology, the vehicle sizing program determines each subsystems' mass, center of gravity, physical envelope, and establishes the overall vehicle center of gravity and physical envelope.

6.4 Analysis Methodology and Findings

As summarized in the "flow-diagram" of Fig. 101, the basic approach employed in this study for the determination and analysis of the merits of the various engine/vehicle systems considered centered on engine/vehicle systems of fixed TOGW being computer modeled and simulated to fly a pre-determined reference trajectory with pre-selected engine mode transition points. With vehicle TOGW held constant, the vehicle mass delivered to local orbital conditions, M2, and ultimately to the target 100 nmi orbital altitude, varied with changing engine performance and vehicle configuration characteristics. This caused the calculated vehicle net

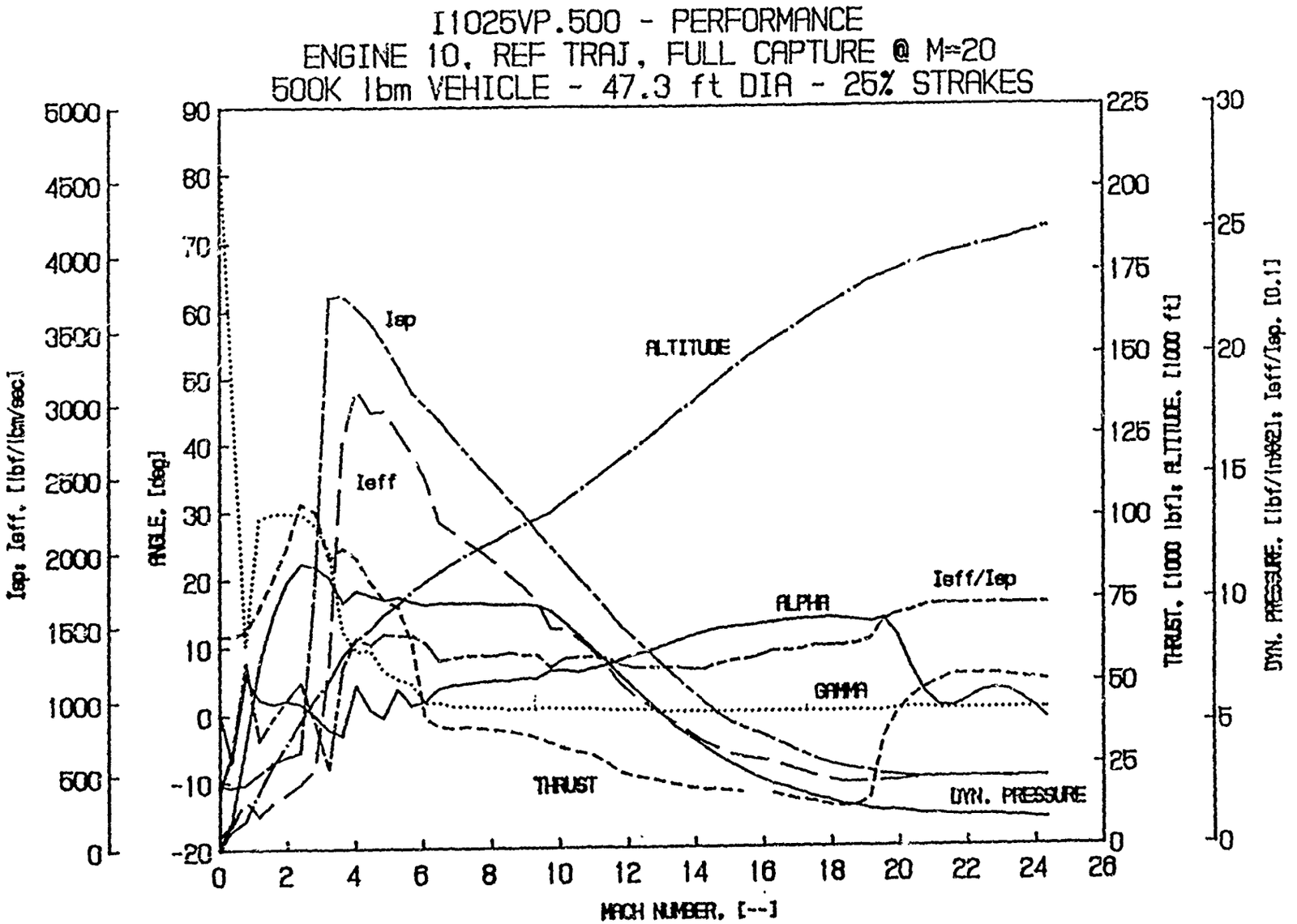


Fig. 98 Performance Graph File Output

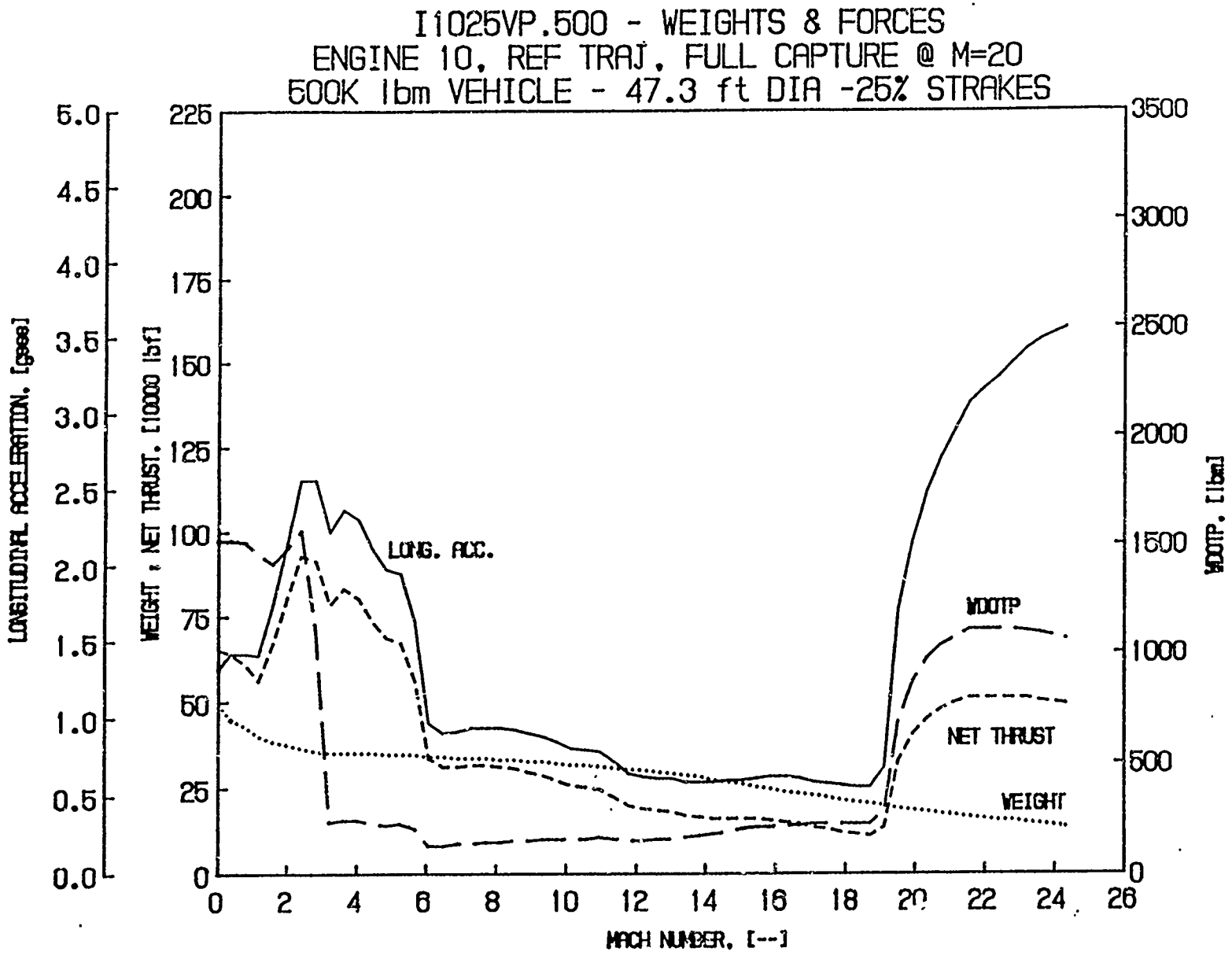


Fig. 99 Weights and Forces Graph File Output

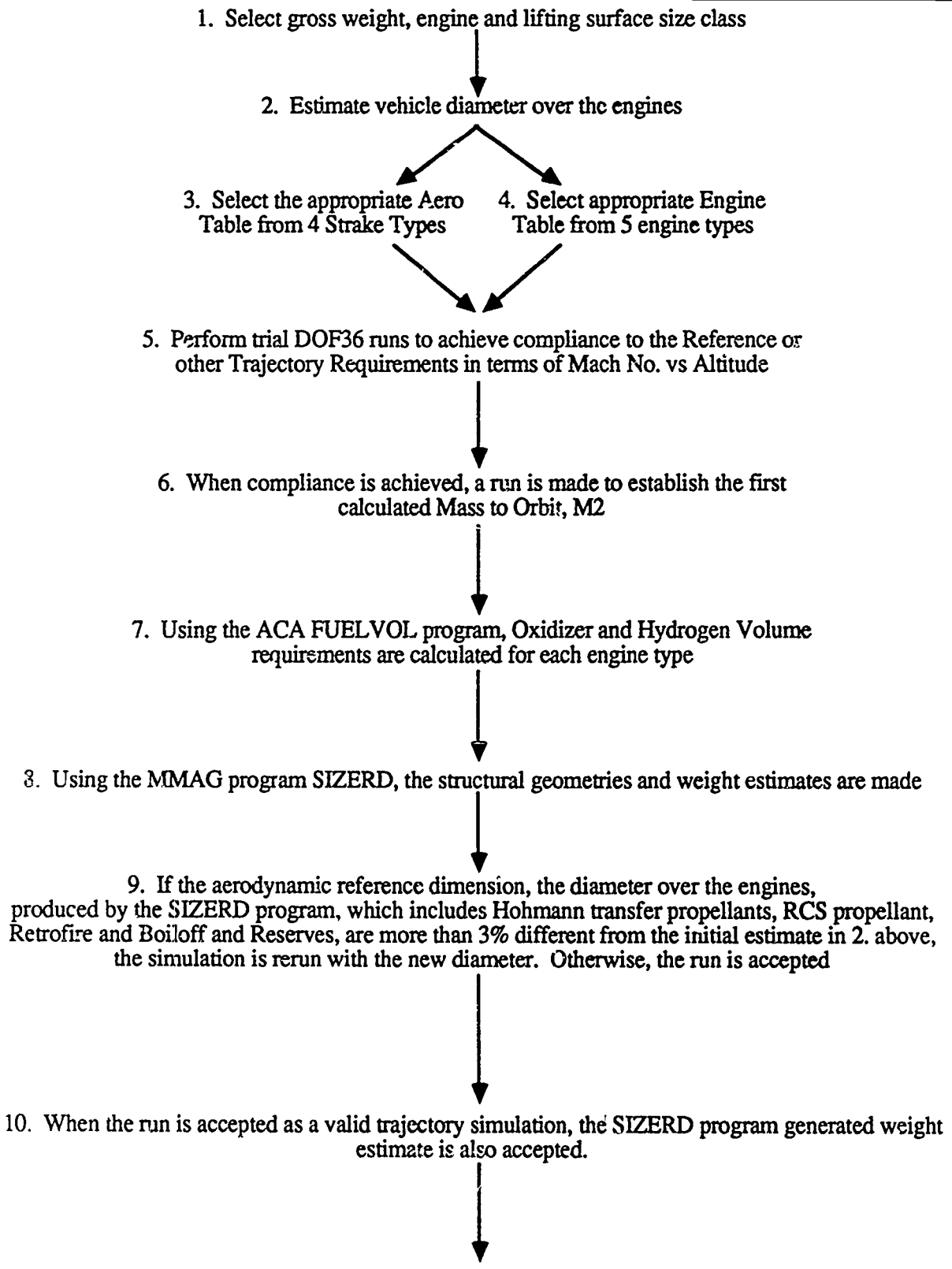


Fig. 101 The Trajectory Analysis Process

```
VEHICLE GTOW IS    956000. LB
WEIGHT AT END OF EJECTOR PHASE IS     908075. LB AT   127.00 SECONDS
WEIGHT AT START OF ROCKET PHASE IS    703390. LB AT   524.00 SECONDS
WEIGHT AT ORBITAL CONDITIONS IS       344768. LB AT   690.00 SECONDS
HALF-ANGLE OF CONICAL FOREBODY IS        8.00 DEGREES
LENGTH OF VEHICLE UP TO THE LOX TANK IS     33.700 FEET
ENGINE NUMBER IS 32 WHICH USES LAIR DURING THE EJECTOR PHASE
AND SLUSH HYDROGEN

DELTA WEIGHT DURING EJECTOR PHASE IS       47925.0 LB
DELTA HYDROGEN WT DURING EJECTOR PHASE IS  47925.0 LB
DELTA WEIGHT DURING R/S JET PHASE IS      204685.0 LB
DELTA HYDROGEN WT DURING R/S JET PHASE IS 204685.0 LB
DELTA WEIGHT DURING ROCKET PHASE IS       358622.0 LB
DELTA HYDROGEN WT DURING ROCKET PHASE IS   51231.7 LB
DELTA LOX WEIGHT DURING ROCKET PHASE IS   307390.3 LB

TOTAL LOX CONSUMED DURING ASCENT          307390.3 LB,   4305.2 CUFT
TOTAL HYDROGEN CONSUMED DURING ASCENT     303841.7 LB,  59113.2 CUFT
THESE TOTALS DO NOT INCLUDE AN ALLOWANCE FOR FLYBACK, ORBITAL MANEUVERS, ETC
LENGTH UP TO LOX TANK IS     33.70 FT
LENGTH OF THE LOX TANK IS    20.00 FT
RADII OF THE LOX TANK ARE    4.74 AND     7.55 FEET
LENGTH OF THE HYDROGEN TANK
FRUSTRUM PORTION IS            79.28 FT
RADII OF THE HYD TANK ARE    7.55 AND    18.69 FEET
```

Fig. 100 Typical FUELVOL Output File

discretionary payload mass to change. Vehicle payload performance was the study's primary figure-of-merit in the engine/vehicle system analysis work conducted.

DOF36 was neither used to model required Hohmann transfer, RCS, and retrofire propellant consumption, nor propellant boiloff and reserve propellant requirements. Since the vehicle hull geometry, which ultimately determined the structural inert weight calculated in the MMAG geometrical sizing program, was that geometry dictated by the propellant consumption characteristics of only the Earth-to-orbit portion of the mission profile, an iterative process was required between the initial estimated geometry and the resulting actual geometry, which included Hohmann transfer propellant, boiloff, reserves, etc. volumes, for each particular simulation case considered. If the critical aerodynamic and engine dimensions obtained in the initial estimation process differed by more than 3% from those obtained from the sizing program with these additional volume requirements, an additional run was made to obtain convergence between the estimated and program calculated values.

This section describes the study's approach to engine performance characteristics estimation, as input to the trajectory simulation program, and provides the rationale used to develop the vehicle mass properties assumed for the post-trajectory simulation analysis. It also details the approach utilized to estimate and implement vehicle aerodynamic characteristics and defines the study's baseline reference trajectory flight path. Most importantly, this section discusses the basic matrix of variables studied and the variable sensitivity studies performed, and presents the results and findings of these respective efforts. The results of the analysis work are presented, to the extent possible, in fixed-scale barchart format and also in various line graphs and data tables. Finally, the results of the study's preliminary vehicle point design effort is presented.

6.4.1 Engine Performance Estimation Approach

This section discusses the air-augmented rocket combined cycle engine specific impulse and thrust data derived from the study's baseline database. This data was tabularized for input to DOF36 in half-Mach number increments from 0 to Mach 10 and in full-Mach number increments above Mach 10.

Study Principle Database

The mid-1960s NAS7-377 study, "A Study of Composite Propulsion Systems for Advanced Launch Vehicle Applications" (Ref. 2), provided the baseline for the present study's engine performance and engine mass properties estimation processes. This earlier effort provided well organized, comprehensive technical information covering a wide range of RBCC propulsion systems for space transportation applications. The Composite Engine Study provided the present study with all five of the fundamental engine concepts, as well as the engine specific impulse and thrust performance estimates for ejector, supercharged ejector, and ramjet modes of engine operation.

Specific Impulse

Tables 14 to 18 present, respectively, engine specific impulse tabulations for all five engines as prepared to support DOF36 engine file creation. It should be noted that the ejector and ramjet mode performance data obtained from NAS7-377 includes the effects of ram-drag; that is, net-jet specific impulse data is presented. Vehicle forebody precompression effects for a 6-degree, two-dimensional wedge were used to estimate the pressure field effects on ramjet mode performance for the reference 3-dimensional, 16-degree, conical vehicle configuration.

The NAS7-377 scramjet data were based on several reference trajectories, all of which differed markedly from this study's reference trajectory. In addition, the database scramjet performance information was limited to a Mach 12 flight speed and was considered to be overly conservative according to contemporary studies as previously discussed in Section 3.0. For these reasons, the available, unclassified, non-proprietary literature was examined in order to obtain a set of composite scramjet performance estimates. The specific impulse estimates resulting from this literature evaluation process can be noted in the scramjet specific impulse tabulations. It should be noted that forebody precompression effects are implicit in scramjet data and that the engine equivalence ratio schedule was required to meet thrust requirements at hypersonic velocities. As a result of this equivalence ratio schedule, a degrading effect on specific impulse is fairly marked at the low- and mid-speed range conditions.

Thrust

DOF36 does not have the capability to accept, as input to the engine file, both specific impulse and thrust. Therefore, engine thrust (T) was converted to fuel or propellant flowrate (W_p) using a modified form of the definition of specific impulse (I_{sp}), where $W_p = T/I_{sp}$. This enabled specific impulse to be entered into the engine file as a function of Mach number, and by the implication of using a reference trajectory, a function of altitude. The fuel flowrate was then entered into an in-house modified version of DOF36 which accepted these values as maximum fuel flowrates in the thus created FFMAX file.

Tables 14 to 18 present thrust tables for all 5 engines configurations studied. As with specific impulse, the data are given for half Mach number increments from 0 to Mach 10 and in full Mach number increments above Mach 10. These values are then subject to linear interpolation within DOF36. These tables show the composite engine study derived engine thrusts for ejector and ramjet modes of engine operation.

Table 14a Specific Impulse Performance for Engine #10 - Ejector Scramjet

ENGINE 10 SPECIFIC IMPULSE PROFILE FOR REFERENCE TRAJECTORY
(FOR A 250 klbf SLS ENGINE)

11 JUNE 87

REFERENCE TRAJECTORY			SPECIFIC IMPULSE, Isp [lbf-s/lbm] **								
MACH NUMBER [—]	ALTITUDE [ft]	q* [psf]	EJECTOR	NO PRESS FIELD RAMJET	4 DEG WEDGE RAMJET	6 DEG WEDGE RAMJET	8 DEG WEDGE RAMJET	@ SCRAMJET	@ ROCKET	REFERENCE Isp ## PROFILE	ENGINE OPERATING MODE
0.0	0	0	430							430	EJECTOR
0.5	7100	240	425							425	"
1.0	17250	700	458							458	"
1.5	28650	1050	571	2600						571	"
2.0	38500	1200	627	3350						627	"
2.5	45500	1400	677	3740						677	"
2.8	50900	1450	733	3890						733	"
3.0	52150	1500		3920	3770	3700	3630			3700	RAMJET
3.5	58650	1500		3930	3825	3765	3705			3765	"
4.0	63150	1500		3800	3730	3685	3640			3685	"
4.5	68000	1500		3610	3570	3535	3500			3535	"
5.0	72500	1500		3340	3370	3350	3330			3350	"
5.5	76500	1500		3100	3135	3135	3135			3135	"
6.0	80000	1500		2790	2900	2900	2900	3000		3000	SCRAMJET
6.5	83500	1500						2900		2900	"
7.0	86500	1500						2750		2750	"
7.5	89500	1500						2625		2625	"
8.0	92000	1500						2500		2500	"
8.5	95000	1500						2400		2400	"
9.0	97500	1500						2300		2300	"
9.5	100000	1500						2175		2175	"
10.0	102000	1400						2050		2050	"
11.0	115000	1300						1725		1725	"
12.0	120000	1000						1450		1450	"
13.0	130000	900						1225		1225	"
14.0	135000	800						1025		1025	"
15.0	140000	750						850	470	470	ROCKET
16.0	145000	700						750	470	470	"
17.0	155000	600						650	470	470	"
18.0	160000	500						550	470	470	"
19.0	165000	450						525	470	470	"
20.0	175000	400						475	470	470	"
21.0		350						450	470	470	"
22.0		250						425	470	470	"
23.0		200						400	470	470	"
24.0		100						400	470	470	"
25.0		50						400	470	470	"
26.0								375	470	470	"
27.0									470	470	"

* AIAA-86-1388
\+ STAARS DATABASE #0211, CAPTURE AREA/CAPTURE AREA @ M=15
\# 51.0 ft DIAMETER VEHICLE, 70% CAPTURE AT M=15
@ STAARS DATABASE # TBD, PRELIMINARY ENGINE INFORMATION ON FIVE COMBINED CYCLE ENGINES
** A STUDY OF COMPOSITE PROPULSION SYSTEMS FOR ADVANCED LAUNCH VEHICLE APPLICATIONS, VOLUME 6
++ A STUDY OF COMPOSITE PROPULSION SYSTEMS FOR ADVANCED LAUNCH VEHICLE APPLICATIONS, VOLUME 4, PAGE 23
ASSUMES 6-DEGREE 2-DIMENSIONAL WEDGE INDUCED PRESSURE FIELD, EJECTOR MODE SHIFT TO RAMJET MODE AT MACH 3, RAMJET MODE SHIFT TO SCRAMJET MODE AT MACH 6, SCRAMJET MODE SHIFT TO ROCKET MODE AT MACH 20

Table 14b Thrust Performance for Engine #10 - Ejector Scramjet

ENGINE 10 THRUST PROFILE FOR REFERENCE TRAJECTORY (FOR A 250 klbf SLS ENGINE)

28 APR 87

REFERENCE TRAJECTORY		THRUST, [lbf] **							+							
MACH NUMBER [--]	* ALTITUDE [ft]	EJECTOR	NO PRESS FIELD RAMJET	4 DEG WEDGE RAMJET	6 DEG WEDGE RAMJET	8 DEG WEDGE RAMJET	*,+,#,@ SCRAMJET	ROCKET	Ac normal [--]	Ac@ [ft**2]	Ct@ [--]	NDOTP T/Isp [lbm/s]	REFERENCE NDOTP [lbm/s]	REFERENCE NDOTO2 [lbm/s]	REFERENCE THRUST ## [lbf]	ENGINE OPERATING MODE
0.0	0	250000										581	1512	1300	650000	EJECTOR
0.5	7100	248000										584	1517	1300	644800	"
1.0	17250	263000										574	1493	1300	683800	"
1.5	28650	306000	116000									536	1393	1300	795600	"
2.0	38500	358000	172000						0.300	429		571	1485	1300	930800	"
2.5	45500	409000	216000						0.327	468		604	1571	1300	1063400	"
2.9	50900	453000	280000						0.348	498		618	1607	1300	1177800	"
3.0	52150		296000	325000	335000	345000			0.354	506		91	235	0	871000	RAMJET
3.5	58650		258000	330000	355000	380000			0.381	545		94	245	0	923000	"
4.0	63150		234000	320000	345000	370000			0.408	583		94	243	0	897000	"
4.5	68000		210000	275000	302500	330000			0.435	622		86	222	0	786500	"
5.0	72500		184000	255000	285000	315000	380796		0.462	660	1.000	85	221	0	741000	"
5.5	76500		162000	250000	280000	310000	386889		0.488	699	0.960	89	232	0	728000	"
6.0	80000						391204		0.515	737	0.920	130	339	0	1017131	SCRAMJET
6.5	83500						380320		0.542	776	0.850	131	341	0	988832	"
7.0	86500						380415		0.569	814	0.810	138	360	0	989079	"
7.5	89500						386111		0.596	853	0.785	147	382	0	1003889	"
8.0	92000						380415		0.623	891	0.740	152	396	0	989079	"
8.5	95000						380764		0.650	930	0.710	159	412	0	989987	"
9.0	97500						374195		0.677	968	0.670	163	423	0	972908	"
9.5	100000						368753		0.704	1007	0.635	170	441	0	958758	"
10.0	102000						337639	200000	0.731	1045	0.600	165	428	0	877961	"
11.0	115000						305766	200000	0.785	1122	0.545	177	461	0	794993	"
12.0	120000						237511	200000	0.838	1199	0.515	164	426	0	617528	"
13.0	130000						216444	200000	0.892	1276	0.490	177	459	0	562755	"
14.0	135000						195678	200000	0.946	1353	0.470	191	496	0	508764	"
15.0	140000						189763	200000	1.000	1430	0.460	426	1106	948	520000	ROCKET
16.0	145000						0	200000			0.450	426	1106	948	520000	"
17.0	155000						0	200000			0.445	426	1106	948	520000	"
18.0	160000						0	200000			0.445	426	1106	948	520000	"
19.0	165000						0	200000			0.450	426	1106	948	520000	"
20.0	175000						0	200000			0.460	426	1106	948	520000	"
21.0							0	200000			0.470	426	1106	948	520000	"
22.0							0	200000			0.480	426	1106	948	520000	"
23.0							0	200000			0.495	426	1106	948	520000	"
24.0							0	200000			0.510	426	1106	948	520000	"
25.0							0	200000			0.530	426	1106	948	520000	"
26.0								200000				426	1106	948	520000	"
27.0								200000				426	1106	948	520000	"

* AIAA-86-1388
\+ STAARS DATABASE #0211, CAPTURE AREA/CAPTURE AREA @ M=15
\# 51.0 ft DIAMETER VEHICLE, 70% CAPTURE AT M=15
\@ STAARS DATABASE # TBD, PRELIMINARY ENGINE INFORMATION ON FIVE COMBINED CYCLE ENGINES
** A STUDY OF COMPOSITE PROPULSION SYSTEMS FOR ADVANCED LAUNCH VEHICLE APPLICATIONS, VOLUME 6
\++ A STUDY OF COMPOSITE PROPULSION SYSTEMS FOR ADVANCED LAUNCH VEHICLE APPLICATIONS, VOLUME 4, PAGE 23
\## ASSUMES 6-DEGREE 2-DIMENSIONAL WEDGE INDUCED PRESSURE FIELD, EJECTOR MODE SHIFT TO RAMJET MODE AT MACH 3, RAMJET MODE SHIFT TO SCRAMJET MODE AT MACH 6, SCRAMJET MODE SHIFT TO ROCKET MODE AT MACH 20

Table 15a Specific Impulse Performance for Engine #12 - Supercharged Ejector Scramjet

ENGINE 12 SPECIFIC IMPULSE PROFILE FOR REFERENCE TRAJECTORY
(FOR A 250 klbf SLS ENGINE)

11 JUNE 87

REFERENCE TRAJECTORY			SPECIFIC IMPULSE, Isp [lbf-s/lbm] **									
MACH NUMBER [—]	* ALTITUDE [ft]	q* [psf]	SUPER-CHARGED EJECTOR	FAN RAMJET	NO PRESS FIELD RAMJET	4 DEG WEDGE RAMJET	6 DEG WEDGE RAMJET	8 DEG WEDGE RAMJET	@ SCRAMJET	@ ROCKET	REFERENCE Isp ## PROFILE	ENGINE OPERATING MODE
0.0	0	0	470								470	EJECTOR
0.5	7100	40	462	1640							462	"
1.0	17250	700	498	2300							498	"
1.5	28650	1050	571	3040	2600						571	"
2.0	38500	1200	664	3620	3350						664	"
2.5	45500	1400	763	3840	3740						763	"
2.9	50900	1450	832	3980	3890						832	"
3.0	52150	1500			3920	3770	3700	3630			3700	RAMJET
3.5	58650	1500			3930	3825	3765	3705			3765	"
4.0	63100	1500			3800	3730	3685	3640			3685	"
4.5	68000	1500			3610	3570	3535	3500			3535	"
5.0	72500	1500			3380	3370	3350	3330			3350	"
5.5	76500	1500			3100	3135	3135	3135			3135	"
6.0	80000	1500			2790	2900	2900	2900	3000		3000	SCRAMJET
6.5	83500	1500							2900		2900	"
7.0	86500	1500							2750		2750	"
7.5	89500	1500							2625		2625	"
8.0	92000	1500							2500		2500	"
8.5	95000	1500							2400		2400	"
9.0	97500	1500							2300		2300	"
9.5	100000	1500							2175		2175	"
10.0	102000	1400							2040		2050	"
11.0	115000	1300							1725		1725	"
12.0	120000	1000							1450		1450	"
13.0	130000	900							1225		1225	"
14.0	135000	800							1025		1025	"
15.0	140000	750							850	470	470	ROCKET
16.0	145000	700							750	470	470	"
17.0	155000	600							650	470	470	"
18.0	160000	500							550	470	470	"
19.0	165000	450							525	470	470	"
20.0	175000	400							475	470	470	"
21.0		350							450	470	470	"
22.0		250							425	470	470	"
23.0		200							400	470	470	"
24.0		100							400	470	470	"
25.0		50							400	470	470	"
26.0									375	470	470	"
27.0										470	470	"

* AIAA-86-1388
\+ STAARS DATABASE #0211, CAPTURE AREA/CAPTURE AREA @ M=15
\# 53.1 ft DIAMETER VEHICLE, 70% CAPTURE AT M=15
@ STAARS DATABASE # TBD, PRELIMINARY ENGINE INFORMATION ON FIVE COMBINED CYCLE ENGINES
** A STUDY OF COMPOSITE PROPULSION SYSTEMS FOR ADVANCED LAUNCH VEHICLE APPLICATIONS, VOLUME 6
++ A STUDY OF COMPOSITE PROPULSION SYSTEMS FOR ADVANCED LAUNCH VEHICLE APPLICATIONS, VOLUME 4, PAGE 23
ASSUMES 6-DEGREE 2-DIMENSIONAL WEDGE INDUCED PRESSURE FIELD, EJECTOR MODE SHIFT TO RAMJET MODE AT MACH 3, RAMJET MODE SHIFT TO SCRAMJET MODE AT MACH 6, SCRAMJET MODE SHIFT TO ROCKET MODE AT MACH 20

Table 15b Thrust Performance for Engine #12 - Supercharged Ejector Scramjet

ENGINE 12 THRUST PROFILE FOR REFERENCE TRAJECTORY (FOR A 250 klbf SLS ENGINE)

29 APR 87

REFERENCE TRAJECTORY		THRUST, [lbf] **								+			WDOTP	REFERENCE	REFERENCE	REFERENCE	ENGINE
MACH NUMBER [--]	* ALTITUDE [ft]	SUPER-CHARGED EJECTOR	FAN RAMJET	NO PRESS FIELD RAMJET	4 DEG WEDGE RAMJET	6 DEG WEDGE RAMJET	8 DEG WEDGE RAMJET	*,+,#,@ SCRAMJET	ROCKET	Ac normal [--]	Ac@ [ft**2]	Ct@ [--]	T/Isp [lbm/s]	WDOTP [lbm/s]	WDOTO2 [lbm/s]	THRUST ## [lbf]	OPERATING MODE
0.0	0	253000											538	1400	2314	657800	EJECTOR
0.5	7100	248000											537	1396	2314	644800	"
1.0	17250	266000	92000										534	1389	2314	691600	"
1.5	28650	305000	148000	116000									534	1389	2314	793000	"
2.0	38500	359000	196000	172000						0.300	465		541	1406	2314	933400	"
2.5	45500	424000	249000	216000						0.327	507		556	1445	2314	1102400	"
2.9	50900	469000		285000						0.348	540		564	1466	2314	1219400	"
3.0	52150			296000	325000	335000	345000			0.354	549		91	235	0	871000	RAMJET
3.5	58650			258000	330000	355000	380000			0.381	590		94	245	0	923000	"
4.0	63100			234000	320000	345000	370000			0.408	632		94	243	0	897000	"
4.5	68000			210000	275000	302500	330000			0.435	674		86	222	0	786500	"
5.0	72500			184000	255000	285000	315000	412855		0.462	716	1.000	85	221	0	741000	"
5.5	76500			162000	250000	280000	310000	419461		0.488	757	0.960	89	232	0	728000	"
6.0	80000							424140		0.515	799	0.920	141	368	0	1102763	SCRAMJET
6.5	83500							412339		0.542	841	0.850	142	370	0	1072081	"
7.0	86500							412442		0.569	883	0.810	150	390	0	1072350	"
7.5	89500							418618		0.596	924	0.785	159	415	0	1088406	"
8.0	92000							412442		0.623	966	0.740	165	429	0	1072350	"
8.5	95000							412821		0.650	1008	0.710	172	447	0	1073334	"
9.0	97500							405699		0.677	1050	0.670	176	459	0	1054817	"
9.5	100000							399798		0.704	1091	0.635	184	478	0	1039476	"
10.0	102000							366065	200000	0.731	1133	0.600	179	464	0	951768	"
11.0	115000							331509	200000	0.785	1217	0.545	192	500	0	861923	"
12.0	120000							257507	200000	0.838	1300	0.515	178	462	0	669518	"
13.0	130000							234667	200000	0.892	1384	0.490	192	498	0	610134	"
14.0	135000							212152	200000	0.946	1467	0.470	207	538	0	551596	"
15.0	140000							205739	200000	1.000	1551	0.460	426	1106	948	520000	ROCKET
16.0	145000								200000			0.450	426	1106	948	520000	"
17.0	155000								200000			0.445	426	1106	948	520000	"
18.0	160000								200000			0.445	426	1106	948	520000	"
19.0	165000								200000			0.450	426	1106	948	520000	"
20.0	175000								200000			0.460	426	1106	948	520000	"
21.0									200000			0.470	426	1106	948	520000	"
22.0									200000			0.480	426	1106	948	520000	"
23.0									200000			0.495	426	1106	948	520000	"
24.0									200000			0.510	426	1106	948	520000	"
25.0									200000			0.530	426	1106	948	520000	"
26.0									200000				426	1106	948	520000	"
27.0									200000				426	1106	948	520000	"

* AIAA-86-1388
\+ STAARS DATABASE #0211, CAPTURE AREA/CAPTURE AREA @ M=15
\# 53.1 ft DIAMETER VEHICLE, 70% CAPTURE AT M=15
@ STAARS DATABASE # TBD, PRELIMINARY ENGINE INFORMATION ON FIVE COMBINED CYCLE ENGINES
** A STUDY OF COMPOSITE PROPULSION SYSTEMS FOR ADVANCED LAUNCH VEHICLE APPLICATIONS, VOLUME 6
++ A STUDY OF COMPOSITE PROPULSION SYSTEMS FOR ADVANCED LAUNCH VEHICLE APPLICATIONS, VOLUME 4, PAGE 23
ASSUMES 6-DEGREE 2-DIMENSIONAL WEDGE INDUCED PRESSURE FIELD, EJECTOR MODE SHIFT TO RAMJET MODE AT MACH 3, RAMJET MODE SHIFT TO SCRAMJET MODE AT MACH 6, SCRAMJET MODE SHIFT TO ROCKET MODE AT MACH 20

Table 16a Specific Impulse Performance for Engine #22 - Ejector ScramLACE

ENGINE 22 SPECIFIC IMPULSE PROFILE FOR REFERENCE TRAJECTORY
(FOR A 250 klbf SLS ENGINE)

11 JUNE 87

REFERENCE TRAJECTORY			SPECIFIC IMPULSE, Isp [lbf-s/lbm] **								
MACH NUMBER [—]	ALTITUDE [ft]	q* [psf]	EJECTOR	NO PRESS FIELD RAMJET	4 DEG WEDGE RAMJET	6 DEG WEDGE RAMJET	8 DEG WEDGE RAMJET	@ SCRAMJET	@ ROCKET	REFERENCE Isp ## PROFILE	ENGINE OPERATING MODE
0.0	0	0	1415							1415	EJECTOR
0.5	7100	240	1379							1379	"
1.0	17250	700	1471							1471	"
1.5	28650	1050	1577	2600						1577	"
2.0	30500	1200	1818	3350						1818	"
2.5	45500	1400	2096	3740						2096	"
2.9	50900	1450	2328	3890						2328	"
3.0	52150	1500		3920	3770	3700	3630			3700	RAMJET
3.5	58650	1500		3930	3825	3765	3705			3765	"
4.0	63100	1500		3800	3730	3685	3640			3685	"
4.5	68000	1500		3610	3570	3535	3500			3535	"
5.0	72500	1500		3380	3370	3350	3330			3350	"
5.5	76500	1500		3100	3135	3135	3135			3135	"
6.0	80000	1500		2790	2900	2900	2900	3000		3000	SCRAMJET
6.5	83500	1500						2900		2900	"
7.0	86500	1500						2750		2750	"
7.5	89500	1500						2625		2625	"
8.0	92000	1500						2500		2500	"
8.5	95000	1500						2400		2400	"
9.0	97500	1500						2300		2300	"
9.5	100000	1500						2175		2175	"
10.0	102000	1400						2050		2050	"
11.0	115000	1300						1725		1725	"
12.0	120000	1000						1450		1450	"
13.0	130000	900						1225		1225	"
14.0	135000	800						1025		1025	"
15.0	140000	750						850	470	470	ROCKET
16.0	145000	700						750	470	470	"
17.0	155000	600						650	470	470	"
18.0	160000	500						550	470	470	"
19.0	165000	450						525	470	470	"
20.0	175000	400						475	470	470	"
21.0		350						450	470	470	"
22.0		250						425	470	470	"
23.0		200						400	470	470	"
24.0		100						400	470	470	"
25.0		50						400	470	470	"
26.0								375	470	470	"
27.0									470	470	"

* AIAA-86-1388
\+ STAARS DATABASE #0211, CAPTURE AREA/CAPTURE AREA @ M=15
\# 55.0 ft DIAMETER VEHICLE, 70% CAPTURE AT M=15
@ STAARS DATABASE # TBD, PRELIMINARY ENGINE INFORMATION ON FIVE COMBINED CYCLE ENGINES
** A STUDY OF COMPOSITE PROPULSION SYSTEMS FOR ADVANCED LAUNCH VEHICLE APPLICATIONS, VOLUME 6
++ A STUDY OF COMPOSITE PROPULSION SYSTEMS FOR ADVANCED LAUNCH VEHICLE APPLICATIONS, VOLUME 4, PAGE 23
ASSUMES 6-DEGREE 2-DIMENSIONAL WEDGE INDUCED PRESSURE FIELD, EJECTOR MODE SHIFT TO RAMJET MODE AT MACH 3, RAMJET MODE SHIFT TO SCRAMJET MODE AT MACH 6, SCRAMJET MODE SHIFT TO ROCKET MODE AT MACH 20

Table 16b Thrust Performance for Engine #22 - Ejector ScramLACE

ENGINE 22 THRUST PROFILE FOR REFERENCE TRAJECTORY (FOR A 250 klbf SLS ENGINE)

DAVID L. DOUGHTY

29 APR 87

REFERENCE TRAJECTORY		THRUST, [lbf] **							+			WDOTP	REFERENCE	REFERENCE	ENGINE
MACH NUMBER [--]	* ALTITUDE [ft]	EJECTOR	NO PRESS FIELD RAMJET	4 DEG WEDGE RAMJET	6 DEG WEDGE RAMJET	8 DEG WEDGE RAMJET	*,+,#,@ SCRAMJET	ROCKET	Ac normal [--]	Ac# [ft**2]	Ct@ [--]	T/Isp [lbm/s]	WDOTP [lbm/s]	THRUST ## [lbf]	OPERATING MODE
0.0	0	253000										179	465	657800	EJECTOR
0.5	7100	205000										149	387	533000	"
1.0	17250	215000										146	380	559000	"
1.5	28650	234000	116000									186	485	764400	"
2.0	38500	318000	172000						0.300	499		175	455	826800	"
2.5	45500	369000	216000						0.327	544		176	458	959400	"
2.9	50900	404000	280000						0.348	580		174	451	1050400	"
3.0	52150		296000	325000	335000	345000			0.354	589		91	235	871000	RAMJET
3.5	58650		258000	330000	355000	380000			0.381	633		94	245	923000	"
4.0	63100		234000	320000	345000	370000			0.408	678		94	243	897000	"
4.5	68000		210000	275000	302500	330000			0.435	723		86	222	786500	"
5.0	72500		184000	255000	285000	315000	442864		0.462	768	1.000	85	221	741000	"
5.5	76500		162000	250000	280000	310000	449950		0.488	812	0.960	89	232	728000	"
6.0	80000						454969		0.515	857	0.920	152	394	1182919	SCRAMJET
6.5	83500						443310		0.542	902	0.850	153	397	1150007	"
7.0	86500						442421		0.569	947	0.810	161	418	1150295	"
7.5	89500						449046		0.596	992	0.785	171	445	1167518	"
8.0	92000						442421		0.623	1036	0.740	177	460	1150295	"
8.5	95000						442827		0.650	1081	0.710	185	480	1151350	"
9.0	97500						435188		0.677	1126	0.670	189	492	1131488	"
9.5	100000						428858		0.704	1171	0.635	197	513	1115032	"
10.0	102000						392673	200000	0.731	1215	0.600	192	499	1020949	"
11.0	115000						355605	200000	0.785	1305	0.545	206	536	924573	"
12.0	120000						276224	200000	0.838	1395	0.515	190	495	718183	"
13.0	130000						251724	200000	0.892	1484	0.490	205	534	654482	"
14.0	135000						227573	200000	0.946	1574	0.470	222	577	591690	"
15.0	140000						220694	200000	1.000	1663	0.460	426	1106	520000	ROCKET
16.0	145000						0	200000			0.450	426	1106	520000	"
17.0	155000						0	200000			0.445	426	1106	520000	"
18.0	160000						0	200000			0.445	426	1106	520000	"
19.0	165000						0	200000			0.450	426	1106	520000	"
20.0	175000						0	200000			0.460	426	1106	520000	"
21.0							0	200000			0.470	426	1106	520000	"
22.0							0	200000			0.480	426	1106	520000	"
23.0							0	200000			0.495	426	1106	520000	"
24.0							0	200000			0.510	426	1106	520000	"
25.0							0	200000			0.530	426	1106	520000	"
26.0								200000				426	1106	520000	"
27.0								200000				426	1106	520000	"

* AIAA-86-1388
\+ STAARS DATABASE #0211, CAPTURE AREA/CAPTURE AREA @ M=15
\# 55.0 ft DIAMETER VEHICLE, 70% CAPTURE AT M=15
@ STAARS DATABASE # TBD, PRELIMINARY ENGINE INFORMATION ON FIVE COMBINED CYCLE ENGINES
** A STUDY OF COMPOSITE PROPULSION SYSTEMS FOR ADVANCED LAUNCH VEHICLE APPLICATIONS, VOLUME 6
++ A STUDY OF COMPOSITE PROPULSION SYSTEMS FOR ADVANCED LAUNCH VEHICLE APPLICATIONS, VOLUME 4, PAGE 23
ASSUMES 6-DEGREE 2-DIMENSIONAL WEDGE INDUCED PRESSURE FIELD, EJECTOR MODE SHIFT TO RAMJET MODE AT MACH 3, RAMJET MODE SHIFT TO SCRAMJET MODE AT MACH 6, SCRAMJET MODE SHIFT TO ROCKET MODE AT MACH 20

Table 17a Specific Impulse Performance for Engine #30 - Supercharged ScramLACE

ENGINE 30 SPECIFIC IMPULSE FOR REFERENCE TRAJECTORY (FOR 250 klbf SLS ENGINE)

11 JUNE 87

REFERENCE TRAJECTORY			SPECIFIC IMPULSE, Isp [lbf-s/lbm] **									
MACH NUMBER [—]	* ALTITUDE [ft]	q* [psf]	SUPER-CHARGED EJECTOR	FAN RAMJET	NO PRESS FIELD RAMJET	4 DEG WEDGE RAMJET	6 DEG WEDGE RAMJET	8 DEG WEDGE RAMJET	@ SCRAMJET	@ ROCKET	REFERENCE Isp ## PROFILE	ENGINE OPERATING MODE
0.0	0	0	1680								1680	EJECTOR
0.5	7100	240	1636	1640							1636	"
1.0	17250	700	1735	2280							1735	"
1.5	28650	1050	1876	3040	2600						1876	"
2.0	38500	1200	2192	3620	3350						2192	"
2.5	45500	1400	2571	3840	3740						2571	"
2.9	50900	1450	2865		3980						2865	"
3.0	52150	1500			3920	3770	3700	3630			3700	RAMJET
3.5	58650	1500			3930	3825	3765	3705			3765	"
4.0	63100	1500			3800	3730	3685	3640			3685	"
4.5	68000	1500			3610	3570	3535	3500			3535	"
5.0	72500	1500			3380	3370	3350	3330			3350	"
5.5	76500	1500			3100	3135	3135	3135			3135	"
6.0	80000	1500			2790	2900	2900	2900	3000		3000	SCRAMJET
6.5	83500	1500							2900		2900	"
7.0	86500	1500							2750		2750	"
7.5	89500	1500							2625		2625	"
8.0	92000	1500							2500		2500	"
8.5	95000	1500							2400		2400	"
9.0	97500	1500							2300		2300	"
9.5	100000	1500							2175		2175	"
10.0	102000	1400							2050		2050	"
11.0	115000	1300							1725		1725	"
12.0	120000	1000							1450		1450	"
13.0	130000	900							1225		1225	"
14.0	135000	830							1025		1025	"
15.0	140000	750							850	470	470	ROCKET
16.0	145000	700							750	470	470	"
17.0	155000	600							650	470	470	"
18.0	160000	500							550	470	470	"
19.0	165000	450							525	470	470	"
20.0	175000	400							475	470	470	"
21.0		350							450	470	470	"
22.0		250							425	470	470	"
23.0		200							400	470	470	"
24.0		100							400	470	470	"
25.0		50							400	470	470	"
26.0									375	470	470	"
27.0										470	470	"

* AIAA-86-1388
\+ STAARS DATABASE #0211, CAPTURE AREA/CAPTURE AREA @ M-15
\# 54.4 ft DIAMETER VEHICLE, 70% CAPTURE AT M-15
@ STAARS DATABASE # TBD, PRELIMINARY ENGINE INFORMATION ON FIVE COMBINED CYCLE ENGINES
** A STUDY OF COMPOSITE PROPULSION SYSTEMS FOR ADVANCED LAUNCH VEHICLE APPLICATIONS, VOLUME 6
++ A STUDY OF COMPOSITE PROPULSION SYSTEMS FOR ADVANCED LAUNCH VEHICLE APPLICATIONS, VOLUME 4, PAGE 23
ASSUMES 6-DEGREE 2-DIMENSIONAL WEDGE INDUCED PRESSURE FIELD, EJECTOR MODE SHIFT TO RAMJET MODE AT MACH 3, RAMJET MODE SHIFT TO SCRAMJET MODE AT MACH 6, SCRAMJET MODE SHIFT TO ROCKET MODE AT MACH 20

Table 17b Thrust Performance for Engine #30 - Supercharged ScramLACE

ENGINE 30 THRUST PROFILE FOR REFERENCE TRAJECTORY (FOR 250 klbf SLS ENGINE)

28 APR 87

REFERENCE TRAJECTORY		THRUST, [lbf] **								+						
MACH NUMBER [—]	* ALTITUDE [ft]	SUPER-CHARGED EJECTOR	FAN RAMJET	NO PRESS FIELD RAMJET	4 DEG WEDGE RAMJET	6 DEG WEDGE RAMJET	8 DEG WEDGE RAMJET	*,+,#,@ SCRAMJET	ROCKET	Ac normal [--]	Ac@ [ft**2]	Ct@ [--]	WDOTP T/Isp [lbm/s]	REFERENCE WDOTP [lbm/s]	REFERENCE THRUST ## [lbf]	ENGINE OPERATING MODE
0.0	0	255000											152	395	663060	EJECTOR
0.5	7100	207000											127	329	538200	"
1.0	17250	217000	130000										125	325	564200	"
1.5	28650	279000	208000	116000									149	387	725430	"
2.0	38500	325000	270000	172000						0.300	488		149	387	967600	"
2.5	45500	390000	308200	216000						0.327	532		152	396	1014000	"
2.9	50900	434000		280000						0.348	567		151	394	1128400	"
3.0	52150			296000	325000	335000	345000			0.354	576		91	235	871000	RAMJET
3.5	58650			258000	330000	355000	380000			0.381	619		94	245	923000	"
4.0	63100			234000	320000	345000	370000			0.408	663		94	243	897000	"
4.5	68000			210000	275000	302500	330000			0.435	707		86	222	786500	"
5.0	72500			184000	255000	285000	315000	433172		0.462	751	1.000	85	221	741000	"
5.5	76500			162000	250000	280000	310000	440102		0.488	795	0.960	89	232	728000	"
6.0	80000							445012		0.515	838	0.920	148	386	1157030	SCRAMJET
6.5	83500							432630		0.542	882	0.850	149	388	1124838	"
7.0	86500							432738		0.569	926	0.810	157	409	1125120	"
7.5	89500							439218		0.596	970	0.785	167	435	1141967	"
8.0	92000							432738		0.623	1014	0.740	173	450	1125120	"
8.5	95000							433136		0.650	1057	0.710	180	469	1126152	"
9.0	97500							425663		0.677	1101	0.670	185	481	1106725	"
9.5	100000							419473		0.704	1145	0.635	193	501	1090629	"
10.0	102000							384079	200000	0.731	1189	0.600	187	487	998605	"
11.0	115000							347822	200000	0.785	1276	0.545	202	524	904338	"
12.0	120000							270179	200000	0.839	1364	0.515	186	484	702465	"
13.0	130000							246215	200000	0.892	1452	0.490	201	523	640158	"
14.0	135000							222592	200000	0.946	1539	0.470	217	565	578740	"
15.0	140000							215864	200000	1.000	1627	0.460	426	1106	520000	ROCKET
16.0	145000							0	200000			0.450	426	1106	520000	"
17.0	155000							0	200000			0.445	426	1106	520000	"
18.0	160000							0	200000			0.445	426	1106	520000	"
19.0	165000							0	200000			0.450	426	1106	520000	"
20.0	175000							0	200000			0.460	426	1106	520000	"
21.0								0	200000			0.470	426	1106	520000	"
22.0								0	200000			0.480	426	1106	520000	"
23.0								0	200000			0.495	426	1106	520000	"
24.0								0	200000			0.510	426	1106	520000	"
25.0								0	200000			0.530	426	1106	520000	"
26.0									200000				426	1106	520000	"
27.0									200000				426	1106	520000	"

* AIAA-86-1388
\+ STAARS DATABASE #0211, CAPTURE AREA/CAPTURE AREA @ M-15
\# 54.4 ft DIAMETER VEHICLE, 70% CAPTURE AT M-15
@ STAARS DATABASE # TBD, PRELIMINARY ENGINE INFORMATION ON FIVE COMBINED CYCLE ENGINES
** A STUDY OF COMPOSITE PROPULSION SYSTEMS FOR ADVANCED LAUNCH VEHICLE APPLICATIONS, VOLUME 6
++ A STUDY OF COMPOSITE PROPULSION SYSTEMS FOR ADVANCED LAUNCH VEHICLE APPLICATIONS, VOLUME 4, PAGE 23
ASSUMES 6-DEGREE 2-DIMENSIONAL WEDGE INDUCED PRESSURE FIELD, EJECTOR MODE SHIFT TO RAMJET MODE AT MACH 3, RAMJET MODE SHIFT TO SCRAMJET MODE AT MACH 6, SCRAMJET MODE SHIFT TO ROCKET MODE AT MACH 20

Table 18a Specific Impulse Performance for Engine #32 - Recycled Supercharged ScramLACE

ENGINE 32 SPECIFIC IMPULSE PROFILE FOR REFERENCE TRAJECTORY (FOR 250 klbf SLS ENGINE)

11 JUNE 87

REFERENCE TRAJECTORY			SPECIFIC IMPULSE, Isp [lbf-s/lbm] **									
MACH NUMBER (—)	ALTITUDE * (ft)	q* (psf)	SUPER-CHARGED EJECTOR	FAN RAMJET	NO PRESS FIELD RAMJET	4 DEG WEDGE RAMJET	6 DEG WEDGE RAMJET	8 DEG WEDGE RAMJET	@ SCRAMJET	@ ROCKET	REFERENCE Isp ## PROFILE	ENGINE OPERATING MODE
0.0	0	0	3320								3320	EJECTOR
0.5	7100	240	3120	1640							3120	"
1.0	17230	700	3119	2300							3119	"
1.5	28650	1050	3554	3040	2600						3554	"
2.0	38500	1200	4081	3620	3350						4081	"
2.5	45500	1400	4424	3840	3740						4424	"
2.9	50900	1450	4595		3890						4595	"
3.0	52150	1500			3920	3770	3700	3630			3700	RAMJET
3.5	58650	1500			3930	3825	3765	3705			3765	"
4.0	63100	1500			3800	3730	3655	3640			3685	"
4.5	68000	1500			3610	3570	3535	3500			3535	"
5.0	72500	1500			3380	3370	3350	3330			3350	"
5.5	76500	1500			3100	3135	3135	3135			3135	"
6.0	80000	1500			2790	2900	2900	2900	3000		3000	SCRAMJET
6.5	83700	1500							2900		2900	"
7.0	86500	1500							2750		2750	"
7.5	89500	1500							2623		2625	"
8.0	92000	1500							2500		2500	"
8.5	95000	1500							2400		2400	"
9.0	97500	1500							2300		2300	"
9.5	100000	1500							2175		2175	"
10.0	102000	1400							2050		2050	"
11.0	115000	1300							1725		1725	"
12.0	120000	1000							1450		1450	"
13.0	130000	900							1225		1225	"
14.0	135000	800							1025		1025	"
15.0	140000	750							850	470	470	ROCKET
16.0	145000	700							750	470	470	"
17.0	155000	600							650	470	470	"
18.0	160000	500							550	470	470	"
19.0	165000	450							525	470	470	"
20.0	175000	400							475	470	470	"
21.0		350							450	470	470	"
22.0		250							425	470	470	"
23.0		200							400	470	470	"
24.0		100							400	470	470	"
25.0		50							400	470	470	"
26.0									375	470	470	"
27.0										470	470	"

* AIAA-86-1388
+ STAARS DATABASE #0211, CAPTURE AREA/CAPTURE AREA @ M-15
# 53.8 ft DIAMETER VEHICLE, 70% CAPTURE AT M-15
@ STAARS DATABASE # TBD, PRELIMINARY ENGINE INFORMATION ON FIVE COMBINED CYCLE ENGINES
** A STUDY OF COMPOSITE PROPULSION SYSTEMS FOR ADVANCED LAUNCH VEHICLE APPLICATIONS, VOLUME 6
++ A STUDY OF COMPOSITE PROPULSION SYSTEMS FOR ADVANCED LAUNCH VEHICLE APPLICATIONS, VOLUME 3, PAGE 23
ASSUMES 6-DEGREE 2-DIMENSIONAL WEDGE INDUCED PRESSURE FIELD, EJECTOR MODE SHIFT TO RAMJET MODE AT MACH 3, RAMJET MODE SHIFT TO SCRAMJET MODE AT MACH 6, SCRAMJET MODE SHIFT TO ROCKET MODE AT MACH 20

Table 18b Thrust Performance for Engine #32 · Recycled Supercharged ScramLACE

ENGINE 32 THRUST PROFILE FOR REFERENCE TRAJECTORY (FOR 250 klbf SLS ENGINE)

28 APR 87

REFERENCE TRAJECTORY		THRUST, T [lbf] **														
MACH NUMBER [--]	* ALTITUDE [ft]	SUPER-CHARGED EJECTOR	FAN RAMJET	NO PRESS FIELD RAMJET	4 DEG WEDGE RAMJET	6 DEG WEDGE RAMJET	8 DEG WEDGE RAMJET	*,+,#,@ SCRAMJET	ROCKET	+ Ac normal [--]	Ac@ [ft**2]	Ct@ [--]	MDOTP T/Isp [lbm/s]	REFERENCE MDOTP [lbm/s]	REFERENCE THRUST ## [lbf]	ENGINE OPERATING MODE
0.0	0	257000											77	201	668200	EJECTOR
0.5	7100	205000											66	171	533000	"
1.0	17250	209000	140000										67	174	543400	"
1.5	28650	270000	214000	116000									76	198	702000	"
2.0	38500	314000	214000	172000						0.300	477		77	200	816400	"
2.5	45500	343000	310950	216000						0.327	520		78	202	891800	"
2.9	50900	351000		280000						0.348	554		76	199	912600	"
3.0	52150			296000	325000	335000	345000			0.354	563		91	235	871000	RAMJET
3.5	58650			258000	330000	355000	360000			0.381	606		94	245	923000	"
4.0	63100			234000	320000	345000	370000			0.408	649		94	243	897000	"
4.5	68000			210000	275000	302500	330000			0.435	692		86	222	786500	"
5.0	72500			184000	255000	285000	315000	423666		0.462	734	1.000	85	221	741000	"
5.5	76500			162000	250000	280000	310000	430444		0.488	777	0.960	89	232	728000	"
6.0	80000							435245		0.515	820	0.920	145	377	1131639	SCRAMJET
6.5	83500							423136		0.542	863	0.850	146	379	1100154	"
7.0	86500							423242		0.569	906	0.810	154	400	1100429	"
7.5	89500							429579		0.596	949	0.785	164	425	1116906	"
8.0	92000							423242		0.623	991	0.740	169	440	1100429	"
8.5	95000							423630		0.650	1034	0.710	177	459	1101439	"
9.0	97500							416322		0.677	1077	0.670	181	471	1082438	"
9.5	100000							410267		0.704	1120	0.635	189	490	1066695	"
10.0	102000							375650	200000	0.731	1163	0.600	183	476	976691	"
11.0	115000							340199	200000	0.785	1248	0.545	197	513	884492	"
12.0	120000							264250	200000	0.838	1334	0.515	182	474	687049	"
13.0	130000							240812	200000	0.892	1420	0.490	197	511	626110	"
14.0	135000							217708	200000	0.946	1505	0.470	212	552	566040	"
15.0	140000							211127	200000	1.000	1591	0.460	426	1106	520000	ROCKET
16.0	145000							0	200000			0.450	426	1106	520000	"
17.0	155000							0	200000			0.445	426	1106	520000	"
18.0	160000							0	200000			0.440	426	1106	520000	"
19.0	165000							0	200000			0.450	426	1106	520000	"
20.0	175000							0	200000			0.460	426	1106	520000	"
21.0								0	200000			0.470	426	1106	520000	"
22.0								0	200000			0.480	426	1106	520000	"
23.0								0	200000			0.495	426	1106	520000	"
24.0								0	200000			0.510	426	1106	520000	"
25.0								0	200000			0.530	426	1106	520000	"
26.0									200000				426	1106	520000	"
27.0									200000				426	1106	520000	"

* AIAA-86-1388
\+ STAARS DATABASE #0211, CAPTURE AREA/CAPTURE AREA @ M=15
\# 53.8 ft DIAMETER VEHICLE, 70% CAPTURE AT M=15
@ STAARS DATABASE # TBD, PRELIMINARY ENGINE INFORMATION ON FIVE COMBINED CYCLE ENGINES
** A STUDY OF COMPOSITE PROPULSION SYSTEMS FOR ADVANCED LAUNCH VEHICLE APPLICATIONS, VOLUME 6
++ A STUDY OF COMPOSITE PROPULSION SYSTEMS FOR ADVANCED LAUNCH VEHICLE APPLICATIONS, VOLUME 4, PAGE 23
ASSUMES 6-DEGREE 2-DIMENSIONAL WEDGE INDUCED PRESSURE FIELD, EJECTOR MODE SHIFT TO RAMJET MODE AT MACH 3, RAMJET MODE SHIFT TO SCRAMJET MODE AT MACH 6, SCRAMJET MODE SHIFT TO ROCKET MODE AT MACH 20

These tables also show the scramjet mode thrust. This thrust was calculated as follows: Using the normalized capture area schedule, the vehicle diameter, and the assumption that 70% of the vehicle frontal area equates to full capture at a selected scramjet/rocket transition velocity, the actual engine capture area schedule, A_c, was developed. Then, using the thrust coefficient schedule (C_T), the dynamic pressure (q) and the engine capture area (A_c), scramjet mode thrust could be calculated from the simple relationship, $T = C_T\, q\, A_c$.

Once the engine thrust performance tabulated in the reference thrust column had been estimated over the entire reference flight path, and for the predetermined engine operating modes shown in the far right-hand column of the tables, the reference fuel or propellant flowrate, W_P, could be calculated from the equation,

$$W_P = T / I_{sp}$$

The NAS7-377 study thrust data, and the thrust performance data previously presented for this study in Tables 14 to 18, is net jet thrust and includes the effects of inlet ram-drag. As with ramjet specific impulse, scramjet thrust augmentation occurs as a result of forebody precompression induced pressure field effects.

6.4.2 Vehicle Mass Properties

The method of development and findings with regard to vehicle mass properties determination was previously discussed in Section 5.0

6.4.3 Vehicle Aerodynamic Analysis Methodology

In order to evaluate the performance of the RBCC/SSTO vehicle, it is necessary to estimate its aerodynamic characteristics. In this study, which was primarily designed to determine the relative merits of a variety of combined cycle engines, the vehicle was "flown" exclusively in the pitch plane. Thus, only longitudinal characteristics were required. In addition, aerodynamic coefficients were supplied in "trimmed" format, because the vehicle control system was not under study. As a result, only trimmed lift and drag coefficients were required to support the vehicle simulation. It was required that these coefficients be supplied at a level of accuracy comparable to the propulsion and mass properties data.

Drag Estimation Methodology

Total vehicle drag was broken down into two components, zero-lift drag (composed of pressure and skin friction drag) and drag due-to-lift (induced drag). Although total drag can be broken down into a multitude of components, this breakdown permitted drag to be estimated with sufficient fidelity using existing theory and empirical data. These two components were estimated for the subsonic, supersonic and hypersonic speeds.

The base drag was not separated as a distinct drag component. Rather, base drag was considered to be an intrinsic component of zero-lift drag. Over the majority of the hypersonic speed regime (Mach > 5), base drag is a relatively small component, as shown in Fig. 102 which was derived for a generic slender delta wing vehicle at NASA Langley (Ref. 25). This is particularly true for the axisymmetric RBCC/SSTO configuration where engine exhaust "fills" the base area, reducing base drag in comparison to non-axisymmetric vehicles. Also, note the rather high base drag at transonic Mach numbers (Fig. 102). The shape of this composite drag curve is emulated in the shape of the zero-lift drag curve of the RBCC/SSTO vehicles (example shown in Fig. 103).

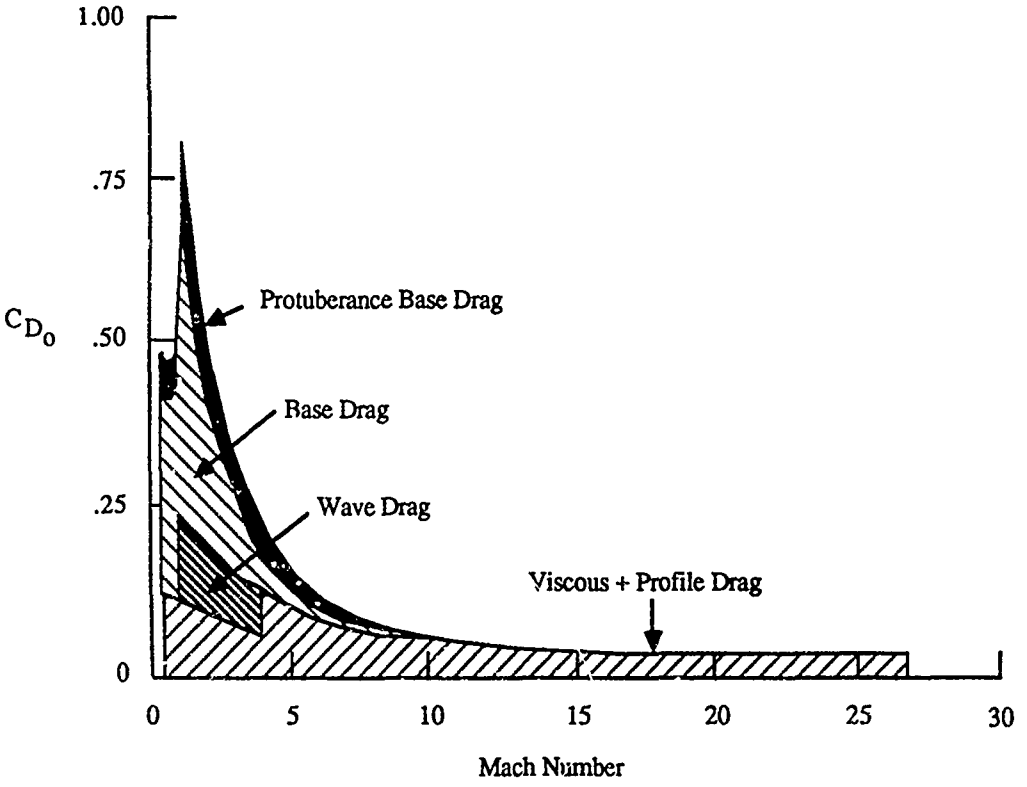
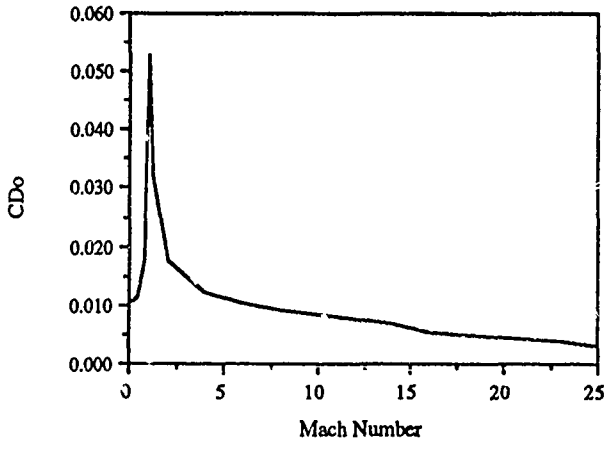


Fig. 102 NASA LaRC Generic Slender Wing Vehicle Drag Breakdown



Notes:

C_{D_0} = Zero-Lift Drag Coefficient
S_{Ref} = 4453 ft^2 (Reference Area)
8° Cone Half-angle
70% Capture at M=25
25% Strakes

Fig. 103 A Zero-Lift Drag Curve for the RBCC/SSTO Vehicles

The selected reference area for each vehicle was the planform area of the eight strakes projected into the horizontal plane of the vehicle. The strake configurations investigated are illustrated in Fig. 104.

Zero Lift Drag (C_{Do})

The supersonic/hypersonic drag coefficients were based on empirically derived data for conical noses presented in "Fluid Dynamic Drag" by S.F. Hoerner (Ref.26). The data is based on experiments on cones between 10 and 40 degrees half-angle at Mach numbers ranging from 1.5 to 8.0. A curve-fit of this experimental data yielded a formula for zero-lift drag as a function of Mach number (M) and cone half-angle (δ). This formula has the form:

$$C_{Do} = 2.1 * \sin\delta + 0.5 * [\sin\delta/(M^2-1)^{1/2}]$$

The subsonic drag coefficients were derived using the previously defined supersonic/hypersonic data. C_{Do} at Mach=0.98 was set equal to C_{Do} at Mach=1.2. The remaining subsonic coefficients were obtained using the Prandtl-Glauret relationship to correct for compressibility effects. This correction yields the following equation:

$$C_{Do} = (C_{Do(M=0.98)} * (1 - (0.98)^2)^{1/2})/(1 - (Mach)^2)^{1/2}$$

Where Mach is the desired subsonic Mach number.

These coefficients were then corrected for drag already accounted for in the propulsion data. This is necessary because the entire forebody of the vehicle acts as an inlet (or compressor). The "ram drag" or drag associated with turning and slowing the flow entering the propulsion system is a large component of total vehicle drag, particularly at hypersonic speeds. This ram drag has already been subtracted from gross engine thrust in the propulsion database. Consequently, only that flow which is not "captured" by the engine inlets must be accounted for by the aerodynamic drag coefficient. The drag associated with the vehicle forebody was therefore corrected based on engine capture ratio. This was accomplished by multiplying the baseline zero-lift C_{Do} by a "drag ratio factor". This factor was defined as:

Drag Ratio Factor = 1 - (Percentage Capture)

Where percentage capture is a function of Mach number as defined in the propulsion section of this report, Section 3.0.

This zero-lift drag coefficient is input to the DOF36 program as a zero-lift axial force coefficient (C_{Ao}). Because zero-lift occurs at zero angle-of-attack on the vehicle, C_{Do} and C_{Ao} are identically equal (i.e. the stability and body axes coincide at zero angle-of-attack). An example plot of C_{Ao} versus Mach number is shown in Fig. 105.

Induced Drag (C_{Di})

Subsonic induced drag coefficients were based on theory described in "Prediction of Vortex-Lift by a Leading Edge Suction Analogy" by E.C. Polhamus (Ref. 27). According to this theory, the drag due to lift of a delta wing with fully developed vortex flow can be expressed as:

$$C_{Di} = C_L * \tan(\alpha)$$

Where α is the angle-of-attack in degrees or radians.

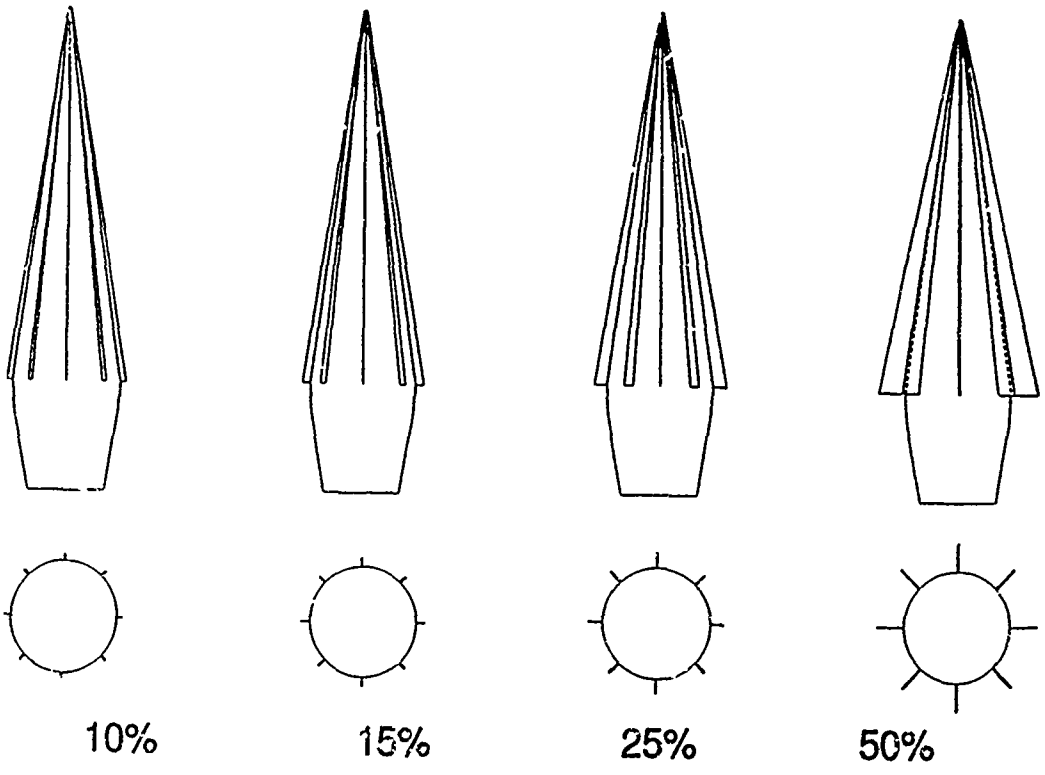


Fig. 104 Various Strake Configurations Studied

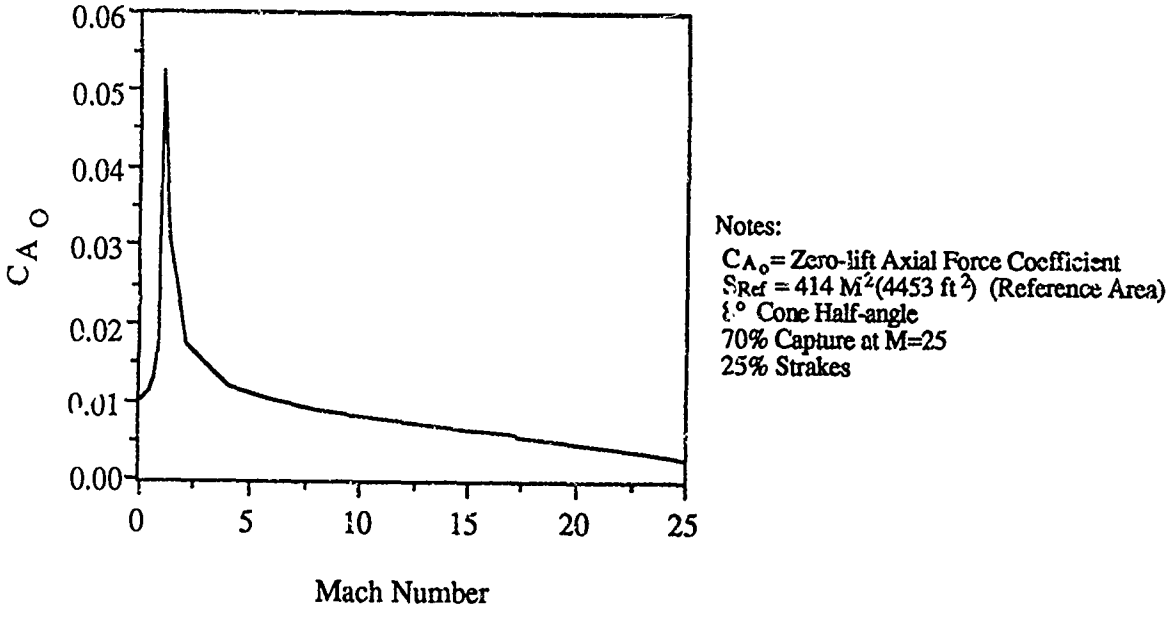


Fig. 105 Axial Force Coefficient of the Axisymmetric Configuration

Supersonic/hypersonic drag coefficients were based on linearized (Ackeret) theory described in "Aerodynamics for Engineers" by Bertin and Smith (Ref. 28). According to linearized theory drag due-to-lift can be expressed as:

$$C_{Di} = C_L * \alpha$$

Where α is the angle-of-attack in radians

The induced drag is input to DOF36 as an axial force coefficient due-to-lift (CA_a) after being transformed from the stability to the body axis system.

Total Drag

At any particular flight condition, total drag is derived by calculating C_{Do} and C_{Di} values for the given cone half-angle, Mach number, and angle-of-attack. The total drag is the sum of these two components or:

$$C_{Dtotal} = C_{Do} + C_{Di}$$

After transformation to the body axis system, total axial force has the form:

$$CAtotal = CAo + CA_a$$

Lift Estimation Methodology

Total vehicle lift characteristics for the vehicles were derived by assuming that the vehicle strakes act as delta wings (i.e. assumed no body effects on the strakes. This was judged to be a reasonable assumption for both subsonic speeds (dominated by vortical flow from strakes) and supersonic/hypersonic speeds for small deflection angles (i.e. small cone angles and small angles-of-attack).

Subsonic lift coefficients were based on delta wing theory developed by Edward C. Polhamus as described in "Predictions of Vortex-lift by a Leading Edge Suction Analogy" (Ref. 27). According to this theory, total lift is the sum of potential and vortex lift as shown in Fig. 106(i.e.):

$$C_{Ltotal} = C_{Lp} + C_{Lv}$$

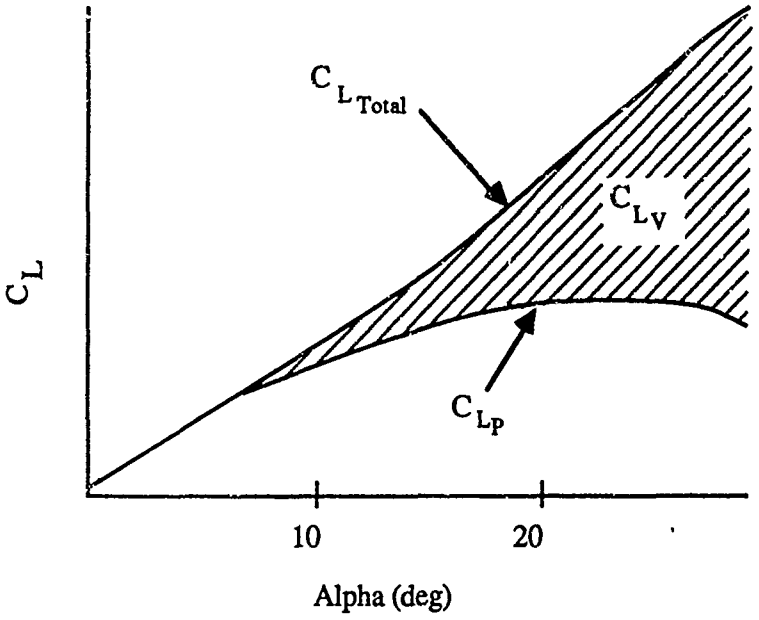
Where: C_{Lp} = Potential Lift and C_{Lv} = Vortex Lift.

Supersonic/hypersonic lift coefficients were based on linearized (Ackeret) theory described in "Aerodynamics for Engineers" by Bertin and Smith (Ref. 28). This theory provides good estimates for small deflection angles and high Mach numbers. According to linearized theory, lift coefficient has the following form:

$$C_L = 4\alpha/(M^2 - 1)^{1/2}$$

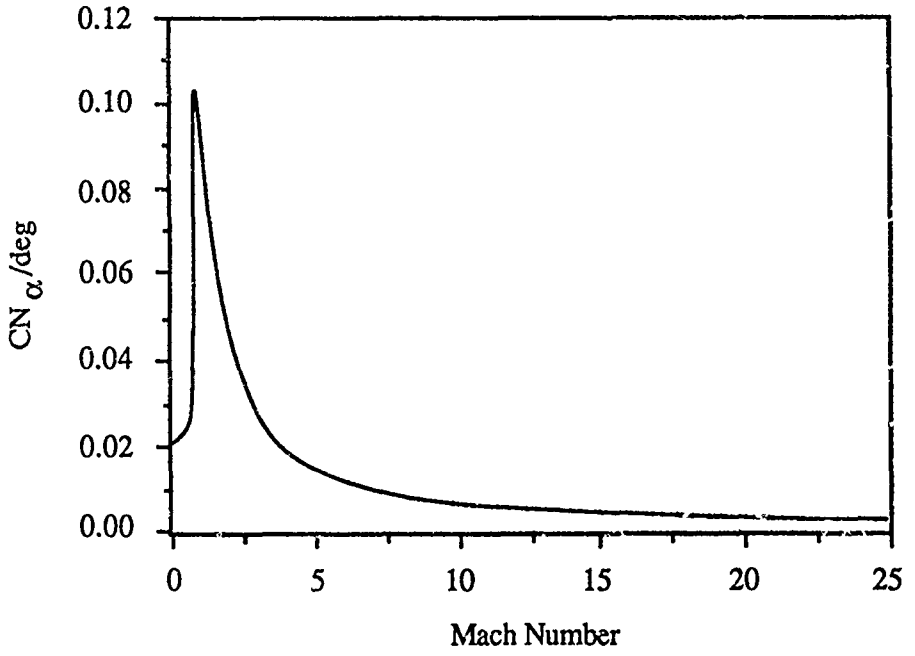
Where α is the angle-of-attack in radians.

The lift coefficients were then transformed from the stability axis system to the body axis system, as required by DOF36. An example plot of C_N (normal force coefficient) versus angle-of-attack is shown in Fig. 107. These normal force coefficients were then divided by the angle-of-attack to yield C_{N_a}, which was the parameter required by the DOF36 aerodynamic subroutine.



$C_{L_{Total}} = C_{L_P} + C_{L_V}$ Where:
C_{L_P} = Potential Lift
C_{L_V} = Vortex Lift

Fig. 106 Subsonic Lift Coefficient Characteristics of Slender Delta Wings



Notes:

CN_α = Slope of Normal Force Coefficient. Versus Angle-of-attack
S_{Ref} = 414 M^2(4453 ft^2) (Reference Area)
8° Cone Half-angle
Alpha=4°
25% Strakes

Fig. 107 Normal Force Coefficient of the Axisymmetric Configuration

DOF36 Aerodynamic Implementation Methodology

The DOF36 program required inputs of C_{D_0}, C_{A_a}, and C_{N_a}. These coefficients were generated in a table format compatible with DOF36 input format. C_{N_a} and C_{A_a} were calculated at angles-of-attack of -12, -8, -4, 0, 4, 8, 12, and 16 degrees. All three coefficients were calculated for Mach numbers of 0.0, 0.2, 0.4, 0.6, 0.8, 0.98, 1.2, 2., 4., 6., 8., 10., 14., 18., 23., and 28. Tables containing these three coefficients (and other data required by DOF36) were computed for the four strakes sizes; 10, 15, 25, and 50% of body diameter.

6.4.4 Definition of Reference Trajectory

It is important to note that the reference trajectory is not an optimum trajectory. Higher and lower q profiles were investigated but no improvements were found over the reference trajectory. Trajectories that were not investigated were higher altitude trajectories during the initial portions of flight and trajectories with lower thrust loading profiles which require data on part throttle performance of the RBCC engines which were not practical to obtain within the study resources.

The reference trajectory and engine mode operating regimes chosen to provide a baseline for comparison of the engine/vehicle systems analyzed in this study is presented in Fig. 108. The initial portion of this trajectory, up to Mach 10, was the optimum trajectory established in the baseline NAS7-377 study. This trajectory was entered with either horizontal or vertical takeoff. The entry flight paths into the reference trajectory for VTO and HTO are illustrated in Fig. 109. The takeoff maneuver was accomplished in ejector mode for Engines 10 and 22, and in supercharged ejector mode for Engines 12, 30, and 32. This event was followed by either a pitch-up (HTO) or a pitch-down (VTO) maneuver in order to allow the vehicle to get on a 1500 psf constant dynamic pressure flight path. The ejector mode, or supercharged ejector mode, depending on engine type, was sustained until a flight Mach number of 3 was reached. At this point, the engine was transitioned into ramjet mode.

The vehicle, with its engines then in the ramjet mode of operation, continued to fly the constant dynamic pressure acceleration profile. At a flight Mach number of 9.5, a point where vehicle surface heating rates were assumed to become critical, the vehicle's trajectory was adjusted to hold an estimated constant radiation temperature flight, i.e., at a decreasing dynamic pressure schedule, profile. The engine's were maintained in scramjet mode and the vehicle continued on the constant equilibrium wall temperature trajectory until the engine transition to rocket mode was performed. The vehicle then ascended under rocket power to local orbital velocity. After orbit circularization, a minimum-energy Hohmann transfer maneuver to a circular 100 nmi orbit was assumed. The propellant requirements for this maneuver were calculated in a post processing step.

6.4.5 Matrix of Core Variables Studied

This section discusses and presents the results of the parametric matrix of core variables analyzed in this study. These core variables include:

- Four strake sizes
- Two takeoff attitudes (HTO and VTO)
- Five engine types for each TOGW vehicle

This results in a matrix of 40 runs at each TOGW, all of which assumed that full capture was attained at a single Mach number with all other variables held constant. When any additional variable value was changed, a matrix of 40 additional runs was required to be run. This created a significant problem and required a judicious selection of the variables studied.

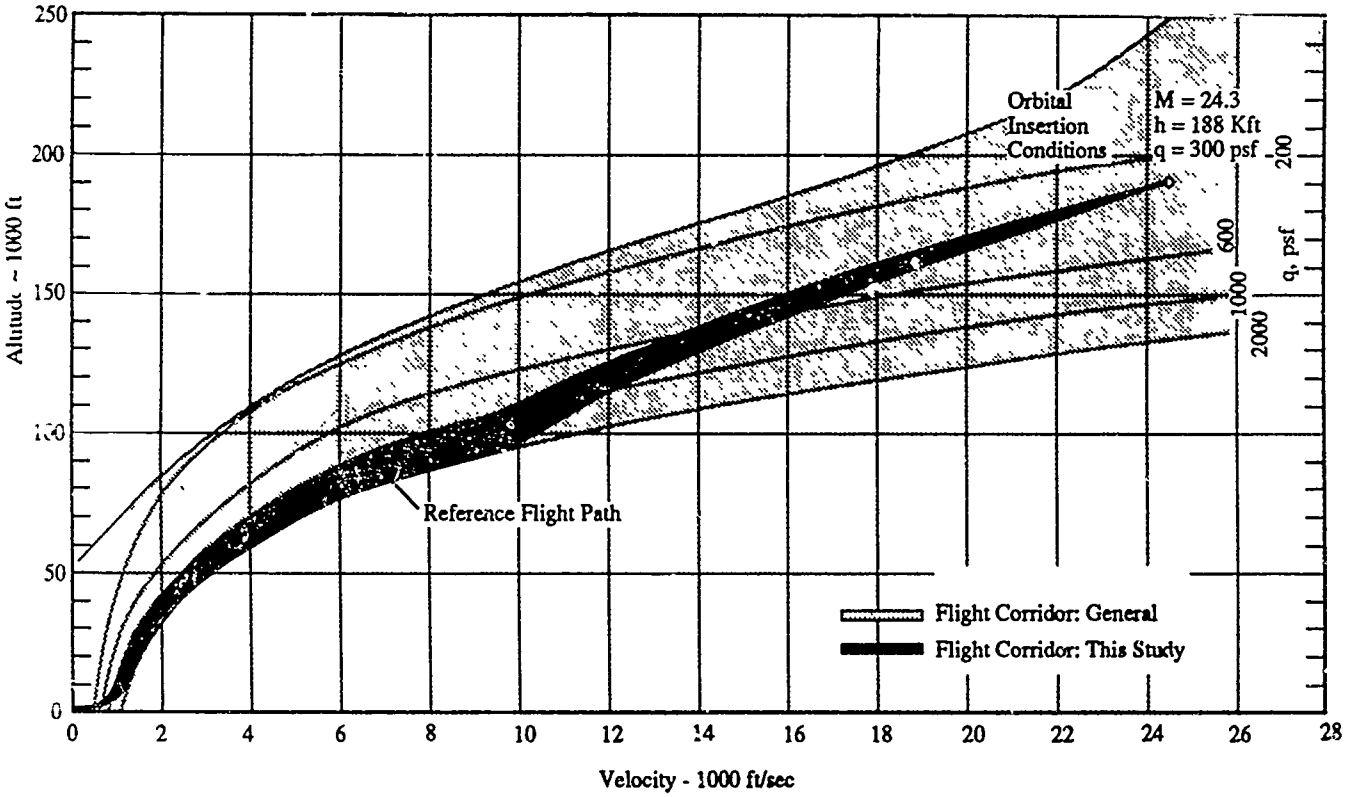


Fig. 108 Reference Ascent Trajectory

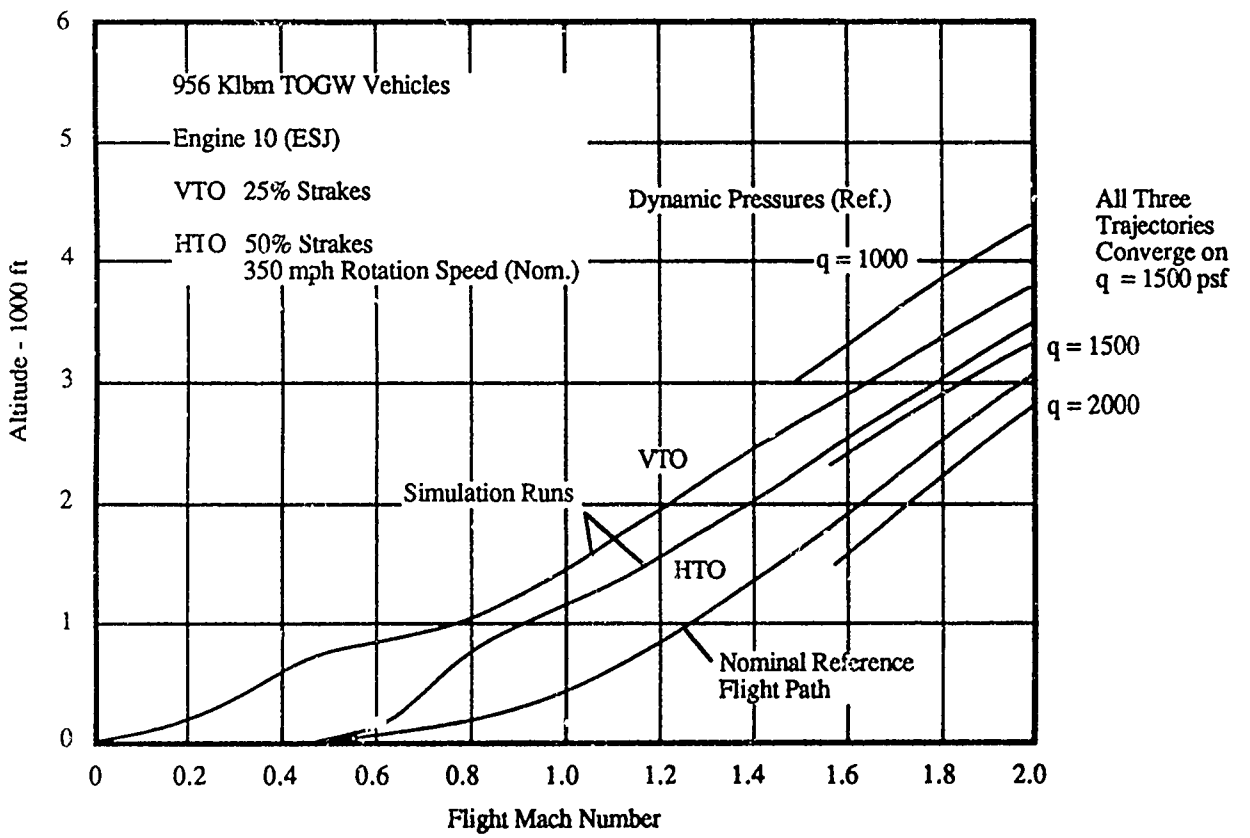


Fig. 109 Initial Portion of the Flight Path for HTO and VTO Modes of Takeoff

The first GLOW analyzed was 956 klbm. Findings of this analysis with full capture design at Mach 25, but rocket transition at Mach 20, are presented in the barcharts of Fig. 110 and 111. The figures present, in an easily comparable, fixed-scale format, the net discretionary payload delivered to the target 100 nmi polar orbit for each of the individual strake sizes and for each of the five engine types studied, with takeoff attitude and technology availability date (TAD) as additional parameters.

Discussion of the study's core variables and the specific findings regarding these variables, which taken together form the parametric matrix, now follow.

Takeoff Attitude

Both VTOHL and HTOHL were considered in the analysis work conducted in this study. From the results presented in Fig. 110 and 111, it appears that no significant payload advantage exists for either VTOHL or HTOHL.

The practicality of vertical takeoff has been demonstrated in both special aircraft designs and rocket vehicles.

The tires, wheels and brakes technology problems that must be resolved are significantly less if the VTOHL option is selected than in the HTOHL case, since the gear for HTO must carry the full vehicle gross weight for taxi and at takeoff whereas the gear for the the VTO case is sized by the empty weight on landing.

Vertical Takeoff

In order to carry out VTO simulation, the Takeoff data section of the DOF36 input file was bypassed and the vehicle attitude or flight path angle (γ) was initialized at 90 degrees.

Engines for both VTO and HTO vehicles were sized to provide 1.3 g initial takeoff acceleration. This value is consistent with vertical rocket practice and consistent with recommendations for VTO aircraft to avoid reingestion of engine effluent and ingestion of debris. Since strakes for a VTO vehicle are not required to be sized for the takeoff/rotation maneuver, as is the case for HTO, strake sizes for VTO were determined by vehicle angle-of-attack requirements after flight speed had been achieved.

Once the takeoff maneuver was accomplished, the vehicle was commanded to pitch over until a 1500 psf constant dynamic pressure flight path was achieved. Each VTO vehicle was required to achieve this constant dynamic pressure condition prior to attaining Mach 3.0 flight speed..

Horizontal Takeoff

In the simulation of horizontal takeoff using DOF36, the velocity at the initiation of pitch rotation and the takeoff commanded vertical plane acceleration were selected such that the actual takeoff speed did not exceed 350 nmi/hr, a speed considered to be the goal of current development efforts. Additionally, the requirement for a nominal 15-degree maximum pitch rotation angle was imposed on the HTO systems in order to insure that runway tail scrape did not occur. Horizontal takeoff vehicle strakes were then sized according to these requirements, while horizontal takeoff/landing gear were assumed to comprise 3% of vehicle TOGW.

The initial vehicle longitudinal acceleration was held constant at 1.3 g's for both VTO and HTO engine/vehicle configurations. While this value is considered high for HTO systems, and

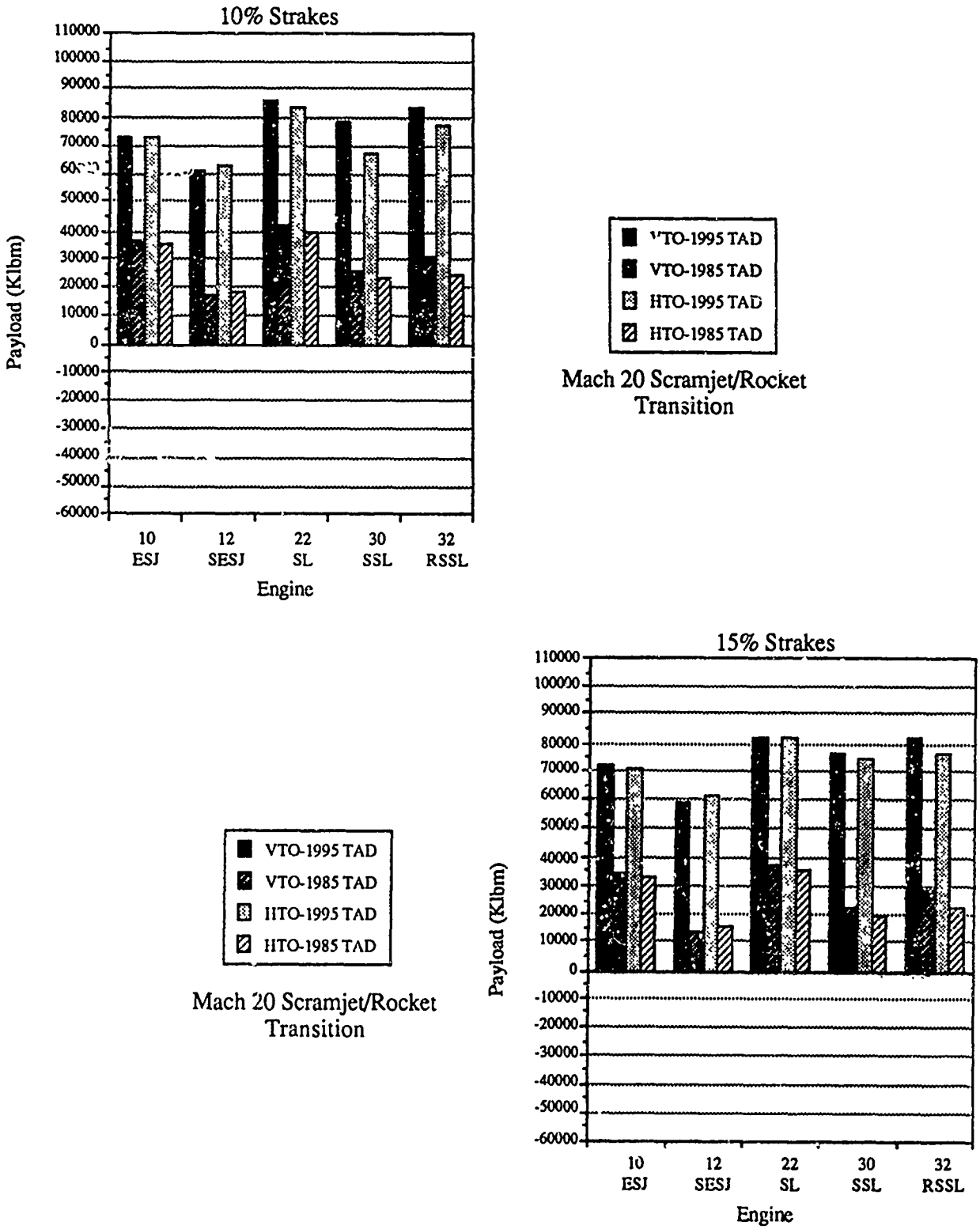


Fig. 110 Payload vs. Engine Type and Strake Size for a 956 klbm Vehicle at 10% and 15% Strake Sizes

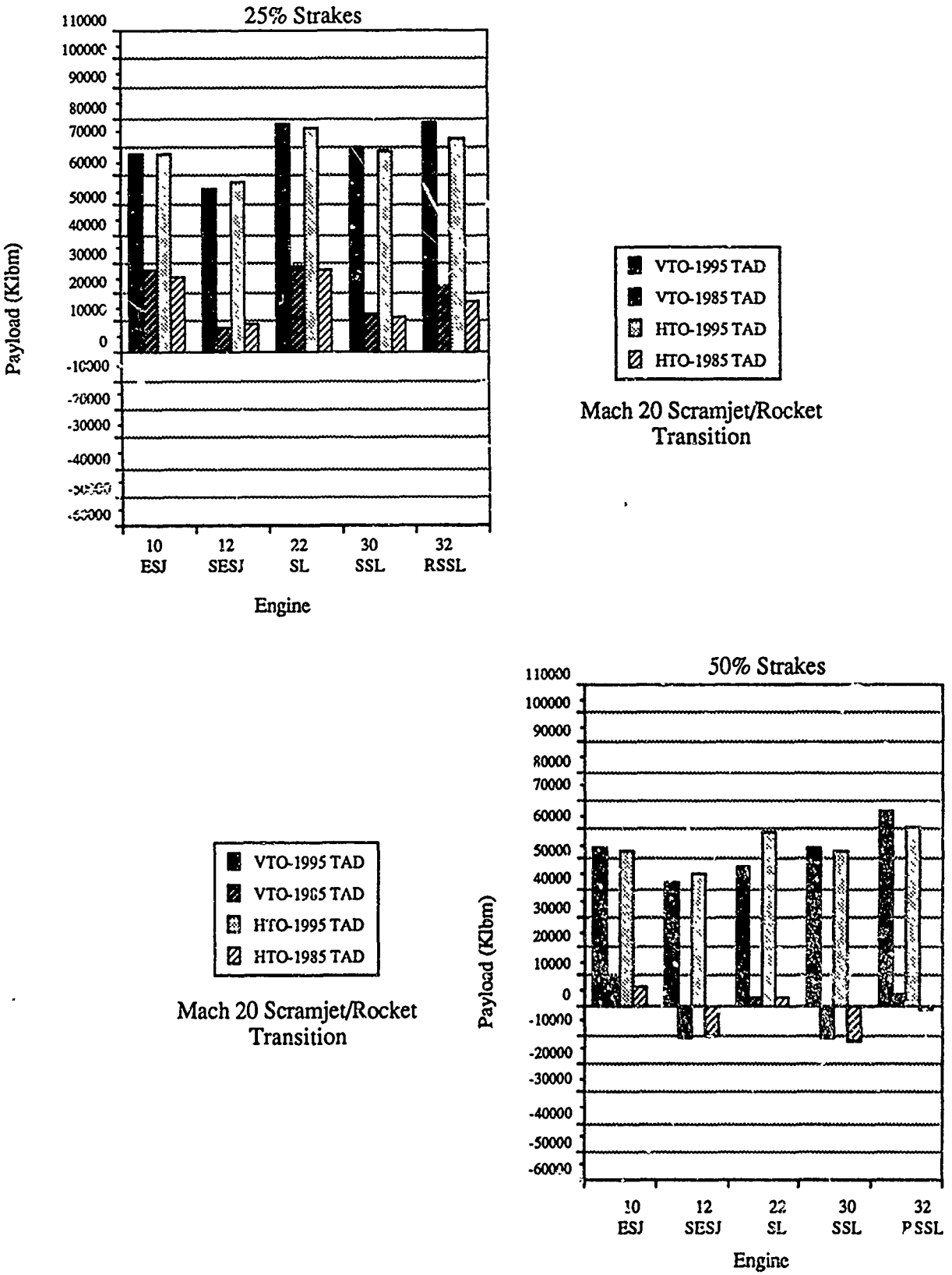


Fig. 111 Payload vs. Engine Type and Strake Size for a 956 klbm Vehicle at 20% and 25% Strake Sizes

lower initial thrust loading should be addressed in future efforts, in the SSTO mission context, engine size is typically driven by intermediate and high Mach range thrust requirements, not takeoff thrust requirements.

Engine Type and Air Liquefaction

The five air-augmented rocket based combined cycle engine types analyzed in this study are discussed in Section 3.0, illustrated in Fig. 112 and briefly described again here for emphasis.

The principle features and components of Engine 10, the Ejector Scramjet engine, form the basic core of the other four engines. These other engines were, therefore, looked upon as simple variants of this engine with increasing degrees of specific impulse performance in ejector mode and technical complexity. Engine 12, the Supercharged Ejector Scramjet, and Engine 22, the ScramLACE, improved upon Engine 10 performance, at the expense of increased engine/vehicle system complexity and weight, by the addition of a supercharging fan subsystem and an air-liquefaction heat-exchanger subsystem, respectively. Engine 30 combined this fan and heat-exchanger into a single engine system which formed the Supercharged ScramLACE. The Recycled Supercharged ScramLACE, Engine 32, further improved upon the baseline performance of Engine 10 by incorporating hydrogen recycle operation into the air-liquefaction subsystem.

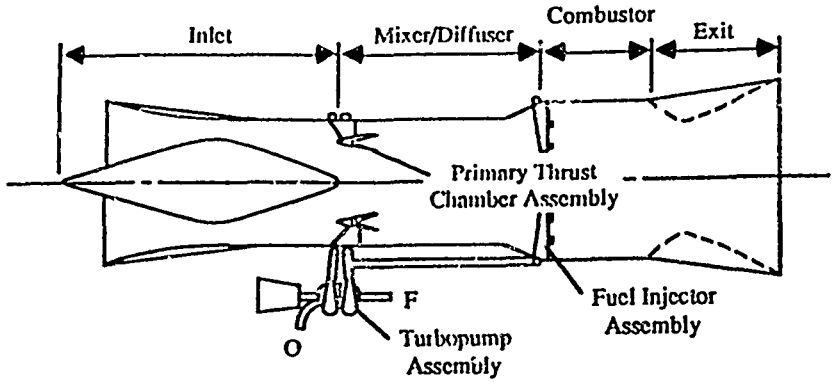
It appears that the air-liquefaction approach, as applied to the combined cycle type air-augmented rocket engines analyzed in the SSTO vehicle context of this study, provides only minimal payload advantages when compared to the non-air-liquefaction engine powered vehicle payload performance. This finding is also in contrast to the NAS7-377 findings (Ref. 2) for two-stage vehicles. This SSTO result can be seen by referring back to the barcharts of Fig. 110 and 111 and comparing, for each strake size, takeoff attitude, or TAD assumption, the net discretionary payload delivered to orbit by the non-air-liquefaction based engines (Engines 10 and 12) and by the air-liquefaction based engines (Engines 22, 30, and 32). Although the air-liquefaction based engines had superior specific impulse, the additional engine weight associated with the air-liquefaction process significantly reduced this advantage in SSTO flight.

Fan Supercharging

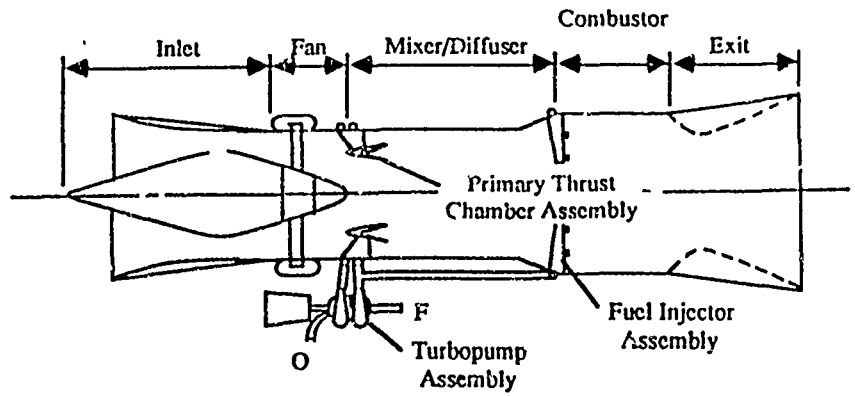
Using Figures 105 and 106, a comparison between Engine 10 and 12 and between Engine 22 and 30 can be made which indicates that, even though the fan subsystem provides thrust augmentation during the supercharged ejector mode at very high levels of specific impulse, the fan subsystem does <u>not</u> "pay its own way" on orbital ascent in a single stage vehicle. This is in contrast to the previous finding in the NAS7-377 study of two-stage HTOHL vehicles where the fan clearly was beneficial to payload capability. In the SSTO vehicle, for any given strake size, takeoff attitude, or TAD assumption, Engines 12 and 30, the fan-equipped engines, deliver less payload to orbit than the respective non-fan-equipped from which they were derived. It should be pointed out, however, that inclusion of the the fan subsystem significantly reduces the fuel requirements for powered flyback, landing and self-ferry capability.

6.4.6 Sensitivity Studies Performed

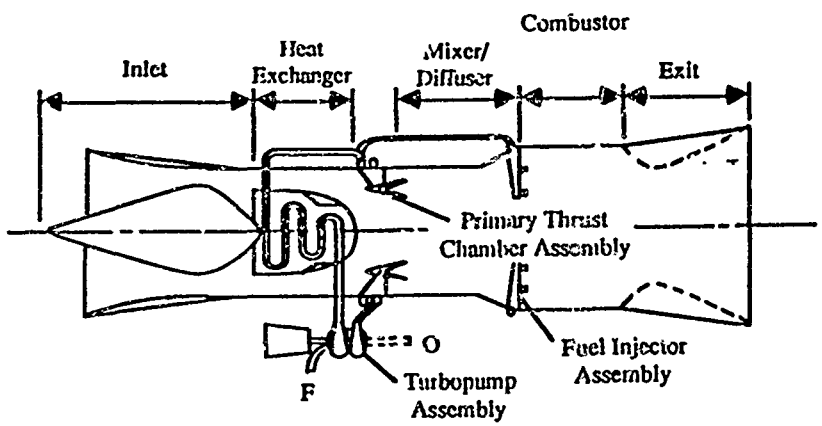
The results of work which characterized the sensitivity to variations in several important parameters not studied in the basic matrix of variables will now be discussed. Several important findings relating to vehicle TOGW and airbreathing termination Mach number resulted from this work.



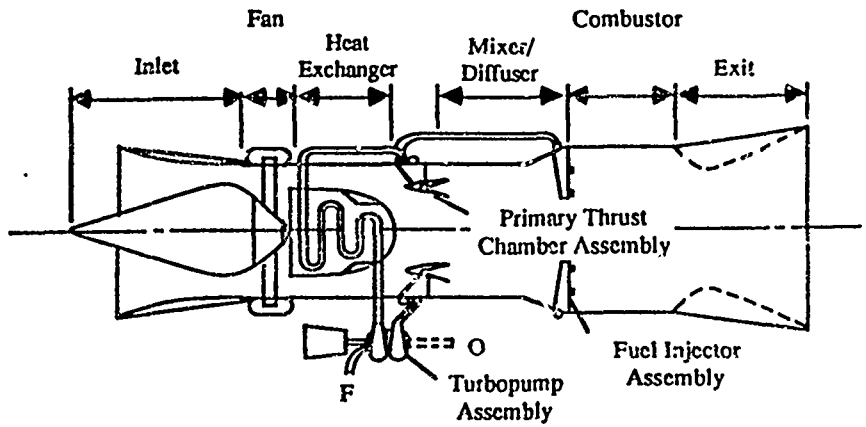
Ejector Scramjet
Engine #10



Supercharged Ejector Scramjet
Engine #12



ScramLACE
Engine #22



Supercharged ScramLACE
(Both Recycled and Non-Recycled)
Engine #30 and #32

Fig. 112 RBCC Engine Types Evaluated

Vehicle Takeoff Gross Weight

Departing from the 956 klbm TOGW vehicle matrix, two other vehicle TOGWs were studied, 500 klbm and 1500 klbm, in order to enable estimation of the TOGW of the target 10 klbm payload capacity vehicle and to determine general payload performance sensitivity to TOGW/GLOW.

Several 500 klbm vehicle configurations were studied. These included both horizontal and vertical takeoff vehicles equipped with 25% strakes for all five engine types. As with the basic 956 klbm vehicle matrix runs, full engine capture was designed to occur at Mach 25 and airbreathing termination at Mach 20. Additional runs were made for these conditions with 50% strakes assumed for HTO.

As shown in Fig. 113, these early runs indicated that a vehicle with a TOGW/GLOW of 500 klbm was required to achieve the 10 klbm payload goal with a safety margin using 1995 TAD weight assumptions. After investigating the effects of airbreathing termination Mach number, it was found that an optimization point occurs at around Mach 15 that increases the payload capability significantly, as illustrated in Fig. 114. It was this combination, 500 klbm with scramjet to rocket transition at Mach 15, that was selected as the target vehicle configuration.

Strake Size and Takeoff Mode

Comparisons in Fig. 110 and 111 between vehicle strake sizes can be made by noting, based on engine type, takeoff attitude, or TAD assumption, the payload capability of each engine/vehicle system between the individual charts contained in the two figures. From these charts, it is clear that the 10% straked engine/vehicle configurations provide the best payload performance. However, when limited to the takeoff conditions previously discussed, the HTOHL systems were required to employ 50% strakes for all subsequent sensitivity analysis work conducted in order to meet the maximum takeoff speed limitation. VTOHL vehicle configurations were required to specify 25% strakes in order to satisfy vehicle angle-of-attack requirements that were then being set for the study. As will be subsequently discussed, the final baseline 500 klbm, VTOHL configuration has larger stake area, 50% of body radius, to meet the maximum angle-of-attack limitation which was subsequently adopted by the project staff.

Scramjet/Rocket Transition Velocity

Additional trajectory analyses were carried out to study variations of vehicle TOGW assuming rocket mode transition at decreasing Mach numbers from 20 down to Mach 10, with full capture at that transition Mach number, in the baseline 956 klbm vehicles A clear optimization point was found in the vicinity of Mach 15. This effect was found to be primarily due to the decrease in tank structural weight due to decreased total vehicle volume from increased vehicle density caused by increasing liquid oxygen loading. A minor contribution was found in reduced aerodynamic drag caused by reduced vehicle cross sectional area.

This effect held true even though the Isp from the scramjet propulsion system was higher then the rocket mode Isp being used to replace it until the Mach 15 optimum was reached.

The findings resulting from additional trajectory analysis work carried out using scramjet/rocket transition to from Mach 25 down to Mach 10 for 1.5 Mlbm, 956 klbm and 500 klbm vehicles are presented in Fig. 115 for Engine 10.

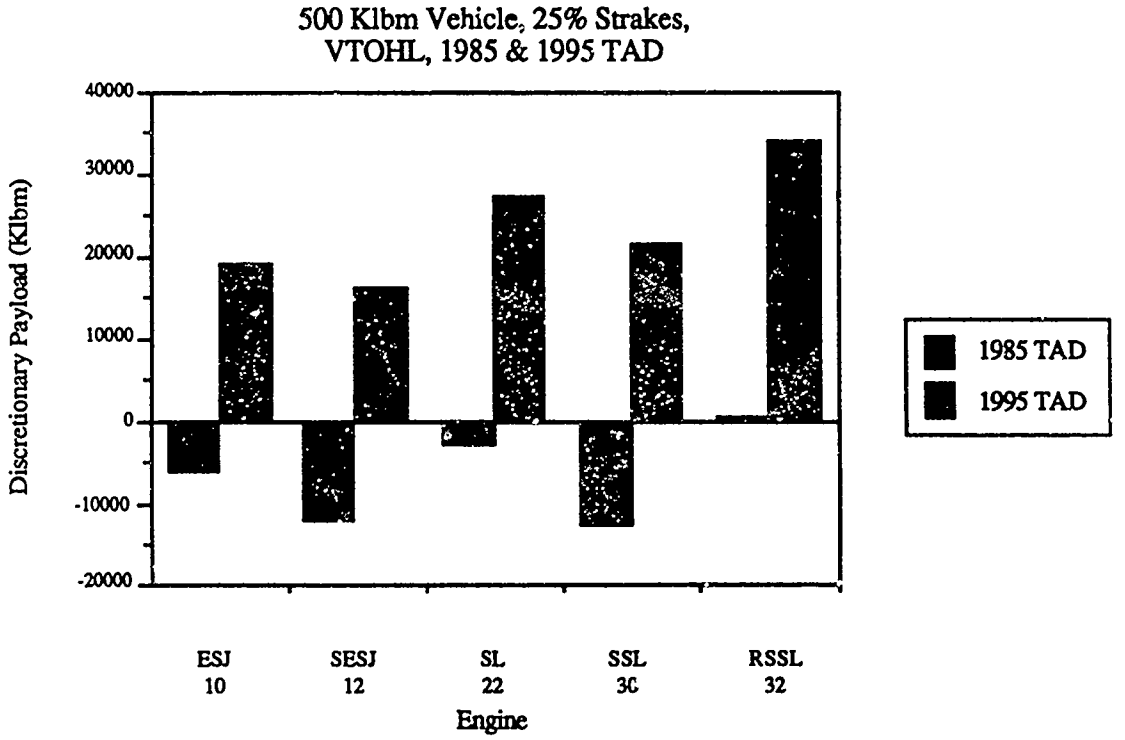


Fig. 113 Payload vs. Engine Type - Airbreathing Termination at Mach 20 with Full Capture at Mach 25

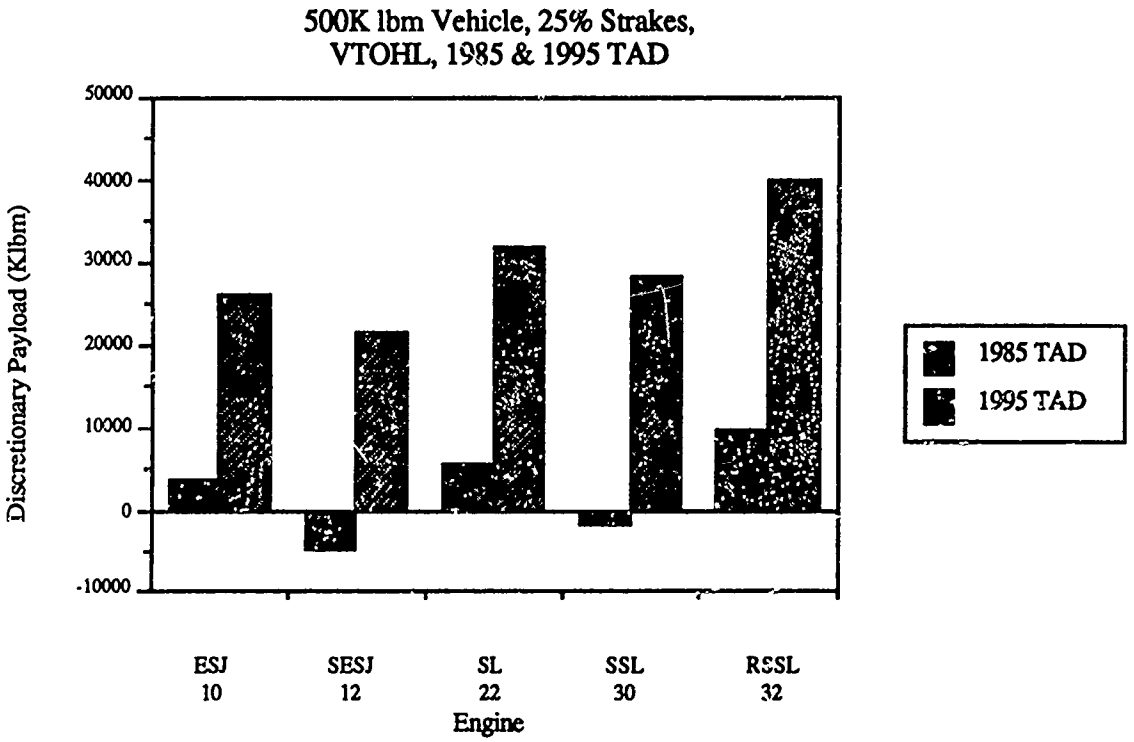


Fig. 114 Payload vs. Engine Type - Airbreathing Termination and Full Capture at Mach 15

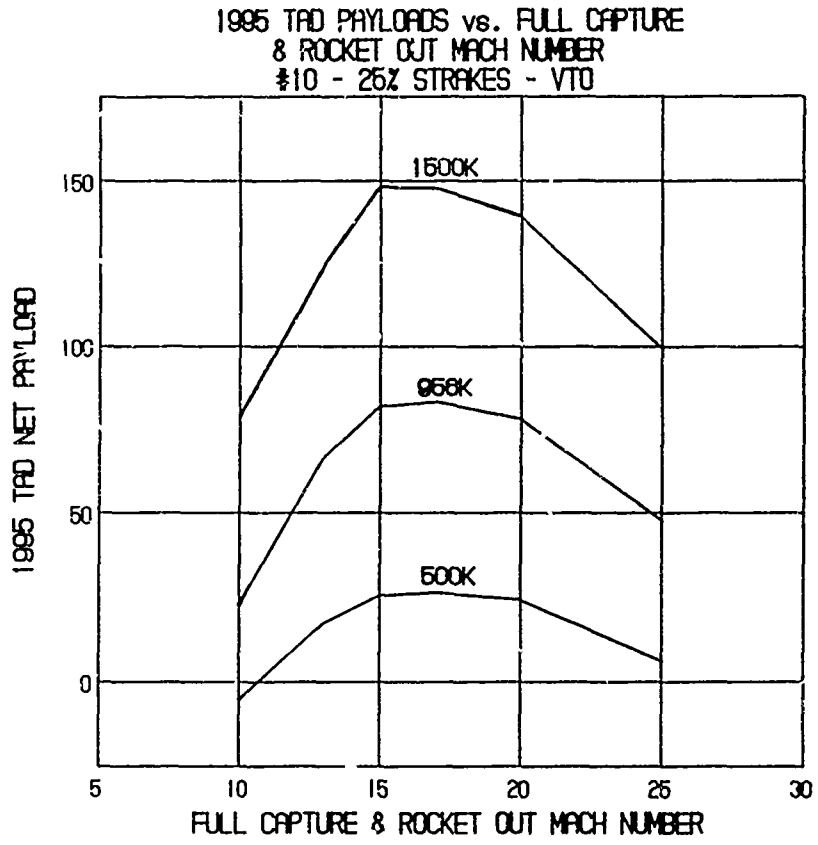


Fig. 115 Payload vs. Full Capture and Rocket Out Mach Number for Varying TOGW/GLOW Weight Classes

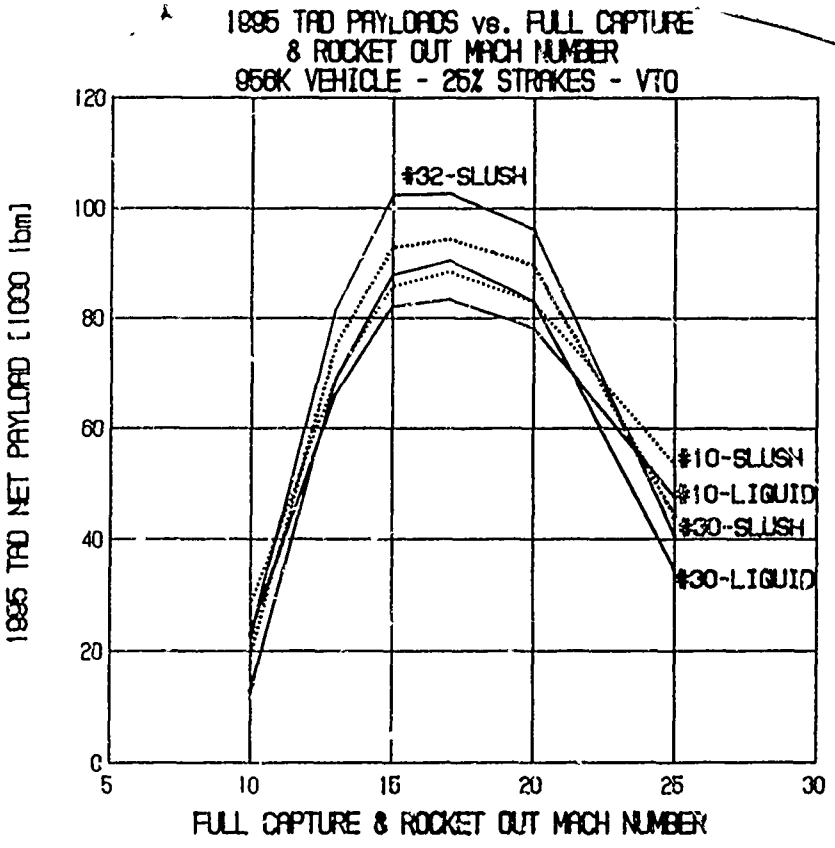


Fig. 116 Payload vs. Full Capture and Rocket Out Mach Number for Various Engine Types

Engine Type and Slush Hydrogen

The variation in payload produced by different engine types using the Mach 15 transition point was analyzed using Engines 10, 30 and 32 in a 956 klbm vehicle with 25% strakes and VTO. These three engines are representative of the "basic" RBCC engine and the more complex, higher performing engines that could be developed through a preplanned product improvement program. The effect of the use of slush hydrogen in both engine types was also investigated. The findings of these trajectory analyses is presented in Fig. 116.

Fig. 116 presents another significant finding of the study. The effect of slush hydrogen was evaluated in the NAS7-377 baseline study on the basis of its providing the means to more closely approach a stoichiometric mixture ratio in rocket ejector mode operation with liquid air systems (specifically the Recycled Supercharged ScramLACE - Engine 32) in two-stage vehicle systems. The findings of the present study indicate that a significant portion of the advantage derived from slush operation comes from decreased propellant tank weights resulting from increased hydrogen density and not from hydrogen recycling to achieve a mixture ratio closer to stoichiometric in Engine 32. The major portion of the slush hydrogen advantage is available to all 5 RBCC engine types in the SSTO mission, not just Engine 32.

Further, this advantage is available to all TOGW/GLOW weight class vehicles. The findings derived from analysis of Engines 10, 30 and 32 using NBP and Slush hydrogen in each of the 3 TOGW/GLOW weight class vehicles are illustrated in Fig. 116.

Payload Sensitivity to Aerodynamic Drag

The aerodynamic data used in POF36 simulations of the RBCC/SSTO vehicle was derived at a conceptual design level, and consequently has a significant level of uncertainty. Because of this uncertainty, it is important to understand the sensitivity of vehicle payload capability to changes in drag level estimates. If the payload to orbit is strongly affected by drag level, then the viability of the vehicle concept is strongly dependent on vehicle drag being near current predictions. If, however, payload capability is not strongly a function of vehicle drag, then current uncertainties in drag estimates pose little threat to the basic practicality of the vehicle design approach presented in this report.

Force Accounting

Before discussing these sensitivities, it is necessary to understand the force accounting scheme being used and what is meant by "aerodynamic drag". The drag forces experienced by the vehicle arise from a number of sources. These drag forces can be broken down into those forces associated with the propulsion system, and those forces strictly associated with, or due to, the external shape of the vehicle. Unlike more "conventional" vehicles, the majority of the external surface area of the axisymmetric RBCC/SSTO vehicle is wetted by propulsion influenced airflow. As a consequence, the propulsion systems operating characteristics assume an important role in the determination of overall vehicle drag. Drag forces which are not associated with the propulsion system play a smaller role in determining resistive forces than on a "conventional" vehicle.

Propulsion System Characteristics

As discussed above, the propulsion system has a strong influence on the flow field around the RBCC/SSTO vehicle. In effect, the entire forebody acts as a compressor for the engines (located at the maximum diameter station). The drag associated with that portion of the forebody that passes flow through the engines is accounted for in net jet based Isp and thrust characteristics of the RBCC engines. This drag is subtracted from the engines gross thrust to yield "net thrust"

which is the thrust value utilized in DOF36. All drag associated with the turning and slowing of flow which passes through the engines is handled within the engine database. As described in Sections 2 and 3, this propulsion performance data has a substantial foundation in the work performed in NAS7-377 (Ref. 2).

Aerodynamic Characteristics

The previous paragraph has described those portions of resistive aerodynamic forces which are contained within the engine database. The forebody drag portion of the aerodynamic database represents only the resistive forces associated with that flow which is not captured (or is spilled) by the engines. Consequently, the "aerodynamic drag" on the forebody is significantly less than in a typical aircraft configuration where a small percentage of the frontal area of the vehicle is capture area. In addition, the base drag associated with the aft end of the vehicle is greatly reduced by the expansion of engine exhaust over the aft cone. This "thrust' force associated with the expansion of engine exhaust on the aftbody is treated as a propulsion force. Just as on the forebody, the base drag is significantly reduced from that of a more "conventional" configuration over the majority of the flight regime.

Consequences of Force Accounting

The preceding paragraphs have indicated that the "aerodynamic drag" accounted for by the aerodynamic database is significantly reduced from that of a more conventional aircraft configuration. As a result of this reduction, the performance of the RBCC/SSTO vehicle (represented by payload to orbit capability) is less sensitive to changes in aerodynamic drag level than such conventional vehicles. This reduced sensitivity is shown clearly in Fig. 117 which presents the results of eight DOF36 simulation runs with varying levels of aerodynamic drag. The drag level was varied from zero aerodynamic drag to a drag level 30% greater than the baseline. As described previously, these drag level variations do not affect those drag forces associated with the propulsion system inlet flow which is included in the caclulations of engine net jet thrust and net jet Isp. Fig. 117 shows that RBCC/SSTO mass to orbit capability is reduced less than 190 pounds for each percent increase in aerodynamic drag in the 956 klbm vehicle. As a result, RBCC/SSTO concept viability is not strongly affected by aerodynamic drag level. It is suggested that the performance results presented, although based on a conceptual design level aerodynamic database, will remain valid even if further study indicates increases in vehicle drag level provided that the capture schedule projected can be achieved and the net-jet thrust and Isp estimates are correct. It is reasonable to expect the the RBCC engines net jet thrust and net jet Isp in ejector mode, ramjet and scramjet mode to Mach 8 will be achieved based on experimental work previously described in Section 2.0. The performance of RBCC engines in the Mach range from 8 to 15 (Scramjet mode) remains to be verified. The thrust and Isp values used in all-rocket mode are not net jet but rocket engine Isp values not dependent on any capture area schedule or inlet drag estimates but will be affected by the ability to achieve very high nozzle area ratio expansion.

Specific Impulse Sensitivity

The specific impulse delivered in each operating mode was varied by +/-10% with the exception of the all-rocket mode. The rocket Isp in all-rocket mode Isp was not investigated above the baseline estimate of 470 sec but was investigated at -10%.

The findings for the 956 klbm vehicle system are presented in Fig. 118 for a vehicle powered by Engine 32, the Recycled Supercharged Ejector ScramLACE.

There is relatively little impact caused by ejector mode Isp variations in this engine. This is due primarily to the fact that this engine is running on LAIR and oxygen mass is not required

to support ejector operation. Thus the increase, or decrease, in hydrogen mass that would be attendant to lower and higher Isp values respectively is all that must be accounted for in an Engine 32 powered vehicle. As will later be seen in the 500 klbm engine #10 powered vehicle, this condition is not the same for ejector operation on LOX/H_2 where a much higher, or lower, payload weight differential was found.

10% increase and decrease in ramjet Isp does not produce a significant change in payload delivery capability. This is due to the high Isp performance being delivered and the comparatively low fuel mass consumed in this mode in comparison to that consumed

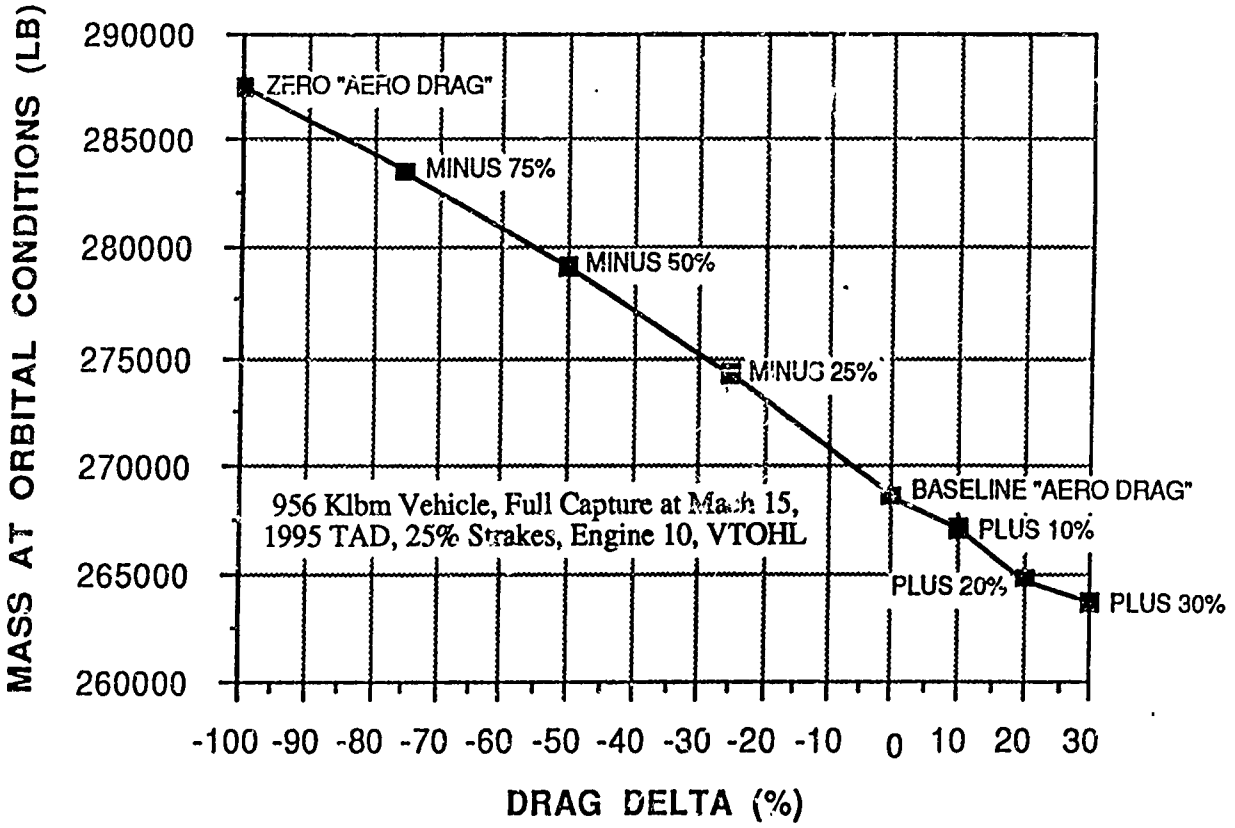


Fig. 117 Sensitivity of Mass Delivered to Orbit to Vehicle Drag

in the other three modes of operation. This same, relatively low, sensitivity will be shown to exist for the 500 klbm Engine 10 vehicle configuration to be discussed subsequently, since ramjet mode operation is the same in both engine configurations.

The maximum sensitivity is found in the scramjet mode where a major portion of the total propellant mass is consumed over a relatively large speed range.

The reader should note that in Fig. 118, a scramjet to rocket mode transition velocity of Mach 20 and a maximum capture schedule at Mach 25 was used. As will be seen from subsequent discussion of the 500 klbm point design vehicle which uses a scramjet to rocket mode

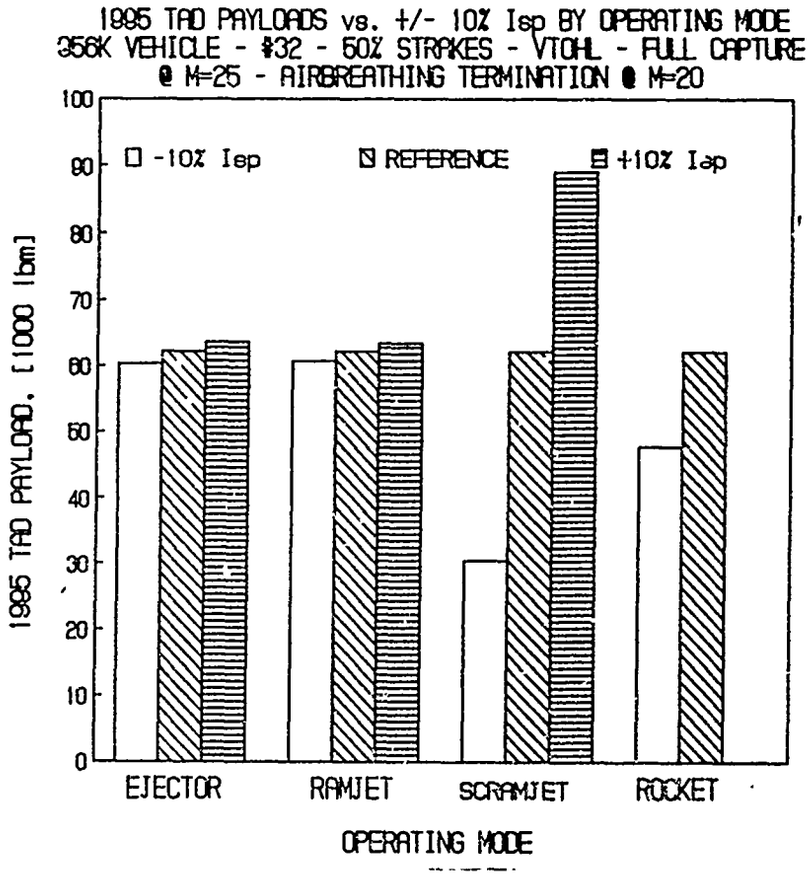


Fig. 118 Effect of +/- 10% Isp by Propulsion Mode on Payload

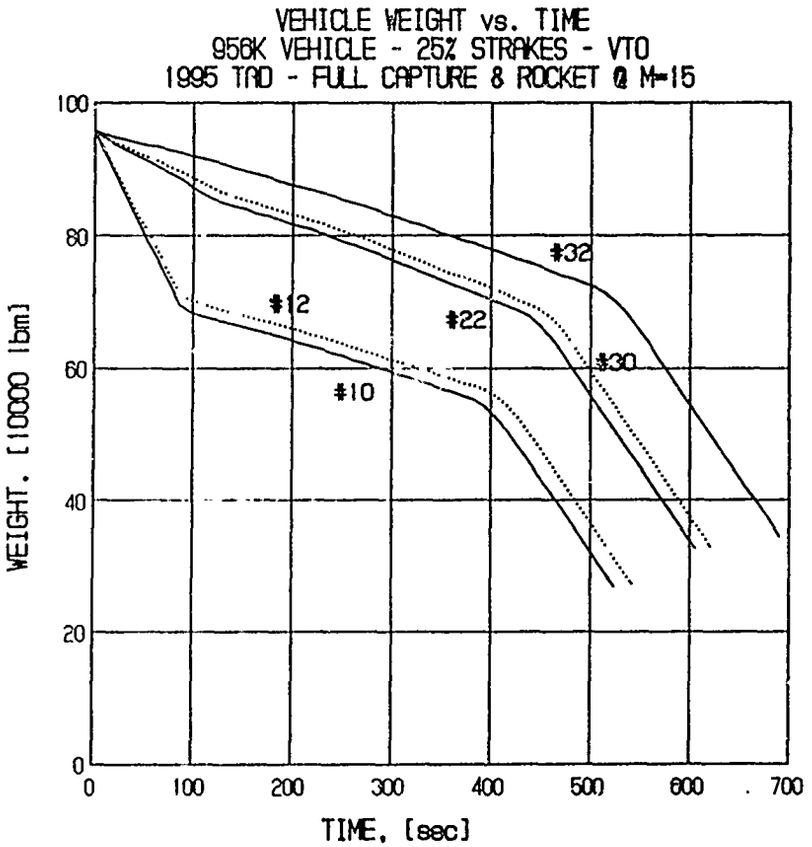


Fig. 119 Vehicle Weight History for all Five RBCC Engine Types Studied

transition velocity of Mach 15, the sensitivity is reduced significantly by the lower transition velocity.

In the rocket mode, LOX is used as the oxidizer in all engines. The payload performance sensitivity is similar with all engine configurations.

In Fig. 119, the ascent flight time history of instantaneous vehicle mass for all five RBCC engines studied for a 1995 TAD is presented. The reader should note that this presentation is based on a scramjet-to-rocket transition velocity of Mach 15, not the Mach 20 case previously discussed. This figure should further illustrate why the Isp sensitivity differences exist between LAIR ejector RBCC engine configurations and LOX ejector RBCC engine configurations.The latter have a higher propellant flow rate because of their lower Isp capability.

Another significant observation that can be made from this illustration is the fact that while the propellant mass flow rate schedule varies significantly between each of the engine types, the mass to orbital insertion, or M2, does not.

Sensitivity to Weight Estimates

Fig. 120 illustrates the sensitivity of payload mass delivered to orbit to vehicle inert or empty weight for 1995 TAD with vehicle inert weight estimates greater than those used in this study. It should be noted that this figure presents this sensitivity for the 956 klbm vehicle with 25% strakes and the point design 500 klbm vehicles with heavier, 50% strakes, both with Mach 15 rocket transition velocity.

This is the most significant sensitivity for a number of reasons. First, increased inert weight subtracts from payload on a pound for pound basis for a given mass M2. Secondly, while many of the element weight estimates comprising the RBCC/SSTO configurations vehicle weight estimates are based upon experience, many are not. In any future studies of this type of vehicle configuration, emphasis should be placed on obtaining as reliable weight estimates as possible through selected engine and vehicle design studies.

Other Characteristics

Fig. 121 presents the I* performance and payload delivery performance of all five RBCC engine systems for a 1995 TAD. As can be seen, all engine types achieve the study goal of over 600 seconds equivalent effective specific impulse based on the assumptions made in this study.

Table 19 presents the flight time and trajectory ground track range for both 956 klbm and 500 klbm vehicles with a 1995 TAD.

Table 20 presents the payload to TOGW/GLOW ratios and payload as a portion of total dry weight for the 956 klbm vehicle with Mach 20 scramjet termination. The measure of payload/total dry weight provides a figure of merit with which to estimate the cost of hardware required to deliver a pound of payload to orbit. The reader should be aware of the fact that this is a good measure with expendable systems, but the systems considered here are reusable systems. In reusable systems, the number of missions that can be flown in the useful life of the reusable vehicle must be known before this characteristic can be used for cost comparison purposes between alternative vehicles. The ratios presented here are significantly superior to those provided by expendable all-rocket booster systems.

Table 21 presents the propellant mass fraction and tanked O/F weight ratio, for the 956 klbm vehicle for a 1995 TAD with Mach 20 scramjet termination. The propellant mass fraction required to achieve the orbital delivery mission is considerably lower for RBCC systems then for

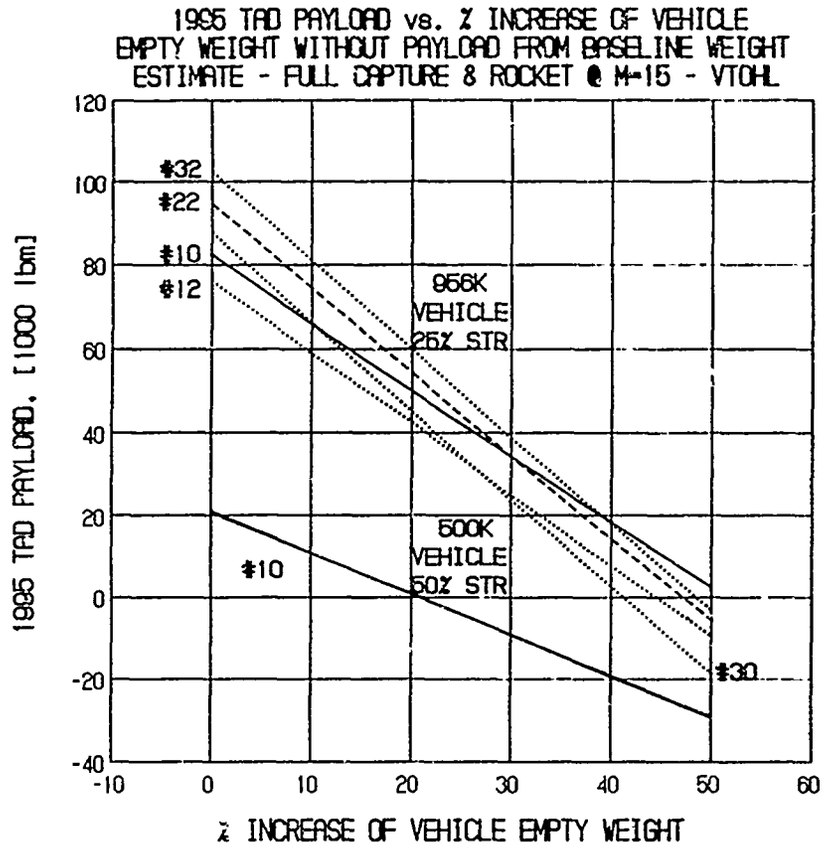


Fig. 120 Payload vs. % Variation in Weight Estimates

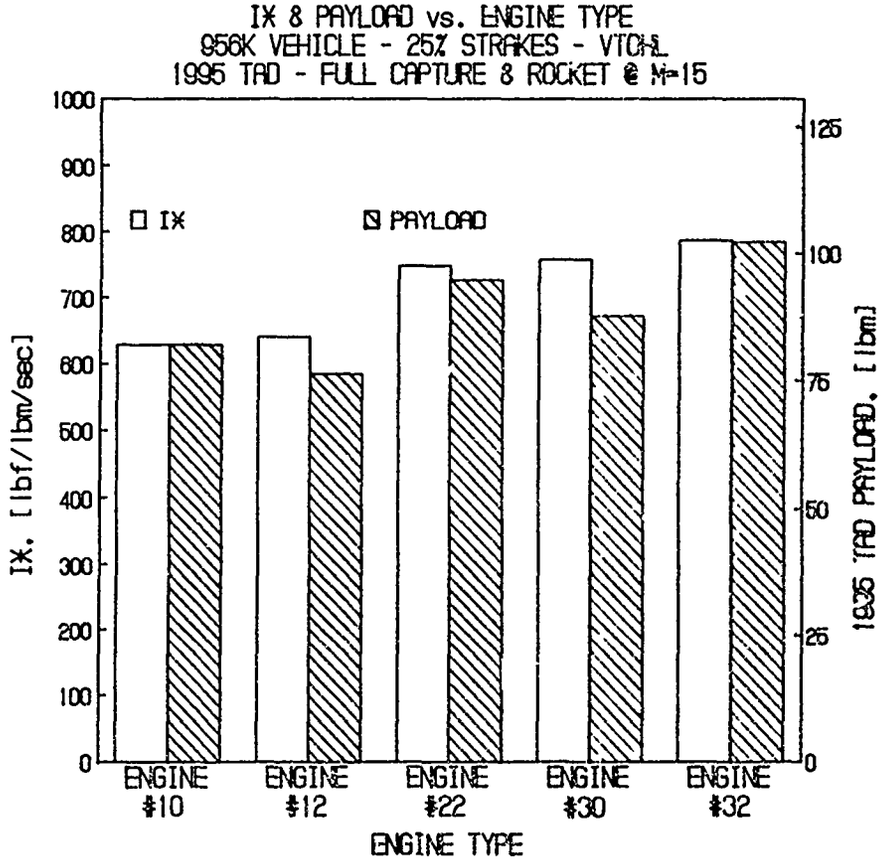


Fig. 121 I* and Payload vs. Engine Types

Table 19 Ascent Flight Time to 50 nmi Orbit Prior to Hohmann Transfer to 100 nmi Orbit

956 Klbm, 25% Strake, Full Capture at Mach=25,
Airbreathing Termination at Mach=20,
1995 TAD

Engine		Ascent Time & Range					
		HTO			VTO		
No.	Type	sec	min	Range nmi	sec	min	Range nmi
10	Ejector Scramjet	802	13.4	1715	773	12.9	1616
12	Supercharged Ejector Scramjet	822	13.7	1764	787	13.1	1646
22	Scramlace	857	14.3	1803	867	14.4	1756
30	Supercharged Scramlace	875	14.6	1849	889	14.8	1804
32	Recycled Supercharged Scramlace	1000	16.7	2129	1021	17.0	2097

VTO

500 Klbm, 25% Strake, Full Capture at Mach=15,
Airbreathing Termination at Mach=15,
1995 TAD

No.	Type	sec	min	Range nmi
10	Ejector Scramjet	474	7.9	840
12	Supercharged Ejector Scramjet	479	8.0	853
22	Scramlace	573	9.6	991
30	Supercharged Scramlace	583	9.7	1018
32	Recycled Supercharged Scramlace	630	10.5	1109

Table 20 Net Payload and Payload Fractions for 956 klbm Vehicle with Mach 25

Vehicle: 956 Klb TOGW, VTOHL, 25% Strakes,
Full Capture at Mach 25, Airbreathing
Termination at Mach 20, 1995 TAD

	Engines	Payload* (lbm)	Payload/ TOGW	Payload/ Dry Weight
	10	67,700	0.07	0.38
H_2/O_2	12	56,400	0.06	0.29
H_2/LAIR	22	77,800	0.08	0.35
(O_2 For Rocket Mode)	30	70,500	.0.07	0.30
	32	79,000	0.08	0.34

* Does Not Include 5000 lbm Flyback Fuel And 440 lbm Crew

Table 21 Total Propellant Mass Fractions and Tanked O/F Ratios for 956 klbm Vehicle

Vehicle: 956 Klb TOGW, VTOHL, 25% Strakes,
Full Capture at Mach 25, Airbreathing
Termination at Mach 20, 1995 TAD

	Engines	Propellant Mass-fraction	Tanked O/F
	#10	74%	0.93
H_2/O_2	#12	74%	0.81
H_2/LAIR	#22	68%	0.22
(O_2 For Rocket Mode)	#30	68%	0.22
	#32	67%	0.23

all-rocket systems; around 70% compared to 80% to 90% in all-rocket systems. This infers that design to the weight goal in RBCC systems might be easier then in all rocket systems. However, RBCC engine systems are considerably heavier then rocket engine systems of equivalent thrust.

6.5 Point Design Vehicle Configuration Selection and Performance

The parametric studies carried out for TOGW/GLOW RBCC/SSTO vehicles of 500 klbm, 956 klbm and 1500 klbm provided the basis for identifying the configuration of the "point design" vehicle, which is the vehicle capable of delivering a 10 klbm payload and a crew of two to a 100 nmi polar orbit and returning that vehicle to a landing point.

6.5.1 Selection of Point Design TOGW/GLOW

Fig. 122 presents the payload performance estimates for 1995 TAD RBCC/SSTO vehicles with scramjet/rocket mode transition at Mach 15 and various engine types. The target payload can be delivered with an Ejector Scramjet powered vehicle of 500 klbm TOGW/GLOW.

The distribution of weight for all vehicles studied included 5000 lbm of flyback and landing propellant. This propellant weight will support only minimal maneuvering during flyback and landing. As will be discussed, flyback and landing maneuvering requirements must be specified before the TOGW/GLOW class can be selected. Selection of the 500 klbm TOGW/GLOW provides additional propellants, beyond the 5000 lbm fixed mass initially used, for flyback and landing maneuvering. These considerations led to the 500 klbm vehicle being selected as the point design candidate rather then .

6.5.2 Point Design Engine Selection

With the selection of the point design TOGW/GLOW, the second issue addressed was engine selection. Fig. 122 presents the payload performance of Engines 10, 30 and 32 which encompasses the performance envelope of all 5 candidate RBCC engine systems. The difference in terms of payload delivery capability between the simplest configuration, Engine 10, and the most complex engine with the highest technological risk, Engine 32, is not large.

The approach taken in this study was to balance payload performance against technological risk. Engine 10 with NBP hydrogen was selected for the point design vehicle primarily on the basis of providing minimum new technology development requirements while also meeting the target mission requirements.

However, if more than minimal flyback and landing capability is required, fan supercharged Engines must be considered.

As can be seen from Fig. 122, the payload performance of any point design vehicle would not be significantly affected by the selection of any of the five RBCC engines in any TOGW/GLOW weight class vehicle. The flyback and landing capability would be positively affected with fan supercharged engines. Thus the selection of Engine 10 in the 500 klbm weight class does not result in a vehicle with radical performance differences from the other four RBCC engine powered SSTO vehicle configurations.

This selection does provide a baseline from which preplanned product improvement efforts can be undertaken to significantly improve flyback and landing performance.

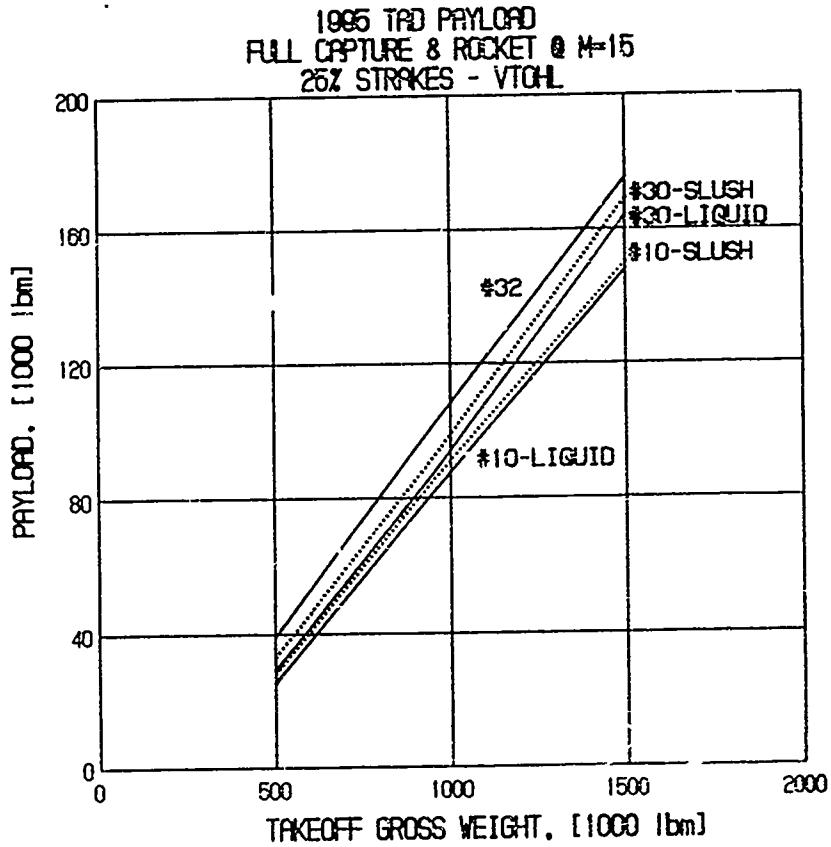


Fig. 122 Payload vs. TOGW and Engine Type

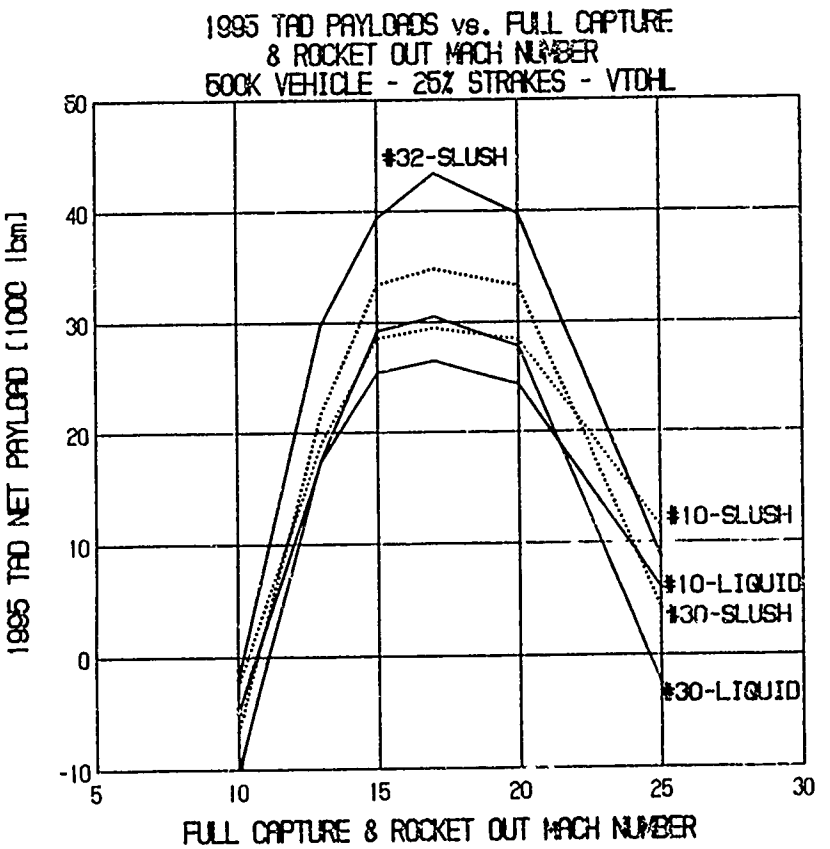


Fig 123 Payload vs. Full Capture Mach Number for Engines #10, #30 and #32

6.5.3 Scramjet/Rocket Transition Velocity Selection

Fig. 123 presents payload performance of 500 klbm vehicles versus full capture design flight speed/transition to rocket flight speed. As can clearly be seen, the optimum transition velocity is Mach 17 in terms of payload consideration only. When the risks associated with payload sensitivity to scramjet Isp were considered, the decision was made to go for the lower transition velocity of Mach 15 which produces only minimal payload performance impact but reduces the scramjet operating regime by 2.5 Mach numbers and reduces the overall vehicle sensitivity to scramjet Isp values that might actually be achieved in practice as has been previously discussed and illustrated in Fig. 118.

6.5.4 Strake Size

The payload performance of the alternative weight classes of RBCC/SSTO vehicle configurations presented in Fig. 122 and 123 were for 25% straked vehicles. As has been previously discussed, in the axisymmetric configuration of RBCC propelled vehicles, an important objective is to minimize forebody angle-of-attack to minimize the development of crossflow and other non-uniform airflow conditions that will be detrimental to RBCC engine inlet performance. Because of this, the effect of strake size on payload for the point design vehicle was analyzed.

The effect of strake size on angle-of-attack for the 1995 TAD RBCC point design vehicle with Mach 15 transition velocity was investigated. The results of these trajectory simulations are presented in Fig. 124.

The payload capability of a 1995 TAD, 500 klbm RBCC/SSTO vehicle with Mach 15 transition was then analyzed for the three strake sizes considered in Fig. 124. The findings of this analysis are presented in Fig. 125.

The 500 klbm, 50% strake size configuration reduces the propellants available for flyback and landing to approximately 16 klbm comprised of the 5 klbm provided as a baseline in all vehicle configurations and approximately 11 klbm available in excess of the 10 klbm payload

Based on these findings, the point design vehicle configuration was selected. This vehicle is a 500 klbm vehicle powered by an Ejector Scramjet propulsion system with 50% strakes, rocket mode transition and full capture at Mach 15 and assuming 1995 technology availability. The vehicle will use vertical takeoff and horizontal landing.

6.6 Point Design Vehicle Sensitivities

6.6.1 Isp Sensitivity

Fig. 126 presents the sensitivity of payload to Isp variation. By selecting the Mach 15 transition point, the sensitivity to scramjet Isp is significantly reduced from the Mach 20 transition point case illustrated in Fig. 118. The sensitivity to all-rocket mode performance is significantly increased as would be expected. However, based on previous experimental work and actual H_2/O_2 engine performance experience as discussed in Section 3.0, it is not reasonable to expect that a 10% lower Isp value for the rocket subsystem, i.e., 423 seconds compared to 470 seconds estimated, would be delivered in actual practice (see Table 1).

Based on the experimental work carried out by The Marquardt Corporation in the USAF Advanced Ramjet Concepts technology program and other efforts in the 1960's, relatively high confidence can be placed in the ejector mode and ramjet mode Isp values used in this study. The principle Isp uncertainty is scramjet Isp between Mach 8 and Mach 15.

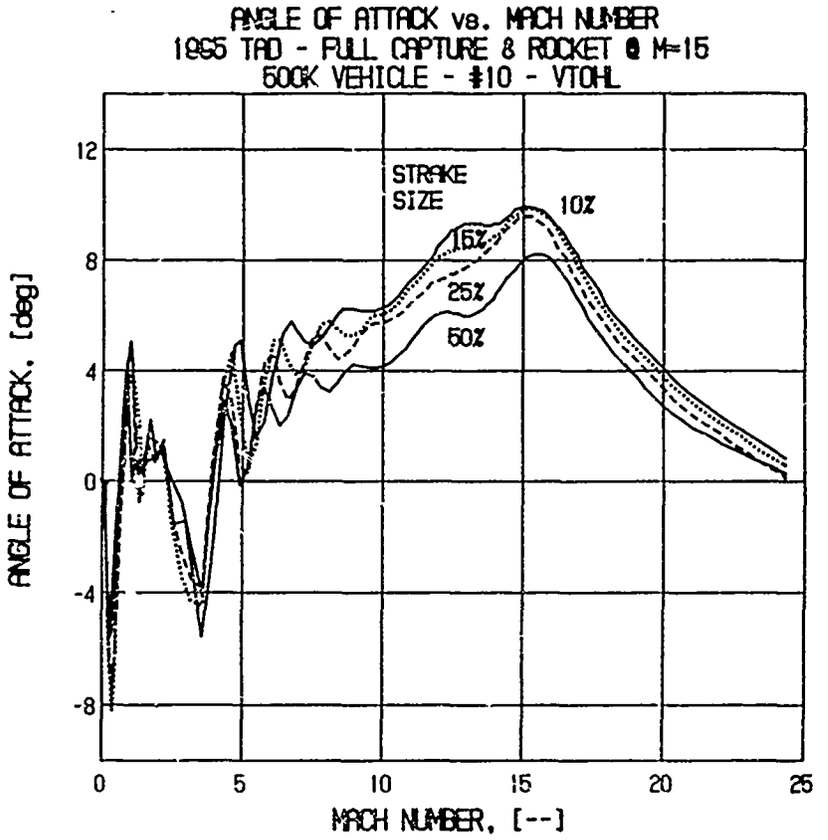


Fig. 124 Angle of Attack vs. Mach Number for Varying Strake Sizes

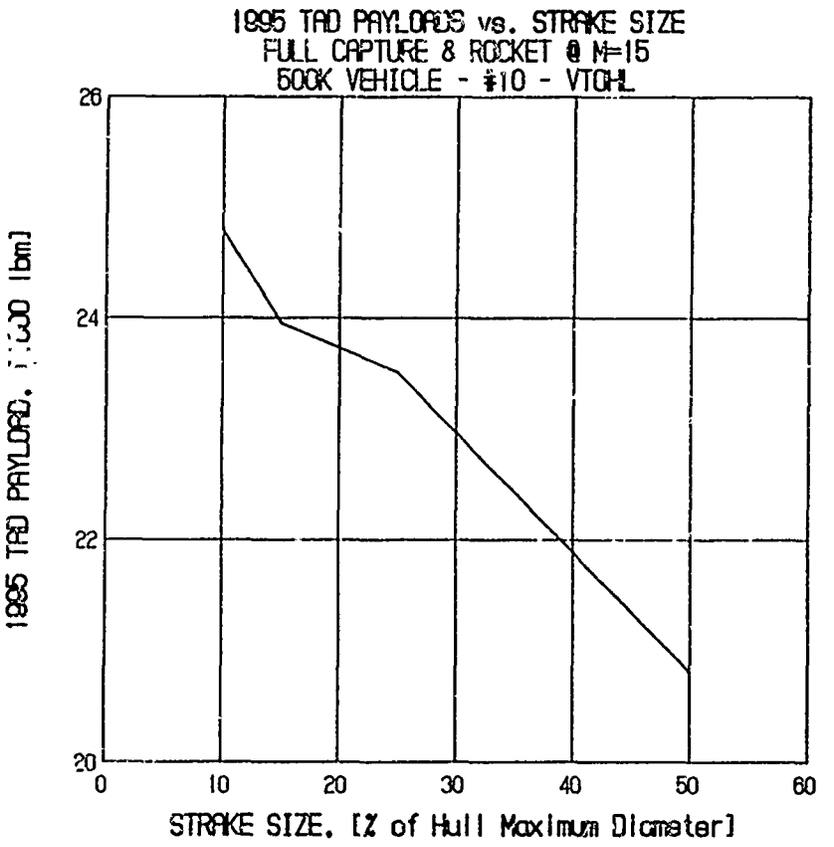


Fig. 125 Payload vs. Strake Size for the Baseline Vehicle

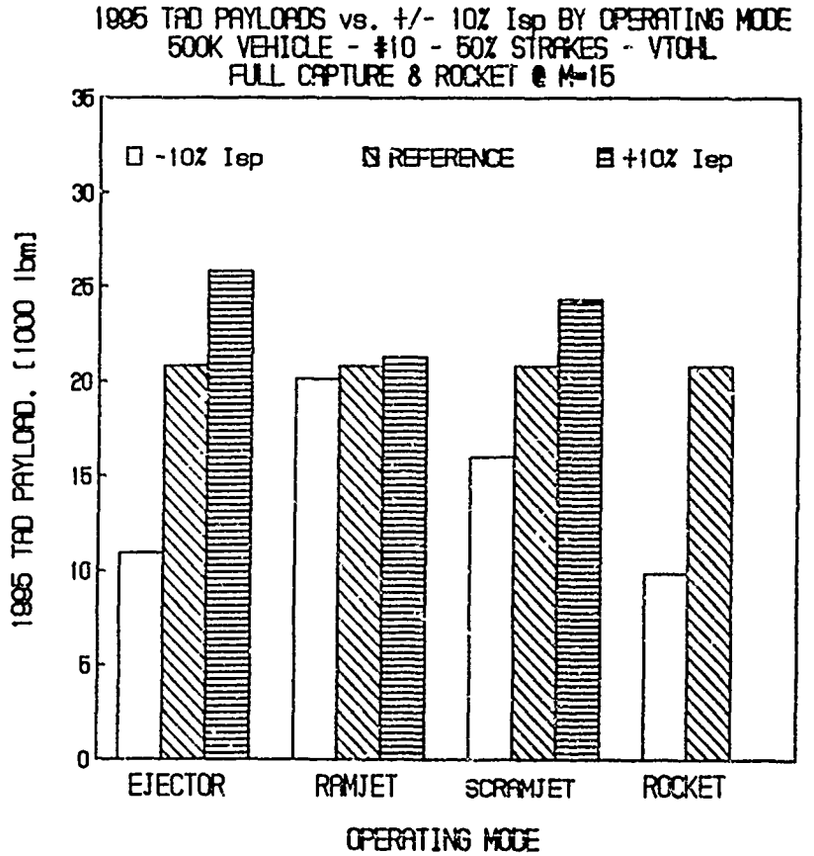


Fig. 126 Effect of +/- 10% Isp Variation on Payload for the Baseline Vehicle

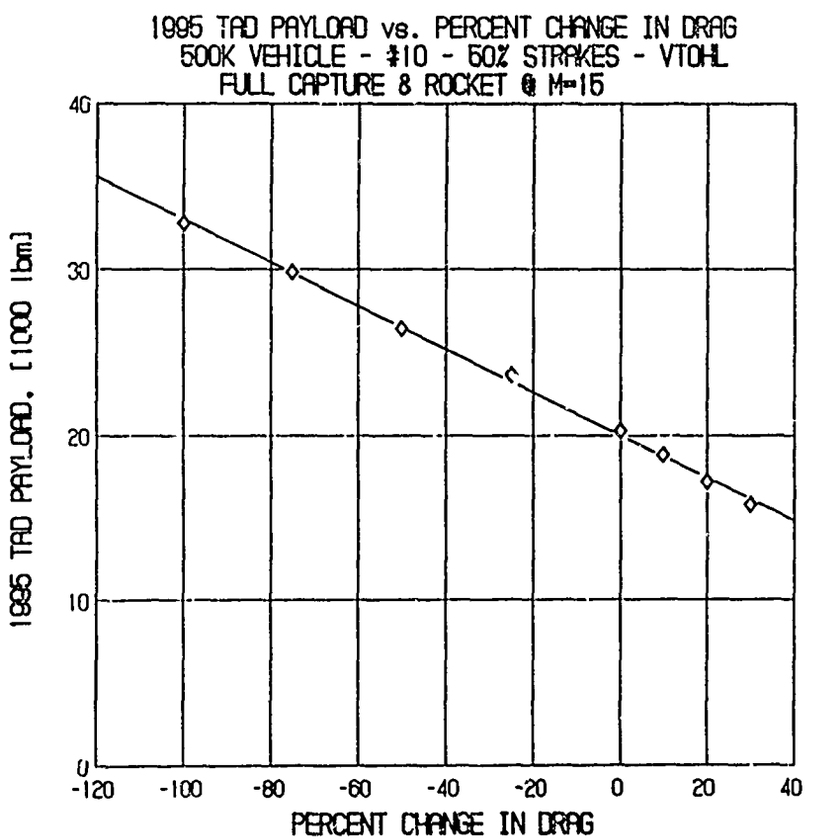


Fig. 127 Payload vs. % Change in Drag Estimates for the Baseline Vehicle

6.6.2 Drag Sensitivity

Fig. 127 presents the study findings with regard to the sensitivity of the point design vehicle to drag. As can be seen from this graph, the target payload is still delivered in a case where actual aerodynamic drag exceeds the estimates used in this study by more than 40%.

6.6.3 Weight Estimate Sensitivity

Fig. 120, previously presented, illustrates the sensitivity of the point design vehicle to weight estimation error for both 956 klbm, 25% straked vehicles and a 500 klbm, Engine 10 powered, 50% straked vehicle.

Weight estimate sensitivity is significant for two reasons. First, increased inert weight subtracts from payload on a pound for pound basis for a given mass M2 delivered to orbit. Secondly, while many of the element weight estimates comprising the RBCC/SSTO configurations vehicle weight estimates are based upon experience but many are not. In any future studies of this type of vehicle configuration, emphasis should be placed on obtaining as accurate weight estimates as possible.

The weight estimates breakdown for an RBCC/SSTO vehicle of 500 klbm TOGW/GLOW were previously presented in Section 5.0. To provide further comparisons between the study weight estimates for RBCC/SSTO vehicles and those developed by other organizations for all-rocket SSTO vehicles, a rough comparison was made between the NASA Langley Research Center's estimates for Shuttle II and the 500 klbm RBCC/SSTO weight estimate developed in this study.

The comparison was developed by directly scaling the weights of the LaRC Shuttle II down to a 500 klbm gross weight. This findings from this comparison are illustrated in Table 22.

This is a rough order of magnitude comparison. The objective of making it was to identify any weights where the study team weight estimates were grossly lower then the Shuttle II estimates for comparable subsystems. Significant differences were found in one instance. This was in Weight Item 28 - Pre-Launch Losses. The Shuttle II system would appear to be designed without a continuous "topping" system active to lift-off. It is proposed that the RBCC/SSTO vehicle would have a continuously active topping system and that pre-launch losses from the flight tank volume would be minimal.

The orbit shown for the 500 klbm RBCC vehicle is a 100 mile orbit with 28.5 degrees northerly inclination. Approximately 5000 lbm should be subtracted from the useful payload to provide for the propellant requirement to achieve the 250 mile orbit base of the Shuttle II weight projection.

6.6.4 Other Characteristics of the Point Design Vehicle

Trajectory Weight History

Fig. 128 presents the ascent trajectory time history of weight of the point design vehicle. This figure illustrates the "energy intensiveness" of each portion of the orbital ascent trajectory. The initial high rate of propellant consumption occurs in the ejector mode followed by the ramjet and scramjet mode at much lower propellant flow rates and the final all-rocket mode with its high propellant flow rate.

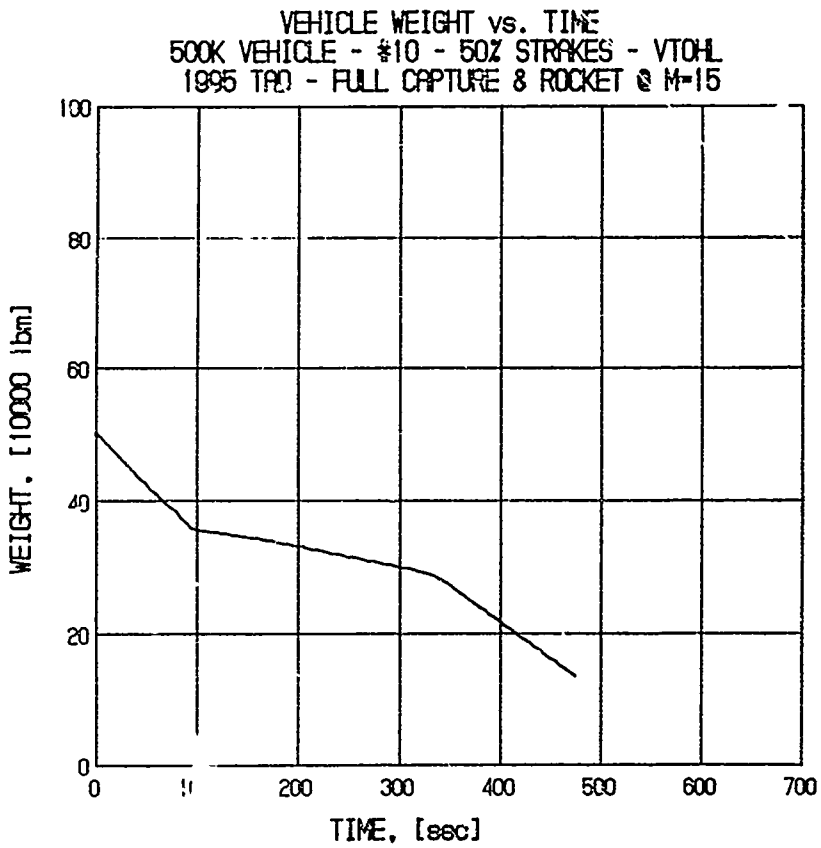


Fig. 128 Baseline Vehicle Weight Characteristics vs. Time

The overall flight characteristics of the ascent trajectory to orbit for the point design vehicle are graphically summarized in Fig. 129 and 130.

The maximum vehicle acceleration was set at 3.5 g based on passenger and crew consideration.

Endurance and Range

In estimating the endurance and one-way range capability of the point design vehicle, the following conditions were set:

- vertical takeoff on the reference trajectory
- ascent on the reference trajectory to that altitude where the flight velocity to be studied was achieved

Shuttle II Weight Statement vs. RBCC/SSTO Weight Estimates
1992 Technology Availability Date
850 psf maximum Q
20 klbm to Space Station
LaRC - January 1987
SSTO - Dual Fuel - Separate Engines
Prepared: 1 January 1988 - R.Foster

	Baseline LaRC 4.2 mlbm TOGW	Referenced to 500 klbm TOGW *	500 klbm RBCC/SSTO ESJ Engine	
1.0 Wing Group	39900	4788	8309	
2.0 Tail or Tip Fin Group	1399	168	0	In wing group
3.0 Body Group	124692	14963	31347	
4.0 Thermal Protection System	41653	4998	0	In body weight
5.0 Landing Gear	12989	1559	10000	
6.0 Propulsion	93437	11212	40880	
7.0 Propulsion, RCS	8423	1011	454	RCS + Control Surfaces
8.0 Propulsion, OMS	2524	303	0	Uses RCS
9.0 Primary Power	1170	140	5000	APU 1% of GLOW
10.0 Electrical Conv. & Dist	9227	1107	382	
11.0 Hydraulic Conv. & Dist	0	0	0	
12.0 Surface Contols	3781	454	0	see RCS
13.0 Avionics	3289	395	3000	Avionics/ECS/Personnel
14.0 Environmental Control	1615	194	0	provisions
15.0 Personnel Provisons	1375	165	0	
16.0 Margin	28004	3360	0	
Dry Weight	373478	44817	99372	
17.0 Personnel	3076	369	440	
18.0 Payload Provisions - Shroud	9920	1190	0	In body group
19.0 Cargo - Returned	20000	2400	20820	
20.0 Residual Fluids	23558	2827	0	3740 lbm in Ascent Prop.
21.0 Reserves	2500	300	5000	
Landed Weight	432532	51904	125632	
22.0 RCS Propellant	1458	175	0	
23.0 ACPS Consumeables - On Orbit	43182	5182	0	5560 lbm in Ascent Prop.
24.0 Cargo Discharged	0	0	0	
25.0 Ascent Reserves	8680	1042	0	
26.0 Inflight Losses	763	92	0	
27.0 Ascent Propellants	3612156	433459	374369	
Launch Weight	4698773	563853	500001	
28.0 Pre-Launch Losses	62494	7499	0	
Gross Weight	4161262	499351	500001	

* - 500000 lbm/4161262 lbm = .120

Table 22 Weight Comparison of the LaRC Shuttle II Directly Scaled to 500 klbm vs. a 500 klbm RBCC/SSTO Vehicle

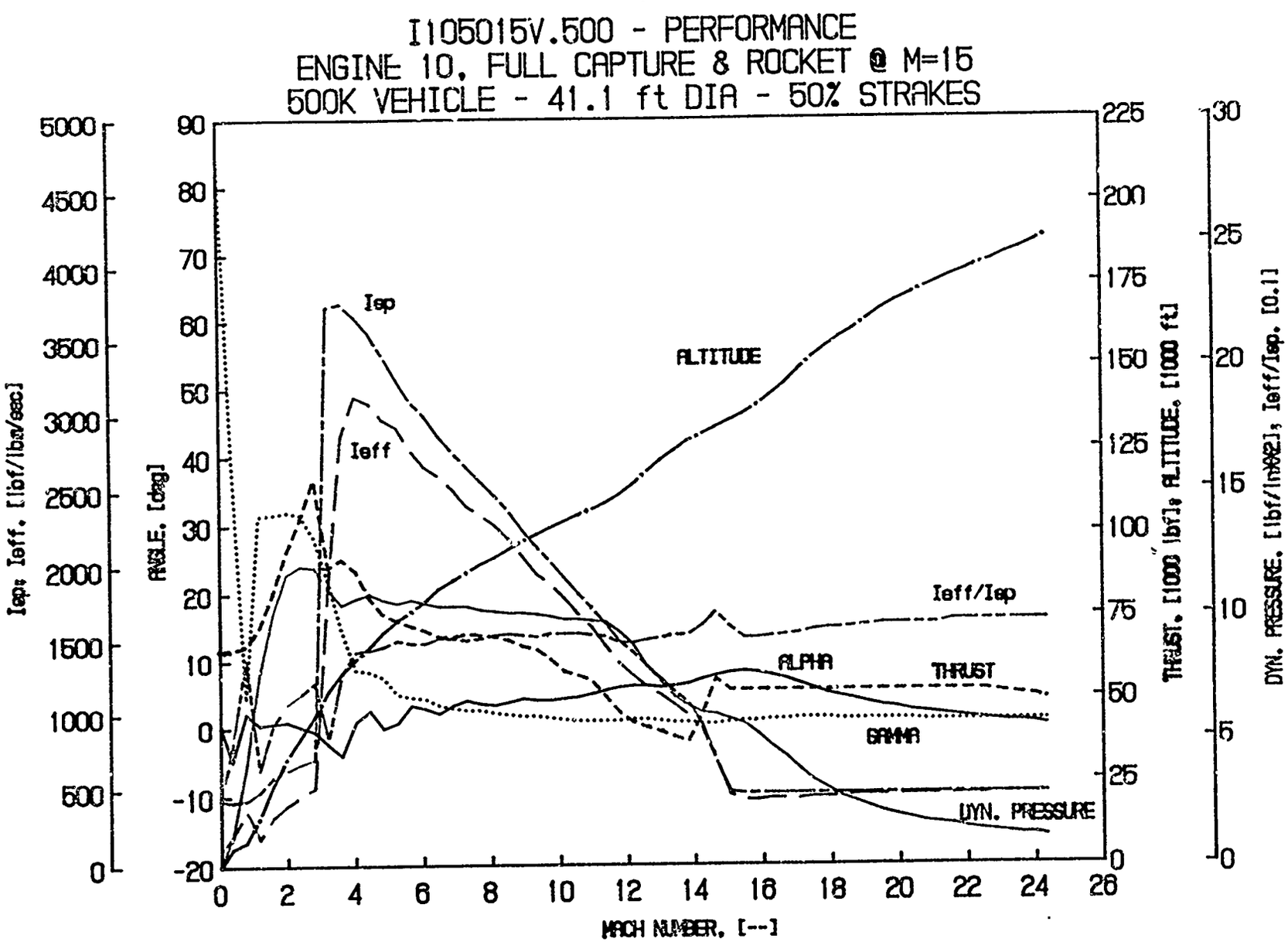


Fig. 129 Baseline Vehicle Performance

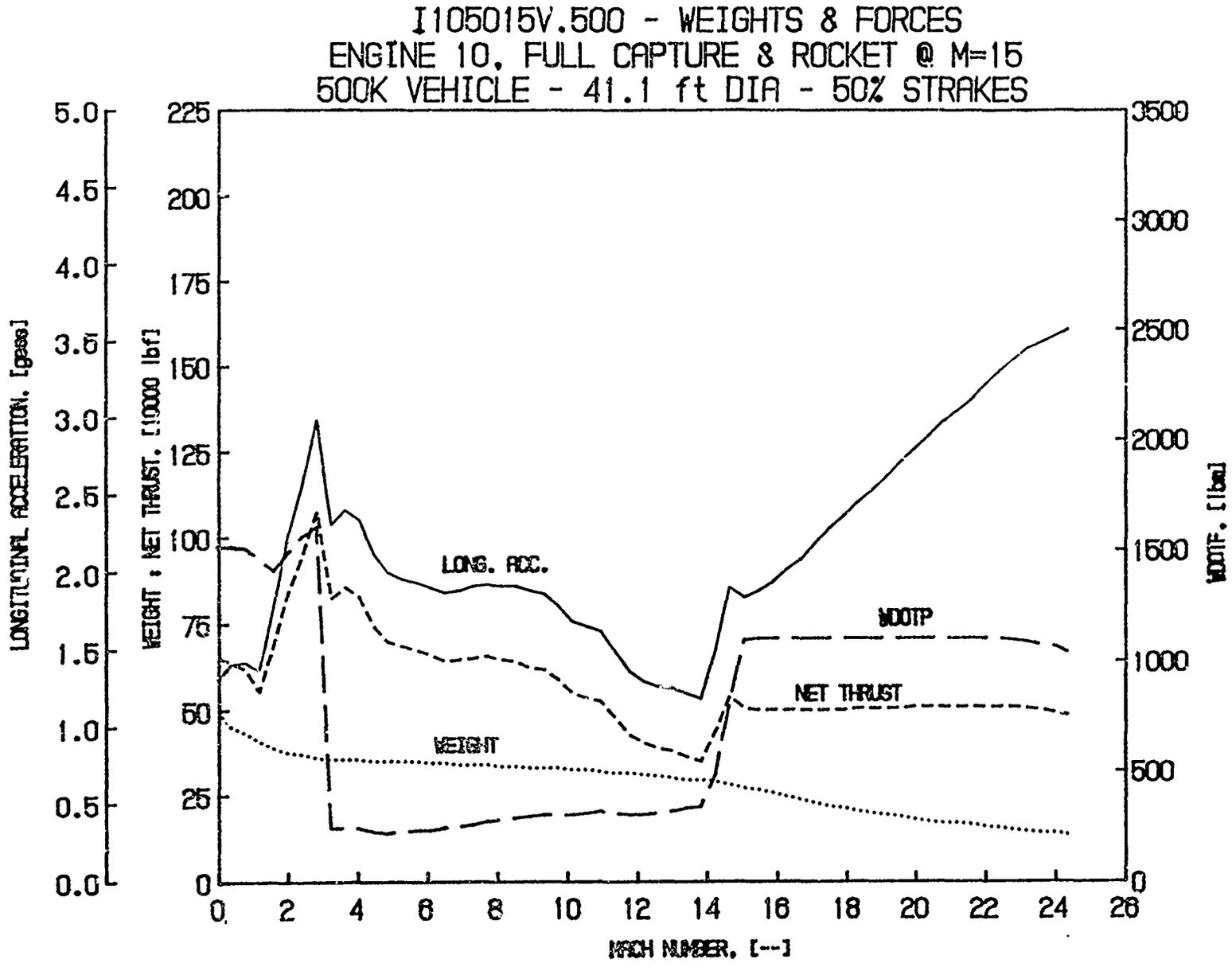


Fig. 130 Baseline Vehicle Weights and Forces

- level flight was initiated at that altitude. It should be noted that this is in all probability not an optimum cruise altitude.
- full payload, crew and 5000 klbm of flyback and landing propellant
- only that number of engines required to produce constant flight velocity at the Mach number and altitude were used
- no capture area effect on drag was used. The vehicle was flown with conventional drag force accounting
- The liquid oxygen required for the orbital ascent trajectory was not loaded.

The findings resulting from this analysis are presented in Fig. 131 and 132 for both 25% straked vehicles and the 50% straked point design vehicle at the optimum flight speed for endurance and range.

Ascent Time and Range Track

The ascent time and range track distance for a 500 klbm vehicle similar to the point design vehicle was previously presented in Table 19. While the vehicle design in that table has 25% strakes, the use of 50% strakes does not make a significant difference.

6.7 Vertical Takeoff Considerations

6.7.1 Thrust Vector Control

In order to carry out both vertical takeoff and vertical landing, as well as in flight trajectory control at altitudes where conventional control surfaces are not effective, thrust vectoring in all three vehicle axes is required. A unique attribute of the multi-engine axisymmetric vehicles is the ability to provide pitch and yaw attitude control by differentially throttling the engine systems on opposing sides of the vehicle. Roll control can be provided in the same fashion, i.e., by differential throttling, if opposing engines are installed with thrust vector alignments that produce roll moments. There must be two such sets, one to produce roll in each direction. If these opposing engine sets are operated at equal thrust level, no roll moment is generated. When a particular set is increased in thrust level, or its counterpart set is run at decreased thrust level, a roll moment is produced.

The thrust loss produced by intentional thrust vector alignment away from the longitudinal axis of the vehicle has been found to be acceptably low for two reasons. First, the degree of displacement from the vehicle longitudinal axis required is usually less then 3 to 4 degrees and the axial thrust component loss is a sine function of this displacement. Secondly, the inertia of a differentially throttled system is the inertia of a fluid control and combustion circuit, not the physical inertia of moving an entire rocket engine assembly , as with a gimbaled rocket engine, or moving a variable geometry

exhaust deflection system, and this provides a higher speed of response to attitude control commands inputs. This higher speed of response results in a lower average thrust vector displacement over the full trajectory which further diminishes the thrust loss due to the intentional misalignment.

An advantage of this system is that there is no weight penalty for the thrust vector control system other then the propellant modulating valve systems. The weight of mechanical thrust vectoring systems can be appreciated from Fig. 133 which shows a single axis thrust vector

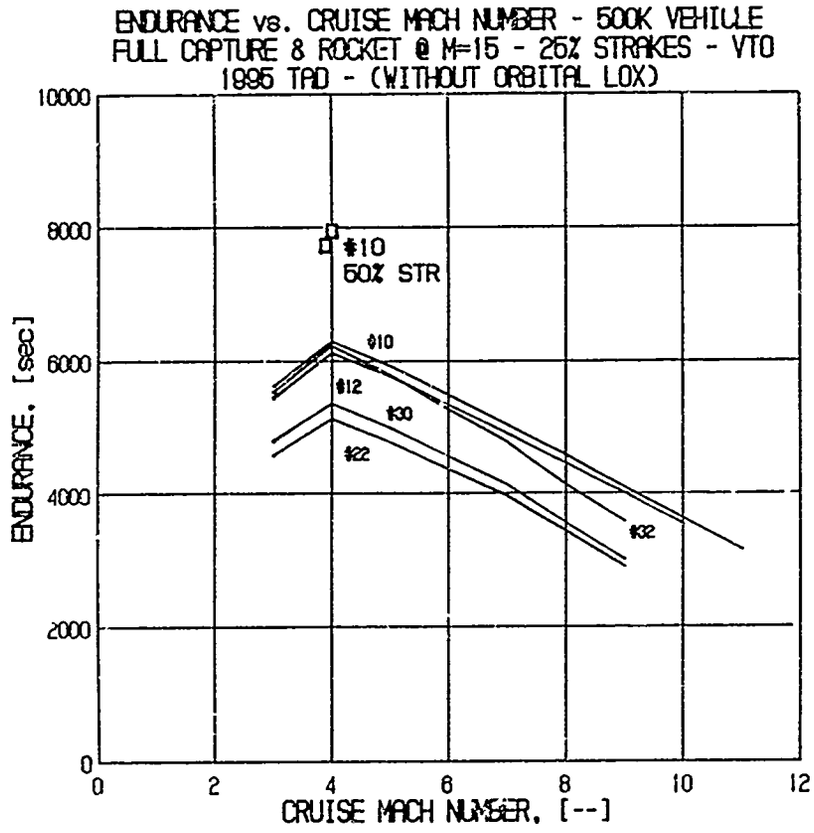


Fig. 131 Baseline Vehicle Endurance vs. Cruise Mach Number

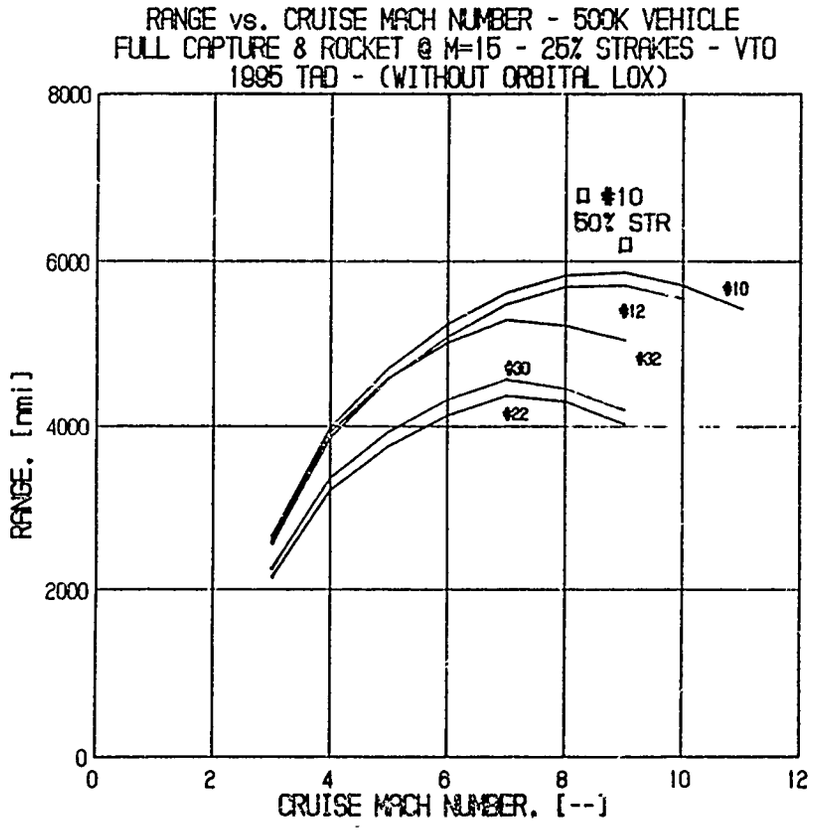


Fig. 132 Baseline Vehicle Range vs. Cruise Mach Number

control system developed as a part of advanced gas turbine development work being carried out under the joint agency "Integrated High Performance Turbine Engine Technology (IHPTET)" program.

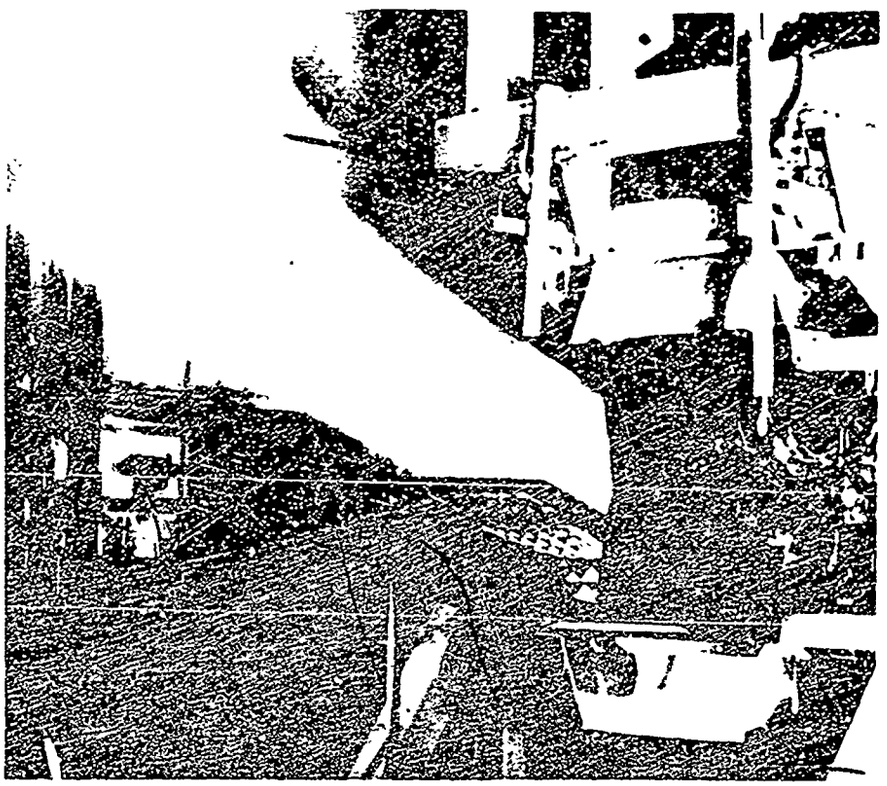


Fig. 133 Single Axis Thrust Vector Control System Demonstrated as Part of the USAF "Integrated High Performance Turbine Engine Technology (IHPTET) Program

6.7.2 Vertical Takeoff and Landing Maneuver

There are two types of VTOVL design approaches. The first is the "Horizontal Attitude" VTOVL, or HA/VTOVL, approach. The second is the "Vertical Attitude" VTOVL , or VA/VTOVL, approach.

The HA/VTOVL is exemplified by the "Harrier" type aircraft. In this approach, the aircraft is always in a horizontal attitude for takeoff and landing and the thrust vector is swung to a vertical orientation thru the center of gravity of the aircraft in both takeoff and landing.

The VA/VTOVL approach is exemplified by the APOLLO Lunar Excursion Module, the Lockheed XFV-1, the Convair XFY-1, the TEMCO Model 39 and the Ryan X-13 aircraft in this country (Ref. 29 and 30). In this approach, the thrust vector and the aircraft longitudinal axis are

always aligned in the basic aircraft structure and the attitude of the vehicle must be oriented to control the thrust vector alignment.

The takeoff and landing maneuvers for these two design approaches are illustrated simplistically in Fig. 134. The thrust vector alignment schedule can be seen for takeoff, flight and landing in this figure.

The key point is that fuselage orientation in relationship to the thrust vector is irrelevant to thrust vector control in both HA/VTOVL and VA/VTOVL. Thrust vector management is a separate problem from attitude control in relation to that thrust vector. Thrust vector control accomplishes VTOVL. This can be seen in the generic VTOVL maneuver illustrated in the bottom of Fig. 134 where the vehicle vertical and horizontal geometry in relation to the thrust vector is omitted.

VA/VTOVL is simpler to control then HA/VTOVL since varying the thrust vector relationship to the vehicle longitudinal axis over 90 degrees jet deflection or jet rotation using an active control subsystem is not required.

6.7.3 Vertical Takeoff and Landing Flight Path

In winged vehicles, the approach to vertical takeoff transitioning to horizontal flight is to increase thrust and develop a vertical velocity component using thrust vector or other reaction control systems for stabilization, then, as lift is developed, the aircraft is pitched down moving the lift vector generation off the engine thrust vector and on to the lifting surfaces lift vector and shifting attitude control to the conventional control surfaces.

There are two different maneuver approaches to vertical landing. The first can be called the "zoom" maneuver and the second the "constantly decreasing altitude" or "Pitch Up" maneuver. These two alternatives are illustrated in Fig. 135 and 136.

6.7.4 Time to Flying Speed

The takeoff and landing maneuvers and time schedules actually performed by the TEMCO Model 39 aircraft are presented in Fig. 137.

At takeoff gross weight, the point design vehicle will reach full flying speed in approximately 60 seconds compared to the the 20 second requirement for the Model 39.

6.8 Propellant Consumption for Both Vertical and Horizontal Landing Maneuvers with or without "Go-Around"

The discussions presented in 6.8.1 and 6.8.2 is based upon a vehicle returning from a Polar orbital mission.

6.8.1 Vertical Landing

The propellant requirements for bringing a 500 klbm vehicle returning from orbit to zero velocity at zero altitude for varying altitudes of initiation of the vertical landing maneuver are presented in Fig. 138. "Initiation" is defined as the flight altitude for the "pitch-up" maneuver and the altitude at which zero vertical velocity is achieved in the "zoom" maneuver with a 300 mph approach speed. This figure assumes full 20,800 lbm payload return with a 5000 lbm landing propellant reserve. Portions of this payload could be used for additional landing propellants.

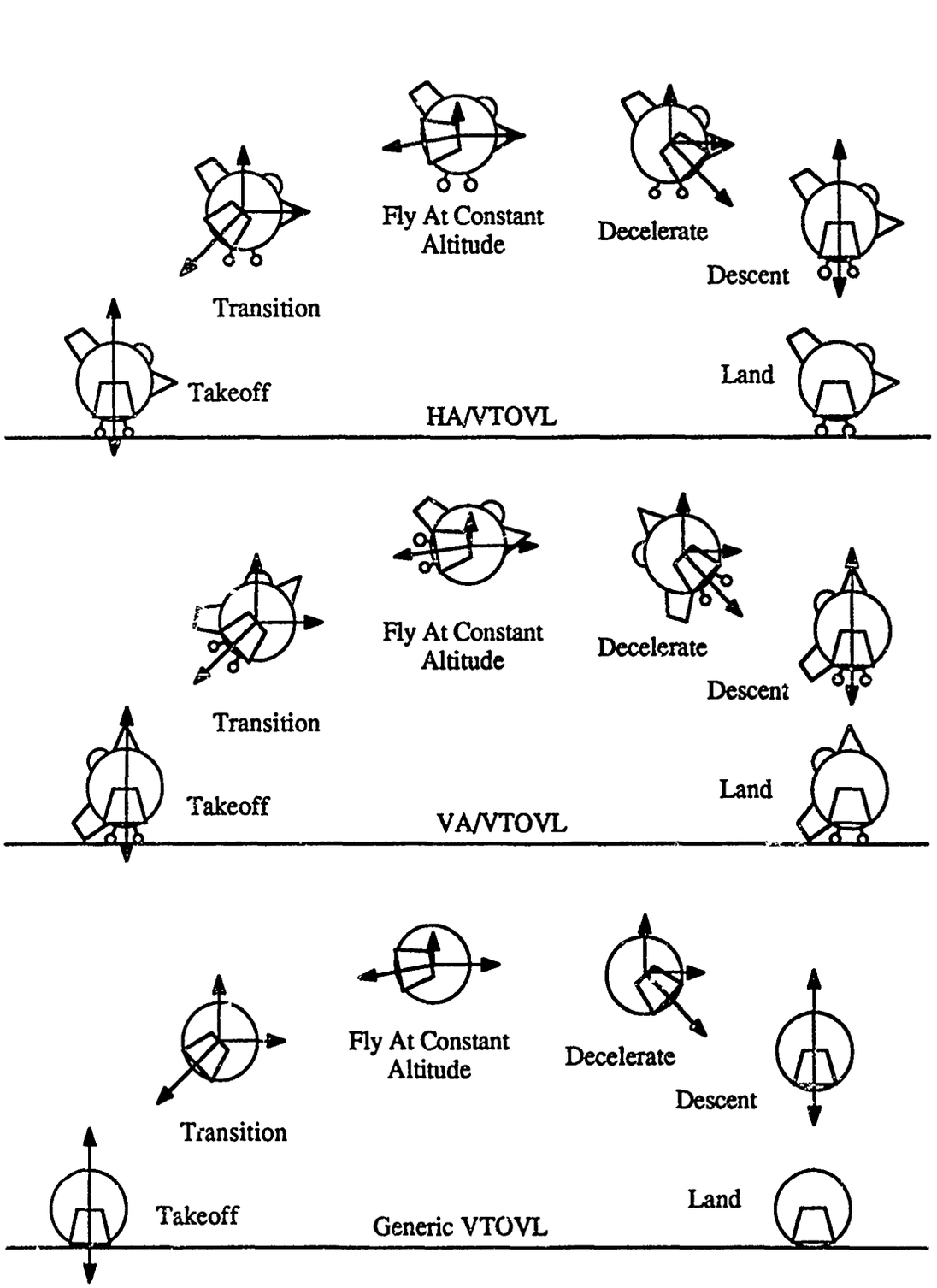


Fig. 134 Vertical Takeoff and Landing Attitude Maneuvers

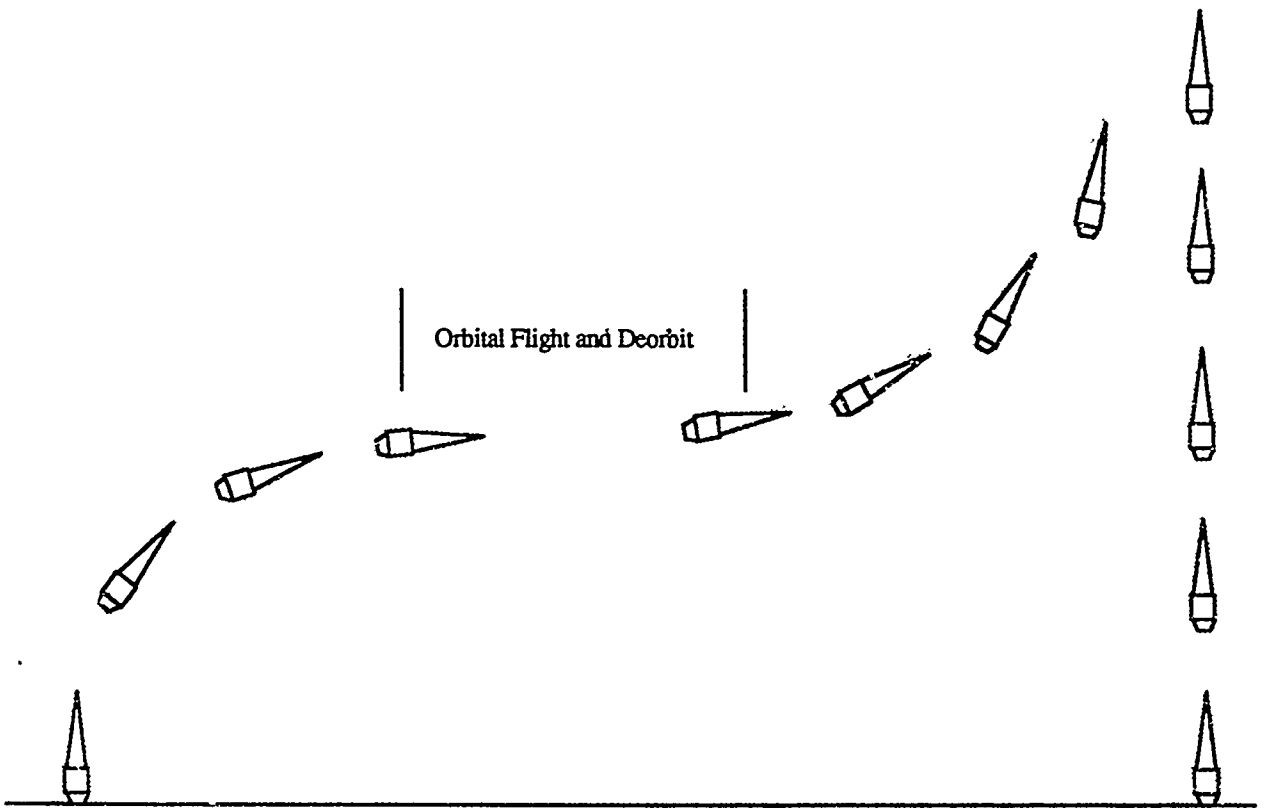


Fig. 135 "ZOOM" Maneuver for Vertical Landing - Minimum Energy Maneuver

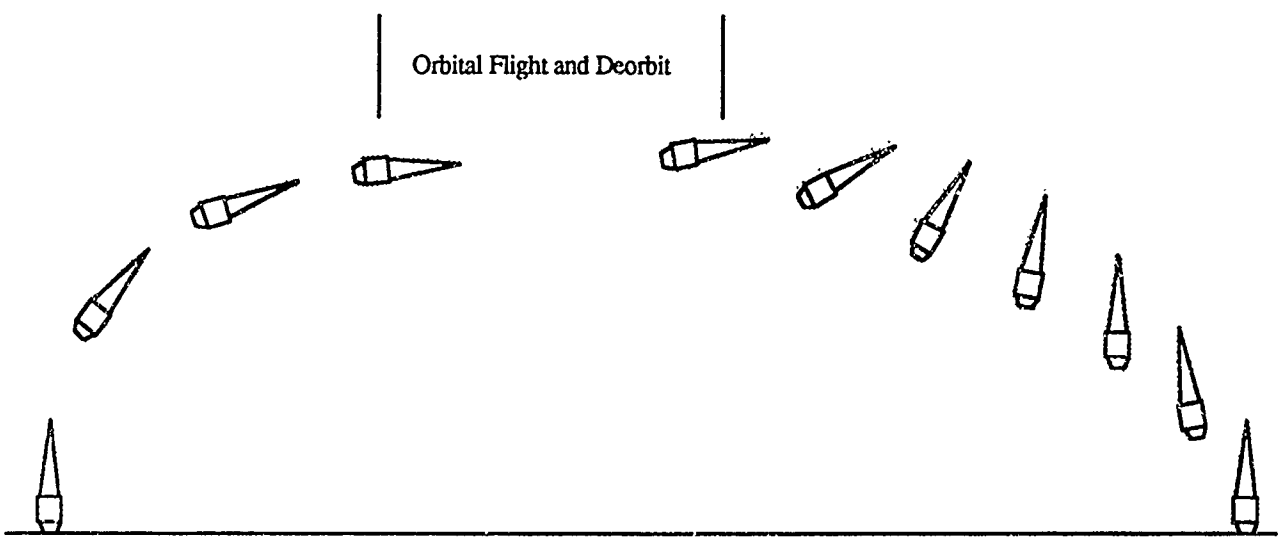
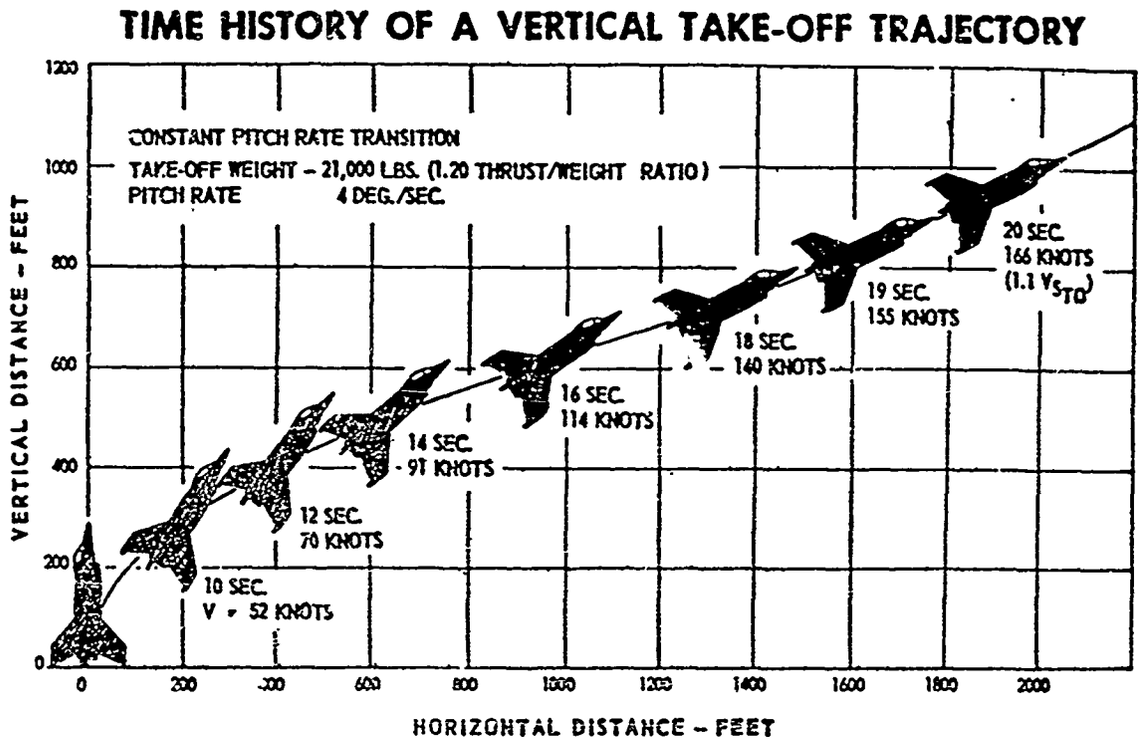


Fig. 136 Constantly Decreasing Altitude Vertical Landing Maneuver



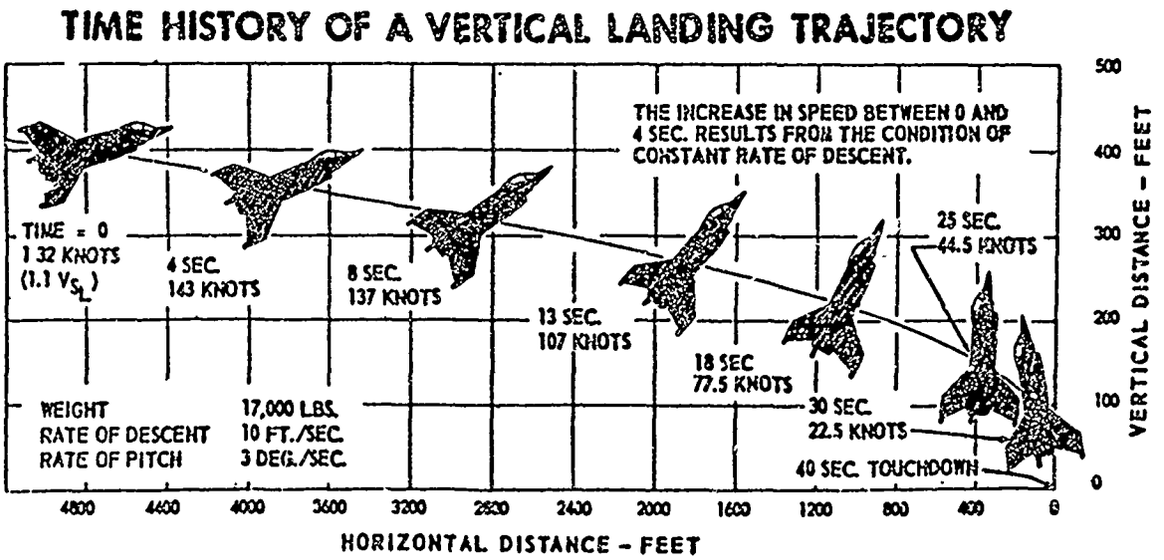


Fig. 137 Time History of Vertical Attitude Takeoff and Landing Maneuvers for the TEMCO Model 39 (Ref. 29)

Fig. 138 should be taken as being only a rough estimate for three reasons. First, attitude control propellant requirements are not included in the estimates developed. Determining attitude control propellant requirements would entail a level of vehicle

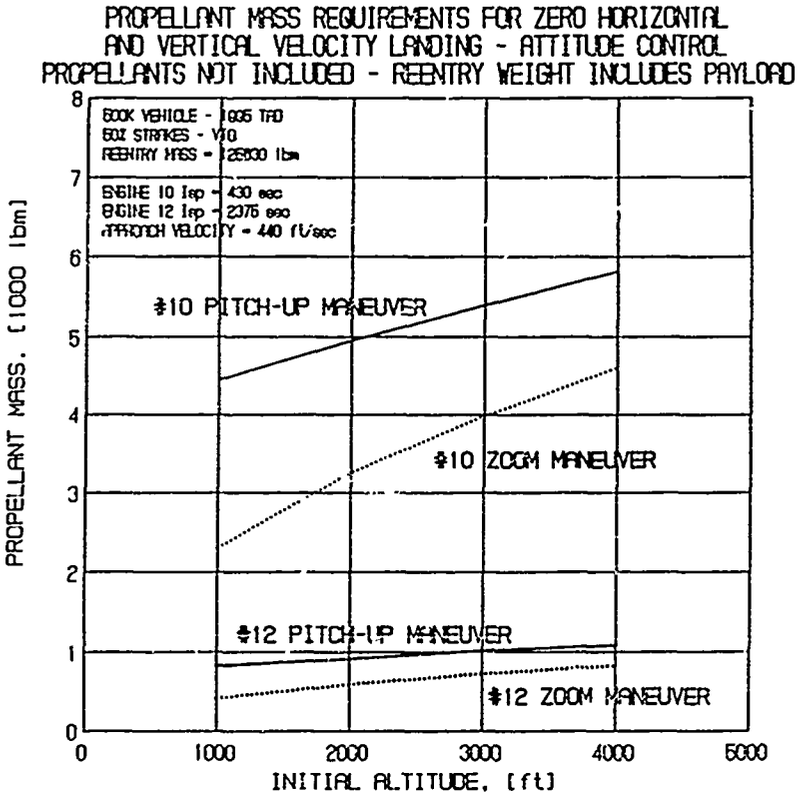


Fig. 138 Propellant Requirements for Zero Horizontal and Vertical Velocity Landing

dynamics analysis that is beyond the level practical for this study. Secondly, a similar level of analysis would be required to determine the minimum entry altitude that would be required and the zero vertical velocity altitude that would result from a "zoom" maneuver. Thirdly, a question remains as to whether or not a 300 mph approach velocity would be adequate to complete a true "zoom" maneuver without stalling.

Additional analyses were run using DOF36 to determine the "go-around" capability of Engine 10 and Engine 12 in the event of an aborted vertical landing maneuver.

With these reservations, the basic conclusions derived from this analysis with regard to vertical landing for the 500 klbm vehicle with 15,800 pounds available over the 10 klbm payload mass used for landing propellants are:

- The "zoom" maneuver is more economical then the "pitch-up" maneuver for both engine types studied

- Engine 12 with fan supercharging and plenum burning consumes significantly less propellant the Engine 10
- Engine 10 would have, with the reservations previously noted, approximately 20 to 30 seconds of hover capability.
- Engine 12 would have, with the reservations previously noted, approximately 200 seconds of hover capability.
- Engine 10 does not have sufficient propellant to abort a vertical landing maneuver.
- Engine 12 using only fan mode with plenum burning might have sufficient propellant to abort one landing attempt and make a second landing attempt after approximately 10 miles of go-around cruise. Further study is definitely required to substantiate this conclusion.

6.8.2 Horizontal Landing Capabilities

- Engine 10 cannot make one go-around attempt at **horizontal** landing.
- Engine 12 might be able to make as many as 3 go-around attempts at **horizontal** landing.

6.9 The Effect of Orbital Inclination on Payload and Landing Capabilities

The discussion that has been presented in 6.8 was based upon a 500 klbm vehicle returning from a **polar** orbital mission.

.10 The Effect of Orbital Inclination on Payload

Fig. 139 presents the effect of orbital inclination on payload for an ETR launch. Note that a 28.5 degree orbital inclination adds some 10,000 pounds to the polar orbit delivery capability

6.11 Post Deorbit Cruise and Landing Effect of Non-Polar Orbits

If Engines 10 and 12 used scramjet propulsion at Mach 8 the 500 klbm RBCC/SSTO vehicle would have about 40 miles post deorbit cruise capability per 1000 lbm of hydrogen propellant allocated for cross range flight. This propellant requirement would have to be traded off against landing and go-around requirements.

In non-polar orbits, if propellant tank capacity were available, this additional fuel weight could be assigned to landing maneuver reserve. Under this condition, the additional propellant could be allocated to post deorbit cruise or go-around fuel reserve.

If this 10,000 lbm were assigned exclusively to the landing maneuver abort, go-around and second landing attempt, Engine 10 might be capable of a second landing attempt at the same landing point. More detailed study will be required to establish this as a possibility.

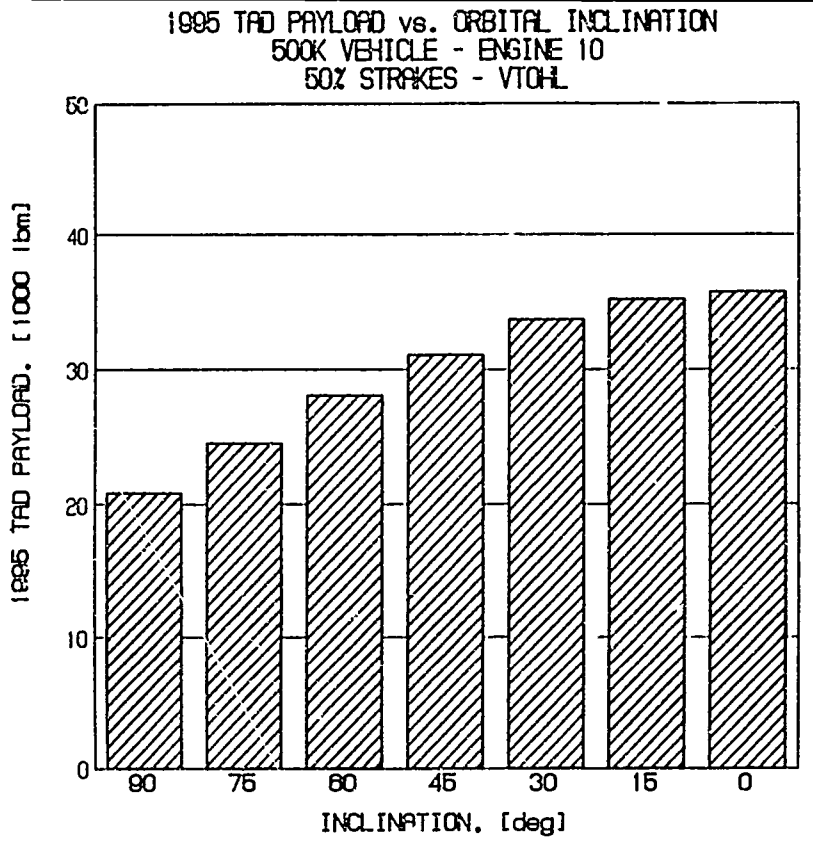


Fig. 139 1995 TAD Payload vs. Orbital Inclination

6.12 On-Orbit Refueling

With on-orbit refueling, depending upon the % of total propellant capacity loaded on-orbit;

- other mission profiles,
- extended post-deorbit cruise at hypersonic, supersonic and subsonic speed,
- landing abort and go-around
- and alternative landing site selection at meaningful distances from the initial site

would be achieveable in both Engine 10 and Engine 12 powered RBCC/SSTO vehicles.

6.13 Aerodynamics and Stability Investigations of Similar Configurations by NASA Langley Research Center

During 1987, NASA's Langley Research Center carried out a program of investigation of an axisymmetric winged conical model to Mach 20. A model with a 12 degree full angle conical forebody and 16 degree full angle aftbody, illustrated in Fig. 140, was investigated to Mach 10 in air and at Mach 20 in LaRC's helium tunnel facility (Ref. 31).

The configuration of the LaRC model, presented in Fig. 140, closely resembles the configuration concept of the RBCC/SSTO vehicle illustrated in Fig. 141 with the exception that

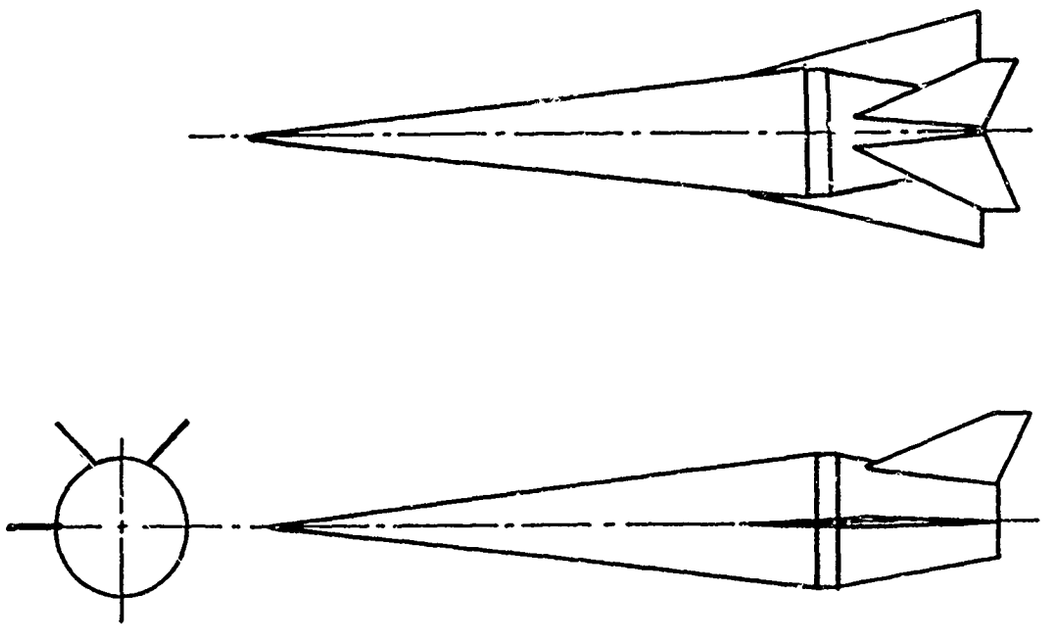


Fig. 140 LaRC Axisymmetric Model Configuration

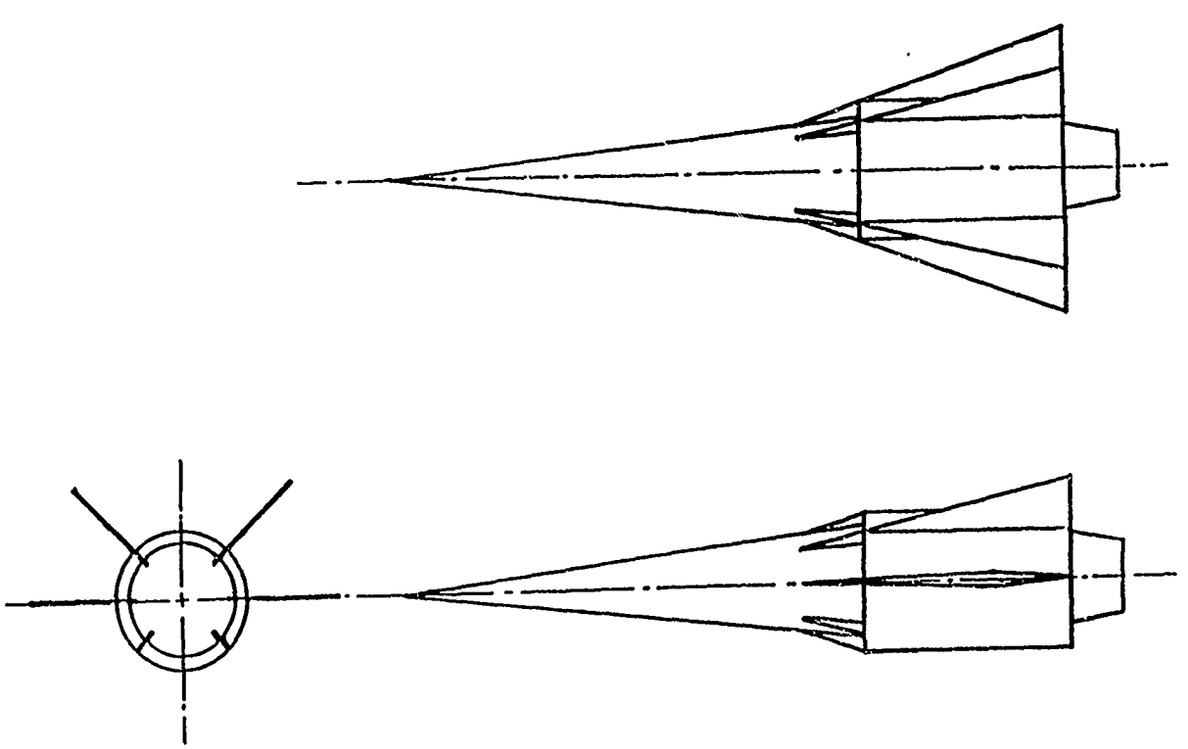


Fig. 141 RBCC/SSTO Vehicle with Annular Engine Installation

the RBCC/SSTO configuration has a 16 degree full angle cone forebody and a 30 degree full angle cone aftbody.

Fig. 142 presents a series of oil flow tests at 6 degrees angle-of-attack on the model. The following observations are made with regard to these model findings and the RBCC/SSTO configuration proposed in this study;

- The flow patterns shown are surface or boundary layer flow patterns. The study team could find no information, in the open literature or available to persons working in this field who were questioned on this subject, on the flow patterns between the vehicle surface and the outside diameter of the inlet system or flow at larger radii that would effect wing and elevon flow. Investigation of these flow patterns over the full range of the orbital ascent trajectory is recommended as a high priority area for future study.

- the flow change which occurs at the wing leading edge would not effect inlet flow on the RBCC/SSTO vehicle because the inlet station of the RBCC/SSTO vehicle is immediately forward of the first leading edge station.

- 6 degrees angle-of-attack is higher then the acceptable angle-of-attack presumed in this study. The limit value assumed, in the abscence of any detailed flow investigation, is from 3 to 4 degrees.

- at the angle-of-attack investigated, flow separation occurred at the maximum body diameter. Downstream of this separation, a recirculation pattern developed that greatly reduced the lift available from the airfoils and the contribution to lateral stability by the elevons. In the RBCC/SSTO configuration, this separation and recirculation should not occur as that configuration becomes a constant diameter section at that diameter.

- this recirculation diminished the longitudinal stability by moving the center of lift of the airfoil forward. Further, it greatly reduced the effectiveness of the elevon system in providing lateral stability as can be seen in the lower left model photo where this recirculation masks nearly 2/3rd of the elevon area available.

- LaRC reported that the vehicle was not laterally stable at any flight speed while is was longitudinally stable to Mach 3.95 with the CG assumed to be at 66% station of the model. In the RBCC/SSTO configuration, the CG remains forward of this 66% station at all times and increased longitudinal stability should result as illustrated in Fig. 143.

It is also reasonable to expect that the RBCC/SSTO elevons, which are also lifting surfaces, will not be masked in as found in the LaRC model due to elimination of flow separation at the major diameter that will be provided by constant diameter engine section characteristic of the RBCC/SSTO configuration proposed in this study. It appears that is is reasonable to the RBCC/SSTO vehicle configuration to have lateral stability in a meaningful portion of the ascent trajectory. The extent to which lateral stability would be availalbe should be determined by computational analysis and wind tunnel testing .

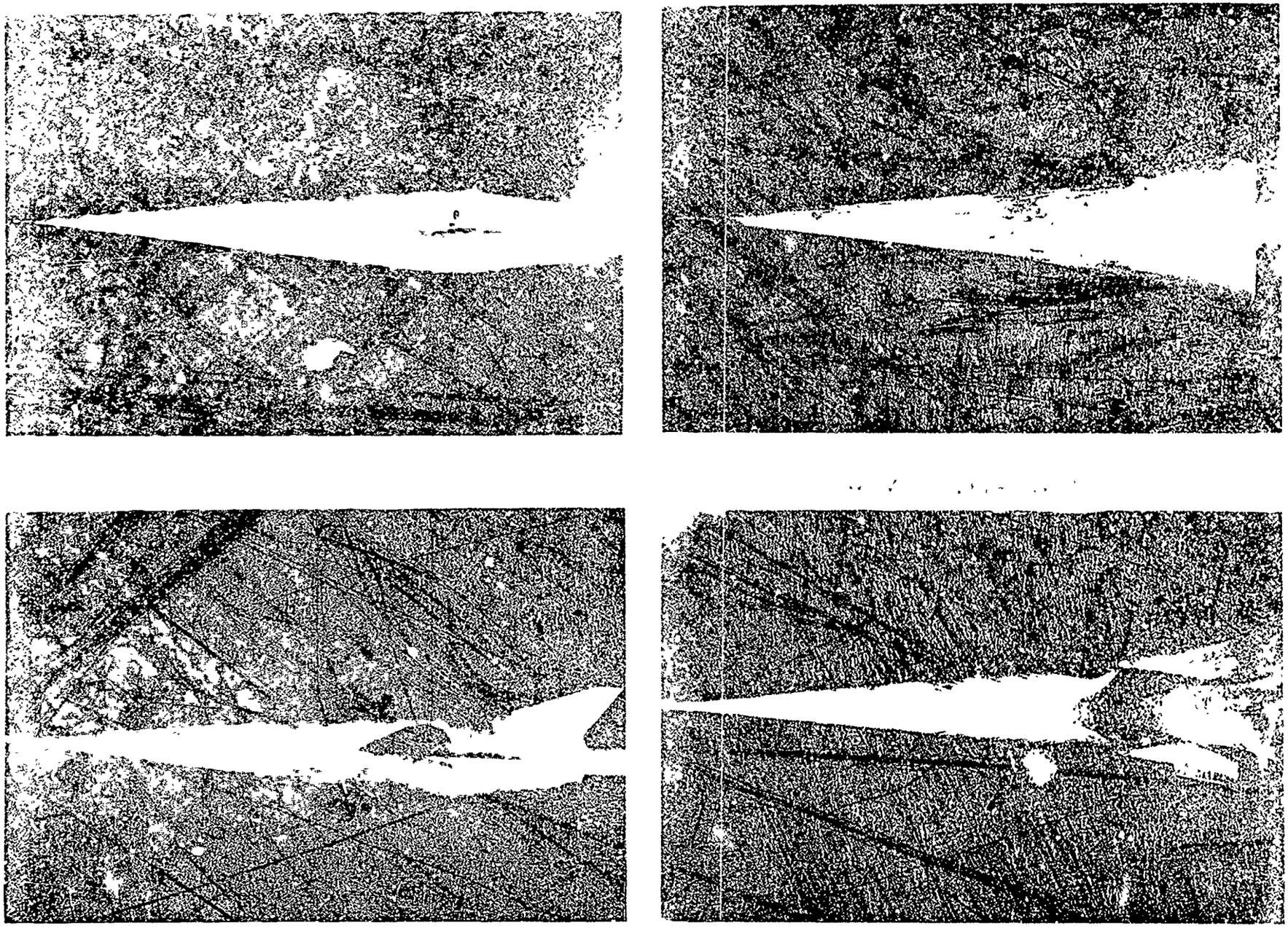
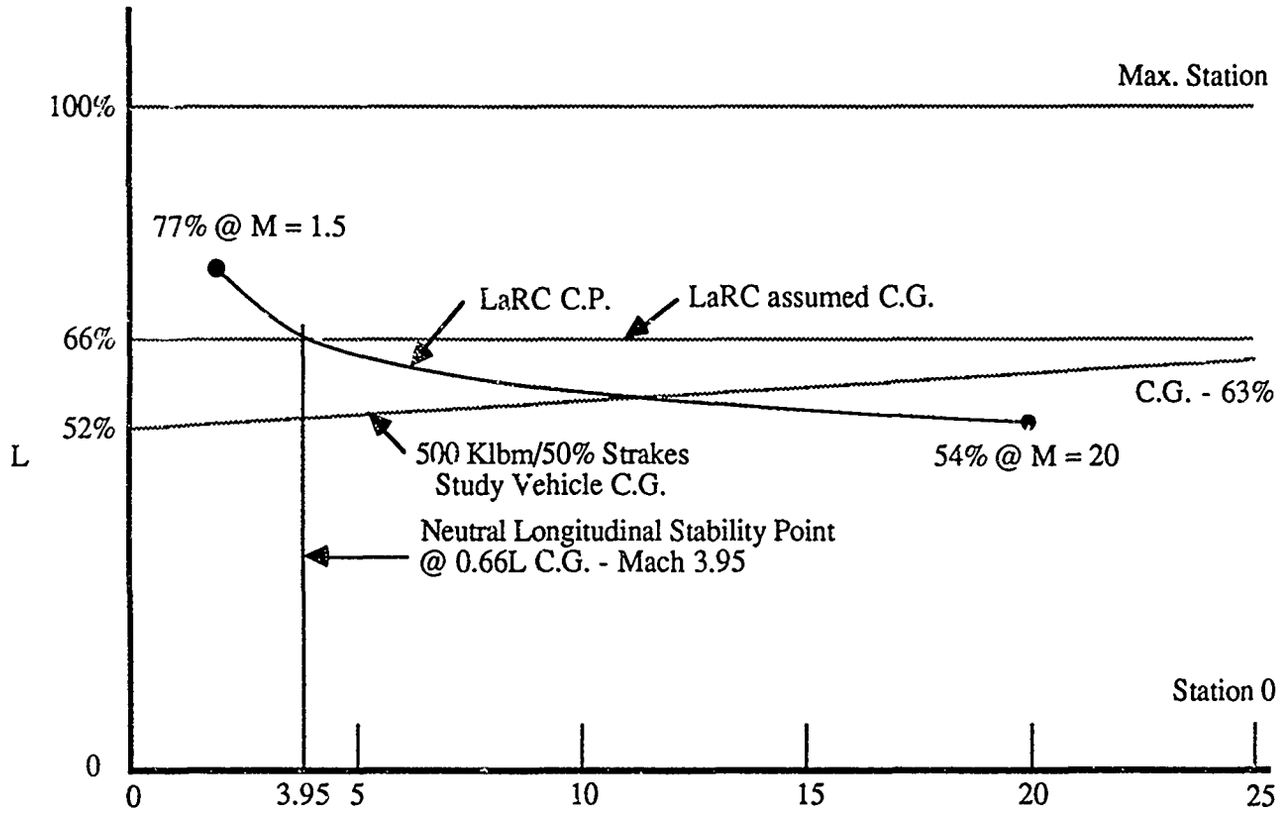


Fig. 142 LaRC Oil Flow Tests at Mach 10 and Varying Angles of Attack



C.P. Shift vs. C.G. Location and Mach Number

Source: AIAA 87-2484

Lateral Control/ Stability - LaRC Configuration is Laterally Unstable at All Mach Numbers

Fig. 143 NASA LaRC Elevoned Cone - Longitudinal Stability

Section 7.0

GROUND OPERATIONS

7.1 Shuttle Ground Operations - Baseline

In Fig. 144 the primary systems comprising a space launch system are presented in a work breakdown structure. The objectives sought here are to reduce the system equipment complexity, reduce the number of support personnel required, reduce the training level that will be required for those personnel and to produce a significant reduction in launch cycle time.

The Shuttle STS launch system, our baseline for comparison, is complicated by the fact that the vehicle is, for all practical purposes, a three stage vehicle comprised of the Solid Rocket Boosters, External Tank and the Orbiter vehicle itself, and requires recovery of two of these stages; the Orbiter and the Solid Rocket Boosters.

Fig. 145 presents the operations flow of a typical Shuttle STS landing and launch operation as it might be carried out at the Vandenberg launch site.

The complexity of the launch operation that derives from the need for processing three major assembly systems for each launch, i.e., the orbital vehicle itself, the external tank assembly and the solid rocket boosters (SRB) combined with two recovery operations is apparent. The same situation exists in all multiple stage vehicles.

A typical Shuttle STS landing to launch operation schedule is presented in Fig. 146. Here again the complexity of ground operations plus the extensive period of time required to carry out those complex operations is apparent.

7.2 The Simplification Due to SSTO Operations

The potential simplification of the landing to launch operation of a Single-Stage-to-Orbit vehicle is illustrated in Fig. 147.

It is suggested that this operations flow could be even further simplified by carrying out all maintenance and launch preparation operations at the launch complex. In the case of a vertical landing vehicle, the launch location would be colocated with the takeoff location and all maintenance and support equipment and facilities. The complete ground system would be comprised of only the landing/launch site and a single support facility or mobile systems that might provide these same services.

If the landing and launch work schedule presented in Fig. 146 for the Shuttle STS is modified for an SSTO vehicle, the operations that are eliminated are significant. This hypothetical ground operation schedule is presented in Fig. 148 without modifying the basic time line to show the first effect; extensive reduction in the number of operations required. It is then appropriate to consider how this schedule might be reorganized to reduce the time line to the maximum extent possible.

7.3 The Five Day Turnaround Goal

For the purposes of this study, a five day, one-shift, launch turnaround cycle goal was set.

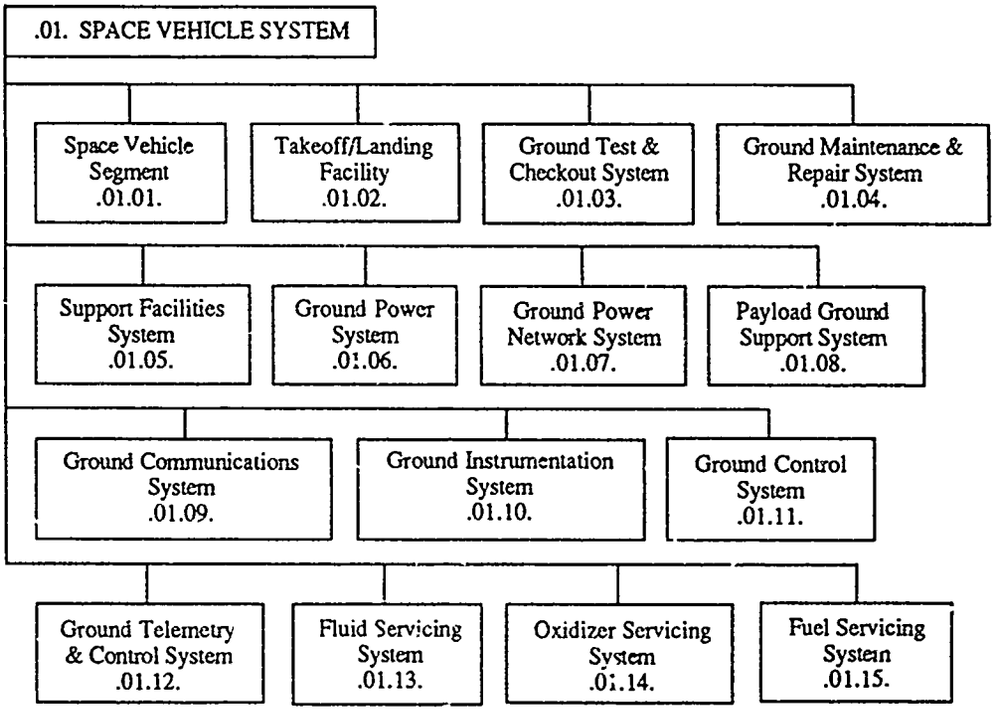


Fig. 144 Baseline Vehicle and Ground System Work Breakdown Structure

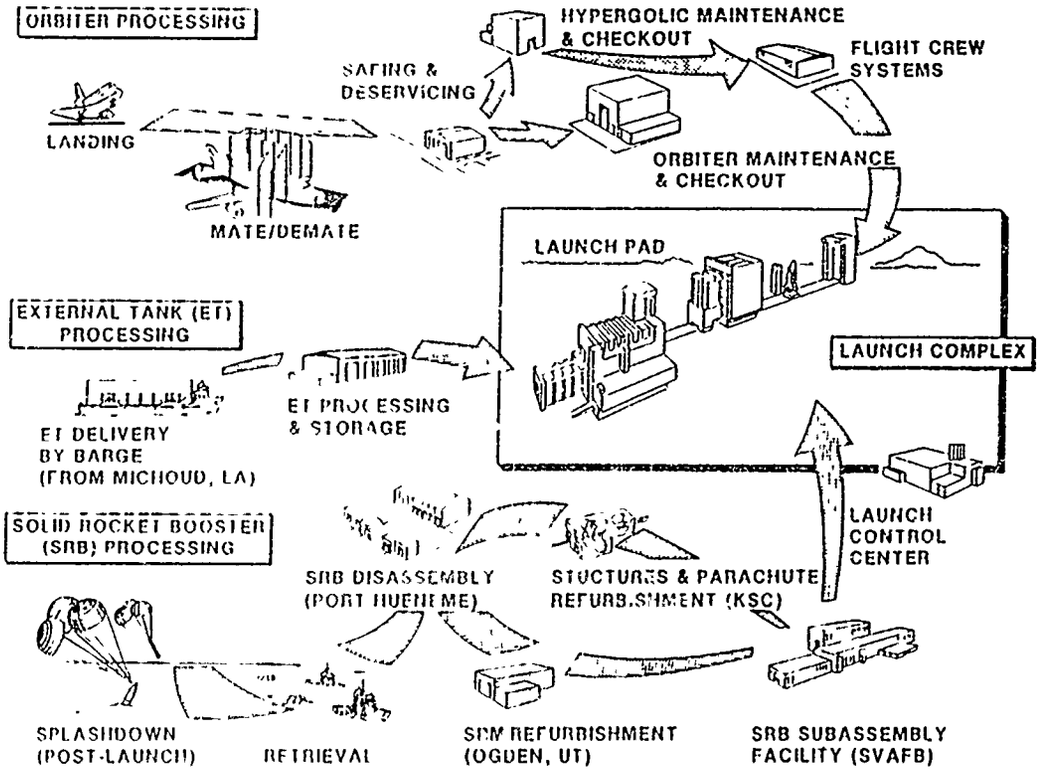


Fig. 145 National Space Transportation System Vandenberg Launch Site Operations Flow

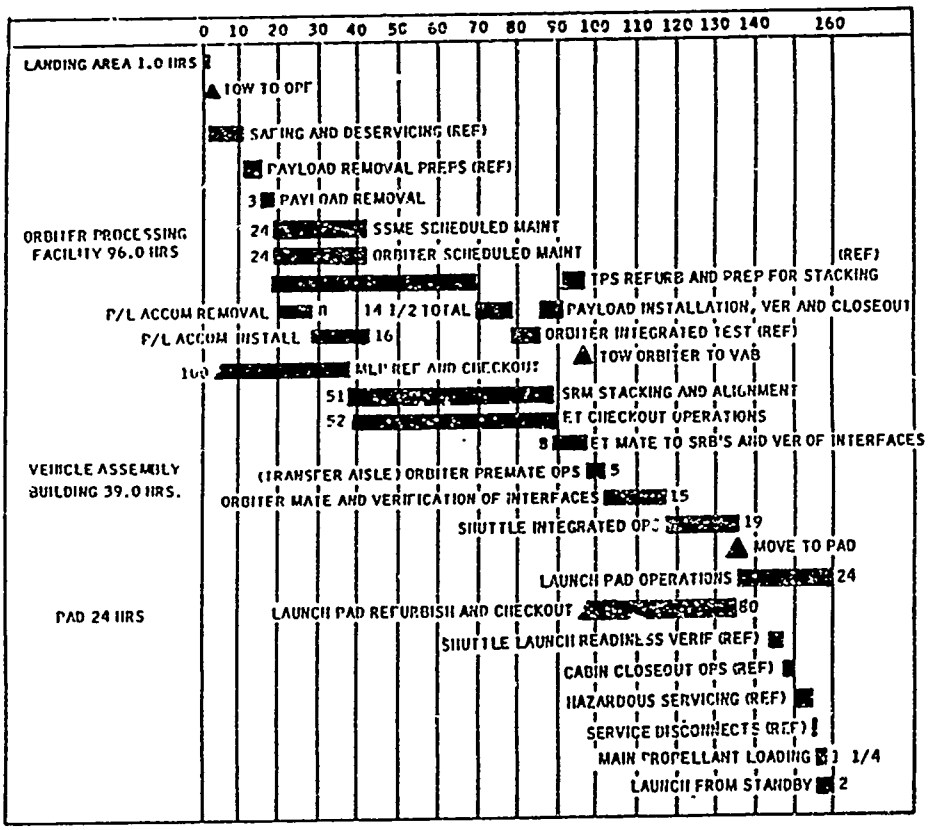


Fig. 146 Shuttle STS Landing and Launch Work Schedule

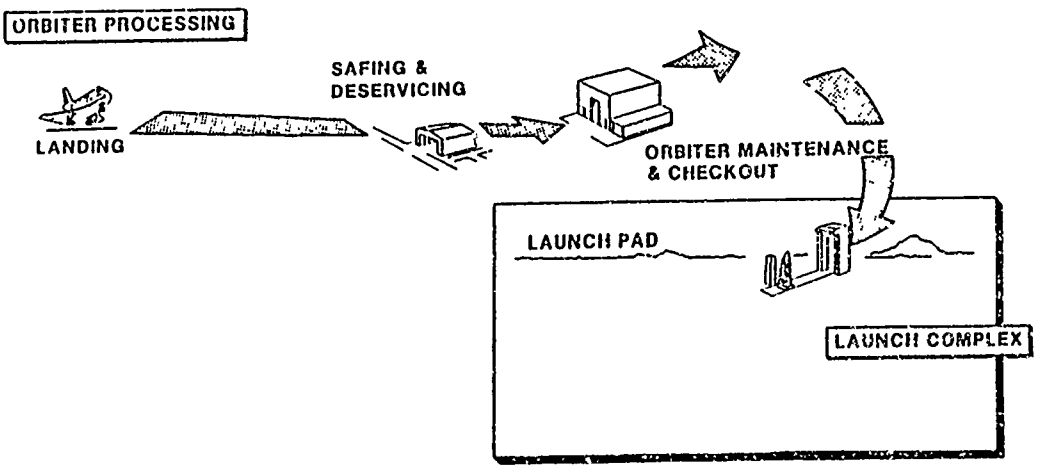


Fig. 147 A Single Stage Orbiter Landing and Launch Operations Flow

Looking at the three major time consuming operations; scheduled maintenance operations, integrated operations and launch pad operations, the operations where a significant reduction in operation time must be achieved if the 5 day goal is to be met are apparent. The integrated operations exercise and launch pad operations are proposed to be eliminated. With a properly maintained vehicle system being available at the end of the scheduled maintenance operation, only a launch readiness verification is proposed to be required.

A principal point of concern would be the scheduled aintenance of the RBCC/SSTO vehicle and the thermal protection system. The goal in thermal protection system design will be to reduce this operation to basic inspection of a system that has a preestablished useful life within the scheduled maintenance program. The extent to which the scheduled maintenance time can be reduced remains to be established and will probably be found to be the most significant time consuming operation in the landing to launch turnaround cycle time.

A number of the operations presented in Fig. 148 can be carried out in parallel with other vehicle checkout and launch preparation operations. Others of these cannot be run in parallel, such as hazardous servicing and main propellant loading operations.

The resulting ground operations schedule is illustrated in Fig. 149 with a goal of five days cycle time.

This landing to launch process simplification cannot be provided, or the 5 day one-shift turnaround goal met, if the present approaches to space vehicle design are carried over into the design and construction of the RBCC/SSTO vehicle system.

To have any hope of achieving the landing to launch process simplification proposed, or the five day turnaround goal, the RBCC/SSTO vehicle will have to be designed to be an almost entirely autonomous system.

7.4 The Concept of Autonomous Operation

In Section 5.0, the concept of operation of the RBCC/SSTO vehicle as an "autonomous" system was briefly discussed. The limited past work done in this field and present activities being undertaken due to renewed interest in this subject were reviewed.

An "automaton" is defined as any set of linked communicating elements that is self controlled to provide some function desired.

If the RBCC/SSTO vehicle is to be an autonomous system, significant technology development, particularly in the field of "artificial intelligence" technology,-- "expert systems" technology and real-time operation of these types of systems must be accomplished over the next several years.

The term "artificial intelligence" creates considerable confusion and should be further clarified in the context we are concerned with. All subsequent discussion will be limited to that specific context. This is a real hardware system that not only includes the RBCC/SSTO vehicle, but all equipment required to support its operation. The exception to this is the crew. Because of the present state of knowledge, it is not possible to discuss the role of the crew in vehicle system control, operational intervention, orbital maintenance and repair or other modes.

In this limited context, a working definition of "intelligence" and "knowledge" can be provided.

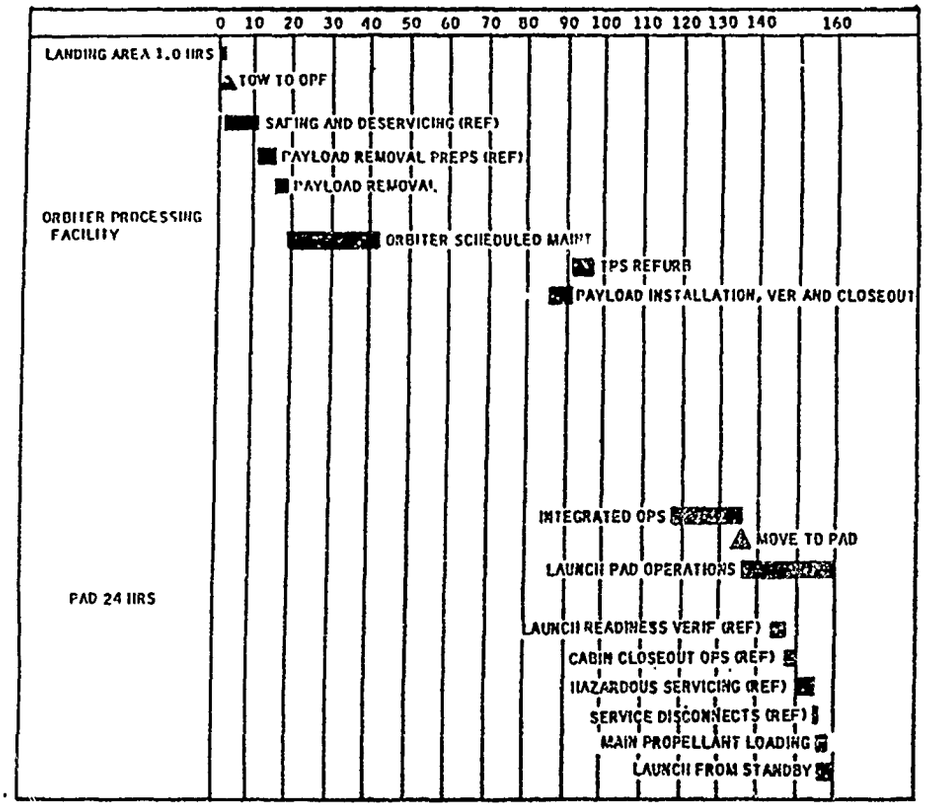


Fig. 148 An SSTO Version of the Shuttle STS Ground Operations Flow

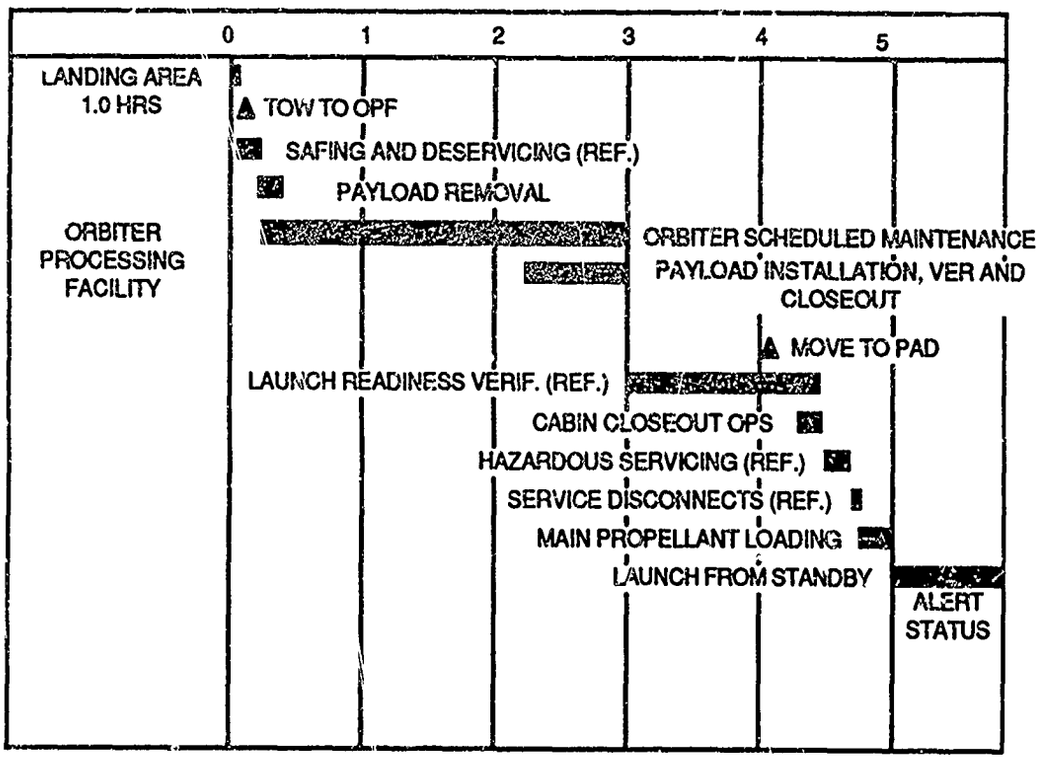


Fig. 149 RBCC/SSTO Landing to Launch Alert Operations Schedule

Considering the previous definition of the RBCC/SSTO system as defining an automaton, "knowledge" can be defined as the measure of the amount of information stored within that automaton. "Intelligence" is the measure of the ability of the automaton to use this stored information to make decisions which benefit the attainment of its goals. In the context here, these goals can be identified for purposes of discussion.

- The first goal would be to maximize the probability of crew survival
- The second goal would be to maximize the probability of survival of both the crew and the vehicle system
- The third goal would be to maximize the probability of crew survival, vehicle survival and mission accomplishment.

The lowest level of "intelligent" automatons are those which are purely passive automatons, which have the "intelligence" to operate with a knowledge base of a particular form and to carry out a set of functions of some value through its communications links. The distinction is that this type of automaton is not capable of taking any direct actions to improve its probability of survival and will simply degrade within its operating environment. It cannot carry out self-repair or change configuration to adapt to component or subsystem failure.

The next level of "intelligence" is defined as an automaton which has the ability to sense its environment, has stored within its knowledge base the effects of previously sensed patterns in that environment, and which is able to take corrective action to increase its probability of survival in its environment based on its knowledge of past experiences. It is capable of learning and self-repair or self-reconfiguration.

The next higher level of "intelligence" in this context is achieved when the autonomous system can anticipate an environment before that environment is actually encountered and to take actions to increase its probability of surviving through that environmental condition.

A general characteristic of the operation of autonomous systems, either conceptual or real, is the fact that they all operate in a temporal domain. That is that the overall system objective of improving its own probability of meeting its goal of operation is more completely defined as improving its probability of survival over time.

There is an additional consideration that must be borne in mind with regard to the temporality of automatons. This is the rate at which events are encountered in the automaton's operating environment over time. In systems of the type discussed here, there are many points in time where a significant number of events, critical to the survival of the automaton, occur over a very short total time period. This creates significant processing speed requirements in the hardware elements comprising the system to meet "real-time" operating requirements.

For all practical purposes of discussion, past space vehicle systems qualify as automatons but only in the lowest class. These systems have had sufficient knowledge contained within them and a level of intelligence sufficient to carry out what are essentially serial sequences of operations. At the present time, there is essentially no experience base upon which to reliably design, construct and operate autonomous systems possessing the level of "intelligence" that is currently being postulated for future space vehicle systems and other types of complex systems. These systems are postulated to have adaptive capability based on both learning and prediction. In our subsequent discussions in this section, it is assumed that such a capability will be available by 1995.

7.5 The Requirements for Autonomous Operation

Within the general field of "artificial intelligence" systems, there is a subclass of systems referred to as "expert" systems. The autonomous control concept being considered here falls, to a great extent, into that subclass. The system will be a portion of the space vehicle. We will refer to the vehicle borne expert system as the "Space Borne Expert System", or SES.

A generic representation of an SES is presented in Fig. 150. It is anticipated that the vehicle borne SES will consist of a central SES working with subsystem level SES's in a distributed architecture.

The generic SES consists of two software components structured to meet the requirements of an autonomous system. The first component of the system is the knowledge base consisting of the vehicle component level knowledge base, mission requirements knowledge base and flight environment knowledge base. The second element of the system is the "expert" program. It is the expert program that applies the knowledge contained in the knowledge base in a manner appropriate to the information input from the system being controlled and which generates the outputs required to control the system operation in such a manner as to meet the SES operating objectives previously discussed.

In order to achieve autonomy to the greatest extent possible, the ideal condition will be one where all vehicle and ground support systems management will be carried out under the control of the SES. This approach is illustrated in Fig. 151. The extent to which this can be accomplished in practice remains to be determined. This problem is a subject of study of a number of organizations as has been discussed in Section 5.0.

A top level systems breakdown for a representative space vehicle system has been presented in Fig. 144. It is appropriate to discuss the impact of autonomous operation as it would effect each of the ground systems.

The RBCC/SSTO vehicle, in autonomous operation, ceases to be a system that is controlled from ground systems during launch preparations and launch operations. It will become the controlling system for all launch preparation operations and the actual launch operation.

The takeoff and landing facility will not be significantly impacted by autonomous operation. However, if vertical landing is a capability of the vehicle system, the size, and expense, of these facilities can be significantly reduced.

The ground test and checkout system will be significantly impacted by autonomous operation. In this mode of operation, vehicle test and checkout capability will be built into the basic vehicle design and will function under the control of the SES.

The ground maintenance and repair system will not be significantly impacted. Scheduled maintenance and repair operations will be required to be carried out. A goal would be to have those ground test and checkout operations required for prelaunch and postlaunch test and checkout to be minimized to such an extent that they can become a part of the routine operation of the ground maintenance and repair system.

The support facilities system should also be greatly reduced along with support manpower requirements.

The ground power system function will be unaffected in terms of the basic problem of delivering power to the vehicle and launch supporting equipment at the launch site. However,

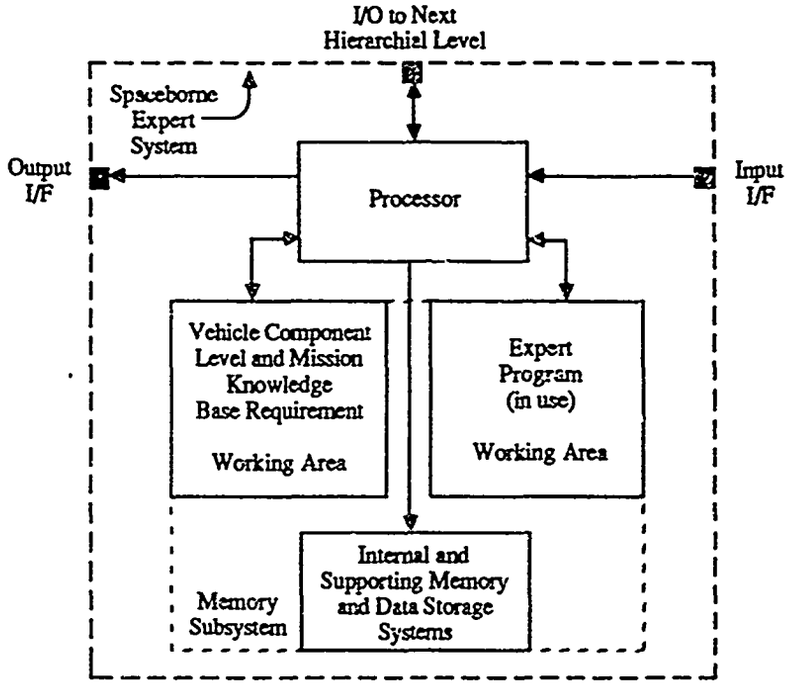


Fig. 150 The Generic Spaceborne Expert System (SES)

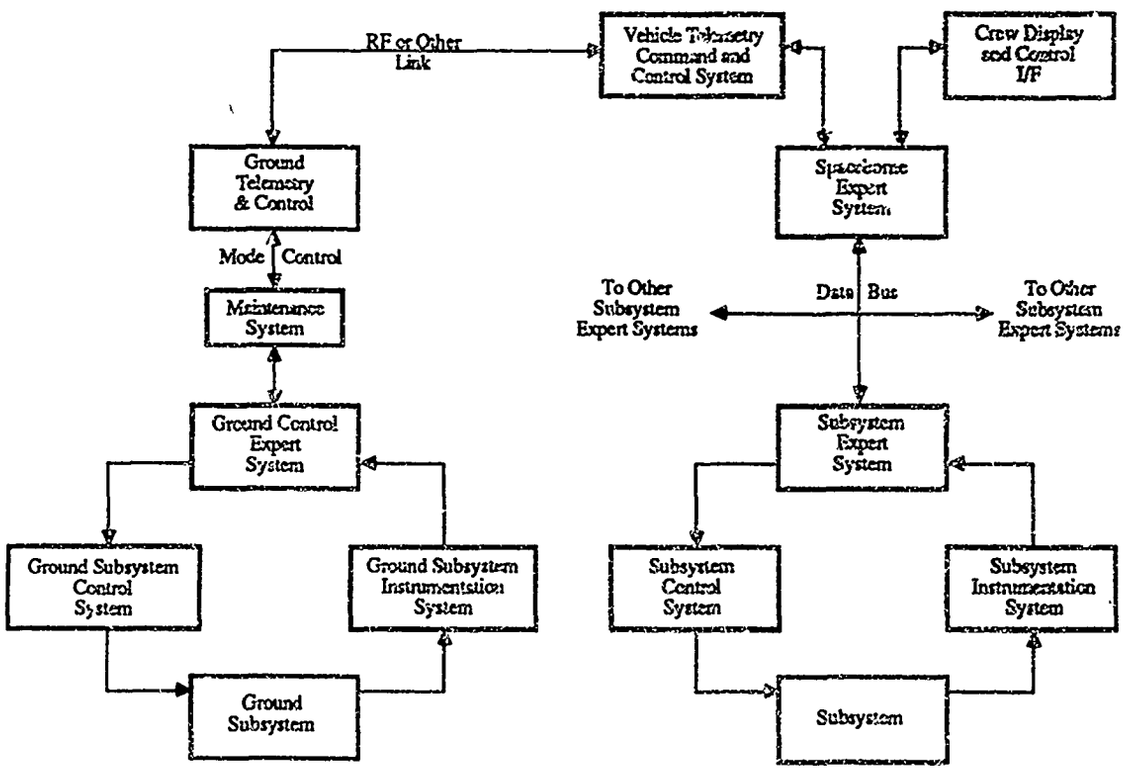


Fig. 151 Interface Between the SES and the Ground Support System

the ground power system control will shift from the ground to the vehicle SES. Similarly the ground power network system should be greatly simplified through the reduction that will be achieved in a general complexity of the ground equipment system.

The payload ground support system may be affected but this condition would be a payload specific one.

The role of ground communications, ground instrumentation and ground control systems will be significantly reduced and preferably eliminated. What should remain are only those ground communications required for operation of the ground maintenance and repair system and the various servicing systems.

Ground telemetry systems at present, are strictly measuring systems. In autonomous operation, this system will become the ground telemetry and control system, a two-way link rather then a one-way link as has been the case historically, and will provide the interface between the SES and ground systems. The ground telemetry and control system will provide information on the status of ground systems to the vehicle and will receive command information through the vehicle telemetry and control system that will be used to control those ground systems.

The oxidizer and fuel servicing system, and any other fluid servicing systems, will remain essentially in their present configuration with the exception of the fact that control of these systems will shift from the ground to the vehicle SES.

A by-product of this design approach should be a significant reduction in both the number of ground personnel required to support launch and landing operations and the skill levels required of those personnel. This will be achieved by designing the ground systems as automated systems and through the use of robotic technology to the greatest extent practical. The use of robotic technologies should be incorporated into the vehicle servicing operation to the greatest extent practical.

Section 8.0

TECHNOLOGY ASSESSMENT

In discussing those areas of RBCC engine and vehicle development which present the greatest technological risk, we will divide the engine and vehicle systems into their constituent technologies. A framework of the technologies which are required by, or enhance, the performance of an RBCC engine system is shown in Fig. 152. This section focuses on discussion of technologies essential to RBCC propulsion system development that must be further advanced before activities comprising the DDT&E phase of an RBCC/SSTO vehicle system can be undertaken. With regard to the total vehicle system, only those technologies specific to the RBCC/SSTO vehicle are discussed in keeping with the propulsion focus of this study.

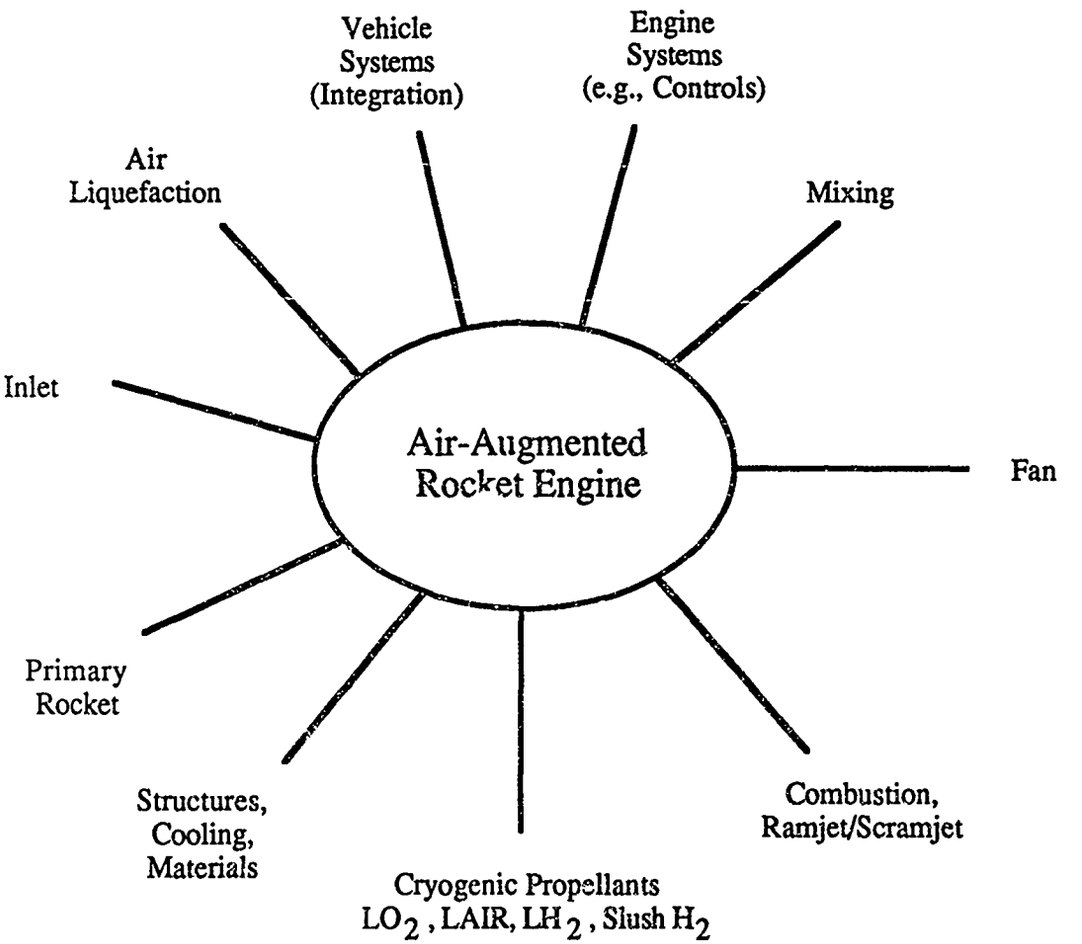


Fig. 152 Technologies Related to Air-Augmented Rocket Systems

8.1 Engine Subsystems

The engine technology development issues will be examined moving from the front of the basic engine to the rear.

8.1.1 Inlet Subsystem

RBCC engine operations will require that the following technology development issues related to the inlet subsystem be resolved.

1) In order to achieve necessary levels of scramjet performance while constraining vehicle size, capture ratios of approximately 70% of vehicle frontal area must be obtained. This will require significant forebody/inlet tailoring through computational and wind tunnel analysis. Due to the lack of flight test data in this speed regime, or on configurations of this type, this capture ratio level cannot be assured at this time.

2) Operation of an axisymmetric vehicle at angle-of-attack (alpha) implies that some engines will be operating with lower forebody compression and non-uniform inlet flow. Numerous problems can occur on the leeward side ranging from a minor thrust loss to engine inlwt "unstarts". The severity of these problems depends on the forebody configuration, the maximum alpha allowed, and other flow parameters such as Mach number and Reynolds number. Problems due to leeward side engine "starvation" or inlet distortion can be minimized through a variety of techniques including higher dynamic pressure trajectories, increased wing area, or high lift devices. These and other methods all reduce the maximum alpha required to fly a given trajectory, thereby reducing the problem. Currently, this problem has been characterized to some extent, but further study must be completed before accurate predictions of alpha effects on leeward engine performance can be made.

3) Efficient RBCC engine operation across the wide speed range desired will require a sophisticated variable geometry inlet/forebody system. The variable geometry system must handle boundary layer bleed, shock positioning, bypass air, and inlet closure as well as a variety of other tasks. At the same time, the system must be mechanized in a practical fashion which will permit reliable operation over an extended lifetime while meeting stringent weight constraints and control response requirements. Portions of such a system fly on current high Mach number aircraft, however, the RBCC system must be significantly more capable (complex) while withstanding considerably harsher environments. Such a system will require extensive analytical, wind tunnel, and flight test development time.

4) The RBCC/SSTO inlet/forebody will experience extremely high temperatures on the leading edge of all components as well as areas of shock impingement. In order to maintain the integrity of these components (utilizing light weight structures) at high temperatures, active cooling will be required in some regions. Although significant operational experience exists for regeneratively cooled rocket and ramjet combustors and nozzles, similar data and experience is lacking for vehicle and inlet structural components. Considerable development will be required to bring this technology to operational status for inlet subsystem use.

5) The variable geometry system described above, and other RBCC engine subsystems, will require numerous high temperature seals between sliding and rotating components. Current seal technology does not allow operation under the pressure and temperature conditions anticipated for the RBCC/SSTO vehicle. Research directed at development of high temperature/strength reliable long-life seals will be needed. Such work is being carried out as "generic technology" in the NASP Technology Maturation Program.

8.1.2 Fan Subsystem

RBCC engine operations will require that the following technology development issues related to the fan subsystem be resolved (if a fan subsytem is used).

1) The use of a fan in the RBCC engine will require that the fan be stowed out of the inlet duct after its use in the low speed regime, subsequently the fan must be redeployed into the

duct prior to use during the flyback phase. There are substantial technical mechanization problems which will require resolution during RBCC engine development. These include; actuation and control, transient airflow distortion, physical integration aspects, and maintaining an acceptable environment while stowed.

2) An RBCC engine fan system will necessitate a high performance hydrogen fueled gas generator. Although the nation's gas turbine industry is making substantial progress towards the development of high performance lightweight turbomachine gas generators, the work is focused on conventional hydrocarbon fuels. Previous efforts have demonstrated hydrogen turbine technology. In the mid 1960's Pratt & Whitney and NASA successfully converted J-57 and J-65 engines to operate on hydrogen. Garrett AiResearch Co. has performed similar work as described in Section 3. At present, the study team knows of no directly applicable developments currently underway with the exception of the "Integrated High Performance Turbine Engine Technology (IHPTET)" program which emphasizes hydrocarbon fuels.

3) Current bearings, seals, and lubricants will not be capable of adequate performance in the environments anticipated for RBCC fan components. Significant work is being conducted to improve the performance of these components in advanced hydrocarbon fueled systems. These developments should be directly applicable to RBCC engine applications, although additional research may be required.

4) An effective fan system will require a compatible augmenter (afterburner) unit in order to provide adequate vertical landing thrust capabilities. The afterburner, which operates in the ramjet mode as well, must interface efficiently with the high expansion ratio exhaust nozzle envisioned for the RBCC/SSTO vehicle. Additionally, it must withstand environmental extremes (pressure, temperature, vibration) which will be more adverse than those experienced by present day augmenters. Application specific investigation will be required to develop these capabilities.

5) In order to provide the performance levels required, there is a potential need for an increased pressure ratio single stage fan (1.3 < P.R. <1.6). Current efforts in engine development, both military and commercial, should lead to fan systems with the required pressure ratios within the desired timeframe. High temperature materials and/or active cooling may be required at the higher mach numbers in which the fan operates. The amenability of these designs to stowage and redeployment will be a critical factor in their utility in RBCC propulsion systems.

8.1.3 Rocket Subsystem

RBCC engine operations will require that the following technology development issues related to the rocket subsystem be resolved.

8.1.3.1 Air-Augmented Rocket (AAR) mode

1) This study has described the merits of the dual concentric annular bell design. Although experimental work was conducted on this concept in the 1960's, additional development will be required to validate performance predictions.

2) High performance AAR mode operation requires high combustion efficiencies at stoichiometric conditions. Detailed analysis and ground test will be needed to demonstrate that high efficiencies can be achieved in the unique, highly integrated RBCC propulsion system.

3) If LAIR systems are to be used, an injector for the rocket combustor system which demonstrates high combustion efficiency while using either LO_2 or LAIR must be developed. Considerable engineering development remains to prove the viability of this dual oxidizer system.

4) Although the transition from AAR to ramjet and from ramjet to scramjet has been shown in laboratory hardware demonstrations, similar experimental data does not exist for the scramjet to rocket transition. This transition could be implemented in a number of ways. Scramjet/rocket systems could be phased out/in in a variety of ways to ensure smooth, reliable transition. A great deal of research must be directed towards characterizing the problems

involved in achieving transition and efficient high area ratio expansion as well as developing implementation methodologies.

8.1.3.2 Rocket Mode

5) Efficient AAR operation necessitates high expansion ratios within the duct. Analytical and experimental work in the 1960s tentatively demonstrated that extendable and staged bell nozzles could provide high expansion ratios in a AAR setting. This experimental database must be expanded to include expansion in large ducts at representative flight conditions (e.g., low back pressures) in order to define RBCC engine all rocket mode performance and design requirements.

6) In addition to expansion within the engine duct, rocket mode performance is also dependent on the feasibility of further exhaust expansion on the aft body. This process increases Isp and decreases base drag. Although this proposed expansion process is based on sound analytical theory, little or no research has been performed on similar configurations at the desired flight conditions. Substantial research will be required to prove the viability of this approach and to provide quantified information on the expansion efficiency and base drag characteristics.

8.1.3.3 Non-Rocket Modes

7) The internal rocket ejector system will experience very high temperatures during hypersonic flight because of its placement in the duct. Consequently, schemes to protect the exposed ejector hardware using high temperature materials and active cooling, for these duct mounted components, will be necessary to ensure the viability of the concept. Extensive testing and analytical development will be needed to create these thermal protection designs.

8) The use of the rocket unit for scramjet fuel injection has been suggested here. Validation of this approach will require substantial computational and wind tunnel tests, followed by flight tests to demonstrate the effectiveness of various design alternatives.

8.1.4 Ramjet Subsystem

RBCC engine operations will require that the following technology development issues related to the ramjet subsystem be resolved.

1) In keeping with the RBCC engine concept of multiple uses for hardware, the ramjet combustor will be used in non-ramjet modes as an AAR afterburner and fan augmenter. This multi-use technology has not been demonstrated to date, and will require further analysis and engineering development.

2) Operation of the RBCC engine in both ramjet and scramjet mode may require the use of retractable ramjet fuel injector/flameholder units or development of alternative approaches. Any approach presents difficulties, either in practical mechanization, or in heating/flow distortion problems. Substantial groundwork remains to be done to demonstrate the validity of any design concept

3) Although ramjet/scramjet mode transition has been demonstrated in the a laboratory environment ("dual-mode" and "convertible" ramjet work), the RBCC engine concept will require reliable, consistent transitions accomplished on a routine basis. This is beyond the current state-of-the-art and will require flight simulation demonstrations with full scale hardware to demonstrate engine system design adequacy.

4) High Mach number ramjet system tests will require the use steady state, true temperature facilities to provide the data fidelity required. Current facilities can supply these needs to a large extent, but facilities upgrades and flight tests will be needed to fully demonstrate and validate ramjet system performance.

3.1.5 Scramjet Subsystem

RBCC engine operations will require that the following technology development issues related to the scramjet subsystem be resolved.

1) Analysis of scramjet systems involves many complex aerothermodynamic problems. Improvement in computational fluid dynamics (CFD) techniques will be required to aid in solving the myriad problems associated with practical scramjet design. Ongoing efforts in this area, associated with the NASP program, should provide the necessary analysis tools as they are required for the design process.

2) Despite advances in CFD, ground and flight test data are needed to validate scramjet theory and design practices. Current scramjet designs are based almost solely on small scale ground tests and CFD results which have not been validated against experimental findings. This lack of relevant test data adds significant risk to the development process. Availability of applicable test data (whether ground based or flight) would greatly reduce scramjet performance uncertainties.

3) Scramjet development will require steady state, true temperature facilities capable of large scale test at Mach numbers up to 25, which is not a reasonable expectation. Current facilities are limited to Mach 8, with Mach 12 facilities under construction. Transient (pulse) tunnels cover the desired speed regime but offer milliseconds of testing time and are limited in scale. Current facilities can supply scramjet test needs to a limited extent, but facilities upgrades and flight tests will be needed to fully demonstrate/validate scramjet system performance.

4) Use of the rocket unit as a fuel injector for scramjet mode makes maximum use of existing hardware, thereby reducing system weight and complexity. However, this technology has not been demonstrated and will present difficulties in optimizing a rocket configuration which must perform this dual function along with dual oxidizer operation and operation with high temperature hydrogen. The development of this multipurpose component will necessitate basic studies to properly characterize the requirements of such a device.

5) The planned operation of the scramjet system in a fuel rich afterburning mode will have significant effects on vehicle thrust, drag, and aeroheating of the aft body. Little or no research has been conducted on the effect of fuel rich operation on a configuration of this type. Characterization of the problem will require basic studies using both CFD and ground tests.

6) The lack of existing test data makes the prediction of scramjet system cooling requirements and fuel thermal management very difficult. Advanced CFD methodologies and high fidelity thermal analysis programs should provide the necessary information, but these findings must be validated against ground and flight test data. Until both the experiments and analytical model fine tuning has been completed, significant questions about scramjet and fuel thermal problems will remain.

7) Development of large scale scramjet engines will require that scale effects be accurately corrected for in the transition from smaller test articles. Such scaling laws are relatively well understood for low speed aero/thermo phenomenon, however high speed phenomenon are not as well understood. Investigation of relevant scaling parameters will be needed to ensure successful transition from test to full scale hardware.

8.1.6 Air Liquefaction Subsystem

RBCC engine operations will require that the following technology development issues related to the use of liquid air be resolved.

1) Use of LAIR in the RBCC engine system will require substantial improvements in heat exchanger fabrication and test procedures. Heat exchangers which meet the stringent weight and reliability goals are beyond the current state-of-the-art. Continuation of ongoing efforts could provide the materials, design, and production techniques necessary for these advanced devices.

2) The use of para to ortho hydrogen shift catalysts significantly enhances the refrigeration effect of cryogenic hydrogen. However, the use of such catalysts (e.g. ruthenium)

increases heat exchanger weight and is subject to deactivation through poisoning or attrition. At present, this technology remains undeveloped, with the majority of basic data having been obtained in the early 1960s. Considerable research and testing will be needed to demonstrate low weight approaches.

3) Heat exchanger fouling by ice formed from atmospheric water content (liquid or vapor), carbon dioxide and argon is a demonstrated real world problem. Limited testing in the 1960's indicated that the problem can be reduced to acceptable levels through a variety of means. This work must be continued and expanded on to define an approach which minimizes anti-fouling weight penalties while guaranteeing consistent, reliable performance.

4) The use of slush LH_2 will allow in-tank reliquefaction (i.e. recycle operation) and/or may be used to increase vehicle fuel density to improve the propellant mass fraction. This process may yield vehicle performance benefits, however, slush hydrogen technology is not well developed and requires substantial experimentation and engineering development.

8.1.7 Slush Hydrogen Subsystem

RBCC engine operations will require that the following technology development issues related to the use of slush hydrogen be resolved.

1) Unlike LH_2, the aerospace industry as a whole has very limited production and handling experience with SLH_2. Numerous physical properties associated with onboard fuel storage and management have not been defined with sufficient detail at present. Additional research and development will be required to permit the routine use of SLH_2 as fuel.

2) A heat leak equivalent to 16% LH_2 boiloff is sufficient to convert SLH_2 to NBP LH_2. This consideration requires the design and use of very high performance fuel tank insulation systems and unique handling and storage procedures in comparison to NBP LH_2. In order to avoid premature transition to NBP LH_2, advanced production, transfer, storage, and maintenance systems must be developed.

8.2 Vehicle Systems

Basic factors affecting the flight mechanics and overall performance of the axisymmetric configuration must be investigated to establish appropriate design approaches and to confirm design validity. The areas needing study are listed below.

8.2.1 Aerodynamic Characteristics

The basic aerodynamic characteristics of the axisymmetric vehicle must be better understood to enable a more detailed assessment of system capabilities. Currently, little published data exists for straked cone configurations, particularly over the speed regime of interest. Even less information is available which includes propulsion system effects on aerodynamic characteristics. Studies which parametrically describe the force and moment coefficients associated with axisymmetric, RBCC engine powered vehicles must be completed to enable more accurate design and system performance evaluation.

8.2.2 Control System

Conceptual studies to this point have emphasized vehicle performance but have not evaluated the requirements for an RBCC/SSTO vehicle control system. Advances must be made in understanding the needs of both engine and flight control systems, as well as the interaction between them. Current aircraft and launch vehicles do not require the level of control sophistication or integration needed in this highly integrated airframe/propulsion system.

8.2.3 Vertical Landing

Although vertical landing maneuvers are well understood for rotary wing and vectored thrust type aircraft (e.g. Harrier), these vehicles are significantly different than the RBCC/SSTO vehicle. The problem of transition from cruise to landing has not been studied in depth up to this time. Research is needed to determine the characteristics of this vehicle during the landing phase, including wind tunnel testing and thorough simulations. This work is necessary to validate the proposed landing method.

8.2.4 Vehicle Structure

The integrated RBCC/SSTO axisymmetric vehicle will undergo structural loads due to aerodynamic forces, propulsion system generated forces which are unique to this type of configuration. Typical designs for both aircraft and launch vehicles are well understood and important design parameters have been identified. Although many or all current structural analysis techniques may be applicable to this vehicle its unconventional design will necessitate new studies to obtain the level of understanding of the structural system necessary for "high confidence" in all structural design aspects.

8.2.5 Aeroheating and Thermal Protection System

Aeroheating that will occur during the ascent and reentry portions of the orbital mission will present materials, design and fabrication technology problems that have not heretofore been addressed. These problems are further complicated by the need for an easily inspected thermal protection system, an easily maintained system and a long-lived system. Research is needed into all these problem areas. This work should consider both active and passive TPS technology development.

8.2.6 Acoustic Environment

A highly integrated engine/airframe system such as the RBCC/SSTO vehicle presents new acoustic problems not experienced in more conventional configurations. These problems must be studied and characterized, enabling system design to proceed with valid acoustic theory and confirming available test data.

Section 9.0

SUBSCALE ENGINE TEST PLAN

9.1 Introduction

As has been previously discussed, the RBCC engine combines four propulsion subsystems into one engine system. These subsystems are the air-augmented rocket ejector subsystem, ramjet subsystem, scramjet subsystem and rocket subsystem. In the RBCC engine design approach considered here, the hardware requirements of the ejector subsystem and rocket subsystem are met by the same engine subsystem, a dual, annular rocket engine. There are three classes of problems that must be further investigated that require subscale engine testing.

The first class of problems are those relating to the performance of individual engine subsystems over the full envelope of conditions to be encountered in the orbital ascent, flyback and landing maneuvers.

The second class of problems are those related to the integration of the propulsion subsystems design and operation control into the vehicle.

The principal propulsion areas where further basic subsystem test and development work is required are in the inlet subsystem, scramjet subsystem and the operation of the dual annular rocket subsystem at very high expansion conditions in the final all-rocket mode of orbital ascent.

As in the case of any aircraft engine system, if a subscale engine system can be demonstrated in flight testing operations, the confidence in its performance potential is greatly increased. However, in the case of the engines being discussed here, flight testing is much more significant. This is due to the fact that a part of the altitude and velocity envelope within which RBCC engine systems must operate cannot be simulated in ground test facilities at the present time or in the foreseeable future.

This same situation exists with regard to engine subsystems integration demonstration over the full flight envelope. Therefore, flight test vehicles must be reasonably expected to be required to investigate engine operation and control of RBCC engines in the upper portions of the flight envelope.

The third set of problems are those related to component and subassembly design and operational evaluation including the engine control system in particular.

9.2 Subscale Engine Size

As a starting point for determining the size of the subscale engine system, consider the 65 Klb sea level static thrust rated Engine 10, the Ejector Scramjet, ten of which are used to power the 500 klbm TOGW/GLOW point design vehicle.

In this thrust rating, Engine 10, in a circular cross section engine will have a basic cylindrical diameter of four feet and an exit nozzle diameter of five feet. The overall length of the engine is 16 feet. With the axisymmetric spike inlet system, the "installed" configuration, the overall length is 25 feet. The weight of the engine is approximately 4,065 lbm.

In downscaling RBCC engines, the circular cross section areas can be downscaled directly, the requirement being that the characteristic area ratios be maintained. In RBCC engine systems, it is expected that engine downscaling will also be essentially a linear process in terms

of the length/diameter ratio of the engine system. In RBCC engine systems, the principle processes that establish the scaling relationship are combustion processes and mixing processes. In hydrocarbon engines, the combustion process dominates and establishes minimum axial distances set by the combustion time requirements of hydrocarbon fuel. In hydrogen powered engines, the combustion process is extremely fast and flame zones quite short, thus engine length is dominated by mixing process considerations. Mixing processes scale predominately by the L/D ratio. It can be anticipated that RBCC engines will scale linearly in circular cross sectional area and close to linearly in length.

The size of the subscale engine should be established with the primary consideration being towards minimizing test operations cost and maximizing the compatibility of the engine dimensions with existing test facilities.

It is recommended that the subscale engine thrust rating be set at approximately 8,000 Klb or a 1/8th scale configuration of the 65 Klb SLS ejector scramjet engine. The subscale engine would be approximately two feet in diameter and 8 to 10 feet in length. This is approximately the size of the Marquardt ejector ramjet subscale engines illustrated in Fig. 13, if the engine were in a direct connect mode configuration. This dimension does not include the inlet length which, if a spike inlet were used, would add an additional 10 to 12 feet to the test engine in free jet testing.

9.3 The Role of Ground and Flight Testing

Sustained hypersonic velocity operating conditions above Mach 12 cannot now be, and probably will not in the near future be, produced in ground test facilities. The upper end of the test envelope that will require exploration probably will only be explorable with flight test vehicles operating under velocity and altitude conditions that will be encountered in actual operation. The basic problem in this is that emulating the altitude and velocity conditions of orbital flight in flight test operations requires achieving orbital velocity and altitude.

Because of this condition, the upper limit of the RBCC engine system will probably have to be explored by larger scale systems with orbital flight capability. In these engine systems, it is suggested that the advanced research engine phase will merge with the DDT&E phase to a greater extent than has been experienced in any aircraft or rocket vehicle systems to date.

9.4 Streamtube Engines

Experience has established the experimental value of "streamtube" engine test rigs. This approach utilizes modular building-block engine elements to provide valid comparative performance information quite economically. Streamtube engines can be constructed, in boilerplate configurations, to explore various duct geometries, subsystem and components design alternatives, combustion dynamic phenomena, etc. under various operating conditions.

These tests can be conducted in established test facilities using both direct-connect and free-jet test configurations. The direct-connect alternative allows the engine operation to be investigated separate from inlet conditions. Inlet systems can be separately tested and the engine and inlet system integrated into a free-jet test facility.

Existing test facilities could be used to evaluate streamtube configuration engines up to Mach 8 and up to Mach 12 in facilities presently under construction. A streamtube engine rig is illustrated in Fig. 153. In Fig. 154, sketches of a variety of "building block modules" that would be used in such a rig are presented.

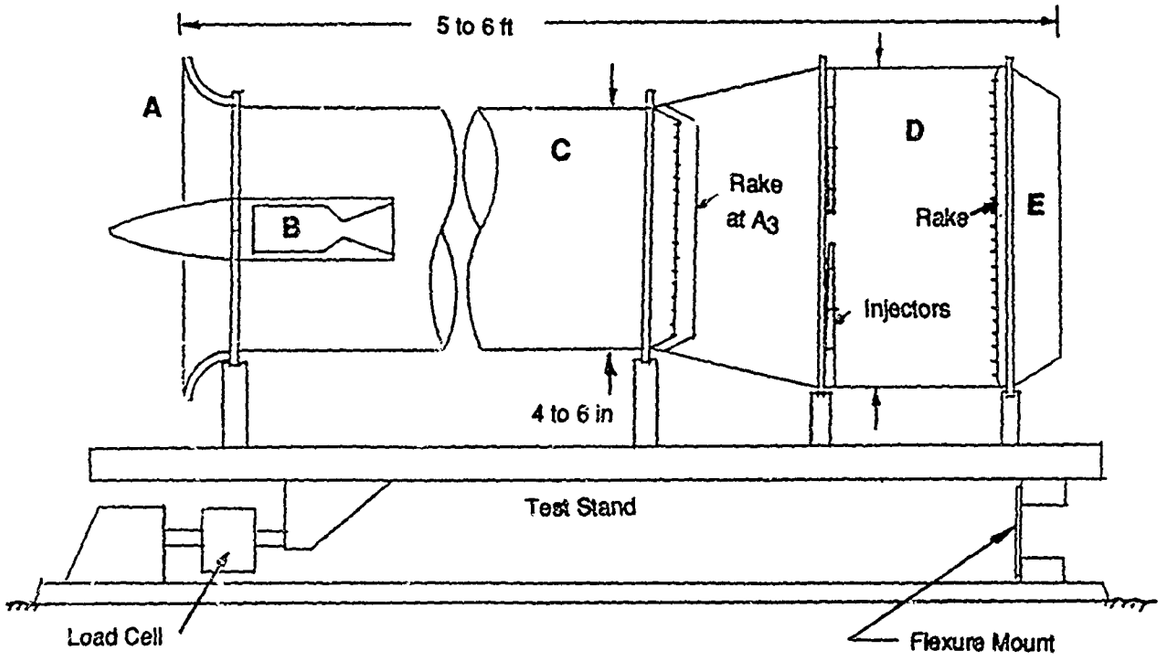


Fig. 153 A Streamtube Engine Rig

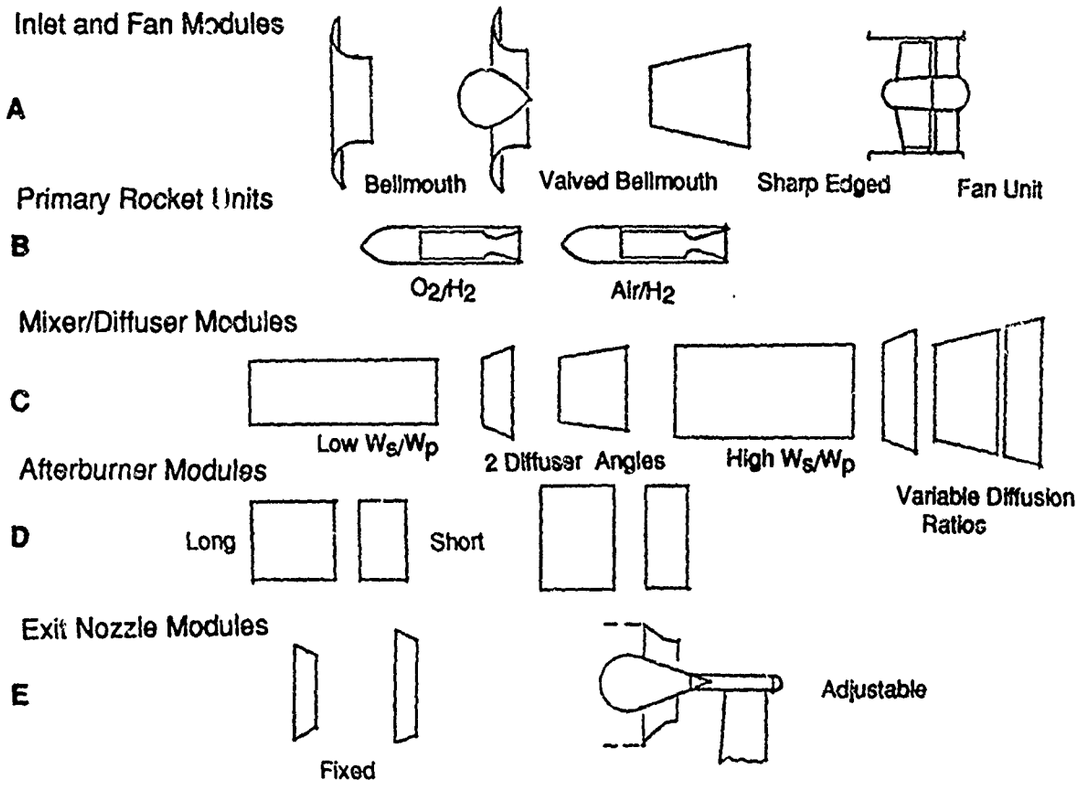


Fig. 154 Various Streamtube Engine Rig Building Blocks

9.5 After Streamtube Engine Research

The use of the modular streamtube engine approach to exploratory investigations of engines of the type under study here is usually found to be very cost beneficial. This is due to the combination of the modular approach with boilerplate construction. As information is developed by the streamtube program, and the questions regarding the final design approaches are further resolved, the next step is usually the construction of portions of the streamtube rig using designs that more closely approach the final operational configuration sought.

In situations where the engine systems can be completely tested in ground installations, the DDT&E work can be carried out with a very heavy reliance on ground testing. This is not the case with RBCC engine systems designed to propel vehicles to earth orbit. The higher velocity environments cannot be duplicated in ground facilities.

This leads to two basically different alternatives in the program under study here:

The first alternative is to implement a flight test program with test vehicles developed specifically for the purpose of obtaining information in these higher flight velocity regimes for the RBCC subscale engine program. This approach will be discussed further in this section. This approach has the weakness previously discussed in that it cannot provide the flight environment near orbital velocity conditions without actually being able to achieve orbital velocity conditions. This cannot be done with the size of engine, 8 Klb, considered here. This approach might be used to extend the investigation of scramjet propulsion up to the Mach 15 regime identified in this study as the optimum transition point for all RBCC vehicles to rocket propulsion. This will represent a significant technological accomplishment.

This second alternative is to consider the research findings that will be developed by the NASP/X-30 program. This vehicle might provide a testbed, if it has orbital capability, that could explore the entire operating envelope of RBCC engine systems. This approach would be similar to that proposed by LaRC in the HRE program, previously discussed in Section 2.0, where those investigators sought to use the X-15 vehicle as a testbed for the HRE. In that instance, delays encountered in the HRE program and the termination of the X-15 program prevented such a flight test program from being carried out. This same approach might be implemented using the Shuttle Orbiter.

If the X-30 or Shuttle Orbiter options cannot be considered, a subscale flight test program involving two types of vehicles is suggested.

The first test vehicle type would consist of expendable, or partially recoverable, vehicles to investigate scramjet operation up to Mach 15 and the initial portions of all-rocket mode operations. This vehicle would be boosted by an expendable rocket, either one or two stage, to hypersonic flight conditions. The engine subsystem could be recoverable. This vehicle is referred to as the Hypersonic Propulsion Test Vehicle or HPTV.

The second flight test would increase the number of subsystems provided in the test article to more closely emulate the full RBCC/SSTO configuration. This would include lifting surfaces and aerodynamic control. The vehicle, substantially larger then the HPTV, would initially use self powered takeoff and landing for lower flight speed regimes followed by expendable rocket boost to achieve higher airbreathing flight termination velocity. This vehicle is referred to as the Self Powered Unmanned Vehicle or SPUV.

The HPTV flight test vehicle and the SPUV flight test vehicle investigations would be integrated with ground test operations to the greatest extent practical. What should also be

considered is the integration of all three of these efforts into the initial portions of the DDT&E program leading to the full-scale RBCC/SSTO vehicle system.

The initial focus of the flight test program would be on the rocket-boosted HPTV vehicle system. The HPTV concept has precedence such as the rocket boosted ramjet powered X-7 vehicle, as well as several planned, but not implemented out, scramjet-powered vehicles which were to be vertically launched on expendable rocket systems as parts of incremental flight-test programs planned by the Marquardt Corporation, General Electric and others.

The primary objective of this HPTV element of the subscale flight-test effort is to conduct testing in those high-speed flight regimes which cannot otherwise be explored in ground-test facilities. Ramjet and scramjet performance will be derived both from internal onboard recorded instrumentation output and from external vehicle tracking station measurements. Recovery, and possibly reuse, of the HPTV may be quite important since telemetry transmission of data may not be practical over some portions of the flight due to plasma-sheath radio blackout effects.

In relation to the SPUV program elements, the HPTV will be maintained configurationally compatible with the larger vehicle system. It will also be flown sufficiently early so that the significant hypersonic flight experience will be in hand prior to the point where SPUV flights covering the "high-speed end" will be beginning.

Following the HPTV program, the SPUV program will also be closely coordinated with the ground-test program as well as with the initial portions of the DDT&E program leading to the full scale vehicle system. There would be a progressive increase in the final end-of-powered flight speed until near-orbital/orbital conditions would be approached. At the same time, this vehicle could provide a testbed for DDT&E subsystems hardware designs since the SPUV will incorporate other subsystems such as a structural system that might closely emulate the full scale vehicle, a guidance and control system, thermal protection system, landing and takeoff gear, etc.

9.6 Costs and Schedule

The similarity between the RBCC subscale engine development program and the LaRC HRE program carried out between 1966 and 1975 provided our basis for cost estimation of the RBCC subscale engine test program.

The finally revised cost estimates for the HRE program which included flight testing provide our benchmark. The funds expended in this program on the engine development itself were approximately $50 million. The projected cost of the complete program with 25 X-15 flights was an additional $125 million in 1975 $.

In the subscale engine test program proposed here, our study indicates that a two to three year program would be required to carry out the ground testing with a four year program required to carry out the flight testing. Both these programs would overlap. The flight test phase would also overlap with the initial part of the DDT&E phase of the full scale vehicle system.

It is estimated that approximately $215M (1987 dollars) would be required for the ground test operations. An additional $285 M would be required for the flight test programs for a total of approximately $500 M for the subscale engine program.

The schedule for the flight-test program, is illustrated in Fig. 155. Including the ground test program, the total subscale program duration is estimated to be approximately six years with a one year overlap between the ground test and flight test portions. The subscale ground test program is not included in this figure.

Note: Supported by Prior Subscale Ground Test Program Element: 3 Years, $215 M

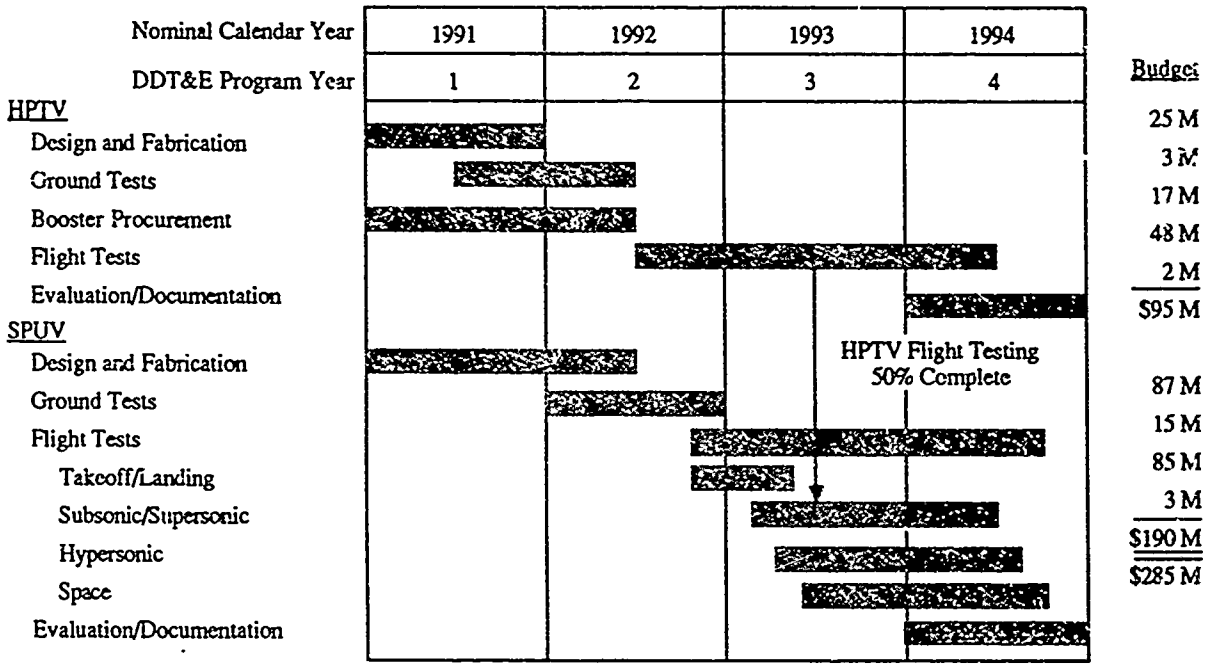


Fig. 155 Flight Test Program Schedule and Budget

Section 10.0

DDT&E PHASE PLAN

10.1 Ground Rules

The engine DDT&E phase, to be described in this section, assumes that the technology development and demonstration phase using subscale engines has been carried out.

The engine proposed is Engine 10, the Ejector Scramjet, using NBP hydrogen. The technology availability date is assumed to be 1995.

The initial guideline cost estimate that must be provided by the government has an overwhelming influence on DDT&E phase planning. This guideline cost estimate should be clearly established with the aid of experienced specialists in engine development cost estimation from industry, non-profit groups, and selected senior management in government. This recommendation was a final recommendation developed by the LaRC HRE program staff management as a result of the experiences encountered in that program.

Fig. 156 presents the DOD R&D categories system that places research and technology development, technology demonstration and system development in an orderly perspective.

Phase	Primary Output	DOD Category	NASA Category
Research and Technology Development	Understanding of Physical Phenomena Creation of New Concepts Design Data and Procedures	6.1 Research 6.2 Exploratory Development 6.3A Advanced Development (Non-systems)	R&T Base Systems Technology
Technology Demonstration	Demonstrated System/ Subsystem Performance	6.3A Advanced Development (Non-systems)	Systems Technology
System Development	Operational Systems	6.3B Advanced Development (Systems) 6.4 Engineering Development	Systems Development



Fig. 156 DOD Research and Development Category System

The DDT&E phase is concerned with activities in category 6.3B, Advanced Development Systems and category 6.4, Engineering Development. These two R&D categories are preceded by category 6.3A, Advanced Development (non-systems) and categories 6.1 to 6.2, which cover,

respectively, research (6.1), and exploratory development (6.2). It is these activities that must precede the Engineering Development Portion, 6.4, of the DDT&E phase.

A ground rule applicable to the DDT&E phase plan is that maximum use will be made of "prior work" and the findings of the subscale ground-test and flight-test activities described in the previous section. It is also assumed that the early phases of the DDT&E phase will overlap and be integrated into the technology development and technology demonstration work carried out in the subscale program.

This background of information and experience includes experience in the liquid propellant rocket field and advanced airbreathing propulsion systems field. In particular, the considerable amount of research and technology development and demonstration work carried out in the original "aerospace plane" program of the late 1950s and the early 1960s, and successor work on hypersonic ramjet and scramjet propulsion development through the 60s is a very significant resource which can be applied here. Specific program examples include:

- USAF/Industry Aerospaceplane efforts of the 1960s
- USAF/Marquardt Advanced Ramjet Concepts (ARC) program
- NASA/Garrett Hypersonic Research Engine (HRE) program
- USAF+NASA/Rocketdyne "Aerospike" Rocket Technology Development
- NASA-LaRC Dual Mode Ramjet/Scramjet Program of 1975-1985
- USN/APL Scramjet Missile Program

Specifically applicable to the RBCC engine system is the theoretical, design and experimental work carried out by the Marquardt Corporation under the NASA Contract NAS7-377.

Based on this existing theoretical and experimental database deriving from these efforts, the subscale engine development ground and flight task program would be carried out to provide the basis for beginning the engine development portion of the DDT&E phase of an RBCC/SSTO vehicle system.

10.2 DDT&E Program

The DDT&E program plan is presented in Fig. 157. These efforts are divided into nine program elements within the DDT&E phase and one element, P-1, which supports engine production. This program element, and the vehicle DDT&E phase and the production phase will be discussed subsequently in this section and the combined cost aspects of the total program will be described in Section 11.0.

Each of the nine work elements will now be described.

10.2.1 Program Element 1

Directed Component Technology

Schedule: Years 1 to 3 (3 years)

Scope: Individual subsystem and component research and technology efforts are undertaken as required to achieve performance and weight goals for the full-scale engine (at IOC). Engine design and analysis work is pursued in parallel and provides overall engine system performance characterization.

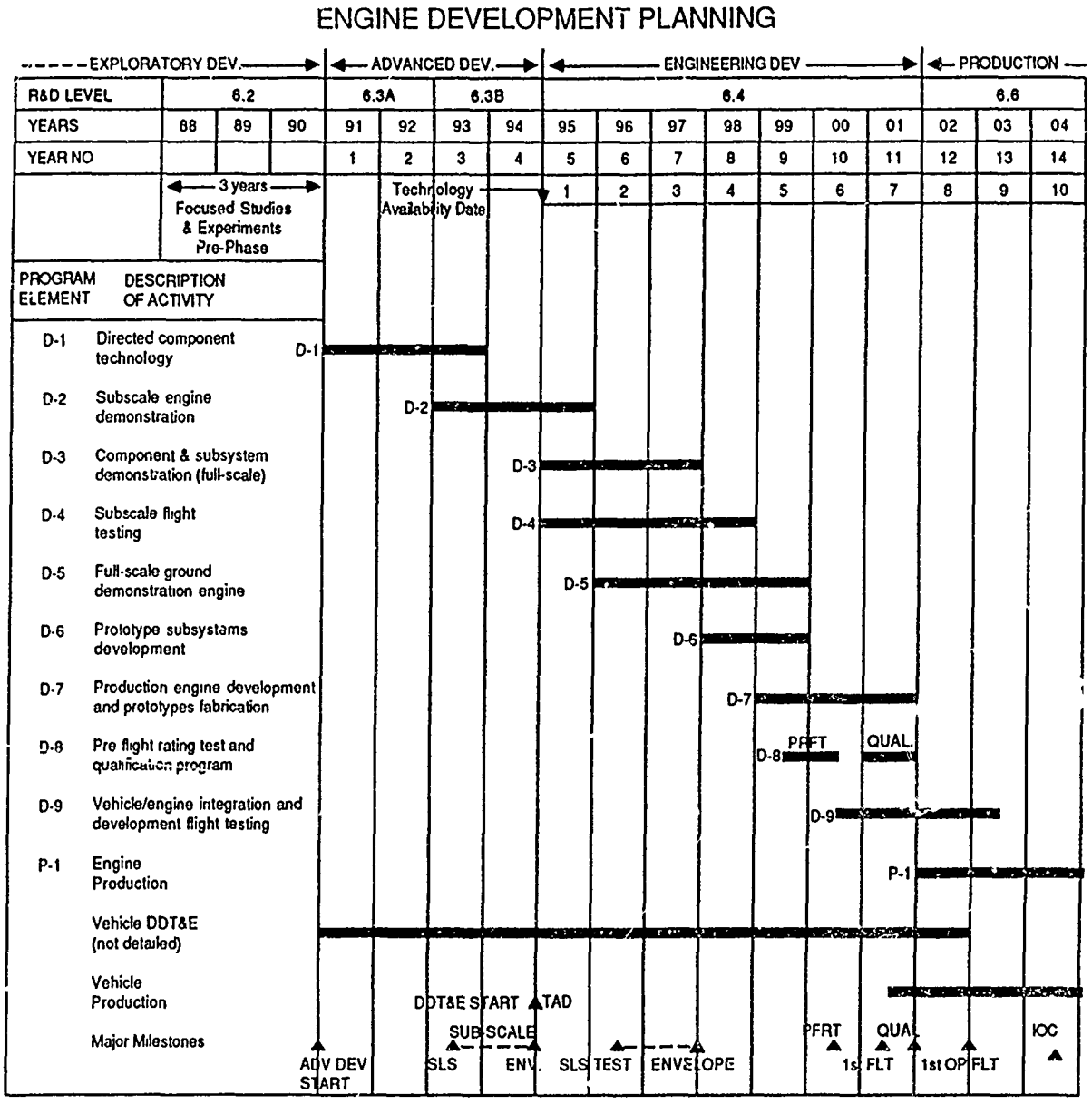


Fig. 157 **Engine DDT&E Program Plan**

Facilities: This work will be performed using existing ground test facilities available to the engine contractor and subcontractors in most cases. If new facilities are necessary, they must be expedited at program startup.

Principal Output: Achieves and demonstrates subsystem/component technology readiness to enable full-scale development to proceed on all subsystems.

Breakdown of Subsystems/Components:

- Engine controls, instrumentation and integration
- Ejector Primary Rocket Subsystem
  - Combustor/nozzle assemblies (2)
  - Turbopumps and drive gas generators
  - Valves, piping and structure
  - Ramjet fuel injection provisions
  - Scramjet fuel injection provisions
  - Subsystems controls, instrumentation and integration
- Mixer/Diffuser/Combustor/Nozzle
  - Regeneratively-cooled duct, centerbody and web structure
  - Fuel injectors and retraction provision
  - Pumps and drives
  - Controls, instrumentation and integration
- Vehicle Interface
  - Structures
  - Electrical and instrumentation connections
  - Fluid connections

10.2.2 Program Element 2

Subscale Engine Demonstration (Previously described in Section 9.0)

Schedule: Years 1-1/2 to 3-1/2 (2 years)

Scope: At a selected scaled-down size (to be heavily influenced by test facility capabilities), several builds of both boiler-plate and semi-flightweight subscale engines are fabricated and tested. Both ground- and flight-test facilities support this effort. Each mode is explored over its applicable flight-speed range. At least one subscale engine will be capable of all modes and will be so tested.

Facilities: Subsonic, supersonic, and hypersonic ground-test facilities, both Government and contractor operated, will be utilized as required. In recognition of the present upper flight-speed simulation limitations (of about Mach 7-8), a hypersonic flight-test vehicle is to be developed and utilized. This could range from a simple solid-rocket boosted vehicle to the new X-30 research aircraft. Utilization of the Space Shuttle system is another possibility.

Principal Output: Demonstrates and validates overall engine design capabilities and achievable levels of performance at the selected scale. Provides a direct development tool for the full-scale engine effort which overlaps the subscale program. Directly supports flight-test phase.

Preliminary Set of Builds:

- Ramjet/Scramjet test unit
- Rocket test unit
- All-mode test unit (ground test)
- All-mode test unit (flight test)

10.2.3 Program Element 3

Component and Subsystems Demonstration (Full Scale)

Schedule: Years 3 to 4-1/2 (1-1/2 years)

Scope: All engine subsystems and components are developed as engineering prototypes, and subsequently as production-type items, and tested over the applicable operating range as subsystems. Interfaces are simulated by facility operations as necessary (flight testing, generally speaking, is not applicable at this stage).

Facilities: To the extent ground-test facilities are available, emphasis will be on full subsystem evaluations. Otherwise, critical components will be separately evaluated. If necessary, individual full-scale elements will be tested (e.g., individual combustor fuel injection struts).

Principal Output: Enables the full-scale Ground Demonstration Engine program element to be implemented in a short time and at an acceptable level of technical risk. Similarly, this activity supports the Pre-Flight Rating Test (PFRT), First Flight, and Qualification Engine efforts by making available continuously improved hardware.

10.2.4 Program Element 4

Subscale Flight Testing

Schedule: Years 4 to 6 (3 years)

Scope: Appropriate set of subscale engine flight test vehicles (e.g., HPTV and SPUV) will be developed and operated to explore and document propulsion system operation outside the flight regime provided by ground test facilities, with overlap for correlation purposes. Flight type engine test hardware is derived from the earlier "Subscale Engine Demonstration" Program Element 2.

Facilities: In addition to the test vehicles to be used in the conduct of this activity, an appropriate flight test operations facility is needed (e.g., EAFB, NASA-KSC).

Principal Output: Experimental assessment and verification of propulsion system performance and operations in flight regimes which cannot be effectively simulated in ground-test facilities. Other engineering aspects of the overall advanced vehicle system under development may be explored and validated by use of the same or similar flight-test vehicle. The data obtained in the context of a flight-test vehicle can be on an installed basis. Thus, vital engine/vehicle integration aspects can be quantified (e.g., further exhaust expansion on the vehicle aft-end).

Suggested Flight-test Regimes of Interest

- Hypersonic flight - Mach 6 to 15, 60 to 150 Kft altitude
- Hypersonic flight - Mach 12 to 15 to near-orbital speed, 110 to 180 Kft altitude
- Space environment - above 200 Kft altitude

10.2.5 Program Element 5

Full Scale Ground Demonstration Engine

Schedule: Years 4-1/2 to 6 (1-1/2 years)

Scope: Several builds of the prototype full-scale engine are ground tested at sea-level static and (to the extent supportable by available facilities) over the operating envelope. Both direct connect and, as appropriate to inlet selection and development status, free-jet tested. These highly instrumented systems will be made up of the components and subsystems deriving from the previous 1-1/2 years effort. Although the engine may not be entirely flightweight, it will closely approach the production engine configuration and overall functions.

Note: In view of ground test facility limitations, and the engine size, the entire operating envelope can only be explored and demonstrated in the later developmental flight testing activity.

Facilities: This program element will make maximal use of available ground test facilities as noted. New and otherwise modified facilities will be needed in all probability. These will continue to serve during the subsequent PFRT and Qualification program elements.

Principal Output. Experimentally determined design improvements and production prototype detailed configuration definition, plus the completion and proofing of ground test facilities for the remainder of the development program.

Anticipated Testing Regimes:

- Sea-level static (initially emphasized)
- Subsonic flight speeds (sea-level and altitude)
- Transonic flight speeds (altitude)
- Supersonic flight speeds (altitude)
- Hypersonic flight speeds (altitude)
- Space environment

10.2.6 Program Element 6

Prototype Subsystems Development

Schedule: Years 6 to 7-1/2 (1-1/2 years)

Scope: Production prototypes of all subsystems and critical components are designed, fabricated and tested in preparation for overall production prototype engine development to follow. This effort proceeds directly from the component and subsystem full-scale demonstration effort, and runs parallel with the ground demonstration program element, from which direct design-impacting feedback is received. This effort will encompass complete specification/configuration management documentation and control, and the establishment of production tooling requirements.

Facilities: Ground-test facilities capable of documenting and validating the resulting production prototype subsystems will be required, as well as basic production facilities for the developmental hardware involved. Contractor, subcontractor and vendor administrative arrangements will be formulated to establish the overall span of facility resources for the remainder of the development and acquisition program.

Principal Output: Production prototypes, followed by production items for all engine subsystems. This program element is the key lead-in activity in support of the subsequent production engine development phase.

10.2.7 Program Element 7

Production Engine Development and Prototypes Fabrication

Schedule: Years 7 to 8-1/2 (2-1/2 years)

Scope: Initially yielding production prototype engines for test and evaluation operations (leading to PFRT and Qualification systems), this program element sees the completion of overall engine development activities. It is directly followed by engine production commencing the acquisition/procurement phase of system life cycle operations. It is directly supported by the preceding prototype subsystem development phase.

Facilities: Engine assembly and subsystem fabrication facilities are required to support this program element as well as the full-production phase to follow. Developmental facilities involved are largely those to support the PFRT and Qualification programs.

Principal Output: Production prototype engine systems, including hardware to be evaluated in meeting PFRT and Qualification goals, as well as first-flight engines for delivery to the associated vehicle contractor's facilities.

Estimated Number of Engines through Qualification

• Pre-PFRT test evaluation	2
• PFRT	5
• Pre-Qualification	3
• Qualification	8
Total	18

10.2.8 Program Element 8

Pre-Flight Rating Test (PFRT) and Qualification Program

Schedule: PFRT: Year 7-1/2+ (5 months)

Qualification: Year 8 (8 months)

Scope: PFRT processing of several production prototype engines assures a competent, low risk first flight capability by suitable "spot-checking" of performance and operations across the operating envelope within the capabilities of ground-test facilities. Upon successful completion of PFRT, the engine type is released for final vehicle/engine integration and initial flight testing.

The Qualification process is substantially more detailed and involves several times the test time of PFRT. Here the engine is checked through testing for total specification adherence, again within the capabilities of available ground test facilities. The Qualification process is to be completed in the developmental flight test sequence following PFRT completion (to make the engines available for this.

Facilities: Qualification follows PFRT in the same set of facilities, spanning the ground-testable envelope of the engine.

Principal Output: PFRT - flightworthy engines for the development flight test phase (not the IOC systems).

Qualification - complete specification adherence demonstration which permits engine production to be initiated with a "finalized" product.

10.2.9 Program Element 9

Vehicle/Engine Integration and Development Flight Testing

Schedule: Years 7-1/2 to 10-1/2 (3 years)

Scope: In this phase, the vehicle/engine engineering liaison process moves to the hardware stage as the prototype vehicles are physically mated with the propulsion systems evolving from the production engine development activity. With the completion of PFRT, first flight-vehicle engines are delivered for installation and overall vehicle system ground testing proceeds toward the first-flight milestone. Developmental flight testing completes the qualification process by exercising the engines over their overall operating envelope (not feasible through ground-testing alone).

Facilities: Facilities capable of supporting the vehicle development and production activity being presumed, the facility requirement associated with this phase of the program is that of experimental flight test support in the field (likely equates to the equivalent of EAFB, NASA-KSC, et al).

Principal Output: As noted, completion of development flight testing completes the engine qualification process (and other subsystems as well, e.g., avionics, flight control). Its completion marks the milestone, "Development Complete".

Estimated Number of Engines Required to Support Flight Testing

First flight vehicle	10
Spares	4
Total	14

Engine Production and Initital Operating Capability (IOC)

One and one half years into thed Program Element 9 activity, engine production begins. This activity must support achieving IOC 2.5 years later. Vehicle production begins 6 months prior to engine production as shown in Fig. 157.

Section 11.0

LIFE CYCLE COSTS ANALYSIS

11.1 Approach

While the subject of this study was a manned vehicle flying a lifting ascent trajectory, the cost model used was not an aircraft cost model. The axisymmetric, vertical takeoff vehicle configuration is a "rocket-like" configuration when judged from the standpoints of the DDT&E phase requirements, production and assembly operations requirements and launch operations and launch operations support requirements. The cost model used was the STAS Cost Model developed by MMAG for axisymmetric "rocket-like" structures and systems.

MMAG has an extensive computerized data base of launch system costs based upon that company's decades of experience in all phases of the life cycle of large rocket systems.

The MMAG Advanced Programs Cost Model uses parametric CER's, cost estimating relationships, derived from MMAGs experience, to calculate life cycle costs (LCC). The model estimates development cost, production and operations costs, and launch manpower requirements based on data provided by MMAG tests and operations personnel. The model was initially developed for STAS and has been used for the RBCC/SSTO study as will be discussed here.

It was not practical to estimate the additional operations and operations support cost reductions that might result from the extensively autonomous design of the RBCC/SSTO vehicle system. No CER's descriptive of the life cycle cost reduction impact of the reduced GSE requirement are available. This situation is approximated by the reduction of the ground operations cycle time between launches, but reduced GSE equipment costs are not considered. Since these costs are not trivial, an additional operations and operations support cost reduction is possible.

11.2 Comparison Base Line

In the discussion to follow, the life cycle costs of an RBCC/SSTO vehicle will be provided for the three phases comprising the overall life cycle. The baseline of comparison of costs is the STS Shuttle operations phase costs in terms of Cost/Flight and Cost/lb payload.

11.3 MMAG Cost Model Description

11.3.1 Applications

The MMAG cost model's primary function is to calculate the life cycle cost for a given launch vehicle and mission model. Up to four launch vehicles may be run at one time to give an overall architecture life cycle cost. The total costs are also broken down into subsystem costs for analysis requiring further detailed costs. The model lends itself very well to running sensitivities and providing cost data for trade studies. Some frequently performed sensitivities as a function of cost are: reliability, vehicle life, vehicle size, flight rates, facilities costs and manpower, IOC, complexity factor, vehicle design parameters, downtime costs, and other variables having an impact on total launch vehicle costs.

11.3.2 Required Inputs

Four types of inputs are required to run the cost model. The first input required, complexity factors, is used to distinguish design and production cost for a new system as compared to existing system characteristics which comprise the data behind the cost estimating relationships (CER's). Each subsystem (e.g., TPS, tanks, etc.) has corresponding stage of design complexity factors and production complexity factors as follows:

- Design complexity factors:
    - Design factor - allows a distinction between existing design with existing design technology and new design with advanced technology.
    - Complexity with respect to CER - comparison of the new subsystem to the data from which the CER was derived.
- Production Complexity Factor:
    - Manufacturing complexity - comparison of new subsystem with respect to CER manufacturing to data from which CER was derived.
    - Material cost - a factor for distinguishing material costs for new subsystems which define the CER (e.g., advanced composites in the new subsystem versus aluminum and other existing materials used in todays existing subsystems comprising the CER).
    - CIM impact - a measure of the benefits of computer integrated manufacturing.
    - Other cost model inputs - the cost impact of including additional systems not part of the CER's.

Table 22 is an example file used to enter complexity factors for each required subsystem. Complexity factors may be entered for each subsystem for launch vehicles having up to four stages.

The second set of required inputs are vehicle design characteristics. Vehicle technical parameters for each subsystem combine with the CER's and complexity factors to generate design and first unit costs. These subsystems categories are:

- Thermal Protection System
- Interface, Attachment and Controls
- Nosecone, Wing, and Tail
- Tanks
- Separation
- Recovery Landing Gear
- Propulsion Subsystems
- Engine Subsystems
- Avionics

The third set of inputs is the annual flight rate. The flight rate is combined with the vehicle type to determine production quantities and cost and operations costs.

The final set of inputs, commonality factors, allow for adjustments in vehicle stage costs due to sharing of common components among launch vehicles in a given architecture.

Table 23 Thermal Protection System

Comp	Sub-item Factor	Value	Rationale
State of Design	Design Factor	0.50	New design-existing technology
	Complexity with relation to CER	1.00	Similar to existing systems
Production Complexity Factor	Complexity with relation to CER	0.75	Less complex to produce
	Material Cost	1.20	Advanced materials
	Computer Integrated Manufacturering impact	0.65	High production rate
	Other systems include	1.10	Additional monitoring

Table 24 LCC Groundrules and Assumptions

- Fiscal Year 1987 Dollars
- Point Design Vehicle - 440 klb TOGW
- Structures and Engines Life = 100 flights
- Engines: Ejector Scramjet (10)
- Stage-Up reliability = 0.996
- Stage-Down reliability = 0.996
- Mission Success = 0.992
- IOC = 2005
- 1997 - 2002 DDT&E
- 5 test vehicle in DDT&E phase
- 7 production vehicles
- 2 main operating bases (WTR & ETR)
- Cost of LH_2 = \$2.00/lb
- Cost of LOX = \$0.05/lb
- Cost of SLH_2 = \$4.00/lb
- Normal turnaround time for ground operations processing = 5 days (1 shift/day)
- Launch site facilties: Vehicle Service Facility
  Operations Control Center
  Propellant Servicing Area
- Payload encapsulation performed off-line (i.e., not in the vehicle-turnaround timeline).
- No pad or landing strip built (assume use of existing runways or pads).
- STAS Mission Model Civil Option II/DOD Option 2
- Vehicle capability 40klb LEO @ 28.5 ° - 100% manifest load factor.
- DDT & E Engines = \$4B, 1st Unit Cost = \$81M
- Payload lost cost is a function of flight rate, payload capability, reliability, and payload \$/lb.

11.3.3 Generated Outputs

Cost outputs may be printed out in various forms. A life cycle cost broken down into the cost categories of DDT&E, facilities, production, and operations and support costs is the most common type of output used. Annual undiscounted funding profile and five percent, ten percent, and fifteen percent discounted funding profiles show present value LCC estimates. $/lb in orbit and $/flight data are available for each cost category for vehicles flying out of the ETR and the WTR. The WBS allows for further cost breakdown to the subsystem level. Ground operations and logistics support costs are also included in the final costs.

11.4 Ground Rules and Assumptions

Table 24 presents the LCC ground rules and assumptions used as input to the MMAG cost model.

11.5 Findings

11.5.1 DDT&E Costs

The DDT&E costs, Fig. 158, are the largest component of the LCC program . This is to be expected because this is the first attempt to put a single stage manned vehicle into orbit with advanced technology airbreathing engines. Engineering design and development of the vehicle system is more than half of the entire DDT&E effort. The simplified ground systems require minimal effort. The flight test hardware is the next largest contributor to DDT&E. This is attributed to the ground rule of five complete test vehicles produced during DDT&E (three flight test vehicles and two structural units). Ground processing facilities are built at the WTR and ETR. Production facilities are also included in DDT&E. The ground processing facilities account for 84% of the total facility construction cost.

11.5.2 Production Phase Costs

The propulsion system productions costs, Fig. 159, are about half of the system production costs. The majority of this can be attributed to the engines themselves with an estimated first unit cost of approximately $81M per unit. The program mission model requires seven vehicles. This is a relatively low number, when compared with aircraft type production, and it is unlikely that much cost reduction will be achieved during the production phase because of this. The auxiliary propulsion segment includes the stability and control elements, the reaction control systems (RCS), the orbital maneuvering systems (OMS), as well as other related components. This overall segment represents 25% of the production phase costs. Structures and mechanisms include the aerosurfaces, tanks, nosecone and crew compartment segments of the vehicle.

11.5.3 Operations Phase

Unlike the operations and support (O&S) costs for existing systems such as the Space Shuttle, the O&S estimates for this system, Fig. 160, are the smallest element of the LCC. Launch operations represent the manpower for a five day turnaround working one shift per day. Processing in the vehicle system facility would consist of several parallel tasks. The payload is integrated in this facility but prepared off-line. The cost of slush hydrogen is approximately twice that of NBP hydrogen used in existing vehicles. Even with this additional cost, the propellant is not a cost driver and only represents 15% of the overall O&S cost. Payload loss costs are computed in the cost model as a function of the flight rate, reliability, payload capability and a payload value of $10,000/lb.

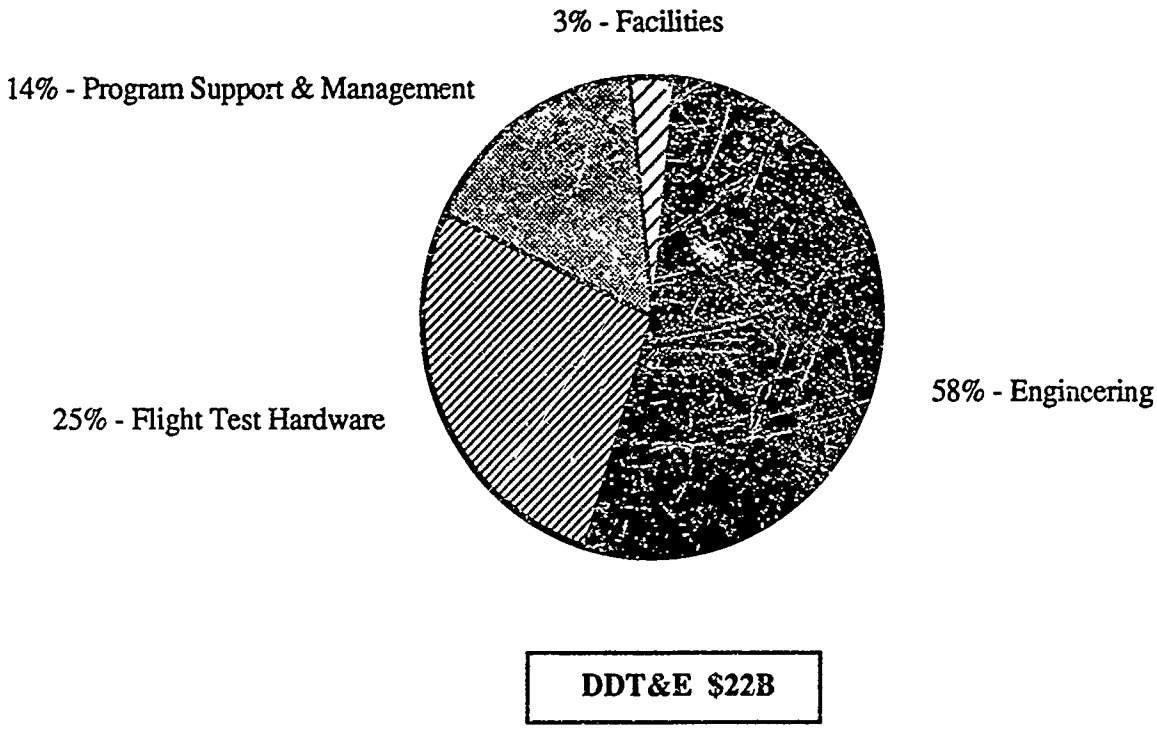


Fig. 158 DDT&E Cost Element

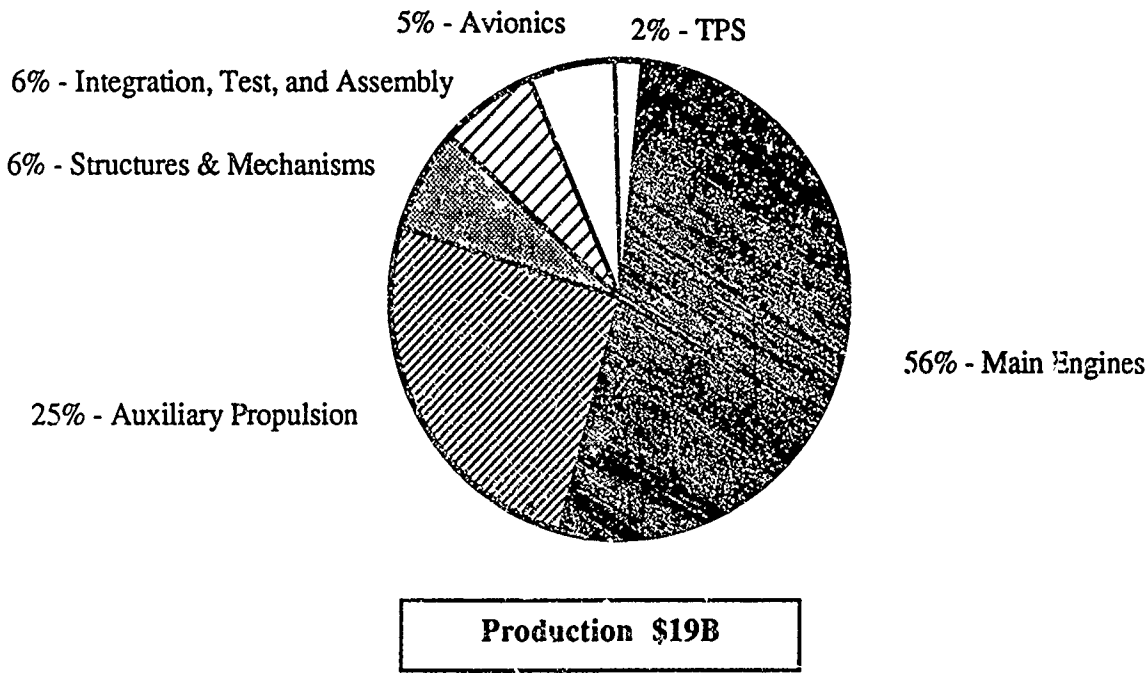
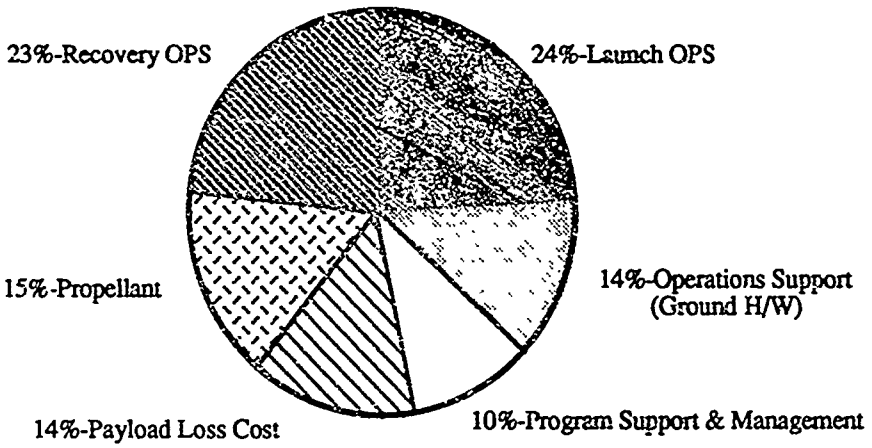
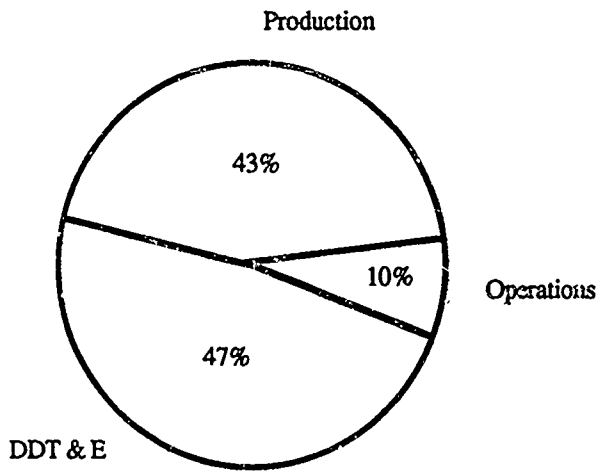


Fig. 159 Vehicle and Engine Production Element



O & S $4B

Fig. 160 Operations and Support Element



ETR (Payload = 40klb 28.5° Inclined)	WTR (Payload = 10 Klb 90° Polar)
Operations $/flt = $7M/flt	Operations $/flt = $15M/flt
Operations $/# = $160	Operations $/# = $1450
LCC $/flt = $88M	LCC $/flt = $98M
LCC $/lb = $2190	LCC $/lb = $9790

Life Cycle Cost = $45 B FY 87

Fig. 161 Vehicle and Engines Life Cycle Cost

11.5.4 Life Cycle Cost

The life cycle cost breakdown for the RBCC/SSTO vehicle, based on the assumptions and guidelines previously discussed, are summarized in Fig. 161. Notice that the DDT&E costs are slightly greater than the production costs for this program. This is due to the relatively small number of operational vehicles (seven total) which would be required to support launch of all 40 K pound payloads in the STAS II/R2 Mission Model. This suggests that if a larger number of vehicles were to be built, based upon the already expended DDT&E costs and production tooling costs, etc., the per vehicle cost, per launch cost, and dollar/lb to orbit costs would be further reduced.

Section 12.0

CONCLUSIONS AND RECOMMENDATIONS

The objective of this study was to assess the feasibility and capabilities of air-augmented rocket-based combined cycle engines applied to single-stage-to-orbit space transportation missions. The specific configuration focused on in this study was an extensively axisymmetric vehicle. The performance characteristics of this particular approach have been measured in terms of payload delivery capability and life cycle costs. The principal finding is that this vehicle design, using any of the five engine configurations studied, appears technically feasible and capable of meeting the performance requirements of an orbital payload delivery mission. It is suggested that this particular design concept deserves further study. This section presents task recommendations for that further study work.

On a life cycle cost basis, this design approach appears to have costs that meet the goals presently sought for the next generation of space transportation systems.

Additional analytical study will be required before an adequate information base can be developed to support any reasonable decision making processes with regard to further development of airbreathing launch vehicles. If the recommended work provides positive findings, the information base should then be available to support a logical decision making process regarding the desirability of proceeding, or not proceeding, with further development of this type of launch vehicle system.

12.1 Principal Conclusions

In the 500 klbm vehicle configuration (Fig. 162), all five engine types appear capable of delivering the target 10 klbm payload to a 100 nmi polar orbit. Ejector Scramjet powered vehicles in the 500 klbm, 1,000 klbm and 1.5 Mlbm TOGW/GLOW weight classes appear to have the capability of delivering 30 klbm, 90 klbm and 150 klbm of payload, respectively, to the 100 nmi polar orbit (Fig. 163).

The Ejector Scramjet engine is the least complex RBCC engine system of the five engine systems studied in the work that has been carried out by ACA. The Ejector Scramjet (ESJ) does not require turbocompressors or power turbine systems.

Air liquefaction technology development does not appear to be required for delivery of meaningful payloads to orbit. Future development of air liquefaction technology can provide improvement in vehicle performance.

Slush hydrogen technology development does not appear to be required for delivery of payloads to orbit. Development of the technology that would enable slush hydrogen to be used in RBCC/SSTO vehicles would provide increased vehicle performance.

The vehicle design optimizes at a scramjet velocity termination at Mach 15. To meet the mission requirements of an RBCC/SSTO vehicle, scramjet technology development may not be required above this velocity (Fig. 164).

Six strakes of approximately 50% body diameter height, or an equivalent lifting surface area, appear to be required to keep the angle-of-attack of the vehicle within reasonable bounds based on engine inlet conditions. Further work is recommended to verify this estimation.

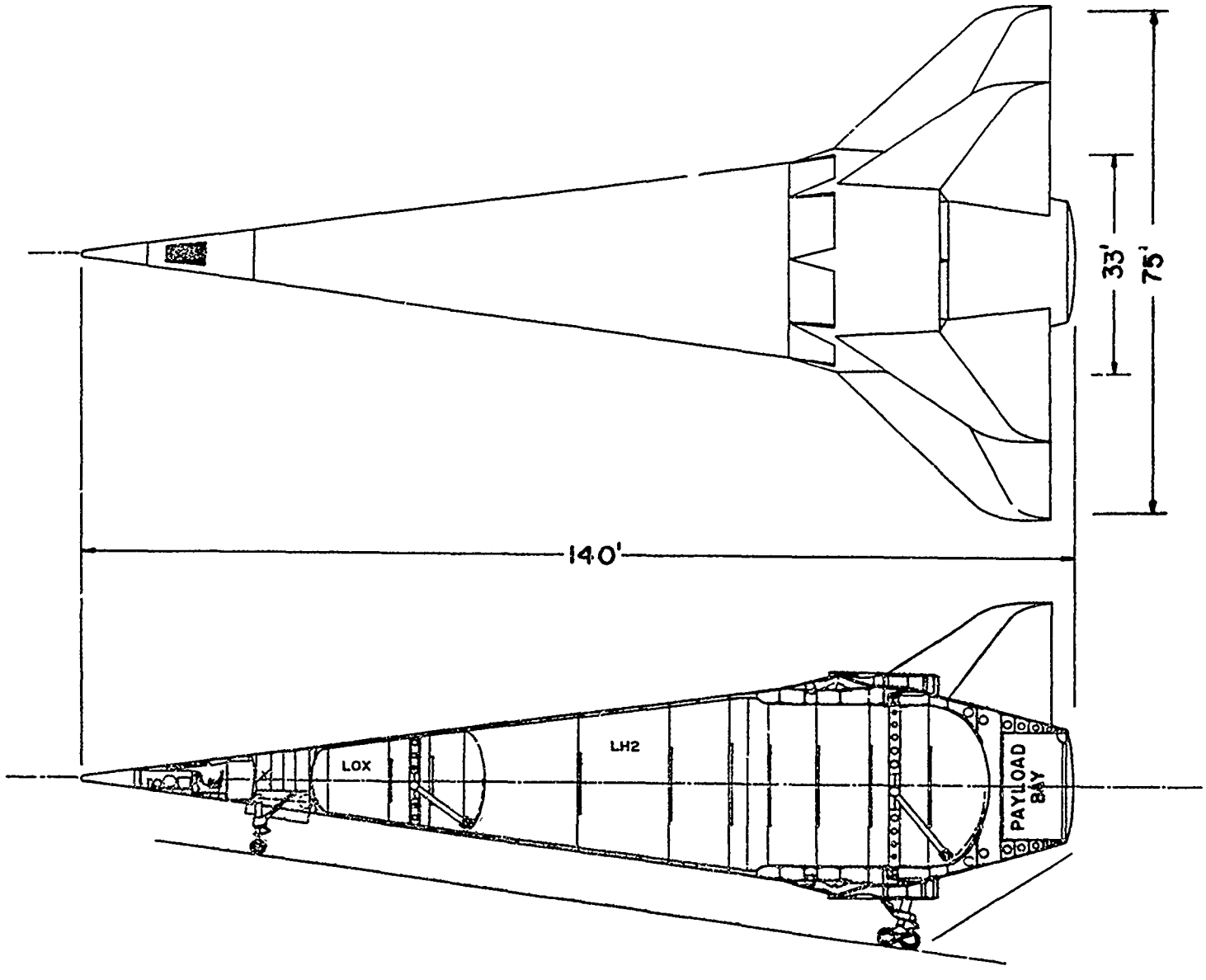


Fig. 162 500 klbm Axisymmetric Baseline Vehicle Configuration

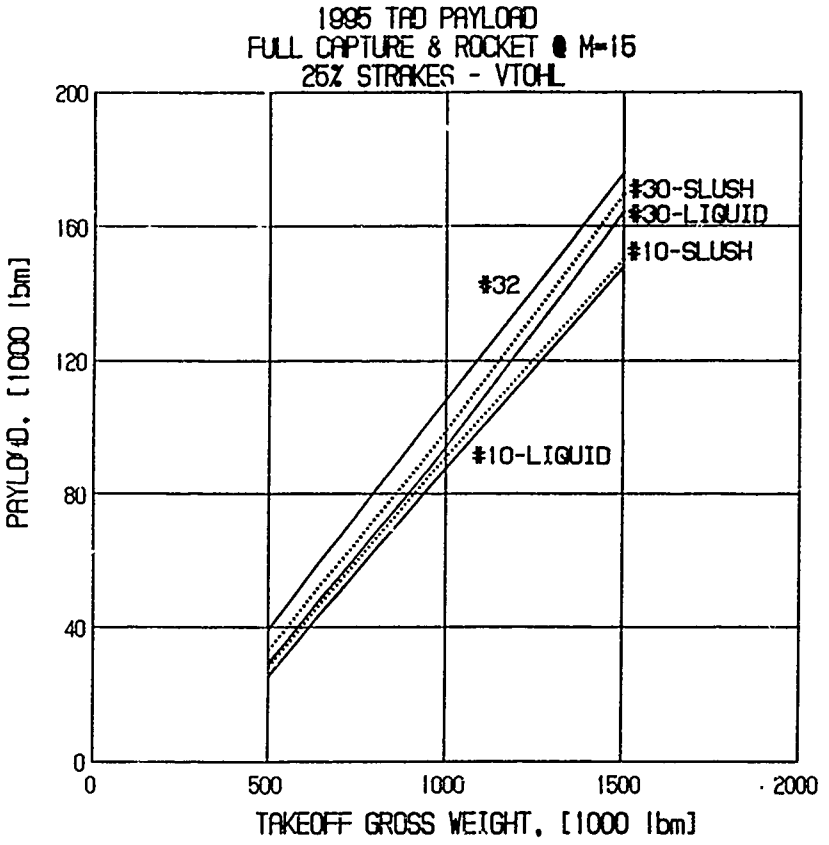


Fig. 163 RBC/SSTO Vehicles Payload vs. TOGW/GLOW

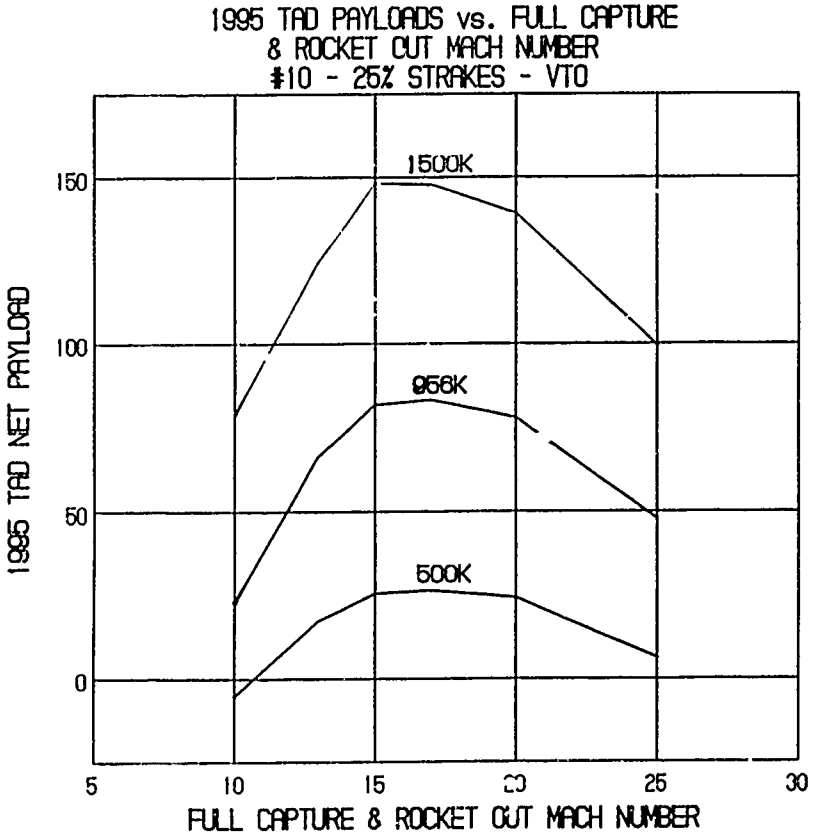


Fig. 164 RBCC/SSTO Vehicles Scramjet Transition Velocity vs. Rocket Out Mach Number for Various TOGW/GLOW Weights

Weight estimates and performance findings are based on technology advances generally expected to be accomplished by 1995. The accuracy of the payload estimates are dependent upon the accuracy of these 1995 TAD weight estimates. Further work in this area of study is recommended.

12.2 Recommended Approach

The objective of the work plan presented here is to carry the investigation of this design approach to a further level of depth and to develop a higher level of confidence in the findings of this conceptual study.

It is recommended that the tasks comprising the proposed program of work be carried out by a multi-contractor team. Firms with demonstrated experience in computational fluid dynamics, rocket ejector, ramjet, scramjet and rocket based combined cycle propulsion systems design, aerospace vehicle and ground systems design and launch vehicle systems life cycle cost analysis should serve as members of the project team.

It is recommended that the study work focus upon three TOGW/GLOW Ejector Scramjet vehicle configurations:

- 500,000 lbm
- 1,000.000 lbm
- 1,500,000 lbm

Using these three TOGW/GLOW class vehicles will permit further evaluation of the potential performance of RBCC/SSTO vehicles in mission scenarios inclusive of heavy lift missions.

It is further recommended that the Supercharged Ejector Scramjet be studied at a second priority level, as part of a preplanned product improvement program.

12.3 Tasks

The tasks to be carried out in the proposed program are:

12.3.1 Task 1 - Thrust Vector Lift/Aerodynamic Lift Study

Problem

The trajectory analysis work accomplished in this study is based upon a vehicle configuration with fixed, parallel thrust vector, lifting surfaces chord lines and vehicle longitudinal axis. The findings made during the study indicate that this does not appear to represent the optimum approach for two reasons. First, high angles of attack on the vehicle forebody act unfavorably on the inlet performance of the forebody. Secondly, the fixed thrust and lift vector geometry results in an expenditure of an as yet undetermined propellant weight to supplement the lifting capabilities of the aerosurfaces. Based on the experience gained in carrying out these analyses, there is an indication that a more optimum approach would trade off increased aerosurface lift, that could be achieved by a number of means, against reduced engine thrust vector lift over the overall trajectory. This should result in lower forebody angle of attack operation and may also result in higher payload capability.

Work Required

This investigation should provide analysis of the effects of varying the relationship between the thrust vector, lift vector, and vehicle longitudinal axis with varying wing areas on payload delivered to orbit.

12.3.2 Task 2 - Upgrade Aerodynamics and Trajectory Analysis Findings

Problem

The fidelity of the aerodynamic characterization of the vehicle should be improved.

Work Required

It is recommended that the an aerodynamic characterization of the extensively axisymmetric RBCC/SSTO vehicle be developed at a higher level of fidelity then that used in this conceptual study. The USAF DATCOM system and the NASA APAS program, and particularly the Hypersonic Arbitrary Body Program (HABP) which is a part of APAS, are examples of existing aerdynamic analysis tools that could usefully be applied to this problem. This aerodynamic characterization cannot be complete without additional information being developed descriptive of the base drag characteristics of the selected study configuration. This will require the work to be described in Task 3 to be carried out in a manner coordinated with this task.

A higher fidelity trajectory analysis program, for example the NASA POST program, should then be used to support more detailed investigation of the trajectory performance of the optimum configuration resulting from the Task 1 work. It is recommended that an aeroheating characterization capability be implemented and the aeroheating characteristics of each trajectory established. Trade studies should then be carried out to identify the trades between payload performance and aeroheating.

12.3.3 Task 3 - Forebody, Base Drag and Rocket Mode Computational Fluid Dynamic Study

Problem

The forebody and aftbody flow characteristics of the axisymmetric RBCC/SSTO vehicle design requires further investigation.

The means of achieving acceptable compression performance on the vehicle forebody is significant to the practicability of the axisymmetric design approach. This performance is effected by variations in vehicle angle of attack, velocity and altitude during air-breathing flight.

Full annular flow of engine exhaust products of combustion on the aftbody is expected to provide significant performance improvement in terms of both thrust augmentation and higher Isp, particularly in scramjet mode, and significant reduction in base drag.

The final all-rocket propulsion mode provides the velocity increment from Mach 15 to Mach 25. High Isp performance in this mode is essential. Obtaining the I_{sp} performace goals will be effected by the extent to which three expansion steps can be achieved in the rocket subsystem beyond the expansion provided by the divergent portions of the rocket subsystem nozzles. With the inlet doors closed, the first efficient expansion that must be achieved is expansion from the rocket subsystem nozzle exhaust conditions to the engine duct wall. The second expansion is in the RBCC engine nozzle section. The third expansion is on the vehicle

aftbody. Analysis is required to determine the nature of the conditions that must be established to successfully achieve these three expansions with the highest efficiency possible.

Work Required

A CFD study of forebody, engine and aftbody flow characteristics at varying angles of attack during air-breathing flight should be carried out. The objective of this work would be to quantify, to the greatest extent practical with analytical tools, the forebody compression performance at various angles of attack, the effectiveness of various means of reducing the effect of angle of attack on inlet flow conditions and the base drag characteristics of the aftbody throughout the complete orbital ascent trajectory.

In order to establish the aftbody flow characteristics during air-breathing flight, engine exhaust station conditions must be established to provide the initial state of flow at the aftbody start station. This suggests that the engine internal flow must also be modeled to permit a full "end-to-end" analysis is be carried out.

Analysis of the engine internal flow and aftbody flow during the all-rocket mode of operation to final orbital conditions should be analyzed as an integral portion of the trajectory analysis.

12.3.4 Task 4 - Vehicle, Propulsion and Ground Support Systems Design

Problem

The depth of design analysis of the propulsion system, all vehicle subsystems and ground support systems should be extended. The objective should be to further refine RBCC engine performance estimates, all weight estimations and all operations and support equipment requirements to provide more specific data to support life cycle cost analysis as described in Task 6.

Work Requirements

It is recommended that this study should involve the activities of a number of subcontractors familiar with rocket, ramjet and scramjet propulsion systems design and manufacture, space vehicle systems and ground support systems design and manufacture, and the specific problem of advanced turbofan technology. The principal objectives of this work should be to provide:

- a more detailed design of the complete vehicle system
- information upon which to refine the aerodynamic description of the vehicle
- improved vehicle weight and balance analyses
- data inputs to a second iteration of the system life cycle costs analysis.

One of the findings of this work has been the relatively small benefit realized from the more complex engine configurations involving:

- liquid air systems
- the use of slush hydrogen to enable the use of hydrogen recycling for air liquefaction

- the use of slush hydrogen to increase vehicle performance

It is recommended that further studies of air liquefaction and slush hydrogen be considered as part of a planned product improvement program.

With regard to fan supercharging systems, the potential benefit of the fan supercharger to vehicle utility in terms of improved cruise, loiter, landing and go-around capability together with vertical landing capability warrants further study.

12.3.5 Task 5 - Takeoff and Landing Mode Trades

Problem

The mode of takeoff and landing used will significantly effect the RBCC/SSTO system design requirements and design approach used. The selection of the particular combination of modes to be used is highly dependent upon the mission to be carried out by a particular vehicle system and is thus "user" dependent. The advantages and disadvantages of various combinations of horizontal takeoff and landing and vertical takeoff and landing needs to be investigated in sufficient detail to permit reasonable decision making by potential "users" of the takeoff and landing modes to be used. System safety studies must be included in any such investigation.

Vertical takeoff and landing capability, which eliminates all runway requirements, can contribute significantly to the reduction of operations costs. In addition, the range of operational scenarios in which this type of vehicle could function would be increased by elimination of the runway requirement. The value of this vehicle system to a "user" might thus be significantly increased by increasing the utility of the vehicle system to that user.

Vertical takeoff and landing capability can be provided in the axisymmetric RBCC/SSTO vehicle because of the thrust to weight ratio of these engines. There is an experience base in vertical takeoff and landing aircraft gathered in the experimental accomplishments in the field of vertical attitude vertical takeoff and vertical attitude vertical landing aircraft during the 1950s and 1960s. However, this experience base is not adequate to anwer the questions that need to be answered with regard to takeoff and landing modes for RBCC/SSTO vehicle systems.

Work Requirements

It is recommended that all takeoff and landing modes and mode combinations that might be used by axisymmetric RBCC/SSTO vehicles be studied with the objective of determining:

1. The stability and control requirements for each mode of takeoff and landing
2. The flight dynamic characteristics of the transition maneuvers and the requirements of optimum transition maneuvers.
3. The fuel weights required for both the takeoff and landing maneuvers combined with reasonable cruise, loiter and go-around capability in a range of scenarios.
4. The vehicle behavior in high wind conditions, including gusting, that might be encountered in all combinations of takeoff and landing maneuvers.
5. The structural implications of each takeoff and landing mode and each practical combination of mode particularly considering landing gear requirements.

6. The safety of each takeoff and landing mode and the means of achieving an acceptable level of system safety. This study should quantify the performance requirements that would have to be met by the vehicle system to provide required system safety levels and a quantitive measure of the probability of vehicle damage, vehicle loss, crew injury or crew loss. These findings should be developed in a manner that would permit safety requirements to be quantitatively defined in a manner that would permit direct comparison to the safety performance equivalent of fixed wing aircraft, helicopters, tilt-rotor aircraft and other air and surface transportation systems.

12.3.6 Task 6 - Upgrade Life Cycle Costs Analysis

It is recommended that the life cycle cost analysis then be upgraded based on the vehicle systems information resulting from the work done in the five preceding tasks described. This life cycle cost analysis should place particular emphasis on determining the CER's associated with axisymmetric construction and the use of an autonomous control system in the vehicle as it impacts on not only operations and operations support costs but upon test and checkout operations during the production phase.

REFERENCES

No.	Reference
1	Dixon, S.C., NASA R&T for Aerospace Plane Vehicles, Langley Research Center, NASA Technical Memorandum 86429, May 1985.
2	Escher, W.J.D., and Flornes, B. J., et al, A Study of Composite Propulsion Systems for Advanced Launch Vehicle Applications, Final Report on NASA Contract NAS7-377, The Marquardt Corporation, Van Nuys, CA, April 1967
3	Anon, Pre-proposal Contractor Briefing Package, ALS, System Contract #F04701-87-C-0101, USAF/AFSC, HQ Space Division, Los Angeles, CA, 5 May 1987
4	Simonson, A.J. and Schmeer, J.W., Static Thrust Augmentation of a Rocket Ejector System with a Heated Supersonic Primary Jet, Langley Research Center, NASA TND-1261, May 1962
5	Mossman, E.A., Rozycki, R.C., and Hoile, G.F., A Summary of Research on a Nozzle-Ejector System, Martin Denver Research Report R-60-31, October 1960
6	Totten, J.K., Final Summary Technical Report on the Calendar Year 1963 Advanced Ramjet Technology Program, The Marquardt Company Final Technical Report under the Aeropropulsion Laboratory Contract AF 33(657)12146
7	Congelliere, J., Prevatte, N. and Lime, J., Advanced Ramjets Concepts, Vol II Ejector Scramjet Technology, The Marquardt Corporation, Report No. AFAPL-TR-67-118, May, 1968
8	Anon., Hypersonic Research Engine Project (Phase II), Final Oral Review Technical Presentation, Garrett AiResearch Report No. 75-1/338, NASA Contract NAS1-6666, 23 March 1975
9	Anon., Final Report - Hydrogen Turbofan Study, Garrett AiResearch Corporation for the Lockheed California Co. under NASA Langley Research Center Contract NAS-1-14614, NASA CR-145369, Vol. I, pp. 32-95, July 1978
10	Kumar, A., and Anderson, G. Y., Study of Hypersonic Inlet Flow Fields with a Three-Dimensional Navier-Stokes Code", AIAA Paper AIAA-86-1426, June 1986
11	Anon, YF-12 Experiments Symposium, NASA Conference Publication 2054, Dryden Research Center, September 1978

No.	Reference
12	Puorto, J. W., SERJ Fan Integration Study, Final Report, The Marquardt Corporation, Report No. 25279, AD500754, February 1969
13	Hosack, G. A. and Stromsta, R. R., Performance of the Aerobell Extendible Nozzle, AIAA Journal of Spacecraft, Vol. 6, No. 12, pp 1416-1423, December 1969
14	Congelliere, J., et al, 1965 Advanced Ramjet Concepts Program Final Report Vol. III - Ejector SCRAMJET Analysis, The Marquardt Corporation AFAPL-TR-66-49, August 1966
15	Congelliere, J., Prevatte, N. and Lime, J., Advanced Ramjets Concepts, Vol II Ejector Scramjet Technology, The Marquardt Corporation, Report No. AFAPL-TR-67-118, May 1968
16	Flornes, B. J., and Davidson, G. R., Advanced Ramjet Concepts, Vol VIII, RamLACE/SCRAMLACE Propulsion Systems Analysis and Design, Technical Report AFAPL-TR-67-188, Vol. VII, The Marquardt Corporation, Van Nuys, CA, February 1968
17	Stull, F. D., Useful Scramjet Curves, a technical graph package obtained from the author, WPAPL, October 1984
18	Anon, Alternate Vehicle/Propulsion Study, Boeing Military Airplane Company and Rockwell International Space Transportation Systems Division presentation package, Jun 1985
19	Billig, F. S., and Beach, L. D., Hypersonic Propulsion, AIAA Sponsored Short Course Notes, Huntsville, AL, June 1985
20	Escher, W. J. D., and Doughty, D. L., Assessment of Cryogenic Hydrogen-Induced Air Liquefaction Technologies, Final Report to Science Applications International Corporation under Subcontract No. 15-860020-82, September 1986
21	Smith, L.R., Summary of Aerospace Program for 1963, The Marquardt. 1963 Annual Project Report under USAF Contract AF33(657)10796, Report No. APL-TDR-64-32, January 1964
22	McCarty, R.D., Hord, J. and Roder, H. M., Selected Properties of Hydrogen (Engineering Design Data), National Bureau of Standards Monograph, National Engineering Laboratory, Boulder, CO, USGPO 1981
23	Watson, K. A, DOF36 Program Users Guide, Air Force Wright Aeronautical Laboratories, Dayton, OH, April 1986
24	Watson, K. A., Analysis Development - 6-DOF Trajectory Simulation, Air Force Wright Aeronautical Laboratory, Dayton, OH, 1986
25	Freeman, Delma A., Advanced Space Transportation Studies Peer Review, NASA LaRC, 28 July 1987

No.	Reference
26	Hoerner, Sighard F., Fluid Dynamic Drag, Hoerner Fluid Dynamics, Brick Town, N.J., 1975
27	Polhamus, Edward C., Predictions of Vortex-Lift Characteristics by a Leading Edge Suction Analogy, Journal of Aircraft, April 1971, Vol 8, No. 4, pp 193-199
28	Bertin, John J. and Smith, Michael L., Aerodynamics for Engineeers, Prentice Hall, Englewood Cliffs, N.J., 1979
29	Lindenbaum, B., V/STOL Concepts and Developed Aircraft, Final Report, AFWAL-TR-86-3071, Air Force Wright Aeronautical Laboratories, November 1986
30	Anon, Special Short Course in V/STOL Aircraft, AGARD Report AGARD-R-710, North Atlantic Treaty Organization Advisory Group for Aerospace Research and Development, May 1984
31	Provided by Mr. W. Pelham Phillips, Experimental Aerodynamics Branch, Space Systems Division, NASA LaRC, December 1987

GLOSSARY

AAR	Air Augmented Rocket
ACA	Astronautics Corporation of America
ACES	Air Collection Enrichment System
ACS	Attitude Control System
Alpha	Angle of Attack
APL	Applied Physics Laboratory of Johns Hopkins University
APU	Auxiliary Power Unit
ALS	Advanced Launch System
CDA	Constantly Decreasing Altitude
CER	Cost Estimating Relationship
CFD	Computational Fluid Dynamics
C.G.	Center of Gravity
CONUS	Continental United States
DAB	Diffusion and Combustion
DOF36	Trajectory Analysis program
ECLSS	Environmental Control and Life Support System
ES	Ejector Scramjet - Engine No. 10
ETR	Eastern Test Range
Gamma	Flight Path Angle
GLOW	Gross Lift Off Weight
GSE	Ground Support Equipment
HA	Horizontal Attitude
HL	Horizontal Landing
HRE	Hypersonic Research Engine
HPTV	Hypersonic Propulsion Test Vehicle
HRSI	High Temperature Reuseable Surface Insulation
HTO	Horizontal Takeoff
I*	Total Mission Effective Specific Impulse
I_{eff}	Effective Specific Impulse
I_{sp}	Specific Impulse
IHPTET	Integrated High Performance Turbine Engine Technology
IOC	Initial Operating Capability
LACE	Liquid Air Cycle Engine - loosely used to refer to RBCC engines using liquid air
L/D	Length/Diamcter
LAIR	Liquid Air
LaRC	NASA Langley Research Center
LCC	Life Cycle Costs
LeRC	NASA Lewis Research Center
LEO	Low Earth Orbit
LOX	Liquid Oxygen
LRSI	Low Temperature Reuseable Surface Insulation

M2	Mass inserted into target orbit
MMAG	Martin Marietta Aerospace Group
MSFC	NASA Marshall Space Flight Center
NASP	National Aerospaceplane Project
NBP	Normal Boiling Point
O/F	Oxidizer/Fuel
OMS	Orbital Manuevering System
O&S	Operations and Support
PFRT	Pre-Flight Readiness Test
Q	Dynamic Pressure
RCS	Reaction Control System
RBCC	Rocket Based Combined Cycle
RENE	Rocket Engine Nozzle Ejector
RP-1	Rocket Propellant 1
RSSL	Recycled Supercharged Scram LACE - Engine No. 32
SSTO	Single Stage to Orbit
SES	Spaceborne Expert System
SES	Supercharged Ejector Scramjet - Engine No. 12
SH2	Slush liquid Hydrogen
SL	ScramLACE - Engine No. 22
SLH2	Slush liquid Hydrogen
SLS	Sea Level Static
SMC	Simultaneous Mixing and Combustion
SPUV	Self Powered Unmanned Vehicle
SSL	Supercharged ScramLACE - Engine No. 30
STAS	Space Transportation Architecture Study
STS	Space Transportation System
TAD	Technology Availability Date
TOGW	Takeoff Gross Weight
TPS	Thermal Protection System
T/W	Thrust to Weight Ratio
VA	Vertical Attitude
VL	Vertical Landing
VTO	Vertical Takeoff
WBS	Work Breakdown Structure
WDOTP	Total Propellant Flow Rate
WTR	Western Test Range